

Alma Mater Studiorum - Università di Bologna

DOTTORATO DI RICERCA IN  
BENI CULTURALI E AMBIENTALI

Ciclo 35

**Settore Concorsuale:** 05/B1 - ZOOLOGIA E ANTROPOLOGIA

**Settore Scientifico Disciplinare:** BIO/05 - ZOOLOGIA

UNLOCKING ECOLOGICAL HISTORY USING FISH REMAINS: ECO-  
EVOLUTIONARY CONSEQUENCES OF EXPLOITATION IN THE ATLANTIC  
BLUEFIN TUNA

**Presentata da:** Adam Jon Andrews

**Coordinatore Dottorato**

Donatella Restani

**Supervisore**

Fausto Tinti

**Co-supervisore**

Alessia Cariani

**Esame finale anno 2023**



# Unlocking ecological history using fish remains

## Eco-evolutionary consequences of exploitation in the Atlantic bluefin tuna

Adam J. Andrews

Dissertation presented for the degree of  
*Philosophiae Doctor (PhD)*  
2023



Dipartimenti di Scienze Biologiche, Geologiche e Ambientali e di Beni Culturali, Campus di Ravenna  
ALMA MATER STUDIORUM - Università di Bologna

**Author's address**

Adam J. Andrews  
MSCA SeaChanges ITN  
Dipartimento di Scienze Biologiche, Geologiche ed  
Ambientali  
Università di Bologna, Ravenna, 48123 Italia  
[adam@palaeome.org](mailto:adam@palaeome.org)

**Main Supervisor**

Prof. Fausto Tinti  
Dipartimento di Scienze Biologiche, Geologiche ed  
Ambientali  
Università di Bologna, Ravenna, 48123 Italia  
[fausto.tinti@unibo.it](mailto:fausto.tinti@unibo.it)

**Co-Supervisor**

Prof. Alessia Cariani  
Dipartimento di Scienze Biologiche, Geologiche ed  
Ambientali  
Università di Bologna, Ravenna, 48123 Italia  
[alessia.cariani@unibo.it](mailto:alessia.cariani@unibo.it)

**Reviewers**

Dr. Canan Çakılar  
University of Groningen  
Faculty of Arts  
Poststraat 6  
9712 ER Groningen, The Netherlands  
[c.cakirlar@rug.nl](mailto:c.cakirlar@rug.nl)

Prof. Brian MacKenzie  
DTU AQUA - Technical University of Denmark  
National Institute of Aquatic Resources  
Section for Oceans and Arctic  
Kemitorvet, 201, 262  
2800 Kgs. Lyngby, Denmark  
[brm@aquu.dtu.dk](mailto:brm@aquu.dtu.dk)

**Cover image**

*Embarking on the ancient DNA analysis of tuna remains, Laboratorio del DNA antico, Ravenna 2019.*

## Abstract

Adam J. Andrews

### **Unlocking ecological history using fish remains**

Eco-evolutionary consequences of exploitation in the Atlantic bluefin tuna

ALMA MATER STUDIORUM - Università di Bologna

Dissertation

During recent decades, the health of ocean ecosystems and fish populations has been threatened by overexploitation, pollution, and anthropogenic-driven climate change. Due to a lack of long-term data, we have a poor understanding of when intensive exploitation began and what impact anthropogenic activities have had on the ecology and evolution of fishes. Such information is crucial to recover degraded and depleted marine ecosystems and fish populations, maximise their productivity in-line with historical levels, and predict their future dynamics. In this thesis, I evaluate anthropogenic impacts on the iconic Atlantic bluefin tuna (*Thunnus thynnus*; BFT), one of the longest and recently most intensely exploited marine fishes, with a tremendous cultural and economic importance. Using a long-time series of archaeological and archived faunal remains (bones) dating back to approximately two millennia ago, I apply morphological, isotopic, and genomic techniques to perform the first studies on long-term BFT size and growth, diet and habitat use, and demography and adaptation, and produce the first genome-wide data on this species. My findings suggest that exploitation had impacted BFT foraging behaviour by the ~16<sup>th</sup> century when coastal ecosystem degradation induced a pelagic shift in diet and habitat use. I reveal that BFT biomass began to decline much earlier than hitherto documented, by the 19<sup>th</sup> century, consistent with intensive tuna trap catches during this period and catch-at-size increasing. I find that BFT juvenile growth had increased by the early 1900s (and more dramatically by the 21<sup>st</sup> century) which may reflect an evolutionary response to size selective harvest—which I find putative genomic signatures of. Further, I observed that BFT foraging behaviours have been modified following overexploitation during the 20<sup>th</sup> century, which previously included a isotopically distinct, Black Sea niche. Finally, I show that despite biomass declining from centuries ago, BFT has retained genomic diversity. This provides confidence for its long-term recovery, suggesting that management plans can be ambitious with their recovery targets. However, the loss of a Black Sea trophic niche, and potential for fisheries-induced evolution is concerning and requires further investigation. Unfortunately, all in all my findings show that modern marine ecosystems may be more heavily modified than previously thought, therefore further multidisciplinary long-term investigations are warranted to study the wide-ranging and far-reaching effects of marine exploitation.

Keywords: exploitation impacts; adaptation; fisheries-induced evolution; historical baselines; long-term population dynamics; fish remains



*José Luis Cort -  
Atlantic bluefin tuna in abundance during antiquity, on their  
annual spawning migration through the Strait of Gibraltar.*

“

If you slaughter sheep instead of shearing them once a year you run out of wool, skin and the future lambs.

”

Fray Martín Sarmiento, 1757.

*On the perceived overexploitation of Atlantic bluefin tuna during the 16<sup>th</sup> century.*

Translated from *De los atunes y sus transmigraciones y conjeturas sobre la decadencia de las almadrabas y sobre los medios para restituirlas. Caixa de Pontevedra, Madrid.*

This thesis is a contribution to the <https://tunaarchaeology.org> project within the framework of the Marie Skłodowska–Curie Actions Innovative Training Network, SeaChanges <https://sites.google.com/york.ac.uk/seachanges> – hosted by the University of York, U.K.



This thesis was funded by the European Union's Horizon 2020 Grant No. 813383





## Contents

<b>Acknowledgements</b> .....	<b>11</b>
<b>Introduction</b> .....	<b>13–19</b>
Fish remains as archives of eco-evolutionary change.....	14
Study system: the eastern Atlantic and Mediterranean bluefin tuna.....	16
Aims and outline.....	17
<b>Chapter 1</b> Exploitation history of Atlantic bluefin tuna in the eastern Atlantic and Mediterranean—insights from ancient bones.....	<b>21–50</b>
<b>Chapter 2</b> Length estimation of Atlantic bluefin tuna ( <i>Thunnus thynnus</i> ) using vertebrae.....	<b>52–80</b>
<b>Chapter 3</b> Vertebrae reveal industrial-era increases in Atlantic bluefin tuna catch-at-size and juvenile growth.....	<b>82–112</b>
<b>Chapter 4</b> Isotopic life-history signatures are retained in modern and ancient Atlantic bluefin tuna vertebrae.....	<b>114–138</b>
<b>Chapter 5</b> Exploitation shifted trophic ecology and habitat preferences of Mediterranean and Black Sea bluefin tuna over centuries.....	<b>140–187</b>
<b>Chapter 6</b> Ancient DNA SNP-panel data suggests stability in bluefin tuna genetic diversity despite centuries of fluctuating catches in the eastern Atlantic and Mediterranean....	<b>189–213</b>
<b>Chapter 7</b> Ancient DNA and genomics reveals exploitation induced pre-industrial biomass declines in Atlantic bluefin tuna but has not limited its adaptive potential.....	<b>215–253</b>
<b>Discussion</b> .....	<b>255–260</b>
Eco-evolutionary consequences of exploitation.....	255
Revising Atlantic bluefin tuna ecology with history.....	257
Digging deeper.....	259
Conclusion.....	260
<b>References</b> .....	<b>261–271</b>

*To my mother and my father, for their love and support without ever expecting*

## Acknowledgements

This thesis documents a series of challenging studies which had little precedent and fell outside of both the fields of marine ecology and archaeology. Therefore, more so here than in any work I have conducted to date, have I been grateful for the collaboration of a large group of wonderful friends and colleagues who each contributed with specific expertise toward the success of the project. Despite the added complications of the global COVID-19 pandemic, I have been fortunate enough to be able to follow (and I think exceed) my research objectives thanks to the personal and professional support given by many, for which I am eternally grateful. First, I would like to recognise my MSc supervisors in Tromsø, Kim, Jørgen and Shripathi for their part in preparing me for this PhD. The training you each provided was invaluable and I am grateful for your support and friendship still. I would like to sincerely thank my supervisors, Fausto, Alessia and Betta for giving me such a rare opportunity to explore my research interests in the most enjoyable of ways at this historical institution, and in such a wonderful part of the world. I am truly grateful for the faith you placed in me, the freedom you gave me and the support you've provided whenever I've needed it. Thank you. I would also like to thank my second team of supervisors (just not on paper), which I also hold dear, Michelle, Arturo, Bastiaan and Tony. Thank you for the knowledge you've imparted during the past few years, for the hard work you've put in, and for kindly hosting me (sometimes for months on end!). A special thanks is warranted to Bastiaan for introducing me to my darling Emma, who at the time was his MSc student studying tuna paleogenomics. As it turns out, ancient tuna DNA is quite the topic to bond over and my publications were not the biggest success of the last few years. While there are too many friends and colleagues to mention, I would like to specifically thank Darío, for his archaeological wisdom, and David for his support and coordination of the SeaChanges ITN. Lastly, I'd like to thank those I studied alongside, Marko, Fra, Paolo, Andrea – I feel very lucky to have shared this experience with you and to have done so laughing every day.



## Introduction

For millennia, ocean ecosystems have been threatened by a myriad of anthropogenic impacts, such as fisheries exploitation, habitat modification, pollution, and climate change (Jackson *et al.*, 2001; Erlandson and Rick, 2010; Lotze, Hoffmann and Erlandson, 2014; Schwerdtner Máñez *et al.*, 2014; Engelhard *et al.*, 2015). During the past century, these have had measurable and increasing consequences for the ecology and evolution of fish populations. Among threats, the development of fisheries has brought about rapid and substantial declines in population biomass (Myers and Worm, 2003). While depleting populations, exploitation has been shown to impact population complexity, through the extinction of sub-populations, the contraction of geographical ranges, the restructuring of age classes, as well as modifying a host of other life-history traits which are intertwined, such as fecundity, maturation, growth, migration and spawning behaviour, and diet use (Jennings, Reynolds and Mills, 1998; Pauly *et al.*, 1998; Rochet, 1998; Casini *et al.*, 2009; Butchart *et al.*, 2010; Worm and Tittensor, 2011; Neubauer *et al.*, 2013; Britten, Dowd and Worm, 2016). As a result, many fish populations are perceived to be less productive, and less reproductively successful (lower fitness), than they were historically (Pauly, 1995; Crozier and Hutchings, 2014; Engelhard *et al.*, 2015). This has generated both immediate economic concerns for the sustainability of industries and food security (Pauly *et al.*, 2002; Pauly, Watson and Alder, 2005; McClanahan, Allison and Cinner, 2015), and ecological ones; for the ability of fish populations to recover, contribute to natural ecosystem functioning, and adapt to dynamic environments (Hilborn *et al.*, 2003; Kuparinen and Hutchings, 2012; Neubauer *et al.*, 2013; Duarte *et al.*, 2020).

Due to a scarcity of long-term empirical data on the historical abundance and complexity of fish populations, the true impact of their exploitation—and anthropogenic activities more broadly—remains unknown. Prior to 1970, and especially 1950, quantitative fishery and ecological data are lacking; prompting questions by many of how recent changes in marine environments scale in a historical perspective, when exploitation rates were lower and when climate conditions were different (Pauly, 1995; Jackson *et al.*, 2001; Finney *et al.*, 2010; Lotze, Hoffmann and Erlandson, 2014; Schwerdtner Máñez *et al.*, 2014; McClatchie *et al.*, 2017). Moreover, a lack of long-term data precludes the opportunity to realise whether anthropogenic impacts have caused more permanent, evolutionary (inherited) responses such as a loss of genetic variability—as observed in overexploited terrestrial taxa (Khan *et al.*, 2021; Femerling *et al.*, 2022; Robin *et al.*, 2022)—and adaptive responses like fisheries -induced evolution (Kuparinen and Merilä, 2007; Heino, Pauli and Dieckmann, 2015), which have large consequences for the resilience of fish populations (Jørgensen *et al.*, 2007; Planque *et al.*, 2010; Kuparinen and Hutchings, 2012; Howarth *et al.*, 2014; Heino, Pauli and Dieckmann, 2015; Kardos *et al.*, 2021).

Despite acknowledgement of recent human impacts, efforts to rebuild marine ecosystems and recover depleted fish populations (Worm *et al.*, 2009; Duarte *et al.*, 2020; Hilborn *et al.*, 2020) are therefore limited (Pauly, 1995). In recent years, the discipline of 'Marine historical ecology' (Box 1) has emerged as a means to uncover past properties of marine ecosystems, populations, and their dynamics; and thereby provide novel perspectives with which to guide recovery targets (Pinnegar and Engelhard, 2008). Indeed, a growing body of research indicates that ocean ecosystems have been more impacted by human exploitation for longer than was previously understood (Jackson *et al.*, 2001; Barrett, Locker and Roberts, 2004;

Lotze, Hoffmann and Erlandson, 2014; Guiry *et al.*, 2021; Atmore *et al.*, 2022). It is therefore of practical significance to investigate the onset of intensive exploitation for fish populations, their past properties under more natural scenarios; and their responses to ecosystem change (Lotze and Worm, 2009; Engelhard *et al.*, 2015; Caswell *et al.*, 2020). This is especially important for those species that bioenergetically dominate and regulate marine ecosystems like apex predators.

#### Box 1. Marine historical ecology

Uncovering past reference points (or historical baselines) for the past properties of fish populations requires the assembling of hard-to-obtain long time-series data, and the combination of qualitative information and reasonable assumptions. In recent years, the discipline of marine historical ecology has developed to address these challenges; allowing for novel perspectives on the “shifting baseline” concept (Pauly, 1995) i.e. that knowledge of natural marine environments has been lost and the condition of modern environments is being measured against more recent, already modified states; which appear to be normal and natural (Jackson *et al.*, 2001; Erlandson and Rick, 2010; Lotze, Hoffmann and Erlandson, 2014; Schwerdtner Mániz *et al.*, 2014; Engelhard *et al.*, 2015).

Therefore, historical baselines of population abundance and complexity have the potential to improve the management and conservation of marine fish populations—especially those which have been recently overexploited yet have a long exploitation history. Indeed, there is a financial and scientific cost of not doing so (Zeller, Froese and Pauly, 2005). Since Pauly (Pauly, 1995), significant interest has developed in the subject, as evidenced by a host of international research programmes including the Oceans Past Initiative, 4-OCEANS, and our own SeaChanges ITN.

It is recognised that even low-level artisanal fisheries had the potential to drive ecological change and that, after a myriad of natural and anthropogenic processes that have occurred across millennia, returning degraded ecosystems to their former states is unlikely (Pinnegar and Engelhard, 2008; Duarte *et al.*, 2020).

#### Fish remains as archives of eco-evolutionary change

A range of sources have been interrogated to investigate the historical abundance and complexity of fish populations, including ethnography, anecdotes, and historical catch records (Ravier and Fromentin, 2001; MacKenzie and Myers, 2007; Pinnegar and Engelhard, 2008; Di Natale, 2014; Thurstan, Hawkins and Roberts, 2014; Bennema, 2018; France, 2021; Schijns *et al.*, 2021). Fish remains (bones, scales, otoliths) excavated from archaeological settlements or archived in osteological and zoological collections offer additional ecological and evolutionary insights, not feasible with qualitative historical and fishery catch data, especially via multidisciplinary applications of biomolecular and morphological analyses (Erlandson and Rick, 2010; Orton, 2016; Morales-Muñiz *et al.*, 2018). That fish remains can reveal long-term population dynamics and marine impacts, at the forefront of marine historical ecology advances, is exemplified by numerous recent studies (Richter *et al.*, 2011; McClatchie *et al.*, 2017; Oosting *et al.*, 2019; Blankholm *et al.*, 2020; Guiry and Hunt, 2020; Llorente-

Rodríguez *et al.*, 2022), spurred from a rich basis of investigations which have already greatly improved our perspectives of the natural world (Finney *et al.*, 2002; Van Neer *et al.*, 2002, 2004; Barrett, Locker and Roberts, 2004).

Among information archived within fish remains are historical size and growth data—measurable from the dimensions of the remains themselves and growth rings preserved across their surface (Bolle *et al.*, 2004; Orton, 2016; Barrett, 2019). While fishes grow, they incorporate biogeochemical signatures from their environment and prey into their body tissues. Some of these can persist for centuries or millennia after post-mortem processes have degraded other components of the body. Stable isotopes have thus emerged as a useful tool to study the diet and habitat use of fishes in past environments, while elements are increasingly studied, though require additional consideration of how degradation and exogenous material from burial or storage environments might affect measurements (Orton, 2016; Tzadik *et al.*, 2017; Guiry and Hunt, 2020). Driven by limited empirical data for fisheries-induced evolution, and expectations on how exploitation impacts genetic variability—which is being born true in terrestrial taxa (Khan *et al.*, 2021; Femerling *et al.*, 2022; Robin *et al.*, 2022), DNA is potentially the most exciting biomolecule archived within fish remains. Ancient DNA—that which is old or that was not intentionally preserved—has been shown to be well preserved within fish remains, depending on the burial environment (Ferrari *et al.*, 2021), and thus offers much potential to investigate demographic and adaptive responses of fish populations.

Some fishes e.g. Atlantic cod (*Gadus morhua*) have become reasonably well-studied in these regards and now have a rich base of long-term population dynamic information gleaned from faunal remains (Barrett *et al.*, 2011; Orton *et al.*, 2011; Ólafsdóttir *et al.*, 2014, 2017, 2021; Bonanomi *et al.*, 2015; Barrett, 2019; Denechaud *et al.*, 2020; Smoliński *et al.*, 2020; Pinsky *et al.*, 2021; Pedersen, Amundsen and Wickler, 2022; Sodeland *et al.*, 2022). Other fishes like Atlantic bluefin tuna (*Thunnus thynnus*; BFT) are poorly studied, despite their importance (Box 2). For BFT, investigations on long-term population dynamics remain limited by genetic marker power and temporal extent (Riccioni *et al.*, 2010). Although, the potential for revealing demographic change, specifically, has been noted (Puncher *et al.*, 2016). Meanwhile, several sources of BFT remains have been documented as ripe for ecological purposes (Puncher *et al.*, 2015), after species ID and DNA preservation was confirmed using genetic methods (Puncher *et al.*, 2019). Only a single other study applying multidisciplinary methods on BFT remains exists (Schloesser *et al.*, 2009), which investigates the stable isotopic composition of archived otoliths—though without ecological insights. Since fishes can be ecologically diverse, with different exploitation histories, it is not often appropriate to apply findings from one species or population to another. Thus, it was my objective to advance knowledge on the historical ecology and evolution of the iconic BFT.

## Box 2. Significance of the Atlantic bluefin tuna

The Atlantic bluefin tuna (*Thunnus thynnus*; BFT) has been hugely culturally important for millennia, not only around the Mediterranean but in northern Europe and America (MacKenzie and Myers, 2007; Fromentin, 2009; Di Natale, 2012, 2014; Longo and Clark, 2012; Örenc *et al.*, 2014; Cort and Abaunza, 2019; Mylona, 2021). Today, it has the highest value among all tunas (Thunnini tribe), comprising a multi-billion-euro industry which is important for food security (Galland, Rogers and Nickson, 2016). Ecologically, as a large marine predator, BFT is considered a keystone species, important for regulating trophic dynamics of multiple marine ecosystems via top-down control (Heithaus *et al.*, 2008; Baum and Worm, 2009; Steneck, 2012). In addition, BFT acts as a sentinel species which indicates ecosystem health (Hazen *et al.*, 2019). There is also a growing recognition of the role that large marine predators play in ecosystem services more broadly, including as biogeochemical regulators important in the current climate crisis (Spiers *et al.*, 2016; Atwood and Hammill, 2018; Bianchi *et al.*, 2021). Furthermore, BFT plays a crucial role as an iconic species for marine conservation, attracting perhaps the greatest societal affinity than any fish since its adoption in World Wildlife Foundation programs (WWF, 2006; Williams, 2007).

## Study system: the eastern Atlantic and Mediterranean bluefin tuna

BFT is a pelagic marine predatory fish characterised by its large size (up to 3.3 m in length and 725 kg in weight), far-reaching and inshore migration behaviour, and slow maturation (between 3-6 years, Piccinetti, Di Natale and Arena, 2013; Heinisch *et al.*, 2014). Since 1980, BFT have been managed by ICCAT (the International Commission for the Conservation of Atlantic Tunas) as two stocks (Fromentin and Powers, 2005), a hypothesis supported by recent isotopic (Rooker *et al.*, 2008) and genomic studies (Puncher *et al.*, 2018). These are a western Atlantic component that spawns predominantly in the Gulf of Mexico (Richardson *et al.*, 2016) and an eastern Atlantic and Mediterranean component that spawns predominantly in the Mediterranean Sea (Piccinetti, Di Natale and Arena, 2013). The majority of individuals undertake diverse feeding migrations to a range of habitats throughout the Atlantic (Sella, 1929; Wilson and Block, 2009; Druon *et al.*, 2016; Mariani *et al.*, 2016) from as early as age one (Dickhut *et al.*, 2009), believed to be mediated by climate (Faillettaz *et al.*, 2019). Adults exhibit a high-degree of natal homing despite high-levels of population mixing (Rooker *et al.*, 2008; Richardson *et al.*, 2016; Puncher *et al.*, 2018; Rodríguez-Ezpeleta *et al.*, 2019; Brophy *et al.*, 2020) and home to oligotrophic spawning grounds between April and July where they batch spawn (they sometimes skip spawning) at temperatures of ~24°C (Rooker *et al.*, 2008; Addis *et al.*, 2016; Aarestrup *et al.*, 2022), when conditions match phytoplankton blooms which sustain larval offspring (Fiksen and Reglero, 2022).

Juvenile and adult BFT primarily inhabit the upper 200 m of neritic habitats (Walli *et al.*, 2009; Wilson and Block, 2009; Druon *et al.*, 2016), feeding on varied combinations of forage fishes, cephalopods and crustaceans (Karakulak, Salman and Oray, 2009; Logan *et al.*, 2011), and occasionally diving offshore to feed at great depths (Wilson and Block, 2009; Battaglia *et al.*, 2013; Olafsdottir *et al.*, 2016). The role of additional contemporary and historical spawning areas such as the Slope Sea (East of Cape Hatteras, USA) (Richardson *et al.*, 2016; Hernández *et al.*, 2022), the Bay of Biscay (Rodríguez, Johnstone and Lozano-Peral, 2021), and the Black Sea (Di Natale, 2010; MacKenzie and Mariani, 2012) are yet to be clearly



defined but BFT born in the Slope Sea appear to be a genetically mixed component of the two populations (Rodríguez-Ezpeleta *et al.*, 2019). Recent tagging data has supported decades old observations (Mather, Mason and Jones, 1995) that a portion of Mediterranean BFT are resident all year round (De Metrio *et al.*, 2004; Fromentin, 2009; Cermeño *et al.*, 2015), yet the function, drivers and consistency of this behaviour remains poorly understood (Medina *et al.*, 2022).

The current work will predominantly focus on the proportionally (~10 times) larger eastern Atlantic and Mediterranean stock, which in 2007 was considered depleted, consistent with i) an estimated 60% decline in spawning biomass (adult fish) from 1970s levels (ICCAT, 2007), ii) a restructuring of the population toward younger individuals (Fromentin, 2009; Siskey *et al.*, 2016), and iii) modelling predictions of impending collapse (MacKenzie, Mosegaard and Rosenberg, 2009). In the past decade, strict quotas have (along with several years of favourable oceanographic conditions for spawning) recovered recruitment and spawning biomass of the eastern Atlantic and Mediterranean stock to 1970s levels (Porch *et al.*, 2019; Juan-Jordá *et al.*, 2022), and therefore, quotas have increased (ICCAT, 2020). However, I suggest that archaeological and historical data may reveal if population abundance and complexity had reduced by 1970, and if so, quantify by how much.

## Aims and outline

It was my aim to contextualise the ecology and evolution of modern BFT with a historical perspective, to understand how natural and anthropogenic impacts in general (but especially exploitation) have modified BFT population(s) in the eastern Atlantic and Mediterranean. I aimed to focus on the eastern stock of BFT because the western (Atlantic) stock was commercially exploited much later, and thus temporal samples would be sparse or non-existent. Therefore, I wanted to know how ecologically and evolutionarily different historical (eastern) BFT were from modern (eastern) BFT. It was my aim to reconstruct the past properties of their population(s) using a long-time series of samples dating back to approximately two millennia ago i.e., at the onset of their commercial exploitation in the Mediterranean. I aimed to investigate these differences by analysing faunal remains from archaeological settlements and archived in museum and private osteological and zoological collections and comparing them with analogous modern samples. Three indicators of eco-evolutionary dynamics were selected for study, with the presumption that exploitation would be the main driver of recent population dynamics. Moreover, exploitation could be specifically tested for, with some pre-emptive expectations of how exploitation might modify populations from the theoretical and recent literature. These indicators were 1) size and growth, 2) diet and habitat use, and 3) demography and adaptation.

As a basis for quantitative investigations on each of these indicators, I first aimed to conduct a state-of-the-art review (**Chapter 1**) of the qualitative archaeological, ecological and fishery data which explains the exploitation history of BFT in the literature; and how multidisciplinary approaches using fish remains might advance knowledge of BFT exploitation history, its eco-evolutionary consequences, and the drivers of long-term population dynamics in BFT. My thesis comprises **Chapter 1** and six further data chapters, detailed in **Table 1**.

**Table 1.** Overview of the Chapters in this thesis, including the methodological approach used and their foci.

Chapter	Methodological approach	Focus
<b>1</b> Exploitation history of Atlantic bluefin tuna in the eastern Atlantic and Mediterranean—insights from ancient bones	Literature review mining zooarchaeological records and qualitative archaeological, ecological and fishery data	>Exploitation history >Sample availability >Analysis opportunities
<b>2</b> Length estimation of Atlantic bluefin tuna ( <i>Thunnus thynnus</i> ) using vertebrae	Morphological analysis of modern BFT reference skeletons	>Ability to reconstruct size of BFT using vertebrae dimensions
<b>3</b> Vertebrae reveal industrial-era increases in Atlantic bluefin tuna catch-at-size and juvenile growth	Morphological analyses of ancient and modern BFT vertebrae growth rings (annuli) and archaeological vertebrae size	>Size and growth dynamics
<b>4</b> Isotopic life-history signatures are retained in modern and ancient Atlantic bluefin tuna vertebrae	Stable isotopic analyses of serially-sectioned and incrementally sampled BFT bone	>Biochemical properties of BFT bone
<b>5</b> Exploitation shifted trophic ecology and habitat preferences of Mediterranean and Black Sea bluefin tuna over centuries	Stable isotopic analysis of ancient and modern BFT bone	>Dynamics in diet and habitat use
<b>6</b> Ancient DNA SNP-panel data suggests stability in bluefin tuna genetic diversity despite centuries of fluctuating catches in the eastern Atlantic and Mediterranean	Genetic analysis of ancient and modern BFT bone DNA using a genotyping assay	>Population genetic structure >Genetic resilience >DNA preservation
<b>7</b> Ancient DNA and genomics reveals exploitation induced pre-industrial biomass declines in Atlantic bluefin tuna but has not limited its adaptive potential	Genomic analysis of ancient and modern BFT bone DNA using whole genome resequencing	>Demographic patterns >Population genomic structure >Genomic resilience >Adaptive responses

Due to the sparse research already conducted on archaeological BFT—and biomolecules archived in fish remains more broadly—components of **Chapters 1, 2 and 4** are produced to facilitate the investigations which address my main research questions. As part of **Chapter 1**, I build an online database of all BFT remains (bones and scales) reported in the literature which were recovered from archaeological settlements. This was vital for a holistic understanding of which specimens were available, and suitable, for analyses in the following chapters. In **Chapter 2**, I produce a tool to estimate the body size (fork length) of BFT with the aim of analysing differences in catch-at-size throughout two millennia in **Chapter 3**. In **Chapter 4**, I study the variation of stable isotope values throughout the growth axis of BFT vertebrae—which vary according to how rapidly BFT bone remodels and incorporates isotopic signatures from the environment as it grows. This was vital information in order to understand whether BFT bone records snapshots into feeding ecology or life history patterns over several years, which aids interpretations of how isotopic values explain diet and habitat use in **Chapter 5**. **Chapter 5** also requires length estimates enabled by Chapter 2 since isotopic values are

known to scale with body size in fishes—otherwise we have no method to disentangle differences in isotope values between size, spatial or temporal effects. Finally, **Chapter 6** is a preliminary genetic investigation to a higher-resolution whole genome approach in **Chapter 7**; which is necessary to understand the preservation levels of DNA in BFT bone and their capacity for whole genome resequencing. Moreover, differences in methodological DNA approaches between **Chapter 6** and **7** reflect novel research opportunities due to DNA sequencing advances and ancient DNA analysis, throughout the study period, and my aim for BFT research to be at the forefront of those advances.

For each eco-evolutionary indicator of long-term BFT dynamics; size and growth; diet and habitat use; and demography and adaptation, I had several research questions—driven by knowledge gaps and expectations of how exploitation modifies populations from the literature. These research questions are summarised in **Table 2**.

**Table 2.** The research questions that we aimed to address within the chapter structure of this thesis and the eco-evolutionary indicator which they relate to.

Chapters	Research Questions	Eco-evolutionary indicator
2 and 3	<ul style="list-style-type: none"> <li>• What was the size-selectivity of BFT fisheries during the past two millennia?</li> <li>• When did the onset of fishing large (&gt;200 cm fork length) BFT commence?</li> <li>• Has size selective fishing induced phenotypic growth changes in BFT, as expected under fisheries-induced evolution theory? i.e. earlier maturation and slow mature growth.</li> </ul>	Size and growth
4 and 5	<ul style="list-style-type: none"> <li>• What was the foraging ecology of Black Sea BFT—which disappeared due to exploitation during the 1980s?</li> <li>• How did Black Sea BFT function trophically and how was it structured in relation to the eastern Atlantic and Mediterranean BFT?</li> <li>• Has the diet and/or migrations of BFT changed throughout the past two millennia as a result of BFT exploitation and marine ecosystem degradation.</li> </ul>	Diet and habitat use
6 and 7	<ul style="list-style-type: none"> <li>• When did BFT biomass begin to decline as a result of intensive exploitation?</li> <li>• Have BFT lost spawning populations or genetic variability as a result of biomass depletion or have they retained their adaptive potential?</li> <li>• Has size-selective exploitation of BFT induced adaptive responses at the genomic level?</li> </ul>	Demography and adaptation

## **Chapter 1**


Exploitation history of Atlantic bluefin tuna in the eastern Atlantic and Mediterranean—insights from ancient bones  
**(pages 21—50)**

“One thing at a time”

- a tired but determined PhD student, 2020

## Review Article

# Exploitation history of Atlantic bluefin tuna in the eastern Atlantic and Mediterranean—insights from ancient bones

Adam J. Andrews <sup>1,2,\*</sup>, Antonio Di Natale<sup>3</sup>, Darío Bernal-Casasola<sup>4</sup>, Veronica Aniceti<sup>5</sup>, Vedat Onar<sup>6</sup>, Tarek Oueslati<sup>7</sup>, Tatiana Theodropoulou<sup>8</sup>, Arturo Morales-Muñiz<sup>9</sup>, Elisabetta Cilli<sup>2,†</sup>, and Fausto Tinti<sup>1,†</sup>

<sup>1</sup>Department of Biological, Geological and Environmental Sciences, University of Bologna, Campus of Ravenna, Ravenna, Italy

<sup>2</sup>Department of Cultural Heritage, University of Bologna, Campus of Ravenna, Ravenna, Italy

<sup>3</sup>Aquastudio Research Institute, Messina, Italy

<sup>4</sup>Department of History, Geography and Philosophy, Faculty of Philosophy and Letters, University of Cádiz, Cádiz, Spain

<sup>5</sup>University of Rome Tor Vergata, Italy

<sup>6</sup>Istanbul University-Cerrahpaşa, Osteoarchaeology Practice and Research Centre and Faculty of Veterinary Medicine, Istanbul, Turkey

<sup>7</sup>CNRS-Université de Lille, Histoire Archéologie Littérature des Mondes Anciens, Lille, France

<sup>8</sup>University of Côte d'Azur, UMR7264 CEPAM CNRS, Team GReNES, Nice, France

<sup>9</sup>Department of Biology, Autonomous University of Madrid, Madrid, Spain

\*Corresponding author: tel: +39 0544 937401; e-mail: [adam@palaome.org](mailto:adam@palaome.org).

†Elisabetta Cilli and Fausto Tinti should be considered joint senior author.

Andrews, A. J., Di Natale, A., Bernal-Casasola, D., Aniceti, V., Onar, V., Oueslati, T., Theodropoulou, T., Morales-Muñiz, A., Cilli, E., and Tinti, F. Exploitation history of Atlantic bluefin tuna in the eastern Atlantic and Mediterranean—insights from ancient bones. – ICES Journal of Marine Science, 79: 247–262.

Received 27 August 2021; revised 23 November 2021; accepted 15 December 2021; advance access publication 18 January 2022.

Overexploitation has directly, negatively affected marine fish populations in the past half-century, modifying not only their abundance but their behaviour and life-history traits. The recovery and resilience of such populations is dependent upon their exploitation history, which often extends back millennia. Hence, data on when exploitation intensified and how populations were composed in historical periods, have the potential to reveal long-term population dynamics and provide context on the baselines currently used in fisheries management and conservation. Here, we setup a framework for investigations on the exploitation history of Atlantic bluefin tuna (*Thunnus thynnus*; BFT) in the eastern Atlantic and Mediterranean by collating records of their zooarchaeological remains and critically reviewing these alongside the literature. Then, we outline how novel multidisciplinary applications on BFT remains may be used to document long-term population dynamics. Our review of literature provides clear evidence of BFT overexploitation during the mid-20th century CE. Furthermore, a strong case could be made that the intensification of BFT exploitation extends back further to at least the 19th century CE, if not the 13th–16th century CE, in the eastern Atlantic and Mediterranean. However, a host of archaeological evidence would suggest that BFT exploitation may have been intensive since antiquity. Altogether, this indicates that by the currently used management baselines of the 1970s, population abundance and complexity was already likely to have declined from historical levels, and we identify how biomolecular and morphometric analyses of BFT remains have the potential to further investigate this.

**Keywords:** biomolecular analyses, fish remains, historical baselines, historical marine ecology, *Thunnus thynnus*, zooarchaeology.

## Introduction

Overexploitation has negatively impacted marine fish populations in various ways during the last half-century (Jackson *et al.*, 2001; Pauly *et al.*, 2002; Butchart *et al.*, 2010). While depleting the abundance of populations, overexploitation has been shown to impact population complexity through e.g. the extinction of sub-populations, the contraction of geographical ranges, the restructuring of age classes, as well as modifying a host of other life-history traits which are intertwined such as fecundity, maturation, growth, migration and spawning behaviour, and diet use (Jennings *et al.*, 1998; Rochet, 1998; Heino *et al.*, 2015; Hutchings and Kuparinen, 2021).

A prerequisite for documenting these changes is the availability of fisheries and ecological data from different time points to be compared. However, prior to 1970 and especially 1950 this data is lacking; precluding the opportunity to contextualize recent change in a historical perspective when exploitation rates were lower and when climate conditions were different (Erlandson and Rick, 2010; Lotze *et al.*, 2014). Accordingly, we have a poor understanding on the long-term drivers of population dynamics (Jackson *et al.*, 2001; Erlandson and Rick, 2010; Schwerdtner Mánuez *et al.*, 2014; Rodrigues *et al.*, 2019), whether exploitation has caused plastic or evolutionary (inherited) responses (Heino *et al.*, 2015; Hutchings and Kuparinen, 2021), and thus, it is unknown how resilient populations are now, compared to their natural potential (Pauly, 1995; Pauly *et al.*, 2002; Butchart *et al.*, 2010; Erlandson and Rick, 2010; Neubauer *et al.*, 2013; Rodrigues *et al.*, 2019).

Therefore, past reference points (or historical baselines) of population abundance and complexity have the potential to improve the management and conservation of marine fish populations—especially those which have been recently overexploited, yet have a long exploitation history (Lotze *et al.*, 2014; Schwerdtner Mánuez *et al.*, 2014). Indeed, population recovery is dependent upon the duration and intensity of exploitation (Neubauer *et al.*, 2013; Hutchings and Kuparinen, 2021), and the sustainability of catches is dependent upon identifying how/when anthropogenic activities and climatic events can negatively impact populations, and minimising these (Hilborn *et al.*, 2003; Berkeley *et al.*, 2004). Here, we critically review archaeological and historical information to qualitatively investigate the exploitation history of Atlantic bluefin tuna (*Thunnus thynnus*; BFT) in the eastern Atlantic and Mediterranean. Furthermore, we setup a framework to enable quantitative investigations of historical exploitation impacts by collating a database of zooarchaeological records and identifying how these as well as archived fish remains may provide novel historical baselines for population abundance and complexity.

Few species have an exploitation history as long and as intensive as BFT, which was famously overexploited since at least the 1980s (Porch *et al.*, 2019) and supported one of the first commercial fisheries (beginning ~8th century BCE; García-Vargas and Florido del Corral, 2010; Di Natale, 2014). The status of the eastern Atlantic and Mediterranean BFT population is currently judged against management baselines from the 1970s, i.e. from when fisheries catch data was more accurately collected for this species. Yet, we hypothesize that exploitation had already impacted BFT by the 1970s according to the huge economic and cultural importance of this population historically, as documented by many reviews (e.g. MacKenzie and Myers, 2007; MacKenzie *et al.*, 2009; Fromentin, 2009; Karakulak and Oray, 2009; Di Natale, 2010, 2014; Longo and

Clark, 2012; Orenc *et al.*, 2014; Cort and Abaunza, 2019; Porch *et al.*, 2019; Di Natale *et al.*, 2020).

The historical exploitation of BFT has predominantly been investigated from historical literature sources, such as the locations of tuna traps (Pagá García *et al.*, 2018), and their catches, from the 16th century CE onwards (Ravier and Fromentin, 2001, 2004; Pagá García *et al.*, 2017). However, the use of zooarchaeological remains (BFT bones and scales) has been neglected and restricted to selected periods and regions (Morales-Muñoz, 1993; Felici, 2018; García-Vargas *et al.*, 2018; Nielsens and Persson, 2020; Mylona, 2021). Despite this, fish remains can offer additional biological insights into past population abundance and complexity, not feasible with fishery catch data, especially *via* multidisciplinary applications of biomolecular and morphometric analyses (Erlandson and Rick, 2010; Orton, 2016; Morales-Muñoz *et al.*, 2018).

Biomolecular applications on fish remains can provide quantitative metrics of demographic and adaptive change over time, as already achieved using genetics/genomics for archaeological (Oosting *et al.*, 2019) but predominantly archived fish samples (Nielsen and Hansen, 2008). Isotopic and element analyses can enable the detection of changes in past environmental conditions, diet, habitat use, and growth (Orton, 2016; Matsubayashi *et al.*, 2017; Blankholm *et al.*, 2020; Guiry *et al.*, 2020). Moreover, archaeological fish bone is a particularly promising archive of information since DNA and proteins can be well preserved and remodelling rates are slow (Ferrari *et al.*, 2020). In addition, morphometric studies offer equally promising opportunities to study growth rate changes over time by studying the growth rings of vertebrae or otoliths (ear bones; Van Neer *et al.*, 1999; Bolle *et al.*, 2004; Ólafsdóttir *et al.*, 2017).

Qualitative metrics produced by traditional zooarchaeology, i.e. observations on the number and sizes of remains found in archaeological assemblages, differ significantly from those derived using biomolecular tools and morphometrics. Traditional zooarchaeological data are vital in providing an indication of when and where species were exploited, how species were distributed (Barrett *et al.*, 2004; Hoffmann, 2005), and which sizes of fish were exploited (Maschner *et al.*, 2008; Barrett, 2019). However, like historical data (e.g. tuna trap catches), raw archaeological data (e.g. the number of fish bones) require interpretation. They are by nature incomplete because of a long series of processes depending on which fish were available, could be fished, were consumed, and how remains were disposed of. In addition, their recovery depends on how well remains preserve, are retrieved and reported.

The objectives of this study were to (1) collate zooarchaeological BFT records, (2) critically assess the extent of historical exploitation based on these records and the literature, and (3) outline how BFT remains might be used to generate quantitative historical baselines for population abundance and complexity. This knowledge is of importance to glean historical insights on the long-term drivers of population dynamics and the impact of exploitation.

## A background on Atlantic bluefin tuna

BFT is a highly migratory pelagic predator (up to 3.3 m in length and 725 kg in weight; Cort *et al.*, 2013), whose populations were under threat from overexploitation until very recently (Porch *et al.*, 2019). Since 1980, BFT have been managed as two stocks (Fromentin and Powers, 2005), a hypothesis supported by recent isotopic (Rooker *et al.*, 2008) and genomic (Puncher *et al.*, 2018) studies. These are a western Atlantic population that spawns predom-

inantly in the Gulf of Mexico, and an eastern Atlantic population that spawns predominantly in the Mediterranean: off the Balearic Islands, Sicily, Malta, Libya, and in the Levantine Sea (García *et al.*, 2005; Piccinetti *et al.*, 2013). Both populations comprise of individuals that migrate into the Atlantic Ocean to feed, including as juveniles (Cort and Abaunza, 2019), exhibiting high-levels of connectivity and homing to spawning grounds between April and July to optimum spawning temperatures of  $\sim 24^{\circ}\text{C}$  (Rooker *et al.*, 2008). The role of additional spawning areas, i.e. the Slope Sea (West of Cape Hatteras, USA: Richardson *et al.*, 2016), the Bay of Biscay (Rodríguez *et al.*, 2021), or other Atlantic areas (Azores, Canary Islands, Ibero-Moroccan, and Gulf of Guinea, Mather *et al.*, 1995; Piccinetti *et al.*, 2013), are yet to be defined.

The current work will deal only with the proportionally ( $\sim 10$  times) larger eastern Atlantic and Mediterranean stock, which in 2007 was considered depleted, consistent with a 60% decline in spawning biomass (adult fish) from 1970s levels (ICCAT, 2007), a restructuring of the population toward younger individuals (Fromentin, 2009; Siskey *et al.*, 2016), and modelling predictions of impending collapse (MacKenzie *et al.*, 2009). These losses in abundance and population complexity were driven by overfishing that occurred especially following the demand of BFT for farming (fattening in cages) from the 1990s onwards (Porch *et al.*, 2019). Thus, the 1990s and early 2000s experienced record annual catches of  $> 60000$  t, before ICCAT (International Commission for the Conservation of Atlantic Tunas) imposed strict quotas to limit catches from 2003 (Fromentin, 2003; ICCAT, 2017). In the last decade, quotas have (along with several years of favourable oceanographic conditions for spawning) recovered recruitment and spawning biomass of the eastern Atlantic and Mediterranean stock to 1970s levels, and therefore, quotas have increased (ICCAT, 2020). However, we suggest that archaeological and historical data may reveal if population abundance and complexity had reduced by 1970, and if so, quantify by how much.

## Materials and methods

Zooarchaeological records were data-mined from reports in multiple languages, including unpublished reports. We accumulated records identified only as BFT or large specimens of the genus *Thunnus* with the caveat that juvenile BFT remains are challenging to distinguish morphologically from albacore (*Thunnus alalunga*). Both species have overlapping distributions in the eastern Atlantic and Mediterranean, although albacore inhabits offshore waters (Bard, 1974) and would not be routinely caught with in-shore fishing methods used to target BFT in any period described herein. In addition, albacore reaches a maximum length of  $\sim 1.5$  m at 13 years (Bard, 1974), whereas the same size BFT is  $\sim 6$  years old (Rodríguez-Marín *et al.*, 2004). Therefore, species can, in theory, be identified by size and vertebral growth rings (Rodríguez-Marín *et al.*, 2006)—unless remains are fragmented. Molecular identification methods, i.e. Zooarchaeology by Mass Spectrometry (ZooMS) collagen protein fingerprinting (Rick *et al.*, 2019) or genetic bar-coding (Puncher *et al.*, 2019) were not utilized by any of the studies included, therefore, we assume that these records are in fact BFT but urge caution in their future use and interpretations.

We mapped the location of archaeological BFT remains alongside fish processing facilities—called *cetariae* in antiquity (active from 550 years BCE to 700 years CE, from the RAMPPA Project: <https://ramppa.uca.es/>), and 16th–20th century CE BFT trap catch

sites (from Pavesi, 1889; Devedjian, 1926; Ravier and Fromentin, 2001; Pagá García *et al.*, 2017) to provide context for zooarchaeological remains and indicate potential new sources of BFT archaeological remains yet to be explored. Our database of zooarchaeological records is unlikely to be absolute due to difficulties in accessing grey literature and because new records are in constant discovery. To tackle this, we established the accessible online portal <https://tunaarchaeology.org/>, allowing researchers to access records and input new records.

## Scavenging and subsistence fishing (140000 years BCE–10th century BCE)

Zooarchaeological evidence is paramount to understand the extent, scale, and development of fishing in prehistory, i.e. before written sources exist. The earliest evidence of BFT are vertebrae dating to the Eemian Period ( $\sim 140000$  years BCE), recovered from near Svenborg, Denmark (SNM Copenhagen, Pers. Comm. K. Kjaer), and vertebrae associated with Neanderthal habitations in Gorham's Cave, Gibraltar (26000–22000 years BCE, Brown *et al.*, 2011). It is unclear if these finds represent fishing, or cases of opportunistic scavenging following episodic beaching events, perhaps caused by orca (*Orcinus orca*, Cort and Abaunza, 2019). Paintings of BFT in Genovesè's Cave on the isle of Levanzo (near Sicily, Italy), dated to  $\sim 9200$  years BCE (Tusa, 1999; Spoto, 2002), are the earliest reliable sources of evidence that BFT fishing had begun in the Mediterranean, and was clearly of some cultural importance by the Mesolithic. This is supported by the recovery of BFT vertebrae from a wide spatial extent of sites dating from 10000–5800 years BCE in modern-day Spain, France, and Croatia (Supplementary Table S1), and especially in the Aegean Sea between 9000 and 3200 years BCE (Figure 1), which we consider to be the result of increased archaeological effort throughout Greece.

Vertebrae recovered from these prehistoric cave sites are mostly few (Supplementary Table S1), yet, at Franchthi and Saliagos (Aegean Sea, Greece), the recovery of hundreds or thousands of vertebrae (Evans and Renfrew, 1968; Rose, 1994) indicate that by the Neolithic, BFT was already being caught at some scale. This may suggest that Neolithic coastal communities were expert fishers (Evans and Renfrew, 1968), but we caution that species identifications from these early excavations might not be reliable. In any case, such catches could simply reflect episodic events where, for example, prey lured BFT into shallow waters and enabled fishing. Likewise, predators such as orca could have beached or corralled BFT into shallow waters as is commonly observed around the Strait of Gibraltar (Wilson and Mittermeier, 2014; Cort and Abaunza, 2019). It is unlikely that Neolithic catches evidence fishing on scale greater than subsistence, because large BFT would be challenging to catch by hook and line or harpoon – the predominant fishing methods in this period (Mylona, 2014; Nielssen and Persson, 2020). Nets were probably not used to target BFT in prehistory due to limitations in the strength of organic yarns (Mylona, 2014), precluding the opportunity to catch BFT on its spawning migration when it does not take bait (Lozano Rey, 1952), other than by spearfishing in a few suitable locations. However, by the 12th century BCE, Mycenaean ceramics depicting early beach-seine fishing of BFT (Hadjianastasiou, 1991; Sarà, 1998), suggest that such fishing methods had developed during the Bronze Age in the Aegean, though a lack of zooarchaeological records are available to corroborate this (Supplementary Table S1). Nonetheless, hook and line boat fishing was still carried out

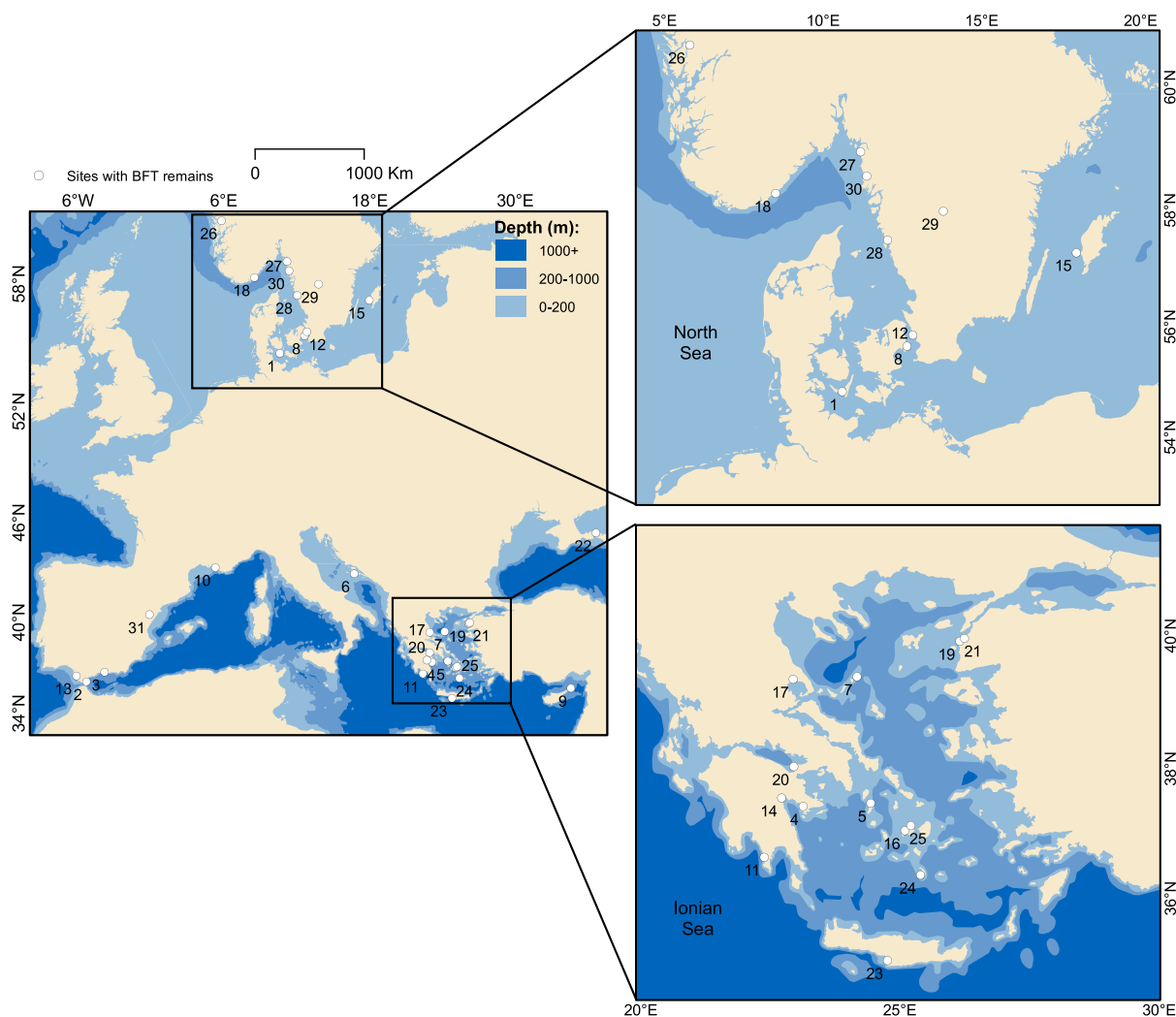


**Figure 1.** Map of Atlantic bluefin tuna (*T. thynnus*; BFT) archaeological remains recovered prior to the 9th century BCE. For numbering refer to Supplementary Table S1.

at least a century later as depicted on Cypriot ceramics (Iacovou, 1988).

It is evident that prehistoric BFT capture also occurred in the northeastern Atlantic, albeit probably on a smaller scale (Supplementary Table S1). Scores of archaeological excavations in Norway, Sweden, and Denmark report BFT remains dating to 6800–3500 years BCE (as reviewed in Enghoff *et al.*, 2007; Nielssen and Persson, 2020; Supplementary Table S1; Figure 1) when conditions in the northeastern Atlantic were warmer than at present and were probably favoured by BFT (Enghoff *et al.*, 2007). Early Nordic fishing appears to have targeted BFT and orca together with harpoons (Nielssen and Persson, 2020), perhaps while orca corralled BFT into shallow waters as we suspect in the Mediterranean. BFT remains have also been found far into the Baltic Sea, at Neolithic Gotland (5200–4000 years BCE; Ericson, 1989; Knape and Ericson, 1983). The Baltic Sea was more saline during this period than today (Enghoff *et al.*, 2007), but BFT would still have exhibited the same low salinity tolerance here as during their residency in the Black Sea, where they were also clearly distributed from at least 2000

years BCE (Rose, 1994; Uerpmann and van Neer, 2000; Lyashenko, 2006; Figure 1).

### Commercial Phoenician-Punic, Greek, and Roman fisheries (9th century BCE–7th century CE)

During the beginning of the 1st millennium BCE, the large-scale trade of goods throughout the Mediterranean was vastly accelerated due to the Phoenician colonization of the western Mediterranean. Accordingly, it is believed that BFT fisheries were commercialized around the 8th century BCE in the western Mediterranean (Di Natale, 2012, 2014; Cort and Abaunza, 2019). The earliest attestable evidence of trade (transport) is from 7th century BCE amphorae containing BFT vertebrae and scales, which were found at an inland site in southern Spain and according to their design, originated from the Malaga region (Aguayo de Hoyos *et al.*, 1987). Remains of Punic-era salting factories at Cadiz and Sicily from the 6th century BCE (Figure 2) also testify this early trade in the Mediterranean. BFT remains have been found at major Punic sites, e.g. Lixus, Ceuta,



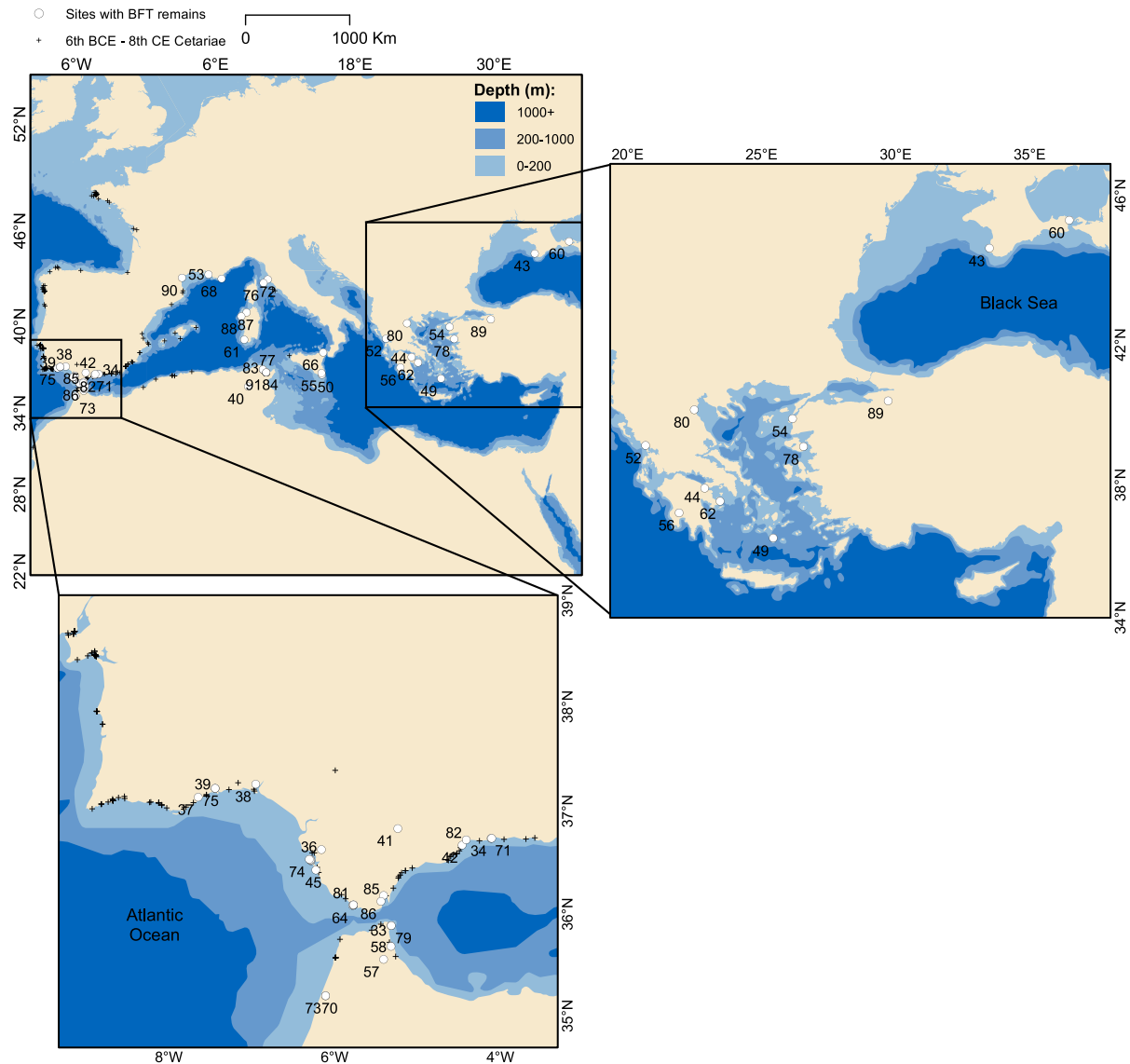


**Figure 2.** Map of Atlantic bluefin tuna (*T. thynnus*; BFT) archaeological remains recovered between the 9th century BCE and 7th century CE in reference to fish processing facilities (*cetariae*, from <https://ramppa.uca.es/>). For numbering refer to Supplementary Table S2.

Carthage (Nobis, 1999), and notably Tavira (Supplementary Table S2). During the same period, Greek BFT trade was developed as evidenced by archaeological finds from the Syracuse area (Bernal-Casasola *et al.*, 2021). Greek coinage from Cyzicus (Mysia, Sea of Marmara) depicting BFT imply that at least local trade of BFT was already well-established by the 6th century BCE (Di Natale, 2014). Undoubtedly, the combination of nets able to intercept spawning (and return) migrations, salting factories able to preserve catches, and amphorae able to transport catches, created the opportunity for commerce across the Mediterranean (Doumenge, 1999; Fromentin and Powers, 2005; Di Natale, 2012). Amphorae containing BFT remains, found in/or off Italy and Greece but originating from modern-day Spain and Morocco (Tailliez, 1961; Delussu and Wilkens, 2000; Zimmerman Munn, 2003; Theodoropoulou, 2014) exemplify this development, indicating that long distance trade of

salted BFT (*salsamentum*) was taking place by at least the 5th century BCE (Supplementary Table S2).

BFT fishing methods developed in Greek and Roman times as variations of the *Almadra* or *Tonnara* techniques (Sarà, 1998; García-Vargas and Florido Del Corral, 2010) that are often aggregated in the literature, and referred to as “tuna traps.” Tuna traps varied, apparently originating as the non-static *Almadra de tiro* (prototypes of beach-seines) before static/fixed *Almadras* (Spanish), *Tonnare* (Italian), or *Madragues* (French), developed, that were semi-permanently weighted to the sea floor, and became the dominant method of BFT exploitation from at least the 16th century CE onwards (García-Vargas and Florido Del Corral, 2010). It is not entirely clear which traps were used in antiquity. Oppian (177 years CE) reports the use of up to five boats, and watch towers (*thynnoskopeion*)—which identified the arrival of BFT (sometimes

by orca sightings), in addition to instructing boats to encircle the catch. The same author appears to describe the “death-chamber” of fixed traps, where “nets like a city” with “gates” filled “the closing net with copious prey” (Oppianus, 1738). Testifying this, mosaics such as those from 3rd century CE Tunisia appear to portray BFT being dispatched inside a weighted net (Yacoub, 1995). Furthermore, the discovery of arranged anchor parts found off a Roman settlement in Morocco, which may have been fixing points for nets (Trakadas, 2010), suggest that both trap methods may in fact have been used in antiquity. The use of both methods enables the capture of BFT in various scenarios (at different migration distances from shores, bottom-types, and target sizes) that concurs with widespread zooarchaeological evidence (Figure 2) and indicates that exploitation rates had increased.

The importance of BFT to Greek and Roman societies between the 5th century BCE and 5th century CE can be clearly observed from coins minted in fishing settlements, which depicted BFT (Di Natale, 2014), multiple historical writings, notably from Aristotle (4th century BCE), Pliny the Elder (1st century CE), and Oppian (2nd century CE), and finds of salting factories (Figure 2). Factories not only produced *salsamentum* for trade but the fish sauce *garum* (or variations; *liquamen*, *muria*, *allec*, and *lymphatum*; Trakadas, 2005). Numerous BFT remains at factories in the Roman coastal settlements of 1st century CE Cadiz and 2nd century BCE–5th century CE Baelo Claudia (Strait of Gibraltar, Figure 2, Morales-Muñiz and Roselló-Izquierdo, 2007; Bernal-Casasola et al., 2016, 2019) further indicate that large-scale BFT exploitation occurred. Salting factories in the eastern Mediterranean are seldom recovered, but classical writings document their existence (Roesti, 1966). Although, their scarce recovery may be the result of a lack of interest in such structures (Theodoropoulou, 2014), we suggest that less BFT exploitation occurred in the eastern Mediterranean than around the Strait of Gibraltar (Figure 1). This is corroborated by all amphorae containing BFT remains evidencing a west-to-east trade in Mediterranean antiquity (Supplementary Table S2).

According to the zooarchaeological remains, BFT exploitation in the eastern Mediterranean occurred mostly in the Aegean in antiquity (Figure 2, Supplementary Table S2). Though as in prehistory, this is likely to be skewed by uneven archaeological effort. BFT migrations through the Dardanelles and Bosphorus to/from the Black Sea were extensively documented by Aristotle, and Strabo (1st century CE in Roesti, 1966). Thus, we might have expected to observe greater numbers of BFT remains around these straits. There is still uncertainty whether BFT migrations through this area were for feeding or spawning in the Black Sea (MacKenzie and Mariani, 2012; Di Natale, 2015). Zooarchaeological evidence of BFT from Greek times at Pantikapaion (Kerch, Ukraine; Morales-Muñiz et al., 2007), and prior to that at Bronze Age Troy (~1000–2000 BCE, Supplementary Table S1; Rose, 1994; Uerpmann and Van Neer, 2000) might address this potential loss of population complexity via reconstructing past population structure and habitat use. BFT was highly valued there as noted from their appearance on coins from several Black Sea and Sea of Marmara fishing centers and classical writings on the scale of export to the Greek mainland (Roesti, 1966; Di Natale, 2014). This indicates the importance of this fishery historically, even if it was not conducted at the same scale as those in the western Mediterranean (Roesti, 1966; Bekker-Nielsen, 2005; Morales-Muñiz et al., 2007).

We find it conceivable that BFT was exploited to sufficient extent across the Mediterranean in antiquity (Figure 2) to potentially have had some impact on population abundance and complexity,

but the extent of this is currently unknown. In Roman times, people were aware that exploitation impacted at least inshore fishes (e.g. Gilthead seabream *Sparus aurata*) and cephalopods in the Tyrrhenian Sea, where they noted that by the 2nd century CE, they had decreased in size, were fewer, and therefore, efficient fishing techniques e.g. torch-fishing were purportedly banned (Trakadas, 2006). Hence, studies are warranted to address this theory as we currently do not have data to quantify the abundance and complexity of BFT populations in this period, and to which extent they might have been impacted by exploitation.

### Middle age transition and intensification (8th–18th century CE)

Evidence of BFT fisheries is lacking between the 8th and 10th century CE. It is probable that the collapse of the Western Roman Empire gradually (over a few centuries) destabilized the parallel industries and trade (Horden and Purcell, 2000) on which BFT fisheries depended, and second, caused economic downturns which induced a greater dependence on localized exploitation throughout the Mediterranean (Montanari, 1979; Squatriti, 2002). The Eastern Roman Empire was revitalized, though there is no evidence that this promoted an increase in BFT exploitation. During the Islamic period in Iberia and Sicily (~8th–13th century CE), Al-Idrisi (1154a, b) wrote of BFT, and noted that in Ceuta (northern Africa), BFT were being caught with harpoons while traps were used elsewhere—specifically in Sicily. During the same century, Benjamin of Tudela noted the economic importance of salted BFT to Palermo (Sicily; Aniceti, 2019). In general, fish diets in Italy are perceived to have shifted to freshwater species between the 7th and 13th century CE (Montanari, 1979), though we doubt that this shifted the diets of coastal communities away from marine fish. In addition, the Spanish name for tuna traps (*Almadrabas*) is of Arabic Andalusian origin (deriving from *تبريض*, a place to strike; or *بريض*, knots) suggesting that some development of BFT exploitation occurred during this period.

Prior to a better documented period when tuna trap catch records were recovered, from 1512 CE onwards (Ravier and Fromentin, 2001; Pagá García et al., 2017), the number and location of BFT remains ought to represent an opportunity to investigate historical exploitation. However, recoveries from the Middle Ages were lacking in comparison with antiquity (Supplementary Table S3, Figure 3). The few BFT remains recovered in this period likely do not represent a decline in exploitation but rather a lack of archaeological effort. One exceptional rescue (i.e. unplanned) excavation at Theodosius' Harbour, Istanbul (Turkey, Onar et al., 2008), recovered 150 BFT vertebrae dating between the 4th and 15th century CE. Likewise, rescue excavations in Sicily recovered scores of BFT vertebrae from the 9th–13th century CE (Aniceti, 2019). This highlights a general lack of archaeological interest in Middle Age coastal contexts (Aniceti, 2019), where the two largest recoveries of this period were unplanned, suggesting that exploitation extent may be underestimated if using observations of BFT remains collated herein as a proxy.

Data on tuna trap presence before 1512 CE indicates that BFT exploitation around Sicily barely increased between the 5th and 12th century CE, from 20 to 25 traps (Pagá García et al., 2018). It was not until the 13th century CE that Sicilian trap numbers noticeably increased, to 104 (Pagá García et al., 2018), clearly documenting an increase in demand for BFT. This was probably spurred on by

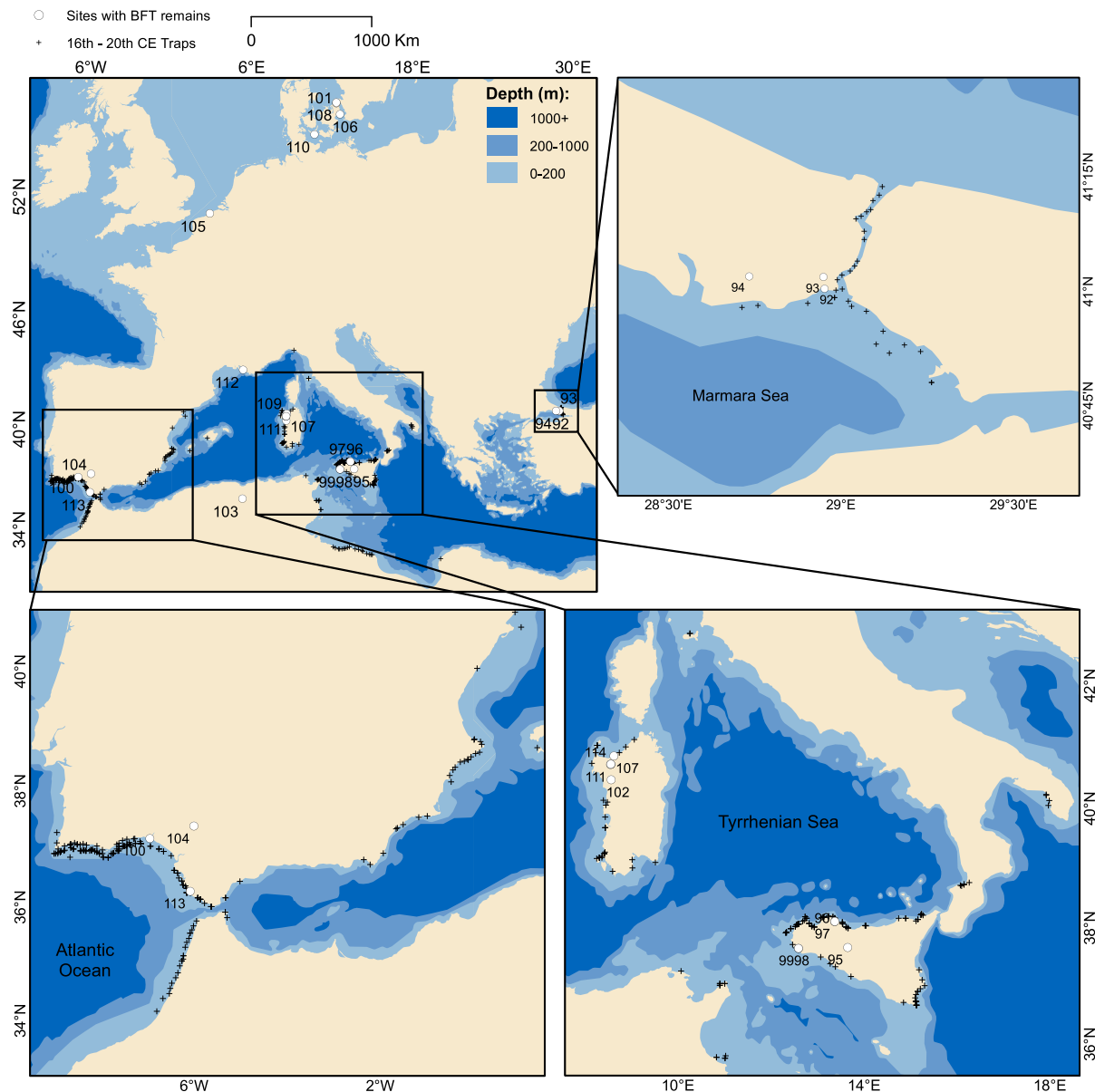


**Figure 3.** Map of Atlantic bluefin tuna (*T. thynnus*; BFT) archaeological remains recovered between the 8th and 19th century CE in relation to tuna trap locations (from Pavese, 1889; Devedjian, 1926; Pagá García *et al.*, 2017). For numbering refer to Supplementary Table S3.

Christianism and aligns well with a Sicilian shift away from Islamic dietary practices. Likewise, from the 13th century CE, a plethora of literary works reference the Andalusian tuna traps (see Ladero Quesada, 1993; Bello León, 2005). This signifies a juncture when exploitation impacts likely increased after King Alfonso X of Castille gave the Knights of Santiago the license to these traps in 1248 CE once they regained (Christian) control in the most historically productive BFT fishing region of Iberia. This apparent increase in demand for BFT is comparatively late, e.g. in northern Europe, increased demand for marine fish had already occurred by the 10th century CE, predominantly for prevalent species, i.e. Atlantic herring (*Clupea harengus*) and cod (Barrett *et al.*, 2004; Oueslati, 2019). Investigation is warranted to clarify if exploitation impacts may

have indeed increased from those during antiquity before the 13th century, for we do not know to which extent metrics such as the Sicilian trap numbers are influenced by pre-13th century data-gaps (Pagá García *et al.*, 2018).

During the 13th century CE, trap numbers probably increased due to more stable demand, in turn promoting the development of more efficient methods of BFT exploitation, i.e. the static traps. These traps (Figure 3) were certainly common by the 16th century CE, and perhaps the 14th century CE (Sarmiento, 1757; Ravier and Fromentin, 2001), and were more efficient because they could target BFT migrating further from the coast and were less dependent the effort of many personnel (Ravier and Fromentin, 2001). Therefore, catch variability probably decreased with well-designed static

traps. Hence, we postulate that exploitation may have substantially increased between the 13th and 16th century CE, when traps also became more numerous (Ravier and Fromentin, 2001; Pagá García *et al.*, 2018).

In support of this theory, by the mid-16th century CE, it is estimated that Spanish traps alone caught 14000 tons of BFT (Ravier and Fromentin, 2001; Pagá García *et al.*, 2017). Spanish catches then decreased significantly between the mid-16th and 18th century CE, which Sarmiento (1757) attributed to their exploitation. García (2016) suggested that despite legislation in 1583 CE against it, prey and juvenile BFT were overexploited, and seabed disturbance close to the traps off the Atlantic coast of Andalusia altered the migration route of BFT further from shore. This would also explain the prevalence of static traps that were able to reach further from shore without disturbing the seabed as a non-static trap/beach-seine would. The legislation reconstituted prescripts established in the 14th century CE (García, 2016), clearly then, exploitation impacts on BFT were evident by this time. Notably, catch variations over this period in Spain could only be explained minimally by climatic conditions (Ganzedo *et al.*, 2009). When looking at a greater temporal spread across the Mediterranean, Ravier and Fromentin (2001) noted 100-year fluctuation cycles in trap catches. These cycles were suspected to be mainly related to climate modifying migration patterns and/or recruitment (Ravier and Fromentin, 2001, 2004; Fromentin, 2009), which surely impacts the abundance and catches of pelagic species such as BFT. However, exploitation is expected to magnify fluctuations in abundance (Anderson *et al.*, 2008).

BFT remains from 15th century CE Belgium, and 13th–17th century CE Scandinavia (Supplementary Table S3, Figure 3) are a reminder that BFT exploitation was not only carried out by tuna traps in this era. This is also true for the Mediterranean where harpooning in the Messina Strait has occurred for millennia (Di Natale *et al.*, 2005). Despite these likely being small-scale activities, they should be considered to avoid underestimating exploitation effort, and this extends to unreported/illegal fisheries which likely affected the historical trap catch records. Fishing, most probably by line and hook, even targeted BFT in the extremes of their modern-day range in 1671 CE East Greenland (Di Natale, 2012; Jansen *et al.*, 2021), and accounts of BFT fishing with harpoons off Norway date to 1762 CE (Lindquist, 1994). It is believed however that pre-20th century CE exploitation of BFT in the northeast Atlantic was sporadic and had negligible commercial value (Bennema, 2018).

From the 16th century CE onwards, the vast distribution of traps (Figure 3) and their catches (Ravier and Fromentin, 2001; Pagá García *et al.*, 2017) offers a more reliable indicator of the extent of exploitation, than the location, number, and size of zooarchaeological remains. Yet, BFT remains from this period are potentially useful to generate quantitative historical baselines (e.g. Alter *et al.*, 2012; Ólafsdóttir *et al.*, 2014) because they may offer additional biological insights into life-history traits and adaptive responses not feasible with trap data. It must also be noted that trap catches were influenced by many factors and therefore do not necessarily reflect population abundance (Di Natale and Idrissi, 2012). The 16th–18th century CE trap locations of Pedras de Fogu (Italy), Conil (Spain), and Marseille Harbour (France) offer some of the most recent zooarchaeological remains (Figure 3). The scientific literature appears to well-understand the distribution of BFT fisheries during these centuries, but a knowledge gap exists in how impactful these fisheries were. Therefore, such pre-industrial remains might offer relevant baselines that could be achievable to return to with sustainable management (Schwerdtner Máñez

*et al.*, 2014; Orton, 2016; Rodrigues *et al.*, 2019), in addition to elucidating the long-term drivers of population dynamics (Jackson *et al.*, 2001; Erlandson and Rick, 2010).

### Industrialisation and expansion throughout the Atlantic (19th–20th century CE)

Only a single BFT remain was recovered from the 19th century CE (Supplementary Table S3), but many 20th century CE archived BFT specimens exist, which might allow for an extension of the application of biomolecular and morphometric tools on fish remains to this era. This is particularly important since 19th and 20th century CE overexploitation is more likely but currently, we lack quantitative metrics to identify what changes occurred to population abundance, structure, and life-history traits during these years. Archived collections, i.e. at public museums (which are not reported in this work), and private collections such as the Massimo Sella Archive are vital in this regard (Supplementary Table S3). Most of the bones in the Sella Archive represent BFT caught in central Mediterranean tuna traps (i.e. off Croatia, Italy, and Libya) between 1911 and 1926 (see Riccioni *et al.*, 2010), including those vertebrae studied by Sella on his seminal work on BFT size-at-age (Sella, 1929). Similar collections probably exist elsewhere and are of clear importance to locate since these specimens offer the potential to investigate the impact of exploitation during the 19th and 20th century CE, when exploitation was clearly intensive, yet remains remarkably understudied.

By 1880, tuna trap effort had increased, when only a fraction of the Spanish, Italian, Portuguese, and Tunisian traps believed to exist at the time landed a combined 22000 t (Ravier and Fromentin, 2001; Pagá García *et al.*, 2017). Therefore, together with missing trap catch data and other gear types, catches in the 19th century CE appear to be comparable to the most intensive decades of BFT exploitation, which occurred a century later with further advances in technology and effort. This coincided with declines in trap tonnage across the Mediterranean, particularly after 1960 (Cort and Abaunza, 2016; Pagá García *et al.*, 2017), in part due to the economic difficulties of re-establishing tuna traps following the World Wars (Roesti, 1966).

Several case studies exemplify this advance in technology and exploitation effort in the early 20th century CE. The first being the expansion of fishing on a large scale in the northeastern Atlantic. By the early 20th century, large (> 2 m TL, total length) BFT migrating during summer from the Mediterranean to feed (Hamre, 1958) near the north of their range in the Atlantic became subject to recreational fishing and by-catch in Norwegian, Danish and Swedish fisheries, which often targeted Atlantic mackerel (*Scomber scombrus*) and herring (MacKenzie and Myers, 2007). Advances in the robustness of the purse seine by 1930 allowed these three nations especially to develop this fishery, which peaked in 1952, when Norwegian catches alone exceeded 10 000 t (Hamre *et al.*, 1966). However, Norwegian catches became rare after 1970 (MacKenzie and Myers, 2007).

Second, commercial fisheries in the western Atlantic developed, especially between Cape Hatteras and Newfoundland (Mather *et al.*, 1995; Porch *et al.*, 2019; Di Natale *et al.*, 2020). By 1960, longlining in the western Atlantic escalated, primarily driven by Japanese demand. This caused the so-called “Brazilian episode”—an appearance of an intensive long-line and drift-gillnet fishery for large BFT off Brazil and the central-southern Atlantic, which then almost disappeared within a decade (Takeuchi *et al.*, 2009; Di Natale *et al.*, 2013, 2020). The provenance of BFT captured off Brazil

is unknown. In total, two individuals tagged off the Bahamas in the 1960s were recaptured off South America (Mather *et al.*, 1995), yet some authors suggest that bite marks of the smalltooth cook-icutter shark (*Isistius brasiliensis*)—which is more common in the South Atlantic—on Mediterranean-caught BFT evidence an eastern Atlantic origin (Arena, 1988; Di Natale, 2010; Di Natale *et al.*, 2013; Quilez-Badia, *et al.*, 2013). Hence, BFT caught in the “Brazilian episode” may have falsely inflated western Atlantic population estimates and masked impacts on the eastern Atlantic and Mediterranean BFT population (Di Natale, 2019).

Third, by 1950, a fishery for juvenile BFT in the Bay of Biscay had developed that originated in the 1860s by handline (Bard, 1981). Here, as elsewhere, the retrofitting of echo sounders to vessels in the 1950s improved fishing efficiency. As a result, approximately 120 bait-boats operated from France and Spain in that decade, generating a historical peak in catch numbers that has not been surmounted since (Cort, 1990; Cort and Abaunza, 2019).

The final case study is that of the Black Sea. At the beginning of the 20th century, tuna traps (locally called *Dalians*) were operating in the Sea of Marmara (Örenç *et al.*, 2014) and Bosphorus, supporting the economy of 26 salting factories (Parona, 1919; Ninni, 1923). Indeed, BFT remains indicate exploitation had occurred here and far into the northern Black Sea for millennia (Lebedev and Lapin, 1954; Lyashenko, 2006; Morales-Muñiz *et al.*, 2007). From 1909 to 1923 up to 500 t of BFT caught in *Dalians* were sold each year in Istanbul market alone (Devedjian, 1926), where most were large BFT caught between April and October (Karakulak and Oray, 2009). Here, exploitation also intensified during the 1950s through the development of a purse-seine fleet (Iyigünger, 1957). After the 1970s, poor catches forced BFT fishing fleets into the Sea of Marmara and the Aegean (Karakulak and Oray, 2009; Ulman *et al.*, 2020) while the ancient *Dalian* fishery ended completely (Karakulak, 2004). BFT are now rare in the Black Sea and in the Sea of Marmara but show signs of recovery (Di Natale, 2019).

There is a consensus that overexploitation was a primary factor driving each of these 20th century case studies (Karakulak and Oray, 2009; Fromentin, 2009; MacKenzie *et al.*, 2009; Di Natale, 2010; Worm and Tittensor, 2011; Di Natale, 2015; Cort and Abaunza, 2016, 2019; Porch *et al.*, 2019). However, studies have been limited in their ability to quantify exploitation impacts in this period because data is lacking prior to when ICCAT collected accurate statistics from the 1970s onwards (ICCAT, 2017), though some data on population status does exist for the 1950s and 1960s (MacKenzie *et al.*, 2009). Other explanations have been proposed, such that oceanographic changes induced poor recruitment and/or altered migration patterns away from Norway (Fromentin, 2009) and Brazil (Fromentin *et al.*, 2014). Yet, MacKenzie and Myers (2007) suggested that the Nordic catches were not driven by environmental conditions. A long absence of BFT from these areas until very recently (Di Natale *et al.*, 2019; Nøttestad *et al.*, 2020) indicates that a lack of prey was not the predominant factor. However, common to all, is that large individuals migrated to these areas (Pusineri *et al.*, 2002; Di Natale, 2010, 2015; Cort *et al.*, 2013) and although mixed size-classes were caught off 1950s Norway (Fromentin and Powers, 2005), only large individuals have returned (Nøttestad *et al.*, 2020). It is evident that both the western and eastern population of BFT was truncated (Fromentin, 2009; MacKenzie *et al.*, 2009; Siskey *et al.*, 2016), which is a symptom of overexploitation (Heino *et al.*, 2015). In support of this, population decline, and cohort loss is theorized to result in a loss of migratory behaviour or collective memory, which takes time to rebuild (Petitgas *et al.*, 2010;

De Luca *et al.*, 2014; Mariani *et al.*, 2016). It is probable that climate, predator–prey dynamics, and overexploitation each contributed to the crashes of these fisheries. Multidisciplinary studies on fish remains offer the potential to disentangle these, thereby furthering the understanding the long-term drivers of population dynamics.

## Discussion

### Insights from traditional zooarchaeology

BFT bones recovered from archaeological excavations demonstrate that BFT exploitation had begun at 10000 years BCE. Despite large recoveries at sites such as Franchthi in the Aegean, basic fishing gear (Mylona, 2014), a lack of preservation facilities and demand suggest that it is unlikely BFT fishing was conducted on a large enough scale to impact population abundance or complexity until at least the Roman era onward. We hypothesize that because BFT are widely distributed and have a relatively large population size in the eastern Atlantic and Mediterranean, considerable exploitation intensity would be required to impact at the population level. It is remarkable that large (> 2 m TL) BFT, commonly caught during the Modern Age, were seldom represented in the archaeological record. We suppose that large individuals would have been readily caught once nets that could intercept spawning migrations were commonly used, i.e. from antiquity. We stress that large BFT especially, but indeed all adults, are cumbersome and would, therefore, not be routinely transported to salting facilities or settlements where most excavations focused. Historically, fish were more often processed close to the shore, and their bones dumped or burnt on beaches (Morales-Muñiz *et al.*, 2007), therefore, we observe and report only a minor fraction of the actual remains. This is attested by refuse dumps at the 2nd century BCE beach site Punta Camarinal where many articulated vertebral columns of large BFT were recovered including fins and tails (Morales-Muñiz and Roselló-Izquierdo, 2007). In comparison, only scattered remains were found at the adjoining city and *cetariae* of Baelo Claudia (Morales-Muñiz *et al.*, 2004c). Indeed, this incomplete nature of zooarchaeological data hinders robust interpretations.

We urge caution when interpreting the distribution and quantity of the remains herein as a proxy of fishing effort or evidence of human behaviour. The aphorism “absence of evidence is not evidence of absence” certainly applies here, especially since Middle Age sites and coastal middens are clearly understudied. There were discrepancies between the estimated size of individuals and their species identifications—for example ~20% of studies reported individuals estimated < 1.5 m in length (i.e. within the size range of albacore), while ~71% of studies did not report size estimations. It should be noted that reliable size reconstruction methods are yet to be established. Moreover, species identification from scales is contentious. Approximately 20% did not report the number of identified specimens (NISP), thus we suggest that NISP is not a good proxy for past population abundance or fishing effort. Another potential bias is that dating was estimated mostly by contextualizing stratigraphic units, with some records spanning multiple centuries, which clouds inferences of exploitation. Hence, further zooarchaeological study is required. The processing and trap locations presented here (from Pavesi, 1889; Devedjian, 1926; Pagá García *et al.*, 2017 and <https://ramppa.uca.es/>) offer plentiful locations for enquiry. In particular, the western Mediterranean *cetariae* collated by the RAMPPA Project, which date between 6th and 7th century CE, show no evidence of fish remains at ~90% of sites ( $n = 303$ ). This further highlights gaps in the archaeological record, which are not

attributed to poor recovery techniques, but specifically in this case, a lack of effort in excavating nearby coastal refuse dumps where BFT remains were discarded, rather than the settlements or *cetariae* themselves.

### Unlocking the potential of fish remains

Considering challenges facing the robustness of traditional zooarchaeological data, the application of biomolecular or morphometric tools on fish remains is vital to unlock their potential to quantify past population abundance and complexity in ways that can reveal long-term ecological trends that are useful for management and conservation (see Orton, 2016). BFT remains are particularly promising for these aims since sites which provide ample material for analyses (NISP > 20) span from 6000 years BCE to the 20th century CE at various periods and locations (Figure 4). Periods and events marking developments in BFT exploitation intensity which should be the focus of future investigations, are; prior to overexploitation case-studies of the mid 20th century CE; prior to the late-19th century CE trap catch peak; prior to the 16th century CE trap catch fluctuations in Spain and shift towards fixed traps; prior to the 14th century CE Spanish fishing regulations and increase in Sicilian trap numbers; and finally; pre-/post-BFT commercialization in antiquity.

Studies will be challenged in disentangling the influences of exploitation, and climate, which surely also effects BFT abundance and complexity (Fromentin, 2009; Reglero *et al.*, 2019), but exploitation is expected to increase with time and exacerbate fluctuations caused by climate (Anderson *et al.*, 2008). Indeed, a long time-series of samples is important in this regard to represent multiple stages of exploitation. Specifically, studies should focus on testing for the erosion of genetic diversity and effective population size as a proxy of abundance (e.g. Alter *et al.*, 2012; Ólafsdóttir *et al.*, 2014; Oosting *et al.*, 2019). The overexploitation of large individuals can be tested by investigating growth rate changes *via* morphometrics (e.g. Ólafsdóttir *et al.*, 2017) and the selection of genes related to maturation, and growth, as suggested by the theory of Fisheries Induced Evolution (Heino *et al.*, 2015; Hutchings and Kuparinen, 2021). Particularly for BFT, three important applications could be: first, testing for the loss of sub-populations as theorized for the Black Sea (Di Natale, 2015) using genomics to reveal past population structure and the selection of genes related to local adaptation (MacKenzie and Mariani, 2012), and isotopes to reconstruct past habitat use (e.g. Alter *et al.*, 2012; Guiry *et al.*, 2020). Second, investigating climate-mediated migration patterns or population components, that have been proposed to cause trap catch fluctuations of the 16th–20th century CE (Fromentin, 2009). These might be best studied using isotopic analyses on bulk bone collagen or individual amino acids to test for ecosystem-level and intra-species shifts in habitat use, and trophic structure (see Orton, 2016; Guiry *et al.*, 2020). Genomic studies on population structure are also expected to help here, and satisfy debate on various hypotheses (Fromentin, 2009; Karakulak and Oray, 2009; Di Natale, 2019; Cort and Abaunza, 2019). Finally, the analyses of isotopes and elements might offer opportunities to assess the onset of heavy metal pollution and changes in migratory behaviour (see Calaprice, 1986; Orton, 2016; Blankholm *et al.*, 2020), as it is hypothesized that during the 20th century, (predominantly) noise pollution drove BFT further from shore and has since limited trap efficiency (Addis *et al.*, 2009).

The preservation of fish remains from the periods proposed is well within the range of success for biomolecular and morphometric studies to date (Orton, 2016; Oosting *et al.*, 2019). The preservation of ancient DNA is of most concern among the techniques proposed. Within fish remains, it is variable (Oosting *et al.*, 2019) and has proved to be poor in BFT bones from arid Iberian sites (Puncher *et al.*, 2019). This may limit the use of poorly preserved remains to demographic analyses only using mitochondrial DNA (Oosting *et al.*, 2019), which is a low-resolution marker for modern population assignment (Carlsson *et al.*, 2004; Boustany *et al.*, 2008) but may offer utility toward genetic diversity changes. However, in general, fish remains show good potential for whole genome applications (Ferrari *et al.*, 2020). In addition to genetics/genomics, bone collagen and amino acids constitutes an important biochemical archive of stable isotopes and should not be hindered by preservation issues (Guiry and Szpak, 2021), at least for BFT remains from post-Roman periods. Element, e.g. heavy metals analyses on ancient bones could also be explored (c.f. Calaprice, 1986; Blankholm *et al.*, 2020) with an awareness of diagenesis and soil bleaching. Finally, studying growth rate changes from vertebrae is challenging, but it is still promising for the large vertebrae of BFT (Van Neer *et al.*, 1999). As a minimum, future studies engaged in BFT zooarchaeology would benefit by applying ZooMS (Rick *et al.*, 2019), or genetic barcoding (Puncher *et al.*, 2019) to provide reliable species identifications from bone and scales.

The approach advocated herein is clearly also relevant for other species and populations subject to intensive fisheries, especially other inshore migrators, e.g. gadids and *Anguilla* spp. (Hoffmann, 2005; Kettle *et al.*, 2008; Barrett, 2019) and those with fragmented populations, e.g. salmonids and sturgeons (Hoffmann, 2005), as these may have been more vulnerable to fishing impacts in pre-industrial periods, and excavations readily reveal their remains (Kettle *et al.*, 2008; Galik *et al.*, 2015; Barrett, 2019). This is particularly important for species which lack a rich base of literature and long-term datasets like the tuna trap catch series (which is often the case), those with populations yet to recover to mid-20th century CE baselines. Several studies have outlined their intent or begun to quantify historical exploitation on marine fishes (Orton, 2016; Morales-Muñiz *et al.*, 2018; Barrett, 2019; Ólafsdóttir *et al.*, 2014, 2017; Guiry *et al.*, 2020).

### The need for historical baselines

Our review suggests that exploitation had the potential to impact BFT populations in the preindustrial era, as has been suggested for a host of fisheries (e.g. Pauly, 1995; Jackson *et al.*, 2001; Hoffmann, 2005; Barrett *et al.*, 2004; Erlandson and Rick, 2010; Lotze *et al.*, 2014; Ólafsdóttir *et al.*, 2014; Morales-Muñiz *et al.*, 2018; Oueslati, 2019). The increase in Sicilian trap numbers by the 13th century CE, the imposition of fishing regulations, and claims of overfishing in the 16th century CE (Sarmiento, 1757; García, 2016) corroborate this, but currently only climate was considered as a regulator of population dynamics in this period (Fromentin, 2009). Rather, we suppose that climate, predator–prey dynamics, and exploitation operated together (with minor other factors, Di Natale and Idrissi, 2012) to promote the fluctuations observed in trap catches from the 16th century CE onwards (see Ravier and Fromentin, 2001; Pagá García *et al.*, 2017). Indeed, it remains to be seen whether exploitation impacts may extend back to antiquity for BFT, as appears the case according to the spread of the zooarchaeological data and classical writings on the importance of tuna in Greek and Roman times.

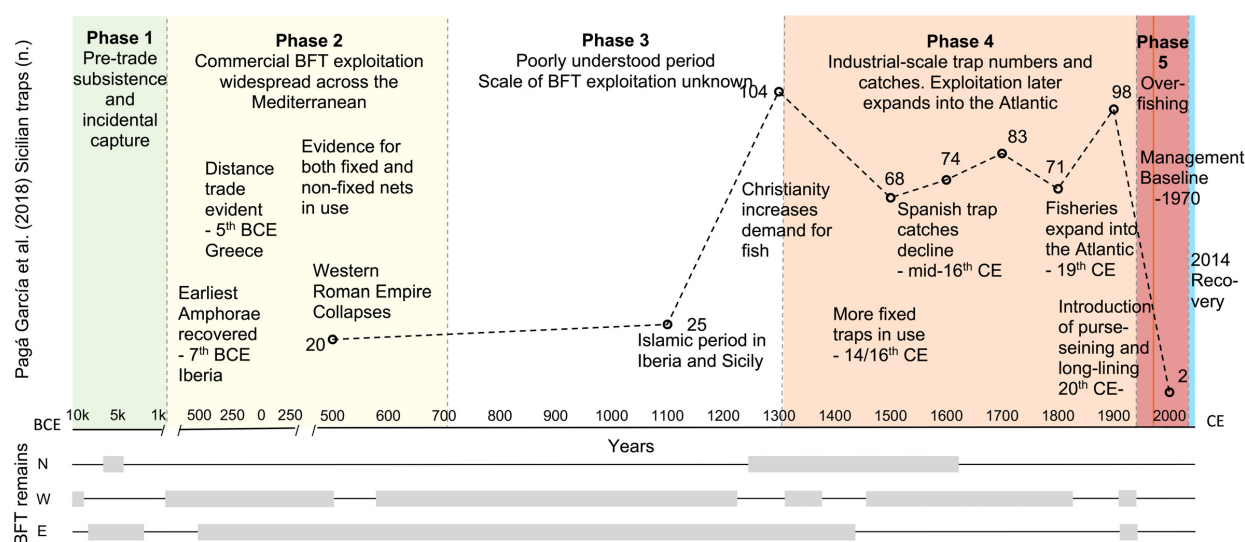


**Figure 4.** Schematic of major events related to the development of Atlantic bluefin tuna (*T. thynnus*; BFT) fisheries over time and the presence of tuna remains in time (grey bars) for three areas; N: northern Europe; W: western Mediterranean and Atlantic; and E: east of Sicily. k: thousand years. The line plot represents variation in the number of Sicilian tuna traps, as collated by Pagá García *et al.* (2018).

By categorizing our observations on exploitation into broad periods (Periods 1–5, Figure 4) we clearly illustrate our theory, despite that changes would have occurred on a much finer scale than is often detectable through inferences on archaeological and historical data due to periods with sparse evidence. Moreover, we highlighted incomplete and biased qualitative archaeological and trap catch data that may underestimate fishing intensity in the Middle Ages (Pagá García *et al.*, 2017, 2018)—in addition to missing data on other gear than traps, i.e. in Scandinavia, the Bay of Biscay, the Sea of Marmara, the Black Sea, and artisanal fisheries, that increased the duration of BFT fishing season from at least the 16th century CE onwards (Devedjian, 1926; Di Natale, 2015; Cort and Abaunza, 2019).

Since recovery and resilience are dependent on exploitation intensity and duration (Pauly, 1995; Neubauer *et al.*, 2013), there is a need to better understand the exploitation history of BFT. Recovery will be overestimated, and resilience underestimated if we do not account for historical exploitation impacts. Even mid-20th century case studies of BFT overexploitation are not accounted for by the 1970s management baselines, despite being fully acknowledged (Fromentin, 2009; MacKenzie *et al.*, 2009; Porch *et al.*, 2019). We suggest that preindustrial exploitation impacts ought to be quantified, especially during the last few centuries, because these may offer more relevant baselines than those of the ancient past, for example (Lotze *et al.*, 2014; Schwerdtner Máñez *et al.*, 2014; Rodrigues *et al.*, 2019). In addition, more recent remains are more likely to be well-preserved, and thus readily provide data. Until these aims are achieved, the use of 1950s and 1960s fisheries catch data might be helpful to explore the current baseline (e.g. MacKenzie *et al.*, 2009) and allow for a greater degree of confidence in the sustainability of BFT catches.

## Conclusion

BFT remains constitute a resource to investigate long-term population dynamics and exploitation impacts. The utility of tradi-

tional zooarchaeology toward this aim is limited due to biases, and spatiotemporal data gaps. Thus, the use of biomolecular and morphometric analyses should be promoted in tandem with increased zooarchaeological effort to understudied periods, i.e. Middle Ages; areas, i.e. coastal sites; and particularly fishing contexts, i.e. trap refuse dumps. Our review of literature provides clear evidence of BFT overexploitation during the mid-20th century CE from Norway (Hamre *et al.*, 1966), Brazil (Takeuchi *et al.*, 2009), the Bay of Biscay (Cort and Abaunza, 2019), and the Black Sea (Karakulak and Oray, 2009). Furthermore, a strong case could be made that the intensification of BFT exploitation extends back further to at least the 19th century CE, if not the 13th–16th century CE, in the eastern Atlantic and Mediterranean. However, a host of archaeological evidence would suggest that BFT exploitation may have been intensive since antiquity, according to the wide spatial extent of sites yielding zooarchaeological remains, among other archaeological evidence. Given this, the use of 1950s metrics as baselines for population status (MacKenzie *et al.*, 2009) might be tried to improve the currently used 1970s management baseline and decrease the uncertainty of future stock declines until quantitative historical baselines are produced for the preindustrial era.

## Funding

This work is a contribution to the MSCA SeaChanges ITN and is funded by EU Horizon 2020 (grant number: 813383).

## Data availability statement

The zooarchaeological records collated herein are available as Supplementary Information to this article. A constantly updated version is available at <https://tunaarchaeology.org/database>.

## Supplementary data

Supplementary material is available at the ICESJMS online.

## Acknowledgements

We are grateful to the RAMPPA Project (<https://ramppa.uca.es/>; PID2019-108948RB-I00/AEI/10.13039/501100011033; FEDER-UCA18-104415; and P18-FR-1483) for access to *cetariae* location data, and Alfonso Pagá García and ICCAT GBYP for access to trap location and number data. Thanks to Canan Çakırlar, Verónica Gomez Fernandez, Gaël Piquès, Barbara Wilkens, and the Natural History Museum of Denmark (Statens Naturhistoriske Museum, Copenhagen) for information on several sources of BFT remains. We thank Athena Trakadas for insights into the impact of Roman era fishing and Richard Hoffmann for insights into the Middle Age transition. We thank the reviewers who greatly improved the quality of this manuscript.

## References

- Addis, P., Locci, I., and Cau, A. 2009. Anthropogenic impacts on bluefin tuna (*Thunnus thynnus*) trap fishery of Sardinia (Western Mediterranean). *Collective Volume of Scientific Papers*, 63, 174–185.
- Aguiayo de Hoyos, P., Carrilero Millán, M., and Martínez Fernández, G. 1987. La presencia fenicia y el proceso de aculturación de las comunidades del bronce final de la depresión de ronda (Málaga). *In Atti II Congresso Internazionale di Studi Fenici e Punici*, 2, Roma, pp. 559571.
- Al-Idrisi al-Qurtubi al-Hasani al-Sabti A.A.A.M. 1154a. *Tabula Rogeriana*.
- Al-Idrisi al-Qurtubi al-Hasani al-Sabti A.A.A.M. 1154b. *De geographia universali* or *Kitāb Nuzhat al-mushtāq fi dhikr al-amṣār wa-al-aqṭār wa-al-buldān wa-al-juzur wa-al-madāʾ in wa-al-āfāq*, Rome (Latin translation of the original work written in Arabic ~1154).
- Alter, S.E., Newsome, S.D., and Palumbi, S.R. 2012. Pre-whaling genetic diversity and population ecology in eastern Pacific gray whales: insights from ancient DNA and stable isotopes. *Plos ONE*, 7, e35039.
- Anderson, C.N., Hsieh, C.H., Sandin, S.A., Hewitt, R., Hollowed, A., Beddington, J., May, R.M., and Sugihara, G. 2008. Why fishing magnifies fluctuations in fish abundance. *Nature*, 452, 835–839.
- Aniceti, V. 2019. *Animals and their roles in the medieval society of Sicily: from Byzantines to Arabs and from Arabs to Norman/Swabians*. Doctoral Thesis, University of Sheffield, UK.
- Arena, P. 1988. *Risultati delle rilevazioni sulle affluenze del tonno nel tirreno e sull'andamento della pesca da parte delle "tonnare volanti" nel triennio 1984-1986*. MMM-CNR. *Atti seminari UU.OO Resp. Prog. Ric.*, Roma: 273–297.
- Aristotle. (343 BC, re-edited in 1635). 1635 *De animalibus*. *In Goza, T. Stagiritae peripatetico rum. Principis de Historia Animalium*. Venezia: 1–843.
- Bard, F. X. 1974. *Etude sur le germon (Thunnus alalunga, bonnaterre 1788) de l'Atlantique nord*. *Elements de dynamique de population*. *Collective Volume of Scientific Papers ICCAT 2*, 198–224.
- Bard, F. X. 1981. *Le thon germon (Thunnus alalunga Bonnaterre 1788) de l'Océan Atlantique*. *Thèse Doctorat*, État Université de Paris. VI. 333.
- Barrett, J.H. 2019. An environmental (pre) history of European fishing: past and future archaeological contributions to sustainable fisheries. *Journal of Fish Biology*, 94: 1033–1044.
- Barrett, J.H., Locker, A.M., and Roberts, C.M. 2004. The origins of intensive marine fishing in medieval Europe: the English evidence. *Proceedings of the Royal Society of London Series B Biological Sciences*, 271: 2417–2421.
- Bekker-Nielsen, T. 2005. (ed.). *Ancient Fishing and Fish Processing in the Black Sea Region*. Aarhus University Press, Aarhus.
- Bello León, J.M. 2005. *Almadrabas andaluzas a finales de la edad media*. *Nuevos datos para su estudio*. *Historia Instituciones Documentos*, 2005: 81–113.
- Bennema, F. P. 2018. Long-term occurrence of Atlantic bluefin tuna *Thunnus thynnus* in the North Sea: contributions of non-fishery data to population studies. *Fisheries Research*, 199, 177–185.
- Berkeley, S. A., Hixon, M. A., Larson, R. J., and Love, M. S. 2004. Fisheries sustainability via protection of age structure and spatial distribution of fish populations. *Fisheries*, 29: 23–32.
- Bernal-Casasola, D. (ed). 2011. *Pescar con arte*. Fenicios y romanos en el origen de los aparejos andaluces. *Monografías del Proyecto Sagena*. 3, Universidad de Cádiz.
- Bernal-Casasola, D., Mazzaglia, D. Malfitana Antonino, J., and Díaz, J. 2021. Tonno e garum nelle cetariae ellenistiche e romane di Poropalò e Vendicari (Siracusa). *Primi risultati interdisciplinari*, *Monografie HEROM*, Catania.
- Bernal-Casasola, D., Vargas Girón, J.M., and Lara Medina, M. 2019. Atunes en salazón y en conserva en las chancas gaditanas: perspectivas desde el olivillo in 7 metros de la historia de Cádiz. *In Arqueología en El Olivillo y en el Colegio Mayor Universitario* (2019). Universidad de Cádiz, Cádiz. 726.
- Blankholm, H.P., Lidén, K., Kovačević, N., and Angerbjörn, K. 2020. Dangerous food. Climate change induced elevated heavy metal levels in younger stone age seafood in northern Norway. *Quaternary International*, 549, 74–83.
- Bolle, L.J., Rijnsdorp, A.D., van Neer, W., Millner, R.S., van Leeuwen, P.I., Eryvnc, A., Ayers, R. et al. 2004. Growth changes in plaice, cod, haddock and saithe in the North Sea: a comparison of (post-) medieval and present-day growth rates based on otolith measurements. *Journal of Sea Research*, 51: 313–328.
- Boustany, A.M., Reeb, C.A., and Block, B.A. 2008. Mitochondrial DNA and electronic tracking reveal population structure of Atlantic bluefin tuna (*Thunnus thynnus*). *Marine Biology*, 156: 13–24.
- Brown, K., Fa, D.A., Finlayson, G., and Finlayson, C. 2011. Small game and marine resource exploitation by Neanderthals: the evidence from Gibraltar. *In Trekking the Shore* pp. 247–272. Springer, New York, NY.
- Butchart, S. H., Walpole, M., Collen, B., Van Strien, A., Scharlemann, J. P., Almond, R. E., and Carpenter, K. E. 2010. Global biodiversity: indicators of recent declines. *Science*, 328: 1164–1168.
- Calaprice, J. R. 1986. Chemical variability and stock variation in northern Atlantic bluefin tuna. *Collective Volume of Scientific Papers ICCAT*, XXIV: 222–254.
- Carlsson, J., McDowell, J. R., Díaz-Jaimes, P., Carlsson, J. E., Boles, S. B., Gold, J. R., and Graves, J. E. 2004. Microsatellite and mitochondrial DNA analyses of Atlantic bluefin tuna (*Thunnus thynnus*) population structure in the Mediterranean Sea. *Molecular Ecology*, 13: 3345–3356.
- Cort, J.L. 1990. *Biología y pesca del atún rojo. Thunnus thynnus (L.) del mar cantábrico* (Tesis doctoral). *Publicaciones Especiales Instituto Español Oceanografía* 4, 1–272.
- Cort, J.L., and Abaunza, P. 2016. The impact of massive fishing of juvenile Atlantic bluefin tunas on the spawning population (1949–2010). *In Proceedings of the ICCAT SCRS/2016/179*, pp. 35.
- Cort, J.L., and Abaunza, P. 2019. The Bluefin Tuna Fishery in the Bay of Biscay: Its Relationship with the Crisis of Catches of Large Specimens in the East Atlantic Fisheries from the 1960s. p. 123. Springer Nature.
- Cort, J.L., Deguara, S., Galaz, T., Mèlich, B., Artetxe, I., Arregi, I., Neilson, J. et al. 2013. Determination of lmax for Atlantic bluefin tuna, *Thunnus thynnus* (L.), from meta-analysis of published and available biometric data, *Reviews in Fisheries Science* 21: 181–212.
- De Luca, G., Mariani, P., MacKenzie, B. R., and Marsili, M. 2014. Fishing out collective memory of migratory schools. *Journal of the Royal Society Interface*, 11: 20140043.
- Delussu, F., and Wilkens, B. 2000. *Le conserve di pesce*. *Alcuni dati da contesti italiani*. *Mélanges de l'école française de Rome*, 112, 17–18.
- Devedjian, K. 1926. *Pêche et Pêcheries en Turquie*, Imprimerie de l'Administration de la Dette Publique Ottomane, Istanbul: 1–480.
- Di Natale, A. 2010. The eastern Atlantic bluefin tuna: entangled in a big mess, possibly far from a conservation red alert. Some comments after the proposal to include bluefin tuna in CITES appendix I. *Collective Volumes of Scientific Papers ICCAT*, 65: 1004–1043.
- Di Natale, A. 2012. New data on the historical distribution of bluefin tuna (*Thunnus thynnus*, L.) in the Arctic Ocean. *Collective Volume of Scientific Papers ICCAT*, 68: 102–114.



- Di Natale, A. 2014. The ancient distribution of bluefin tuna fishery: how coins can improve our knowledge. *Collective Volume of Scientific Papers ICCAT*, 70: 2828–44.
- Di Natale, A. 2015. Review of the historical and biological evidences about a population of bluefin tuna (*Thunnus thynnus* L.) in the eastern Mediterranean and the Black Sea. *Collective Volume of Scientific Papers ICCAT*, 71: 1098–1124.
- Di Natale, A. 2019. Due to the new scientific knowledge, is it time to reconsider the stock composition of the Atlantic bluefin tuna?. *Collective Volume of Scientific Papers ICCAT*, 75: 1282–1292.
- Di Natale, A., Celona, A., and Mangano, A. 2005. A series of catch records by the harpoon fishery in the Strait of Messina from 1976 to 2003. *Collective Volume of Scientific Papers ICCAT*, 58, 1348–59.
- Di Natale, A., and Idrissi, M. 2012. Factors to be taken into account for a correct reading of tuna trap catch series. *Collective Volume of Scientific Papers ICCAT*, 67: 242–261.
- Di Natale, A., Idrissi, M.H., and Rubio, A.J. 2013. The mystery of bluefin tuna (*Thunnus thynnus*) presence and behaviour in central-south Atlantic in recent years. *Collective Volume of Scientific Papers ICCAT*, 69: 857–868.
- Di Natale, A., Macias, D., and Cort, J.L. 2020. Atlantic bluefin tuna fisheries: temporal changes in the exploitation pattern, feasibility of sampling, factors that can influence our ability to understand spawning structure and dynamics. *Collective Volume of Scientific Papers ICCAT*, 76: 354–388.
- Di Natale, A., Tensek, S., and García, A.P. 2019. Is the bluefin tuna slowly returning to the Black Sea? Recent evidences. *Collective Volume of Scientific Papers ICCAT*, 75: 1261–1277.
- Doumenge, F. 1999. 'La storia delle pesche tonniere'. *Biologia Marina Mediterranea*, 6, 5–106.
- Enghoff, I. B., MacKenzie, B. R., and Nielsen, E. E. 2007. The Danish fish fauna during the warm Atlantic period (ca. 7000–3900 BC): fore-runner of future changes? *Fisheries Research*, 87: 167–180.
- Ericson, P. G. P. 1989. Faunahistoriskt intressanta stenålderfrån stora karlsö. *Flora och Fauna* 84: 192–198.
- Erlandson, J.M., and Rick, T.C. 2010. Archaeology meets marine ecology: the antiquity of maritime cultures and human impacts on marine fisheries and ecosystems. *Annual Review of Marine Science*, 2, 231–251.
- Evans, J., and Renfrew, C. 1968. Excavations at Saliagos: Near Antiparos. *British School of Archaeology at Athens*, 227pp.
- Felici, E. 2018. *Thynnus*. *Archeologia della tonnara mediterranea*. Edipuglia, Bari. 1–270pp.
- Ferrari, G., Cuevas, A., Gondek-Wyrozemska, A.T., Ballantyne, R., Kersten, O., Pálsdóttir, A.H., van der Jagt, I. *et al.* 2020. The preservation of ancient DNA in archaeological fish bone. *Journal of Archaeological Science*, 126, 105317.
- Fromentin, J. M. 2009. Lessons from the past: investigating historical data from bluefin tuna fisheries. *Fish and Fisheries* 10, 197–216.
- Fromentin, J. M., Reygondeau, G., Bonhommeau, S., and Beaugrand, G. 2014. Oceanographic changes and exploitation drive the spatio-temporal dynamics of Atlantic bluefin tuna (*Thunnus thynnus*). *Fisheries Oceanography*, 23: 147–156.
- Fromentin, J.M. 2003. Why uncertainty in the management of the east Atlantic bluefin tuna has constantly increased in the past few years. *Scientia Marina*, 67: 51–62.
- Fromentin, J.M., and Powers, J.E.. 2005. Atlantic bluefin tuna: population dynamics, ecology, fisheries and management. *Fish and Fisheries* 5, 281–306.
- Galik, A., Haidvogel, G., Bartosiewicz, L., Guti, G., and Jungwirth, M. 2015. Fish remains as a source to reconstruct long-term changes of fish communities in the Austrian and Hungarian Danube. *Aquatic Sciences*, 77: 337–354.
- Ganzedo, U., Zorita, E., Solari, A.P., Chust, G., Del Pino, A.S., Polanco, J., and Castro, J.J. 2009. What drove tuna catches between 1525 and 1756 in southern Europe?. *ICES Journal of Marine Science*, 66: 1595–1604.
- García, A., Alemany, F., Velez-Belchi, P., López Jurado, J. L., Cortés, D., De la Serna, J. M., and Ramírez, T. 2005. Characterization of the bluefin tuna spawning habitat off the Balearic Archipelago in relation to key hydrographic features and associated environmental conditions. *Collective Volume of Scientific Papers ICCAT*, 58: 535–549.
- García, F.D.L.C.G. 2016. Doñana en su historia: cuatro siglos entre la explotación y la conservación bajo la posesión de la Casa de los Guzmanes. *Organismo Autónomo Parques Nacionales*.
- García-Vargas, E. A., and Florido del Corral, D. 2010. The origin and development of tuna fishing nets (Almadrabas). *In Proceedings of the International Workshop on "Ancient Nets and Fishing Gear in Classical Antiquity. A First Approach"*. Ed. by Bekker-Nielsen, T., and Bernal-Casasola, D., Aarhus – Cádiz, 205–227.
- García-Vargas, E., Roselló-Izquierdo, E., Bernal-Casasola, D., and Morales-Muñiz, A. 2018. Salazones y salsas de pescado en la antigüedad. Un primer acercamiento a las evidencias de paleocon-tenidos y depósitos primarios en el ámbito euro-mediterráneo. *In Las cetariae de Iulia Traducta. Resultados de las excavaciones arqueológicas en la calle San Nicolás de Algeciras (2001-2006)*, pp. 287–312. Ed. by Bernal-Casasola, D., and Jiménez-Camino, R., Universidad de Cádiz y Ayuntamiento de Algeciras, Cádiz.
- Guiry, E., Royle, T.C., Matson, R.G., Ward, H., Weir, T., Waber, N., Brown, T.J. *et al.* 2020. Differentiating salmonid migratory ecotypes through stable isotope analysis of collagen: archaeological and ecological applications. *Plos ONE*, 15: e0232180.
- Guiry, E., and Szpak, P. 2021. Improved quality control criteria for stable carbon and nitrogen isotope measurements of ancient bone collagen. *Journal of Archaeological Science* 132:104516.
- Hadjianastasiou, O. 1991. A mycenaean pictorial vase from naxos. *In De Miro, E., Godart, L., and Sacconi, A.* (eds). *Atti e memorie del secondo congresso internazionale di micenologia*. Gruppo Editoriale Internazionale, Roma. 1433–1441pp.
- Hamre, J. 1958. Tuna investigations in Norwegian coastal waters 1954–1958. *Annales Biologiques*, 15: 197–211.
- Hamre, J., Lozano, F., Rodriguez-Roda, J., and Tiews, K. 1966. Report from the bluefin tuna working group. *ICES Statistical News letters*, 26, 1–34.
- Heino, M., Diaz Pauli, B., and Dieckmann, U. 2015. Fisheries-induced evolution. *Annual Review of Ecology, Evolution, and Systematics*, 46, 461–480.
- Hilborn, R., Quinn, T. P., Schindler, D. E., and Rogers, D. E. 2003. Bio-complexity and fisheries sustainability. *Proceedings of the National Academy of Sciences*, 100: 6564–6568.
- Hoffmann, R.C. 2005. A brief history of aquatic resource use in medieval Europe. *Helgoland Marine Research*, 59: 22–30.
- Horden, P., and Purcell, N. 2000. *The Corrupting Sea: A Study of Mediterranean History*. Wiley-Blackwell.
- Hutchings, J. A., and Kuparinen, A. 2021. Throwing down a genomic gauntlet on fisheries-induced evolution. *Proceedings of the National Academy of Sciences*, 118: e2105319118.
- Iacovou, M. 1988. *The Pictorial Pottery of Eleventh Century B.C. Cyprus (Studies in Mediterranean Archaeology)*. Paul Forlag Astroms. 79p.
- ICCAT. 2007. Report of the 2006 Atlantic bluefin tuna stock assessment session (SCRS/2006/013). International Commission for the Conservation of Atlantic Tuna, Madrid.
- ICCAT. 2017. Report of the 2017 ICCAT bluefin stock assessment meeting. International Commission for the Conservation of Atlantic Tuna, Madrid.
- ICCAT. 2020. Report of the 2020 second ICCAT intersessional meeting of the bluefin tuna species group. International Commission for the Conservation of Atlantic Tuna, Madrid. Online, 20-28 July 2020.
- Iyigunçor, D. 1957. Méthodes et moyens de pêche au thon actuellement en usage en Turquie. No. 4, Document Technique No. 33. FAO, The General Fisheries Commission for the Mediterranean, Rome, Italy, 251–255pp.
- Jackson, J. B., Kirby, M. X., Berger, W. H., Bjorndal, K. A., Botsford, L. W., Bourque, B. J., and Warner, R. R. 2001. Historical overfishing and the recent collapse of coastal ecosystems. *Science*, 293: 629–637.

- Jansen, T., Nielsen, E. E., Rodríguez-Ezpeleta, N., Arrizabalaga, H., Post, S., and MacKenzie, B. R. 2021. Atlantic bluefin tuna (*Thunnus thynnus*) in Greenland—mixed-stock origin, diet, hydrographic conditions, and repeated catches in this new fringe area. *Canadian Journal of Fisheries and Aquatic Sciences*, 99: 1–9.
- Jennings, S., Reynolds, J. D., and Mills, S. C. 1998. Life history correlates of responses to fisheries exploitation. *Proceedings of the Royal Society of London Series B Biological Sciences*, 265: 333–339.
- Karakulak, F. S. 2004. Catch and effort of the bluefin tuna purse-seine fishery in Turkish waters. *Fisheries Research*, 68: 361–366.
- Karakulak, F. S., and Oray, I. K. 2009. Remarks on the fluctuations of bluefin tuna catches in Turkish waters. *Collective Volume of Scientific Papers ICCAT*, 63, 153–160.
- Kettle, A. J., Heinrich, D., Barrett, J. H., Benecke, N., and Locker, A. 2008. Past distributions of the European freshwater eel from archaeological and palaeontological evidence. *Quaternary Science Reviews*, 27: 1309–1334.
- Knappe, A., and Ericson, P. G. P. 1983. Återupptäckta fund från grotta stora förvar. *Fornvännen* 78: 192–198.
- Ladero Quesada, M.A. 1993. Las almadrabas de Andalucía (siglos XIII–XVI). *Boletín de la Real Academia de la Historia*, 190: 345–354.
- Lebedev, V.D., and Lapin, U.E. 1954. Kvprouso o rybalovstve u bosforoskom tsarstve (in Russian: on the issue of fishing in the Bosphorus). *MIA*, 33: 197–214.
- Lindquist, O. 1994. Whales, dolphins and porpoises in the economy and culture of peasant fishermen of Norway, Orkney, Shetland, Faroe Islands and Iceland, ca. 900–1900 AD., and Norse Greenland, ca. 1000–1500 A.D. (Vol I). PhD Thesis, Faculty of Arts, University of St. Andrew, St. Andrews.
- Longo, S. B., and Clark, B. 2012. The commodification of bluefin tuna: the historical transformation of the Mediterranean fishery. *Journal of Agrarian Change*, 12: 204–226.
- Lotze, H. K., Hoffmann, R., and Erlandson, J. 2014. Lessons from historical ecology and management. *In The Sea—Marine Ecosystem-Based Management. Ideas and Observations on Progress in the Study of the Seas*, 16, 17–55 pp. Harvard University Press.
- Lozano Rey, L. 1952. Peces Fisoclistos – Subserie Roracicos. *Memorias de la Real Academia de Ciencias Exactas, 3, Físicas y Naturales de España*, Madrid. ISBN: 1LA20NABG1520.
- Lyashenko, Yu. N. 2006. Fauna material from the Gleiki II settlement in the eastern Crimea. *Starozhytnosti Stepovogo Prychornomyria i Krymu* 13: 68–74.
- MacKenzie, B. R., and Mariani, P. 2012. Spawning of bluefin tuna in the Black Sea: historical evidence, environmental constraints and population plasticity. *Plos ONE*, 7: e39998.
- MacKenzie, B. R., and Myers, R. A. 2007. The development of the northern European fishery for north Atlantic bluefin tuna *Thunnus thynnus* during 1900–1950. *Fisheries Research*, 87: 229–239.
- MacKenzie, B.R., Mosegaard, H., and Rosenberg, N.A. 2009. Impending collapse of bluefin tuna in the northeast Atlantic and Mediterranean. *Conservation Letters* 2, 25–34.
- Mariani, P., Krivan, V., MacKenzie, B.R., and Mullon, C. 2016. The migration game in habitat network: the case of tuna. *Theoretical Ecology*, 9: 219–232.
- Maschner, H. D., Betts, M. W., Reedy-Maschner, K. L., and Trites, A. W. 2008. A 4500-year time series of Pacific cod (*Gadus macrocephalus*) size and abundance: archaeology, oceanic regime shifts, and sustainable fisheries. *Fishery Bulletin*, 106: 386–394.
- Mather, F.J., Mason, J.M., and Jones, A.C.. 1995. Historical document: life history and fisheries of Atlantic bluefin tuna. 1995. NOAA Technical Memorandum NMFS-SEFSC-370. National Oceanic and Atmospheric Administration. 165.
- Matsubayashi, J., Saitoh, Y., Osada, Y., Uehara, Y., Habu, J., Sasaki, T., and Tayasu, I. 2017. Incremental analysis of vertebral centra can reconstruct the stable isotope chronology of teleost fishes. *Methods in Ecology and Evolution*, 8: 1755–1763.
- Montanari, M. 1979. *L'alimentazione contadina nell'alto Medioevo*, 11, Liguori Publications.
- Morales Muñiz, A. 1993. Where are the tunas? Ancient Iberian fishing industries from an archeozoological perspective. *In Skeletons in her Cupboard*, pp. 135–141. Ed. by Clason, A., Payne, S., and Uerpmann, H.P., Oxbow, Oxford.
- Morales-Muñiz, A., and Roselló-Izquierdo, E. 2007. *Los atunes de baelo claudia y punta camarinal (s. II d.C.). Apuntes preliminares*. In *Las Cetariae de Baelo Claudia. Avance de las Investigaciones arqueológicas en el barrio meridional (2000–2004)*, pp. 355–374. Ed. by Arévalo-González, A., and Bernal-Casasola, D, Sevilla.
- Morales-Muñiz, A., Antipina, E., and Roselló-Izquierdo, E. 2007. An ichthyoarchaeological survey of the ancient fisheries from the northern Black Sea. *Archaeofauna*, 16, 117–172.
- Morales-Muñiz, A., de Agüero, E.G.G., Fernández-Rodríguez, C., Rey, F.S., Llorente-Rodríguez, L., López-Arias, B., and Roselló-Izquierdo, E. 2018. Hindcasting to forecast. An archaeological approach to the European hake (*Merluccius merluccius*, Linnaeus 1758) fishery: Iberia and beyond. *Regional Studies in Marine Science*, 21, 21–29.
- Morales-Muñiz, A., Roselló-Izquierdo, E., Bernal Casasola, D., and Arévalo González, A. 2004c. Garum y salazones en el Círculo del Estrecho. *Catálogo de la Exposición (Algeciras)*, Granada, 254–255.
- Porch, C.E., Bonhommeau, S., Diaz, G.A., Arrizabalaga, H., and Melvin, G. 2019. The journey from overfishing to sustainability for Atlantic bluefin tuna, *Thunnus thynnus*. *In The Future of Bluefin Tunas: Ecology, Fisheries Management, and Conservation*, Ed. by Block, B. John Hopkins University Press.
- Mylona, D. 2014. Aquatic animal resources in prehistoric Aegean, Greece. *Journal of Biological Research-Thessaloniki*, 21: 2.
- Mylona, D. 2021. Catching tuna in the Aegean: biological background of tuna fisheries and the archaeological implications. *Anthropozoologica* 56: 23–37.
- Neubauer, P., Jensen, O.P., Hutchings, J.A., and Baum, J.K. 2013. Resilience and recovery of overexploited marine populations. *Science*, 340: 347–349.
- Nielsen, E.E., and Hansen, M.M. 2008. Waking the dead: the value of population genetic analyses of historical samples. *Fish and Fisheries*, 9: 450–461.
- Nielssen, S. V., and Persson, P. 2020. The Jortveit farm wetland: a neolithic fishing site on the Skagerrak coast, Norway. *Journal of Wetland Archaeology*, 20, 1–24.
- Ninni, E. 1923. Primo contributo allo studio dei pesci e della pesca nelle acque dell'Impero Ottomano, *In Missione italiana per l'esplorazione dei mari di levante*, 5, pp. 1–53. Premiate officine grafiche Carlo Ferrari.
- Nobis, G. 1999. *Die Tierreste von Karthago*, pp. 574–632. Ed. by Rakob, F. Philipp von Zabern, Mainz.
- Nøttestad, L., Bøge, E., and Ferter, K. 2020. The comeback of Atlantic bluefin tuna (*Thunnus thynnus*) to Norwegian waters. *Fisheries Research*, 231, 105689.
- Ólafsdóttir, G. Á., Pétursdóttir, G., Bárðarson, H., and Edvardsson, R. 2017. A millennium of north-east Atlantic cod juvenile growth trajectories inferred from archaeological otoliths. *Plos ONE*, 12: e0187134.
- Ólafsdóttir, G.Á., Westfall, K.M., Edvardsson, R., and Pálsson, S. 2014. Historical DNA reveals the demographic history of Atlantic cod (*Gadus morhua*) in medieval and early modern Iceland. *Proceedings of the Royal Society B Biological Sciences*, 281: 20132976.
- Onar, V., Pazvant, G., and Armutak, A. 2008. Radiocarbon dating results of the animal remains uncovered at Yenikapı excavations. *In Istanbul Archaeological Museums, Proceedings of the 1st Symposium on Marmaray-Metro Salvage Excavations*. 249–256.
- Oosting, T., Star, B., Barrett, J.H., Wellenreuther, M., Ritchie, P.A., and Rawlence, N.J. 2019. Unlocking the potential of ancient fish DNA in the genomic era. *Evolutionary Applications*, 12: 1513–1522.
- Oppianus (177 CE). 1738. *Aliuticon*. *In Della Caccia e della Pesca*, pp. 510. Ed. by Salvini, A.M., Firenze, Italy.
- Örenç, A.F., Ünver, M., Düzçü, L., and Di Natale, A. 2014. Tentative GBYP bluefin tuna recovery from the Ottoman archives, the maritime museum archives and the archives of the Istanbul municipality. *Collective Volume of Scientific Papers ICCAT*, 70: 447–458.
- Orton, D.C. 2016. Archaeology as a tool for understanding past marine resource use and its impact. *In Perspectives on Oceans Past*, pp. 47–69. Springer, Dordrecht.

- Oueslati, T. 2019. A French fish event at the turn of the 10th century? Environment, economy, and ethnicity in Maritime Flanders. *International Journal of Osteoarchaeology*, 29: 443–451.
- Pagá García, A., Di Natale, A., Tensek, S., and Palma, C. 2018. Historical and recent data of Sicilian traps: the complexity of data recovery and interpretation. *Collective Volume of Scientific Papers ICCAT*, 74: 2873–2886.
- Pagá García, A., Palma, C., Di Natale, A., Tensek, S., Parrilla, A., and de Bruyn, P. 2017. Report on revised trap data recovered by ICCAT GBYP from phase 1 to phase 6. *Collective Volume of Scientific Papers ICCAT*, 73: 2074–2098.
- Parona, C. 1919. Il Tonno e la sua pesca. *Premiate officine grafiche Carlo Ferrari*. R. Comit. Talass. Ital. Venezia, Mem. LXVIII, 1–259.
- Pauly, D. 1995. Anecdotes and the shifting baseline syndrome of fisheries. *Trends in ecology & evolution*, 10: 430.
- Pauly, D., Christensen, V., Guénette, S., Pitcher, T.J., Sumaila, U.R., Walters, C.J., Watson, R., and Zeller, D. 2002. Towards sustainability in world fisheries. *Nature*, 418: 689–695.
- Pavesi, P. 1889. L'industria del Tonno. *Relazione alla Commissione Reale per le Tonnare*. Ministero di agricoltura, industria e commercio, Roma, Tip. Eredi Botta, 1–254.
- Petitgas, P., Secor, D.H., McQuinn, I., Huse, G., and Lo, N. 2010. Stock collapses and their recovery: mechanisms that establish and maintain life-cycle closure in space and time. *ICES Journal of Marine Science*, 67: 1841–1848.
- Piccinetti, C., Di Natale, A., and Arena, P. 2013. Eastern bluefin tuna (*Thunnus thynnus*, L.) reproduction and reproductive areas and season. *Collective Volume of Scientific Papers ICCAT*, 69: 891–912.
- Plinius, C.S. (65 CE, re-edited in 1553), 1553 *Historia mundi*. In *Naturalis Historia*, pp. 1–882. Ed. by Vicentino, A., Ludguni.
- Puncher, G. N., Cariani, A., Cilli, E., Massari, F., Leone, A., Morales-Muñiz-Muñiz, A., and Tinti, F. 2019. Comparison and optimization of genetic tools used for the identification of ancient fish remains recovered from archaeological excavations and museum collections in the Mediterranean region. *International Journal of Osteoarchaeology*, 29: 365–376.
- Puncher, G. N., Cariani, A., Maes, G. E., Van Houdt, J., Hertens, K., Cannas, R., and Hanke, A. 2018. Spatial dynamics and mixing of bluefin tuna in the Atlantic ocean and Mediterranean Sea revealed using next-generation sequencing. *Molecular Ecology Resources*, 18: 620–638.
- Pusineri, C., Ravier, C., and Fromentin, J.M. 2002. Retrospective analysis of the bluefin tuna Nordic fisheries data. *Collective Volume of Scientific Papers ICCAT*, 54, 517–526.
- Quilez-Badia, G., Cermeño, P., Sainz Trápaga, S., Tudela, S., Di Natale, A., Idrissi, M., and Abid, N. 2013. 2012 ICCAT-GBYP pop-up tagging activity in Larache (Morocco). *Collective Volume of Scientific Papers ICCAT*, 69: 869–877. ICCAT-SCRS/2012/143.
- Ravier, C., and Fromentin, J. M. 2001. Long-term fluctuations in the eastern Atlantic and Mediterranean bluefin tuna population. *ICES Journal of Marine Science*, 58: 1299–1317.
- Ravier C., Fromentin J. M. 2004. Are the long-term fluctuations in Atlantic bluefin tuna (*Thunnus thynnus*) population related to environmental changes?. *Fisheries Oceanography*, 13(3): 145–160.
- Reglero, P., Balbín, R., Abascal, F. J., Medina, A., Alvarez-Berastegui, D., Rasmuson, L., and Hidalgo, M. 2019. Pelagic habitat and offspring survival in the eastern stock of Atlantic bluefin tuna. *ICES Journal of Marine Science*, 76: 549–558.
- Riccioni, G., Landi, M., Ferrara, G., Milano, I., Cariani, A., Zane, L., Sella, M. *et al.* 2010. Spatio-temporal population structuring and genetic diversity retention in depleted Atlantic bluefin tuna of the Mediterranean Sea. *Proceedings of the National Academy of Sciences*, 107: 2102–2107.
- Richardson, D.E., Marancik, K.E., Guyon, J.R., Lutcavage, M.E., Galuardi, B., Lam, C.H., Walsh, H.J. *et al.* 2016. Discovery of a spawning ground reveals diverse migration strategies in Atlantic bluefin tuna (*Thunnus thynnus*). *PNAS USA* 113, 3299–3304.
- Rick, T., Harvey, V.L., and Buckley, M. 2019. Collagen fingerprinting and the chumash billfish fishery, Santa Barbara Channel, California, USA. *Archaeological and Anthropological Sciences*, 11: 6639–6648.
- Rochet, M. J. 1998. Short-term effects of fishing on life history traits of fishes. *ICES Journal of Marine Science*, 55: 371–391.
- Rodrigues, A. S., Monsarrat, S., Charpentier, A., Brooks, T. M., Hoffmann, M., Reeves, R., and Turvey, S. T. 2019. Unshifting the baseline: a framework for documenting historical population changes and assessing long-term anthropogenic impacts. *Philosophical Transactions of the Royal Society B*, 374: 20190220.
- Rodríguez, J. M., Johnstone, C., and Lozano-Peral, D. 2021. Evidence of Atlantic bluefin tuna spawning in the Bay of Biscay, NE Atlantic. *Journal of Fish Biology*. 99, 964–969, In press. doi: 10.1111/jfb.14782.
- Rodríguez-Marín, E., Landa, J., Ruiz, M., Godoy, D., and Rodríguez-Cabello, C. 2004. Age estimation of adult bluefin tuna (*Thunnus thynnus*) from dorsal spine reading. *Collective Volume of Scientific Papers ICCAT*, 56, 1168–1174.
- Rodríguez-Marín, E., Olafsdottir, D., Valeiras, J., Ruiz, M., Chosson-Pampoulie, V., and Rodríguez-Cabello, C. 2006. Ageing comparison from vertebrae and spines of bluefin tuna (*Thunnus thynnus*) coming from the same specimen. *Collective Volume of Scientific Papers ICCAT*, 59: 868–876.
- Roesti, R. M. 1966. The declining economic role of the Mediterranean tuna fishery. *The American Journal of Economics and Sociology*, 25: 77–90.
- Rooker, J. R., Secor, D. H., De Metrio, G., Schloesser, R., Block, B. A., and Neilson, J. D. 2008. Natal homing and connectivity in Atlantic bluefin tuna populations. *Science*, 322: 742–744.
- Rose, M. 1994. With line and glittering bronze hook: fishing in the Aegean Bronze Age. PhD Dissertation, Indiana University, Ann Arbor, Bloomington.
- Sarà, R. 1998. Dal Mito all' Aliscafo: Storie di Tonni e di Tonnare. Messina.
- Sarmiento, F. M. 1757. De los atunes y sus transmigraciones y conjeturas sobre la decadencia de las almadrabas y sobre los medios para restituirlas. *Caixa de Pontevedra*, Madrid.
- Schwerdtner Máñez, K., Holm, P., Blight, L., Coll, M., MacDiarmid, A., Ojaveer, H. *et al.* 2014. The future of the oceans past: towards a global marine historical research initiative. *Plos ONE* 9: e101466.
- Sella, M. 1929. Migrazioni ed habitat del tonno (*Thunnus thynnus* L.) studiati col metodo degli ami, con osservazioni sull'accrescimento, sul regime delle tonnare, ecc. *Memorie Comitato Talassografico Italiano*, 16: 3–24.
- Siskey, M.R., Wilberg, W.J., Allman, R.J., Barnett, B.K., and Secor, D.H.. 2016. Forty years of fishing: changes in age structure and stock mixing in northwestern Atlantic bluefin tuna (*Thunnus thynnus*) associated with size-selective and long-term exploitation. *ICES Journal of Marine Science* 73, 2518–2528.
- Spoto, S. 2002. Sicilia Antica: usi, costumi e personaggi dalla preistoria alla società greca, nell'isola culla della civiltà europea, pp. 352. Ed. by Compton, N.E.. Newton & Compton, Roma.
- Squatriti, P. 2002. *Water and Society in Early Medieval Italy, AD 400–1000*. Cambridge University Press.
- Tailliez, P. 1961. Travaux de l'été 1958 sur l'épave du Titan a l'île du Levant (Toulon), Actes du iie Congrès International d'archéologie sous marines, Bordighera, 175–178.
- Takeuchi, Y., Oshima, K., and Suzuki, Z.. 2009. Inference on the nature of Atlantic bluefin tuna off Basil caught by Japanese longline fishery around the early 1960s. *Collective Volume of Scientific Papers ICCAT*, 63, 186–94.
- Theodoropoulou, T. 2014. Salting the east: evidence for salted fish and fish-products from the Aegean Sea in Roman times. In *Fish & Ships Production and commerce of salsamenta during Antiquity*. éditions errance, Centre Camille Jullian, pp. 213–227.
- Trakadas, A. 2005. The archaeological evidence for fish processing in the western Mediterranean. In *Ancient Fishing and Fish Processing in the Black Sea Region*, pp. 47–82. Aarhus.
- Trakadas, A. 2006. "Exhausted by fishermen's nets" Roman sea fisheries and their management. *Journal of Mediterranean Studies*, 16: 259–272.

- Trakadas, A. 2010. Archaeological Evidence for Ancient Fixed-Net Fishing in Northern Morocco. Universidad de Cádiz - Servicio de Publicaciones.
- Tusa, S. 1999. *La Sicilia Nella Preistoria* 1983. Sellerio, Palermo, Italia. 106.
- Uerpmann, M., and Van Neer, W. 2000. Fischreste aus den neuen grabungen in troia (1989-1999). *Studia Troica*, 10, 145–179.
- Ulman, A., Zengin, M., Demirel, N., and Pauly, D. 2020. The lost fish of Turkey: a recent history of disappeared species and commercial fishery extinctions for the Turkish Marmara and Black Seas. *Frontiers in Marine Science*, 7: 650.
- Van Neer, W., Löugas, L., and Rijnsdorp, A.D. 1999. Reconstructing age distribution, season of capture and growth rate of fish from archaeological sites based on otoliths and vertebrae. *International Journal of Osteoarchaeology*, 9: 116–130.
- Wilson, D.E., and Mittermeier, R.A. 2014. *Handbook of the Mammals of the World: Sea Mammals*, 4, Lynx Edicions, Barcelona, Spain.
- Worm, B., and Tittensor, D.P. 2011. Range contraction in large pelagic predators. *Proceedings of the National Academy of Sciences*, 108: 11942–11947.
- Yacoub, M. 1995. *Splendeurs des mosaïques de Tunisie*, Ministère de la Culture, de la Jeunesse et des Loisirs, Tunis.
- Zimmerman Munn, M.-L. 2003. Corinthian trade with the Punic West in the Classical period. *In* *Corinth. The Centenary 1896–1996. Results of Excavations conducted by the American School of Classical Studies at Athens*, pp. 195–217. Ed. by Williams, C. K., and Bookidis, N., Princeton University Press, Princeton.

*Handling Editor: Bo Poulsen*

## Exploitation history of Atlantic bluefin tuna in the eastern Atlantic and Mediterranean—insights from ancient bones

Adam J. Andrews, Antonio Di Natale, Darío Bernal-Casasola, Veronica Aniceti, Vedat Onar

Tarek Oueslati, Tatiana Theodoropoulou, Arturo Morales-Muñiz, Elisabetta Cilli, Fausto Tinti

### Supplementary Tables

**Table S1.** Archaeological bluefin tuna (*Thunnus thynnus*) records dating prior to the 9<sup>th</sup> century BCE. Site numbering refers to the map reference (Figure 1).

Site	Date (years)	NISP	Size (TL cm)	Reference
1 Svendborg, Denmark	140,000 BCE	2	150	Pers. Comm. Statens Naturhistoriske Museum (SNM), Copenhagen
2 Gorham's Cave, Gibraltar	26,000-22,000 BCE	2		Brown et al., 2011
3 Cueva de Nerja, Malaga, Spain	10,000 BCE	1		Morales-Muñiz et al., 1998
4 Franchthi Cave, Greece	9,000 BCE	500	50-200	Rose, 1994, 1995
5 Maroulas, Kythnos, Greece	8,800-8,600 BCE	12		Mylona, 2010
6 Vela Spila, Korčula Island, Croatia	8,000 BCE	7		Rainsford et al., 2014
7 Youra, Greece	7,700-6,900 BCE			Mylona, 2011; Powell 2011
8 Copenhagen, Denmark	6,800-5,400 BCE	1		Enghoff et al., 2007
9 Cape Andreas Kastros, Cyprus	6,000 BCE	27		Desse & Desse-Berset, 1994
10 Grotte du Cap Ragnon, Bouche-du-Rhône, France	6,000-5,800 BCE	4	3 years of age	Courtin et al., 1972
11 Alepotrypa Cave, Greece	6,000-3,200 BCE	27		Theodoropoulou, 2019
12 Tägerup, Sweden	5,800 BCE			Karsten & Knarrström, 2003
13 El Retamar, Spain	5,000 BCE	4	Medium	Soriguer Escofet et al., 2002
14 Lerna, Greece	5,300-2,200 BCE	1		Gejvall, 1969; Rose, 1994

15 Stora Förvar, Sweden	5,200-4,000 BCE			Ericson, 1989
16 Saliagos Cave, Paros, Greece	4,300 BCE	2608 scombridae bones	Large scombrids: <i>T.thynnus</i> or <i>T.alalunga</i>	Evans & Renfrew, 1968
17 Pefkakia, Volos, Greece	4,300-2,500 BCE	69		Hinz, 1979; von den Driesch, 1987; Rose, 1994
18 Jortveit, Norway	3,500 BCE	17		Nielssen & Persson, 2020
19 Besik Tepe, Turkey	3,000-2,550 BCE	2		von den Driesch & Boessneck, 1984; Boessneck, 1986; Rose, 1994
20 Perachora, Greece	2,650-2,200 BCE	2		Rose, 1994
21 Troy, Turkey	2,250-1,700 BCE	100		Rose, 1994; Uerpmann & van Neer, 2000
22 Gleika II, Crimea	2,000 BCE			Lyashenko, 2006
23 Kommos, Greece	1,700-1,600 BCE	2		Rose, 1994
24 Akrotiri, Greece	1,500 BCE	5	100	Mylona, 2008a
25 Koukounaries, Paros, Greece	1,300-1,150 BCE	1		Rose, 1994
26 Skipshelleren, Norway	Neolithic			Olsen, 1976
27 Ånneröd, Sweden	Neolithic			Alin, 1955
28 Gröninge, Sweden	Neolithic			Särilvik, 1976
29 Sandhem, Sweden	Neolithic			Jonsson, 2007
30 Hakeröd, Sweden	Neolithic			Jonsson, 2002
31 Cova Fosca, Castellón, Spain	Neolithic	1	150	Roselló-Izquierdo et al., 2015

NISP: Number of identified specimens, i.e., counts of bones or scales and often counts of individuals when recovered articulated. TL: Total length.

**Table S2.** Archaeological records bluefin tuna (*Thunnus thynnus*) records dating from the 9<sup>th</sup> century BCE to the 7<sup>th</sup> century CE. Site numbering refers to the map reference (Figure 2). Records listed in bold are examples of transport/trade.

Source	Date	NISP	Size (TL cm)	Reference
32 Utica, Tunisia	Punic	1	122	Fentress, unpublished report
33 Ceuta, Spain	8 <sup>th</sup> -7 <sup>th</sup> BCE	3		Zabala et al., 2011
34 Toscanos, Málaga, Spain	8 <sup>th</sup> -7 <sup>th</sup> BCE			Lepiksaar, 1973

35 Carthage, Tunisia	8 <sup>th</sup> -6 <sup>th</sup> BCE	Multiple	100-150	Nobis, 1999
36 Castillo de Doña Blanca, Spain	750-500 years BCE	52		Roselló-Izquierdo & Morales-Muñiz 1994
37 Tavira, Portugal	8 <sup>th</sup> BCE-1 <sup>st</sup> CE	1,176		Roselló-Izquierdo & Morales-Muñiz, unpublished report
38 Huelva, Spain	8 <sup>th</sup> BCE-1 <sup>st</sup> CE	11		Roselló-Izquierdo & Morales-Muñiz, 1990
39 Castro Marim, Portugal	8 <sup>th</sup> -4 <sup>th</sup> BCE	194		Roselló-Izquierdo & Morales-Muñiz, unpublished report
40 Althiburos, Tunisia	700-750 years BCE	1		Valenzuela, unpublished report
41 <b>Acinipo, Spain</b>	7 <sup>th</sup> BCE	Multiple		Aguayo de Hoyos et al., 1987
42 Cerro del Villar Malaga, Spain	600-575 years BCE			Rodríguez Santana, 1999
43 Chersonesos, Crimea	6 <sup>th</sup> -5 <sup>th</sup> BCE	1		Lebedev & Lapin, 1954
44 <b>Corinth, Greece</b>	460-440 years BCE	Multiple		Zimmerman Munn, 2003; Saez Romero & Theodoropoulou, in press
45 Camposoto, Spain	450 years BCE	234		Sáez et al., 2004
46 Plaza de Asdrúbal, Spain	5 <sup>th</sup> BCE	45		Bernal-Casasola et al., 2014a
47 Carthage, Tunisia	5 <sup>th</sup> -4 <sup>th</sup> BCE	Multiple	80-200	Nobis, 1999
48 Carthage, Tunisia	5 <sup>th</sup> -4 <sup>th</sup> BCE	5	Large	Van Neer & Wouters, 2009
49 Pilarou Cave, Thera, Santorini, Greece	5 <sup>th</sup> -1 <sup>st</sup> BCE	1	80	Mylona, 2008b
50 Portopalo, Sicily, Italy	5 <sup>th</sup> BCE-1 <sup>st</sup> BCE	Multiple	50-100	Bernal-Casasola et al., 2021
51 Palacio de Justicia, Cadiz, Spain	5 <sup>th</sup> BCE-2 <sup>nd</sup> CE			Bernal-Casasola, 2011
52 Kassopi, Greece,	4 <sup>th</sup> BCE			Boessneck, 1994
53 Place Jules Verne, Marseille, France	4 <sup>th</sup> -3 <sup>rd</sup> BCE	Multiple		Sternberg, 1998
54 Besik Tepe, Turkey	4 <sup>th</sup> -1 <sup>st</sup> BCE	15		von den Driesch & Boessneck, 1984; Boessneck 1986; Rose, 1994
55 Vendicari, Sicily, Italy	4 <sup>th</sup> BCE-1 <sup>st</sup> CE	Multiple		Basile, 1992
56 Messene, Greece	3 <sup>rd</sup> -2 <sup>nd</sup> BCE	1		Rose, 2000
57 Tamuda, Morocco	3 <sup>rd</sup> BCE-1 <sup>st</sup> CE			Trakadas, 2018

58 Costa Rincon, Morocco	3 <sup>rd</sup> BCE-1 <sup>st</sup> CE			Trakadas, 2018
59 Teatro Andalucía, Cádiz, Spain	3 <sup>rd</sup> BCE-3 <sup>rd</sup> CE	Multiple		Bernal-Casasola et al., 2014b
60 Pantikapaion, Crimea	250 years BCE	5		Morales-Muñiz et al., 2007
61 Sant'Antioco, Sardinia, Italy	2 <sup>nd</sup> BCE	2	100	Carenti, 2013
62 Kalaureia, Poros, Greece	2 <sup>nd</sup> BCE	6		Mylona, 2008b; Mylona, 2021
63 Baelo Claudia, Spain	2 <sup>nd</sup> BCE	20	100-200	Morales-Muñiz et al., 2004a
64 Punta Camarinal, Baelo Claudia, Spain	2 <sup>nd</sup> BCE	1052	96-391	Morales-Muñiz et al., 2004b; Morales-Muñiz & Roselló-Izquierdo, 2007
65 Baelo Claudia, Spain	2 <sup>nd</sup> BCE	Multiple		Morales-Muñiz et al., 2004c
66 Milazzo, Sicily, Italy	2 <sup>nd</sup> BCE-2 <sup>nd</sup> CE	500		Mangano, 2009
67 Baelo Claudia, Spain	1 <sup>st</sup> BCE	Multiple		Morales-Muñiz et al., 2004d
68 <b>Titán Wreck, Isle of Levant, France</b>	1 <sup>st</sup> BCE	Multiple		Tailliez, 1961
69 Carthage, Tunisia	Pre-Roman			Weinstock, 1995
70 Lixus, Morocco	Pre-Roman			Rodriguez Santana & Rodrigo García, 2005
71 Cerro del Mar, Vélez-Málaga, Spain	1 <sup>st</sup> BCE-1 <sup>st</sup> CE	150+	200	von den Driesch, 1980
72 Populonia, Italy	1 <sup>st</sup> BCE-1 <sup>st</sup> CE	64		De Grossi, 2006
73 Lixus, Morocco	1 <sup>st</sup> CE	1		Oueslati, unpublished report
74 Olivillo, Cadiz, Spain	1 <sup>st</sup> CE	50-100	20-150	Bernal-Casasola et al., 2019
75 Castro Marim, Portugal	1 <sup>st</sup> CE	13		Roselló-Izquierdo & Morales-Muñiz unpublished report
76 <b>Chiessi Wreck, Isle of Elba, Italy</b>	1 <sup>st</sup> CE	Multiple		Delussu & Wilkens, 2000
77 Carthage, Tunisia	1 <sup>st</sup> -3 <sup>rd</sup> CE	Multiple	Large	Nobis, 1999



78 Mytilene, Lesvos, Greece	1 <sup>st</sup> -4 <sup>th</sup> CE			Ruscillo, 1993
79 Puerta Califal, Ceuta, Spain	1 <sup>st</sup> -5 <sup>th</sup> CE	Multiple		Bernal-Casasola et al., 2012
80 <b>Dion, Greece</b>	2 <sup>nd</sup> -3 <sup>rd</sup> CE	2		Theodoropoulou, 2014
81 Baelo Claudia, Spain	5 <sup>th</sup> -6 <sup>th</sup> CE	50-100	50-150	Bernal-Casasola et al., 2016; Brassous et al., 2017
82 Teatro Romano, Malaga, Spain	5 <sup>th</sup> CE	2		Lozano-Francisco, 2017
83 Utica, Tunisia	Roman	2	86-200	Fentress, unpublished report
84 Carthage, Tunisia	5 <sup>th</sup> CE	Multiple	90-100	Nobis, 1999
85 Carteia, Spain	5 <sup>th</sup> -6 <sup>th</sup> CE	2		Exposito & García Pantoja, 2020
86 San Nicolás, Algeciras, Spain	5 <sup>th</sup> -6 <sup>th</sup> CE	3	100-150	Roselló-Izquierdo & Morales-Muñiz, 2018
87 Santa Filítica, Sardinia, Italy	5 <sup>th</sup> -7 <sup>th</sup> CE	1		Wilkins, 2020
88 Sant'Imbenia, Sardinia, Italy	5 <sup>th</sup> -7 <sup>th</sup> CE	1		Wilkins, 2020
89 İznik Roman Theatre, Turkey	5 <sup>th</sup> -7 <sup>th</sup> CE	1		Onar, unpublished report
90 Gruissan, France	6 <sup>th</sup> CE	1		Piques, in press
91 Carthage, Tunisia	6 <sup>th</sup> -7 <sup>th</sup> CE	1		Van Neer & Wouters, 2009

NISP: Number of identified specimens, i.e., counts of bones or scales and often counts of individuals when recovered articulated. TL: Total length.

**Table S3.** Archaeological and archival records of bluefin tuna (*Thunnus thynnus*) dating to the Middle and Modern Ages. \* = archived collection not shown on map. Site numbering refers to the map reference (Figure 3). Records listed in bold are examples of transport/trade.

Source	Date	NISP	Size (TL cm)	Reference
92 Yenikapi, Istanbul, Turkey	4 <sup>th</sup> -15 <sup>th</sup> CE	150	>150	Onar et al., 2008
93 Balat, Istanbul, Turkey	4 <sup>th</sup> -15 <sup>th</sup> CE	21		Onar, unpublished report
94 Bathonea, Istanbul, Turkey	4 <sup>th</sup> -15 <sup>th</sup> CE	2		Onar, unpublished report
95 Casale San Pietro, Sicily	8 <sup>th</sup> -9 <sup>th</sup> CE	4		Aniceti, 2019

96 Sant'Antonino, Sicily	9 <sup>th</sup> -10 <sup>th</sup> CE	12	100-200	Aniceti, 2019
97 Corso dei Mille, Sicily	9 <sup>th</sup> -10 <sup>th</sup> CE	16	100-200	Aniceti, 2019
98 Mazara del Vallo, Sicily	10 <sup>th</sup> -11 <sup>th</sup> CE	10	100-200	Aniceti, 2019
99 Mazara del Vallo, Sicily	13 <sup>th</sup> CE	10	100-250	Aniceti, 2019
100 Saltes, Huelva, Spain	12 <sup>th</sup> -14 <sup>th</sup> CE			Morales-Muñiz et al., 1994
101 Søborg, Gribskov, Denmark	13 <sup>th</sup> -14 <sup>th</sup> CE			Pers. Comm. SNM, Copenhagen
102 Monteleone, Sardinia, Italy	14 <sup>th</sup> CE	1		Wilkens, 2020
103 Ceuta, Spain	14 <sup>th</sup> CE	4		Lozano-Francisco, 2010
104 La Cartuja, Seville, Spain	14 <sup>th</sup> -15 <sup>th</sup> CE	1	>150	Roselló-Izquierdo et al., 1994
105 Raversijde, Oostende, Belgium	15 <sup>th</sup> CE	165		Pieters et al., 2013
106 Tårnby Torv, Copenhagen, Denmark	13 <sup>th</sup> -17 <sup>th</sup> CE			Pers. Comm. SNM, Copenhagen
107 Pedras de Fogu, Sardinia, Italy	16 <sup>th</sup> -18 <sup>th</sup> CE	767	Ages 4- 11	Wilkens & Delussu, 2001
108 Østergade, Gilleleje, Denmark	1600 CE			Pers. Comm. SNM, Copenhagen
109 Cappuccine, Sassari, Sardinia, Italy	17 <sup>th</sup> CE	1		Wilkens, 2020
110 Ågabet, Bagenkop, Denmark	1550-1620 years CE			Pers. Comm. SNM, Copenhagen
111 Sassari, Sardinia, Italy	17 <sup>th</sup> -19 <sup>th</sup> CE	5		Wilkens, 2020
112 Leca Harbour, Marseille, France	1750-1850 years CE	46		Piques, 2020
113 Conil de la Frontera, Spain	1755 CE	100+	>150	Gutierrez-Mas et al., 2016
114 Palazzo Ducale, Sassari, Sardinia, Italy	19 <sup>th</sup> CE	1		Wilkens, 2020

*Central Mediterranean Tonnare	1911-1941 years CE	300+	Complete range	Riccioni et al., 2010
--------------------------------	--------------------	------	----------------	-----------------------

NISP: Number of identified specimens, i.e., counts of bones or scales and often counts of individuals when recovered articulated. TL: Total length.

## Glossary Table

Term	Description
BCE/CE	Before Common Era/Common Era. Secular version of BC/AD.
Mesolithic	Period comprising the middle of the Stone Age, circa 15,000 – 7,000 BCE throughout the Mediterranean
Neolithic	Period comprising the late Stone Age, circa 7,000 - 3,000 BCE throughout Europe
Antiquity	Period comprising the civilisations of ancient Greece and Rome, circa 8 <sup>th</sup> century BCE – 5 <sup>th</sup> century CE
Phoenician	Period comprising the colonisation of the western Mediterranean by Phoenician peoples, who originated from the eastern Mediterranean, circa 10 <sup>th</sup> – 9 <sup>th</sup> century BCE
Punic	Period comprising Phoenician colonies in the western Mediterranean, circa 8 <sup>th</sup> century BCE – 1 <sup>st</sup> century BCE
Greek	Period comprising the ancient Greek civilisation, circa 8 <sup>th</sup> century BCE – 1 <sup>st</sup> century BCE
Roman	Period comprising the Roman Empire, circa 1 <sup>st</sup> century BCE – 5 <sup>th</sup> century CE
Middle Ages	Period comprising the fall of the western Roman Empire (5 <sup>th</sup> century CE) to the Modern Ages (16 <sup>th</sup> century CE)
Islamic Period	Period comprising the Islamic political rule of regions within Iberia and Sicily, dates of which are region specific, circa 8 <sup>th</sup> century CE – 13 <sup>th</sup> century CE. Usage herein ignores the Emirate of Granada, which was the final Iberian region to be dissolved, in the 15 <sup>th</sup> century CE.

## Supplementary only references

Alin, J. (1955). Förteckning över stenåldersboplatser i norra Bohuslän. *Göteborgs och Bohuslänns Fornminnesförening*, Göteborg.  
 Basile, B. (1992). Stabilimenti per la lavorazione del pesce lungo le coste siracusane: Vendicari e Portopalo. *V Rassegna di Archeologia Subacquea* (Giardini Naxos 1990), Messina, 1992, 55- 86.

Bernal-Casasola, D., Marlasca, R., Rodríguez Santana, C.G., Villada, F. (2012). *Los atunes de la Tingitana. Un contexto excepcional de las factorías salazoneras salazoneras de Septem Fratres*, Convegno Internazionale di Studi sull'Africa Romana XIX (Sassari – Alghero, 2010), Trasformazione dei paesaggi del potere nell'Africa settentrionale fino alla fine del mondo antico, 3, 2507-2534, Sassari, 2012.

Bernal-Casasola, D., Muñoz Vicente, Á., Marlasca Martín, R., Cantillo Duarte, J. J., Vargas Girón, J. M., Lara Medina, M. (2014a). *Atunes ronqueados y conchas de la plaza de Asdrúbal. Novedades haliéuticas en los saladeros gadiritas*. In Cantillo Duarte, J.J. Bernal-Casasola, D. & Ramos Muñoz, J. (eds.), *Moluscos y púrpura en contextos arqueológicos atlántico-mediterráneos: nuevos datos y reflexiones en clave de proceso histórico*, Cádiz, pp. 205-228.

Bernal-Casasola, D., Cobos Rodríguez, L., Marlasca, R., Cantillo Duarte, J. J., Vargas Girón, J.M., Lara Medina, M. (2014b). *De las fogatas profilácticas púnicas a las chancas romanas. Moluscos y escómbrios en el antiguo Teatro Andalucía de Cádiz*. In Cantillo Duarte, J.J. Bernal Casasola, D. & Ramos Muñoz, J. (eds.), *Moluscos y púrpura en contextos arqueológicos atlántico-mediterráneos: nuevos datos y reflexiones en clave de proceso histórico*, Cádiz, pp. 179-204.

Bernal-Casasola, D., Expósito Álvarez, J.A., Díaz Rodríguez, J.J., Marlasca Martín, R., Riquelme Cantal, J.A., Lara Medina, M., Vargas Girón, J.M, Bustamante Álvarez, M., Pascual Sánchez, M. (2016). *Saladeros romanos en Baelo Claudia: nuevas investigaciones arqueológicas*. In *Un Estrecho de Conservas. Del garum de Baelo Claudia a la melva de Tarifa. Catálogo de la Exposición*, Cádiz, 43-69.

Boessneck, J. (1986). Die Weichtieresser vom Besik-Sivritepe. *Archäologischer Anzeiger*, 329-338.

- Boessneck, J. (1994). Zooarchaeologische Ergebnisse an den Tierkochen- und Molluskenfunden in W. Hoepfner & E.-L. Schwandner. Haus und Stadt im Klasischen Griechenland, Munchen; Deutcher Kunstverlag, 175-179.
- Brassous, L., Deru, X., Oliva Rodríguez Gutiérrez, Dananai, A., Dienst, S., Doyen, J.-M., Florent, G., Gomes, M., Lemaître, S., Louvion, C., Oueslati, T., Renard, S. (2017). *Baelo Claudia dans l'Antiquité tardive. L'occupation du secteur sud-est du forum entre les IIIe et VIe siècles*. Mélanges de la Casa de Velázquez Nouvelle série 47, 167-200.
- Carenti, G. (2013). San't Antioco (SW Sardinia, Italy): Fish and Fishery Resource Exploitation in a Western Phoenician Colony. *Archaeofauna*, 22, 37-49.
- Desse, J., & Desse-Berset, N. (1994). Stratégies de pêche au 8ème millénaire: les poissons de Cap Andreas Kastros (Chypre). *Fouilles recentes a Khirokitia Editions Recherche sur Civilisations*, Paris, 335-360.
- Exposito, J.A. & García Pantoja, M.E. (2020). Consumo de moluscos marinos en las cetariae romanas del barrio salazonero de Carteia (San Roque, Cádiz). In Vicens, M.A. & Pons, G.X. (eds). *Avances en Arqueomalacología. Nuevos conocimientos sobre las sociedades pasadas y su entorno natural gracias a los moluscos*, Monografies de la Societat de Historia Natural de les Balears, 32, Palma de Mallorca.
- Gejvall N.-J. (1969). *Lerna: a Preclassical Site in the Argolid. Results of Excavations Conducted by the American School of Classical Studies at Athens. Vol. I: The Fauna*. ASCSA Publications, Princeton.
- Gutiérrez-Mas, J.M., Gómez Fernández, V., García-López, S., Morales-Muñiz, J.A. y Ibáñez Ageitos, J.M. (2016). Comparative analysis of the deposits left by the tsunami that followed to the Lisbon Earth-quake (1755 AD), on the Castilnovo beach and the Old Tuna Factory of La Chança (Conil de la Frontera, SW Spain). *Revista de la Sociedad Geológica de España*, 29(1), 21-33.
- Hinz, G. (1979). *Neue Tierknochenfunde aus der Magula. Pevkakia in Thessalien, i. Die Nichtwiederkduer* (Unpublished Dissertation, University of Munich 1979).
- Jonsson, L. (2002). Animal bones from the Middle Neolithic site Hakeröd in Bohuslän, Sweden. *ANL rapport 2002:1*, Institutionen för Arkeologi, Göteborgs universitet, Göteborg.
- Jonsson, L. (2007). Djurbenen från Sandhem. Tidigare undersökningar av djurben från kökkenmöddingar i Västsverige, in: Lönn, M., Claesson, P. (Eds.), *Vistelser Vid Vatten. Gropkeramiska Platser Och Kokgropar Från Bronsålder Och Järnålder*. Riksantikvarieämbetet & Bohusläns museum, Ödeshög, 231–235.
- Karsten, P., and Knarrström, B. (2003). *The Tågerup Excavation*. National Heritage Board. Lund: National Heritage Board.
- Lepiklaaar, J. (1973). *Fischknochenfunde aus der Phönozischen Faktorei von toscanos*, Studien über frühe Tier Knochenfunde von der Iberischen Halbinsel 4, Munich, 109-119.
- Lozano-Francisco, M.C. (2010). *Paleobiología de los restos orgánicos desechados por la comunidad ceutí del siglo XIV*, in J.M. Hita, J. Suarez, F. Villada eds., *Comer en Ceuta en el siglo XIV*. La alimentación durante la época marina, Ceuta, 39-56.
- Lozano-Francisco, M.C. (2017). *Estudio ictiológico de los residuos encontrados en las cetariae malacitanas*. A propósito de las factorías del teatro romano de Málaga. In Corrales Aguilar, M. (ed.), *Aportaciones a la Malaca tardorromana y bizantina. Excavaciones en la factoría de salazones del teatro romano de Málaga (siglos iv-vi d C.)*, Sevilla, 143-164.
- Mangano, G. (2009). *I resti faunistici del sito di Contrada Vaccarella a Milazzo*. In Tigano, G. (ed) Mylai II. *Scavi e ricerche nell'area urbana (1996–2005)*. Regione Siciliana, Messina, 271.
- Morales-Muñiz, A., Roselló-Izquierdo, E., Lenfacker, A., & Morales-Muñiz, D.C. (1994). Archaeozoological research in medieval Iberia: fishing and fish trade on almohad sites. *Trabalhos de Antropologia e Etnologia* 34 (1-2), 453-475.
- Morales-Muñiz, A., Roselló-Izquierdo, E. and Hernández, F. (1998). Late Upper Paleolithic subsistence strategies in southern Iberia: tardiglacial faunas from Cueva de Nerja (Málaga, Spain). *European Journal of Archaeology*, 1(1), 9-50.
- Morales-Muñiz, A., Roselló-Izquierdo, E., Bernal Casasola, D., Arévalo González, A. (2004a). *Proceso de despiece de túnidos*. In *Garum y salazones en el Círculo del Estrecho*. Catálogo de la Exposición (Algeciras), Granada, 176-177.
- Morales-Muñiz, A., Roselló-Izquierdo, E., Bernal Casasola, D., Arévalo González, A. (2004b). *Conjunto de túnidos*. In *Garum y salazones en el Círculo del Estrecho*. Catálogo de la Exposición (Algeciras), Granada, 82-83.
- Morales-Muñiz, A., Roselló-Izquierdo, E., Bernal Casasola, D., Arévalo González, A. (2004d). *Paleocontenido de ánfora púnica (tipo Ramon T-7.4.3.2)*. In *Garum y salazones en el Círculo del Estrecho*. Catálogo de la Exposición (Algeciras).

- Mylona, D. (2008a). 'Cooking' Installations in LC IA Akrotiri on Thera: A preliminary Study of the 'Kitchen' in Pillar Shaft 65: Appendix C. In Brodie, N., Doole, J., Gavalas, G. and Renfrew, C., 2008. *Horizon: A Colloquium on the Prehistory of the Cyclades*. McDonald Institute for Archaeological Research.
- Mylona, D. (2008b). *Fish-eating in Greece from the fifth century BC to the seventh century AD. A story of impoverished fishermen or luxurious fish banquets?* Archaeopress.
- Mylona, D. (2010). Mesolithic Fishers at Maroulas kythnos. The fish bones. The Prehistory of the island of Kythnos (Cyclades, Greece) and the Mesolithic settlement at Maroulas, 151-162.
- Mylona, D. (2011) in Sampson, A. (ed.). 2011. *The Cave of the Cyclops: Mesolithic and Neolithic Networks in the Northern Aegean, Greece. Volume II: Bone Tool Industries, Dietary Resources and the Paleoenvironment, and Archeometrical Studies, Prehistory Monographs*, vol. 31, INSTAP Academic Press, Philadelphia, 237-266.
- Piques, G. (2020). *Etude de l'ichtyofaune : déchets de préparation de thons et autres restes de poissons*. In Richier (ed.), *Avant le port de la Joliette, Le Castel, 22 rue Jean-François Leca, Marseille*, Rapport final d'opération de fouille archéologique, INRAP Midi-Méditerranée, SRA PACA, 448-452.
- Powell, J. (2011). Non-vertebral fish bones. In A. Sampson (Ed.), *The cave of Cyclops. Mesolithic and Neolithic networks in the Northern Aegean, Greece, vol. II. Bone tool industry, dietary resources and the paleoenvironment, and archaeometrical studies/ Prehistory Monographs 31*, 151-236, Philadelphia: INSTAP Academic Press. <https://doi.org/10.2307/j.ctt3fgwb5.9>
- Rainsford, C., O'Connor, T. and Miracle, P. (2014). Fishing in the Adriatic at the Mesolithic–Neolithic transition: Evidence from Vela Spila, Croatia. *Environmental Archaeology*, 19(3), 311-320.
- Rose, M. (1995). Fishing at Franchthi Cave, Greece: Changing Environments and Patterns of Exploitation. *Old World Archaeology Newsletter* 18, 21-26
- Rose, M. (2000). *The fish remains*. In Shaw, J.W. and Shaw, M.C. (eds). *Kommos IV. The Greek sanctuary*. Princeton: Princeton University Press, 495-560.
- Roselló-Izquierdo, E. & Morales-Muñiz, A. (1990). La ictiofauna del yacimiento tartésico de la calle del Puerto, número 10 (Huelva): consideraciones generales. *Espacio, Tiempo y Forma, S. I, Prehist. y Arqueol.*, t. 3, 1990, 291-298
- Roselló-Izquierdo, E., Morales-Muñiz, A. and Carmen Morales-Muñiz, D., 1994. La Cartuja/Spain: anthropogenic ichthyocenosis of culinary nature in a paleocultural context. *Offa*, 51, 323-331.
- Roselló-Izquierdo, E., and Morales-Muñiz, A. (1994). The Fishes. In Castillo de Doña Blanca: Archaeoenvironmental Investigations in the Bay of Cadiz, Spain (750–500 BC), edited by E. Roselló-Izquierdo and A. Morales-Muñiz, pp. 91–142. BAR International Series 593. *British Archaeological Reports*, Oxford.
- Roselló-Izquierdo, E. Llorente-Rodríguez, L., & Morales-Muñiz, A. (2015). The fishes from Cova Fosca (Castellón, Spain): Lost signatures of a hunter gatherer tradition? *CuPAUAM* 41, 87-96.
- Roselló-Izquierdo, E. & Morales-Muñiz, A. (2018). *Vertebrados de las factorías de la calle San Nicolás y reflexiones zoológicas sobre las factorías romanas de salazones*. In Bernal-Casasola, D. and Jiménez-Camino Álvarez, R., 2018. *Las cetariae de Ivlia Tradvcta. Resultados de las excavaciones arqueológicas en la calle San Nicolás de Algeciras (2001-2006)*, 279-286.
- Ruscillo, D. (1993). Faunal remains from the Akropolis site, Mytilene. *Echoes du Monde Classique*, 37, 201-210.
- Sáenz-Arroyo, A., Roberts, C.M., Torre, J., Cariño-Olvera, M. and Hawkins, J.P. (2006). The value of evidence about past abundance: marine fauna of the Gulf of California through the eyes of 16th to 19th century travellers. *Fish and Fisheries*, 7(2), 128-146.
- Sáez Romero, A.M., Sáez Espligares, A., Ramon Torres, J., Muñoz Vicente, Á. (2004). *Paleo contenido de ánfora púnica (tipo Ramon T-11.2.1.3)*. In *Garum y salazones en el Círculo del Estrecho. Catálogo de la Exposición (Algeciras)*, Granada, 252-253.
- Sáez Romero, A. M. & Theodoropoulou, T. In press. *Salting and consuming fish in the Classical Mediterranean. A review of the archaeological evidence from the Punic Amphora Building (Corinth, Greece)*, in D. Bernal-Casasola, M. Bonifay & A. Pecci (eds), *Roman amphorae contents: reflecting on maritime trade of food stuffs in antiquity*, Proceedings of the RAC International Interactive Conference, Cadiz Spain, 5-7 October 2015, Roman and Late Antique Mediterranean Pottery International Series, Archaeopress, Oxford.
- Sternberg, M. (1998). Les produits de la pêche et la modification des structures halieutiques en Gaule Narbonnaise du IIIe siècle av. J.-C. au Ier siècle ap. J.-C. Les données de Lattes (Hérault), Marseille (Bouches-du-Rhône) et Olbia-de-Provence (Var). *Mélanges de l'école française de Rome*, 110(1), 81-109.

Särilvik, I. (1976). Fornlämning 72 och 116, stenåldersboplats, Gröninge, Tölö sn, Halland. Vol. 9. *Riksantikvarieämbetet Rapport 1976 B*, Stockholm.

Theodoropoulou, T. (2019). Fishing together, fishing on its own: Fish exploitation patterns at the Neolithic Alepotrypa cave (Diros, Greece) and Aegean prehistoric fishing traditions. *International Journal of Osteoarchaeology*, 29(3), 395-406.

Trakadas, A. (2018). In *Mauretaniae maritimas*: marine resource exploitation in a Roman North African province. Geographica Historica series. Franz Steiner Verlag: Stuttgart.

Van Neer, W. and Wouters, W. (2009). *Fish remains from the Bir Messaouda excavations 2000/2001 and other Carthaginian settlement contexts*. 65-74.

von den Driesch, A. (1980). Osteoarchäologische Auswertung von Garum-Resten des Cerro del Mar, Madrider Mitteilungen 21, 151-154.

von den Driesch, A. & Boessneck, J. (1984). Vorläufiger Bericht über die Untersuchungen an Tierknochenfunden (Besik Tepe, Grabung 1982). *Archäologischer Anzeiger*, 186-192.

von den Driesch, A. (1987). 'Haus- und Jagdtiere im vorgeschichtlichen Thessalien', *Prähistorische Zeitschrift*, 62, 1-21.

Weinstock, J. (1995). *Some Bone Remains from Carthago, 1991 Excavation Season*. In Buitenhuis, H., & Uerpmann, H.P. (eds.). *Archaeozoology of the near East II* (Leiden 1995), 113-118.

Wilkens, B. and Delussu, F., 2001. Analisi dei resti ossei della tonnara di Pedras de Fogu. *Archeologia Postmedievale*, 5, pp.214-222.

Wilkens, B. (2020). *Fishing in Sardinia, Middle and Modern Ages*, Poster. FRWG 19th Meeting.

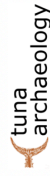
Zabala, C. Soriguer, M., Hernando, J.A. (2011), *Apéndice 2. La fauna marina del yacimiento protohistórico Catedral de Ceuta*. In Villada, F., Ramon, J., Suárez, J. (eds.), *El asentamiento protohistórico de Ceuta*. Indígenas y fenicios en la orilla norteafricana del Estrecho de Gibraltar, Ceuta, 381-419.

Investigate **past fishing impacts and population dynamics to inform the present**

**Resources** for the **Atlantic bluefin tuna research community:**

Access an **updatable database of archaeological bluefin tuna remains**

**Estimate the size of archaeological tuna** using vertebrae



A sub-project of the **MSCA SeaChanges ITN**, initiated by the University of Bologna

**Atlantic bluefin tuna** has been one of the most important resources to Mediterranean civilisations for millennia.

Our aim is to **collate archaeological data** for Atlantic bluefin tuna, and **promote multidisciplinary collaborations** between the fields of archaeology and marine ecology

Latest records:

Maroulas, Kythnos, Greece – 8800-8600 BCE.

Myliona, D.  
In Myliona, 2010

Cape Andreas Kastros, Cyprus – 6000 BCE

Myliona, D.  
In Desse & Desse-Berset, 1994



Contact us:

**Project Supervisor:**  
Prof. Fausto Tinti, University of Bologna: [fausto.tinti@unibo.it](mailto:fausto.tinti@unibo.it)

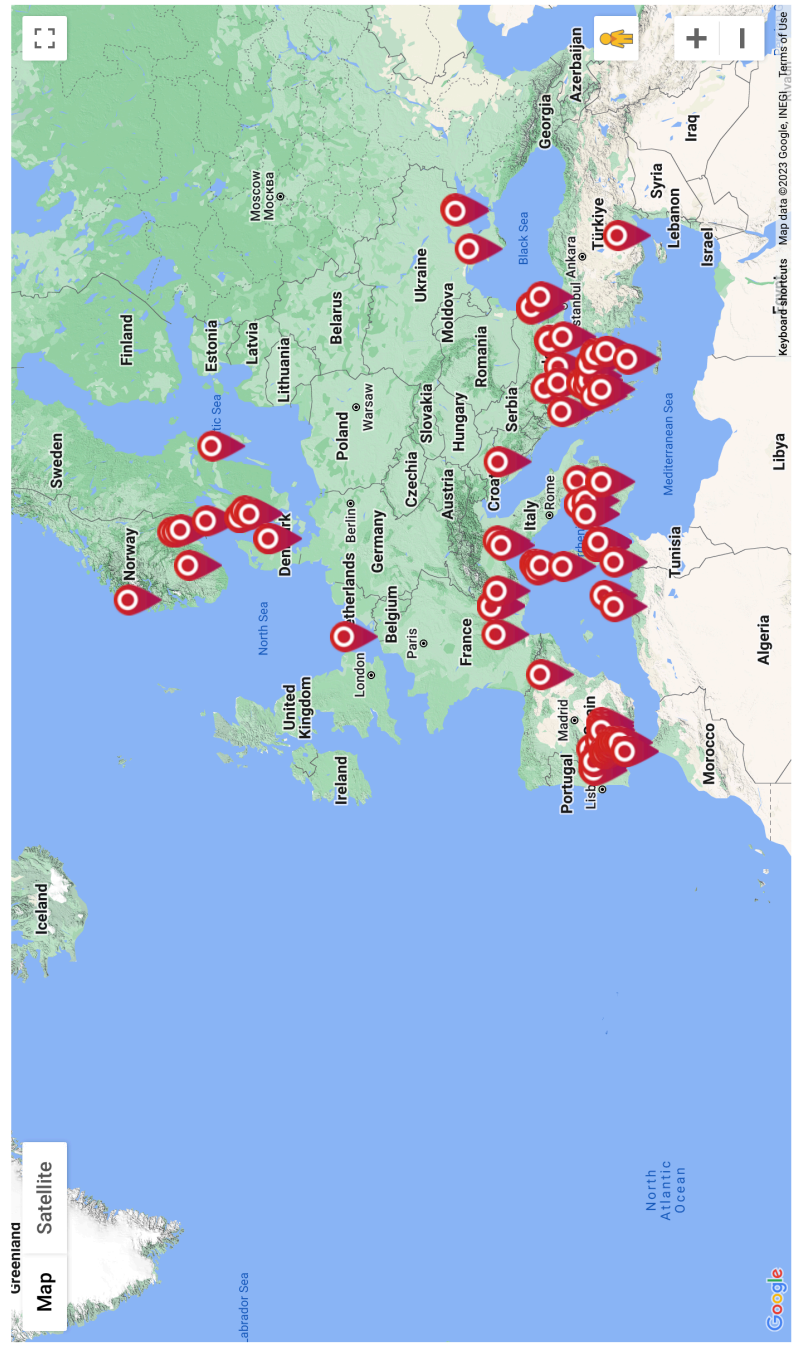
**Researcher & Website Manager:**  
Adam J. Andrews, University of Bologna: [adam@palaeome.org](mailto:adam@palaeome.org)



This project has received funding from the European Union's Horizon 2020 research and innovation programme under the Marie Skłodowska-Curie grant agreement No 813383. The European Research Agency is not responsible for any use that may be made of the information it contains.



We collated archaeological records of Atlantic bluefin tuna (*Thunnus thynnus*) bones and scales from reports in multiple languages including unpublished reports. Please see **Andrews et al. 2022: ICES Journal of Marine Science** for details. Here, the records are mapped. Click on each record for details.





We collated archaeological records of Atlantic bluefin tuna (*Thunnus thynnus*) bones and scales from reports in multiple languages including unpublished reports. Please see **Andrews et al. 2022: ICES Journal of Marine Science** for details.

**Click here** to download the latest version of the database

Show 10 entries

Search:

Source	Collection	Latitude	Longitude	Date	Era	Type	Imported?	NISP	Reference(s)
								Size or TL (cm)	

Svendborg, Denmark	SNM Copenhagen	54.838388	10.597225	140000	Paleolithic	Vertebrae		2	150 Unpublished
Gorham's Cave, Gibraltar	Gibraltar National Museum	36.117572	-5.341995	22000-26000 BCE	Paleolithic	Vertebrae		2	Brown, K., Fa, D.A., Finlayson, G. and Finlayson, C. (2011) Small game and marine resource exploitation by Neanderthals: the evidence from Gibraltar. In Trekkini, the Shore (pp. 247-272). Springer, New York, NY.
Cueva de Nerja, Malaga, Spain	Unknown	36.762194	-3.844262	10000 BCE	Mesolithic	Vertebrae		1	Morales-Muñiz, A., Roselló-Izquierdo, E and Hernández, F. (1998). Late Upper Paleolithic subsisten strategies in souther



Your collaboration is vital to improving the resource for the community.

**Please use the below form to submit records of archaeological tuna remains that will be incorporated into the database.**

If you prefer, submit records in an excel file with column names as per the **database** to: [adam@palaeome.org](mailto:adam@palaeome.org)

**Your name \***

**Your email \***

You will not be contacted unless to clarify data you have submitted. Your email will not be displayed on this website.

**Archaeological site name and country \***

**Site longitude and latitude**

If you can please submit coordinates in decimal format - if you don't know these please try to submit the site name, region and any other indicators of location that might be useful.

**Where are the specimens stored?**

i.e. Museum/institute, Country etc.

**Specimen ID \***

**Specimen type \***

Vertebrae  Scales  Cranial Elements  Multiple, please define in comments





**NISP \***

## **Chapter 2**

Length estimation of Atlantic bluefin tuna (*Thunnus thynnus*)  
using vertebrae  
**(pages 52—80)**

## RESEARCH ARTICLE

# Length estimation of Atlantic bluefin tuna (*Thunnus thynnus*) using vertebrae

Adam J. Andrews<sup>1,2</sup>  | Dimitra Mylona<sup>3</sup> | Lucia Rivera-Charún<sup>4,5</sup>  |  
Rachel Winter<sup>6</sup> | Vedat Onar<sup>7</sup> | Abu B. Siddiq<sup>8</sup>  | Fausto Tinti<sup>1</sup>  |  
Arturo Morales-Muniz<sup>5</sup>

<sup>1</sup>Department of Biological, Geological and Environmental Sciences, University of Bologna, Ravenna, Italy

<sup>2</sup>Department of Cultural Heritage, University of Bologna, Ravenna, Italy

<sup>3</sup>Institute for Aegean Prehistory Study Center for East Crete, Pachia Ammos, Greece

<sup>4</sup>Institute of Marine Research, Spanish National Research Council, Vigo, Spain

<sup>5</sup>Department of Biology, Autonomous University of Madrid, Madrid, Spain

<sup>6</sup>Groningen Institute of Archaeology, University of Groningen, Groningen, Netherlands

<sup>7</sup>Osteoarchaeology Practice and Research Centre and Faculty of Veterinary Medicine, Istanbul University-Cerrahpaşa, Istanbul, Turkey

<sup>8</sup>Department of Anthropology, Mardin Artuklu University, Mardin, Turkey

## Correspondence

Adam J. Andrews and Fausto Tinti,  
Department of Biological, Geological and Environmental Sciences, University of Bologna, Campus of Ravenna, Ravenna, Italy.  
Email: [adam@palaeome.org](mailto:adam@palaeome.org);  
Email: [fausto.tinti@unibo.it](mailto:fausto.tinti@unibo.it)

## Funding information

H2020 Marie Skłodowska-Curie Actions, Grant/Award Number: 813383

## Abstract

Atlantic bluefin tuna (*Thunnus thynnus*; BFT) is a large (up to 3.3 m in length) pelagic predator which has been exploited throughout the eastern Atlantic and Mediterranean since prehistoric times, as attested by its archeological remains. One key insight derivable from these remains is body size, which can indicate past fishing abilities, the impact of fishing, and past migration behavior. Despite this, there exists no reliable method to estimate the size of BFT found in archeological sites. Here, 13 modern *Thunnus* spp. skeletons were studied to provide power regression equations that estimate body length from vertebra dimensions. In modern specimens, the majority of BFT vertebrae can be differentiated by their morphological features, and thus, individual regression equations can be applied for each rank (position in vertebral column). In an archeological context, poor preservation may limit one's ability to identify rank; hence, "types" of vertebrae were defined, which enable length estimates when rank cannot be determined. At least one vertebra dimension, height, width, or length correlated highly with body length when vertebrae were ranked ( $R^2 > 0.97$ ) or identified to types ( $R^2 > 0.98$ ). Whether using rank or type, length estimates appear accurate to approximately  $\pm 10\%$ . Finally, the method was applied to a sample of Roman-era BFT vertebrae to demonstrate its potential. It is acknowledged that further studies with larger sample sizes would provide more precision in BFT length estimates.

## KEYWORDS

Atlantic bluefin tuna, osteometry, size estimation, vertebrae, zooarchaeology

## 1 | INTRODUCTION

Archeological fish remains are vital when investigating the role that fish have played in cultural developments and, conversely, how such developments have impacted fish populations themselves (Colley, 1990; Erlandson & Rick, 2010; Orton, 2016). Studies on fish

remains typically utilize a number of methodologies to do this, for example, recording the location, identity, and number of remains recovered (Colley, 1990; Hoffmann, 2005); analysis of their taphonomy and archeological context (Çakırlar et al., 2016; Prieto, 2021; van Neer et al., 2004); their morphological identification, provenance, and genetics inferred by applications of biomolecular tools (Andrews et al.,

This is an open access article under the terms of the [Creative Commons Attribution](https://creativecommons.org/licenses/by/4.0/) License, which permits use, distribution and reproduction in any medium, provided the original work is properly cited.

© 2022 The Authors. *International Journal of Osteoarchaeology* published by John Wiley & Sons Ltd.

2021, 2022; Orton, 2016; Richter et al., 2011; Winter et al., 2021); and the estimation of fish size from measurements on fish remains (Casteel, 1976; Desse et al., 1989; Wheeler & Jones, 1989).

Methods to estimate size are particularly useful to identify which fishing methods were used in the past, since different techniques target different sizes of fish (Gabriel et al., 2012; Greenspan, 1998; Owen & Merrick, 1994). It is used to investigate how size classes were distributed spatially (Sanchez, 2020) and to assess exploitation impacts, since a symptom of overfishing is the truncation of size classes (Barrett, 2019; Morales-Muniz & Roselló-Izquierdo, 2007; Plank et al., 2018). Size information can also be useful in biomolecular studies since biochemical compounds, for example, stable isotopes, vary with body size (see Barrett et al., 2011, and references therein). Moreover, size information can be used as an additional species identification criterion and to assess the minimum number of individuals (MNI) recovered in excavations (Orchard, 2005). The need for archeological size metrics to inform present-day sustainability is particularly important for one key species, Atlantic bluefin tuna (*Thunnus thynnus*, hereafter BFT), since it appears to have had a long and intense history of exploitation yet the impact on the population is unknown (Andrews et al., 2022). Despite much interest in BFT archeology (Felici, 2018; García Vargas et al., 2018; Mylona, 2021; Nielsen & Persson, 2020), there are currently no reliable methods to estimate BFT size from archeological remains. Here, a method is developed to estimate BFT straight fork length (hereafter FL) from measurements of isolated (and sometimes poorly preserved) vertebrae recovered in archeological excavations.

Size estimations on archeological fish bones are achieved by comparing their measurements to those of reference specimens of known lengths or weights (Casteel, 1976; Desse et al., 1989; Wheeler & Jones, 1989). Cranial elements are sometimes used as the reference of choice because these are readily identified and produce good estimations of body size (Desse & Desse-Berset, 1996; Jiménez-Cano & Masson, 2016; Thieren & van Neer, 2016). Given the rarity with which BFT cranial elements are recovered in archeological contexts (Andrews et al., 2022), vertebrae—a robust and well-preserved element—were chosen as an alternative. Size estimations have been seldom applied to BFT, namely, by Rose (1994), who developed a coarse method of estimating length from a single vertebra (also applied by Mylona, 2018, and Morales-Muniz & Roselló-Izquierdo, 2007, who developed a precursor to the current study). Development of a reliable BFT size estimation tool in these studies has been precluded by a difficulty in obtaining numerous modern reference specimens of known lengths or weights because large adult BFT are expensive and challenging to process. Studies of this type, on any fish species, face two further challenges: (a) how to identify isolated vertebrae found in archeological excavations and assign them to rank (i.e., position in the vertebral column) and (b) how to select the best statistical model of estimation suited to fish growth and account for variation observed within this model.

Taphonomic damage sometimes makes it difficult to establish vertebra rank in archeological specimens (Lambrides & Weisler, 2015; Sinha et al., 2019). Due to size variation throughout the vertebral column in fishes, length estimates will be less accurate if rank cannot be

determined. As an alternative, it is possible estimate length using sections of similar vertebrae, herein called types. One way to discover types is to study which vertebrae are morphologically similar and assess whether these similarities would hold true in an archeological context. Another is to apply the Global Rachidian Profiles (GRP) method (sensu Desse et al., 1989) that identifies which sections of the vertebral column contain vertebrae that do not differ greatly in size (Lambrides & Weisler, 2015; Lidour et al., 2018; Thieren et al., 2012). Regardless of the method used, it is necessary to measure the variation between vertebrae within each type, as this is sometimes too large for meaningful estimates (Jelu et al., 2021). In addition, there is a need to attempt rank or type identification from as much of the vertebral column as possible; otherwise, estimations may be hindered if particular vertebrae are required and not recovered in excavations.

When dealing with vertebrae rank or type, the use of power regression equations has become common in estimating body length, where model fit is often assessed by the coefficient of determination ( $R^2$ ) and standard error values (Gabriel et al., 2012; Jelu et al., 2021; Marrast & Béarez, 2019; Martínez-Polanco & Béarez, 2020; Rurua et al., 2020). Because fish growth is considered allometric, that is, the relationship between body length and vertebrae dimensions is not linear, power regression models are optimal because they account for this (Reitz et al., 1987).

The accuracy of size estimates also needs to be taken into account, because for all fishes, but especially BFT and other tuna (*Thunnus* spp.), intraspecific variation exists in, for example, body length, vertebral length, size-at-age, and in length-weight relationships (Cort, 1989; Perçin & Akyol, 2009; Rodríguez-Marin et al., 2015; Rodríguez-Roda, 1964; Santamaria et al., 2009) because individuals experience varied life histories within a single population or generation (Mather et al., 1995). Therefore, size estimates can be expected to deviate from true values, and this error must be measured and considered when interpreting estimated values.

This study aimed to (1) identify which BFT vertebrae can be identified to rank if found isolated and which “types” of BFT vertebrae exist that can be used to group potentially poorly preserved archeological vertebrae if rank identification is too challenging; (2) develop power regression equations to estimate FL from vertebra measurements and concurrently identify which vertebra dimensions should be selected for estimations; and (3) assess method’s accuracy. As an illustration, a case study is presented, where the method is applied to 59 BFT vertebrae recovered from a second century BCE refuse site Punta Camarinal (near the Roman city of Baelo Claudia, Andalusia, Spain). A guide to identify BFT vertebrae to rank or type was developed to aid length estimations (Appendix S2). An online calculator was also established at <https://tunaarchaeology.org/lengthestimations>, allowing researchers to retrieve length estimates for each vertebra measurement.

## 2 | MATERIALS AND METHODS

Nine BFT vertebral columns were collected from specimens fished or stranded throughout the eastern Atlantic, Mediterranean, and Sea of

Marmara between 1987 and 2020 (Table 1). These were complemented with vertebral columns of two albacore tuna (*Thunnus alalunga*, hereafter ALB) and two bigeye tuna (*Thunnus obesus*, hereafter BET) to better represent intra- and inter-specific variation, as the current study dealt with relatively few reference specimens. BFT specimens comprised a range of growth stages from juveniles to large adults, between 26.5 and 220 cm FL. The ALB and BET fall into this size range with a FL between 45 and 190 cm FL (Table 1).

Morphological features unique to each vertebra were inspected to determine which vertebrae could be identified to rank if found disarticulated. Subsequently, vertebrae that would likely be indistinguishable from each other if damaged due to taphonomic processes were grouped into vertebra types. These identification criteria were illustrated using photographs of vertebrae from one reference specimen and constitute a guide to identify rank and type in BFT which can be found in Appendix S2.

FL was chosen as the preferred measurement of fish size for BFT because it is the most accurate and frequently used length measure in tuna fisheries, more readily enabling comparisons between lengths estimated from archeological remains and modern fishery data. Conversion factors to standard length (SL) and total length (TL) are supplied following published equations (Table S1). A conversion factor for weight is supplied (Table S1), but it is not estimated here because it is highly seasonally variable and estimates would be subject to wide error margins (Cort, 1989; Rodriguez-Marín et al., 2015). Caution should generally be taken when applying length-weight relationships for archeological specimens because fattening rates vary spatially (Cort & Estruch, 2016) and are unknown for the ancient past.

Using digital calipers, the posterior height, posterior width, and length of all 39 vertebrae centra were measured to the nearest 0.01 mm (Figure 1). Exceptions were the first vertebra (V1), where length was not measured since it is fused to the skull in adults, and

the last vertebra (urostyle; V39), where only anterior height and width could be measured. Measurements were sometimes missing hampered by butchery marks. For simplicity, vertebrae are referred to by their rank (i.e., V1 to V39). For the main analysis, the greatest length measurement (comparing left and right side) for each vertebra centrum was used; however, length was recorded on both sides of vertebrae in specimen V8 to assess its variation. Anterior height and width were also measured in specimen V8 to assess variation compared with the posterior dimensions.

When deciding on a regression model to use, linear and logarithmic models were considered (see Lernau & Ben-Horin, 2016, but these did not provide satisfactory fits (data not shown). Since BFT length relationships appear to follow allometric growth patterns (Santamaria et al., 2009), the power regression approach was adopted herein, which provided more appreciable results. Power regression equations for each vertebrae rank and type were defined using measurements from all 13 *Thunnus* spp. specimens and the core function ( $lm$  [formula =  $\log(\text{response variable}) \sim \log(\text{predictor variable})$ ]) in R (Team RC, 2013), applied to each dimension separately. Standard deviation (SD) observed in height, width, and length across vertebrae within each type was assessed by calculating the standard deviation between vertebrae of each specimen before averaging across specimens. The best model fit for each vertebral rank and type was judged according to the vertebral measurement with the highest coefficient of determination ( $R^2$ ) and lowest residual standard error (RSE) values. Where SD between vertebrae measurements was high for the model of best fit identified using  $R^2$  and RSE, the dimension with the highest  $R^2$  value and lowest SD combination was selected as the best model.

There was a need to understand the error associated with estimates produced by our method, because this would give some indication of how reliable inferences might be based on them. Therefore, prediction accuracy for each of the best scoring models was tested by

**TABLE 1** Modern reference specimens of Atlantic bluefin tuna (*Thunnus thynnus*; BFT), albacore tuna (*Thunnus alalunga*; ALB), and bigeye tuna (*Thunnus obesus*; BET) used to produce length estimate equations

	Species	Catch date	Origin	Sex	FL (cm)	TL (cm)	Weight (kg)
1	BFT	1987	Torre Vieja, Spain	-	26.5	32.5	-
2	ALB	1988	Gijón, Spain	-	54	59	-
3	ALB	2006	Gijón, Spain	M	85	91	-
4	BFT	2010	Istanbul, Turkey	-	113	-	-
5	BFT	2015	Istanbul, Turkey	-	120	-	-
6	BET	2020	Barbate, Spain	-	122	135	38
7	BFT	1988	Huelva, Spain	-	124	130	-
8	BFT	2020	Fano, Italy	-	130	137	-
9	BFT	2015	Istanbul, Turkey	-	170	-	90
10	BET	2001	Gijón, Spain	M	190	-	138
11	BFT	2015	Barbate, Spain	M	200	208	190
12	BFT	2012	Chryssi Island, Crete, Greece	-	212	-	-
13	BFT	1993	Southern Crete, Greece	F	220	232	200

Note: Origin refers to the location each specimen was landed or stranded (in the case of specimen 12).

Abbreviations: F, female; FL, straight fork length; M, male; TL, total length; -, not available.

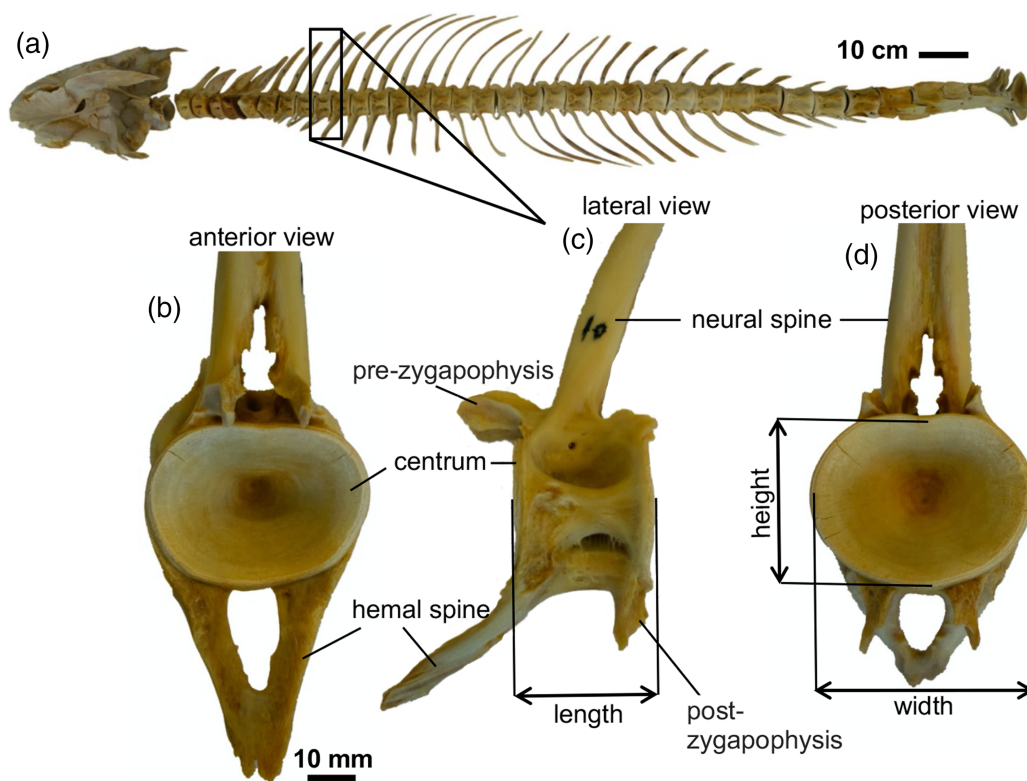


**FIGURE 1** (a) Lateral view of a complete 200 cm straight fork length (FL) Atlantic bluefin tuna (*Thunnus thynnus*) skull and vertebral column showing all 39 vertebrae. V10 is shown as an example to illustrate anatomical features and measurements in (b) anterior view, (c) lateral view, and (d) posterior view. The scales (black bars) are approximations only [Colour figure can be viewed at [wileyonlinelibrary.com](https://onlinelibrary.wiley.com/doi/10.1002/for.3092)]

comparing predicted values to reference values for each specimen using the statistical model with the greatest  $R^2$  for each vertebrae rank and type. For each type, measurements were taken at random from one of the vertebrae, for each specimen.

Interspecific variation was inspected visually within types by projecting ALB and BET measurements onto a BFT power regression line fit for the vertebrae measurement with the greatest  $R^2$  within each type by using *stat\_smooth* (*method = nls*, *formula = y ~ a\*x^b*) in the *ggplot2* package (Wickham, 2011) in R. Independent *t* tests were performed in R to test for differences between the left- versus right-sided centrum length measurements and anterior versus posterior centrum height and width measurements.

### 3 | RESULTS

All except 4 or 5 (V19–22/23) of 39 BFT reference vertebrae could be distinguished by their morphological features (Appendix S2). The discrepancy at V19–V22/23 was caused by a transverse foramen on V23 not being consistently present among all specimens. Nonetheless, our observations suggest that when spines are excessively damaged by taphonomic processes, it will be too challenging to identify vertebral rank in most BFT vertebrae, except V1 and V36–39, which are especially unique (Appendix S2). We described six vertebral types

which can be differentiated from each other by morphological features (Appendix S1, Table S3). Note that V23, V30, and V31 are present in multiple types because they sometimes exhibit a transverse foramen (see Appendix S2 details on which to select). Differences in standard deviation were found between measurements on vertebrae grouped into types. This should influence decisions on which measurement should be selected for size reconstructions so that error can be minimized when using types. Variation between vertebral measurements within types was generally acceptable at  $\leq 5\%$  but was higher in the vertebrae type V33–35 (Table S3). Though, it is likely researchers can identify rank for V33–35 in most cases due to their distinctive morphological features (Appendix S2).

Power regression models for vertebrae identifiable to rank and each of the types reliably described the data where  $R^2$  values  $>0.98$  and  $>0.97$  were reported, respectively (Tables S2 and S3). RSE correlated with  $R^2$  values in all cases. Variations in model fit for each vertebrae rank or type were evident between vertebrae dimensions, though for each vertebral rank or type at least one high scoring model ( $>0.97$ ) was identified (Tables S2 and S3).

Estimated FL values calculated using the reference dataset deviated from their true reference FL value at a mean range between  $-9.6\%$  and  $6.8\%$  across ranked vertebrae in reference specimens  $>30$  cm. Estimations on the single BFT reference specimen  $<30$  cm deviated to a greater extent (range 2.3% to 21.4%). A

similar pattern was observed for types across all individuals >30 cm (mean range -7.0% to 3.2%) and for the <30 cm BFT (range -10.5% to 18.8%) (Figure 2). There was no correlation between deviation and vertebra type nor notable difference in deviation between reference and predicted values for each *Thunnus* species (Table 1; Figure 2).

Vertebral measurements of BET and ALB fit the BFT power regression line well for each type, falling within the variation observed between BFT reference specimens (Figure S1). Differences between posterior and anterior height were not significant ( $p = 0.676$ ,  $t[65] = 0.421$ ), but percentage differences were greater in some vertebrae than others (V6-32: mean 0.9%, range -0.1% to 3.7%, V2-3 and V33-36: range -14.3% to 0.1%). No significant differences were observed between posterior and anterior width ( $p = 0.799$ ,  $t[65] = 0.256$ ), but again, percentage differences were greater in some vertebrae than others (V6-32: mean 0.4%, range -4.8% to 4.1%, V2-3 and V33-36: range -11.1% to 11.0%). No significant differences were found between length measurements on the left and right side

of vertebrae centra ( $p = 0.859$ ,  $t[66] = 0.179$ ), and percentage differences were small (mean 0.88%, range 0.2% to 3.6%).

## 4 | DISCUSSION

In theory, all except four or five (i.e., V19-22/23) BFT vertebrae can be identified to rank. However, our observations suggest that in an archeological context, poor preservation will hinder rank identification. Poorly preserved vertebrae could, however, be identified to type, and in some cases, for example, V1 and V36-39, types should not be needed when vertebrae are especially unique (Appendix S2). It is important for researchers to be able to utilize all vertebrae for BFT size estimations since recoveries of BFT vertebrae are usually few, articulated vertebrae are rare, and recovered BFT vertebrae often vary significantly in rank depending upon their archeological context (Andrews et al., 2022). Seldom can all vertebrae be used for archeological size estimations of fishes. One good example is another large

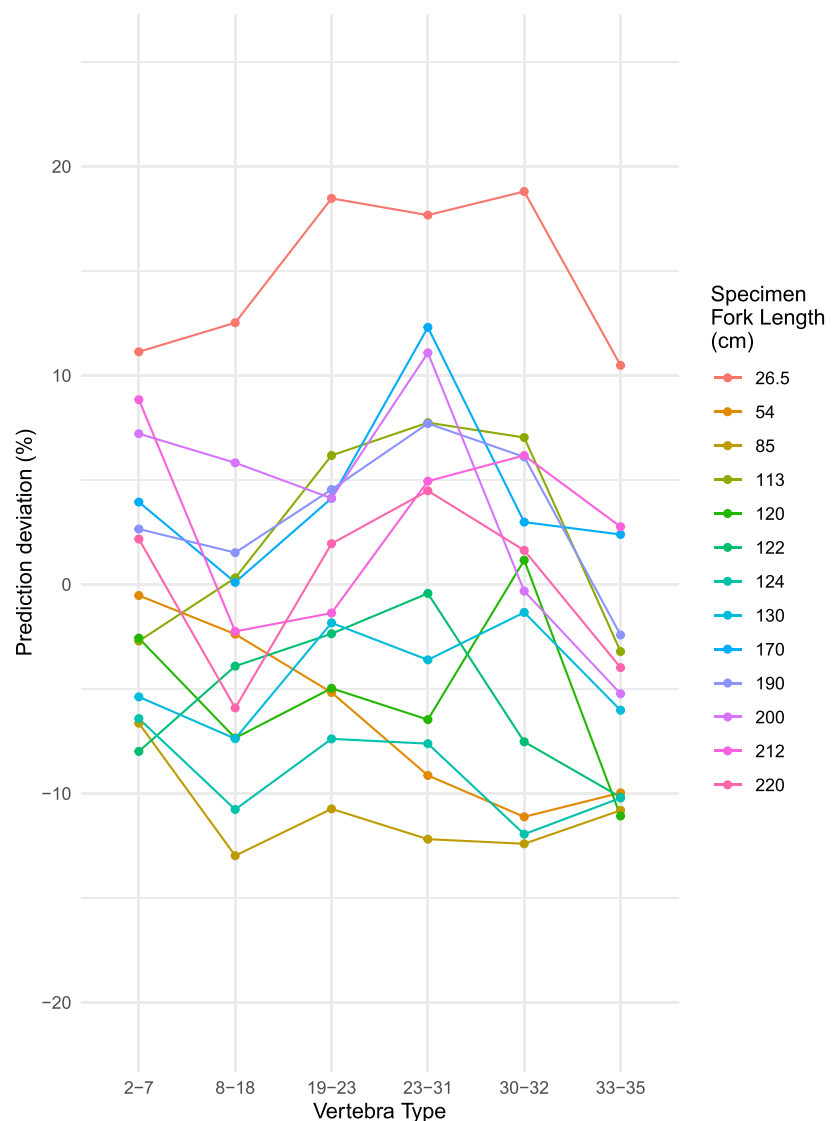


**FIGURE 2** Deviation between the estimated and true reference straight fork length (cm) values for each reference specimen, using types. The best performing model was applied to each type as judged from Table S2 [Colour figure can be viewed at [wileyonlinelibrary.com](https://onlinelibrary.wiley.com)]



species, meager (*Argyrosomus regius*; Gabriel et al., 2012). Studies on the majority of other fishes must necessarily use particular vertebrae or sections of vertebral columns (Jelu et al., 2021; Marrast & Béarez, 2019; Martínez-Polanco & Béarez, 2020; Rurua et al., 2020). Clearly, the extent to which researchers will be able to identify rank or type in BFT will depend on the preservation of vertebrae. Despite obvious challenges, our methods account for the degree of taphonomic damage expected in the majority of archeological BFT recovered (as summarized in Andrews et al., 2022). Moreover, if vertebrae cannot be identified into one of the types described here, their size ought not to be estimated since vertebrae centra are thus likely too damaged for accurate measurements.

To understand how reliable our method is, and thus how readily interpretations can be drawn from these size estimations, it would be useful to compare the accuracy of our equations with those published. Since the majority of studies have not reported prediction error, that is, difference between actual and predicted values (sometimes called back-calculations), it is challenging to do this. Some studies (e.g., Desse & Desse-Berset, 1996; Jelu et al., 2021; Lidour et al., 2018) have only reported  $R^2$  values, to which our  $R^2$  values of  $>0.97$  and  $>0.98$  compare favorably. Others (Gabriel et al., 2012; Marrast & Béarez, 2019; Martínez-Polanco & Béarez, 2020; Rurua et al., 2020; Thieren et al., 2012) report standard error of estimate (SEE) values without defining how they are calculated, which limits comparisons with our RSE values. In any case,  $R^2$  and standard error values are prone to be skewed if sampling is uneven across a given size range and if error is not normally distributed.

Similar to the current study, Thieren et al. (2012) calculated prediction error, reporting that the majority of their best-fitting equations for each element estimated fish length to an error of  $\leq 10\%$  for  $\sim 80\%$  of reference specimens, which is congruent with our findings for BFT. Such levels of variation are expected in BFT. Even early biological studies (e.g., Rodríguez-Roda, 1964) noted this when comparing V35 radius with FL. Our estimates showed that no one element, dimension, or section of the vertebral column is free from this potential source of bias. Moreover, as Lernau (2016) states, archeological size estimations are approximations only, and error margins of at least 10% can be expected. This degree of error will limit some studies interested in detecting fine-scale differences, but assuming this is a component of all archeological estimation methods, it has not limited studies in estimating gear types and target sizes (Blevis et al., 2021; Gabriel et al., 2012; Greenspan, 1998; Lernau, 2016; Owen & Merrick, 1994), how size cohorts were distributed spatially (Sanchez, 2020), or potential shifts in size structure over time (Barrett, 2019; Maschner et al., 2008; Plank et al., 2018). Our results suggest that interspecific variation (differences between *Thunnus* species) in vertebra-FL relationships is small. It might therefore be possible for future studies to apply our methods to suspected BET and ALB, which is useful since their distributions overlap with BFT (Pérez Bielsa et al., 2021), and morphologically, their vertebrae are indistinguishable.

It is acknowledged that using such few reference specimens (compared to usually around 20–70 individuals in other species; Jelu

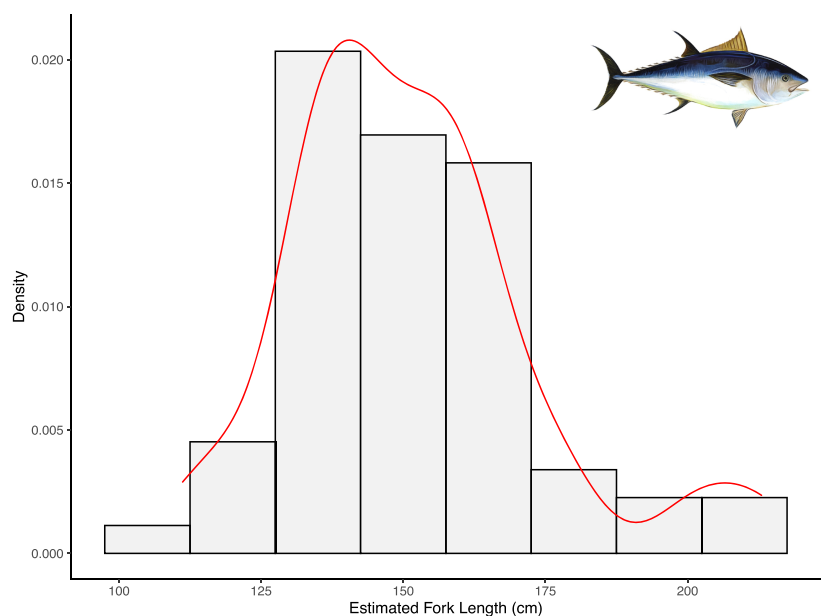
et al., 2021; Marrast & Béarez, 2019; Thieren et al., 2012) may underestimate error in the current study. It is possible that the full extent of intraspecific variation might not have been observed and, therefore, caution should be taken in that the prediction error observed herein should be interpreted as an absolute minimum upon which further studies with greater sample sizes should elaborate on. However, because our reference specimens originated from different locations and years, including a range of sizes, and sister-species, a good degree of intraspecific variation is probably present in our reference dataset (see Gabriel et al., 2012). The need to extrapolate from the BFT regression models might be an issue (Lernau & Ben-Horin, 2016), despite that reference specimens covered a wide size range (26.5–220 cm FL), large BFT reference specimens were missing. BFT of  $\sim 300$  cm might be occasionally recovered in archeological assemblages, and these would fall outside of the regression, which may affect the accuracy of estimations on very large specimens. In any case, a 10% error margin should be applied for all estimations  $>50$  cm FL produced using these equations. Applying this error to very large specimens especially may provide more confidence in extrapolated estimates. According to our prediction accuracy, this error margin should be increased to 20% for BFT estimated  $<50$  cm FL using our methods. Nonetheless, the proportion of this juvenile size class is expected to be small since BFT are  $\sim 50$  cm FL at age 2 (Santamaria et al., 2009), and historical fishing was likely to have targeted spawning migrations (García Vargas & Florido del Corral, 2010).

It is cautioned that despite not being significant, if the anterior surface (instead of posterior) vertebral measurements, or the shorter side (instead of the longer side) of vertebral length measurements are used, estimation accuracy is expected to decrease. This applies also if one of the poorer scoring models for each vertebrae rank or type is used. This error is notwithstanding user error and biases from using archeological bones that, even in the best cases of preservation, will be damaged and likely affect the accuracy of measurements.

## 5 | APPLICATION OF THE METHOD IN THE FIELD: A CASE STUDY

Fifty-nine BFT vertebrae recovered from a second century BCE layer at Punta Camarinal, Andalusia, Spain, were studied to estimate length. Punta Camarinal is a refuse dump (midden) site at the rear of a beach adjacent to the Roman-era city and salting factories of Baelo Claudia (González et al., 2006; Morales-Muniz & Roselló-Izquierdo, 2007). This site is unique in being one of the few BFT midden sites located to date. This is important because large BFT are seldom recovered in settlements and salting factories where most excavations have focused on, probably because processing was more practical at the shore (Andrews et al., 2022). Midden sites might therefore provide a more representative sample of BFT fishing in any given region or period. Punta Camarinal is one of many sites in the key location of the Strait of Gibraltar where the spawning (and return) migrations of BFT can be intercepted annually between April and October. At this location and period, fishing for BFT is theorized to have been conducted

**FIGURE 3** Density curve and histogram of estimated FL (cm) for 59 archeological BFT vertebrae recovered from a second century BCE layer at Punta Camarinal, Baelo Claudia (Andalusia, Spain). Each histogram size class is 15 cm wide [Colour figure can be viewed at [wileyonlinelibrary.com](https://onlinelibrary.wiley.com/doi/10.1002/oa.3092)]



by nets, specifically the *Almadra de tiro* (beach seine tuna trap) method (García Vargas & Florido del Corral, 2010).

Morphological features were studied for each of the vertebrae following Appendix S2. Vertebrae were measured as depicted in Section 2 and Figure 1. The vertebrae recovered from the second century BCE context of Punta Camarinal were estimated to represent BFT between 111 and 213 cm FL, with most specimens at ~150 cm FL (Table S4; Figure 3). Vertebrae were well preserved and could be identified to rank in 55 out of 59 cases. In four cases, types were required to perform the estimations. Preservation was also sufficient that the vertebral dimension with the best power model fit could be applied to all but two of the vertebrae.

The length estimates suggest that Roman-era fisheries at Punta Camarinal would have mainly targeted mature (age ~4+) BFT migrating to and from Mediterranean spawning sites. As is the case with other schooling fishes, BFT associate with fish of equal size when migrating (Mather et al., 1995). Those recorded here reflect several cohorts, which evidence fishing in several different episodes. This might suggest that fixed *Almadras* (weighted to the seabed) were used to capture the various cohorts, as is suspected but not currently shown for the Roman era (Andrews et al., 2022; García Vargas & Florido del Corral, 2010). This hints at a more complex fishing scenario than hitherto postulated, an issue in need of further exploration (Morales-Muniz & Roselló-Izquierdo, 2007).

## 6 | CONCLUSION

BFT historical size data have utility to inform on a variety of ecological and anthropological research questions. Archeological BFT vertebrae can be readily identified to type, but rank identifications might prove challenging. In any case, regression equations were defined for each BFT type and rank. The regression models appear to estimate fork

length within error ranges of approximately  $\pm 10\%$ , in line with expectations for archeological size estimations. This method can be readily applied by researchers with little experience, according to its simplicity, which is aided by the supporting information (Appendix S2) and online calculator. It is acknowledged that in cases where vertebrae are excessively damaged, even type identifications might not be achieved and that the reliability of the methods might be improved by further studies with larger reference sample sizes.

## ACKNOWLEDGMENTS

Antonio Di Natale is thanked for his advice on modern length-weight metrics, as is Corrado Piccinetti for the acquisition of one of the reference specimens. We are grateful for the comments of three anonymous reviewers, which improved the quality of this manuscript. This work is a contribution to the MSCA SeaChanges ITN and was funded by EU Horizon 2020 (H2020 Marie Skłodowska-Curie Actions, Grant Number: 813383). Open Access Funding provided by Università degli Studi di Bologna within the CRUI-CARE Agreement. [Correction added on 25 May 2022, after first online publication: CRUI funding statement has been added.]

## CONFLICT OF INTEREST


No conflict of interest exists related the funding of this work.

## DATA AVAILABILITY STATEMENT

Raw reference measurement data are uploaded as supporting information.

## ORCID

Adam J. Andrews  <https://orcid.org/0000-0002-9000-6523>

Lucia Rivera-Charún  <https://orcid.org/0000-0002-3507-0039>

Abu B. Siddiq  <https://orcid.org/0000-0001-5838-2695>

Fausto Tinti  <https://orcid.org/0000-0002-8649-5387>

## REFERENCES

- Andrews, A. J., Di Natale, A., Bernal-Casasola, D., Aniceti, V., Onar, V., Oueslati, T., Theodoropoulou, T., Morales-Muñiz, A., Cilli, E., & Tinti, F. (2022). Exploitation history of Atlantic bluefin tuna in the eastern Atlantic and Mediterranean—insights from ancient bones. *ICES Journal of Marine Science*. <https://doi.org/10.1093/icesjms/fsab261>
- Andrews, A. J., Puncher, G. N., Bernal-Casasola, D., Di Natale, A., Massari, F., Onar, V., Toker, N., Hanke, A., Pavey, S. A., Savojardo, C., Martelli, P. L., Casadio, R., Cilli, E., Morales-Muñiz, A., Mantovani, B., Tinti, F., & Cariani, A. (2021). Ancient DNA SNP-panel data suggests stability in bluefin tuna genetic diversity despite centuries of fluctuating catches in the eastern Atlantic and Mediterranean. *Scientific Reports*, 11, 20744. <https://doi.org/10.1038/s41598-021-99708-9>
- Barrett, J. H. (2019). An environmental (pre)history of European fishing: Past and future archaeological contributions to sustainable fisheries. *Journal of Fish Biology*, 94, 1033–1044. <https://doi.org/10.1111/jfb.13929>
- Barrett, J. H., Orton, D., Johnstone, C., Harland, J., van Neer, W., Eryvnyck, A., Roberts, C., Locker, A., Amundsen, C., Enghoff, I. B., Hamilton-Dyer, S., Heinrich, D., Hufthammer, A. K., Jones, A. K. G., Jonsson, L., Makowiecki, D., Pope, P., O'Connell, T. C., de Roo, T., & Richards, M. (2011). Interpreting the expansion of sea fishing in medieval Europe using stable isotope analysis of archaeological cod bones. *Journal of Archaeological Science*, 38, 1516–1524. <https://doi.org/10.1016/j.jas.2011.02.017>
- Blevis, R., Bar-Oz, G., Tepper, Y., & Zohar, I. (2021). Fish in the desert: Identifying fish trade routes and the role of Red Sea parrotfish (Scaridae) during the byzantine and early Islamic periods. *Journal of Archaeological Science: Reports*, 36, 102808. <https://doi.org/10.1016/j.jasrep.2021.102808>
- Çakırlar, C., Ikram, S., & Gates, M.-H. (2016). New evidence for fish processing in the ancient eastern Mediterranean: Formalised Epinephelus butchery in fifth century BC Kinet Höyük, Turkey. *International Journal of Osteoarchaeology*, 26, 3–16. <https://doi.org/10.1002/oa.2388>
- Casteel, R. W. (1976). *Fish remains in archaeology and Palaeoenvironmental studies*. Academic Press.
- Colley, S. M. (1990). The analysis and interpretation of archaeological fish remains. *Archaeological Method and Theory*, 2, 207–253. <http://www.jstor.org/stable/20170208>
- Cort, J. L. (1989). *Biología y pesca del atún rojo, Thunnus thynnus (L.), del Mar Cantábrico*. Universidad Complutense de Madrid.
- Cort, J. L., & Estruch, V. D. (2016). Analysis of the length-weight relationships for the Western Atlantic bluefin tuna, *Thunnus thynnus* (L.). *Reviews in Fisheries Science & Aquaculture*, 24, 126–135. <https://doi.org/10.1080/23308249.2015.1112359>
- Desse, J., & Desse-Berset, N. (1996). Archaeozoology of groupers (Epinephelinae). Identification, osteometry and keys to interpretation. *Archaeofauna*, 5, 121–127.
- Desse, J., Desse-Berset, N., & Rocheteau, M. (1989). Les profils rachidiens globaux. Reconstitution de la taille des poissons et appréciation du nombre minimal d'individus à partir des pièces rachidiennes. *Revue de Paléobiologie*, 8, 89–94. [https://horizon.documentation.ird.fr/exl-doc/pleins\\_textes/pleins\\_textes\\_6/colloques1/35934.pdf](https://horizon.documentation.ird.fr/exl-doc/pleins_textes/pleins_textes_6/colloques1/35934.pdf)
- Erlandson, J. M., & Rick, T. C. (2010). Archaeology meets marine ecology: The antiquity of maritime cultures and human impacts on marine fisheries and ecosystems. *Annual Review of Marine Science*, 2, 231–251. <https://doi.org/10.1146/annurev.marine.010908.163749>
- Felici, E. (2018). *Thynnos: Archeologia Della Tonnara Mediterranea*. Edipuglia. <https://doi.org/10.4475/872>
- Gabriel, S., Prista, N., & Costa, M. J. (2012). Estimating meagre (*Argyrosomus regius*) size from otoliths and vertebrae. *Journal of Archaeological Science*, 39, 2859–2865. <https://doi.org/10.1016/j.jas.2012.04.046>
- García Vargas, E., & Florido del Corral, D. (2010). The origin and development of tuna fishing nets (*Almadrabas*). In T. Bekker-Nielsen & D. B. Casasola (Eds.), *Ancient nets and fishing gear: Proceedings of the international workshop on 'Nets and Fishing Gear in Classical Antiquity: A First Approach'*, Cádiz, November 15–17, 2007 (pp. 205–227). Servicio de Publicaciones de la Universidad de Cádiz Aarhus University Press.
- García Vargas, E., Roselló-Izquierdo, E. R., Casasola, D. B., Morales-Muniz, A. M., Izquierdo, E. R., Casasola, D. B., & Muñiz, A. M. (2018). Salazones y salsas de pescado en Antigüedad: un primer acercamiento a las evidencias de paleocontenidos y depósitos primarios en el ámbito euro-Mediterráneo. In D. B. Casasola & R. J.-C. Álvarez (Eds.), *Las cetariae de Iulia Traducta Resultados de Las Excavaciones Arqueológicas en la Calle San Nicolás de Algeciras (2001–2006)* (pp. 287–312). Editorial UCA.
- González, A. A., Casasola, D. B., & Martínez, L. L. (2006). La explotación de recursos marinos en época Romano-Republicana. Resultados de la actuación arqueológica en Punta Camarinal-El Anclón (Bolonia, Tarifa, Cádiz). *Almoraima: Revista de Estudios campogibraltareños*, 33, 221–234. <https://institutoecg.es/wp-content/uploads/2019/03/Almoraima33-221-233.pdf>
- Greenspan, R. L. (1998). Gear selectivity models, mortality profiles and the interpretation of archaeological fish remains: A case study from the Harney Basin, Oregon. *Journal of Archaeological Science*, 25, 973–984. <https://doi.org/10.1006/jasc.1998.0276>
- Hoffmann, R. C. (2005). A brief history of aquatic resource use in Medieval Europe. *Helgoland Marine Research*, 59, 22–30. <https://doi.org/10.1007/s10152-004-0203-5>
- Jelu, I., Wouters, W., & Van Neer, W. (2021). The use of vertebral measurements for body length and weight reconstruction of pike (*Esox lucius*) from archaeological sites. *Archaeological and Anthropological Sciences*, 13(5), 72–81. <https://doi.org/10.1007/s12520-021-01325-0>
- Jiménez-Cano, N. G., & Masson, M. A. (2016). Estimation of fish size from archaeological bones of hardhead catfishes (*Ariopsis felis*): Assessing pre-Hispanic fish acquisition of two Mayan sites. *Journal of Archaeological Science: Reports*, 8, 116–120. <https://doi.org/10.1016/j.jasrep.2016.05.063>
- Lambrides, A. B. J., & Weisler, M. I. (2015). Applications of vertebral morphometrics in Pacific Island archaeological fishing studies. *Archaeology in Oceania*, 50, 53–70. <https://doi.org/10.1002/arco.5059>
- Lernau, O. (2016). Chapter 50: The fish remains. In A. Mazar & N. Panitz-Cohen (Eds.), *Tel Rehov The 1997–2012 excavations volumes I–V preprint* (pp. 1–24). QEDM Monographs of the Institute of Archaeology: The Hebrew University of Jerusalem.
- Lernau, O., & Ben-Horin, M. (2016). Estimations of sizes of fish from sub-fossil bones with a logarithmic regression model. *Environmental Archaeology*, 21, 133–136. <https://doi.org/10.1080/14614103.2016.1157676>
- Lidour, K., Vorenger, J., & Béarez, P. (2018). Size and weight estimations of the spangled emperor (Teleostei: Lethrinidae: *Lethrinus nebulosus*) from bone measurements elucidate the fishing grounds exploited and ancient seasonality at Akab (United Arab Emirates). *International Journal of Osteoarchaeology*, 28, 681–694. <https://doi.org/10.1002/oa.2683>
- Marrast, A., & Béarez, P. (2019). Osteometry and size reconstruction of the Indian and Pacific Oceans' *Euthynnus* species, *E. affinis* and *E. lineatus* (Scombridae). *Cybius: Revue Internationale d'Ichthyologie*, 43, 187–198. <https://doi.org/10.26028/CYBIUM/2019-423-007>
- Martínez-Polanco, M. F., & Béarez, P. (2020). An osteometric approach to reconstruct the length and weight of *Lutjanus argentiventris* (Perciformes: Lutjanidae) for archaeological and ecological purposes. *Neotropical Ichthyology*, 18. <https://doi.org/10.1590/1982-0224-2019-0106>
- Maschner, H. D., Betts, M. W., Reedy-Maschner, K. L., & Trites, A. W. (2008). A 4500-year time series of Pacific cod (*Gadus macrocephalus*)

- size and abundance: Archaeology, oceanic regime shifts, and sustainable fisheries. *Fishery Bulletin*, 106(4), 386–394.
- Mather, F. J., Mason, J. M., & Jones, A. C. (1995). Historical document: life history and fisheries of Atlantic bluefin tuna. *NOAA Technical Memorandum NMFS-SEFSC*, 370, 1–165. <https://doi.org/10.5962/bhl.title.4783>
- Morales-Muniz, A., & Roselló-Izquierdo, E. (2007). Los atunes de Baelo Claudia y Punta Camarinal (s. II aC): Apuntes preliminares. In A. Arévalo & D. Berna (Eds.), *Las cetariae de baelo claudia avance de las investigaciones arqueológicas en el barrio meridional (2000–2004)* (pp. 489–498). Junta De Andalucía, Consejería de Cultura.
- Mylona, D. (2018). Fish processing in the Mediterranean: Varying traditions, technologies and scales of production with particular reference to the Eastern Mediterranean. *Journal of Maritime Archaeology*, 13(3–4), 419–436. <https://doi.org/10.1007/s11457-018-9217-z>
- Mylona, D. (2021). Catching tuna in the Aegean: Biological background of tuna fisheries and the archaeological implications. *Anthropozoologica*, 56(2), 23–37. <https://doi.org/10.5252/anthropozoologica2021v56a2>
- Nielsen, S. V., & Persson, P. (2020). The Jortveit farm wetland: A Neolithic fishing site on the Skagerrak coast, Norway. *Journal of Wetland Archaeology*, 20(1–2), 1–24. <https://doi.org/10.1080/14732971.2020.1776495>
- Orchard, T. J. (2005). The use of statistical size estimations in minimum number calculations. *International Journal of Osteoarchaeology*, 15, 351–359. <https://doi.org/10.1002/oa.793>
- Orton, D. C. (2016). Archaeology as a tool for understanding past marine resource use and its impact. In K. Schwerdtner Máñez & B. Poulsen (Eds.), *Perspectives on Oceans Past* (pp. 47–69). Dordrecht; Springer.
- Owen, J. F., & Merrick, J. R. (1994). Analysis of coastal middens in southeastern Australia: Selectivity of angling and other fishing techniques related to Holocene deposits. *Journal of Archaeological Science*, 21, 11–16. <https://doi.org/10.1006/jasc.1994.1003>
- Perçin, F., & Akyol, O. (2009). Length-weight and length-length relationships of the bluefin tuna, *Thunnus thynnus* L., in the Turkish part of the eastern Mediterranean Sea. *Journal of Applied Ichthyology*, 25(6), 782–784. <https://doi.org/10.1111/j.1439-0426.2009.01288.x>
- Pérez Bielsa, N., Ollé, J., Macías, D., Saber, S., & Viñas, J. (2021). Genetic validation of the unexpected presence of a tropical tuna, bigeye tuna (*Thunnus obesus*), in the Mediterranean. *Journal of Fish Biology*, 99, 1761–1764. <https://doi.org/10.1111/jfb.14866>
- Plank, M. J., Allen, M. S., Nims, R., & Ladefoged, T. N. (2018). Inferring fishing intensity from contemporary and archaeological size-frequency data. *Journal of Archaeological Science*, 93, 42–53. <https://doi.org/10.1016/j.jas.2018.01.011>
- Prieto, G. (2021). Shark fisheries during the second millennium BC in Gramalote, north coast of Peru. *The Journal of Island and Coastal Archaeology*, 1–31. <https://doi.org/10.1080/15564894.2021.1910386>
- Reitz, E. J., Quitmyer, I. R., Stephen Hale, H., Scudder, S. J., & Wing, E. S. (1987). Application of allometry to zooarchaeology. *American Antiquity*, 52(2), 304–317. <https://doi.org/10.2307/281782>
- Richter, K. K., Wilson, J., Jones, A. K. G., Buckley, M., van Doorn, N., & Collins, M. J. (2011). Fish 'n chips: ZooMS peptide mass fingerprinting in a 96 well plate format to identify fish bone fragments. *Journal of Archaeological Science*, 38(7), 1502–1510. <https://doi.org/10.1016/j.jas.2011.02.014>
- Rodríguez-Marin, E., Ortiz, M., Ortiz de Urbina, J. M., Quelle, P., Walter, J., Abid, N., Addis, P., Alot, E., Andrushchenko, I., Deguara, S., di Natale, A., Gatt, M., Golet, W., Karakulak, S., Kimoto, A., Macías, D., Saber, S., Santos, M. N., & Zarrad, R. (2015). Atlantic bluefin tuna (*Thunnus thynnus*) biometrics and condition. *PLoS ONE*, 10, e0141478. <https://doi.org/10.1371/journal.pone.0141478>
- Rodríguez-Roda, J. (1964). Biología del atún, *Thunnus thynnus* (L.), de la costa sudatlántica de España. *Investigación Pesqueras*, 25, 33–146. <https://digital.csic.es/handle/10261/189198>
- Rose, M. J. (1994). *With line and glittering bronze hook: Fishing in the Aegean Bronze Age*. PhD Thesis, Ann Arbor, United States: Indiana University.
- Rurua, V., Béarez, P., Hermann, A., & Conte, E. (2020). Length and weight reconstruction of *Chlorurus microrhinos* (Scaridae) from isolated cranial bones and vertebrae. *Cybium*, 44, 61–68. <https://doi.org/10.26028/CYBIUM/2020-441-008>
- Sanchez, G. M. (2020). Indigenous stewardship of marine and estuarine fisheries?: Reconstructing the ancient size of Pacific herring through linear regression models. *Journal of Archaeological Science: Reports*, 29, 102061. <https://doi.org/10.1016/j.jasrep.2019.102061>
- Santamaria, N., Bello, G., Corriero, A., Deflorio, M., Vassallo-Agius, R., Bök, T., & De Metrio, G. (2009). Age and growth of Atlantic bluefin tuna, *Thunnus thynnus* (Osteichthyes: Thunnidae), in the Mediterranean Sea. *Journal of Applied Ichthyology*, 25(1), 38–45. <https://doi.org/10.1111/j.1439-0426.2009.01191.x>
- Sinha, S., Brinkman, D. B., & Murray, A. M. (2019). A morphological study of vertebral centra in extant species of pike, Esox (Teleostei: Esociformes). *Vertebrate Anatomy Morphology Palaeontology*, 7, 111–128. <https://doi.org/10.18435/vamp29357>
- Team RC. (2013). R: A language and environment for statistical computing.
- Thieren, E., & van Neer, W. (2016). New equations for the size reconstruction of sturgeon from isolated cranial and pectoral girdle bones. *International Journal of Osteoarchaeology*, 26, 203–210. <https://doi.org/10.1002/oa.2407>
- Thieren, E., Wouters, W., van Neer, W., & Ervynck, A. (2012). Body length estimation of the European eel *Anguilla anguilla* on the basis of isolated skeletal elements. *Cybium*, 36, 551–562.
- van Neer, W., Lernau, O., Friedman, R., Mumford, G., Poblóme, J., & Waelkens, M. (2004). Fish remains from archaeological sites as indicators of former trade connections in the Eastern Mediterranean. *Paléorient*, 30(1), 101–147. <https://doi.org/10.3406/paleo.2004.4775>
- Wheeler, A., & Jones, A. K. G. (1989). *Fishes*. Cambridge manuals in archaeology (March 2009, pp. 1–228). Cambridge University Press.
- Wickham, H. (2011). Ggplot2. *Wiley Interdisciplinary Reviews. Computational Statistics*, 3, 180–185. <https://doi.org/10.1002/wics.147>
- Winter, R. M., de Kock, W., Palsbøll, P. J., & Çakırlar, C. (2021). Potential applications of biomolecular archaeology to the ecohistory of sea turtles and groupers in Levant coastal antiquity. *Journal of Archaeological Science: Reports*, 36, 102872. <https://doi.org/10.1016/j.jasrep.2021.102872>

## SUPPORTING INFORMATION

Additional supporting information may be found in the online version of the article at the publisher's website.

**How to cite this article:** Andrews, A. J., Mylona, D., Rivera-Charún, L., Winter, R., Onar, V., Siddiq, A. B., Tinti, F., & Morales-Muniz, A. (2022). Length estimation of Atlantic bluefin tuna (*Thunnus thynnus*) using vertebrae. *International Journal of Osteoarchaeology*, 32(3), 645–653. <https://doi.org/10.1002/oa.3092>

Length estimation of Atlantic bluefin tuna (*Thunnus thynnus*) using vertebrae: Appendix 1

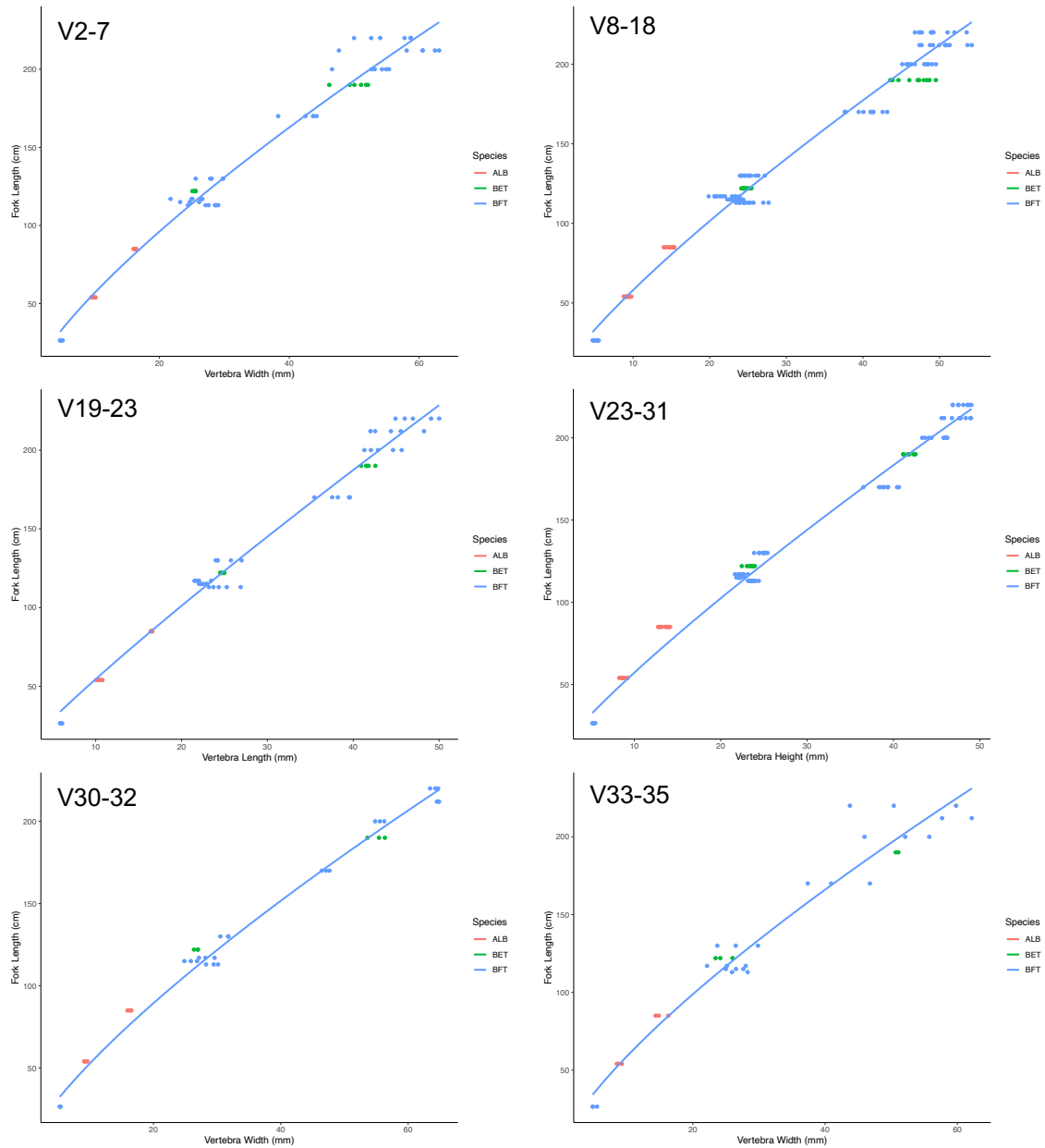


**Figure S1.** Scatterplot for each vertebrae type defined (panels) showing the relationship between vertebra dimensions and fork length for each species (coloured dots: Atlantic bluefin tuna (*Thunnus thynnus*; BFT), albacore tuna (*Thunnus alalunga*; ALB), and bigeye tuna (*Thunnus obesus*; BET)) used in the reference dataset. The best performing model was used for each type as judged from Table S1, S2. The blue line represents the power regression line of BFT reference specimens.

**Table S1.** Conversion factors for length-length, length-weight and caudal fin height-length relationships in BFT as per published sources. Fork Length (FL), Total Length (TL) and Standard Length (SL) are in cm. Weight (round weight RWT) is in kg.

Formula	a	b	R2	FL Range (cm)	Source
<b>Length-length relationships <math>Y=aX-b / Y = a+bX</math>,</b>					
TL = aFL - b	-0.081	1.026	0.996	114-256	Perçin & Akyol 2009
SL = a+bFL	-0.119	1.044	0.998	114-256	Perçin & Akyol 2009
<b>Length-weight relationship <math>Y = aFL^b</math></b>					
RWT = a*FL <sup>b</sup>	0.0000351	2.8785	-	27-300	Rodriguez-Marin et al. 2015

**Table S2.** Power ( $FL = aX^b$ ) equation elements developed herein to estimate fork length (FL, cm) at each vertebra centra dimension (X) measured: Height (H), Width (W) and Length (L) in each vertebra distinguishable in rank (position along vertebral column). n = the number of observations. Dimensions in bold are those representing the best model fit, according to their highest coefficient of determination ( $R^2$ ) and lowest residual standard error (RSE) values. N.B. a values have been raised out of their natural log.

Vertebra Rank	Dimension	a	b	RSE	R <sup>2</sup>	n
1	H	7.988635746	0.92177	0.1248	0.9668	8
<b>1</b>	<b>W</b>	<b>7.90574729</b>	<b>0.86976</b>	<b>0.09612</b>	<b>0.9803</b>	8
2	H	8.397717981	0.92733	0.1101	0.9711	11
<b>2</b>	<b>W</b>	<b>7.378940023</b>	<b>0.85548</b>	<b>0.0613</b>	<b>0.991</b>	11
2	L	5.783158577	1.05325	0.07206	0.9868	12
3	H	8.091142946	0.96959	0.1104	0.969	12
3	W	8.194965481	0.80754	0.05829	0.9914	12
<b>3</b>	<b>L</b>	<b>5.938936043</b>	<b>1.04392</b>	<b>0.05742</b>	<b>0.9916</b>	12
4	H	7.663202674	0.99311	0.09384	0.9796	11
<b>4</b>	<b>W</b>	<b>7.980252081</b>	<b>0.81166</b>	<b>0.06419</b>	<b>0.9905</b>	11
4	L	5.896270309	1.05275	0.07511	0.9869	11
5	H	8.020173058	0.96617	0.0995	0.9726	13
<b>5</b>	<b>W</b>	<b>8.364947013</b>	<b>0.79856</b>	<b>0.0661</b>	<b>0.9879</b>	13
5	L	6.035326777	1.0323	0.07977	0.9826	12
6	H	6.887856958	1.01818	0.1224	0.9585	13
6	W	8.125197211	0.81314	0.07905	0.9827	13
<b>6</b>	<b>L</b>	<b>6.176674377</b>	<b>1.01239</b>	<b>0.0776</b>	<b>0.9833</b>	13
7	H	7.772407796	0.96181	0.1057	0.969	13
7	W	7.878834604	0.83761	0.08406	0.9804	13
<b>7</b>	<b>L</b>	<b>5.635410539</b>	<b>1.04008</b>	<b>0.08267</b>	<b>0.9811</b>	13
8	H	7.417187929	0.96236	0.1125	0.9649	13

8	W	7.592189337	0.86107	0.07926	0.9826	13
<b>8</b>	<b>L</b>	<b>4.801363788</b>	<b>1.0834</b>	<b>0.06799</b>	<b>0.9872</b>	13
9	H	7.344560711	0.95448	0.09362	0.9757	13
<b>9</b>	<b>W</b>	<b>8.098671209</b>	<b>0.8481</b>	<b>0.07864</b>	<b>0.9829</b>	13
9	L	4.629597818	1.09158	0.08176	0.9815	13
10	H	7.287058743	0.9406	0.09215	0.9765	13
<b>10</b>	<b>W</b>	<b>7.953642501</b>	<b>0.8534</b>	<b>0.07283</b>	<b>0.9853</b>	13
10	L	4.507307642	1.095	0.08666	0.9792	13
11	H	6.981403702	0.94195	0.0847	0.9801	13
<b>11</b>	<b>W</b>	<b>7.820668212</b>	<b>0.85645</b>	<b>0.07825</b>	<b>0.983</b>	13
11	L	4.161351911	1.11201	0.09149	0.9768	13
12	H	7.260872495	0.92006	0.0874	0.9788	13
<b>12</b>	<b>W</b>	<b>7.750132965</b>	<b>0.85552</b>	<b>0.07638</b>	<b>0.9838</b>	13
12	L	4.364789659	1.0861	0.08901	0.9781	13
13	H	6.609513166	0.94199	0.09047	0.9773	13
13	W	7.214551297	0.8745	0.08282	0.981	13
<b>13</b>	<b>L</b>	<b>4.277206031</b>	<b>1.0815</b>	<b>0.07303</b>	<b>0.9852</b>	13
14	H	6.751400737	0.93271	0.09411	0.9755	13
14	W	7.166662034	0.87165	0.08114	0.9818	13
<b>14</b>	<b>L</b>	<b>4.372784537</b>	<b>1.0663</b>	<b>0.07195</b>	<b>0.9857</b>	13
15	H	6.547871271	0.941	0.08717	0.979	13
15	W	7.37657914	0.86163	0.08536	0.9798	13
<b>15</b>	<b>L</b>	<b>4.394087995</b>	<b>1.05586</b>	<b>0.06464</b>	<b>0.9884</b>	13
16	H	6.828260801	0.92352	0.09144	0.9768	13
16	W	7.448405629	0.85448	0.08509	0.9799	13
<b>16</b>	<b>L</b>	<b>4.663657446</b>	<b>1.0341</b>	<b>0.07632</b>	<b>0.9839</b>	13
17	H	6.698408762	0.92572	0.08354	0.9807	13
17	W	7.268282363	0.85894	0.07994	0.9823	13
<b>17</b>	<b>L</b>	<b>4.629134882</b>	<b>1.02848</b>	<b>0.07925</b>	<b>0.9826</b>	13
18	H	6.863036622	0.91707	0.07728	0.9835	13
18	W	7.169816059	0.86095	0.08067	0.982	13
<b>18</b>	<b>L</b>	<b>5.003061375</b>	<b>1.00366</b>	<b>0.05969</b>	<b>0.9901</b>	13
<b>23</b>	<b>H</b>	<b>6.720348411</b>	<b>0.9076</b>	<b>0.07232</b>	<b>0.9855</b>	13
23	W	8.171888233	0.8102	0.09523	0.9749	13
23	L	5.636030468	0.94206	0.07474	0.9845	13
<b>24</b>	<b>H</b>	<b>7.043463334</b>	<b>0.8927</b>	<b>0.07547</b>	<b>0.9842</b>	13
24	W	8.679118776	0.79319	0.09755	0.9736	13
24	L	5.905652836	0.9273	0.07989	0.9823	13
25	H	7.205538742	0.88304	0.08848	0.9783	13
25	W	8.657274931	0.7901	0.1074	0.968	13
<b>25</b>	<b>L</b>	<b>6.018451498</b>	<b>0.91202</b>	<b>0.08387</b>	<b>0.9805</b>	13
<b>26</b>	<b>H</b>	<b>7.425425578</b>	<b>0.87549</b>	<b>0.08628</b>	<b>0.9794</b>	13

26	W	8.858256837	0.785	0.1056	0.9691	13
26	L	6.265134145	0.89993	0.1032	0.9705	13
<b>27</b>	<b>H</b>	<b>7.217221175</b>	<b>0.8817</b>	<b>0.08989</b>	<b>0.9776</b>	13
27	W	8.507856239	0.79451	0.1013	0.9716	13
27	L	6.336395033	0.8902	0.1017	0.9713	13
28	H	7.686380527	0.86231	0.1001	0.9722	13
28	W	8.610048918	0.78917	0.1011	0.9717	13
<b>28</b>	<b>L</b>	<b>6.87052141</b>	<b>0.85857</b>	<b>0.07855</b>	<b>0.9829</b>	13
29	H	7.88577103	0.85646	0.09521	0.9749	13
29	W	8.774677355	0.78223	0.09352	0.9758	13
<b>29</b>	<b>L</b>	<b>6.72317155</b>	<b>0.86037</b>	<b>0.09292</b>	<b>0.9761</b>	13
30	H	7.699304499	0.86506	0.09913	0.9728	13
<b>30</b>	<b>W</b>	<b>8.509387791</b>	<b>0.78787</b>	<b>0.08861</b>	<b>0.9783</b>	13
30	L	6.884895816	0.84766	0.09429	0.9754	13
31	H	8.073361998	0.85251	0.09845	0.9732	13
<b>31</b>	<b>W</b>	<b>8.547766323</b>	<b>0.78202</b>	<b>0.08572</b>	<b>0.9796</b>	13
31	L	7.040153684	0.83476	0.09857	0.9731	13
32	H	7.639254348	0.87513	0.09597	0.9745	13
<b>32</b>	<b>W</b>	<b>8.158170986</b>	<b>0.79462</b>	<b>0.07408</b>	<b>0.9848</b>	13
32	L	7.339274531	0.81819	0.09734	0.9738	13
<b>33</b>	<b>H</b>	<b>7.651104374</b>	<b>0.88258</b>	<b>0.08047</b>	<b>0.9821</b>	13
33	W	7.907961209	0.81034	0.08388	0.9805	13
33	L	7.23289955	0.81931	0.08243	0.9812	13
34	H	8.426992948	0.87458	0.1081	0.9676	13
34	W	8.607208071	0.80661	0.08443	0.9803	13
<b>34</b>	<b>L</b>	<b>6.034542235</b>	<b>0.87371</b>	<b>0.04951</b>	<b>0.9934</b>	12
35	H	7.91991125	0.94079	0.142	0.9505	10
35	W	7.42334675	0.88146	0.08755	0.9812	10
<b>35</b>	<b>L</b>	<b>5.933652741</b>	<b>0.90953</b>	<b>0.04465</b>	<b>0.9951</b>	11
36	H	7.078910417	1.00301	0.1425	0.9526	9
36	W	7.678467631	0.9159	0.1572	0.9422	9
<b>36</b>	<b>L</b>	<b>6.787346026</b>	<b>0.94079</b>	<b>0.05372</b>	<b>0.9929</b>	11
37	H	8.15254379	0.9814	0.1147	0.9728	9
<b>37</b>	<b>W</b>	<b>8.001587824</b>	<b>0.96501</b>	<b>0.1131</b>	<b>0.9736</b>	9
37	L	15.02236364	0.94755	0.13	0.9626	10
38	H	9.418256627	0.97263	0.1144	0.9696	10
<b>38</b>	<b>W</b>	<b>8.07433086</b>	<b>1.00703</b>	<b>0.11</b>	<b>0.9719</b>	10
38	L	18.38950277	1.01962	0.1391	0.9525	11
<b>39</b>	<b>H</b>	<b>8.49459433</b>	<b>1.00735</b>	<b>0.1009</b>	<b>0.9754</b>	9
39	W	10.78299116	0.94514	0.1216	0.9643	9



**Table S3.** Power ( $FL = aX^b$ ) equation elements developed herein to estimate fork length (FL, cm) at each vertebra centra dimension (X) measured: Height (H), Width (W) and Length (L) in each vertebra distinguishable by type (groups of vertebrae with similar features). n = the number of observations. Dimensions in bold are those representing the best model fit, according to their highest coefficient of determination ( $R^2$ ) and lowest residual standard error (RSE) values. Standard deviation (SD) of vertebrae measurements is expressed as a percentage mean across all specimens. When SD was high for the model of best fit as identified by  $R^2$  and RSE, the dimension with the next highest  $R^2$  value was selected if its SD was lower. N.B. a values have been raised out of their natural log.

Vertebra type	Dimension	a	b	RSE	$R^2$	STDEV %	n
2-7	H	7.86710388	0.96903	0.1063	0.9686	5.467	73
<b>2-7</b>	<b>W</b>	<b>8.06069676</b>	<b>0.8174</b>	<b>0.07227</b>	<b>0.9855</b>	<b>5.019</b>	<b>73</b>
2-7	L	5.94933828	1.03609	0.07589	0.9839	4.912	73
8-18	H	7.25484847	0.92233	0.1095	0.9643	7.806	143
<b>8-18</b>	<b>W</b>	<b>7.57732322</b>	<b>0.857608</b>	<b>0.07931</b>	<b>0.9813</b>	<b>4.056</b>	<b>143</b>
8-18	L	4.79143524	1.04754	0.1044	0.9676	7.674	143
<b>19-23</b>	<b>H</b>	<b>6.74667641</b>	<b>0.91378</b>	<b>0.07224</b>	<b>0.9846</b>	<b>2.277</b>	<b>65</b>
19-23	W	7.88947821	0.82717	0.08999	0.9761	2.431	65
19-23	L	5.26878613	0.97314	0.06916	0.9859	3.248	65
<b>23-31</b>	<b>H</b>	<b>6.74667641</b>	<b>0.91378</b>	<b>0.07224</b>	<b>0.9846</b>	<b>2.373</b>	<b>65</b>
23-31	W	7.88947821	0.82717	0.08999	0.9761	2.831	65
23-31	L	5.26878613	0.97314	0.06916	0.9859	6.29	65
30-32	H	7.81222645	0.86378	0.09318	0.9746	2.262	39
<b>30-32</b>	<b>W</b>	<b>8.40973531</b>	<b>0.78795</b>	<b>0.07899</b>	<b>0.9818</b>	<b>2.083</b>	<b>39</b>
30-32	L	7.10543511	0.83265	0.09298	0.9747	2.762	39
33-35	H	7.81222645	0.86378	0.09318	0.9746	9.182	39
<b>33-35</b>	<b>W</b>	<b>8.40973531</b>	<b>0.78795</b>	<b>0.07899</b>	<b>0.9818</b>	<b>7.748</b>	<b>39</b>
33-35	L	7.10543511	0.83265	0.09298	0.9747	7.294	39

**Table S4.** Details of 59 2<sup>nd</sup> century BCE *Thunnus thynnus* specimens recovered from Punta Camarinal (Andalusia, Spain) and their length estimations. The measure of vertebra Height, Width and Length dimensions was done as described in Materials and Methods. The power equation ( $FL=aX^b$ ) used to produce fork length (FL, cm) estimates used dimensions in bold, according to the Height, Width or Length dimension (X) with the highest coefficient of determination ( $R^2$ ) value for each vertebra rank or type as Table S1. N.B. a values have been raised out of their natural log.

Specimen ID	Vertebrae Rank or Type	Height (mm)	Width (mm)	Length (mm)	a	b	Fork Length estimate (cm)
1.811	10	28.13	<b>33.33</b>	25.4	7.9536	0.8534	158.5
1186	9	22.92	<b>44.42</b>	26.74	8.0987	0.8481	202.2
1187	7	23.47	40.11	<b>26.42</b>	5.6354	1.0401	169.8
1188	6	22.24	43.92	<b>25.35</b>	6.1767	1.0124	163.0
1189	30	30.47	38.02	<b>36.81</b>	8.5094	0.7879	145.8
10701	7		32.09	<b>21.97</b>	5.6354	1.0401	140.1

11301	39	<b>15.31</b>	15.53		8.4946	1.0074	132.7
11302	39	<b>16.49</b>	17.69		8.4946	1.0074	143.0
11305	30	38.23	46.67	<b>47.93</b>	8.5094	0.7879	179.5
11308	28	34.02	37.21	<b>37.9</b>	6.8705	0.8586	155.7
11309	25	<b>34.87</b>	40.96		6.0185	0.9120	153.5
11310	26	<b>29.86</b>	33.02	29.1	7.4254	0.8755	145.3
11311	19-23	<b>30.92</b>	35.98	31.25	6.7467	0.9138	155.2
11312	26	<b>30.26</b>	34.75	30.34	7.4254	0.8755	147.0
11313	5	21.42	<b>41.08</b>	24.56	8.3649	0.7986	162.6
11315	29	22.82	27.7	<b>28.66</b>	6.7232	0.8604	120.6
11316	10	26.22	<b>29.92</b>	24.08	7.9536	0.8534	144.6
11318	9	22.95	<b>33.43</b>	23.27	8.0987	0.8481	158.9
11319	14	23.27	26.95	<b>21.37</b>	4.3728	1.0663	114.5
11320	8		28.26	<b>21.47</b>	4.8014	1.0834	133.1
11321	9	20.39		<b>21.86</b>	4.6296	1.0916	134.2
11323	7	28.25	37.28	<b>24.08</b>	5.6354	1.0401	154.2
11331	11	30.06	<b>36.61</b>	30.2	7.8207	0.8565	170.8
11406	8-18	23.02	<b>26.76</b>	22.02	7.5773	0.8576	127.0
11702	6	17.6	32.24	<b>20.9</b>	6.1767	1.0124	134.0
11703	3	19.31	33.68	<b>20.3</b>	5.9389	1.0439	137.6
11704	13	18.66	24.72	<b>20.33</b>	4.2772	1.0815	111.2
11705	10	24.95	<b>30.71</b>	23.89	7.9536	0.8534	147.8
11706	17	25.15	29.19	<b>26.55</b>	4.6291	1.0285	134.9
11707	26	<b>29.03</b>	34.03	29.74	7.4254	0.8755	141.7
11708	17	29.84	36.06	<b>31.22</b>	4.6291	1.0285	159.4
11709	8-18	29.72	<b>36.57</b>	30.03	7.5773	0.8576	166.0
11710	35	23.45	30.26	<b>30.06</b>	5.9337	0.9095	131.1
11714	32			<b>36.19</b>	7.3393	0.8182	138.3
11715	32	27.46	<b>34.89</b>	35.4	8.1582	0.7946	137.2
11716	32	29.12	<b>33.33</b>	33.91	8.1582	0.7946	132.3
11717	27	<b>37.64</b>	43.43	37.41	7.2172	0.8817	176.9
11718	28	33.87	42.14	<b>36.58</b>	6.8705	0.8586	151.1
11719	26	<b>30.72</b>	37.27	33.52	7.4254	0.8755	148.9
11720	5		<b>45.5</b>	24.28	8.3649	0.7986	176.4
11810	23-28	<b>32.9</b>	36.77	33.75	6.7467	0.9138	164.2
11811	31	29.8	<b>36.02</b>	37.55	8.5478	0.7820	141.0
11812	33	<b>28.24</b>		39.96	7.6511	0.8826	146.0
11814	35	23.74	29.34	<b>30.84</b>	5.9337	0.9095	134.2
11816	37		<b>29.67</b>	21.89	8.0016	0.9650	210.9
11817	39	<b>15.98</b>	15.57		8.4946	1.0074	138.5
11818	39	<b>16.17</b>	18.3		8.4946	1.0074	140.2
11901	34			<b>59.08</b>	6.0345	0.8737	213.0

11904	23-31	<b>26.68</b>	30.35	26.17	6.7467	0.9138	135.6
11908	37	19.9	<b>28.14</b>	21.16	8.0016	0.9650	200.3
11909	37	19.58	<b>21.94</b>	12.3	8.0016	0.9650	157.6
11911	37	20.84	<b>22.3</b>	12.28	8.0016	0.9650	160.1
11912	37	19.49	<b>22.15</b>	11.7	8.0016	0.9650	159.0
11914	39	<b>18.52</b>	18.1		8.4946	1.0074	160.7
11965	15	23.42	26.8	<b>22.72</b>	4.3941	1.0559	118.9
12101	28	37.27	44.13	<b>40.03</b>	6.8705	0.8586	163.2
12102	28	31.55	37.51	<b>31.95</b>	6.8705	0.8586	134.5
12103	24	<b>31.78</b>	36.38	32.06	7.0435	0.8927	154.4
12104	10	26.81	<b>30.88</b>	24.24	7.9536	0.8534	148.5

Length estimation of Atlantic bluefin tuna (*Thunnus thynnus*) using vertebrae: Appendix 2  
Guide to identifying *Thunnus* spp. vertebrae rank or type

This guide aims to illustrate morphological features present on *Thunnus* vertebrae which allow for the identification of vertebrae (V) recovered in archaeological assemblages to rank (sequential position in vertebral column) or type (grouping of vertebrae with similar morphologies) level. Spines or articular processes (zygapophyses) are often broken or eroded in archaeological vertebrae. As such, here there is a particular focus on the joining position, and angle of, spines and articular processes in relation to the vertebral body, instead of the height of spines, arch of spines or the length of articular processes. Variation between individuals is likely to produce differences in the appearance of vertebrae, compared to the figures below, although, the characteristics described herein hold true for all 13 reference specimens studied.

In the genus *Thunnus*, the total number of vertebrae is 39, including the first vertebra (V1, Figure S2) which often fuses with the skull (at the basioccipital) in adults (~100+ cm FL), and the ultimate centra (V39) connected to the urostyle.

Prior to rank or type identification, it is advised to identify anterior and posterior centra. All lateral views of vertebrae shown here are arranged from anterior (left) to posterior (right). It is possible to differentiate between anterior and posterior surfaces as parapophyses are pronounced at the anterior in V2-32 (also in V1 for juvenile specimens), because hemal spines are attached at the anterior in V8-23 and because in V33-39 spines are directed towards the posterior.

Vertebrae in this guide are grouped into types (V2-7, V8-18, V19-23, V24-31, V30-32) which can be used when it is difficult to identify rank. Error in size estimations will increase if rank/type is misidentified, therefore care should be taken at this step. It is advisable to make identifications checkable by providing identification criteria and photographic evidence where possible. Note that identifying rank is challenging and ought to take considerable time.

V1 may simply be identified if found disarticulated, or unfused in juvenile specimens, by the centra heavily narrowing anteriorly and in adult specimens as the anterior centrum is absent.



Figure S2. First vertebra in *Thunnus* spp., fused to the skull in adults. In ventral view (left) and latero-posterior view (right).

V2-7 (Figure S3) can be recognised by 1) their shorter length-width relation in comparison with other vertebrae and 2) their lack of a hemal spine. The rank of vertebrae 2-7 can be identified when assessing their posterior and ventral view, but the lateral view is optimal where:

In V2, the neural spine is more separated from its anterior articular process than in V3-5, and its parapophysis is barely developed and more anterior than V3-5. In V3, the neural spine stretches across the whole length of the vertebrae and has a proportionally large parapophysis. In V4 and V5, the neural spine is separated from its posterior articular process, more so in V5 and now parapophyses have a protruding costal articulation (see Figure S4, S5), increasing in size to V6. In V6 and V7, vertebra length is increased compared with V2-5 and the neural spine is more distinct from the posterior portion of the centrum than in V2-5, especially for V7. If well preserved, the neural spine is more rounded in V6 and V7 than V2-5, especially for V7. If also well preserved, the parapophyses are enlarged in V5-7, increasing with rank. Parapophyses have protruding articulations that become compressed in V7, especially V8 and on. The parapophyses are best assessed from the anterior or posterior or ventral view (Figure S4, S5).

In addition, three easily identifiable fossae (depressions) can be used when assessing ventral view to distinguish between vertebrae V1-6 and V7-8. Fossae are formed along the midline and laterally (Figure S5) and decrease in size with rank.



Figure S3. Lateral view of V2-7, as labelled on the neural spine in order from V2 (left) to V7 (right). N.B. Images of vertebrae V6-7 are cropped at the neural spine.

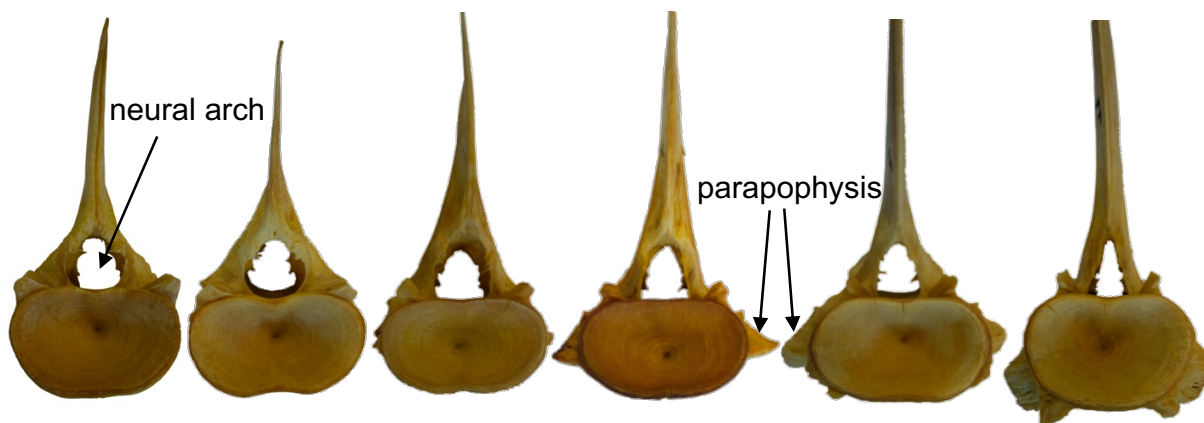


Figure S4. Posterior view of V2-7 in order from V2 (left) to V7 (right). N.B. Images of vertebrae V4-7 are cropped at the neural spines.

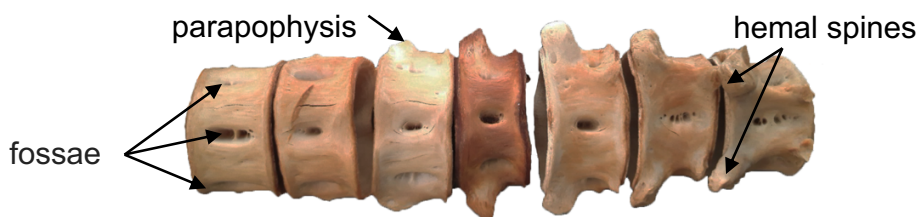


Figure S5. Ventral view of V2-8 in order from V2 (left) to V8 (right). V8 shown to illustrate compressed parapophyses in comparison with V5-7. V8 is the first vertebra to develop anteriorly-projecting hemal spines.

V8-18 are particularly challenging to differentiate. They can principally be recognised by the presence of both neural and hemal spines, which are much broader than in V19 onwards. If well preserved, V8-18 can, if it is sufficiently preserved, be identified according to the angle of the hemal spine in relation to the vertebral body as it is less anteriorly angled with each rank (Figure S6). In V8-13 the hemal spine is orientated anteriorly—particularly so in V8-10 which should make V8-10 more readily identifiable than others of this type. In V14 and V15, the hemal spine is oriented vertically, whereas in V16-18 the hemal spine is posteriorly angled.

V8-18 can also be somewhat identified by the width of their neural spines as these decrease with each rank. Note a particular distinction in neural spine width between V8-13 and V14-18 (Figure S7).



Figure S6. Lateral view of V8-18, as labelled on the neural spine V8 (top left) to V13 (top right), V14 (bottom left) to V18 (bottom right). N.B. Images are cropped at the neural and hemal spines.

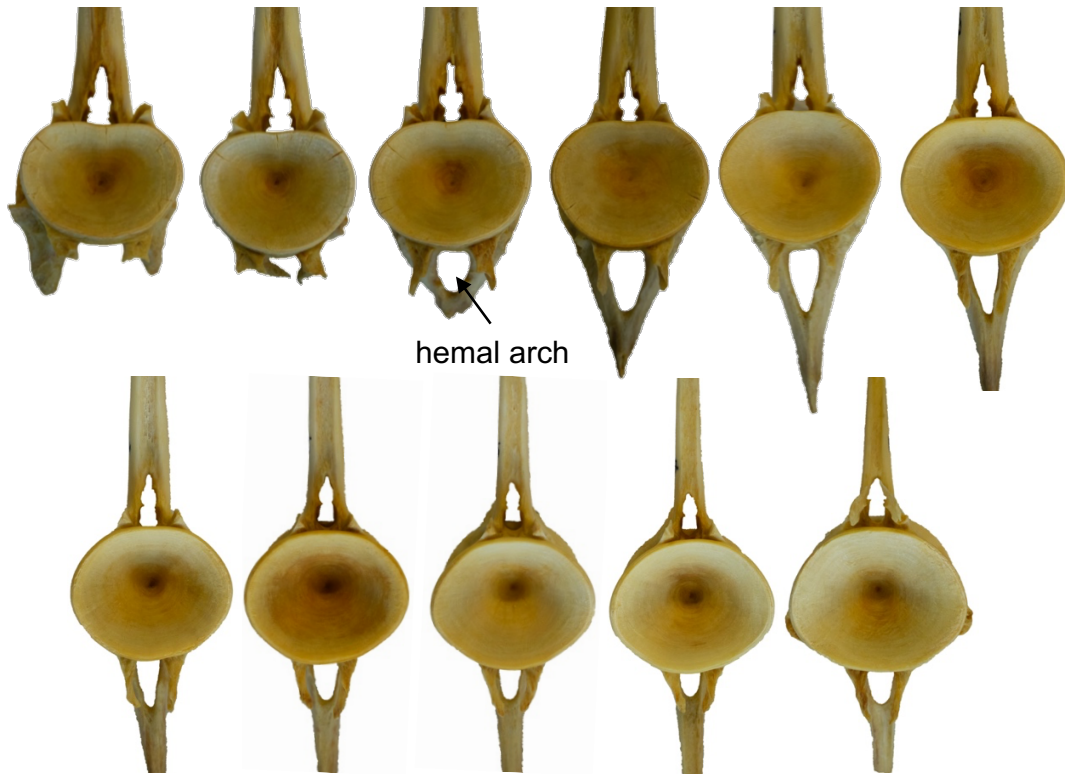


Figure S7. Posterior view of V8-18 in order from V8 (top left) to V13 (top right), V14 (bottom left) to V18 (bottom right). N.B. Images are cropped at the neural and hemal spines.



V19-22/23 were perceived as too morphologically similar to be differentiated. Therefore, their type equation must be applied. V19-22/23 may be recognised by the presence of neural and hemal spines where the neural spine is narrower than in V8-18 (Figure S8, S9). Furthermore, they lack a transverse foramen which is present on V23/24-31 and otherwise appear similar. Variation exists between V22 and V23 because vertebrae V23 sometimes carries a transverse foramen (small hole at the base of the hemal spine). The cause of this variation is unknown.



Figure S8. Lateral view of V19-23, as labelled on the neural spine V19 (left) to V23 (right). N.B. Images are cropped at the neural and hemal spines.



Figure S9. Posterior view of V19-23, in order from V19 (left) to V23 (right). N.B. Images are cropped at the neural and hemal spines.

V23/24-29/31 may be recognised by the presence of a transverse foramen at the base of the hemal spine. Note that a transverse foramen is not always present on V23, V30 and V31. If a transverse foramen is missing, apply the type equation for V19-23 or V30-32, respectively.

V23-31 may be recognised according to the neural and hemal spines, which are more posteriorly positioned, and more posteriorly angled with each rank. Vertebral length can also be used to identify rank since length increases with rank in these vertebrae (Figure S10). The posterior view may be of little use to aid rank identification (Figure S11).



Figure S10. Lateral view of V24-31, as labelled on the neural spine V24 (top left) to V27 (top right), and V28 (bottom left) to V31 (bottom right). N.B. Images are cropped at the neural and hemal spines.



Figure S11. Posterior view of V24-31, in order from V24 (top left) to V27 (top right), and V28 (bottom left) to V31 (bottom right). N.B. Images are cropped at the neural and hemal spines.

V30-32 are challenging to differentiate. They may be recognised due to being elongated, similar to V28 and V29, with posteriorly positioned neural and hemal spines but V30 and V31 may not carry a transverse foramen as is present in the reference specimens shown (Figure S12). If well preserved, each may be identified by the angle of the neural and hemal spines, which is more acute with each subsequent rank (Figure S12, S13).



Figure S12. Lateral view of V30-32, in order from V30 (left) to V31 (right). N.B. the spines of V31 were eroded in this reference specimen.



Figure S13. Posterior view of V30-32, in order from V30 (left) to V31 (right). N.B. the spines of V31 were eroded in this reference specimen.

V33-39 are considered unique and able to be identified to rank, as follows:

V33-35 may be differentiated according to the height of their parapophyses, which are now pronounced in comparison with all other vertebrae, and increase towards the posterior in V33, are at their greatest and more horizontal in V34, and decrease towards the posterior in V35 (Figure S14, S15, S16).

V36 may be differentiated from V33-35 by the obtuse angle of its neural and hemal spines, and because its centra is shortened (Figure S14).

V37 can be differentiated from 38 because vertebral length is notably shortened in V38 (Figure S14).

V39, the final vertebra is attached to the urostyle.



Figure S14. Lateral view of V33-39, in order from V33 (top left) to V35 (top right), V36 (bottom left) to V39 (bottom right).



Figure S15. Dorsal view of V33-36 in order from V33 (left) to V36 (right).

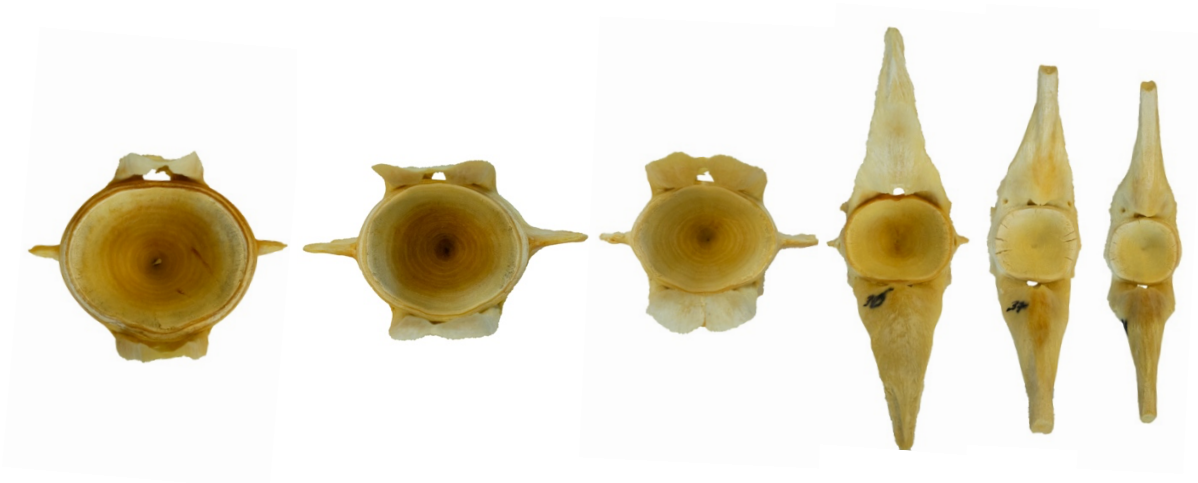


Figure S16. Posterior view of V33-38, in order from V33 (left) to V38 (right).

### Vertebra identification and size estimation tips

- First identify anterior and posterior surfaces and orientate vertebrae as per the figures (anterior, left and posterior, right).
- Attempt identification to rank level where possible as variation between vertebrae in types will decrease the accuracy of estimates.
- Once vertebral rank or type has been identified, measure on the posterior surface of centra where possible using the optimal dimension (H, W or L) for the vertebra rank or type in question (as indicated in Table S2 & S3). Measurements should be made as per Figure 1.
- If measurements can only be made on the anterior surface of centra be aware that slight variation will further affect the accuracy of estimates, particularly for V2-3 and V33-36. Likewise, the accuracy of estimates will decrease if using a vertebra dimension that is not the best fitting (as indicated in Table S2 & S3).
- Apply regression equations using the formula ( $FL=aX^b$ , where X is your appropriate vertebra measurement in mm) and values in Table S2 & S3.
- Alternatively, visit <https://tunaarchaeology.org/lengthestimations> and input your rank or type and measurement where your estimate will be calculated. Note estimates are straight fork lengths, in cm.
- Consider that measurements require the identification of the edge of the vertebrae centra. Thus, if spines and processes are heavily eroded to make difficult the identification of vertebrae to rank or type level, the centra edge is likely to be damaged too and will lead to underestimated measurements.
- To improve the reliability of size estimations: provide criteria for rank or type identification, evidenced by a photograph and any notes of uncertainty when publishing.
- At any time, the corresponding author will welcome queries on rank or type identification.



Calculate fork length estimates for archaeological tuna specimens using vertebrae measurements and equations defined in **Andrews et al. 2022: International Journal of Osteoarchaeology**

N.B. This form does not store user input data

Vertebra Rank or Type

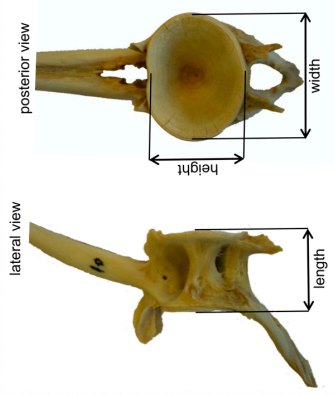
**The optimal dimension is**

Dimension measured

Vertebra measurement (mm)

---

**Estimated Fork Length (cm)**



We recommend applying atleast  $\pm 10\%$  error to the estimated value.

For more information, see our **Publication** including its **Supplementary Materials**



### **Chapter 3**

Vertebrae reveal industrial-era increases in Atlantic bluefin tuna  
catch-at-size and juvenile growth  
**(pages 82—112)**

# Vertebrae reveal industrial-era increases in Atlantic bluefin tuna catch-at-size and juvenile growth

Adam J. Andrews<sup>1,\*</sup>, Antonio Di Natale<sup>2</sup>, Piero Addis<sup>3</sup>, Federica Piattoni<sup>1</sup>, Vedat Onar<sup>4</sup>, Darío Bernal-Casasola<sup>5</sup>, Veronica Aniceti<sup>6</sup>, Gabriele Carenti<sup>7</sup>, Verónica Gómez-Fernández<sup>8</sup>, Fulvio Garibaldi<sup>9</sup>, Arturo Morales-Muñoz<sup>10,\*</sup> and Fausto Tinti<sup>1</sup>

<sup>1</sup>Department of Biological, Geological and Environmental Sciences, University of Bologna, 48123 Ravenna, Italy

<sup>2</sup>Aquastudio Research Institute, 98121 Messina ME, Italy

<sup>3</sup>Department of Life and Environmental Sciences, University of Cagliari, 09124 Cagliari, Sardinia, Italy

<sup>4</sup>Osteoarchaeology Practice and Research Centre, Faculty of Veterinary Medicine, Istanbul University-Cerrahpaşa, 34320 Istanbul, Turkey

<sup>5</sup>Department of History, Geography and Philosophy, Faculty of Philosophy and Letters, University of Cádiz, 11003. Cádiz, Spain

<sup>6</sup>Museum of Natural History, University of Bergen, 5007 Bergen, Norway

<sup>7</sup>CEPAM, CNRS, Université Côte d'Azur, 06357 Nice, France

<sup>8</sup>I.N.I.C.E.—Instituto Nacional de investigaciones científicas y ecológicas, 37008 Salamanca, Spain

<sup>9</sup>Department of Earth, Environment and Life Sciences (DISTAV), University of Genoa, 16182 Genoa, Italy

<sup>10</sup>Department of Biology, Autonomous, University of Madrid, 28049 Madrid, Spain

\*Corresponding authors: tel: +39 0544 937311; e-mails: [adam@palaeome.org](mailto:adam@palaeome.org), [arturo.morales@uam.es](mailto:arturo.morales@uam.es).

Climate change and size-selective overexploitation can alter fish size and growth, yet our understanding of how and to what extent is limited due to a lack of long-term biological data from wild populations. This precludes our ability to effectively forecast population dynamics and support sustainable fisheries management. Using modern, archived, and archaeological vertebrae dimensions and growth rings of one of the most intensely exploited populations, the eastern Atlantic and Mediterranean bluefin tuna (*Thunnus thynnus*, BFT), we estimated catch-at-size and early-life growth patterns from the 3<sup>rd</sup> century BCE to the 21<sup>st</sup> century CE to understand responses to changes in its environment. We provide novel evidence that BFT juvenile growth increased between the 16<sup>th</sup>–18<sup>th</sup>, 20<sup>th</sup>, and 21<sup>st</sup> centuries, and is correlated with a warming climate and likely a decrease in stock biomass. We found it equally plausible that fisheries-induced evolution has acted to increase juvenile BFT growth, driving earlier maturation as a result of size-selective exploitation. Coincidentally, we found limited evidence to suggest a long history of large (>200 cm FL) BFT capture. Instead, we found that the catch-at-size of archaeological BFT was relatively small in comparison with more intensive, 20<sup>th</sup> and 21<sup>st</sup> century tuna trap fisheries which operated further from shore. This complex issue would benefit from studies using fine-scale biochronological analyses of otoliths and adaptation genomics, throughout the last century especially, to determine evolutionary responses to exploitation, and further disentangle the influence of temperature and biomass on fish growth.

**Keywords:** climate change, fisheries-induced evolution, fish trait plasticity, growth of fishes, historical baselines, historical fish size, *Thunnus thynnus*.

## Introduction

In light of ocean warming and the recent overexploitation of fish stocks, long-term investigations into how climate and exploitation affected fish trait plasticity and adaptation in the past are crucial to predict population dynamics and thereby support sustainable fisheries management (Law, 2000; Jørgensen *et al.*, 2007; Lotze *et al.*, 2014; Rodrigues *et al.*, 2019). In particular, the key traits of fish size and growth affect many metrics used to assess stocks, such as size at maturation, fecundity, recruitment, and biomass (Fromentin, 2003; Jørgensen *et al.*, 2007), and display various responses in relation with climatic and exploitation conditions on decadal and centennial scales (Bolle *et al.*, 2004; Enberg *et al.*, 2012; van der Sleen *et al.*, 2016; Ólafsdóttir *et al.*, 2017; Barrett, 2019; Denechaud *et al.*, 2020; Vieira *et al.*, 2020). One of the most intensely and longest exploited fishes is the Atlantic bluefin tuna (*Thunnus thynnus*; BFT); commercial exploitation began ca. 8<sup>th</sup> c. BCE for its eastern Atlantic and Mediterranean stock (Di Natale, 2014; Porch *et al.*, 2019; Andrews *et al.*, 2022b), and by 2007, this stock was considered depleted (ICCAT, 2007). Moreover,

its spawning and feeding habitats rank among the fastest-warming ocean regions (Giorgi, 2006). Despite this, there is hitherto no information on the long-term temporal variation in BFT size or growth.

Here, we fill this data gap by reconstructing pre-industrial catch-at-size data using archaeological vertebrae, and by analysing the early-life growth of archaeological, archived, and modern specimens using vertebrae annuli (annual growth ring) measurements, spanning centuries, to determine how and why growth varies over time for the eastern Atlantic and Mediterranean stocks of BFT. A lack of temporal samples for the western Atlantic stock, owing to the later onset of its commercial exploitation (Andrews *et al.*, 2022b), precludes its inclusion here.

Historical catch-at-size data, collated from records or reconstructed using archaeological bone measurements, inform on the gears used and sizes targeted in historical fisheries, in addition to stock age or size shifts over time (Maschner *et al.*, 2008; Plank *et al.*, 2018; Barrett, 2019; Sanchez, 2020). Size-selective overexploitation appears to have truncated the

Received: October 3, 2022. Revised: January 18, 2023. Accepted: January 19, 2023

© The Author(s) 2023. Published by Oxford University Press on behalf of International Council for the Exploration of the Sea. This is an Open Access article distributed under the terms of the Creative Commons Attribution License (<https://creativecommons.org/licenses/by/4.0/>), which permits unrestricted reuse, distribution, and reproduction in any medium, provided the original work is properly cited.

size-structure of eastern BFT during the last 70 years (Fromentin, 2009; MacKenzie *et al.*, 2009; Siskey *et al.*, 2016b), and since this has the potential to alter fish growth (Law, 2000; Jørgensen *et al.*, 2007; Hollins *et al.*, 2018), pre-industrial catch-at-size baselines are vital to investigate demographics when the stock was less exploited and assess potential evolutionary impacts on growth.

Several decadal- and centennial-scale studies have shown that temporal changes in fish growth may result from plastic responses to ecological or environmental factors like biomass (Vieira *et al.*, 2020; Pedersen *et al.*, 2022), predator-prey interactions (Smoliński, 2019), or temperature (Geffen *et al.*, 2011; van der Sleen *et al.*, 2016; Denechaud *et al.*, 2020; Smoliński *et al.*, 2020), as well as evolutionary ones like fisheries-induced evolution (FIE) (Edeline *et al.*, 2007; Mollet *et al.*, 2007; Swain *et al.*, 2007; Neuheimer and Taggart, 2010; Saura *et al.*, 2010). FIE is the artificial selection of traits (early maturation and/or slow mature growth) that enhance survival and the number of offspring of individuals subject to fishing that commences above a certain size-threshold (Law, 2000; Enberg *et al.*, 2012). Empirical evidence of FIE is still lacking at the genomic level (with two exceptions: Therkildsen *et al.* 2019 and Czorlich *et al.* 2022); however, challenges in detecting polygenic adaptation and the infancy of historical genomic methods (Pinsky *et al.*, 2021) mean that FIE cannot be ruled out for intensely exploited marine fishes (Hutchings and Kuparinen, 2021). Yet, long-term phenotypic perspectives on how long size-selective harvesting has occurred and what impact this may have on growth remain scarce due to difficulties in obtaining temporal samples.

Typically, temporal patterns in fish growth are studied by assessing size-at-age (e.g. Campana 1990) or the increment width of annuli (e.g. Morrongiello and Thresher 2015) using otoliths; collected between years, decades, or centuries. Because archaeological BFT otoliths are yet to be recovered (Andrews *et al.*, 2022b), and we had access to archived BFT vertebrae (but no otoliths), collected ~100 years ago by the ecologist Massimo Sella for his seminal size-at-age work (Sella, 1929), vertebrae were chosen as an alternative. Given that the reliability of size-at-age would be hindered by a  $\pm 10\%$  error in reconstructing size using vertebrae (Andrews *et al.*, 2022a), and that BFT vertebra annuli are difficult to distinguish at vertebra centra edges, we opted for an increment size approach inspired by (Lee *et al.*, 1983). This required some consideration given that vertebrae (unlike otoliths) are subject to resorption (Campana and Thorrold, 2001). However, there is some precedent in using bone elements subject to resorption in long-term growth studies, such as vertebrae (Van Neer *et al.*, 1999) and scales (Guillaud *et al.*, 2017), indeed BFT fin-spine annuli have also been used to good effect to study growth (Landa *et al.*, 2015).

Since annuli have been validated as annual formations in BFT otoliths (Rodríguez-Marín *et al.*, 2007; Neilson and Campana, 2008; Siskey *et al.*, 2016a), and since vertebrae and otolith annuli closely correspond (until age 10) in southern bluefin tuna (*Thunnus maccoyii*, Gunn *et al.*, 2008), vertebra growth rings are likely annual in BFT at least until age 10. Given that BFT vertebra centra are highly correlated with fork length (FL) (Rodríguez-Roda, 1964; Lee *et al.*, 1983; Andrews *et al.*, 2022a), vertebra annuli increment sizes can also be considered to be proportional to somatic growth. A lack of sex information for historical specimens should also not be a hinderance to our study since sexual dimorphism only occurs

between large BFT (Santamaria *et al.*, 2009; Addis *et al.*, 2014; Stewart *et al.*, 2022). Therefore, we find no reason to omit the opportunity to study long-term growth in BFT, provided that we assess the relationship between increment size and vertebrae size to ensure interpretations can be made of increment sizes from different sized vertebrae in BFT.

Despite considerable interest in this large (up to 3.3 m in length and 725 kg in weight: Cort *et al.* 2013), highly migratory species, as detailed in several solid reviews (Mather *et al.*, 1995; Cort, 2003; Fromentin, 2003, 2009; Cort *et al.*, 2013; Murua *et al.*, 2017), long-term growth data is lacking. Long-term insights on growth patterns in BFT would be of practical significance due to their consequences for fisheries management. Size-at-age has been well-studied in BFT since Sella's time (Sella, 1929), most notably by (Rodríguez-Roda, 1964; Cort, 1989; Rodríguez-Marín *et al.*, 2006), and published growth-curves for the eastern BFT stock (summarized in Cort *et al.* 2014) reveal variation between studies but no temporal trend (Supplementary Figure 1, Restrepo *et al.* 2007). Due to the biological trade-off between fish growth and maturation (Enberg *et al.*, 2012), studying one of these traits can be indicative of the other; however, no study has addressed temporal age-at-maturation changes in eastern BFT, either, where the original theory persists, that is, maturation beginning at age 3, while all individuals are mature by age 5 (Rodríguez-Roda, 1967; Mather *et al.*, 1995; Corriero *et al.*, 2005). Fromentin (2003) is the only study on BFT to note temporal variation in size-at-age, noting that juvenile weight-at-age decreased between 1982 and 1998, which we hope to shed light on here.

In the present study, we investigate pre-industrial BFT catch-at-size to inform on the size-selectivity and impact of their exploitation history and test the hypothesis that BFT growth varies temporally in response to environmental conditions or size-selective exploitation (FIE). To this end, our objectives were to (1) reconstruct the size of archaeological BFT using vertebra measurements and discuss these in relation with those collated in recent decades by ICCAT, and (2) assess changes in early-life BFT growth using archaeological, archived, and modern vertebrae annuli and attempt to characterize these in terms of plastic or evolutionary responses.

## Materials and methods

### Historical catch-at-size estimation

To obtain catch-at-size estimates for the historical era, 286 BFT vertebrae were sampled from nine archaeological sites in the eastern Atlantic and Mediterranean, each dated by archaeological context or radiocarbon, between the 3<sup>rd</sup> century BCE–18<sup>th</sup> century CE (Table 1, Figure 1: for details see Supplementary Materials). Care was taken to avoid sampling the same individual twice by selecting a single vertebra when several were in anatomical position, and vertebrae of different sizes and levels of preservation (assessed visually) when selecting from each stratigraphic unit. Small (<100 cm FL) specimens were not sampled because their morphological identification to species level is not considered reliable, as they may represent albacore (*Thunnus alalunga*) and were thus excluded.

FL of archaeological specimens was estimated following Andrews *et al.* (2022a) using the online resource <https://tu.naarchaeology.org/lengthestimations>. Briefly, vertebrae were

**Table 1.** Summary of modern, archival, and archaeological Atlantic bluefin tuna (*T. thynnus*) vertebra sample details used in FL estimations and growth analyses in the current study. V35: 35<sup>th</sup> ranked vertebra, V36: 36<sup>th</sup> ranked vertebra.

Sample ID/Year	Archaeological sample site or fishing location	Long.	Lat.	<i>n</i> vertebrae sampled for growth	<i>n</i> V35 specimens analysed for growth	<i>n</i> V36 specimens analysed for growth	<i>n</i> vertebrae used in FL estimation	FL min-max (mean) cm
2020 CE	Carloforte, Sardinia, Italy	8.31	39.18	58	29	29	–	98–197 (124)
2020 CE	Ligurian Sea, Italy	8.21	43.62	56	28	27	–	104–165 (131)
1926 CE	Venice, Veneto, Italy	14.59	43.93	46	18	15	–	114–187 (143)
1925 CE	Zliten, Libya	14.66	33.25	42	20	15	–	115–249 (182)
1911–1912 CE	Pizzo/Messina, Italy	15.34	38.97	45	21	20	–	78–154 (107)
16 <sup>th</sup> –18 <sup>th</sup> c. CE	Pedras de Fogu, Sardinia, Italy	8.62	40.86	21	13	8	38	99–232 (153)
1755 CE	La Chanca, Conil, Spain	–6.09	36.28	23	13	10	30	140–228 (182)
13 <sup>th</sup> c. CE	Mazara del Vallo, Sicily, Italy	12.58	37.65	–	–	–	6	140–230 (172)
9 <sup>th</sup> –13 <sup>th</sup> c. CE	Yenikapi, Istanbul, Turkey	28.95	41.01	–	–	–	60	131–284 (200)
10 <sup>th</sup> –11 <sup>th</sup> c. CE	Palermo*, Sicily, Italy	13.37	38.11	–	–	–	20	101–185 (138)
4 <sup>th</sup> –5 <sup>th</sup> c. CE	Baelo Claudia, Spain	–5.77	36.09	–	–	–	21	107–210 (137)
1 <sup>st</sup> –4 <sup>th</sup> c. CE	Portopalo, Sicily, Italy	15.13	36.68	–	–	–	14	118–227 (159)
1 <sup>st</sup> c. CE	Olivillo, Spain	–6.31	36.53	–	–	–	24	90–164 (132)
2 <sup>nd</sup> c. BCE	Punta Camarinal, Spain	–5.77	36.09	6	3	3	59	138–213 (151)
3 <sup>rd</sup> c. BCE	Portopalo, Sicily, Italy	15.13	36.68	7	4	3	14	103–261 (178)

\*Palermo samples pertain to two different archaeological sites (see Supplementary Materials for details). *n* = number. Lat. = Latitude. Long. = Longitude.

identified to rank or type (see Andrews *et al.* 2022a), vertebrae centra length, width, and height were measured using digital callipers to the nearest 0.01 mm, and the best-fitting power regression model was applied for each specimen (Figure 1, Supplementary Table S1), which predicts FL to ca. 90% accuracy. When centra were damaged by post-mortem processes, prohibiting the measurement of one or more dimensions, the next-best scoring dimension model was applied. A comparative FL dataset for the 20<sup>th</sup>–21<sup>st</sup> century CE tuna trap fishery (Supplementary Table S2) was obtained from ICCAT ([www.iccat.int/en/accessingdb.html](http://www.iccat.int/en/accessingdb.html)), including 1915–1927 FL data (*n* = 253) from Italian and Libyan tuna traps, initially published by (Pagá Garcia *et al.*, 2017).

### Growth estimation: sample collection

To estimate temporal variation in BFT growth, we identified archaeological, archived, and modern BFT vertebrae to rank (see Andrews *et al.* 2022a) and collected the 35<sup>th</sup> (V35) and 36<sup>th</sup> (V36) vertebrae as these often show clearly-defined annuli (growth rings) and thus have a long history of use in BFT ageing (Sella, 1929; Galtsoff, 1952; Rodríguez-Roda, 1964; Lee *et al.*, 1983; Rodríguez-Marín *et al.*, 2006). A total of 57 archaeological specimens with sufficient preservation were collected from four sites and two periods, namely the 3<sup>rd</sup>–2<sup>nd</sup> c. BCE (Portopalo and Punta Camarinal) and 16<sup>th</sup>–18<sup>th</sup> c. CE (La Chanca and Pedras de Fogu) (Table 1, Figure 1: for details see Supplementary Materials).

A total of 133 archival BFT vertebrae (Massimo Sella Archive, University of Bologna) were selected, pertaining to three central Mediterranean tuna trap sites/years during the early 20<sup>th</sup> c. (Table 1, Figure 1). These sample groups were 1911–1912 (Pizzo and Messina, Italy), 1925 (Venice, Italy), and 1926 (Zliten, Libya). Archived vertebrae were stored dry

after the removal of soft tissues by unknown means. A total of 121 modern specimens were obtained from longlines off Sanremo and Imperia (Italy, *n* = 28) as bycatch of a swordfish (*Xiphias gladius*) longline fishery, and tuna-trap off Isola Piana (Carloforte, Sardinia: Carloforte Tonnare PIAM srl., Italy, *n* = 29), in June–October 2020, and May 2020, respectively. Modern vertebrae were mechanically cleaned of soft tissues, macerated in ambient-temperature water for up to 2 months to remove soft tissues by microbial decomposition, then dried before analyses were conducted to mimic the treatment of archaeological and archival specimens.

### Growth estimation: specimen preparation and measurement

To estimate the FL of individuals used in growth analyses and to study the relationship between vertebrae size and annuli increment widths, measurements of vertebra centra length, width, and height were made using digital callipers to the nearest 0.01 mm. The height and width of vertebrae were measured on the posterior centrum of V35 and the anterior centrum of V36. Vertebra length was recorded from the vertebra side that provided the greater measurement. FL was subsequently estimated using these measurements for all specimens as above.

Vertebra annuli were observed and measured by an experienced reader on the posterior centra of V35 and the anterior centra of V36. Annuli were interpreted as per Galtsoff (1952), Lee *et al.* (1983) and Rodríguez-Marín *et al.* (2006), such that one annulus was one groove (summer growth) and one ridge (winter growth). Because small growth increments and crowding at centrum edges result in difficulties differentiating BFT annuli at ages >8 (Rodríguez-Marín *et al.*, 2006), we adopted a conservative approach, measuring increment

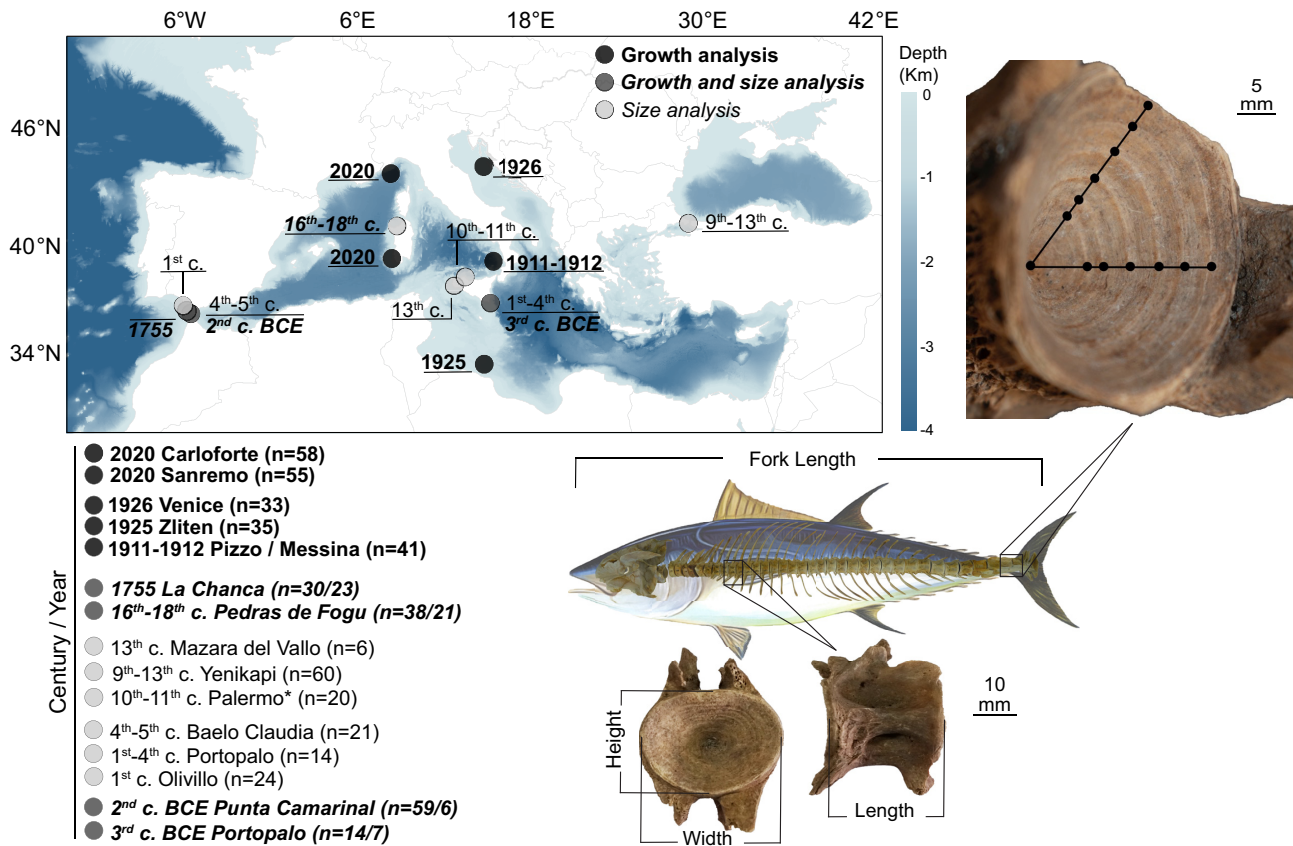


**Figure 1.** Map of modern, archival, and archaeological Atlantic bluefin tuna (*T. thynnus*) sample sites for length estimations (italic, light grey) and growth analyses (bold typeface, black) or both (italic boldface, dark grey). Map created using ESRI ArcMap (v.10.6, <https://arcgis.com>). Numbers (*n*) represent those used in growth analyses/length estimations. Points of annuli measurement (black dots) across distal and focal planes of vertebrae are illustrated using an example archaeological vertebra (35<sup>th</sup>) from 1755 CE Spain. The illustration indicates the FL measurements used and provides an example of a vertebra related to its vertebral position and measurements (height, width, and length) used to reconstruct FL. The scale bar (black bars) is an approximation only due to camera angle distortion. \*Palermo samples pertain to two different archaeological sites (see Supplementary Materials for details).

size between annuli 1–6 (Figure 1, Supplementary Figure S2). Staining was prohibited for the archaeological and archival samples, though experimentation with silver nitrate staining (Stevens, 1975) on modern specimens did not improve annuli readability. We found that illumination provided sufficient conditions for the interpretability of annuli by eye, which was occasionally further aided by rinsing centra with distilled water when annuli were less pronounced.

The study of archaeological and archived specimens also prohibited the cutting of vertebrae and thus increment size could not be measured using straight-edged digital callipers. The increment size was thus measured with specimens intact using a pair of dental callipers (curved, 20 mm max span) to the nearest 0.25 mm. The increment size was measured from the centrum apex (age 0), measuring to the outer winter ridge of the first annuli, then to the next outer winter ridge, and so on, thus recording annual growth from summer to summer. The increment size was measured and averaged across centrum focal and distal planes to account for variability in deformities, variability in the angle of measurement, and to ensure that annuli were complete throughout the centra following (Cullen *et al.*, 2021). Care was taken to avoid the measurement of false annuli, interpreted as being (1) less pronounced than annuli, (2) representing slower growth than expected, and (3) often not complete throughout the centrum. If annuli were not

clearly observed, the specimen was not used in analyses (8 out of 121, 6%, modern, and 24 out of 133, 18% archived specimens collected). Sample groups were measured under the same conditions in random order to ensure measurement accuracy was not biased by space or time. To assess the reproducibility of our dataset, a second reader measured the increment size as above for a subset of specimens (93 out of 372, 25%), which reported high levels of correlation ( $R^2 = 0.95$ ), and a measurement deviation of less than  $\pm 0.75$  mm.

### Growth estimation: statistical analyses

To statistically investigate significant differences in increment size at each age, we pooled samples into century groups (due to sample size limitations), applied one-way ANOVAs to V35 and V36 data separately, and interpreted the outputs using Tukey's Post-Hoc HSD test (except for the 3<sup>rd</sup>-2<sup>nd</sup> c. BCE samples due to small sample size). All statistical analyses were done using R v.4.1.3 (Team, 2013), thresholding significance at  $p < 0.05$ .

Variance in increment size was assessed using increasingly complex linear mixed-effects models (Morrongiello and Thresher, 2015) applied to V35 and V36 separately with the lmer function in the R package lme4 (Bates *et al.*, 2015). First, the optimal random model was determined: random effects

terms included intercept terms of the individual vertebra specimen (FishID), random effect term (Weisberg *et al.*, 2010), and sample (year, Table 1), and/or random slope terms of sample and age (of formation). Models were assessed using AICc (AIC corrected for small sample sizes, Burnham and Anderson, 2004) computed with the `model.sel` function in the `AICcmodavg` R package (Mazerolle, 2017). Mixed-effect models were then defined using the best-scoring random effect model, which included the intercept term FishID and slope of sample and age, for both the V35 and V36 dataset. Mixed-effect models were analysed for intrinsic effects and temporal effects, separately. First, intrinsic-effect models included vertebra length, width, or height (Figure 1). Second, temporal-effect models included sample or century. Century groupings combined 3<sup>rd</sup> c. BCE and 2<sup>nd</sup> c. BCE specimens together, and 1755 and 16<sup>th</sup>–18<sup>th</sup> c. specimens together. Full definition of random and mixed-effect terms can be found in the Supplementary (Supplementary Table S4). ANOVA and 95% confidence intervals were calculated for each model using the core functions `anova` and `confint` in R.

To qualitatively explore the influence of temperature on BFT growth, we collated a series of paleotemperature proxies and measurements to represent the spatiotemporal range of BFT statistically analysed. A western Mediterranean (Minorca Basin) sea surface temperature (SST) proxy was obtained from (Cisneros *et al.*, 2016), representing the stacked anomaly of 5 substrate core profiles. SST proxies were supplemented by the Hadley v4.1 SST northern Hemisphere anomaly for the years 1850–2021 CE (Kennedy *et al.*, 2019). Finally, a North Atlantic Oscillation (NAO) index proxy was obtained from (Faust *et al.*, 2016) and was supplemented by Hurrell's winter NAO index for the years 1865–2019 CE (Hurrell, 1995), which is presented as binned 3-year averages to maintain consistency with the temporal density of the NAO proxy. Temperature proxies and measurements were smoothed using the loess method in the `ggplot2` function `geom_smooth` in R and illustrated with 95% CIs.

To assess the effect of resorption of bone on increment size and the ability to compare vertebrae of different sizes or ages, we first investigated the correlation between (log) vertebra centrum length, width, height, and (log) increment size. Second, we downsampled the 2020 sample, which had a lower mean FL than the other sample groups (Table 1, Supplementary Figure S5). We therefore removed the bottom 50% of individual FLs for the 2020 group and present these data for comparison (Supplementary Figure S6). Third, we included centra dimensions in intrinsic-effect models, detailed above.

## Results

### Historical catch-at-size estimation

FL was estimated for a total of 286 individuals (archaeological vertebrae), which illustrates that 3<sup>rd</sup> c. BCE to 18<sup>th</sup> c. BFT captured in eastern Atlantic and Mediterranean locations were between 90–284 cm FL (Figure 2, left) and were predominantly smaller than those captured in trap fisheries during the 20<sup>th</sup> and 21<sup>st</sup> centuries (Figure 2, right). In general, archaeological catch-at-size estimates range greatly at each site, and between all sites a tri-modal distribution is observed, with no clear temporal or spatial trend where the majority of BFT are distributed around peaks at ca. 120, 180 and 210 cm FL. Although the data are comparatively few, we note the catch of

giant (250–300 cm FL) BFT in pre-Roman (Portopalo, Sicily) and Byzantine (Istanbul, Turkey) fisheries.

Pre-1950 ICCAT-collated BFT measurements (1915–1927) form a bi-modal distribution with peaks at ca. 110 and 220 cm FL (Figure 2, top right). BFT measured at these early 20<sup>th</sup> c. traps represent a similar range to those captured throughout the 20<sup>th</sup> and 21<sup>st</sup> c. trap fisheries; however, during the periods 1956–1980 and 1980–2000, there is a greater relative catch of small (<100 cm FL) and very large (250 cm FL) BFT compared with the mean size frequency of these groups. After 1980, spatial variation was observed, in that Mediterranean trap catches contain a greater relative presence of small individuals (Figure 2, right). This is likely to be an artefact of the data where few traps are active and are in eastern Atlantic and Mediterranean locations known to be predominated by smaller adult individuals, for example, Sardinia (Addis *et al.*, 2016; Secci *et al.*, 2021).

### Growth estimation

We produced a total of 1676 individual growth measurements across 372 samples spanning over two millennia and found that 21<sup>st</sup> c. BFT grew significantly ( $p < 0.03$ ) faster at ages 1 and 2 than in the 20<sup>th</sup> c., and 16<sup>th</sup>–18<sup>th</sup> c., and that 20<sup>th</sup> c. BFT grew significantly faster at age 2 than the in the 16<sup>th</sup>–18<sup>th</sup> c. (Figure 3, Table S3a and b). This pattern is consistent across both V35 and V36 and coincides with stepwise SST and NAO increases with each period (Figure 3c). In general, the 16<sup>th</sup>–18<sup>th</sup> c. period comprises mostly of a negative NAO phase (Figure 3c, bottom), while estimates of SST (Figure 3c, top) are variable, but like those during the 1911–1926 period our archived samples pertain to. The early 20<sup>th</sup> c. sample dates, however, correspond to a positive NAO phase, which becomes more extreme at the 21<sup>st</sup> c., when SST measurements suggest conditions were a lot warmer than during both the 16<sup>th</sup>–18<sup>th</sup>, and early 20<sup>th</sup> century.

Across all samples, growth generally and logically decreased with age, where the biggest decreases were observed between the ages 1, 2, and 3, corresponding to annuli size measurements of ca. 4–5, 2.5–3.5, and 2–2.5 mm, respectively (Figure 3a and b). The increment sizes were consistent between V35 and V36. However, using V35, we detected a significantly ( $p < 0.03$ ) slower growth at age 3 for the 16<sup>th</sup>–18<sup>th</sup> century group, and using V36, we detected a significantly faster growth for the 20<sup>th</sup> century group at age 4 (Figure 3a and b, Supplementary Table S3a, b). We observed a general pattern of similar but slower growth for the 3<sup>rd</sup>–2<sup>nd</sup> c. BCE group, compared with the remaining centuries. Large CIs and inconsistent patterns between V35 and V36 between the ages 3–6 hindered the interpretation of differences in growth between centuries, though growth between the ages 4–6 in 20<sup>th</sup> c. samples was increased compared with the remaining samples, and the general trajectory of the 21<sup>st</sup> c. samples was increased at ages 1, 2, and 3 but is decreased at ages 4, 5, and 6 (Figure 3a and b). Mean increment sizes, significance, and standard error bars for each sample group are presented in the Supplementary (Supplementary Figure S3, Table S3a and b).

Linear models with random effects (Supplementary Table S4, S5a) suggested that the variable century significantly explains increment size for the V35 ( $F = 5.6$ , 95% CI range:

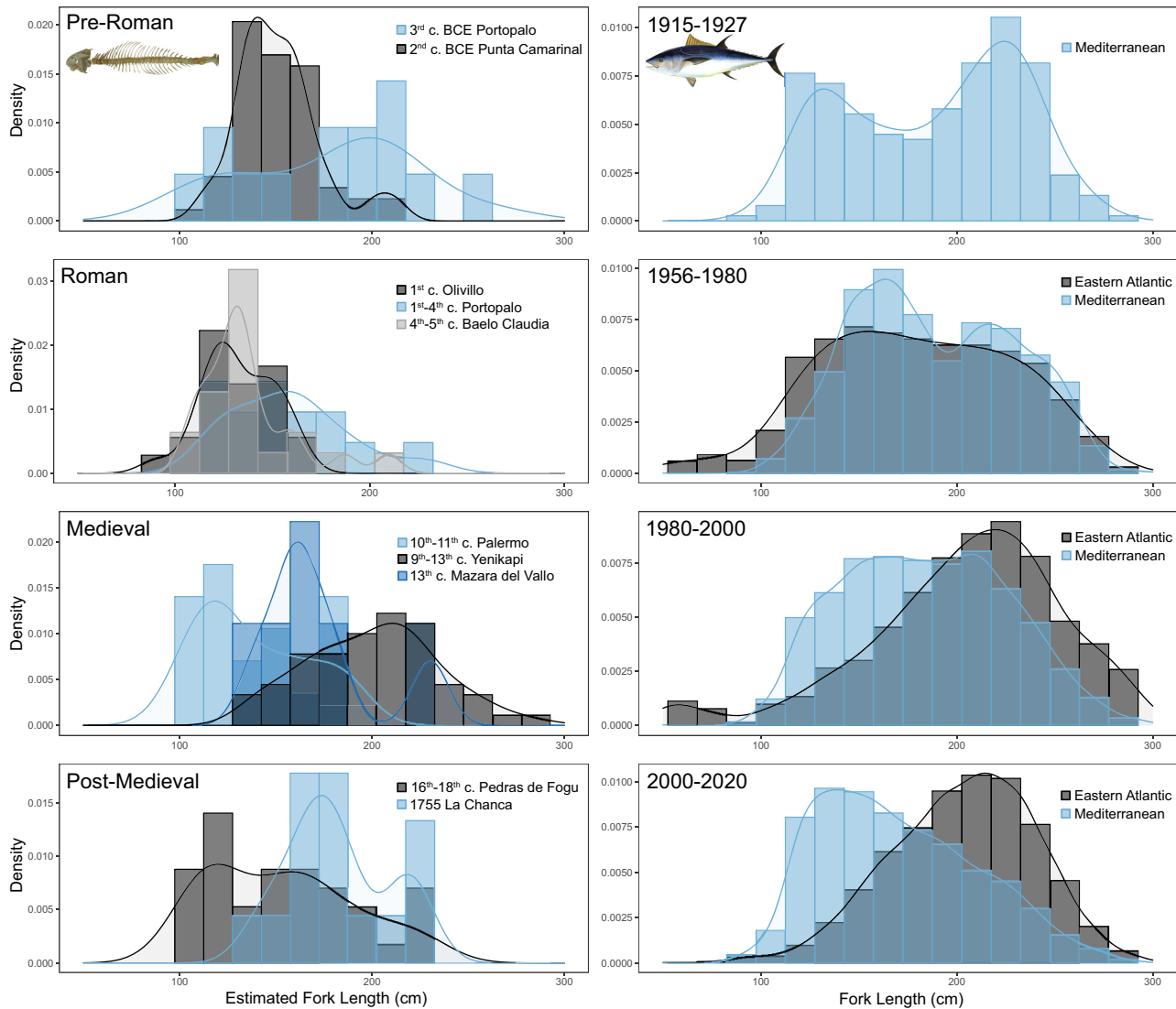


**Figure 2.** Size-at-capture density curves and histograms of estimated FL (cm) for archaeological Atlantic bluefin tuna (*T. thynnus*; BFT) vertebrae (left), shown per site and historical era (Pre-Roman, Roman, Medieval, Post-Medieval), and comparative density curves and histograms of BFT captured in trap fisheries, measured using straight FL from the ICCAT database and separated into multi-decadal groups (years CE). Each histogram size-class is 15 cm wide to approximately represent the ( $\pm 10\%$ ) error in the length estimation methods for archaeological specimens. Mediterranean archaeological sites and historical and modern trap data are illustrated in colour, whereas eastern Atlantic and Bosphorus archaeological sites and historical and modern trap data are illustrated in greyscale. For more details see Supplementary Table S2.

$-0.27, 0.08$ ) and V36 datasets ( $F = 9.6$ , 95% CI range  $-0.21, 0.23$ ), as does sample (year), but to a slightly lower extent for both the V35 ( $F = 3.5$ , 95% CI range:  $-0.65, 0.51$ ) and V36 dataset ( $F = 5.2$ , 95% CI range:  $-0.27, 0.23$ , Supplementary Table S5c). Linear models suggested no effect of vertebra length ( $F = 0.06-0.42$ , 95% CI range:  $-0.08, 0.16$ ), width ( $F = 0.14-0.79$ , 95% CI range:  $-0.08, 0.16$ ), or height ( $F = 0.05-0.17$ , 95% CI range:  $-0.12, 0.12$ ) on Increment size (Supplementary Table S5b), which was also supported by the low variance explained by vertebra dimensions on increment size across all ages ( $R^2 = 0.01$ , Supplementary Figure S3). By altering the size composition of the dataset (removing small 21<sup>st</sup> c. individuals), we noted no change in the interpretation of our results (Supplementary Figure S4).

## Discussion

### Temporal changes in BFT growth

Our results show that juvenile growth of BFT has sequentially and significantly increased between the 16<sup>th</sup>-18<sup>th</sup>, 20<sup>th</sup>, and 21<sup>st</sup> centuries. Our findings contradict those of Fromentin (2003), whose decrease in juvenile BFT weight-at-age appears not to be supported by the general trend of increasing juvenile fish growth over centuries found in the literature. We suspect this is because weight is a heavily variable trait, depending on sampling time, prey composition, and habitats foraged (Cort and Estruch, 2016). Likewise, we contradict evidence of no temporal change in BFT growth supposed by a century of length-at-age data (Cort *et al.*, 2014), probably because length-at-age studies used a variety of different elements and methods (Campana and Thorrold, 2001; Cullen *et al.*, 2021).

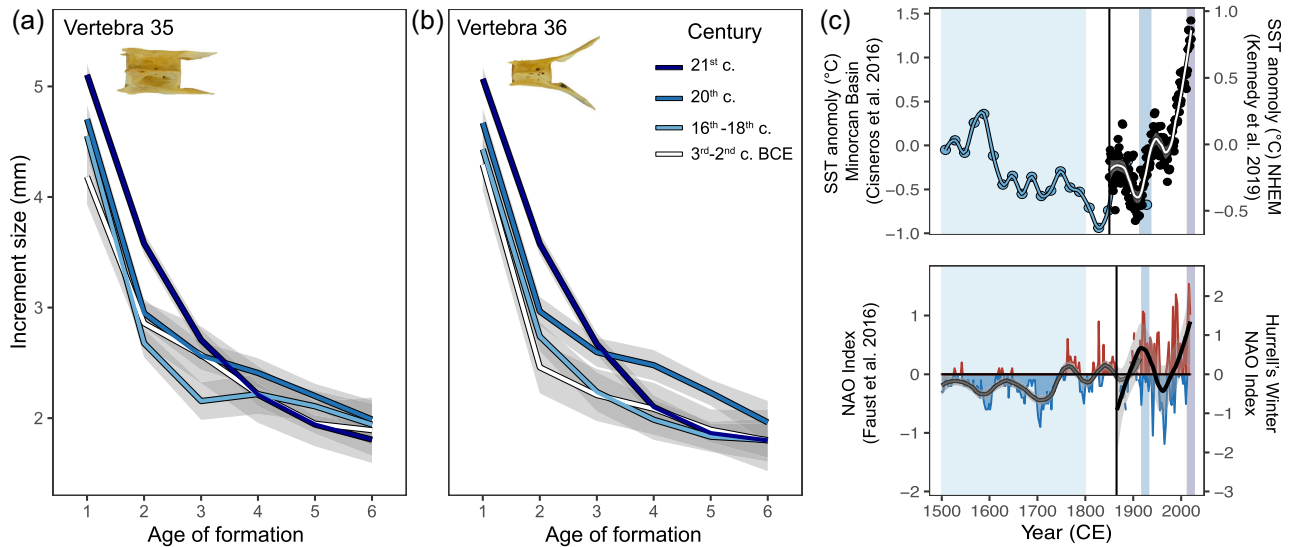


**Figure 3.** Temporal early-life growth estimates for Atlantic bluefin tuna (*T. thynnus*) using vertebra annuli measurements (a, b) and temperature proxies (c) for the Atlantic and Mediterranean presented as potential drivers of growth from the 16<sup>th</sup> c. to the present. (a, b) Smoothed increment sizes (mm) for each annuli (age of formation) measured in the 35<sup>th</sup> (a) and 36<sup>th</sup> (b) vertebrae (insets) are illustrated per “century” grouping, using the loess method `geom_smooth` function in R, grey shading indicates 95% confidence intervals. (c) The temperature proxies, collated between the years 1500–2019 CE (at the top panel) are; a SST proxy (blue dots and line, Cisneros *et al.*, 2016) and measurements (black dots, white line, Kennedy *et al.*, 2019) for the western Mediterranean and averages across the northern Hemisphere, respectively; and (at the bottom panel) a NAO proxy (grey line, Faust *et al.*, 2016) and Hurrell’s Winter NAO Index (black line, Hurrell, 1995), positive values red, negative values blue: bottom panel, presented as smoothed using the same method as (a, b). Century sample time-points are indicated as whiskers between panels, and dashed lines (approximate sample dates: top, bottom panels) matching colours in b, using 1755 CE for the 16<sup>th</sup>–18<sup>th</sup> c. group, though the dating of the entire group is defined as between 16<sup>th</sup> and 18<sup>th</sup> century.



**Figure 4.** Depictions of Atlantic bluefin tuna (*T. thynnus*) from various artists, cropped to illustrate catch-at-size in (a) an ancient Greek era (6<sup>th</sup> c. BCE) vase exhibited at the State Museum of Berlin (Germany), (b) 13<sup>th</sup> c. engraving depicting a tuna trap at Zahara de los Atunes (Spain) © Fundación Casa Medina Sidonia, (c) 16<sup>th</sup> c. engraving depicting a tuna trap at Cadiz (Spain) by the artist Georg Hoefnagel in 1572, (d) 18<sup>th</sup> c. engraving depicting a tuna trap at Trapani (Sicily, Italy) by the artist Jean-Pierre Louis Laurent Houël in (1782) and (e), an early 20<sup>th</sup> c. print in the newspaper “La Domenica del Corriere,” published in Milan (Italy), 8<sup>th</sup> June 1900, depicting a tuna trap at Isola Piana (Sardinia, Italy). Depictions can be observed in full in Di Natale (2012).

Increased juvenile fish growth has been associated with increased temperature and decreased stock biomass in paleoecological studies on marine fishes (Geffen *et al.*, 2011; van der Sleen *et al.*, 2016; Denechaud *et al.*, 2020; Smoliński *et al.*, 2020; Vieira *et al.*, 2020; Pedersen *et al.*, 2022), supporting long-observed monthly and yearly trends that higher temperatures increase primary productivity (Moreno *et al.*, 2004) and the metabolic rate of fishes, while decreased com-

petition at lower population densities increases fish growth (Brett, 1979; Beverton, 1995). A recent modelling study supports that BFT growth has increased during the past 60 years, driven by warming temperatures (Zhou, 2022). We find it equally plausible that recent increased growth at age 1 may reflect earlier spawning ontogenies because growth is enhanced during spring and summer months when BFT spawn (Mather *et al.*, 1995; Medina, 2020). This is a theory deserving of inves-



tigation due to its temperature-driven component (Fiksen and Reglero, 2022) and consequences on the reproductive output of BFT as a multiple-batch spawner (Medina, 2020).

In the closely-related southern bluefin tuna, increased juvenile growth was observed during 1960–90s, and was purportedly tightly linked with a reduction in biomass, rather than temperature (Jenkins *et al.*, 1991; Farley and Gunn, 2007). Indeed, early-life biomass will be even more reduced in size-truncated stocks since reproductive output scales strongly with body size (Medina, 2020). While we have no information on the biomass of eastern BFT during the 16<sup>th</sup>–18<sup>th</sup> c. and the early 20<sup>th</sup> c., it is reasonable to assume that BFT biomass has sequentially decreased in recent centuries due to the intensive trap catches and expansion of their fisheries into the Atlantic during the 19<sup>th</sup> c., and the extreme overexploitation that occurred especially during the late 20<sup>th</sup> c. (Porch *et al.*, 2019). While the eastern stock has recovered to 1970s levels in recent years, we suspect that it remains decreased from early 20<sup>th</sup> c. and pre-industrial levels both in abundance and mean body size (Andrews *et al.*, 2022b). Therefore, while increasing ocean temperatures and the prevalence of positive NAO phases coincide with the increases in juvenile we observed, we are unable to disentangle these effects from stock biomass, or indeed any other covariate for which data is unavailable, such as the eastern Mediterranean Transient, prey abundance, or predation (Di Natale *et al.*, 2017; Smoliński, 2019).

FIE is expected to, and has been shown to, increase juvenile growth and decrease mature growth due to an energetic trade-off favouring earlier maturation and increased reproductive investment management (Law, 2000; Edeline *et al.*, 2007; Jørgensen *et al.*, 2007; Mollet *et al.*, 2007; Swain *et al.*, 2007; Neuheimer and Taggart, 2010; Saura *et al.*, 2010; Enberg *et al.*, 2012; Hollins *et al.*, 2018). FIE is therefore another potential explanator of increases in juvenile growth between the 16<sup>th</sup>–21<sup>st</sup> century. Given that we observed similar BFT growth between centuries at ages 4–6 (the first ages affected by reproductive investment), our data suggest that evolutionary forcing on BFT mature growth during the past five centuries related to size-selective harvesting is less likely. Although, as is often the case with limited paleoecological data and methods, these results must be interpreted with caution.

Increased growth, associated with plasticity responses to favourable environmental conditions, could, in theory, cancel out evolutionary size-selective harvesting effects; which decrease mature growth (Swain *et al.*, 2007; Heino *et al.*, 2008; Hutchings and Kuparinen, 2021). Furthermore, we cannot exclude the possibility that our methods, which necessarily limited our sample size and measurement precision, hindered the observation of a decrease in growth. Indeed, we observe a (non-significant) decrease in growth at ages 4–6 between the 20<sup>th</sup> and 21<sup>st</sup> c. but not between the 16<sup>th</sup>–18<sup>th</sup> c. and the 20<sup>th</sup> c., which appears to support our archaeological size estimations, such that large BFT were not preferentially extracted during the pre-industrial era. Given that the early 20<sup>th</sup> c. IC-CAT size-frequency data resemble those of the latter 20<sup>th</sup> c., stock age or size composition had likely not been truncated by the early 20<sup>th</sup> century. Whereas by the 21<sup>st</sup> c., it appears to have been (Fromentin, 2009; MacKenzie *et al.*, 2009; Siskey *et al.*, 2016b).

Therefore, FIE may have indeed decreased growth for 21<sup>st</sup> c. ages 4–6 BFT, acting against enhanced growth at these ages as observed in the 20<sup>th</sup> c. BFT, which would be driven by

other factors like temperature and biomass as for juvenile growth, or others such as skipped-spawning, which impact growth at reproductive ages (Jørgensen *et al.*, 2006; Aarestrup *et al.*, 2022). This pattern of increased juvenile growth and decreased mature growth is not unique to BFT among over-exploited fish stocks (Smoliński *et al.*, 2020), and is deserving of careful consideration if we are to disentangle plastic and evolutionary effects on fish growth.

### Smaller catch-at-size for the pre-industrial era

Our catch-at-size estimates preclude assessments of stock size structure because of estimation error ( $\pm 10\%$  FL), small sample size, and biases associated with archaeological recoveries (which sites and vertebra were available to study, and the number of fishing episodes they represent). Rather than being population-representative size-frequency data, instead these data inform us that prior to the 19<sup>th</sup> c., BFT catch-at-size was likely smaller than during the 20<sup>th</sup> and 21<sup>st</sup> c., which consequently implies that BFT exploitation was less intense prior to the 19<sup>th</sup> century. Historical depictions of BFT appear to support this thesis of a predominantly ca. 150 cm FL catch-at-size between ancient Greek and post-Medieval times (Figure 4 a–d), whereas BFT are depicted noticeably larger (ca. 200 cm FL), from the mid-19<sup>th</sup> c. onwards (Figure 4e). Indeed, this trend is consistent across scores of depictions summarized in Di Natale (2012).

We postulate that in locations other than narrow channels (e.g. the Bosphorus), where large BFT (>200 cm FL) were well-known to frequent and migrate close to coasts (Cort *et al.*, 2013), large BFT were not routinely targeted and captured prior to the 19<sup>th</sup> c., probably due to gear or worker limitations and market demand. From the Phoenician era onwards the predominant method of BFT capture in the Mediterranean was via tuna trap (for a review see García Vargas and Florido Corral 2007), which were nets fixed or cast perpendicular to coasts, which intercepted migrations of BFT. During the 19<sup>th</sup> and 20<sup>th</sup> c., we postulate that tuna traps were extended further from the shore, facilitating the capture of deeper-migrating individuals. We suggest that at the sites studied herein, the largest BFT were not targeted due to the use of traps cast from the shore, or fixed in shallower waters where smaller BFT predominate (Mather *et al.*, 1995; Wilson and Block, 2009), but we cannot exclude the unlikely possibility other capture methods used for millennia such as handlines and driftnets, which would also target smaller, inshore individuals (Andrews *et al.*, 2022b).

We cannot rule out that the largest BFT bones were discarded on beaches, and are not represented in the archaeological record, or simply that large BFT did not migrate to the sites studied. Two of the sites studied (2<sup>nd</sup> c. BCE Punta Camarinal and 16<sup>th</sup>–18<sup>th</sup> c. Pedras de Fogu) were indeed processing centres directly on the back of beaches where BFT were captured, yet these sites did not yield large BFT. Sardinian sites (such as 16<sup>th</sup>–18<sup>th</sup> c. Pedras de Fogu) are however predominated by smaller BFT in modern traps (Addis *et al.*, 2016; Secci *et al.*, 2021), so clearly, archaeological approaches like ours limited by the number of individuals and sites require cautious interpretation. We suggest that further exploration of catch-at-size at additional post-medieval trap sites, especially during the 19<sup>th</sup> c., would better define the onset of a more-intense fixed trap fishery when large BFT were fished in greater frequency.

## Study limitations

Due to the challenges of working with temporal samples, and the methods we were limited to, we could not produce growth rates to compare with other studies. Though our growth trajectories certainly resemble those of modern samples (e.g. Megalofonou and De Metrio 2000), the methods we employed of measuring intact vertebrae up to age 6, result in reliable intra-study assessments of growth at each age only. Temporal studies of well-preserved otoliths will be required to estimate archaeological growth rates for BFT (e.g. Denechaud *et al.* 2020, Smoliński *et al.* 2020, Vieira *et al.* 2020). The use of otoliths will also aid in removing uncertainties about vertebra resorption. We found that increment size was not influenced by vertebra size, which on the one hand implies that annuli widths are not modified to a detectable level during resorption in BFT, but on the other hand that increment increases do not necessarily translate to increases in size for the whole vertebra and therefore FL. One explanation may be that increases in juvenile growth are met with decreased mature growth (see Smoliński 2019). It is possible we have largely escaped the effects of resorption due to working mostly with samples at early-life stages, since resorption has been shown to increase with age in BFT fin-spines (Santamaria *et al.*, 2015). Given that western and eastern BFT growth is not statistically different (Stewart *et al.*, 2022), it is unlikely that temporal trends were conflated by spatial differences within the eastern stock—though we cannot rule this out entirely. We attempted to limit spatial effects by collecting samples caught in relatively similar locations, and by pooling samples into century groupings. Albeit, no consistent spatial growth patterns have been observed in eastern BFT (Restrepo *et al.*, 2007; Cort *et al.*, 2014), likely as a result of wide-ranging migrations from age 1 (Dickhut *et al.*, 2009).

## Conclusion

In summary, we provide novel evidence that BFT juvenile growth significantly increased between the 16<sup>th</sup>–18<sup>th</sup>, 20<sup>th</sup>, and 21<sup>st</sup> centuries and is correlated with warming SST's and NAO phases, and probably a decrease in stock biomass. An equally plausible explanation is that FIE contributed to increases in juvenile growth in favour of earlier maturation for the 20<sup>th</sup> and 21<sup>st</sup> century. Indeed, we found sparse evidence to suggest a long history of large (>200 cm FL) BFT capture. Rather, we postulate that size-selective fishing of BFT occurred from ca. 19<sup>th</sup> century onwards when tuna traps were set further from the shore, and offshore fisheries developed. BFT growth remains a complex issue in need of further exploration to better define the onset of exploitation impacts and therefore, the recovery of the eastern BFT stock. Specifically, further study is required using fine-scale methods, that is, biochronological analyses of otoliths and adaptation genomics from 1900 onwards, to determine whether FIE is the driver of growth changes we observed between the early 20<sup>th</sup> and 21<sup>st</sup> century.

## Acknowledgements

We would like to thank ICCAT and the GBYP Project, for collating and making available a database of BFT size records. Thanks to Jose Luis Cort for inspiration and assistance with size-at-age equations. Thanks to Ana Rita Viera for advice on linear modelling. Finally, we thank Emma Falkeid Eriksen for

thoughtful discussions and the reviewers who improved the quality of this manuscript.

## Supplementary Material

Supplementary material is available at the ICESJMS online version of the manuscript.

## Data availability statement

Size estimation data is available in the Supplementary File Table S1. Raw growth data is available from the corresponding authors upon reasonable request.

## Author contributions

A.J.A. designed the study. All authors collected samples for the study. A.J.A. performed the laboratory work. A.J.A. performed the statistical analyses. A.J.A., A.M.M., and F.T. wrote the paper. All authors reviewed the paper.

## Funding

This work is a contribution to the <https://tunaarchaeology.org> project within the framework of the MSCA SeaChanges ITN, which was funded by EU Horizon 2020 (Grant Number: 813383). This work also benefited from Spanish Ministry of Science funding (Grant Number: PID2020-118662GB-I00).

## Conflicts of interest

The authors declare no conflicts of interest exist.

## References

- Aarestrup, K., Baktoft, H., Birnie-Gauvin, K., Sundelöf, A., Cardinale, M., Quilez-Badia, G., Onandia, I. *et al.* 2022. First tagging data on large Atlantic bluefin tuna returning to Nordic waters suggest repeated behaviour and skipped spawning. *Scientific reports*, 12: 11772.
- Addis, P., Secci, M., Pishedda, M., Laconcha, U., and Arrizabalaga, H. 2014. Geographic variation of body morphology of the Atlantic bluefin tuna, (*Thunnus thynnus*, Linnaeus, 1758). *Journal of Applied Ichthyology*, 30: 930–936.
- Addis, P., Secci, M., Biancacci, C., Loddò, D., Cuccu, D., Palmas, F., and Sabatini, A. 2016. Reproductive status of Atlantic bluefin tuna, *thunnus thynnus*, during migration off the coast of Sardinia (western Mediterranean). *Fisheries research*, 181: 137–147.
- Andrews, A. J., Mylona, D., Rivera-Charún, L., Winter, R., Onar, V., Sidiq, A. B., Tinti, F. *et al.* 2022a. Length estimation of Atlantic bluefin tuna (*Thunnus thynnus*) using vertebrae. *International Journal of Osteoarchaeology*, 32:645–653.
- Andrews, A. J., Di Natale, A., Bernal-Casasola, D., Aniceti, V., Onar, V., Oueslati, T., Theodropoulou, T. *et al.* 2022b. Exploitation history of Atlantic bluefin tuna in the eastern Atlantic and Mediterranean—insights from ancient bones. *ICES Journal of Marine Science*, 79: 247–262.
- Barrett, J. H. 2019. An environmental (pre)history of European fishing: past and future archaeological contributions to sustainable fisheries. *Journal of Fish Biology*, 94: 1033–1044.
- Bates, D., Mächler, M., Bolker, B., and Walker, S. 2015. Fitting linear mixed-effects models using lme4. *Journal Statistical. Software*, 67: 1–48.
- Beverton, R. J. H. 1995. Spatial limitation of population size; the concentration hypothesis. *Netherlands Journal of Sea Research*, 34: 1–6.

- Bolle, L. J., Rijnsdorp, A. D., van Neer, W., Millner, R. S., van Leeuwen, P. I., Ervynck, A., Ayers, R. *et al.* 2004. Growth changes in plaice, cod, haddock and saithe in the North Sea: a comparison of (post-)medieval and present-day growth rates based on otolith measurements. *Journal of Sea Research*, 51: 313–328.
- Brett, J. R. 1979. Environmental factors and growth. *Fish Physiology*, Vol. VIII. Bioenergetics and Growth. 599–677, Academic Press. New York, USA.
- Burnham, K. P., and Anderson, D. R. 2004. Multimodel inference: understanding AIC and BIC in model selection. *Sociological Methods and Research*, 33: 261–304.
- Campana, S. E. 1990. How reliable are growth back-calculations based on otoliths? *Canadian Journal of Fisheries and Aquatic Sciences*, 47: 2219–2227.
- Campana, S. E., and Thorrold, S. R. 2001. Otoliths, increments, and elements: keys to a comprehensive understanding of fish populations? *Canadian Journal of Fisheries and Aquatic Sciences*, 58: 30–38.
- Cisneros, M., Cacho, I., Frigola, J., Canals, M., Masqué, P., Martrat, B., Casado, M. *et al.* 2016. Sea surface temperature variability in the central-western Mediterranean Sea during the last 2700 years: a multi-proxy and multi-record approach. *Climate of the Past*, 12: 849–869.
- Corriero, A., Karakulak, S., Santamaria, N., Deflorio, M., Spedicato, D., Addis, P., Desantis, S. *et al.* 2005. Size and age at sexual maturity of female bluefin tuna (*Thunnus thynnus* L. 1758) from the Mediterranean Sea. *Journal of Applied Ichthyology*, 21: 483–486.
- Cort, J. L. 1989. *Biología y pesca del atún rojo, Thunnus thynnus* (L.), del Mar Cantábrico. Doctoral Thesis. Universidad Complutense de Madrid. Madrid, Spain.
- Cort, J. L. 2003. Age and growth of the bluefin tuna (*Thunnus thynnus*) of the Northeast Atlantic. *Cahiers Options Méditerranéennes (CIHEAM)*, 60: 45–49.
- Cort, J. L., Deguara, S., Galaz, T., Mèlich, B., Artetxe, I., Arregi, I., Neilson, J. *et al.* 2013. Determination of L max for Atlantic bluefin Tuna, *Thunnus thynnus* (L.), from meta-analysis of published and available biometric data. *Reviews in Fisheries Science*, 21: 181–212.
- Cort, J. L., Arregui, I., Estruch, V. D., and Deguara, S. 2014. Validation of the growth equation applicable to the Eastern Atlantic bluefin tuna, *Thunnus thynnus* (L.), using Lmax, tag-recapture, and first dorsal spine analysis. *Reviews in Fisheries Science & Aquaculture*, 22: 239–255.
- Cort, J. L., and Estruch, V. D. 2016. Analysis of the length–weight relationships for the Western Atlantic Bluefin Tuna, *Thunnus thynnus* (L.). *Reviews in Fisheries Science & Aquaculture*, 24: 126–135.
- Cullen, T. M., Brown, C. M., Chiba, K., Brink, K. S., Makovicky, P. J., and Evans, D. C. 2021. Growth variability, dimensional scaling, and the interpretation of osteohistological growth data. *Biology Letters*, 17: 20210383.
- Czorlich, Y., Aykanat, T., Erkinaro, J., Orell, P., and Primmer, C.R., 2022. Rapid evolution in salmon life history induced by direct and indirect effects of fishing. *Science*, 376: 420–423.
- Denechaud, C., Smoliński, S., Geffen, A. J., Godiksen, J. A., and Campana, S. E. 2020. A century of fish growth in relation to climate change, population dynamics and exploitation. *Global Change Biology*, 26: 5661–5678.
- Dickhut, R. M., Deshpande, A. D., Cincinelli, A., Cochran, M. A., Coriolini, S., Brill, R. W., Secor, D. H. *et al.* 2009. Atlantic bluefin tuna (*Thunnus thynnus*) population dynamics delineated by organochlorine tracers. *Environmental Science & Technology*, 43: 8522–8527.
- Di Natale. 2012. The iconography of tuna traps: essential information for the understanding of the technological evolution of this ancient fishery. *Col. Vol. Sci. Pap. ICCAT*, 67: 33–74.
- Di Natale, A. 2014. The ancient distribution of bluefin tuna fishery: how coins can improve our knowledge. *Col. Vol. Sci. Pap. ICCAT*, 70: 2828–2844.
- Di Natale, A., Tensek, S., and Paga, G. A. 2017. The disappearance of young-of-the-year bluefin tuna from The Mediterranean Coast in 2016: is it an effect of The climate change. *Col. Vol. Sci. Pap. ICCAT*, 74: 2850–2860.
- Edeline, E., Carlson, S. M., Stige, L. C., Winfield, I. J., Fletcher, J. M., James, J. B., Haugen, T. O. *et al.* 2007. Trait changes in a harvested population are driven by a dynamic tug-of-war between natural and harvest selection. *Proceedings of the National Academy of Sciences of the United States of America*, 104: 15799–15804.
- Enberg, K., Jørgensen, C., Dunlop, E. S., Varpe, Ø., Boukal, D. S., Baulier, L., Eliassen, S. *et al.* 2012. Fishing-induced evolution of growth: concepts, mechanisms and the empirical evidence. *Marine Ecology*, 33: 1–25.
- Farley, J. H., and Gunn, J. S. 2007. Historical changes in juvenile southern bluefin tuna *Thunnus maccoyii* growth rates based on otolith measurements. *Journal of Fish Biology*, 71: 852–867.
- Faust, J. C., Fabian, K., Milzer, G., Giraudeau, J., and Knies, J. 2016. Norwegian fjord sediments reveal NAO related winter temperature and precipitation changes of the past 2800 years. *Earth and Planetary Science Letters*, 435: 84–93.
- Fiksen, Ø., and Reglero, P. 2022. Atlantic bluefin tuna spawn early to avoid metabolic meltdown in larvae. *Ecology*, 103: e03568.
- Fromentin, J.-M. 2003. The East Atlantic and Mediterranean bluefin tuna stock management: uncertainties and alternatives. *Scientia Marina*, 67: 51–62.
- Fromentin, J.-M. 2009. Lessons from the past: investigating historical data from bluefin tuna fisheries. *Fish and Fisheries*, 10: 197–216.
- Galtsoff, P. S. 1952. Staining of growth rings in the vertebrae of Tuna (*Thunnus thynnus*). *Copeia*, 1952: 103–105.
- García Vargas, E., and Florido Corral, D. 2007. *The origin and development of tuna fishing nets (Almadrabas)*. In *Proceedings of the International Workshop on Ancient Nets and Fishing Gear in Classical Antiquity. A First Approach*. 205–227. Ed. by T. Bekker-Nielsen, and D. Bernal-Casasola Aarhus – Cádiz.
- Geffen, A. J., Høie, H., Folkvord, A., Hufthammer, A. K., Andersson, C., Ninnemann, U., Pedersen, R. B. *et al.* 2011. High-latitude climate variability and its effect on fisheries resources as revealed by fossil cod otoliths. *ICES Journal of Marine Science: Journal du Conseil*, 68: 1081–1089.
- Giorgi, F. 2006. Climate change hot-spots. *Geophysical Research Letters*, 33: 1–4.
- Guillaud, E., Elleboode, R., Mahé, K., and Béarez, P. 2017. Estimation of age, growth and fishing season of a palaeolithic population of grayling (*Thymallus thymallus*) using scale analysis. *International Journal of Osteoarchaeology*, 27: 683–692.
- Gunn, J. S., Clear, N. P., Carter, T. I., Rees, A. J., Stanley, C. A., Farley, J. H., and Kalish, J. M. 2008. Age and growth in southern bluefin tuna, *Thunnus maccoyii* (Castelnau): direct estimation from otoliths, scales and vertebrae. *Fisheries Research*, 92: 207–220.
- Heino, M., Baulier, L., Boukal, D. S., Dunlop, E. S., Eliassen, S., Enberg, K., Jørgensen, C. *et al.* 2008. Evolution of growth in Gulf of St Lawrence cod? *Proceedings of the Royal Society B: Biological Sciences*, 275: 1111–1112.
- Hollins, J., Thambithurai, D., Koeck, B., Crespel, A., Bailey, D. M., Cooke, S. J., Lindström, J. *et al.* 2018. A physiological perspective on fisheries-induced evolution. *Evolutionary applications*, 11: 561–576.
- Hurrell, J. W. 1995. Decadal trends in the north Atlantic oscillation: regional temperatures and precipitation. *Science*, 269: 676–679.
- Hutchings, J. A., and Kuparinen, A. 2021. Throwing down a genomic gauntlet on fisheries-induced evolution. *Proceedings of the National Academy of Sciences of the United States of America*, 118: e2105319118.
- ICCAT. 2007. Report of the 2006 Atlantic bluefin tuna stock assessment session. *Col. Vol. Sci. Pap. ICCAT*, 60: 652–880.
- Jenkins, G. P., Young, J. W., and Davis, T. L. O. 1991. Density dependence of larval growth of a marine fish, the southern bluefin tuna, *Thunnus maccoyii*. *Canadian Journal of Fisheries and Aquatic Sciences*, 48: 1358–1363.
- Jørgensen, C., Ernande, B., Fiksen, Ø., and Dieckmann, U. 2006. The logic of skipped spawning in fish. *Canadian Journal of Fisheries and Aquatic Sciences*, 63: 200–211.

- Jørgensen, C., Enberg, K., Dunlop, E. S., Arlinghaus, R., Boukal, D. S., Brander, K., Ernande, B. *et al.* 2007. Ecology: managing evolving fish stocks. *Science*, 318: 1247–1248.
- Kennedy, J. J., Rayner, N. A., Atkinson, C. P., and Killick, R. E. 2019. An ensemble data set of sea surface temperature change from 1850: the met office Hadley centre HadSST4.0.0.0 data set. *Journal of Geophysical Research*, 124: 7719–7763.
- Landa, J., Rodríguez-Marín, E., Luque, P. L., Ruiz, M., and Quelle, P. 2015. Growth of bluefin tuna (*Thunnus thynnus*) in the North-eastern Atlantic and Mediterranean based on back-calculation of dorsal fin spine annuli. *Fisheries Research*, 170: 190–198.
- Law, R. 2000. Fishing, selection, and phenotypic evolution. *ICES Journal of Marine Science: Journal du Conseil*, 57: 659–668.
- Lee, D.W., Prince, E.D., and Crow, M.E., 1983. Interpretation of growth bands on vertebrae and otoliths of Atlantic bluefin tuna, *Thunnus thynnus*. In *Proceedings of the International Workshop on Age Determination of Oceanic Pelagic Fishes: Tunas, Billfishes, and Sharks*, 8: 61–70. US Dep. Commer., NOAA Technical Report NMFS. Washington D.C., USA.
- Lotze, H. K., Hoffmann, R., and Erlandson, J. 2014. Lessons from historical ecology and management. In *The Sea, Volume 19: Ecosystem-Based Management*. Harvard University Press. Massachusetts, USA.
- MacKenzie, B. R., Mosegaard, H., and Rosenberg, A. A. 2009. Impending collapse of bluefin tuna in the northeast Atlantic and Mediterranean. *Conservation letters*, 2: 26–35.
- Maschner, H. D. G., Betts, M. W., Reedy-Maschner, K. L., and Trites, A. W. 2008. A 4500-year time series of Pacific cod (*Gadus macrocephalus*) size and abundance: archaeology, oceanic regime shifts, and sustainable fisheries. *Fishery Bulletin*, 104: 386–394.
- Mather, F. J., Mason, J. M., and Jones, A. C. 1995. . NOAA Technical Memorandum NMFS-SEFSC-370. National Oceanic and Atmospheric Administration. 165. <https://repository.library.noaa.gov/view/noaa/8461>. (last accessed October 1, 2022).
- Mazerolle. 2017. AICcmodavg: model selection and multimodel inference based on (Q) AIC (c) (version 1.28). R Package. <https://cran.r-project.org/web/packages/AICcmodavg/AICcmodavg.pdf>. (last accessed October 1, 2022).
- Medina, A. 2020. Reproduction of Atlantic bluefin tuna. *Fish and Fisheries*, 21: 1109–1119.
- Megalofonou, P., and De Metrio, G. 2000. Age estimation and annulus formation in dorsal spines of juvenile bluefin tuna, *Thunnus thynnus*, from the Mediterranean Sea. *Journal of the Marine Biological Association of the United Kingdom*, 80: 753–754.
- Mollet, F. M., Kraak, S. B. M., and Rijnsdorp, A. D. 2007. Fisheries-induced evolutionary changes in maturation reaction norms in North Sea sole *Solea solea*. *Marine Ecology Progress Series*, 351: 189–199.
- Moreno, A., Cacho, I., Canals, M., Grimalt, J. O., and Sanchez-Vidal, A. 2004. Millennial-scale variability in the productivity signal from the Alboran Sea record, Western Mediterranean Sea. *Palaeogeography, Palaeoclimatology, Palaeoecology*, 211: 205–219.
- Morrongiello, J. R., and Thresher, R. E. 2015. A statistical framework to explore ontogenetic growth variation among individuals and populations: a marine fish example. *Ecological Monographs*, 85: 93–115.
- Murua, H., Rodríguez-Marín, E., Neilson, J. D., Farley, J. H., and Juan-Jordá, M. J. 2017. Fast versus slow growing tuna species: age, growth, and implications for population dynamics and fisheries management. *Reviews in Fish Biology and Fisheries*, 27: 733–773.
- Neilson, J. D. N., and Campana, S. E. C. 2008. A validated description of age and growth of western Atlantic bluefin tuna (*Thunnus thynnus*). *Canadian Journal of Fisheries and Aquatic Sciences*, 65, 1523–1527.
- Neuheimer, A. B., and Taggart, C. T. 2010. Can changes in length-at-age and maturation timing in Scotian Shelf haddock (*Melanogrammus aeglefinus*) be explained by fishing? *Canadian Journal of Fisheries and Aquatic Sciences*, 67: 854–865.
- Ólafsdóttir, G. Á., Pétursdóttir, G., Bárðarson, H., and Edwardsson, R. 2017. A millennium of north-east Atlantic cod juvenile growth trajectories inferred from archaeological otoliths. *PLoS ONE*, 12: e0187134.
- Pagá Garcia, A., Palma, C., Di Natale, A., Tensek, S., Parrilla, A., and de Bruyn, P. 2017. Report on revised trap data recovered by ICCAT GBYP from phase 1 to phase 6. *Col. Vol. Sci. Pap. ICCAT*, 73: 2074–2098.
- Pedersen, T., Amundsen, C., and Wickler, S. 2022. Characteristics of early Atlantic cod (*Gadus morhua* L.) catches based on otoliths recovered from archaeological excavations at medieval to early modern sites in northern Norway. *ICES Journal of Marine Science: Journal du Conseil*, 79, 2667–2681.
- Pinsky, M. L., Eikeset, A. M., Helmersen, C., Bradbury, I. R., Bentzen, P., Morris, C., Gondek-Wyrozemska, A. T. *et al.* 2021. Genomic stability through time despite decades of exploitation in cod on both sides of the Atlantic. *Proceedings of the National Academy of Sciences of the United States of America*, 118:e2025453118.
- Plank, M. J., Allen, M. S., Nims, R., and Ladefoged, T. N. 2018. Inferring fishing intensity from modern and archaeological size-frequency data. *Journal of Archaeological Science*, 93: 42–53.
- Porch, C. E., Bonhommeau, S., Diaz, G. A., Haritz, A., and Melvin, G. 2019. The journey from overfishing to sustainability for Atlantic bluefin tuna, *Thunnus thynnus*. In *The future of bluefin tunas: ecology, fisheries management, and conservation*, pp.3–44. Johns Hopkins University Press. Maryland, USA.
- Restrepo, V. R., Rodríguez-Marín, E., Cort, J. L., and Rodríguez-Cabello, C. 2007. Are the growth curves currently used for Atlantic bluefin tuna statistically different? *Col. Vol. Sci. Pap. ICCAT*, 60: 1014–1026.
- Rodrigues, A. S. L., Monsarrat, S., Charpentier, A., Brooks, T. M., Hoffmann, M., Reeves, R., Palomares, M. L. D. *et al.* 2019. Unshifting the baseline: a framework for documenting historical population changes and assessing long-term anthropogenic impacts. *Philosophical transactions of the Royal Society of London. Series B, Biological sciences*, 374: 20190220.
- Rodríguez-Marín, E., Olafsdóttir, D., Valeiras, J., Ruiz, M., Chosson-Pampoulie, V., and Rodríguez-Cabello, C. 2006. Ageing comparison from vertebrae and spines of bluefin tuna (*Thunnus thynnus*) coming from the same specimen. *Col. Vol. Sci. Pap. ICCAT*, 59: 868–876.
- Rodríguez-Marín, E., Clear, N., Cort, J. L., Megalofonou, P., Neilson, J. D., dos Santos, M. N., Olafsdóttir, D. *et al.* 2007. Report of the 2006 ICCAT workshop for bluefin tuna direct ageing. *Col. Vol. Sci. Pap. ICCAT*. 60: 1349–1392.
- Rodríguez-Roda, J. 1964. *Biología del atún, Thunnus thynnus* (L.), de la costa sudatlántica de España. Consejo Superior de Investigaciones Científicas (España).
- Rodríguez-Roda, J. 1967. *Fecundidad del atún, Thunnus thynnus* (L.), de la costa sudatlántica de España. Consejo Superior de Investigaciones Científicas (España).
- Sanchez, G. M. 2020. Indigenous stewardship of marine and estuarine fisheries?: Reconstructing the ancient size of Pacific herring through linear regression models. *Journal of Archaeological Science: Reports*, 29: 102061.
- Santamaria, N., Bello, G., Corriero, A., Deflorio, M., Vassallo-Agius, R., Bök, T., and De Metrio, G. 2009. Age and growth of Atlantic bluefin tuna, *Thunnus thynnus* (Osteichthyes: thunnidae), in the Mediterranean Sea. *Journal of Applied Ichthyology*, 25: 38–45.
- Santamaria, N., Bello, G., Pousis, C., Vassallo-Agius, R., de la Gándara, F., and Corriero, A. 2015. Fin spine bone resorption in Atlantic bluefin tuna, *Thunnus thynnus*, and comparison between wild and captive-reared specimens. *PLoS One*, 10: e0121924.
- Saura, M., Morán, P., Brotherstone, S., Caballero, A., Álvarez, J., and Villanueva, B. 2010. Predictions of response to selection caused by angling in a wild population of Atlantic salmon (*Salmo salar*). *Freshwater Biology*, 55: 923–930.
- Secci, M., Palmas, F., Giglioli, A. A., Pasquini, V., Culurgioni, J., Sabatini, A., and Addis, P. 2021. Underwater tagging of the Atlantic bluefin tuna in the trap fishery of Sardinia (W Mediterranean). *Fisheries Research*, 233: 105747.

- Sella, M. 1929. Migrazioni e habitat del tonno (*Thunnus thynnus*, L.) studiati col metodo degli ami, con osservazioni su l'accrescimento, sul regime delle tonnare ecc. Memoria, R. Comitato Talassografico Italiano, 156: 511–542.
- Siskey, M. R., Lyubchich, V., Liang, D., Piccoli, P. M., and Secor, D. H. 2016a. Periodicity of strontium: calcium across annuli further validates otolith-ageing for Atlantic bluefin tuna (*Thunnus thynnus*). Fisheries Research, 177: 13–17.
- Siskey, M. R., Wilberg, M. J., Allman, R. J., Barnett, B. K., and Secor, D. H. 2016b. Forty years of fishing: changes in age structure and stock mixing in northwestern Atlantic bluefin tuna (*Thunnus thynnus*) associated with size-selective and long-term exploitation. ICES Journal of Marine Science: Journal du Conseil, 73: 2518–2528.
- Smoliński, S. 2019. Sclerochronological approach for the identification of herring growth drivers in the Baltic Sea. Ecological Indicators, 101: 420–431.
- Smoliński, S., Deplanque-Lasserre, J., Hjörleifsson, E., Geffen, A. J., Godiksen, J. A., and Campana, S. E. 2020. Century-long cod otolith biochronology reveals individual growth plasticity in response to temperature. Scientific Reports, 10: 16708.
- Stevens, J. D. 1975. Vertebral rings as a means of age determination in the blue shark (*Prionace glauca* L.). Journal of the Marine Biological Association of the United Kingdom, 55: 657–665.
- Stewart, N. D., Busawon, D. S., Rodriguez-Marin, E., Siskey, M., and Hanke, A. R. 2022. Applying mixed-effects growth models to back-calculated size-at-age data for Atlantic bluefin tuna (*Thunnus Thynnus*). Fisheries Research, 250: 106260.
- Swain, D. P., Sinclair, A. F., and Mark Hanson, J. 2007. Evolutionary response to size-selective mortality in an exploited fish population. Proceedings. Biological sciences / The Royal Society, 274: 1015–1022.
- Team, R. C. 2013. R development core team. RA Lang Environ Stat Comput, 55: 275–286.
- Therkildsen, N. O., Wilder, A. P., Conover, D. O., Munch, S. B., Baumann, H., and Palumbi, S. R. 2019. Contrasting genomic shifts underlie parallel phenotypic evolution in response to fishing. Science, 365: 487–490.
- van der Sleen, P., Dzaugis, M. P., Gentry, C., Hall, W. P., Hamilton, V., Helser, T. E., Matta, M. E. et al. 2016. Long-term Bering Sea environmental variability revealed by a centennial-length biochronology of Pacific ocean perch *Sebastes alutus*. Climate Research, 71: 33–45.
- Van Neer, W., Löugas, L., and Rijnsdorp, A. D. 1999. Reconstructing age distribution, season of capture and growth rate of fish from archaeological sites based on otoliths and vertebrae. International Journal of Osteoarchaeology, 9 : 116–130.
- Vieira, A. R., Dores, S., Azevedo, M., and Tanner, S. E. 2020. Otolith increment width-based chronologies disclose temperature and density-dependent effects on demersal fish growth. ICES Journal of Marine Science: Journal du Conseil, 77: 633–644.
- Weisberg, S., Spangler, G., and Richmond, L. S. 2010. Mixed effects models for fish growth. Canadian Journal of Fisheries and Aquatic Sciences, 67: 269–277.
- Wilson, S. G., and Block, B. A. 2009. Habitat use in Atlantic bluefin tuna *Thunnus thynnus* inferred from diving behavior. Endangered Species Research, 10: 355–367.
- Zhou, C., 2022. Somatic growth of Atlantic bluefin tuna (*Thunnus thynnus*) under global climate variability: evidence from over 60 years of daily resolved growth increments with a simulation study. Canadian Journal of Fisheries and Aquatic Sciences, 79: 642–651.

Handling Editor: Allen Hia Andrews

## Supplementary Materials

### Vertebrae reveal industrial-era increases in Atlantic bluefin tuna catch-at-size and juvenile growth

Adam J. Andrews\*<sup>1</sup>, Antonio Di Natale<sup>2</sup>, Piero Addis<sup>3</sup>, Federica Piattoni<sup>1</sup>, Vedat Onar<sup>4</sup>, Darío Bernal-Casasola<sup>5</sup>, Veronica Aniceti<sup>6</sup>, Gabriele Carenti<sup>7</sup>, Verónica Gómez-Fernández<sup>8</sup>, Fulvio Garibaldi<sup>9</sup>, Arturo Morales-Muñiz\*<sup>10</sup>, Fausto Tinti<sup>1</sup>

<sup>1</sup>Department of Biological, Geological and Environmental Sciences, University of Bologna, Ravenna, Italy

<sup>2</sup>Aquastudio Research Institute, Messina, Italy

<sup>3</sup>Department of Life and Environmental Sciences, University of Cagliari, Cagliari, Sardinia, Italy

<sup>4</sup>Osteoarchaeology Practice and Research Centre, Faculty of Veterinary Medicine, Istanbul University-Cerrahpaşa, Istanbul, Turkey

<sup>5</sup>Department of History, Geography and Philosophy, Faculty of Philosophy and Letters, University of Cádiz, Cádiz, Spain

<sup>6</sup>Museum of Natural History, University of Bergen, Bergen, Norway

<sup>7</sup>Department of Nature and Environmental Sciences, University of Sassari, Sardinia, Italy

<sup>8</sup>I.N.I.C.E - Instituto Nacional de investigaciones científicas y ecológicas, Salamanca, Spain

<sup>9</sup>Department of Earth, Environment and Life Sciences (DISTAV), University of Genoa, Genoa, Italy

<sup>10</sup>Department of Biology, Autonomous University of Madrid, Madrid, Spain

\*Corresponding authors: [adam@palaeome.org](mailto:adam@palaeome.org), [arturo.morales@uam.es](mailto:arturo.morales@uam.es)

Keywords: *Thunnus thynnus*, fish trait plasticity, fisheries induced evolution, historical baselines, historical fish size, growth of fishes, climate change

### *Archaeological sample details*

16<sup>th</sup>-18<sup>th</sup> century CE Pedras de Fogu, Sardinia, Italy

A total of 38 vertebrae samples were obtained from the archaeological site of 'Pedras de Fogu' (Sassari, Sardinia, Italy). A tuna trap (tonnara) operated at this location from the 16<sup>th</sup> to the end of the 18<sup>th</sup> century where BFT vertebrae have been recovered in a midden at the back of the beach after they were revealed by coastal erosion (Delussu and Wilkens, 2001).

1755 CE La Chanca, Conil, Spain

Thirty vertebrae samples were obtained from the archaeological site of 'La Chanca' (Conil de la Frontera, Spain). La Chanca is a small salting factory belonging to the Duchy of Medina Sidonia that was built in the 16<sup>th</sup> century and was in operation until the 19<sup>th</sup> century. On November 1, 1755, an earthquake occurred with an epicentre in the Gulf of Cádiz, which generated a tsunami in the southeast of Andalusia (Huelva and Cádiz) and along the whole Iberian coast, leaving La Chanca completely destroyed, mid-operation. Excavations (Gutiérrez-Mas *et al.*, 2016) confirmed the strata destroyed by the tsunami, where BFT vertebrae, scales and spines were recovered with an anatomical connection, although separated where presumably BFT were cut into spinal sections in preparation for the salting process. The dating of 1755 is corroborated by a letter from Miguel of Aragón and Serrano, who held the position of Corregidor of Conil in 1755 when he wrote to the Duke of Medina Sidonia detailing that BFT were in the salting piles at the time the catastrophe occurred, that the wave dragged them and that they remained buried under the ruins of the building, with no possibility of recovery (document 2326 of the General Archive of the Medina Sidonia Foundation, Spain).

13<sup>th</sup> century CE Mazara del Vallo, Sicily, Italy

A total of 6 samples were obtained from the archaeological site of 'Mazara del Vallo' situated in the town itself (southwest Sicily, Italy). Samples were recovered from urban 13<sup>th</sup> century layers, each dated by context as detailed in (Aniceti, 2019), and identified as different individuals according to their range of sizes.

9<sup>th</sup>-13<sup>th</sup> century CE Yenikapi, Istanbul, Turkey

60 vertebrae specimens were selected for analyses from a rescue excavation at a Byzantine era site in the Yenikapi neighbourhood of Istanbul, Turkey. The Port of Theodosius operated at this site from 4<sup>th</sup>-11<sup>th</sup> century CE before being filled in at the 15<sup>th</sup> century CE (Onar *et al.*, 2008). The 9<sup>th</sup>-13<sup>th</sup> c. origin of the samples is proposed from carbon dating achieved in a separate study (Andrews *et al.* in review). It is unknown whether specimens were fished locally or transported to the city of Constantinople, which was a major trading hub throughout the Byzantine period.

9<sup>th</sup>-10<sup>th</sup> century CE Palermo, Sicily, Italy

A total of 20 vertebrae were selected for analyses from urban 9<sup>th</sup>-10<sup>th</sup> century layers in two different excavations in settlements in the city of Palermo, Sicily; Sant'Antonino and Corso

dei Mille. The layers were dated by context as detailed in (Aniceti, 2019). Samples were estimated to represent individuals believed to have been caught locally.

4<sup>th</sup>-5<sup>th</sup> century CE Baelo Claudia, Andalusia, Spain

A total of 21 vertebrae specimens were analysed from the Roman-era city of Baelo Claudia, Andalusia, Spain). Using the archaeological context of stratigraphic units, samples were dated to the late Roman era (4<sup>th</sup>-5<sup>th</sup> century CE) from various stratigraphic units and contexts within the city, predominantly associated with the fish processing/salting facilities—called *cetariae* (Bernal-Casasola *et al.*, 2018).

1<sup>st</sup> century CE Olivillo, Cadiz, Spain

24 samples were selected for analysis from the archaeological site 'Olivillo', an Imperial Roman fish processing/salting facility within the city of Cádiz (Bernal-Casasola *et al.*, 2020). Samples were selected from various stratigraphic units, dated by context to the 1st century CE.

2<sup>nd</sup> century BCE Punta Camarinal, Andalusia, Spain

59 BFT vertebrae recovered from a second century BCE layer at Punta Camarinal, Andalusia, Spain. Punta Camarinal is a refuse dump (midden) site at the rear of a beach adjacent to the Roman-era city and salting factories of Baelo Claudia and were previously published (Andrews *et al.*, 2022).

3<sup>rd</sup> century BCE - 4<sup>th</sup> century CE Portopalo, Siracusa, Sicily

28 vertebrae were sampled from the ancient Greek and Roman salting vats of Portopalo, Sicily (Bernal-Casasola *et al.*, 2021), which were dated by context to two periods (3<sup>rd</sup> c. BCE and 1<sup>st</sup>-4<sup>th</sup> c. CE). A large tuna trap industry operated adjacent to the salting vats until the mid-20<sup>th</sup> c. and would thus suggest that archaeological specimens were captured from the very beach where the archaeological structures remain today.



Supplementary Tables and Figures

**Table S1** - Fork Length estimations - external file.

**Table S2.** Summary Table of ICCAT-collated tuna trap data plotted using histograms for the 20th and 21st century CE, accessed from [www.iccat.int/en/accesingdb.html](http://www.iccat.int/en/accesingdb.html)

Decade CE	Area	Countries	Number of individuals	Mean Fork Length	Min Fork Length	Max Fork Length
1910	Mediterranean	Italy	119	213	123	278
1920	Mediterranean	Italy, Libya	134	165	96	263
1950	Eastern Atlantic	Spain, Portugal	142	171	45	280
1950	Mediterranean	Italy	305	182	83	262
1960	Eastern Atlantic	Spain	83	192	120	265
1960	Mediterranean	Italy	1620	167	45	299
1970	Mediterranean	Italy	1923	208	95	330
1980	Eastern Atlantic	Spain	441	211	128	296
1980	Mediterranean	Italy	1184	196	78	304
1990	Eastern Atlantic	Spain, Portugal	519	198	38	315
1990	Mediterranean	Italy, Tunisia	2170	178	50	315
2000	Eastern Atlantic	Spain, Portugal	1349	197	75	315
2000	Mediterranean	Italy	3354	171	84	335
2010	Eastern Atlantic	Spain, Portugal	4693	205	50	345
2010	Mediterranean	Italy	408	162	84	288

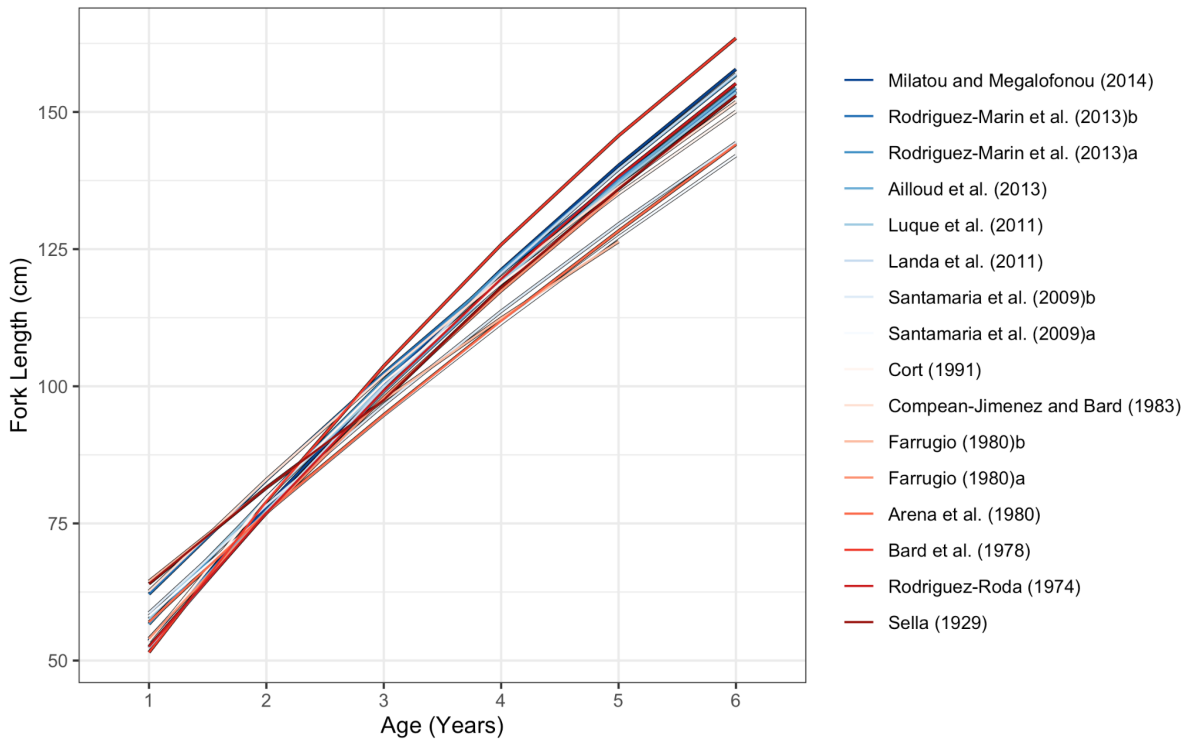


**Figure S1.** Published length-at-age curves for the eastern Atlantic and Mediterranean population of Atlantic bluefin tuna (*Thunnus thynnus*) from various studies, presented in temporal order from oldest (darkest red) to most recent (dark blue) analyses, for ages 1-6.

**Table S3a.** Tukey HSD Means testing results on Century and Age pairs. Significant ( $p < 0.05$ ) pairs are presented in boldface.

Sample group / Age (Years) pair	Difference	Lower	Upper	$p$	Vertebra
<b>20th Century Age 1 - 21st Century Age 1</b>	<b>-4.76E-01</b>	<b>-0.839</b>	<b>-0.113</b>	<b>0.001</b>	<b>35</b>
<b>16-18th Century Age 1 - 21st Century Age 1</b>	<b>-5.84E-01</b>	<b>-1.020</b>	<b>-0.147</b>	<b>0.000</b>	<b>35</b>
<b>3-2nd Century BCE Age 1 - 21st Century Age 1</b>	<b>-9.30E-01</b>	<b>-1.619</b>	<b>-0.240</b>	<b>0.000</b>	<b>35</b>
16-18th Century Age 1 - 20th Century Age 1	-1.07E-01	-0.496	0.282	1.000	35
3-2nd Century BCE Age 1 - 20th Century Age 1	-4.53E-01	-1.114	0.207	0.670	35
3-2nd Century BCE Age 1 - 16-18th Century Age 1	-3.46E-01	-1.050	0.358	0.983	35
<b>20th Century Age 2 - 21st Century Age 2</b>	<b>-4.26E-01</b>	<b>-0.789</b>	<b>-0.063</b>	<b>0.005</b>	<b>35</b>
<b>16-18th Century Age 2 - 21st Century Age 2</b>	<b>-8.65E-01</b>	<b>-1.302</b>	<b>-0.429</b>	<b>0.000</b>	<b>35</b>
<b>3-2nd Century BCE Age 2 - 21st Century Age 2</b>	<b>-7.68E-01</b>	<b>-1.457</b>	<b>-0.078</b>	<b>0.011</b>	<b>35</b>
<b>16-18th Century Age 2 - 20th Century Age 2</b>	<b>-4.40E-01</b>	<b>-0.829</b>	<b>-0.051</b>	<b>0.009</b>	<b>35</b>
3-2nd Century BCE Age 2 - 20th Century Age 2	-2.01E+04	-1.003	0.319	0.970	35
3-2nd Century BCE Age 2 - 16-18th Century Age 2	9.75E-02	-0.606	0.801	1.000	35
20th Century Age 3 - 21st Century Age 3	-9.38E-02	-0.456	0.268	1.000	35
<b>16-18th Century Age 3 - 21st Century Age 3</b>	<b>-5.02E-01</b>	<b>-0.939</b>	<b>-0.066</b>	<b>0.007</b>	<b>35</b>
3-2nd Century BCE Age 3 - 21st Century Age 3	-8.48E-02	-0.774	0.605	1.000	35
<b>16-18th Century Age 3 - 20th Century Age 3</b>	<b>-4.09E-01</b>	<b>-0.797</b>	<b>-0.021</b>	<b>0.026</b>	<b>35</b>
3-2nd Century BCE Age 3 - 20th Century Age 3	8.93E-03	-0.651	0.669	1.000	35
3-2nd Century BCE Age 3 - 16-18th Century Age 3	4.18E-01	-0.286	1.121	0.885	35
20th Century Age 4 - 21st Century Age 4	1.81E-01	-0.188	0.550	0.984	35
16-18th Century Age 4 - 21st Century Age 4	-1.21E-01	-0.557	0.316	1.000	35
3-2nd Century BCE Age 4 - 21st Century Age 4	-1.23E-02	-0.702	0.677	1.000	35
16-18th Century Age 4 - 20th Century Age 4	-3.02E-01	-0.696	0.093	0.444	35
3-2nd Century BCE Age 4 - 20th Century Age 4	-1.93E-01	-0.857	0.471	1.000	35
3-2nd Century BCE Age 4 - 16-18th Century Age 4	1.09E-01	-0.595	0.812	1.000	35
20th Century Age 5 - 21st Century Age 5	1.08E-01	-0.282	0.498	1.000	35

16-18th Century Age 5 - 21st Century Age 5	-4.04E-02	-0.492	0.411	1.000	35
3-2nd Century BCE Age 5 - 21st Century Age 5	-9.11E-02	-0.826	0.644	1.000	35
16-18th Century Age 5 - 20th Century Age 5	-1.48E-01	-0.579	0.282	1.000	35
3-2nd Century BCE Age 5 - 20th Century Age 5	-1.99E-01	-0.922	0.523	1.000	35
3-2nd Century BCE Age 5 - 16-18th Century Age 5	-5.07E-02	-0.808	0.707	1.000	35
20th Century Age 6 - 21st Century Age 6	1.98E-01	-0.246	0.642	0.995	35
16-18th Century Age 6 - 21st Century Age 6	1.47E-01	-0.343	0.636	1.000	35
3-2nd Century BCE Age 6 - 21st Century Age 6	1.30E-01	-0.680	0.940	1.000	35
16-18th Century Age 6 - 20th Century Age 6	-5.11E-02	-0.518	0.416	1.000	35
3-2nd Century BCE Age 6 - 20th Century Age 6	-6.77E-02	-0.864	0.729	1.000	35
3-2nd Century BCE Age 6 - 16-18th Century Age 6	-1.67E-02	-0.839	0.806	1.000	35

**Table S3b.** Tukey HSD Means testing results on Century and Age pairs. Significant ( $p < 0.05$ ) pairs are presented in boldface.

Sample group / Age (Years) pair	Difference	Lower	Upper	p	Vertebra
<b>20th Century Age 1 - 21st Century Age 1</b>	<b>-0.440</b>	<b>-0.815</b>	<b>-0.065</b>	<b>0.005</b>	<b>36</b>
<b>16-18th Century Age 1 - 21st Century Age 1</b>	<b>-0.624</b>	<b>-1.097</b>	<b>-0.151</b>	<b>0.000</b>	<b>36</b>
<b>3-2nd Century BCE Age 1 - 21st Century Age 1</b>	<b>-0.818</b>	<b>-1.514</b>	<b>-0.123</b>	<b>0.005</b>	<b>36</b>
16-18th Century Age 1 - 20th Century Age 1	-0.184	-0.604	0.236	0.996	36
3-2nd Century BCE Age 1 - 20th Century Age 1	-0.378	-1.039	0.282	0.915	36
3-2nd Century BCE Age 1 - 16-18th Century Age 1	-0.194	-0.915	0.526	1.000	36
<b>20th Century Age 2 - 21st Century Age 2</b>	<b>-0.395</b>	<b>-0.770</b>	<b>-0.020</b>	<b>0.025</b>	<b>36</b>
<b>16-18th Century Age 2 - 21st Century Age 2</b>	<b>-0.832</b>	<b>-1.305</b>	<b>-0.359</b>	<b>0.000</b>	<b>36</b>
<b>3-2nd Century BCE Age 2 - 21st Century Age 2</b>	<b>-0.902</b>	<b>-1.597</b>	<b>-0.206</b>	<b>0.001</b>	<b>36</b>
<b>16-18th Century Age 2 - 20th Century Age 2</b>	<b>-0.437</b>	<b>-0.858</b>	<b>-0.017</b>	<b>0.031</b>	<b>36</b>
3-2nd Century BCE Age 2 - 20th Century Age 2	-0.507	-1.167	0.154	0.436	36
3-2nd Century BCE Age 2 - 16-18th Century Age 2	-0.069	-0.790	0.651	1.000	36
20th Century Age 3 - 21st Century Age 3	-0.045	-0.420	0.330	1.000	36
16-18th Century Age 3 - 21st Century Age 3	-0.404	-0.877	0.069	0.225	36
3-2nd Century BCE Age 3 - 21st Century Age 3	-0.432	-1.127	0.264	0.831	36
16-18th Century Age 3 - 20th Century Age 3	-0.359	-0.779	0.061	0.226	36
3-2nd Century BCE Age 3 - 20th Century Age 3	-0.387	-1.047	0.274	0.896	36
3-2nd Century BCE Age 3 - 16-18th Century Age 3	-0.028	-0.749	0.693	1.000	36
<b>20th Century Age 4 - 21st Century Age 4</b>	<b>0.398</b>	<b>0.016</b>	<b>0.779</b>	<b>0.030</b>	<b>36</b>
16-18th Century Age 4 - 21st Century Age 4	-0.095	-0.575	0.386	1.000	36
3-2nd Century BCE Age 4 - 21st Century Age 4	0.003	-0.692	0.699	1.000	36
<b>16-18th Century Age 4 - 20th Century Age 4</b>	<b>-0.492</b>	<b>-0.928</b>	<b>-0.057</b>	<b>0.009</b>	<b>36</b>
3-2nd Century BCE Age 4 - 20th Century Age 4	-0.394	-1.059	0.270	0.883	36
3-2nd Century BCE Age 4 - 16-18th Century Age 4	0.098	-0.628	0.824	1.000	36
20th Century Age 5 - 21st Century Age 5	0.203	-0.205	0.611	0.981	36
16-18th Century Age 5 - 21st Century Age 5	-0.138	-0.611	0.334	1.000	36
3-2nd Century BCE Age 5 - 21st Century Age 5	-0.080	-0.829	0.669	1.000	36
16-18th Century Age 5 - 20th Century Age 5	-0.341	-0.792	0.109	0.463	36
3-2nd Century BCE Age 5 - 20th Century Age 5	-0.283	-1.018	0.453	0.999	36
3-2nd Century BCE Age 5 - 16-18th Century Age 5	0.058	-0.715	0.831	1.000	36
20th Century Age 6 - 21st Century Age 6	0.279	-0.205	0.763	0.910	36
16-18th Century Age 6 - 21st Century Age 6	0.037	-0.482	0.556	1.000	36
3-2nd Century BCE Age 6 - 21st Century Age 6	0.003	-0.766	0.771	1.000	36
16-18th Century Age 6 - 20th Century Age 6	-0.242	-0.749	0.266	0.988	36
3-2nd Century BCE Age 6 - 20th Century Age 6	-0.276	-1.037	0.485	1.000	36
3-2nd Century BCE Age 6 - 16-18th Century Age 6	-0.034	-0.818	0.749	1.000	36

**Table 4a.** Random effects model selection summary statistics. The best supported model is highlighted in bold, based on AICc. Random Age slopes for variables are denoted by “Age|variable”. df, degrees of freedom; wAICc, Akaike weights.

Dataset	Model	df	AICc	$\Delta$ AICc	wAICc
Vertebra 35	log(Growth_mm) ~ log(Age) + (1 ID)	4	-278.9	10.4	0.004
Vertebra 36	log(Growth_mm) ~ log(Age) + (1 ID)	4	-311	19.85	0
Vertebra 35	log(Growth_mm) ~ log(Age) + (1 ID) + (1 Cohort)	5	-286.6	2.72	0.186
Vertebra 36	log(Growth_mm) ~ log(Age) + (1 ID) + (1 Cohort)	5	-321.6	9.27	0.01
<b>Vertebra 35</b>	<b>log(Growth_mm) ~ log(Age) + (1 ID) + (log(Age) Cohort)</b>	<b>7</b>	<b>-289.3</b>	<b>0.00</b>	<b>0.726</b>
<b>Vertebra 36</b>	<b>log(Growth_mm) ~ log(Age) + (1 ID) + (log(Age) Cohort)</b>	<b>7</b>	<b>-330.8</b>	<b>0.00</b>	<b>0.99</b>
Vertebra 35	log(Growth_mm) ~ log(Age) + (log(Age) Cohort)	6	-285.0	4.32	0.084
Vertebra 36	log(Growth_mm) ~ log(Age) + (log(Age) Cohort)	6	-315.1	15.78	0.00

**Table 4b.** Mixed effects model selection summary statistics for each intrinsic variable (in bold) including ANOVA F value and 95% confidence intervals (CI).

Dataset	Variable / Model	Estimate	residual df	t value	F value	5% CI	95% CI
	<i>Intrinsic effects</i>						
Vertebra 35	log(Growth_mm) ~ <b>log(Age)</b> + (1 ID) + (log(Age) Year)	-0.53	492	-41.02	456.41	-0.57	-0.48
Vertebra 36	log(Growth_mm) ~ <b>log(Age)</b> + (1 ID) + (log(Age) Year)	-0.54	404	-18.57	344.78	-0.60	-0.49
Vertebra 35	log(Growth_mm) ~ log(Age) + (1 ID) + <b>log(Width)</b> + (log(Age) Year)	0.01	488	0.25	0.06	-0.08	0.11
Vertebra 36	log(Growth_mm) ~ log(Age) + (1 ID) + <b>log(Width)</b> (log(Age) Year)	0.03	403	0.65	0.42	-0.06	0.16
Vertebra 35	log(Growth_mm) ~ log(Age) + (1 ID) + <b>log(Length)</b> + (log(Age) Year)	0.02	488	0.38	0.14	-0.08	0.12
Vertebra 36	log(Growth_mm) ~ log(Age) + (1 ID) + <b>log(Length)</b> (log(Age) Year)	0.05	403	0.89	0.79	0.05	0.16
Vertebra 35	log(Growth_mm) ~ log(Age) + (1 ID) + <b>log(Height)</b> + (log(Age) Year)	-0.02	488	0.04	0.17	-0.122	0.07
Vertebra 36	log(Growth_mm) ~ log(Age) + (1 ID) + <b>log(Height)</b> (log(Age) Year)	0.01	403	0.23	0.05	-0.09	0.12

**Table 4c.** Mixed effects model selection summary statistics for each temporal variable (in bold) including ANOVA F value and 95% confidence intervals (CI).

Dataset	Variable / Model	Estimate	df	t value	F value	5% CI	95% CI	
	<i>Temporal effects</i>	<i>Slope</i>						
Vertebra 35	log(Growth_mm) ~ log(Age) * <b>Century</b> + (1 ID)	<b>16<sup>th</sup>-18<sup>th</sup> c.</b>	-0.08	486	-0.795	5.58	-0.24	0.08
		<b>20<sup>th</sup> c.</b>	-0.05		-0.755		-0.17	0.06
		<b>21<sup>st</sup> c.</b>	-0.16		-2.190		-0.27	-0.03
Vertebra 36	log(Growth_mm) ~ log(Age) * <b>Century</b> + (1 ID)	<b>16<sup>th</sup>-18<sup>th</sup> c.</b>	-0.01	401	-0.14	9.34	-0.18	0.15
		<b>20<sup>th</sup> c.</b>	0.08		0.9		-0.06	0.23
		<b>21<sup>st</sup> c.</b>	-0.07		-0.76		-0.21	0.07
Vertebra 35	log(Growth_mm) ~ log(Age) * <b>Cohort</b> + (1 ID)	<b>2<sup>nd</sup> c. BCE</b>	0.28	478	2.03	3.54	0.05	0.51
		<b>16<sup>th</sup>-18<sup>th</sup> c.</b>	0.09		0.73		-0.12	0.32
		<b>1911-1912</b>	0.08		0.69		-0.11	0.28
		<b>1925</b>	0.13		1.09		-0.65	0.32
		<b>1926</b>	0.15		1.26		-0.05	0.34
		<b>2019</b>	0.05		0.43		-0.14	0.24
		<b>2020</b>	-0.02		-0.15		-0.21	0.17
Vertebra 36	log(Growth_mm) ~ log(Age) * <b>Cohort</b> + (1 ID)	<b>16<sup>th</sup>-18<sup>th</sup> c.</b>	-0.01	395	-0.13	5.25	-0.18	0.15
		<b>1911-1912</b>	0.08		0.88		-0.07	0.23
		<b>1925</b>	0.08		0.95		-0.06	0.23
		<b>1926</b>	0.07		0.78		-0.07	0.21
		<b>2019</b>	-0.03		-0.34		-0.18	0.12
		<b>2020</b>	-0.12		-1.32		-0.27	0.03

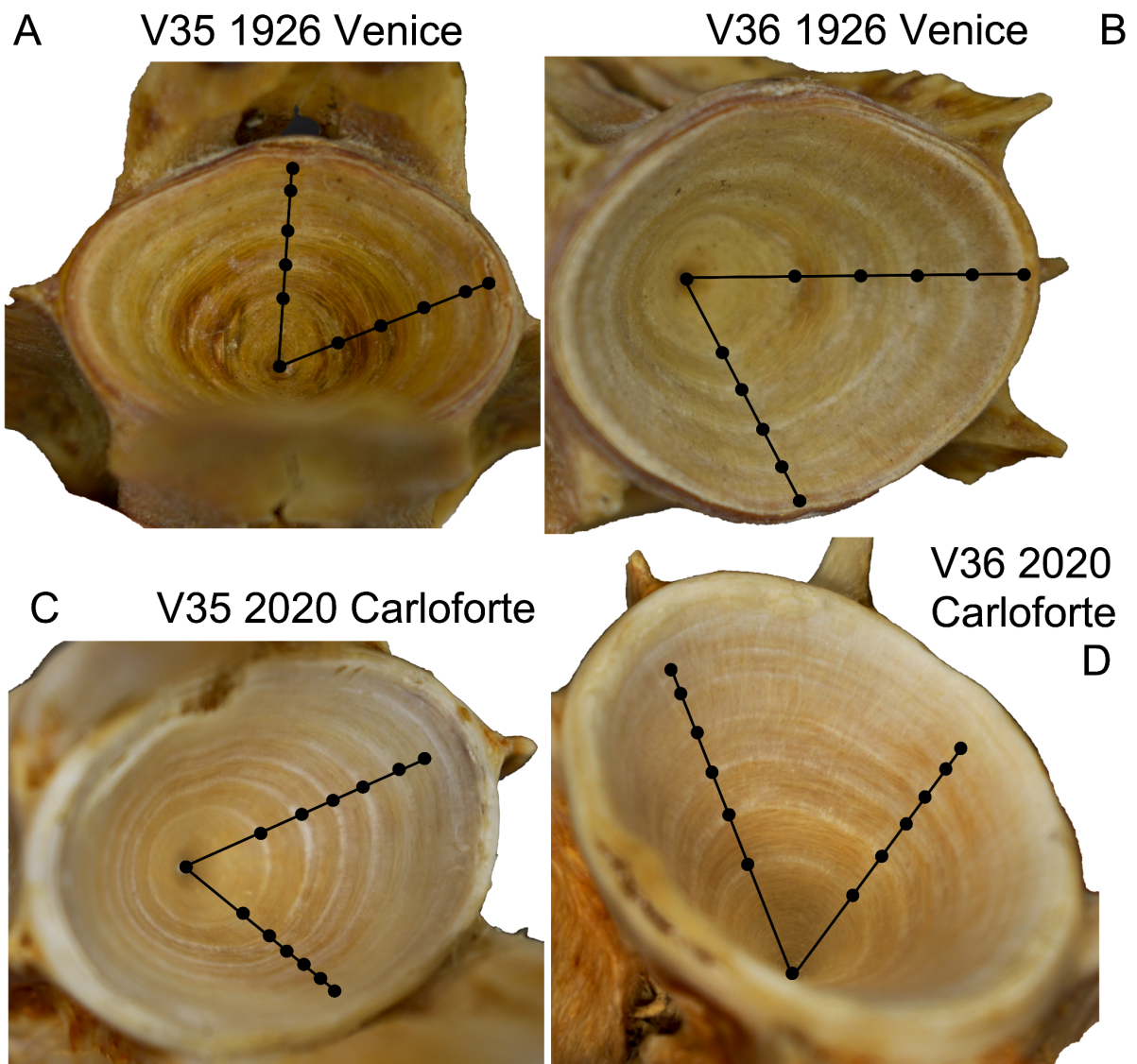


**Figure S2.** Examples of archived (1926, A, B) and contemporary (2020, C, D) specimens indicating annuli (denoted with black circles) measurements taken across the distal and focal plains (black lines). V35 = Vertebra 35, V36 = Vertebra 36. Place names indicate catch locations. For sample details see Figure 1 and Table 1.

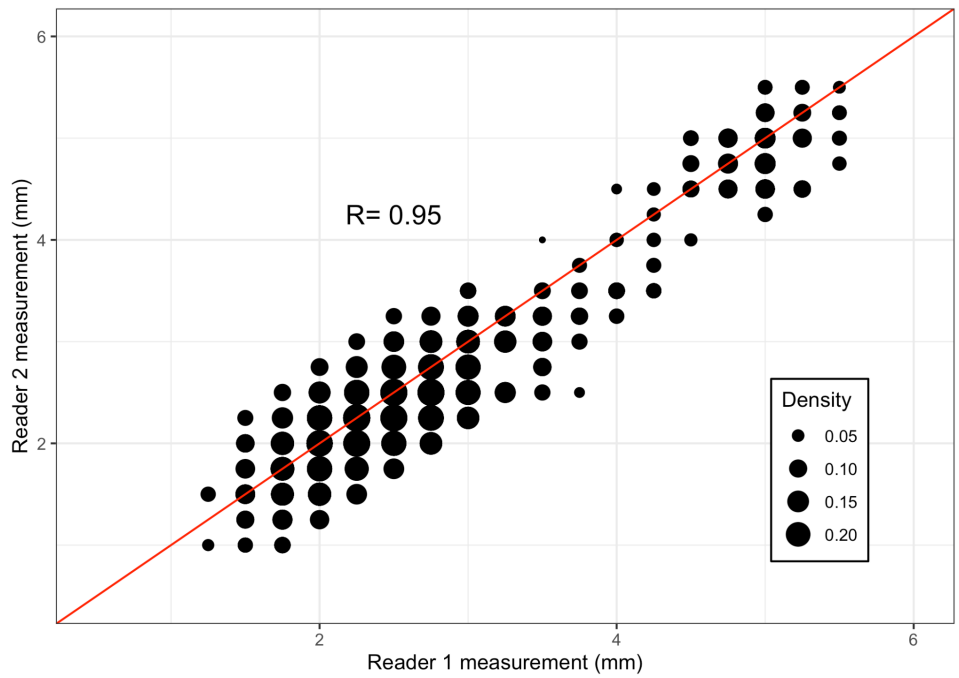


**Figure S3.** Correlation between a subset (25%) of annuli increment size measurements (mm) read by the main reader (1) and a second reader (2) to explore the reproducibility of the dataset.

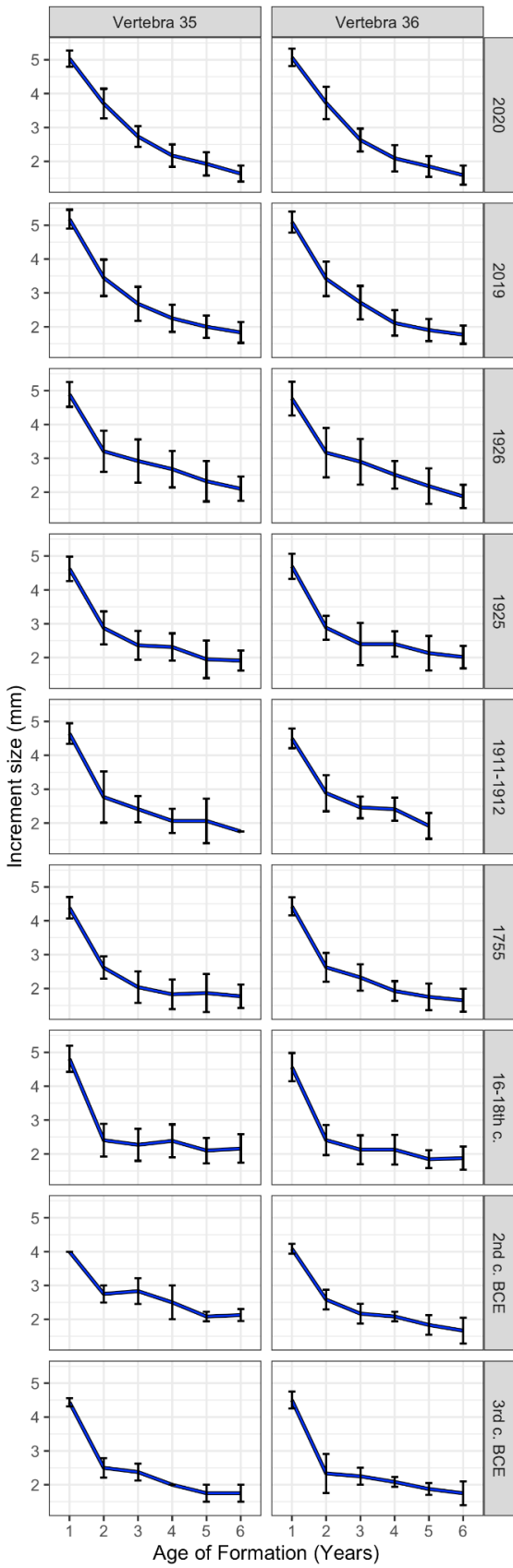


**Figure S4.** Increment size (mm) means (blue lines) with standard error bars (black bars) grouped by cohort (each panel) for Vertebra 35 (left) and Vertebra 36 (right).



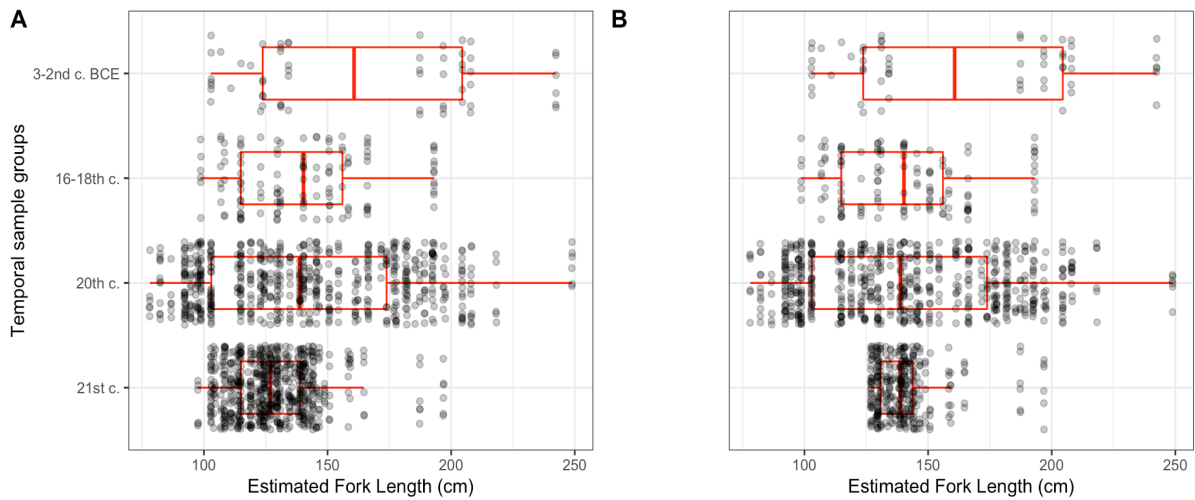


**Figure S5.** Boxplots depicting the variation of specimen sizes used in growth analyses. Fork length FL estimations constructed using all specimens analysed within pooled ‘century’ groups (A) and all except the bottom 50% of FL for the 21<sup>st</sup> c. sample group (B), to investigate the impact of sample size variation on increment sizes. Samples (grey scattered circles) are depicted with boxplots (red boxes) including group means, 25<sup>th</sup> and 75<sup>th</sup> percentile as outer edges and outliers illustrated outside of 95<sup>th</sup> percentiles (black whiskers).

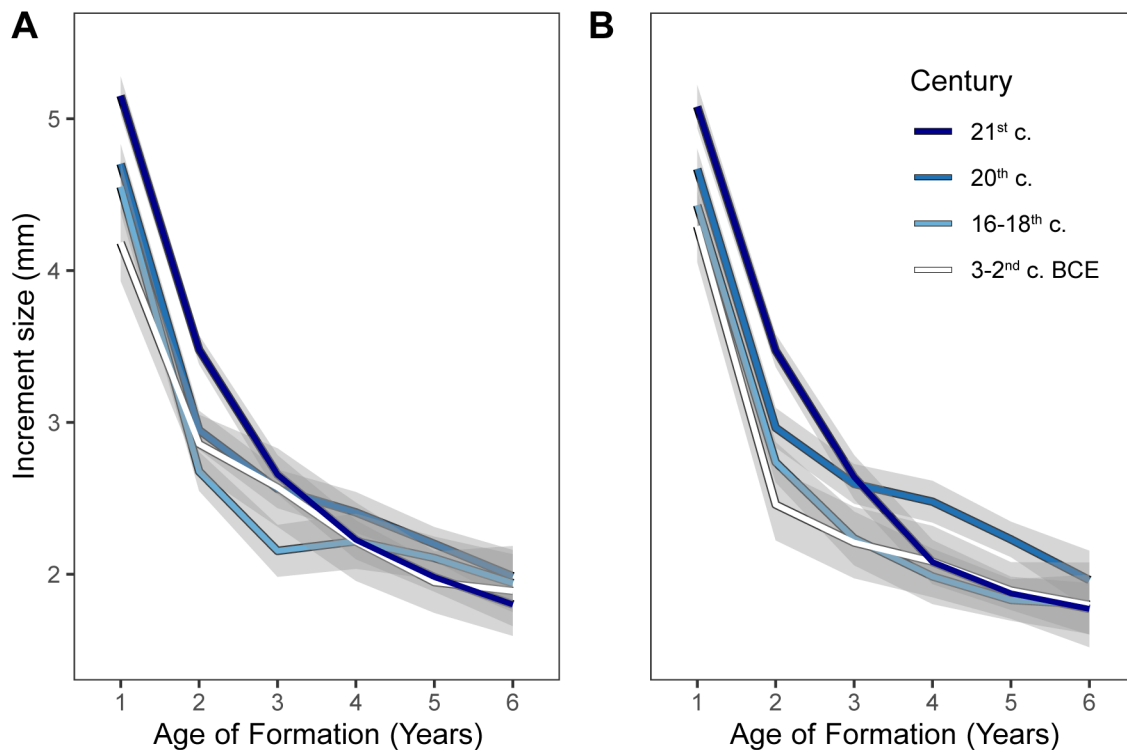


**Figure S6.** Temporal early-life growth estimates for Atlantic bluefin tuna (*Thunnus thynnus*) using vertebrae annuli measurements (A, B) without the bottom 50% of 2020 FL specimens to identify the effect of analysing individuals of different sizes. Smoothed increment sizes (mm) for each annuli (age in years) measured in the 35<sup>th</sup> (A) and 36<sup>th</sup> (B) vertebrae are illustrated per ‘century’ grouping, using the loess method `geom_smooth` function in R, grey shading indicates 95% confidence intervals.

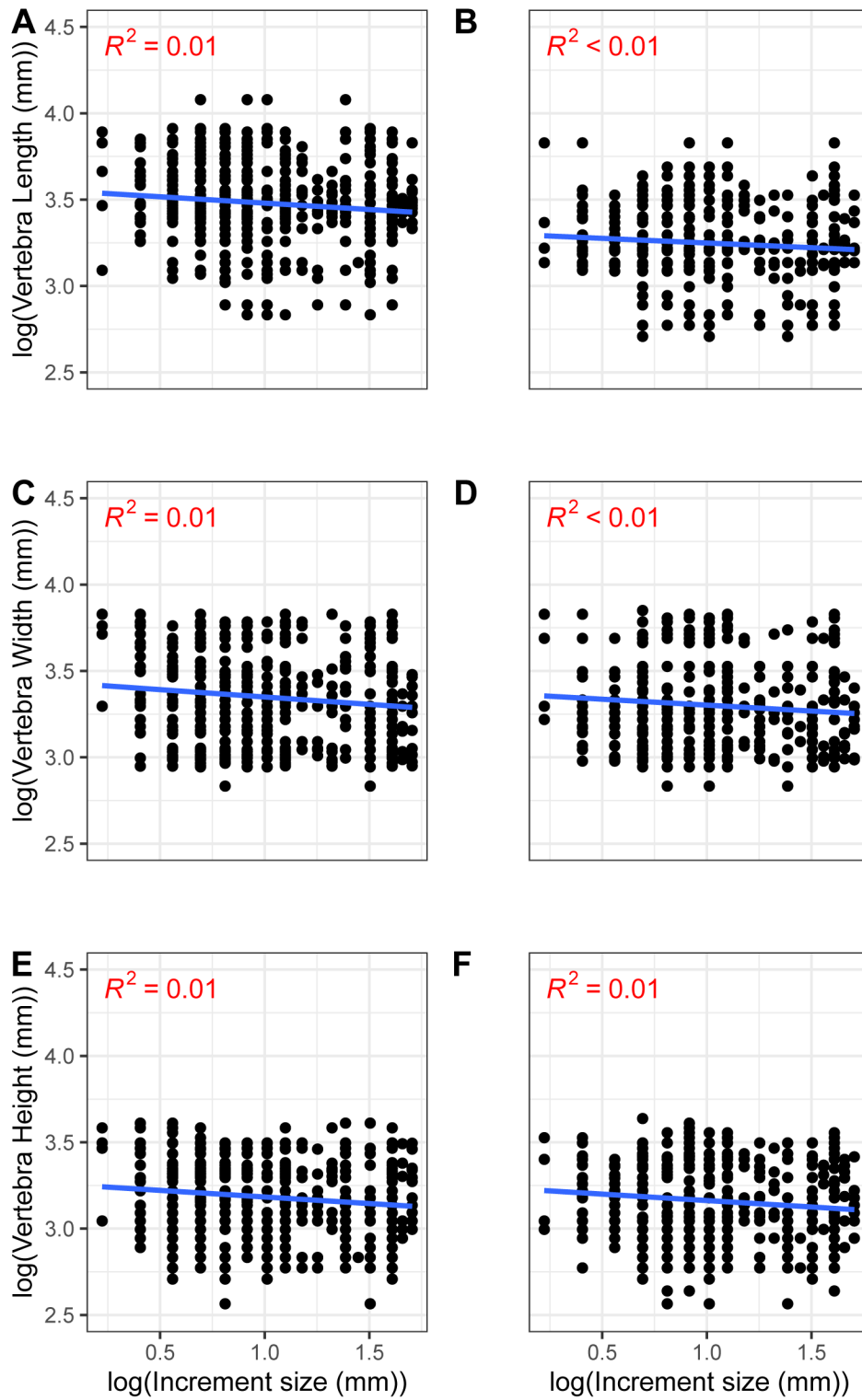


**Figure S7.** Correlation between Increment size (mm) and vertebra dimensions (height, width, length) for vertebra 35 (A, C, E) and vertebra 36 (B, D, F). Measurements (black dots) are presented smoothed (blue line) using the `loess` function in `ggplot2`, grey shading indicates 95% CI's.

## Supplementary-only references

Andrews A.J., Cariani, A., Cilli, E., Addis, P., Bernal-Casasola, D., Di Natale, A., Aniceti, A., Carenti, G., Gómez-Fernández, V., Chosson, V., Ughi, A., Von Tersch, M., Siddiq, A.B., Onar, V., Karakulak, F.S., Oray, I., Tinti, F., Alexander, M. Exploitation shifts trophic ecology and habitat preferences of Mediterranean and Black Sea bluefin tuna over centuries. *In review*.

Ailloud, L. E., M. V. Lauretta, J. M. Hoenig, and J. F. Walter. (2013). Growth of Atlantic bluefin tuna determined from the ICCAT tagging database: A reconsideration of methods. *ICCAT, SCRS/2013/093*, 16.

Aniceti, V. 2019. Animals and their roles in the medieval society of Sicily: from Byzantines to Arabs and from Arabs to Norman/Swabians. Doctoral Thesis. University of Sheffield.

Arena, P., A. Cefali, and F. Munao. (1980). Analisi sull'età, peso lunghezza ed accrescimento de *Thunnus thynnus* (L.) catturati nei mari della Sicilia. *Mem. Biol. Mar. Ocean.*, 10(5): 120–134.

Bard, F. X., J. L. Cort, and J. C. Rey. (1978). Commentaires sur la composition démographique des pecheries de thon rouge (*Thunnus thynnus*) de l'Est Atlantique et de la Méditerranée, 1960–1976. *Col. Vol. Sci. Pap. ICCAT*, 7: 355–365.

Bernal-Casasola, D., Expósito, J. A., and Díaz, J. J. 2018. The Baelo Claudia paradigm: The exploitation of marine resources in Roman cetariae. *Journal of Maritime Archaeology*, 13: 329–351.

Bernal-Casasola, D., Vargas Girón, J. M., and Lara Medina, Y. 2020. Atunes en salazón y en conserva en las chancas gaditanas: perspectivas desde El Olivillo in *7 metros de la Historia de Cádiz*. Darío Bernal, José Manuel Vargas y Macarena Lara (eds.). Arqueología en el Olivillo y en el Colegio Mayor Universitario, 517–534.

Bernal-Casasola, D., Malfitana, D., Mazzaglia, A., and Diaz, J. J. 2021. Le cetariae ellenistiche e romane di Portopalo (Siracusa). Primi studi da ricerche interdisciplinari. HEROM. *Journal of Hellenistic and Roman Material Culture*, Supplement 1.

Compean-Jimenez, G., and F. X. Bard. (1983). Growth increments on dorsal spines of eastern Atlantic bluefin tuna (*Thunnus thynnus* (L.)) and their possible relation to migrations patterns. *NOAA, Tech. Rep. NMFS*, 8: 77–86.

Delussu, F., and Wilkens, B. 2001. Analisi dei resti ossei della tonnara di Pedras de Fogu. *Archeologia Postmedievale*, 5: 214.

Farrugio, H. (1980). Age et croissance du thon rouge (*Thunnus thynnus*) dans la pecherie française de surface en Méditerranée. *Cybium*, 9: 45–59.

Gutiérrez-Mas, J. M., Gómez Fernández, V., García López, S., Morales González, J. A., Ibáñez Ageitos, J. M., and Others. 2016. Comparative analysis of the deposits left by the

tsunami that followed to the Lisbon earthquake (1755 ad), on the Castilnovo beach and the old tuna factory of la Chança (Conil de la Frontera, SW Spain). *Revista de la Sociedad Geológica de España*, 29: 21–33.

Landa, J., E. Rodríguez-Marin, P. L. Luque, M. Ruiz, and P. Quelle. (2011). Growth of bluefin tuna (*Thunnus thynnus*) in the North-eastern Atlantic and Mediterranean based on back-calculation of dorsal spine annuli. *ICCAT, SCRS/2011/178*, 12.

Luque, P., E. Rodríguez-Marin, M. Ruiz, P. Quelle, J. Landa, and D. Macias. (2011). A review of direct ageing methodology using dorsal fin spine from Atlantic bluefin tuna (*Thunnus thynnus*). *ICCAT, SCRS/2011/176*, 22.

Milatou, N., and P. Megalofonou. (2014). Age structure and growth of bluefin tuna (*Thunnus thynnus*, L.) in the capture-based aquaculture in the Mediterranean Sea. *Aquaculture*, 425: 35–44.

Onar, V., Pazvant, G., and Armutak, A. 2008. Radiocarbon dating results of the animal remains uncovered at Yenikapı Excavations. In *Istanbul Archaeological Museums, Proceedings of the 1st Symposium on Marmaray-Metro Salvage Excavations*, 249–256.

Rodríguez-Roda, J. (1974). Present state of tuna fishery with trap in South Spain. *International Council for the Exploration of the Sea (ICES), C. M.* 1974/J:8, 7.

Rodríguez-Marin, E., P. L. Luque, P. Quelle, M. Ruiz, and B. Perez. (2013a). Age determination analysis of Atlantic Bluefin Tuna (*Thunnus thynnus*) within the biological and genetic sampling and analysis contract (GBYP). *ICCAT, SCRS/2013/080*, 13.

Rodríguez-Marin, E., P. L. Luque, D. Busawon, S. Campana, W. Golet, E. Koob, J. Neilson, P. Quelle, and M. Ruiz. (2013b). An attempt of validation of Atlantic Bluefin Tuna (*Thunnus thynnus*) ageing using dorsal fin spines. *ICCAT, SCRS/2013/081*, 14.

Table S1. Supplementary file

Sample ID	Era	Site	Origin	Height	Width	Length	Estimated	Vertebra
SAN_BF2	10-11th CE	10th-11th c. CE Palermo	Sicily, Italy	<b>28</b>		26	156.8	8-18
SAN_BF3	10-11th CE	10th-11th c. CE Palermo	Sicily, Italy	26	<b>22</b>	20	100.8	2-7
SAN_BF6	10-11th CE	10th-11th c. CE Palermo	Sicily, Italy	29	<b>37</b>	27	173.6	7
SAN_BF7	10-11th CE	10th-11th c. CE Palermo	Sicily, Italy	<b>37.5</b>	31.6	25.7	185.1	19-23
SAN_BF8	10-11th CE	10th-11th c. CE Palermo	Sicily, Italy	<b>26</b>		26	184.9	2-7
CDM_BF1	10-11th CE	10th-11th c. CE Palermo	Sicily, Italy	20.34	25.92	<b>27.05</b>	119.1	35
CDM_BF3	10-11th CE	10th-11th c. CE Palermo	Sicily, Italy	<b>32</b>	37	31	160.1	19-23
CDM_BF4	10-11th CE	10th-11th c. CE Palermo	Sicily, Italy	<b>25.04</b>	29.39	22.7	128	19-23
CDM_BF5a	10-11th CE	10th-11th c. CE Palermo	Sicily, Italy	<b>21.12</b>	25.01	21.56	109.5	19-23
CDM_BF6	10-11th CE	10th-11th c. CE Palermo	Sicily, Italy	<b>22.05</b>	28.6	22.78	113.9	19-23
CDM_BF7	10-11th CE	10th-11th c. CE Palermo	Sicily, Italy	<b>23.5</b>	28.87	19.79	120.8	24-31
CDM_BF8	10-11th CE	10th-11th c. CE Palermo	Sicily, Italy	<b>20.67</b>	22.57	20.85	107.4	19-23
CDM_BF10	10-11th CE	10th-11th c. CE Palermo	Sicily, Italy	31.04	35.68	<b>22.4</b>	126.5	36
CDM_BF11	10-11th CE	10th-11th c. CE Palermo	Sicily, Italy	<b>21</b>		19	150.3	2-7
CDM_BF12	10-11th CE	10th-11th c. CE Palermo	Sicily, Italy	20	<b>22</b>	23	107.3	8-18
CDM_BF14	10-11th CE	10th-11th c. CE Palermo	Sicily, Italy	27.02	<b>30.21</b>	25.09	120.2	8-18
CDM_BF15	10-11th CE	10th-11th c. CE Palermo	Sicily, Italy	31.83	<b>40.82</b>	28.81	185.8	7
CDM_BF16	10-11th CE	10th-11th c. CE Palermo	Sicily, Italy			19.8	131.2	2-7
CDM_BF17	10-11th CE	10th-11th c. CE Palermo	Sicily, Italy	<b>29.4</b>		29	148.2	19-23
M1	1st CE	1st c. CE Olivillo	Cadiz, Spain	32.46	35.78	<b>34.05</b>	142	28
M3	1st CE	1st c. CE Olivillo	Cadiz, Spain	22	26	<b>26</b>	163.8	8
M4	1st CE	1st c. CE Olivillo	Cadiz, Spain	<b>24.54</b>		35.02	124	30-32
M5	1st CE	1st c. CE Olivillo	Cadiz, Spain	26.42	<b>32.17</b>	25.47	137.6	2-7
M6	1st CE	1st c. CE Olivillo	Cadiz, Spain	21	<b>26</b>	20	115.6	2-7
M7	1st CE	1st c. CE Olivillo	Cadiz, Spain	<b>28</b>	35	39	144.9	33
M8	1st CE	1st c. CE Olivillo	Cadiz, Spain	<b>26.34</b>	33.67	31.12	134	19-23
M9	1st CE	1st c. CE Olivillo	Cadiz, Spain	<b>30</b>	34	32	151	24-31
M10	1st CE	1st c. CE Olivillo	Cadiz, Spain			<b>32.04</b>	153.8	19-23
M11	1st CE	1st c. CE Olivillo	Cadiz, Spain	35	37	<b>35</b>	145.4	28
M12	1st CE	1st c. CE Olivillo	Cadiz, Spain	26	28	<b>31</b>	121.2	34
M13	1st CE	1st c. CE Olivillo	Cadiz, Spain	<b>24.56</b>	27.05	26	125.7	19-23
M14	1st CE	1st c. CE Olivillo	Cadiz, Spain	28	<b>26</b>	23	115.6	2-7
M15	1st CE	1st c. CE Olivillo	Cadiz, Spain			<b>20.34</b>	112.5	8-18
M16	1st CE	1st c. CE Olivillo	Cadiz, Spain	31.02	35.67	<b>29.34</b>	123.1	29
M17	1st CE	1st c. CE Olivillo	Cadiz, Spain	<b>17.06</b>	24.89	18.43	90.1	19-23
M18	1st CE	1st c. CE Olivillo	Cadiz, Spain	22	<b>29</b>	22	126.4	2-7
M19	1st CE	1st c. CE Olivillo	Cadiz, Spain	27	<b>32</b>	29	129.1	30-32
M20	1st CE	1st c. CE Olivillo	Cadiz, Spain	27	<b>30</b>	26	122.7	30-32
M21	1st CE	1st c. CE Olivillo	Cadiz, Spain	32	34	<b>36</b>	149	28
M22	1st CE	1st c. CE Olivillo	Cadiz, Spain	<b>32</b>	35	32	160.1	19-23
M23	1st CE	1st c. CE Olivillo	Cadiz, Spain	<b>32.53</b>	38.23	33.74	155.5	27
M24	1st CE	1st c. CE Olivillo	Cadiz, Spain	<b>21</b>	25	22	109	19-23
M25	1st CE	1st c. CE Olivillo	Cadiz, Spain	<b>25</b>	29	26	127.8	19-23
BC_5C_01	4th-5th CE	4th-5th c. CE Baelo Claudia	Andalucia, Spain	25	<b>33</b>		161.8	35
BC_5C_02	4th-5th CE	4th-5th c. CE Baelo Claudia	Andalucia, Spain	<b>26</b>	29	28	132.5	19-23
BC_5C_03	4th-5th CE	4th-5th c. CE Baelo Claudia	Andalucia, Spain	<b>43</b>		38	209.8	19-23
BC_5C_04	4th-5th CE	4th-5th c. CE Baelo Claudia	Andalucia, Spain	30.59	34.03	<b>31.92</b>	132.2	29
BC_5C_05	4th-5th CE	4th-5th c. CE Baelo Claudia	Andalucia, Spain	<b>22.35</b>	25.67	22.1	115.4	19-23
BC_5C_06	4th-5th CE	4th-5th c. CE Baelo Claudia	Andalucia, Spain	23.42	<b>29.06</b>	22.45	139.7	8
BC_5C_07	4th-5th CE	4th-5th c. CE Baelo Claudia	Andalucia, Spain	25	32	<b>37</b>	131.1	33
BC_5C_08	4th-5th CE	4th-5th c. CE Baelo Claudia	Andalucia, Spain	25	33	<b>37</b>	131.1	33
BC_5C_09	4th-5th CE	4th-5th c. CE Baelo Claudia	Andalucia, Spain	32		<b>29</b>	187	7
BC_5C_10	4th-5th CE	4th-5th c. CE Baelo Claudia	Andalucia, Spain	17	<b>19</b>	9	137.1	37
BC_5C_11	4th-5th CE	4th-5th c. CE Baelo Claudia	Andalucia, Spain	22	<b>25</b>	21	121.7	12
BC_5C_12	4th-5th CE	4th-5th c. CE Baelo Claudia	Andalucia, Spain	<b>22</b>	20	19	113.7	19-23
BC_5C_13	4th-5th CE	4th-5th c. CE Baelo Claudia	Andalucia, Spain	21		<b>24</b>	106.8	35
BC_5C_14	4th-5th CE	4th-5th c. CE Baelo Claudia	Andalucia, Spain		31	<b>25</b>	139	13
BC_5C_15	4th-5th CE	4th-5th c. CE Baelo Claudia	Andalucia, Spain	<b>25.18</b>	28.18	25.79	128.6	19-23
BC_5C_16	4th-5th CE	4th-5th c. CE Baelo Claudia	Andalucia, Spain	19.34		<b>19.18</b>	109.3	36
BC_5C_17	4th-5th CE	4th-5th c. CE Baelo Claudia	Andalucia, Spain		<b>22.64</b>		119.2	1
BC_5C_18	4th-5th CE	4th-5th c. CE Baelo Claudia	Andalucia, Spain	26.05	29	<b>23.69</b>	127.8	14
BC_5C_19	4th-5th CE	4th-5th c. CE Baelo Claudia	Andalucia, Spain	27.41		<b>37.41</b>	160	35
BC_5C_20	4th-5th CE	4th-5th c. CE Baelo Claudia	Andalucia, Spain	27	33	<b>24</b>	150.2	8
BC_5C_21	4th-5th CE	4th-5th c. CE Baelo Claudia	Andalucia, Spain	<b>26</b>	31	27	132.5	19-23
LC_1755_1a	1755 CE	1755 CE La Chanca	Conil, Spain	38.35	48.68	<b>34.18</b>	220.3	8
LC_1755_1b	1755 CE	1755 CE La Chanca	Conil, Spain	39	<b>50</b>	38	217.1	8-18
LC_1755_3a	1755 CE	1755 CE La Chanca	Conil, Spain	<b>32</b>	38	40	160.1	19-23
LC_1755_3b	1755 CE	1755 CE La Chanca	Conil, Spain	32	<b>49</b>	30	219.2	11
LC_1755_11a	1755 CE	1755 CE La Chanca	Conil, Spain	43	<b>51</b>	42	220.8	8-18
LC_1755_11b	1755 CE	1755 CE La Chanca	Conil, Spain	38	45	<b>45</b>	228.3	18
LC_1755_12a	1755 CE	1755 CE La Chanca	Conil, Spain	<b>28</b>	34	29	141.7	19-23

LC_1755_12b	1755 CE	1755 CE La Chanca	Conil, Spain	38	<b>46</b>	50	171.8	30-32
LC_1755_13	1755 CE	1755 CE La Chanca	Conil, Spain	21	<b>41</b>	23	162.3	5
LC_1755_8a	1755 CE	1755 CE La Chanca	Conil, Spain	35	<b>41</b>	38	188.2	11
LC_1755_8b	1755 CE	1755 CE La Chanca	Conil, Spain	30	<b>35</b>	30	159.9	8-18
LC_1755_9a	1755 CE	1755 CE La Chanca	Conil, Spain	<b>45</b>	58	49	218.7	19-23
LC_1755_9b	1755 CE	1755 CE La Chanca	Conil, Spain	<b>36</b>	44	42	178.3	24-31
LC_1755_10a	1755 CE	1755 CE La Chanca	Conil, Spain	41	<b>52</b>	53	188.4	32
LC_1755_10b	1755 CE	1755 CE La Chanca	Conil, Spain	31.02	<b>37.06</b>	39.89	144.1	31
LC_1755_6b	1755 CE	1755 CE La Chanca	Conil, Spain	30	36	<b>22</b>	140.3	7
LC_1755_6a	1755 CE	1755 CE La Chanca	Conil, Spain	<b>42</b>	50	44	205.3	19-23
LC_1755_5a	1755 CE	1755 CE La Chanca	Conil, Spain	<b>35</b>	41	38	166.9	26
LC_1755_7	1755 CE	1755 CE La Chanca	Conil, Spain	<b>45</b>	53	45	218.7	24-31
LC_1755_14	1755 CE	1755 CE La Chanca	Conil, Spain	29.65	37.62	<b>29.13</b>	185.3	8
LC_1755_15	1755 CE	1755 CE La Chanca	Conil, Spain	31	<b>39</b>	31	150.8	30-32
LC_1755_16	1755 CE	1755 CE La Chanca	Conil, Spain	<b>38</b>	47	41	187.4	24-31
LC_1755_17	1755 CE	1755 CE La Chanca	Conil, Spain	33.04	39.79	<b>32.26</b>	183.1	13
LC_1755_4	1755 CE	1755 CE La Chanca	Conil, Spain	33	<b>38</b>	30	177.1	9
LC_1755_36	1755 CE	1755 CE La Chanca	Conil, Spain	30.23	<b>35.67</b>	28.73	162.5	8-18
LC_1755_55	1755 CE	1755 CE La Chanca	Conil, Spain	32.12	<b>37.85</b>	29.56	171	8-18
LC_1755_62	1755 CE	1755 CE La Chanca	Conil, Spain	<b>34.44</b>	41.22	34.77	171.2	19-23
LC_1755_90	1755 CE	1755 CE La Chanca	Conil, Spain	33.8	40.89	<b>32.93</b>	173.3	16
LC_1755_138	1755 CE	1755 CE La Chanca	Conil, Spain	30.42	36.56	<b>27.4</b>	173.4	8
LC_1755_202	1755 CE	1755 CE La Chanca	Conil, Spain	<b>33.6</b>		31.71	179.1	8-18
PF_1618_1	16th-18th CE	16th-18th c. CE Pedras de Fogu	Sassari, Sardinia, Italy	38.64	<b>54.82</b>	53.58	195.8	31
PF_1618_2	16th-18th CE	16th-18th c. CE Pedras de Fogu	Sassari, Sardinia, Italy	<b>23</b>	25	23	118.4	19-23
PF_1618_3	16th-18th CE	16th-18th c. CE Pedras de Fogu	Sassari, Sardinia, Italy	19	<b>24</b>	22	108	24
PF_1618_4	16th-18th CE	16th-18th c. CE Pedras de Fogu	Sassari, Sardinia, Italy	<b>22.27</b>	26.71	22.74	115	19-23
PF_1618_5	16th-18th CE	16th-18th c. CE Pedras de Fogu	Sassari, Sardinia, Italy	<b>35</b>	39	35	173.8	19-23
PF_1618_6	16th-18th CE	16th-18th c. CE Pedras de Fogu	Sassari, Sardinia, Italy	<b>33</b>	44	40	164.7	23-31
PF_1618_7	16th-18th CE	16th-18th c. CE Pedras de Fogu	Sassari, Sardinia, Italy	<b>31</b>	37	30	155.5	19-23
PF_1618_8	16th-18th CE	16th-18th c. CE Pedras de Fogu	Sassari, Sardinia, Italy	<b>47.96</b>	60.88	47.8	231.8	19-23
PF_1618_9	16th-18th CE	16th-18th c. CE Pedras de Fogu	Sassari, Sardinia, Italy	<b>29.5</b>	35.8	30.87	177.4	19-23
PF_1618_10	16th-18th CE	16th-18th c. CE Pedras de Fogu	Sassari, Sardinia, Italy	25	30	<b>24</b>	153.6	7
PF_1618_11	16th-18th CE	16th-18th c. CE Pedras de Fogu	Sassari, Sardinia, Italy	<b>19</b>	22	22	106.7	26
PF_1618_12	16th-18th CE	16th-18th c. CE Pedras de Fogu	Sassari, Sardinia, Italy	19	<b>24</b>	24	119.8	10
PF_1618_16	16th-18th CE	16th-18th c. CE Pedras de Fogu	Sassari, Sardinia, Italy	53.82	64.18	<b>57.13</b>	221.5	28
PF_1618_17	16th-18th CE	16th-18th c. CE Pedras de Fogu	Sassari, Sardinia, Italy	44	49	<b>34</b>	219.4	6
PF_1618_18	16th-18th CE	16th-18th c. CE Pedras de Fogu	Sassari, Sardinia, Italy	<b>32.53</b>	35.92	32.94	178	19-23
PF_1618_19	16th-18th CE	16th-18th c. CE Pedras de Fogu	Sassari, Sardinia, Italy	25.6	<b>28.58</b>	26.94	124	24
PF_1618_20	16th-18th CE	16th-18th c. CE Pedras de Fogu	Sassari, Sardinia, Italy	32	49	<b>34</b>	219.1	8
PF_1618_21	16th-18th CE	16th-18th c. CE Pedras de Fogu	Sassari, Sardinia, Italy	24	39	<b>27</b>	173.6	7
PF_1618_22	16th-18th CE	16th-18th c. CE Pedras de Fogu	Sassari, Sardinia, Italy	21	<b>22</b>	19	110.4	11
PF_1618_23	16th-18th CE	16th-18th c. CE Pedras de Fogu	Sassari, Sardinia, Italy	<b>31.59</b>	36.68	34.7	158.3	26
PF_1618_25	16th-18th CE	16th-18th c. CE Pedras de Fogu	Sassari, Sardinia, Italy	26	<b>33</b>	25	152	8-18
PF_1618_26	16th-18th CE	16th-18th c. CE Pedras de Fogu	Sassari, Sardinia, Italy	40.19	<b>53.06</b>	42.53	202.6	24
PF_1618_27	16th-18th CE	16th-18th c. CE Pedras de Fogu	Sassari, Sardinia, Italy	25	32	39	166.1	35
PF_1618_28	16th-18th CE	16th-18th c. CE Pedras de Fogu	Sassari, Sardinia, Italy	25	34	35	150.6	35
PF_1618_29	16th-18th CE	16th-18th c. CE Pedras de Fogu	Sassari, Sardinia, Italy	27		37	158.4	35
PF_1618_30	16th-18th CE	16th-18th c. CE Pedras de Fogu	Sassari, Sardinia, Italy	21		30	130.9	35
PF_1618_31	16th-18th CE	16th-18th c. CE Pedras de Fogu	Sassari, Sardinia, Italy	16		24	106.8	35
PF_1618_32	16th-18th CE	16th-18th c. CE Pedras de Fogu	Sassari, Sardinia, Italy			22	98.7	35
PF_1618_33	16th-18th CE	16th-18th c. CE Pedras de Fogu	Sassari, Sardinia, Italy	22		28	122.9	35
PF_1618_34	16th-18th CE	16th-18th c. CE Pedras de Fogu	Sassari, Sardinia, Italy	25		26	114.9	35
PF_1618_35	16th-18th CE	16th-18th c. CE Pedras de Fogu	Sassari, Sardinia, Italy	27		46	193	35
PF_1618_36	16th-18th CE	16th-18th c. CE Pedras de Fogu	Sassari, Sardinia, Italy			46	193	35
PF_1618_37	16th-18th CE	16th-18th c. CE Pedras de Fogu	Sassari, Sardinia, Italy	21	27	23	129.7	36
PF_1618_38	16th-18th CE	16th-18th c. CE Pedras de Fogu	Sassari, Sardinia, Italy	26	33	26	145.5	36
PF_1618_39	16th-18th CE	16th-18th c. CE Pedras de Fogu	Sassari, Sardinia, Italy	27		39	166.1	35
PF_1618_40	16th-18th CE	16th-18th c. CE Pedras de Fogu	Sassari, Sardinia, Italy	20	22	26	114.9	35
PF_1618_41	16th-18th CE	16th-18th c. CE Pedras de Fogu	Sassari, Sardinia, Italy	17		26	114.9	35
PF_1618_42	16-18th CE	16th-18th c. CE Pedras de Fogu	Sassari, Sardinia, Italy			25	140.2	36
MZ_BF12	13th CE	13th c. CE Mazara del Vallo	Palermo, Sicily, Italy	24	<b>30</b>	25	140.1	8-18
MZ_BF13	13th CE	13th c. CE Mazara del Vallo	Palermo, Sicily, Italy	30.6	44.4	<b>35.6</b>	230.3	8
MZ_BF14	13th CE	13th c. CE Mazara del Vallo	Palermo, Sicily, Italy	35	<b>41</b>	37	167.7	2-7
MZ_BF15	13th CE	13th c. CE Mazara del Vallo	Palermo, Sicily, Italy	29	<b>34</b>	29	155.9	8-18
MZ_BF16	13th CE	13th c. CE Mazara del Vallo	Palermo, Sicily, Italy	30	36	<b>28</b>	180.3	7
MZ_BF20	13th CE	13th c. CE Mazara del Vallo	Palermo, Sicily, Italy	41.1	47.4	<b>39.1</b>	160	28
PP_1BC_01	3-1st BCE	3rd-1st c. BCE Portopalo	Sicily, Italy	22	28	<b>27</b>	114.6	29
PP_1BC_02	3-1st BCE	3rd-1st c. BCE Portopalo	Sicily, Italy	<b>37</b>	47	37	182.8	19-23
PP_1BC_03	3-1st BCE	3rd-1st c. BCE Portopalo	Sicily, Italy	40	48	<b>48</b>	188	29
PP_1BC_08	3-1st BCE	3rd-1st c. BCE Portopalo	Sicily, Italy	49	<b>60</b>	59	211.8	30-32
PP_1BC_09	3-1st BCE	3rd-1st c. BCE Portopalo	Sicily, Italy	35	46	<b>34</b>	219.1	8
PP_1BC_11	3-1st BCE	3rd-1st c. BCE Portopalo	Sicily, Italy	39	48	<b>38</b>	211.5	14

PP_1BC_13	3-1st BCE	3rd-1st c. BCE	Portopalo	Sicily, Italy	25	31	<b>29</b>	121.8	29
PP_1BC_15	3-1st BCE	3rd-1st c. BCE	Portopalo	Sicily, Italy	42	52	<b>40</b>	261.3	7
PP_1BC_18	3-1st BCE	3rd-1st c. BCE	Portopalo	Sicily, Italy	18	<b>36</b>	19	150.8	2-7
PP_1BC_19	3-1st BCE	3rd-1st c. BCE	Portopalo	Sicily, Italy	19	<b>32</b>	19	137	2-7
PP_1BC_Box10	3-1st BCE	3rd-1st c. BCE	Portopalo	Sicily, Italy	32	44	<b>47</b>	196.9	35
PP_1BC_Box16a	3-1st BCE	3rd-1st c. BCE	Portopalo	Sicily, Italy	29	40	34	187.3	36
PP_1BC_Box16b	3-1st BCE	3rd-1st c. BCE	Portopalo	Sicily, Italy	16	22	18	103	36
PP_1BC_Box15	3-1st BCE	3rd-1st c. BCE	Portopalo	Sicily, Italy		43	<b>49</b>	204.5	35
PP_1AD_01	1-4th CE	1st-4th c. CE	Portopalo	Sicily, Italy	31.5	24	<b>24.5</b>	157	7
PP_1AD_02	1-4th CE	1st-4th c. CE	Portopalo	Sicily, Italy	25	<b>42</b>	23	165.8	4
PP_1AD_03	1-4th CE	1st-4th c. CE	Portopalo	Sicily, Italy	32	<b>55</b>	34	227.4	2
PP_1AD_05	1-4th CE	1st-4th c. CE	Portopalo	Sicily, Italy	<b>27</b>	32	23.5	137.1	19-23
PP_1AD_07	1-4th CE	1st-4th c. CE	Portopalo	Sicily, Italy	<b>23</b>	28	22.5	118.4	19-23
PP_1AD_08	1-4th CE	1st-4th c. CE	Portopalo	Sicily, Italy	<b>24</b>	28	22	123.1	19-23
PP_1AD_11	1-4th CE	1st-4th c. CE	Portopalo	Sicily, Italy	<b>30.5</b>	37	32	153.3	19-23
PP_1AD_12	1-4th CE	1st-4th c. CE	Portopalo	Sicily, Italy	38	43	<b>40</b>	163.1	28
PP_1AD_13	1-4th CE	1st-4th c. CE	Portopalo	Sicily, Italy	29.5	34.5	25	157	8
PP_4AD_01	1-4th CE	1st-4th c. CE	Portopalo	Sicily, Italy	31	<b>39</b>	30	175.4	8-18
PP_4AD_02	1-4th CE	1st-4th c. CE	Portopalo	Sicily, Italy	26.5	30	<b>25</b>	126.8	17
PP_4AD_05	1-4th CE	1st-4th c. CE	Portopalo	Sicily, Italy	31.5	43	<b>47</b>	196.9	35
PP_4AD_06	1-4th CE	1st-4th c. CE	Portopalo	Sicily, Italy	28	<b>33</b>	39	139	24
PP_4AD_08	1-4th CE	1st-4th c. CE	Portopalo	Sicily, Italy	32	37	<b>29</b>	184.4	8
1.811	2nd BCE	2nd c. BCE	Punta Camarinal	Andalucia, Spain	28.13	<b>33.33</b>	25.4	158.5	10
1186	2nd BCE	2nd c. BCE	Punta Camarinal	Andalucia, Spain	22.92	<b>44.42</b>	26.74	202.2	9
1187	2nd BCE	2nd c. BCE	Punta Camarinal	Andalucia, Spain	23.47	40.11	<b>26.42</b>	169.8	7
1188	2nd BCE	2nd c. BCE	Punta Camarinal	Andalucia, Spain	22.24	43.92	<b>25.35</b>	163	6
1189	2nd BCE	2nd c. BCE	Punta Camarinal	Andalucia, Spain	30.47	38.02	<b>36.81</b>	145.8	30
10701	2nd BCE	2nd c. BCE	Punta Camarinal	Andalucia, Spain		32.09	<b>21.97</b>	140.1	7
11301	2nd BCE	2nd c. BCE	Punta Camarinal	Andalucia, Spain	<b>15.31</b>	15.53		132.7	39
11302	2nd BCE	2nd c. BCE	Punta Camarinal	Andalucia, Spain	<b>16.49</b>	17.69		143	39
11305	2nd BCE	2nd c. BCE	Punta Camarinal	Andalucia, Spain	38.23	46.67	<b>47.93</b>	179.5	30
11308	2nd BCE	2nd c. BCE	Punta Camarinal	Andalucia, Spain	34.02	37.21	<b>37.9</b>	155.7	28
11309	2nd BCE	2nd c. BCE	Punta Camarinal	Andalucia, Spain	<b>34.87</b>	40.96		153.5	25
11310	2nd BCE	2nd c. BCE	Punta Camarinal	Andalucia, Spain	<b>29.86</b>	33.02	29.1	145.3	26
11311	2nd BCE	2nd c. BCE	Punta Camarinal	Andalucia, Spain	<b>30.92</b>	35.98	31.25	155.2	19-23
11312	2nd BCE	2nd c. BCE	Punta Camarinal	Andalucia, Spain	<b>30.26</b>	34.75	30.34	147	26
11313	2nd BCE	2nd c. BCE	Punta Camarinal	Andalucia, Spain	21.42	<b>41.08</b>	24.56	162.6	5
11315	2nd BCE	2nd c. BCE	Punta Camarinal	Andalucia, Spain	22.82	27.7	<b>28.66</b>	120.6	29
11316	2nd BCE	2nd c. BCE	Punta Camarinal	Andalucia, Spain	26.22	<b>29.92</b>	24.08	144.6	10
11318	2nd BCE	2nd c. BCE	Punta Camarinal	Andalucia, Spain	22.95	<b>33.43</b>	23.27	158.9	9
11319	2nd BCE	2nd c. BCE	Punta Camarinal	Andalucia, Spain	23.27	26.95	<b>21.37</b>	114.5	14
11320	2nd BCE	2nd c. BCE	Punta Camarinal	Andalucia, Spain		28.26	<b>21.47</b>	133.1	8
11321	2nd BCE	2nd c. BCE	Punta Camarinal	Andalucia, Spain	20.39		<b>21.86</b>	134.2	9
11323	2nd BCE	2nd c. BCE	Punta Camarinal	Andalucia, Spain	28.25	37.28	<b>24.08</b>	154.2	7
11331	2nd BCE	2nd c. BCE	Punta Camarinal	Andalucia, Spain	30.06	<b>36.61</b>	30.2	170.8	11
11406	2nd BCE	2nd c. BCE	Punta Camarinal	Andalucia, Spain	23.02	<b>26.76</b>	22.02	127	8-18
11702	2nd BCE	2nd c. BCE	Punta Camarinal	Andalucia, Spain	17.6	32.24	<b>20.9</b>	134	6
11703	2nd BCE	2nd c. BCE	Punta Camarinal	Andalucia, Spain	19.31	33.68	<b>20.3</b>	137.6	3
11704	2nd BCE	2nd c. BCE	Punta Camarinal	Andalucia, Spain	18.66	24.72	<b>20.33</b>	111.2	13
11705	2nd BCE	2nd c. BCE	Punta Camarinal	Andalucia, Spain	24.95	<b>30.71</b>	23.89	147.8	10
11706	2nd BCE	2nd c. BCE	Punta Camarinal	Andalucia, Spain	25.15	29.19	<b>26.55</b>	134.9	17
11707	2nd BCE	2nd c. BCE	Punta Camarinal	Andalucia, Spain	<b>29.03</b>	34.03	29.74	141.7	26
11708	2nd BCE	2nd c. BCE	Punta Camarinal	Andalucia, Spain	29.84	36.06	<b>31.22</b>	159.4	17
11709	2nd BCE	2nd c. BCE	Punta Camarinal	Andalucia, Spain	29.72	<b>36.57</b>	30.03	166	8-18
11710	2nd BCE	2nd c. BCE	Punta Camarinal	Andalucia, Spain	23.45	30.26	<b>30.06</b>	131.1	35
11714	2nd BCE	2nd c. BCE	Punta Camarinal	Andalucia, Spain			<b>36.19</b>	138.3	32
11715	2nd BCE	2nd c. BCE	Punta Camarinal	Andalucia, Spain	27.46	<b>34.89</b>	35.4	137.2	32
11716	2nd BCE	2nd c. BCE	Punta Camarinal	Andalucia, Spain	29.12	<b>33.33</b>	33.91	132.3	32
11717	2nd BCE	2nd c. BCE	Punta Camarinal	Andalucia, Spain	<b>37.64</b>	43.43	37.41	176.9	27
11718	2nd BCE	2nd c. BCE	Punta Camarinal	Andalucia, Spain	33.87	42.14	<b>36.58</b>	151.1	28
11719	2nd BCE	2nd c. BCE	Punta Camarinal	Andalucia, Spain	<b>30.72</b>	37.27	33.52	148.9	26
11720	2nd BCE	2nd c. BCE	Punta Camarinal	Andalucia, Spain		<b>45.5</b>	24.28	176.4	5
11810	2nd BCE	2nd c. BCE	Punta Camarinal	Andalucia, Spain	<b>32.9</b>	36.77	33.75	164.2	23-28
11811	2nd BCE	2nd c. BCE	Punta Camarinal	Andalucia, Spain	29.8	<b>36.02</b>	37.55	141	31
11812	2nd BCE	2nd c. BCE	Punta Camarinal	Andalucia, Spain	<b>28.24</b>		39.96	146	33
11814	2nd BCE	2nd c. BCE	Punta Camarinal	Andalucia, Spain	23.74	29.34	<b>30.84</b>	134.2	35
11816	2nd BCE	2nd c. BCE	Punta Camarinal	Andalucia, Spain		<b>29.67</b>	21.89	210.9	36
11817	2nd BCE	2nd c. BCE	Punta Camarinal	Andalucia, Spain	<b>15.98</b>	15.57		138.5	39
11818	2nd BCE	2nd c. BCE	Punta Camarinal	Andalucia, Spain	<b>16.17</b>	18.3		140.2	39
11901	2nd BCE	2nd c. BCE	Punta Camarinal	Andalucia, Spain			<b>59.08</b>	213	35
11904	2nd BCE	2nd c. BCE	Punta Camarinal	Andalucia, Spain	<b>26.68</b>	30.35	26.17	135.6	23-31
11908	2nd BCE	2nd c. BCE	Punta Camarinal	Andalucia, Spain	19.9	<b>28.14</b>	21.16	200.3	37
11909	2nd BCE	2nd c. BCE	Punta Camarinal	Andalucia, Spain	19.58	<b>21.94</b>	12.3	157.6	37

11911	2nd BCE	2nd c. BCE Punta Camarinal	Andalucia, Spain	20.84	<b>22.3</b>	12.28	160.1	37
11912	2nd BCE	2nd c. BCE Punta Camarinal	Andalucia, Spain	19.49	<b>22.15</b>	11.7	159	37
11914	2nd BCE	2nd c. BCE Punta Camarinal	Andalucia, Spain	<b>18.52</b>	18.1		160.7	39
11965	2nd BCE	2nd c. BCE Punta Camarinal	Andalucia, Spain	23.42	26.8	<b>22.72</b>	118.9	15
12101	2nd BCE	2nd c. BCE Punta Camarinal	Andalucia, Spain	37.27	44.13	<b>40.03</b>	163.2	28
12102	2nd BCE	2nd c. BCE Punta Camarinal	Andalucia, Spain	31.55	37.51	<b>31.95</b>	134.5	28
12103	2nd BCE	2nd c. BCE Punta Camarinal	Andalucia, Spain	<b>31.78</b>	36.38	32.06	154.4	24
12104	2nd BCE	2nd c. BCE Punta Camarinal	Andalucia, Spain	26.81	<b>30.88</b>	24.24	148.5	10
MET10092	9-13th CE	9-13th c. CE Yenikapi	Istanbul, Turkey	27.27	<b>35.64</b>	27.2	138.4	23-31
MET11176	9-13th CE	9-13th c. CE Yenikapi	Istanbul, Turkey	36.9	<b>44.39</b>	35.11	179	2-7
MET13029	9-13th CE	9-13th c. CE Yenikapi	Istanbul, Turkey	45.29	55.37	44.35	209.5	24 or 25
MET13186	9-13th CE	9-13th c. CE Yenikapi	Istanbul, Turkey	46.02	57.54	46.55	246.9	24-31
MET13280	9-13th CE	9-13th c. CE Yenikapi	Istanbul, Turkey	<b>38.2</b>	44.45	38.5	188.3	24-31
MET13687	9-13th CE	9-13th c. CE Yenikapi	Istanbul, Turkey	34.37	43.62	42.04	164.7	30-32
MET14112	9-13th CE	9-13th c. CE Yenikapi	Istanbul, Turkey	49.83	62.07	47.65	240	19-23
MET14118	9-13th CE	9-13th c. CE Yenikapi	Istanbul, Turkey	40.58	47.65	41.14	192.8	24-31
MET14129	9-13th CE	9-13th c. CE Yenikapi	Istanbul, Turkey	<b>33.9</b>	42	31.6	168.8	24-31
MET14266	9-13th CE	9-13th c. CE Yenikapi	Istanbul, Turkey	42.28	52.07	36.98	224.7	8-18
MET14321	9-13th CE	9-13th c. CE Yenikapi	Istanbul, Turkey	40.8	50.54	40.03	190.9	26
MET14369	9-13th CE	9-13th c. CE Yenikapi	Istanbul, Turkey	43.41	56.6	40.58	211.6	19-23
MET14541	9-13th CE	9-13th c. CE Yenikapi	Istanbul, Turkey	45.97	53.73	43.2	210.9	27
MET15144	9-13th CE	9-13th c. CE Yenikapi	Istanbul, Turkey	<b>34.11</b>	43.28	35.1	197.3	19-23
MET16672	9-13th CE	9-13th c. CE Yenikapi	Istanbul, Turkey	44.14	52.99	38.7	231.4	12 or 13
MET16688	9-13th CE	9-13th c. CE Yenikapi	Istanbul, Turkey	50.79	63.74	41.3	267.1	6 or 7
MET17473	9-13th CE	9-13th c. CE Yenikapi	Istanbul, Turkey	48.24	<b>55.22</b>	51.37	198.4	30-32
MET18542	9-13th CE	9-13th c. CE Yenikapi	Istanbul, Turkey	45.01	<b>54.99</b>	37.58	235.5	8-18
MET2083	9-13th CE	9-13th c. CE Yenikapi	Istanbul, Turkey	<b>44.81</b>	53.54	43.76	217.8	19-23
MET20830	9-13th CE	9-13th c. CE Yenikapi	Istanbul, Turkey	26.66	<b>35.95</b>	32.1	141.4	33-35
MET4041	9-13th CE	9-13th c. CE Yenikapi	Istanbul, Turkey	<b>45.43</b>	55	47.15	214.6	23
MET57084	9-13th CE	9-13th c. CE Yenikapi	Istanbul, Turkey	33.41	41.05	<b>33</b>	146	25 or 26
MET57505	9-13th CE	9-13th c. CE Yenikapi	Istanbul, Turkey	39.1	46.1	<b>31.94</b>	204.7	8
MET59646	9-13th CE	9-13th c. CE Yenikapi	Istanbul, Turkey	36.09	<b>43.11</b>	38.76	171.8	24 or 25
MET6052	9-13th CE	9-13th c. CE Yenikapi	Istanbul, Turkey	<b>40.59</b>	X	37.71	220.9	8-18
MET7173	9-13th CE	9-13th c. CE Yenikapi	Istanbul, Turkey	46.34	58.34	<b>44.8</b>	177.1	29
MET7386	9-13th CE	9-13th c. CE Yenikapi	Istanbul, Turkey	46.84	56.83	48.61	215.4	26
MET7848	9-13th CE	9-13th c. CE Yenikapi	Istanbul, Turkey	33.5	<b>39</b>	35	150.8	30-32
MRY10178	9-13th CE	9-13th c. CE Yenikapi	Istanbul, Turkey	42.23	48.76	<b>33.56</b>	217.7	7
MRY10902	9-13th CE	9-13th c. CE Yenikapi	Istanbul, Turkey	42.45	51.18	39.87	221.4	8-18
MRY10963	9-13th CE	9-13th c. CE Yenikapi	Istanbul, Turkey	46.83	<b>56.79</b>	41.73	213.8	24
MRY11030	9-13th CE	9-13th c. CE Yenikapi	Istanbul, Turkey	34.94	44.87	<b>43.98</b>	185.3	35
MRY11060	9-13th CE	9-13th c. CE Yenikapi	Istanbul, Turkey	47	57.59	<b>43.26</b>	284.4	8
MRY11407	9-13th CE	9-13th c. CE Yenikapi	Istanbul, Turkey	37.48	<b>45.98</b>	30.97	208.6	10
MRY11604	9-13th CE	9-13th c. CE Yenikapi	Istanbul, Turkey	36.52	<b>43.78</b>	32.55	193.7	8-18
MRY11617	9-13th CE	9-13th c. CE Yenikapi	Istanbul, Turkey	37.26	45.55	34.15	179.5	24
MRY11675	9-13th CE	9-13th c. CE Yenikapi	Istanbul, Turkey	44.42	54.95	45.61	182.6	28
MRY12298	9-13th CE	9-13th c. CE Yenikapi	Istanbul, Turkey	31.73	<b>38.74</b>	30.85	174.4	8-18
MRY12450	9-13th CE	9-13th c. CE Yenikapi	Istanbul, Turkey	25.83	<b>29.5</b>	21.1	138.1	8-18
MRY12888	9-13th CE	9-13th c. CE Yenikapi	Istanbul, Turkey	<b>48.31</b>	59.68	45.92	226.9	23
MRY13127	9-13th CE	9-13th c. CE Yenikapi	Istanbul, Turkey	<b>29.04</b>	33.8	26.46	146.5	19-23
MRY13139	9-13th CE	9-13th c. CE Yenikapi	Istanbul, Turkey	48.84	<b>60.3</b>	43.46	254.9	8-18
MRY13166	9-13th CE	9-13th c. CE Yenikapi	Istanbul, Turkey	37.28	44.14	<b>38.33</b>	165.2	28
MRY1704	9-13th CE	9-13th c. CE Yenikapi	Istanbul, Turkey	34.13	<b>44.86</b>	41.47	168.4	30 or 31
MRY1772	9-13th CE	9-13th c. CE Yenikapi	Istanbul, Turkey	52.98	<b>66.87</b>	53.58	230.7	30 or 31
MRY2790	9-13th CE	9-13th c. CE Yenikapi	Istanbul, Turkey	36.42	<b>46.41</b>	35.4	203.6	8-18
MRY3068	9-13th CE	9-13th c. CE Yenikapi	Istanbul, Turkey	43.6	50.14	40.93	163.9	29
MRY3074	9-13th CE	9-13th c. CE Yenikapi	Istanbul, Turkey	40.56	45.79	<b>38.43</b>	155.2	29
MRY3208	9-13th CE	9-13th c. CE Yenikapi	Istanbul, Turkey	39.83	<b>48.98</b>	43.5	180.5	30 or 31
MRY3572	9-13th CE	9-13th c. CE Yenikapi	Istanbul, Turkey	<b>38.28</b>	45.28	39.13	188.6	23-31
MRY3964	9-13th CE	9-13th c. CE Yenikapi	Istanbul, Turkey	43.23	<b>54.81</b>	38.75	241.6	9
MRY4226	9-13th CE	9-13th c. CE Yenikapi	Istanbul, Turkey	<b>45.16</b>	55.89	43.63	219.4	23-31
MRY4452	9-13th CE	9-13th c. CE Yenikapi	Istanbul, Turkey	<b>51.94</b>	67.04	51.24	249.3	24-31
MRY4524	9-13th CE	9-13th c. CE Yenikapi	Istanbul, Turkey	62.49	<b>77.55</b>	66.2	259.2	30-31
MRY5106	9-13th CE	9-13th c. CE Yenikapi	Istanbul, Turkey	<b>47</b>	58.14	59.9	215.1	27
MRY5112	9-13th CE	9-13th c. CE Yenikapi	Istanbul, Turkey	<b>41.22</b>	52.81	42.54	201.8	23-31
MRY5277	9-13th CE	9-13th c. CE Yenikapi	Istanbul, Turkey	45.51	<b>55.66</b>	46.48	199.6	30 or 31
MRY7601	9-13th CE	9-13th c. CE Yenikapi	Istanbul, Turkey	41.79	48.08	<b>37.06</b>	205.9	14
MRY8553	9-13th CE	9-13th c. CE Yenikapi	Istanbul, Turkey	30.92	<b>34.7</b>	24.67	164	9
MRY9361	9-13th CE	9-13th c. CE Yenikapi	Istanbul, Turkey	45.99	55.17	38.99	223	19-23



#### **Chapter 4**

Isotopic life-history signatures are retained in  
modern and ancient Atlantic bluefin tuna vertebrae  
**(pages 114—138)**

# Isotopic life-history signatures are retained in modern and ancient Atlantic bluefin tuna vertebrae

Adam J. Andrews<sup>\*1</sup>, David Orton<sup>2</sup>, Vedat Onar<sup>3</sup>, Piero Addis<sup>4</sup>, Fausto Tinti<sup>1</sup>, Michelle Alexander<sup>\*2</sup>

<sup>1</sup>Department of Biological, Geological and Environmental Sciences, University of Bologna, Campus of Ravenna, Ravenna, Italy

<sup>2</sup>BioArCh, Department of Archaeology, University of York, York, U.K.

<sup>3</sup>Osteoarchaeology Practice and Research Centre and Faculty of Veterinary Medicine, Istanbul University-Cerrahpaşa, Istanbul, Turkey

<sup>4</sup>Department of Life and Environmental Sciences, University of Cagliari, Cagliari, Sardinia, Italy

\*Corresponding authors: [adam@palaeome.org](mailto:adam@palaeome.org), [michelle.alexander@york.ac.uk](mailto:michelle.alexander@york.ac.uk)

Keywords: serial sectioning, stable isotope analysis, fish bone turnover, life histories of fishes, historical ecology

## Abstract

Isotopic, tagging and diet studies of modern-day teleosts lack the ability to contextualise life-histories and trophic dynamics with a historical perspective, when exploitation rates were lower and climatic conditions differed. Isotopic analysis of vertebrae, the most plentiful hard-part in archaeological and museum collections, can potentially fill this data-gap. Chemical signatures of habitat and diet use during growth are retained by vertebrae during bone formation. However, to fulfil their potential to reveal life-history and trophic dynamics, we need a better understanding of the time-frame recorded by vertebrae, currently lacking due to a poor understanding of fish bone remodelling. To address this issue, we serially-sectioned four vertebral centra of the highly migratory Atlantic bluefin tuna (*Thunnus thynnus*; BFT) captured off Sardinia (Italy) and analysed their isotopic composition. We show how carbon ( $\delta^{13}\text{C}$ ), nitrogen ( $\delta^{15}\text{N}$ ) and sulfur ( $\delta^{34}\text{S}$ ) isotope values can vary significantly across BFT vertebrae growth-axes, revealing patterning in dietary life-histories. Further, we find similar patterns are revealed through incremental isotopic analysis of inner and outer vertebrae centra samples from thirteen archaeological BFT vertebrae dating between the 9<sup>th</sup>-13<sup>th</sup> century CE. Our results indicate that multi-year foraging signatures are retained in vertebrae and allow for the study of life-histories in both modern and paleo-environments. These novel methods can be extended across teleost taxa owing to their potential to inform management and conservation on how teleost trophic dynamics change over time and what their long-term environmental, ecological, and anthropological drivers are.

## 1. Introduction

Retrospective ecological studies are increasingly analysing the stable isotopic composition of teleost vertebrae due to the predominance of these bones in the archaeological record and potential to reveal how trophic dynamics respond to environmental, ecological and cultural shifts (Barrett *et al.*, 2011; Guiry *et al.*, 2020; Ólafsdóttir *et al.*, 2017). However, little is known about how tissue turnover influences isotopic variation across the growth axes of teleost vertebrae and thus whether isotope values represent short-term snapshots into the foraging ecology of fishes immediately before they were caught, or long-term averages across their entire life-span (Tzadik *et al.*, 2017). This information has important

This article has been accepted for publication and undergone full peer review but has not been through the copyediting, typesetting, pagination and proofreading process which may lead to differences between this version and the [Version of Record](#). Please cite this article as doi: [10.1111/jfb.15417](https://doi.org/10.1111/jfb.15417)

consequences for their interpretation, comparison with isotope measurements from other tissue types and biogeochemical data, as well as for the sampling of teleost vertebrae prior to analysis.

For highly migratory species, such as the Atlantic bluefin tuna (*Thunnus thynnus*, hereafter BFT), the ability to trace temporal changes in life-histories using isotopic variation across the growth axes of vertebra represents an additional novel opportunity; otherwise only possible when using otoliths, which are metabolically inert and not subject to turnover (Campana & Thorrold, 2001; Tzadik *et al.*, 2017). Given that otoliths are not as prevalent in the archaeological record or museum collections, and are generally only analysed for a few elements (e.g.,  $\delta^{13}\text{C}$ ,  $\delta^{18}\text{O}$  and  $^{87/86}\text{Sr}$ ) due to being composed primarily of calcium carbonate, vertebrae might offer a practical solution to obtaining isotopic life-history signatures from protein including those of additional elements (e.g.,  $\delta^{15}\text{N}$ ,  $\delta^{34}\text{S}$ ,  $\delta^2\text{H}$ ; Andrews *et al.*, 2022b; Barrett *et al.*, 2011; McCormack *et al.*, 2021; Nehlich *et al.*, 2013). Importantly, this would enhance investigations into how feeding patterns and migrations change in the marine environment over time and what their environmental, ecological and anthropological drivers are (Guiry & Hunt, 2020).

Two factors will influence the degree of isotopic variation within teleost bone: 1) the variation in isotope signatures between habitats and diets utilised across the individual's lifespan, and 2) how rapidly the protein containing those signatures is remodelled and reabsorbed. Teleost bone is mainly composed of hydroxyapatite ( $\text{Ca}_{10}(\text{PO}_4)_6(\text{OH})_2$ ), a type of calcium phosphate which is deposited onto collagen fibrils. Teleost bone turnover has long been considered slow relative to soft tissues such as muscle and liver (Buchheister & Latour, 2010; Madigan *et al.*, 2012; Tzadik *et al.*, 2017) following assumptions from better-studied taxa (e.g., mammals and birds (Hobson & Clark, 1992; Tieszen *et al.*, 1983)). Since fish growth continues throughout life, resorption (the repair of damaged tissue by osteoclasts) and remodelling (the incorporation of new tissue by osteoblasts) are ongoing processes, which are expected to vary between bone elements and species, depending on their growth and damage rates, but these are largely unknown (Bas & Cardona, 2018; Davesne *et al.*, 2019; Witten & Villwock, 1997). Complications further arise since these two processes may function differently depending on whether fishes have acellular bone (lacking osteocytes, e.g., Atlantic cod, *Gadus morhua*) or cellular bone (containing osteocytes e.g., BFT), despite osteocytes being more heavily involved in mineral homeostasis, rather than remodelling, in teleosts (Davesne *et al.*, 2019; Meunier, 2011; Witten *et al.*, 2000; Witten & Huysseune, 2009).

The cellular bone of BFT can be further distinguished by two types; cortical (dense, surface) bone, which retains annuli (annual growth layers) and cancellous (spongy, interior) bone, where growth layers are more rapidly resorbed (Matsubayashi & Tayasu, 2019; Santamaria *et al.*, 2018; Turner Tomaszewicz *et al.*, 2016). Cortical vertebral bone is well-evidenced to retain life-history isotopic signatures in Elasmobranchs (e.g., sharks). These are ca. 1-2‰ variation in both  $\delta^{13}\text{C}$  and  $\delta^{15}\text{N}$  values over the life-span of 10-15 year old individuals, which studies generally agree represents a multi-year signal instead of a perfect chronology (Carlisle *et al.*, 2015; Estrada *et al.*, 2006; Kerr *et al.*, 2006; Shen *et al.*, 2022). In teleosts, investigations are more recent and are as yet restricted to mostly anadromous Salmonidae spp., Pleuronectidae spp., and Clupeidae spp. from a confined Pacific locality (Kato *et al.*, 2021; Matsubayashi *et al.*, 2017, 2019, 2020), reporting variability of ca. 1-5‰ in  $\delta^{13}\text{C}$ ,  $\delta^{15}\text{N}$

and  $\delta^{34}\text{S}$  across growth axes of adult fishes, suggesting that juvenile signatures can be fully or partially retained into adulthood.

A range of ecological and environmental variables will affect the  $\delta^{13}\text{C}$ ,  $\delta^{15}\text{N}$  and  $\delta^{34}\text{S}$  values retained at each life-history stage.  $\delta^{15}\text{N}$  values increase with each trophic level and are thus used to estimate the trophic position of an organism in a food web (Sigman *et al.*, 2009). In contrast,  $\delta^{13}\text{C}$  and  $\delta^{34}\text{S}$  values pass between primary producers and consumers with low levels of fractionation. This lends them to being good indicators of provenance because distinct  $\delta^{13}\text{C}$  and  $\delta^{34}\text{S}$  signatures are generally maintained across trophic levels (DeNiro & Epstein, 1978; Guiry, 2019; Thode, 1991). Typically, coastal habitats (and those heavily influenced by cold or low-salinity water) are lower in  $\delta^{13}\text{C}$  than oceanic habitats, partially due to increased terrestrially-derived (low- $\delta^{13}\text{C}$ ) carbon inputs and lower quantities of resuspended (remineralized, high- $\delta^{13}\text{C}$ ) carbon from the benthos and deep-ocean (Barnes *et al.*, 2009; Magozzi *et al.*, 2017). For these reasons, pelagic consumers often contain lower  $\delta^{13}\text{C}$  than benthic ones (Amiriaux *et al.*, 2023; DeNiro & Epstein, 1978).

It is important to note that multiple factors govern the variation in  $\delta^{15}\text{N}$  and  $\delta^{13}\text{C}$  between consumers, including the environmental conditions, levels of benthic-pelagic coupling and the production in each habitat foraged (Barnes *et al.*, 2009; Jennings *et al.*, 2008; Sigman *et al.*, 2009). One useful technique is to use additional isotopes (such as  $\delta^{34}\text{S}$ ) to disentangle these effects. For example, low  $\delta^{34}\text{S}$  values often reflect increased foraging on benthic or neritic prey while higher values indicate a greater degree of energy incorporated from pelagic production (Fry & Chumchal, 2011; Szpak & Buckley, 2020). Distance from shore also influences  $\delta^{34}\text{S}$  values, not because of freshwater input (even brackish water is dominated by marine high  $\delta^{34}\text{S}$  signatures) (Cobain *et al.*, 2022; Fry & Chumchal, 2011; Guiry *et al.*, 2022), but rather the greater extent of sulfide-rich (low  $\delta^{34}\text{S}$ ) production in coastal areas, such as in seagrass beds, salt marshes and mudflats (Guiry *et al.*, 2022; Szpak & Buckley, 2020; Thode, 1991). Since ecological and environmental variables governing production change over time (e.g., following production dynamics, and sources such as pollution), there is often intra- and inter-annual variation at the base of marine food-webs, which one needs to be aware of when drawing conclusions from temporal isotopic data—especially over the long-term (Jardine *et al.*, 2014; Solomon *et al.*, 2008). However, some degree of temporal variation can be accounted for, like the long-term decrease in oceanic  $\delta^{13}\text{C}$  following industrialisation (Suess Effect: Gruber *et al.* (1999).

BFT is a large ( $\leq 3.3$  m in length and  $\leq 725$  kg in weight: Cort *et al.* (2013)) pelagic predator, which spawns from ages 3-4 (Mather *et al.*, 1995; Piccinetti *et al.*, 2013); predominantly in the Mediterranean and in the Gulf of Mexico. The majority of individuals undertake diverse feeding migrations to a range of habitats throughout the Atlantic (Druon *et al.*, 2016; Mariani *et al.*, 2016; Wilson & Block, 2009) from as early as age one (Dickhut *et al.*, 2009), though tagging evidence suggests that a portion of the population are resident in the Mediterranean all-year-round (Cermeño *et al.*, 2015). Juvenile and adult BFT primarily inhabit the upper 200 m of neritic habitats (Druon *et al.*, 2016; Walli *et al.*, 2009; Wilson & Block, 2009), feeding mostly on varied combinations of teleost fishes, cephalopods and crustaceans (Karakulak *et al.*, 2009; Logan *et al.*, 2011) and occasionally undertaking divergent offshore feeding strategies at great depths (Battaglia *et al.*, 2013; Olafsdottir *et al.*, 2016; Wilson & Block, 2009). The greatest shift in BFT foraging strategy appears to be at age two, once the

predation of zooplankton ends and the predation of fishes begins, after which, year classes become more isotopically similar (Rumolo *et al.*, 2020; Sarà & Sarà, 2007).

The aim of this study was to determine isotopic variation across the growth axis of BFT vertebrae to explore if the degree of tissue turnover is sufficiently slow to expand chronological studies of isotopic life-history signatures in retrospective ecological contexts. We hypothesised that BFT vertebrae would document limited isotopic variation because the diets and habitats of BFT are rather isotopically homogeneous (Brophy *et al.*, 2020), and the cellular bone of BFT in addition to their endothermy and rapid growth rates would promote more rapid resorption and remodelling than other teleosts (Davesne *et al.*, 2019). Our objectives were to (1) serial-section modern BFT vertebral cortical bone, (2) sample inner and outer archaeological BFT vertebrae centra, and (3) determine and analyse the  $\delta^{13}\text{C}$ ,  $\delta^{15}\text{N}$  and  $\delta^{34}\text{S}$  collagen isotope values of samples.

## 2. Methods

### 2.1 Serial-sectioning of modern specimens

Modern BFT were sampled off Isola Piana (Carloforte, Sardinia, Italy) in July 2020 by tuna trap (Carloforte Tonnare PIAM srl, Table 1). Vertebrae were mechanically cleaned of soft-tissues, macerated in ambient-temperature water for up to 3 months to remove the remaining soft-tissues by microbial decomposition, then rinsed using distilled water and dried.

**Table 1.** Details of the modern Atlantic bluefin tuna (*Thunnus thynnus*) specimens serially-sectioned in the current study. Age was estimated by counting annuli following Lee *et al.* (1983) and Andrews *et al.* (2023), as described in the methods. Height, Width and Length correspond to 35<sup>th</sup> vertebra measurements on the posterior centra as per Andrews *et al.* (2022a).

Sample	Location	Capture date	Coordinates	FL (cm)	Age (yrs)	Element analysed	Height (mm)	Width (mm)	Length (mm)	No. Sections
CF_2020_588	Carloforte tonnara, Sardinia	July 2020	39.18 E, 8.31 N	196	9	35 <sup>th</sup> vertebra	33.01	43.42	46.89	18
CF_2020_810	Carloforte tonnara, Sardinia	July 2020	39.18 E, 8.31 N	158	8	35 <sup>th</sup> vertebra	25.10	33.4	37.12	12
CF_2020_667	Carloforte tonnara, Sardinia	July 2020	39.18 E, 8.31 N	149	5	35 <sup>th</sup> vertebra	20.12	27.26	28.96	9
CF_2020_673	Carloforte tonnara, Sardinia	July 2020	39.18 E, 8.31 N	124	7	35 <sup>th</sup> vertebra	17.74	22.5	25.05	8

The 35<sup>th</sup> vertebra of each specimen was isolated, pertaining to one of the penultimate vertebrae in BFT which have a total of 39 vertebrae (for a guide on BFT vertebra identification see Andrews *et al.* (2022a)). The 35<sup>th</sup> vertebra was selected for consistency between specimens and due to the fact that annuli (growth rings) are often more clearly interpreted in these vertebrae. We aged specimens by counting annuli (Figure 1A) on the posterior centra of the 35<sup>th</sup> vertebra for each specimen, without staining and with illumination

only, following Lee *et al.* (1983) and Andrews *et al.* (2023), where one year pertained to one groove (summer growth) and one ridge (winter growth).

Vertebrae (Table 1) were prepared for sectioning, whereby the outer surface of each specimen was mechanically cleaned to remove exogenous residues. Specimens were then cut using a band-saw, by halving first along the lateral plane (Figure 1A), and second along the ventral plane to obtain a posterior centrum cross-section, such that all annual layers of growth in each specimen were represented (Figure 2B). A cross-section sample (ca. 250 to 1000 mg) was obtained for each specimen by again cutting along the lateral plane. The band saw was then set to cut ca. 1 mm (0.1 mm error) increments starting at the centre of the centrum (age 0) (Figure 1B). Each increment was trimmed using a scalpel to remove cancellous bone, retaining cortical bone for analyses (Figure 1C). The first and second increment sections from the centre were combined in all instances to provide sufficient mass for analyses.

### 2.2 Incremental sampling of archaeological specimens

A total of 13 archaeological BFT vertebrae were analysed from a Byzantine-era site in the Yenikapi neighbourhood of Istanbul, Turkey (Table S2). The Port of Theodosius operated at this site from the 4<sup>th</sup>-11<sup>th</sup> century CE before being filled in during the 15<sup>th</sup> century CE (Onar *et al.*, 2008). The 9<sup>th</sup>-13<sup>th</sup> century origin of the samples is proposed from <sup>14</sup>C dating taking into account reservoir effects for habitats foraged (Andrews *et al.*, in review). Fork length (FL) of archaeological specimens was estimated following Andrews *et al.* (2022a) using the online resource <https://tunaarchaeology.org/lengthestimations>. Briefly, vertebrae were identified to rank or type (see (Andrews *et al.*, 2022a), vertebral centrum length, width and height was measured using digital callipers to the nearest 0.01 mm, and the best-fitting power regression model was applied for each specimen (Table S1, S2). Age estimation was not attempted due to the poor visibility of annuli in these archaeological specimens. Size estimation was not attempted for three individuals due to inability to reliably identify vertebrae rank or type due to preservation (Table S2).

Due to national restrictions in the invasive sampling of archaeological materials in Turkey, the cutting of archaeological vertebrae was prohibited, thus we drilled into each vertebra at inner (close to the centrum centre) and outer (close to the centrum edge) positions (Figure 3). First, drilling sites at the inner and outer edges of vertebrae centra were mechanically cleaned for each specimen to remove exogenous residues. Then, we drilled into vertebrae at these inner and outer positions with 6 mm stainless-steel drill bits, maintaining a low speed. We collected 50-150 mg bone powder from each position, pertaining to both cortical and cancellous bone in roughly similar proportions as modern cross-section samples.

### 2.3 Collagen extraction

Bone collagen was extracted following a modified Longin method (Brown *et al.*, 1988). Modern samples were defatted by sonication for 15 minutes in a 2:1 dichloromethane/methanol solution (Colonese *et al.*, 2015), repeated a minimum of three times until the solution remained clear. Solvents were then evaporated overnight before samples were rinsed three times with milli-Q water to remove residual solvents. All samples were demineralised at +4°C, using 8 ml of 0.6 M HCl for modern samples and a gentler 0.4 M HCl for archaeological samples. Once completely demineralised, collagen was gelatinised

at 80°C for 48 hours in 0.001 M HCl. Gelatinised collagen was filtered (60 to 90 µm; Ezee filters, Elkay, U.K.) and then freeze-dried.

#### 2.4 Stable isotope analysis

To determine the carbon and nitrogen isotopic values, collagen (0.4-0.6 mg) was analysed in duplicate using a Sercon continuous flow 20-22 IRMS interfaced with a Universal Sercon gas solid liquid elemental analyser (Sercon, U.K.). Sulfur isotope values were determined for the serial sections of one of the specimens (CF\_2020\_810) by analysing collagen (0.9-1.2 mg), 20% in duplicate using a Delta V Advantage continuous-flow IRMS coupled via a ConFloIV to an IsoLink elemental analyser (Thermo Scientific, Germany) at SUERC (East Kilbride, U.K.) as described in Sayle *et al.* (2019). The obtained values were corrected from the isotopic ratio of the international standards, Vienna Pee Dee Belemnite (VPDB) for carbon, air (AIR) for nitrogen, and Vienna Cañon-Diablo Troilite (VCDT) for sulfur, using the  $\delta$  (‰) notation. Accuracy was determined using a two-point calibration curve taking into account uncertainty for duplicate samples (Tables S1, S2 and Supplementary Appendix).

Uncertainties on the measurements were calculated by combining the SDs of the sample replicates and those of International Atomic Energy Agency (IAEA) reference material according to Kragten (Kragten, 1994) for carbon and nitrogen, and (Sayle *et al.*, 2019) for sulfur. The international standards used as reference material in analytical runs were; caffeine (IAEA-600), ammonium sulfate (IAEA-N-2), and cane sugar (IA-Cane) for carbon and nitrogen; and silver sulfide (IAEA-S-2 and IAEA-S-3) for sulfur. International standard average values and SD across the runs were as follows: IAEA-600 ( $n = 18$ ),  $\delta^{13}\text{C}$  raw =  $-27.65 \pm 0.1\text{‰}$  ( $\delta^{13}\text{C}$  true =  $-27.77 \pm 0.04\text{‰}$ ) and  $\delta^{15}\text{N}$  raw =  $+0.77 \pm 0.16\text{‰}$  ( $\delta^{15}\text{N}$  true =  $1 \pm 0.2\text{‰}$ ); IAEA-N-2 ( $n = 18$ ),  $\delta^{15}\text{N}$  raw =  $+20.13 \pm 0.18\text{‰}$  ( $\delta^{15}\text{N}$  true =  $20.3 \pm 0.2\text{‰}$ ); and IA-CANE ( $n = 18$ ),  $\delta^{13}\text{C}$  raw =  $-11.72 \pm 0.08\text{‰}$  ( $\delta^{13}\text{C}$  true =  $-11.64 \pm 0.03\text{‰}$ ); IAEA-S-2 ( $n=9$ ),  $\delta^{34}\text{S}$  was calibrated relative to VCDT using internal standards GS2 and GAS2 (themselves calibrated to international standards IAEA-S-2 and IAEA-S-3). The maximum uncertainty across all samples was  $\pm 0.18\text{‰}$  for  $\delta^{13}\text{C}$  and  $0.22\text{‰}$  for  $\delta^{15}\text{N}$  ( $n = 56$ ), and  $\pm 0.41\text{‰}$  for  $\delta^{34}\text{S}$  ( $n = 21$ ). For more information on calibration and analytical uncertainty see Supplementary Appendix (Tables S3-S5).

The quality of  $\delta^{13}\text{C}$  and  $\delta^{15}\text{N}$  values was confirmed by assessing that atomic C:N ratios (3.0-3.3) fell within the accepted ranges for archaeological and modern samples (Guiry & Szpak, 2020, 2021), while  $\delta^{34}\text{S}$  quality was confirmed by assessing %S, C:S and N:S against acceptable standards (Nehlich & Richards, 2009). The quality of archaeological samples was further confirmed by assessing that collagen yields ( $>1\%$ , Table S2) represented an adequate state of preservation. A modern bovine control which was processed and analysed alongside the archaeological sample batch yielded expected isotopic values ( $-23.2\text{‰}$   $\delta^{13}\text{C}$ ,  $6.2\text{‰}$   $\delta^{15}\text{N}$ , 3.2 C:N) and collagen yield (17.5%).

#### 2.5 Statistical analysis

Logarithmic regressions were performed in R (R Team, 2013) to assess the significance of the relationship between section number and isotope value, per specimen. Prior to testing, negative  $\delta^{13}\text{C}$  values were transformed to positive equivalents. Paired Wilcoxon tests were performed in R to test the significance of difference between inner and outer isotope values. Significance was judged at the 5% level.

### 3. Results

#### 3.1 Serial-sectioning of modern specimens

Modern BFT specimens varied between 124-196 cm FL, ages 5-9, 18-33 mm centrum height, and yielded between 7 and 17 vertebra sections for isotopic analyses.  $\delta^{13}\text{C}$  values were generally between  $-15\text{‰}$  and  $-14\text{‰}$ , except for CF\_2020\_810, where values varied between  $-14\text{‰}$  and  $-13\text{‰}$  (Figure 2B).  $\delta^{13}\text{C}$  values generally increased from the center to the edges of vertebrae, by ca.  $1\text{‰}$  for the largest individuals (CF\_2020\_588, 810) with 11-17 serial sections and ca.  $0.5\text{‰}$  for the smaller individuals (CF\_2020\_667, 673) with 7-8 serial sections (Figure 2A). Cross-sections of growth axes generally had  $\delta^{13}\text{C}$  values ca.  $0.2\text{‰}$  greater than the outermost serial sections of each individual, the exception being CF\_2020\_673, which was ca.  $0.2\text{‰}$  lower than outermost serial sections values. A significant relationship between  $\delta^{13}\text{C}$  and vertebra sections was found for three of the four individuals, CF\_2020\_673 ( $F_5 = 8.2$ ,  $R^2 = 0.55$ ,  $p < 0.05$ ), CF\_2020\_588 ( $F_{15} = 12.1$ ,  $R^2 = 0.41$ ,  $p < 0.01$ ) and CF\_2020\_810 ( $F_9 = 123.3$ ,  $R^2 = 0.92$ ,  $p < 0.001$ ).

Serial section  $\delta^{15}\text{N}$  values were stochastic but overall increased from the center to the edges of vertebrae (Figure 2C) by ca.  $0.5\text{‰}$  for all individuals.  $\delta^{15}\text{N}$  values of cross-sections of growth axes more closely matched the outermost serial sections of each individual except CF\_2020\_667, whose outermost serial section value appears to be an outlier. The oldest aged individual analysed (CF\_2020\_588, 9 yrs) had  $\delta^{15}\text{N}$  value of ca.  $10\text{‰}$  whereas the remaining three individuals (ages 5, 7, 8 yrs) had  $\delta^{15}\text{N}$  values of ca.  $6\text{--}7\text{‰}$  expected for juveniles (ages 1-2) (Figure 2C). A significant relationship between  $\delta^{15}\text{N}$  and vertebra sections was found for three of the four individuals, CF\_2020\_667 ( $F_6 = 11.2$ ,  $R^2 = 0.59$ ,  $p < 0.05$ ), CF\_2020\_673 ( $F_5 = 24.3$ ,  $R^2 = 0.79$ ,  $p < 0.01$ ) and CF\_2020\_588 ( $F_{15} = 8.3$ ,  $R^2 = 0.31$ ,  $p < 0.05$ ).

$\delta^{34}\text{S}$  values increased for the individual CF\_2020\_810 by ca.  $2\text{‰}$  from the center to the edge of its vertebra (Figure 2F), showing three distinct periods of feeding at ca.  $17.5\text{‰}$  (sections 2-4),  $18.5\text{‰}$  (sections 5-8) and ca.  $19\text{‰}$  (sections 9-12) throughout its 8 years of life (Figure 2E).  $\delta^{34}\text{S}$  and  $\delta^{13}\text{C}$  demonstrated strong covariance throughout the growth axis (Figure 2B, 2F), suggesting a stepwise enrichment in  $^{34}\text{S}$  and  $^{13}\text{C}$  after the fourth and eighth serial section respectively. A significant relationship between  $\delta^{34}\text{S}$  and vertebra sections was found for this individual ( $F_9 = 23.8$ ,  $R^2 = 0.69$ ,  $p < 0.001$ ).

#### 3.2 Incremental sampling of archaeological specimens

Archaeological BFT vertebrae specimens varied between 166-242 cm estimated FL and corresponded to post-cranial, abdominal, and pre-caudal positions in the vertebral column. Specimens yielded 13 inner and outer centrum samples for  $\delta^{13}\text{C}$  and  $\delta^{15}\text{N}$  isotope analysis and 10 inner and outer centrum samples for  $\delta^{34}\text{S}$  isotope analysis. There was no significant difference between C:N ratios of inner and outer vertebra samples ( $p = 0.26$ , Figure S1).

In agreement with observations on modern serial-sections,  $\delta^{13}\text{C}$  values were significantly greater at the outer of archaeological vertebrae, by ca.  $1\text{‰}$  when compared with inner samples ( $p < 0.001$ , Figure 3A). Overall, this resulted in a mean ca.  $0.5\text{‰}$  increase in  $\delta^{13}\text{C}$  values across all outer samples (mean ca.  $-15.0$  to  $-14.5\text{‰}$ ). Likewise,  $\delta^{15}\text{N}$  values were significantly greater in outer samples (mean ca.  $7.2\text{‰}$ ) compared with inner samples (mean  $6.9\text{‰}$ ,  $p = 0.01$ , Figure 3B), yet to a smaller degree than  $\delta^{13}\text{C}$ , reflecting the lower degree of



$\delta^{15}\text{N}$  variation observed across modern serial-sections.  $\delta^{34}\text{S}$  values were not significantly different between inner and outer vertebrae samples, around a mean distribution of 14‰ (Figure 3C). This mirrored the observation of  $\delta^{34}\text{S}$  values in modern serial-sections where the cross-section sample (containing cancellous bone) presented  $\delta^{34}\text{S}$  values at approximately the mean of cortical bone serial-sections.

#### 4. Discussion

Our results show  $\delta^{13}\text{C}$ ,  $\delta^{15}\text{N}$  and  $\delta^{34}\text{S}$  isotope values can vary significantly throughout the growth axes of BFT vertebrae, probably reflecting the environments and prey foraged by fish over several years prior to capture. Clearly, like elasmobranch vertebrae (Carlisle *et al.*, 2015; Shen *et al.*, 2022), BFT vertebrae do not record a perfect isotopic chronology because juvenile bone collagen and muscle signatures (e.g., ca. 16‰  $\delta^{13}\text{C}$ , 5‰  $\delta^{15}\text{N}$ ) reflecting Mediterranean planktonic diets (Rumolo *et al.*, 2020; Sarà & Sarà, 2007) were not measured in serial-sections. Therefore, we propose, using our age five specimen, that a maximum of four years of life-history signatures may be retained while early-life signatures are lost due to resorption during bone growth. In support, the degree of significant variation we observed across vertebral centra (e.g., in  $\delta^{13}\text{C}$ ) was similar to those published across multiple annuli in the otoliths and fin-spines of tunas (Fraile *et al.*, 2016; Luque *et al.*, 2020), and indeed the recent but few serial-section isotope studies corroborate a theory of >3 year isotopic retention in teleost vertebrae (Kato *et al.*, 2021; Matsubayashi *et al.*, 2017, 2019, 2020). In addition to these studies, we show that significant isotopic variation can be observed across archaeological and modern vertebral centra of a highly mobile species inhabiting a wider range of marine habitats than those previously studied in this fashion. This methodology offers an important advance to investigating diet and habitat use dynamics since spatial variation in marine isotopes is highly complex (Guiry, 2019; Magozzi *et al.*, 2017; Sigman *et al.*, 2009), and residency times per life-history stage remain poorly understood for migratory teleosts like BFT (Cermeño *et al.*, 2015).

Significant isotopic variation in BFT vertebrae is noteworthy since BFT is supposed to have relatively high rates of bone resorption and remodelling due to its cellular bone, endothermy and rapid growth (Davesne *et al.*, 2019). Further study is therefore required to assess resorption and remodelling rates in teleost bone, and its influence on their chemical recording properties. To do this, at least two methods could be employed: a direct comparison of otolith (non-remodelling) and bone isotope values at each age (e.g., Matsubayashi *et al.* (2017)), or a controlled feeding experiment with regular sampling of cohorts (bone) throughout life. Until a better understanding of teleost bone remodelling is achieved, studies should be cautious in assuming which years of growth are being represented by isotopic measurements.

Isotopic variation across archaeological and modern vertebral centra reflected an increasing degree of oceanic (higher  $\delta^{13}\text{C}$ ), pelagic (higher  $\delta^{34}\text{S}$ ) and higher trophic level (higher  $\delta^{15}\text{N}$ ) foraging throughout the life history of individuals. This is well supported by knowledge on BFT biology shown by diet and migration studies (Druon *et al.*, 2016; Karakulak *et al.*, 2009; Logan *et al.*, 2011; Walli *et al.*, 2009; Wilson & Block, 2009) in addition to isotope values published on multiple age-classes (Estrada *et al.*, 2005; Logan, 2009; Medina *et al.*, 2015; Rumolo *et al.*, 2020; Sarà & Sarà, 2007; Varela *et al.*, 2019). How these life-history patterns vary across time and space, however, remains poorly understood, and thus the methodology

used herein provides a novel means with which to identify this variation. Modern cross-section  $\delta^{13}\text{C}$  and  $\delta^{15}\text{N}$  values were more similar with outer, than inner, serial-section  $\delta^{13}\text{C}$  and  $\delta^{15}\text{N}$  values. This may be best explained by cancellous bone, which was present in cross-sections but not serial-sections, being more rapidly remodelled compared with cortical bone (Matsubayashi & Tayasu, 2019; Santamaria *et al.*, 2018; Turner Tomaszewicz *et al.*, 2016). While it is challenging to draw conclusions on a single sample, a rapid remodelling of cancellous bone might also explain why modern cross-section  $\delta^{34}\text{S}$  values were approximately the mean of serial-sections  $\delta^{34}\text{S}$  values if the individual sporadically foraged on neritic or benthic prey during its final period of life. Such dynamic seasonal foraging behaviours are well evidenced in BFT (Battaglia *et al.*, 2013; Olafsdottir *et al.*, 2016). In general, these findings suggest that vertebrae are suitable candidates for life history signatures, however caution should be taken to standardise sampling methodologies to minimise technical effects.

#### 4.1 Consequences for paleoecological isotopic studies

As has long been best practice, we reiterate that isotope studies must sample teleost vertebrae using methodologies which obtain similar proportions of cortical and/or cancellous bone across growth axes to avoid a minimal (but significant) bias which might result from comparing samples representing different life stages. This bias is likely to be less significant in species with rapid remodelling rates and less variation in habitat and diet use throughout life such as BFT (than e.g., Salmonids: Matsubayashi *et al.* (2017)). We recommend cross-sectioning bone as achieved herein to obtain roughly equal proportions of bone types and growth layers which ought to largely eliminate concerns that isotopic signatures from different life stages have been sampled. Studies ought to then incorporate size data to assess relationships between isotope values and body size if specimens vary in size and age. As an example, such methodological biases may have resulted in the increases in  $\delta^{34}\text{S}$  and decreases in  $\delta^{13}\text{C}$  between 9<sup>th</sup>-13<sup>th</sup> century and modern samples; and rather than draw conclusions herein, a full-scale independent study is required to assess these. It is important to note that when conclusions are based on a large degree of isotopic variation (e.g., Guiry *et al.* (2021)), bias from bone type/remodelling (ca.  $\leq 1\%$  in BFT) will clearly not be an issue.

While lower resolution is achieved when analysing vertebrae chemistry due to sample quantity requirements than that achieved by, for example, micro-milling calcium carbonate in fin spines and otoliths (Fraile *et al.*, 2016; Luque *et al.*, 2020; Rooker *et al.*, 2008); vertebrae open up the opportunity for study in spatiotemporal contexts where other tissue types are lacking (Andrews *et al.*, 2022b; Guiry & Hunt, 2020). In addition, bone protein offers the potential to study additional isotopes (e.g.,  $\delta^{15}\text{N}$ ,  $\delta^{34}\text{S}$ ,  $\delta^2\text{H}$ ) than calcium carbonate, which also extends to the analysis of individual amino acids (CSIA, e.g., Bradley *et al.* (2015)), meaning that in theory, source and trophic level effects can be explored across the life-history of individuals. However, due to the sample quantity requirements (usually  $>0.4$  mg collagen), limitations will be placed on which species are large enough to sample, and how ancient specimens can be sampled and used due to sample degradation and institutional regulations on invasive sampling.

Thus far, studies have applied isotopic analysis to archaeological and archived teleost bone to reveal the extinction of a resident trophic niche in Atlantic salmon (*Salmo salar*: Guiry *et*

*al.* (2016), indicate potential millennial-scale diet shifts in the highly exploited Atlantic cod (*Gadus morhua*; Ólafsdóttir *et al.*, 2021)—and Atlantic hake (*Merluccius merluccius*; Llorente-Rodríguez *et al.*, 2022)—and suggest potential habitat productivity or usage shifts in Atlantic and Pacific fishes during the last 500 years compared with the previous centuries (Misarti *et al.*, 2009; Ólafsdóttir *et al.*, 2021). Serial-sectioning of ancient and modern teleost vertebrae has the potential to advance these investigations to reveal changes in life-histories, complementing modern tagging studies which is especially important for juveniles which are difficult to tag (Walli *et al.*, 2009). Examples of research gaps for BFT that we are confident vertebrae exist to evidence, and that may stimulate thought for those studying a variety of systems are:

- Was/is there a resident Mediterranean population? Might there be an isotopic niche that is not only distinct from others but consistent throughout life? *sensu* Cermeño *et al.* (2015) and Di Natale (2015).
- What was unique to BFT that migrated to Atlantic extremes such as Norway and Brazil then disappeared during the 1960s; what was their population origin and which isotopic habitats did these individuals explore throughout their life? *sensu* Fromentin *et al.* (2014).
- What is the extent of BFT site fidelity across several years? How much interannual variability is there in habitats and prey foraged and has this been shaped by industrial-era habitat degradation? *sensu* Andrews *et al.* (2022b).

## 5. Conclusions

Ancient and modern BFT vertebrae appear to retain multi-annual isotopic life-history signatures across their growth axes. These findings are likely reproducible in many commercial and threatened teleosts because the biological features of BFT such as cellular bone, endothermic regulation and rapid growth rates are likely to promote more rapid bone resorption and remodelling than other teleosts. Accordingly, studies should take caution when sampling to avoid interpreting isotopic data from samples which contain varying components of cortical and cancellous bone across the growth axis. We recommend that the analysis of cortical-bone, serial-sectioned across vertebrae centra is likely to provide the highest resolution in reconstructing life-histories. The ability of vertebrae to record life-history signatures highlights their potential as environmental and ecological archives and suggests that teleost bone chemistry is a powerful tool to investigate the drivers of ecological change to support management and conservation. However, further study is required to estimate bone remodelling rates and accurately define the isotopic time-frame being recorded.

## Author Contributions

AJA, DO and MA designed the study. AJA, VO, PA and FT collected vertebrae samples for analysis. AJA conducted the laboratory work. AJA and MA analysed the data. AJA, FT, DO and MA wrote the paper.

## Acknowledgements

We thank Matt Von Tersch and Maria Fontanals-Coll for laboratory assistance. We are grateful to the Istanbul Archaeological Museum, and the General Directorate of Cultural Heritage and Museums of the Ministry of Culture in Turkey for permission and support given to Prof. Vedat Onar -143362 / 01.09.2006 related to the analyses of remains from the archaeological site of Yenikapi. This work is a contribution to the <https://tunaarchaeology.org> project within the framework of the MSCA SeaChanges ITN, which was funded by EU Horizon 2020 (Grant Number: 813383).

## Funding Information

This project was funded by the EU Horizon 2020 Grant Number 813383 as part of the MSCA ITN SeaChanges.

## Conflict of Interest

No conflicts of interest exist.

## Figure Legends

**Figure 1.** A schematic of the serial-sectioning procedure for modern Atlantic bluefin tuna (*Thunnus thynnus*) vertebra specimens, using the individual CF\_2020\_673 as an example. Growth axes of the 35<sup>th</sup> vertebrae (A) were sectioned in 1 mm increments from inner (early) to outer (later) bone growth before cancellous bone (B) was removed prior to obtaining numbered sections for isotopic analyses (C). N.B Section 1 and 2 were pooled for each individual to provide sufficient material for analyses.

**Figure 2.** Variation of stable isotope values across vertebrae growth axes of modern Atlantic bluefin tuna (*Thunnus thynnus*; BFT). Carbon (‰, A, B), Nitrogen (‰, C, D) and Sulfur (‰, E, F) stable isotope ratios of vertebra centra serial-sections from four specimens; CF\_2020\_588 (red), CF\_2020\_810 (black), CF\_2020\_667 (grey), CF\_2020\_673 (beige), captured off Carloforte, Sardinia. Isotope values (‰) represent absolute ratios ( $\delta^{13}\text{C}$ : A,  $\delta^{15}\text{N}$ : C,  $\delta^{34}\text{S}$ : E) and deviations (dev.) from the mean value of all sections from each isotope and individual ( $\Delta^{13}\text{C}$ : B,  $\Delta^{15}\text{N}$ : D,  $\Delta^{34}\text{S}$ : F). Solid lines indicate the isotope values of the cross-sections of each individual. Vertebral bone sections start at the centre of the centrum (early life) and increase toward the margin (later life). Grey error bars represent measurement error.

**Figure 3.** Carbon (‰, A), Nitrogen (‰, B) and Sulfur (‰, C) stable isotope ratios of inner vertebrae and outer vertebrae samples from thirteen archaeological Atlantic bluefin tuna (*Thunnus thynnus*; BFT) specimens, dated to between the 9<sup>th</sup>-13<sup>th</sup> century CE from the site of Yenikapi, Turkey. Inset (center) shows approximate drilling positions of inner (left, grey) and outer (right, beige) samples, using specimen MET12545 with 41 mm centrum height, as an example. The significance (*p*) of Paired Wilcoxon tests is shown for each stable isotope.

## References

- Andrews A.J., Cariani, A., Cilli, E., Addis, P., Bernal-Casasola, D., Di Natale, A., Aniceti, A., Carenti, G., Gómez-Fernández, V., Chosson, V., Ughi, A., Von Tersch, M., Onar, V., Karakulak, F.S., Oray, I., Tinti, F., Alexander, M. Exploitation shifted trophic ecology and habitat preferences of Mediterranean and Black Sea bluefin tuna over centuries. In review.
- Amiriaux, R., Mundy, C. J., Pierrejean, M., Niemi, A., Hedges, K. J., Brown, T. A., ... Yurkowski, D. J. (2023). Tracing carbon flow and trophic structure of a coastal Arctic marine food web using highly branched isoprenoids and carbon, nitrogen and sulfur stable isotopes. *Ecological Indicators*, 147, 109938.

- Andrews, A. J., Mylona, D., Rivera-Charún, L., Winter, R., Onar, V., Siddiq, A. B., ... Morales-Muniz, A. (2022a). Length estimation of Atlantic bluefin tuna (*Thunnus thynnus*) using vertebrae. *International Journal of Osteoarchaeology*, *32*, 645–653.
- Andrews, A. J., Di Natale, A., Bernal-Casasola, D., Aniceti, V., Onar, V., Oueslati, T., ... Tinti, F. (2022b). Exploitation history of Atlantic bluefin tuna in the eastern Atlantic and Mediterranean—insights from ancient bones. *ICES Journal of Marine Science*, *79*, 247–262.
- Andrews, A. J., Di Natale, A., Addis, P., Piattoni, F., Onar, V., Bernal-Casasola, D., ... & Tinti, F. (2023). Vertebrae reveal industrial-era increases in Atlantic bluefin tuna catch-at-size and juvenile growth. *ICES Journal of Marine Science*, fsad013. doi: 10.1093/icesjms/fsad013.
- Barnes, C., Jennings, Barry, J. T., & Simon. (2009). Environmental correlates of large-scale spatial variation in the  $\delta^{13}\text{C}$  of marine animals. *Estuarine, Coastal and Shelf Science*, *81*, 368–374.
- Barrett, J. H., Orton, D., Johnstone, C., Harland, J., Van Neer, W., Eryvynck, A., ... Richards, M. (2011). Interpreting the expansion of sea fishing in medieval Europe using stable isotope analysis of archaeological cod bones. *Journal of Archaeological Science*, *38*, 1516–1524.
- Bas, M., & Cardona, L. (2018). Effects of skeletal element identity, delipidation and demineralization on the analysis of stable isotope ratios of C and N in fish bone. *Journal of Fish Biology*, *92*, 420–437.
- Battaglia, P., Andaloro, F., Consoli, P., Esposito, V., Malara, D., Musolino, S., ... Romeo, T. (2013). Feeding habits of the Atlantic bluefin tuna, *Thunnus thynnus* (L. 1758), in the central Mediterranean Sea (Strait of Messina). *Helgoland Marine Research*, *67*, 97–107.
- Bradley, C. J., Wallsgrave, N. J., Choy, C. A., Drazen, J. C., Hetherington, E. D., Hoen, D. K., & Popp, B. N. (2015). Trophic position estimates of marine teleosts using amino acid compound specific isotopic analysis. *Limnology and Oceanography, Methods / ASLO*, *13*, 476–493.
- Brophy, D., Rodríguez-Ezpeleta, N., Fraile, I., & Arrizabalaga, H. (2020). Combining genetic markers with stable isotopes in otoliths reveals complexity in the stock structure of Atlantic bluefin tuna (*Thunnus thynnus*). *Scientific Reports*, *10*, 14675.
- Brown, T. A., Nelson, D. E., Vogel, J. S., & Southon, J. R. (1988). Improved Collagen Extraction by Modified Longin Method. *Radiocarbon*, *30*, 171–177.
- Buchheister, A., & Latour, R. J. (2010). Turnover and fractionation of carbon and nitrogen stable isotopes in tissues of a migratory coastal predator, summer flounder (*Paralichthys dentatus*). *Canadian Journal of Fisheries and Aquatic Sciences*, *67*, 445–461.
- Campana, S. E., & Thorrold, S. R. (2001). Otoliths, increments, and elements: keys to a comprehensive understanding of fish populations? *Canadian Journal of Fisheries and Aquatic Sciences*, *58*, 30–38.
- Carlisle, A. B., Goldman, K. J., Litvin, S. Y., Madigan, D. J., Bigman, J. S., Swithenbank, A. M., ... Block, B. A. (2015). Stable isotope analysis of vertebrae reveals ontogenetic changes in habitat in an endothermic pelagic shark. *Proceedings. Biological sciences / The Royal Society*, *282*, 20141446.
- Cermeño, P., Quílez-Badia, G., Ospina-Alvarez, A., Sainz-Trápaga, S., Boustany, A. M., Seitz, A. C., ... Block, B. A. (2015). Electronic tagging of Atlantic bluefin tuna (*Thunnus thynnus*, L.) reveals habitat use and behaviors in the Mediterranean Sea. *PloS One*, *10*, e0116638.
- Cobain, M. R. D., McGill, R. A. R., & Trueman, C. N. (2022). Stable isotopes demonstrate seasonally stable benthic-pelagic coupling as newly fixed nutrients are rapidly transferred through food chains in an estuarine fish community. *Journal of Fish Biology*, doi.org/10.1111/jfb.15005.
- Colonese, A. C., Farrell, T., Lucquin, A., Firth, D., Charlton, S., Robson, H. K., ... Craig, O.

- E. (2015). Archaeological bone lipids as palaeodietary markers. *Rapid Communications in Mass Spectrometry: RCM*, 29, 611–618.
- Cort, J. L., Deguara, S., Galaz, T., Mèlich, B., Artetxe, I., Arregi, I., ... Idrissi, M. (2013). Determination of L max for Atlantic Bluefin Tuna, *Thunnus thynnus* (L.), from Meta-Analysis of Published and Available Biometric Data. *Reviews in Fisheries Science*, 21, 181–212.
- Davesne, D., Meunier, F. J., Schmitt, A. D., Friedman, M., Otero, O., & Benson, R. B. J. (2019). The phylogenetic origin and evolution of acellular bone in teleost fishes: insights into osteocyte function in bone metabolism. *Biological Reviews of the Cambridge Philosophical Society*, 94, 1338–1363.
- DeNiro, M. J., & Epstein, S. (1978). Influence of diet on the distribution of carbon isotopes in animals. *Geochimica et cosmochimica acta*, 42, 495–506.
- Dickhut, R. M., Deshpande, A. D., Cincinelli, A., Cochran, M. A., Corsolini, S., Brill, R. W., ... Graves, J. E. (2009). Atlantic bluefin tuna (*Thunnus thynnus*) population dynamics delineated by organochlorine tracers. *Environmental Science & Technology*, 43, 8522–8527.
- Di Natale, A. (2015). Review of the historical and biological evidences about a population of bluefin tuna (*Thunnus thynnus* L.) in The Eastern Mediterranean and the black sea. *Collect. Vol. Sci. Pap. ICCAT.*, 71, 1098–1124.
- Druon, J.-N., Fromentin, J.-M., Hanke, A. R., Arrizabalaga, H., Damalas, D., Tičina, V., ... Addis, P. (2016). Habitat suitability of the Atlantic bluefin tuna by size class: An ecological niche approach. *Progress in Oceanography*, 142, 30–46.
- Estrada, J. A., Rice, A. N., Natanson, L. J., & Skomal, G. B. (2006). Use of isotopic analysis of vertebrae in reconstructing ontogenetic feeding ecology in white sharks. *Ecology*, 87, 829–834.
- Estrada, J. A., Lutcavage, M., & Thorrold, S. R. (2005). Diet and trophic position of Atlantic bluefin tuna (*Thunnus thynnus*) inferred from stable carbon and nitrogen isotope analysis. *Marine Biology*, 147, 37–45.
- Fraile, I., Arrizabalaga, H., Santiago, J., Goñi, N., Arregi, I., Madinabeitia, S., ... Rooker, J. R. (2016). Otolith chemistry as an indicator of movements of albacore (*Thunnus alalunga*) in the North Atlantic Ocean. *Marine and Freshwater Research*, 67, 1002–1013.
- Fromentin, J.-M., Reygondeau, G., Bonhommeau, S., & Beaugrand, G. (2014). Oceanographic changes and exploitation drive the spatio-temporal dynamics of Atlantic bluefin tuna (*Thunnus thynnus*). *Fisheries Oceanography*, 23, 147–156.
- Fry, B., & Chumchal, M. M. (2011). Sulfur stable isotope indicators of residency in estuarine fish. *Limnology and Oceanography*, 56, 1563–1576.
- Gruber, N., Keeling, C. D., Bacastow, R. B., Guenther, P. R., Lueker, T. J., Wahlen, M., ... Stocker, T. F. (1999). Spatiotemporal patterns of carbon-13 in the global surface oceans and the oceanic suess effect. *Global Biogeochemical Cycles*, 13, 307–335.
- Guiry, E. (2019). Complexities of Stable Carbon and Nitrogen Isotope Biogeochemistry in Ancient Freshwater Ecosystems: Implications for the Study of Past Subsistence and Environmental Change. *Frontiers in Ecology and Evolution*, 7, 313.
- Guiry, E. J., & Hunt, B. P. V. (2020). Integrating fish scale and bone isotopic compositions for 'deep time' retrospective studies. *Marine Environmental Research*, 160, 104982.
- Guiry, E. J., Needs-Howarth, S., Friedland, K. D., Hawkins, A. L., Szpak, P., Macdonald, R., ... Richards, M. P. (2016). Lake Ontario salmon (*Salmo salar*) were not migratory: A long-standing historical debate solved through stable isotope analysis. *Scientific Reports*, 6, 36249.
- Guiry, E. J., & Szpak, P. (2020). Quality control for modern bone collagen stable carbon and nitrogen isotope measurements. *Methods in Ecology and Evolution / British Ecological Society*, 11, 1049–1060.
- Guiry, E. J., & Szpak, P. (2021). Improved quality control criteria for stable carbon and nitrogen isotope measurements of ancient bone collagen. *Journal of Archaeological Science*, 132, 105416.

- Guiry, E. J., Kennedy, J. R., O'Connell, M. T., Gray, D. R., Grant, C., & Szpak, P. (2021). Early evidence for historical overfishing in the Gulf of Mexico. *Science Advances*, 7.
- Guiry, E. J., Orchard, T. J., Needs-Howarth, S., & Szpak, P. (2022). Freshwater wetland-driven variation in sulfur isotope compositions: Implications for human paleodiet and ecological research. *Frontiers in Ecology and Evolution*. 2022, doi:10.3389/fevo.2022.953042.
- Guiry, E., Royle, T. C. A., Matson, R. G., Ward, H., Weir, T., Waber, N., ... Szpak, P. (2020). Differentiating salmonid migratory ecotypes through stable isotope analysis of collagen: Archaeological and ecological applications. *PLoS One*, 15, e0232180.
- Hobson, K. A., & Clark, R. G. (1992). Assessing Avian Diets Using Stable Isotopes I: Turnover of  $^{13}\text{C}$  in Tissues. *The Condor*, 94, 181–188.
- Jardine, T. D., Hadwen, W. L., Hamilton, S. K., Hladyz, S., Mitrovic, S. M., Kidd, K. A., ... Bunn, S. E. (2014). Understanding and overcoming baseline isotopic variability in running waters. *River Research and Applications*, 30, 155–165.
- Jennings, S., Barnes, C., & Sweeting, C. J. (2008). Application of nitrogen stable isotope analysis in size-based marine food web and macroecological research. *in Mass Spectrometry*, 22(11), 1673-1680.
- Karakulak, F. S., Salman, A., & Oray, I. K. (2009). Diet composition of bluefin tuna (*Thunnus thynnus* L. 1758) in the Eastern Mediterranean Sea, Turkey. *Journal of Applied Ichthyology*, 25, 757–761.
- Kato, Y., Togashi, H., Kurita, Y., Osada, Y., Amano, Y., Yoshimizu, C., ... Tayasu, I. (2021). Segmental isotope analysis of the vertebral centrum reveals the spatiotemporal population structure of adult Japanese flounder *Paralichthys olivaceus* in Sendai Bay, Japan. *Marine Biology*, 168, 57.
- Kerr, L. A., Andrews, A. H., Cailliet, G. M., Brown, T. A., & Coale, K. H. (2006). Investigations of  $\Delta^{14}\text{C}$ ,  $\delta^{13}\text{C}$ , and  $\delta^{15}\text{N}$  in vertebrae of white shark (*Carcharodon carcharias*) from the eastern North Pacific Ocean. In Age and Growth of Chondrichthyan Fishes: New Methods, Techniques and Analysis, Carlson, J.K, and Goldman, K.J. (eds), 337–353.
- Kragten, J. (1994). Tutorial review. Calculating standard deviations and confidence intervals with a universally applicable spreadsheet technique. *The Analyst*, 119, 2161–2165.
- Lee, Prince, & Crow. (1983). Interpretation of growth bands on vertebrae and otoliths of Atlantic bluefin tuna, *Thunnus thynnus*. In Proceedings of the International Workshop on Age Determination of Oceanic Pelagic Fishes: Tunas, Billfishes, and Sharks, 8, 61–70. US Dep. Commer., NOAA Technical Report NMFS, USA.
- Llorente-Rodríguez, L., Craig, O. E., Colonese, A. C., Tersch, M., Roselló-Izquierdo, E., González Gómez de Agüero, E., ... Morales Muñoz, A. (2022). Elucidating historical fisheries' networks in the Iberian Peninsula using stable isotopes. *Fish and Fisheries*.
- Logan, J. (2009). Tracking diet and movement of Atlantic bluefin tuna (*Thunnus thynnus*) using carbon and nitrogen stable isotopes. University of New Hampshire, Durham. Doctoral thesis. <https://core.ac.uk/download/pdf/215517272.pdf>.
- Logan, J. M., Rodríguez-Marín, E., Goñi, N., Barreiro, S., Arrizabalaga, H., Golet, W., & Lutcavage, M. (2011). Diet of young Atlantic bluefin tuna (*Thunnus thynnus*) in eastern and western Atlantic foraging grounds. *Marine Biology*, 158, 73–85.
- Luque, P. L., Sakai, S., Murua, H., & Arrizabalaga, H. (2020). Protocol for Sampling Sequential Fin Spine Growth Intervals for Isotope Analysis in the Atlantic Bluefin Tuna. *Frontiers in Marine Science*, 7.
- Madigan, D. J., Litvin, S. Y., Popp, B. N., Carlisle, A. B., Farwell, C. J., & Block, B. A. (2012). Tissue turnover rates and isotopic trophic discrimination factors in the endothermic teleost, pacific bluefin tuna (*Thunnus orientalis*). *PLoS One*, 7, e49220.
- Magozzi, S., Yool, A., Vander Zanden, H. B., Wunder, M. B., & Trueman, C. N. (2017). Using ocean models to predict spatial and temporal variation in marine carbon isotopes. *Ecosphere*, 8, e01763.
- Mariani, P., Křivan, V., MacKenzie, B. R., & Mullon, C. (2016). The migration game in habitat network: the case of tuna. *Theoretical Ecology*, 9, 219–232.

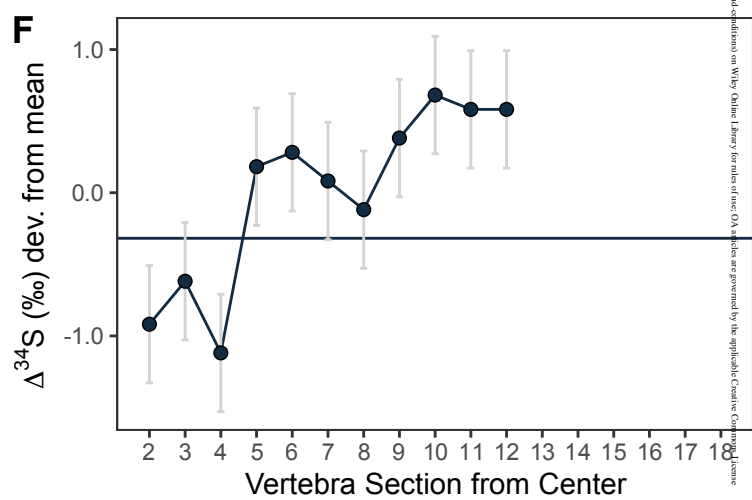
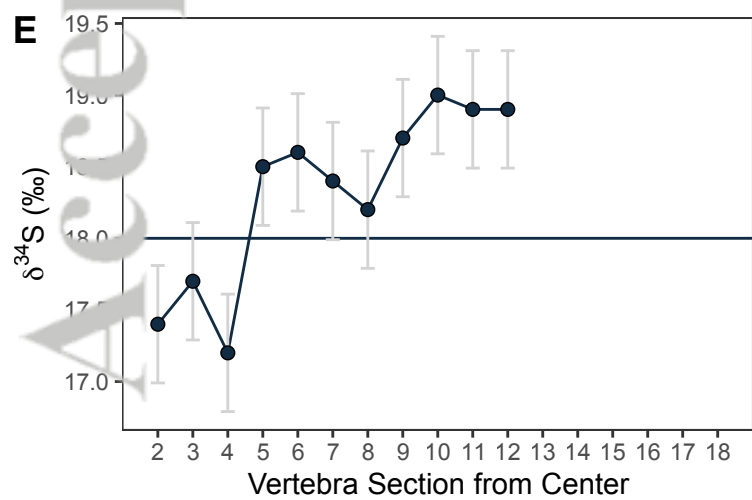
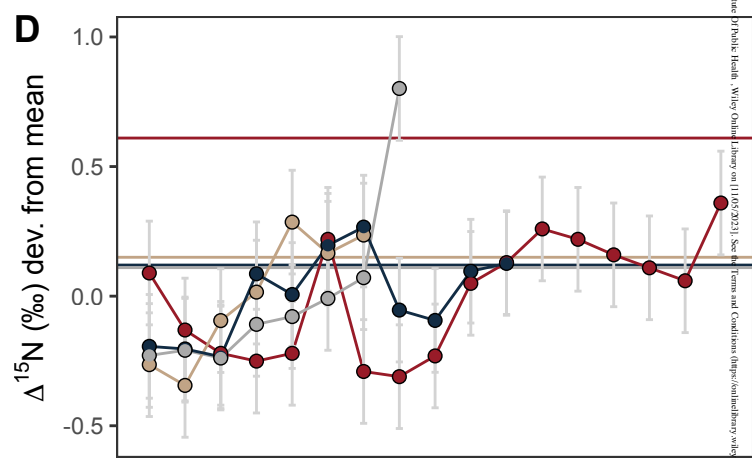
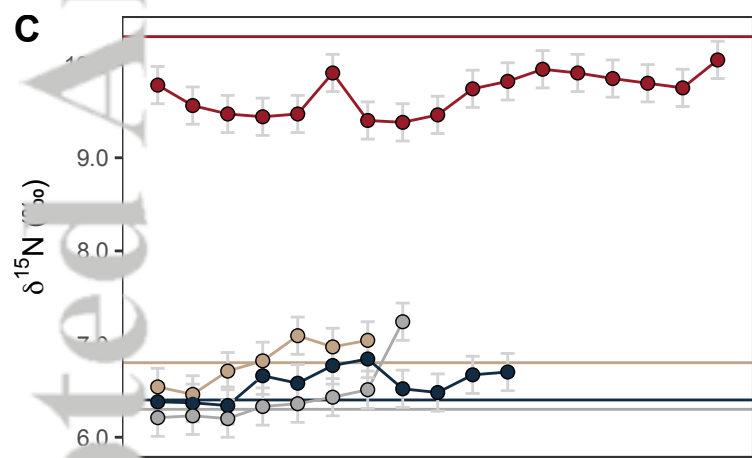
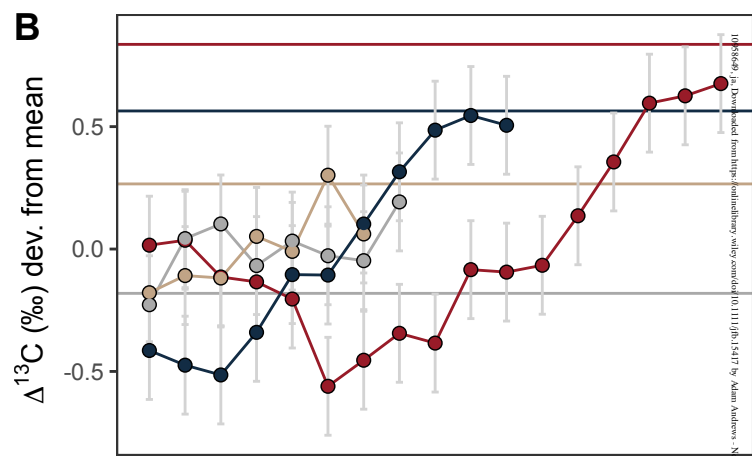
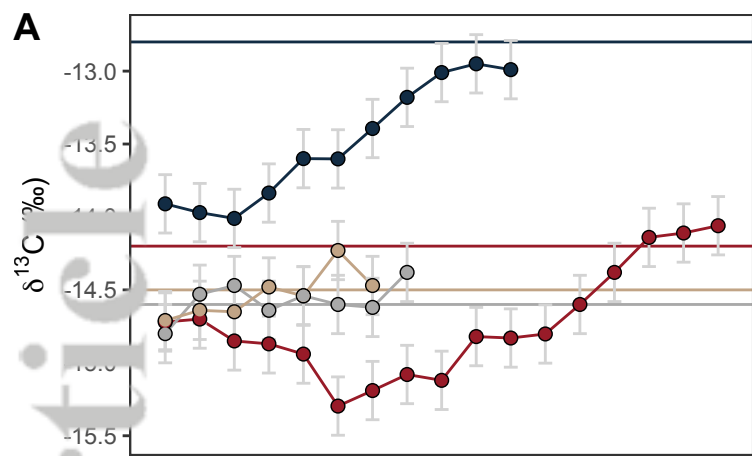
- Mather, F. J., Mason, J. M., & Jones, A. C. (1995). Historical document: life history and fisheries of Atlantic bluefin tuna. *NOAA Technical Memorandum NMFS-SEFSC-370*. National Oceanic and Atmospheric Administration, 165. <https://repository.library.noaa.gov/view/noaa/8461>.
- Matsubayashi, J., & Tayasu, I. (2019). Collagen turnover and isotopic records in cortical bone. *Journal of Archaeological Science*, *106*, 37–44.
- Matsubayashi, J., Saitoh, Y., Osada, Y., Uehara, Y., Habu, J., Sasaki, T., & Tayasu, I. (2017). Incremental analysis of vertebral centra can reconstruct the stable isotope chronology of teleost fishes. *Methods in Ecology and Evolution / British Ecological Society*, *8*, 1755–1763.
- Matsubayashi, J., Umezawa, Y., Matsuyama, M., Kawabe, R., Mei, W., Wan, X., ... Tayasu, I. (2019). Using segmental isotope analysis of teleost fish vertebrae to estimate trophic discrimination factors of bone collagen. *Limnology and Oceanography, Methods / ASLO*, *17*, 87–96.
- Matsubayashi, J., Osada, Y., Tadokoro, K., Abe, Y., Yamaguchi, A., Shirai, K., ... Tayasu, I. (2020). Tracking long-distance migration of marine fishes using compound-specific stable isotope analysis of amino acids. *Ecology Letters*, *23*, 881–890.
- McCormack, J., Szpak, P., Bourgon, N., Richards, M., Hyland, C., Méjean, P., ... Jaouen, K. (2021). Zinc isotopes from archaeological bones provide reliable trophic level information for marine mammals. *Communications Biology*, *4*, 1–11.
- Medina, A., Goñi, N., Arrizabalaga, H., & Varela, J. L. (2015). Feeding patterns of age-0 bluefin tuna in the western Mediterranean inferred from stomach-content and isotope analyses. *Marine Ecology Progress Series*, *527*, 193–204.
- Meunier, F. J. (2011). The Osteichthyes, from the Paleozoic to the extant time, through histology and palaeohistology of bony tissues. *Comptes rendus. Palevol*, *10*, 347–355.
- Misarti, N., Finney, B., Maschner, H., & Wooller, M. J. (2009). Changes in northeast Pacific marine ecosystems over the last 4500 years: evidence from stable isotope analysis of bone collagen from archeological middens. *Holocene*, *19*, 1139–1151.
- Nehlich, O., & Richards, M. P. (2009). Establishing collagen quality criteria for sulphur isotope analysis of archaeological bone collagen. *Archaeological and Anthropological Sciences*, *1*, 59–75.
- Nehlich, O., Barrett, J. H., & Richards, M. P. (2013). Spatial variability in sulphur isotope values of archaeological and modern cod (*Gadus morhua*). *Rapid Communications in Mass Spectrometry*, *27*, 2255–2262.
- Ólafsdóttir, D., MacKenzie, B. R., Chosson-P, V., & Ingimundardóttir, T. (2016). Dietary Evidence of Mesopelagic and Pelagic Foraging by Atlantic Bluefin Tuna (*Thunnus thynnus* L.) during Autumn Migrations to the Iceland Basin. *Frontiers in Marine Science*, *3*.
- Ólafsdóttir, G. Á., Pétursdóttir, G., Bárðarson, H., & Edvardsson, R. (2017). A millennium of north-east Atlantic cod juvenile growth trajectories inferred from archaeological otoliths. *PloS One*, *12*, e0187134.
- Ólafsdóttir, G. Á., Edvardsson, R., Timsic, S., Harrison, R., & Patterson, W. P. (2021). A millennium of trophic stability in Atlantic cod (*Gadus morhua*): transition to a lower and converging trophic niche in modern times. *Scientific Reports*, *11*, 12681.
- Onar, V., Pazvant, G., & Armutak, A. (2008). Radiocarbon dating results of the animal remains uncovered at Yenikapı Excavations. *Istanbul Archaeological Museums, Proceedings of the 1st Symposium on Marmaray-Metro Salvage Excavations*, 249–256.
- Piccinetti, C., Di Natale, A., & Arena, P. (2013). Eastern bluefin tuna (*Thunnus thynnus*, L.) reproduction and reproductive areas and season. *Col. Vol. Sci. Pap. ICCAT.*, *69*, 891–912.
- Rooker, J. R., Secor, D. H., DeMetrio, G., Kaufman, A. J., Belmonte Ríos, A., & Ticina, V. (2008). Evidence of trans-Atlantic movement and natal homing of bluefin tuna from stable isotopes in otoliths. *Marine Ecology Progress Series*, *368*, 231–239.
- R Team, Core. (2013). R development core team. *RA Lang Environ Stat Comput*, *55*, 275–286.

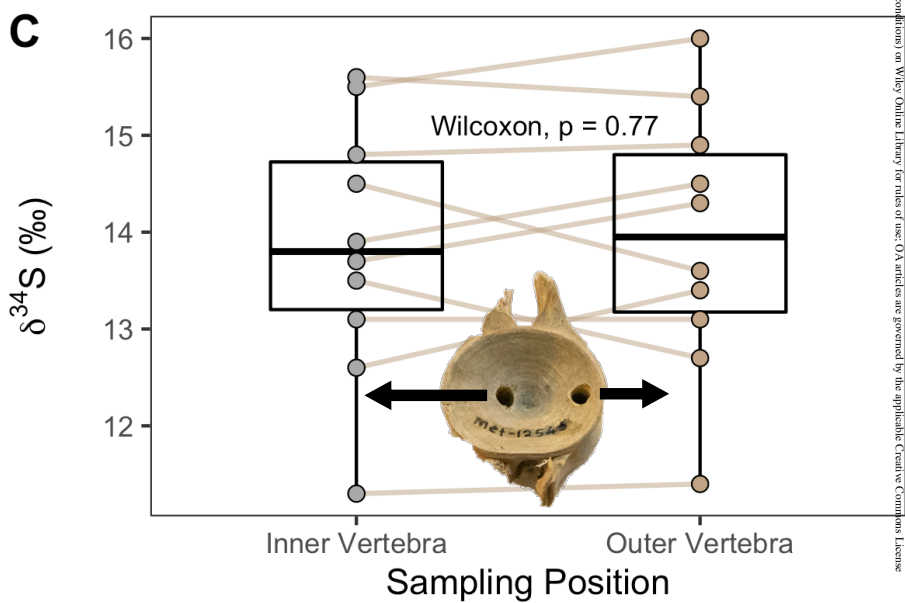
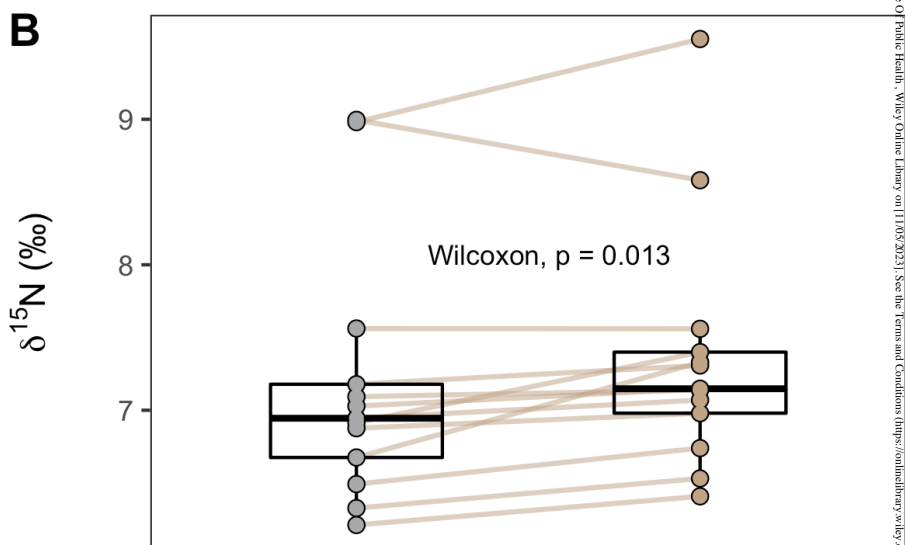
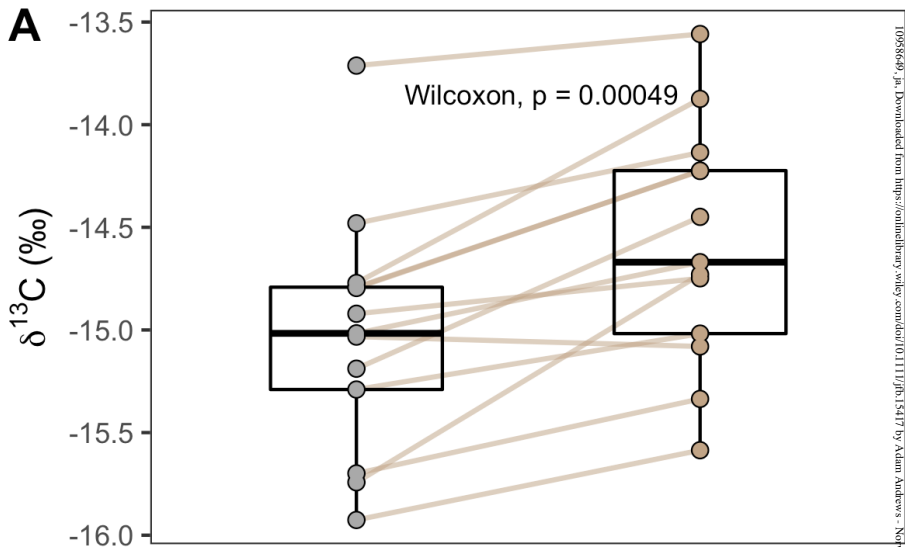


- Rumolo, P., Bonanno, A., Genovese, S., Romeo, T., Mazzola, S., Basilone, G., ... Barra, M. (2020). Growth-related trophic changes of *Thunnus thynnus* as evidenced by stable nitrogen isotopic values in the first dorsal spine. *Scientific Reports*, *10*, 9899.
- Santamaria, N., Bello, G., Passantino, L., Di Comite, M., Zupa, R., Pousis, C., ... Corriero, A. (2018). Micro-anatomical structure of the first spine of the dorsal fin of Atlantic bluefin tuna, *Thunnus thynnus* (Osteichthyes: Scombridae). *Annals of Anatomy: Official Organ of the Anatomische Gesellschaft*, *219*, 1–7.
- Sarà, G., & Sarà, R. (2007). Feeding habits and trophic levels of bluefin tuna *Thunnus thynnus* of different size classes in the Mediterranean Sea. *Journal of applied ichthyology*, *23*, 122–127.
- Sayle, K. L., Brodie, C. R., Cook, G. T., & Hamilton, W. D. (2019). Sequential measurement of  $\delta^{15}\text{N}$ ,  $\delta^{13}\text{C}$  and  $\delta^{34}\text{S}$  values in archaeological bone collagen at the Scottish Universities Environmental Research Centre (SUERC): A new analytical frontier. *Rapid Communications in Mass Spectrometry*, *33*, 1258–1266.
- Shen, Y., Gong, Y., Wu, F., & Li, Y. (2022). Retrospective stable isotopes of vertebrae reveal sexual ontogenetic patterns and trophic ecology in oceanic whitetip shark, *Carcharhinus longimanus*. *Ecology and Evolution*, *12*, e8452.
- Sigman, D. M., Karsh, K. L., & Casciotti, K. L. (2009). Nitrogen Isotopes in the Ocean. *Encyclopedia of Ocean Sciences*. 2009, pp. 40–54, doi:10.1016/b978-012374473-9.00632-9.
- Solomon, C. T., Carpenter, S. R., Rusak, J. A., & Vander Zanden, M. J. (2008). Long-term variation in isotopic baselines and implications for estimating consumer trophic niches. *Canadian Journal of Fisheries and Aquatic Sciences*, *65*, 2191–2200.
- Szpak, P., & Buckley, M. (2020). Sulfur isotopes ( $\delta^{34}\text{S}$ ) in Arctic marine mammals: indicators of benthic vs. pelagic foraging. *Marine Ecology Progress Series*, *653*, 205–216.
- Thode, H. G. (1991). Sulphur isotopes in nature and the environment: An overview. In H. R. Krouse & V. A. Grinenko (Eds.), *Stable Isotopes in the Assessment of Natural and Anthropogenic Sulphur in the Environment*, *43*, 1–26.
- Tieszen, L. L., Boutton, T. W., Tesdahl, K. G., & Slade, N. A. (1983). Fractionation and turnover of stable carbon isotopes in animal tissues: Implications for  $\text{d}^{13}\text{C}$  analysis of diet. *Oecologia*, *57*, 32–37.
- Turner Tomaszewicz, C. N., Seminoff, J. A., Avens, L., & Kurle, C. M. (2016). Methods for sampling sequential annual bone growth layers for stable isotope analysis. *Methods in Ecology and Evolution / British Ecological Society*, *7*, 556–564.
- Tzadik, O. E., Curtis, J. S., Granneman, J. E., Kurth, B. N., Pusack, T. J., Wallace, A. A., ... Stallings, C. D. (2017). Chemical archives in fishes beyond otoliths: A review on the use of other body parts as chronological recorders of microchemical constituents for expanding interpretations of environmental, ecological, and life-history changes. *Limnology and Oceanography, Methods / ASLO*, *15*, 238–263.
- Varela, J. L., Carrera, I., & Medina, A. (2019). Seasonal feeding patterns of Atlantic bluefin tuna (*Thunnus thynnus*) in the Strait of Gibraltar. *Marine Environmental Research*, 104811.
- Walli, A., Teo, S. L. H., Boustany, A., Farwell, C. J., Williams, T., Dewar, H., ... Block, B. A. (2009). Seasonal movements, aggregations and diving behavior of Atlantic bluefin tuna (*Thunnus thynnus*) revealed with archival tags. *PloS One*, *4*, e6151.
- Wilson, S. G., & Block, B. A. (2009). Habitat use in Atlantic bluefin tuna *Thunnus thynnus* inferred from diving behavior. *Endangered Species Research*, *10*, 355–367.
- Witten, P. E., Villwock, W., Peters, N., & Hall, B. K. (2000). Bone resorption and bone remodelling in juvenile carp, *Cyprinus carpio* L. *Journal of Applied Ichthyology*, *16*, 254–261.
- Witten, P. E., & Huysseune, A. (2009). A comparative view on mechanisms and functions of skeletal remodelling in teleost fish, with special emphasis on osteoclasts and their function. *Biological Reviews of the Cambridge Philosophical Society*, *84*, 315–346.
- Witten, P. E., & Villwock, W. (1997). Growth requires bone resorption at particular skeletal

elements in a teleost fish with acellular bone (*Oreochromis niloticus*, Teleostei: Cichlidae). *Journal of Applied Ichthyology*, 13, 149–158.







## Appendix

### Isotopic life-history signatures are retained in modern and ancient Atlantic bluefin tuna vertebrae

Adam J. Andrews<sup>\*1</sup>, David Orton<sup>2</sup>, Vedat Onar<sup>3</sup>, Piero Addis<sup>4</sup>, Fausto Tinti<sup>1</sup>, Michelle Alexander<sup>\*2</sup>

1Department of Biological, Geological and Environmental Sciences, University of Bologna, Campus of Ravenna, Ravenna, Italy

2BioArCh, Department of Archaeology, University of York, York, U.K.

3Osteoarchaeology Practice and Research Centre and Faculty of Veterinary Medicine, Istanbul University-Cerrahpaşa, Istanbul, Turkey

4Department of Life and Environmental Sciences, University of Cagliari, Cagliari, Sardinia, Italy

\*Corresponding authors: [adam@palaeome.org](mailto:adam@palaeome.org), [michelle.alexander@york.ac.uk](mailto:michelle.alexander@york.ac.uk)

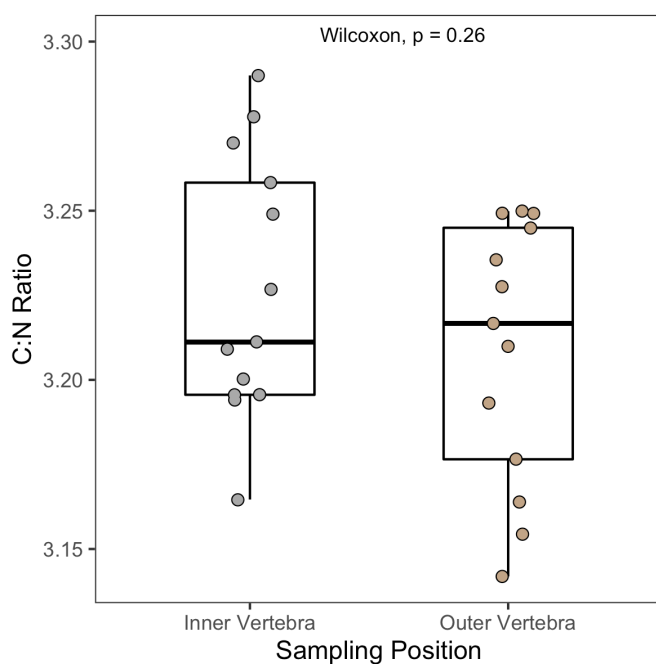


**Figure S1.** Boxplots showing non-significant differences in C:N ratios of inner vertebrae and outer vertebrae samples from thirteen archaeological Atlantic bluefin tuna (*Thunnus thynnus*) specimens, dated to between the 9-13<sup>th</sup> c. CE from the site of Yenikapi, Istanbul, Turkey. The significance ( $p$ ) of a paired Wilcoxon test was tested in R.

## Calibration and Analytical Uncertainty for Isotopic Measurements

Stable carbon, nitrogen isotope compositions were calibrated relative to VPDB ( $\delta^{13}\text{C}$ ), AIR ( $\delta^{15}\text{N}$ ) using IAEA-600, IAEA-N-2, IA-R006. Sulfur ( $\delta^{34}\text{S}$ ) was calibrated relative to VCDT using internal standards GS2 and GAS2 (themselves calibrated to IAEA-S-2, silver sulfide,  $\delta^{34}\text{S}$  VCDT =  $22.62 \pm 0.08$  ‰ and IAEA-S-3, silver sulfide,  $\delta^{34}\text{S}$  VCDT =  $-32.49 \pm 0.08$  ‰) (Table S3).

**Table S3.** Standard reference materials used for calibration of  $\delta^{13}\text{C}$  relative to VPDB,  $\delta^{15}\text{N}$  relative to AIR and  $\delta^{34}\text{S}$  relative to VCDT.

Standard	Material	Accepted $\delta^{13}\text{C}$ (‰, VPDB)	Accepted $\delta^{15}\text{N}$ (‰, AIR)	Accepted $\delta^{34}\text{S}$ (‰, VCDT)
IAEA-600	Caffeine	-27.771	+1.0	
IAEA-N-2	Ammonium Sulfate		+20.41	
IA-R006	Cane Sugar	-11.64		
GS2	Gelatine, sulfanilamide, 13C- glycine			-10.28 ± 0.18
GAS2	Gelatine, acetanilide, sulfanilamide, 15N- glycine			18.56 ± 0.10

The following standard was used to monitor analytical uncertainty (Table S4). The isotopic compositions reported here for internal standards represent long term averages calibrated to VPDB and AIR with IAEA-600, IAEA-N-2, and IA-R006.

**Table S4.** Standard reference materials used to monitor internal accuracy and precision.

Standard	Material	Mean $\delta^{13}\text{C}$ (‰, VPDB)	Mean $\delta^{15}\text{N}$ (‰, AIR)	Mean $\delta^{34}\text{S}$ (‰, VCDT)
ISO_12	SIGMA Fish Gelatine	-15.29±0.11	+15.23±0.28	
USGS88	Marine Collagen			+17.10±0.44
USGS89	Porcine Collagen			+3.86±0.56
B2215	IRMS Fish Gelatine			+1.21±0.24

Table S5 presents the means and standard deviations of the  $\delta^{13}\text{C}$  and  $\delta^{15}\text{N}$  values for the check and calibration standards, as well as the number of standards included in each analytical session. On the basis of the check and calibration standards, measurement precision (the pooled standard deviation of the check and calibration standards) was  $\pm 0.08$  ‰ for  $\delta^{13}\text{C}$ ,  $\pm 0.23$  ‰ for  $\delta^{15}\text{N}$  ( $n=13$ ) and  $\pm 0.38$  ‰ for  $\delta^{34}\text{S}$  ( $n=9$ ). Measurement accuracy (bias) was evaluated by comparing the known and measured  $\delta^{13}\text{C}$  and  $\delta^{15}\text{N}$  values for ISO\_12 and factoring in the long-term uncertainty in these known measurements. Measurement bias due to systematic error (accuracy) was determined to be  $\pm 0.11$  ‰ for  $\delta^{13}\text{C}$ ,  $\pm 0.28$  ‰ for  $\delta^{15}\text{N}$  and  $\pm 0.41$  ‰ for  $\delta^{34}\text{S}$ .

**Table S5.** Mean and/or standard deviation of all check and calibration standards for all analytical sessions containing data presented in this paper.

Session ID	Standard	n	$\delta^{13}\text{C}$ (‰, VPDB)	$\delta^{15}\text{N}$ (‰, AIR)	$\delta^{34}\text{S}$ (‰, VCDT)
Session 1	ISO_12	5	-15.18±0.12	15.15±0.13	
Session 1	IA-R006	5	±0.11		
Session 1	IAEA-600	5	±0.06	±0.06	
Session 1	IAEA-N-2	5		±0.25	
Session 2	ISO_12	5	-15.42±0.06	15.23±0.15	
Session 2	IA-R006	5	±0.10		
Session 2	IAEA-600	5	±0.10	±0.10	
Session 2	IAEA-N-2	5		±0.11	
Session 3	ISO_12	3	-15.40±0.11	14.99±0.17	
Session 3	IA-R006	3	±0.04		
Session 3	IAEA-600	3	±0.07	±0.07	
Session 3	IAEA-N-2	3		±0.13	
Session 4	ISO_12	5	-15.25±0.07	15.03±0.20	
Session 4	IA-R006	5	±0.08		
Session 4	IAEA-600	5	±0.05	±0.13	
Session 4	IAEA-N-2	5		±0.10	
Session 5	USGS88	6			16.96±0.37
Session 5	USGS89	7			4.92±0.64
Session 5	B2215	4			1.26±0.21
Session 6	USGS88	5			17.02±0.34
Session 6	USGS89	4			4.28±0.38
Session 6	B2215	4			0.96±0.40
Session 6	B2215	4			0.78±0.29



Table S1. Modern sample measurements and details. A/B for isotope measurements refers to individual replicates per sample. SD = standard deviation.

Site	Date	Specimen	Section	%C	%N	CN_Ratio	Replicates	d13C_A	d13C_B	d13C_SD	d13C_mea	d15N_A	d15N_B	d15N_SD	d15N_mea	%S	CS_Ratio	NS_Ratio	Replicates_d34S_A	d34S_B	d34S_mear	d34S_SD	d34S_mear	Rank or Tyr	Height (mm)	Width (mm)	Length (mm)	Estimated F	Estimated Age	
Carloforte, I	Jul-20	CF_588	2	40.2	14.4	3.25	2	-14.73	-14.7	0.02	-14.72	9.77	9.8	0.02	9.78									35	33.01	43.42	46.89	196	9	
Carloforte, I	Jul-20	CF_588	3	38.6	14	3.23	2	-14.71	-14.68	0.02	-14.71	9.55	9.58	0.03	9.56										35	33.01	43.42	46.89	196	9
Carloforte, I	Jul-20	CF_588	4	41.1	14.9	3.21	2	-14.85	-14.84	0.01	-14.85	9.47	9.48	0.01	9.47										35	33.01	43.42	46.89	196	9
Carloforte, I	Jul-20	CF_588	5	41.8	15.1	3.24	2	-14.88	-14.87	0.01	-14.87	9.44	9.45	0.01	9.44										35	33.01	43.42	46.89	196	9
Carloforte, I	Jul-20	CF_588	6	43.8	15.3	3.33	2	-14.95	-14.94	0	-14.94	9.45	9.48	0.02	9.47										35	33.01	43.42	46.89	196	9
Carloforte, I	Jul-20	CF_588	7	42.3	14.7	3.37	2	-15.3	-15.29	0.02	-15.3	9.89	9.93	0	9.91										35	33.01	43.42	46.89	196	9
Carloforte, I	Jul-20	CF_588	8	43.9	15.2	3.38	2	-15.2	-15.18	0	-15.19	9.39	9.4	0	9.4										35	33.01	43.42	46.89	196	9
Carloforte, I	Jul-20	CF_588	9	42.9	15.1	3.32	2	-15.08	-15.08	0.05	-15.08	9.35	9.41	0.04	9.38										35	33.01	43.42	46.89	196	9
Carloforte, I	Jul-20	CF_588	10	44.1	15.5	3.32	2	-15.16	-15.09	0.05	-15.12	9.44	9.47	0.02	9.46										35	33.01	43.42	46.89	196	9
Carloforte, I	Jul-20	CF_588	11	43.3	15.1	3.34	2	-14.83	-14.82	0.01	-14.82	9.7	9.78	0.06	9.74										35	33.01	43.42	46.89	196	9
Carloforte, I	Jul-20	CF_588	12	43	15.3	3.28	2	-14.84	-14.82	0.01	-14.83	9.81	9.83	0.02	9.82										35	33.01	43.42	46.89	196	9
Carloforte, I	Jul-20	CF_588	13	42.7	15.3	3.26	2	-14.81	-14.79	0.02	-14.8	9.93	9.98	0.03	9.95										35	33.01	43.42	46.89	196	9
Carloforte, I	Jul-20	CF_588	14	43.9	15.7	3.27	2	-14.62	-14.58	0.03	-14.6	9.89	9.93	0.03	9.91										35	33.01	43.42	46.89	196	9
Carloforte, I	Jul-20	CF_588	15	42.2	15.3	3.22	2	-14.39	-14.37	0.01	-14.38	9.83	9.87	0.03	9.85										35	33.01	43.42	46.89	196	9
Carloforte, I	Jul-20	CF_588	16	41.1	15.2	3.16	2	-14.15	-14.13	0.01	-14.14	9.77	9.82	0.04	9.8										35	33.01	43.42	46.89	196	9
Carloforte, I	Jul-20	CF_588	17	39.8	14.9	3.12	2	-14.12	-14.11	0.01	-14.11	9.74	9.76	0.02	9.75										35	33.01	43.42	46.89	196	9
Carloforte, I	Jul-20	CF_588	18	40.4	15.2	3.11	2	-14.08	-14.04	0.03	-14.06	10.04	10.06	0.01	10.05										35	33.01	43.42	46.89	196	9
Carloforte, I	Jul-20	CF_673	2	41	15.2	3.14	2	-14.74	-14.67	0.05	-14.71	6.48	6.59	0.07	6.54										35	17.74	22.5	25.05	124	5
Carloforte, I	Jul-20	CF_673	3	39.8	14.8	3.13	2	-14.64	-14.63	0.01	-14.64	6.45	6.47	0.02	6.46										35	17.74	22.5	25.05	124	5
Carloforte, I	Jul-20	CF_673	4	39.3	14.7	3.12	2	-14.65	-14.65	0.01	-14.65	6.71	6.71	0	6.71										35	17.74	22.5	25.05	124	5
Carloforte, I	Jul-20	CF_673	5	38.2	14.5	3.08	2	-14.49	-14.47	0.02	-14.48	6.78	6.86	0.05	6.82										35	17.74	22.5	25.05	124	5
Carloforte, I	Jul-20	CF_673	6	39.4	14.8	3.11	2	-14.55	-14.53	0.01	-14.54	7.07	7.11	0.02	7.09										35	17.74	22.5	25.05	124	5
Carloforte, I	Jul-20	CF_673	7	38.2	14.7	3.03	2	-14.23	-14.23	0	-14.23	6.94	7	0.04	6.97										35	17.74	22.5	25.05	124	5
Carloforte, I	Jul-20	CF_673	8	38.9	14.7	3.09	2	-14.52	-14.41	0.08	-14.47	7.02	7.06	0.03	7.04										35	17.74	22.5	25.05	124	5
Carloforte, I	Jul-20	CF_810	2	37	13.8	3.12	2	-13.91	-13.91	0	-13.91	6.36	6.39	0.02	6.38	0.45	211	67	1	17.45				17.45	35	25.1	33.4	37.12	158	8
Carloforte, I	Jul-20	CF_810	3	37.2	13.9	3.11	2	-13.98	-13.95	0.02	-13.97	6.37	6.37	0	6.37	0.49	202	63	1	17.73				17.73	35	25.1	33.4	37.12	158	8
Carloforte, I	Jul-20	CF_810	4	41.5	15.3	3.16	2	-14.02	-14	0.02	-14.01	6.32	6.36	0.03	6.34	0.59	187	57	1	17.23				17.23	35	25.1	33.4	37.12	158	8
Carloforte, I	Jul-20	CF_810	5	41.6	15.6	3.12	2	-13.85	-13.82	0.02	-13.84	6.65	6.66	0.01	6.66	0.55	203	62	1	18.46				18.46	35	25.1	33.4	37.12	158	8
Carloforte, I	Jul-20	CF_810	6	42.2	15.6	3.14	2	-13.62	-13.59	0.02	-13.6	6.57	6.59	0.01	6.58	0.51	221	67	1	18.58				18.58	35	25.1	33.4	37.12	158	8
Carloforte, I	Jul-20	CF_810	7	40.9	15.4	3.1	2	-13.62	-13.58	0.03	-13.6	6.78	6.78	0.01	6.77	0.53	213	64	1	18.36				18.36	35	25.1	33.4	37.12	158	8
Carloforte, I	Jul-20	CF_810	8	39.5	14.9	3.09	2	-13.39	-13.39	0	-13.39	6.83	6.85	0.01	6.84	0.52	207	63	1	18.21				18.21	35	25.1	33.4	37.12	158	8
Carloforte, I	Jul-20	CF_810	9	40.2	15.2	3.08	2	-13.21	-13.15	0.04	-13.18	6.5	6.54	0.02	6.52	0.55	206	62	1	18.66				18.66	35	25.1	33.4	37.12	158	8
Carloforte, I	Jul-20	CF_810	10	38.4	14.5	3.09	2	-13.01	-13.01	0	-13.01	6.47	6.49	0.02	6.48	0.48	225	70	1	18.96				18.96	35	25.1	33.4	37.12	158	8
Carloforte, I	Jul-20	CF_810	11	37.9	14.3	3.1	2	-12.99	-12.91	0.06	-12.95	6.64	6.7	0.04	6.67	0.45	230	72	2	18.93	18.93	18.93	0	18.93	35	25.1	33.4	37.12	158	8
Carloforte, I	Jul-20	CF_810	12	37.7	14.1	3.12	2	-13	-12.98	0.01	-12.99	6.7	6.71	0	6.7	0.47	219	68	2	18.94	18.86	18.9	0.03	18.86	35	25.1	33.4	37.12	158	8
Carloforte, I	Jul-20	CF_667	2	40.4	14.7	3.21	2	-14.82	-14.78	0.03	-14.8	6.21	6.21	0	6.21										35	20.12	27.26	28.96	149	7
Carloforte, I	Jul-20	CF_667	3	40.8	15.1	3.15	2	-14.53	-14.52	0.01	-14.53	6.2	6.26	0.04	6.23										35	20.12	27.26	28.96	149	7
Carloforte, I	Jul-20	CF_667	4	40.7	15.3	3.11	2	-14.5	-14.45	0.04	-14.47	6.18	6.22	0.03	6.2										35	20.12	27.26	28.96	149	7
Carloforte, I	Jul-20	CF_667	5	42	15.6	3.15	2	-14.72	-14.57	0.11	-14.64	6.32	6.34	0.01	6.33										35	20.12	27.26	28.96	149	7
Carloforte, I	Jul-20	CF_667	6	42.7	16	3.12	2	-14.57	-14.51	0.04	-14.54	6.32	6.4	0.05	6.36										35	20.12	27.26	28.96	149	7
Carloforte, I	Jul-20	CF_667	7	43	16	3.12	2	-14.61	-14.6	0.01	-14.6	6.41	6.46	0.03	6.43										35	20.12	27.26	28.96	149	7
Carloforte, I	Jul-20	CF_667	8	40.6	15.3	3.1	2	-14.63	-14.61	0.02	-14.62	6.48	6.54	0.04	6.51										35	20.12	27.26	28.96	149	7
Carloforte, I	Jul-20	CF_667	9	39.2	14.5	3.16	2	-14.38	-14.37	0.01	-14.38	7.24	7.24	0	7.24										35	20.12	27.26	28.96	149	7
Carloforte, I	Jul-20	CF_588	cross-sectc	43.9	15.8	3.24	2	-14.53	-14.56	0.02	-14.55	10.33	10.31	0.01	10.32										35	33.01	43.42	46.89	196	9
Carloforte, I	Jul-20	CF_673	cross-sectc	42.9	16.2	3.08	2	-14.22	-14.27	0.04	-14.2	6.27	6.24	0.02	6.3										35	17.74	22.5	25.05	124	5
Carloforte, I	Jul-20	CF_810	cross-sectc	43.2	16.2	3.08	2	-12.75	-12.9	0.11	-12.82	6.83	6.79	0.03	6.81										35	25.1	33.4	37.12	158	8
Carloforte, I	Jul-20	CF_667	cross-sectc	52.9	20	3.1	2	-14.5	-14.54	0.03	-14.52	6.37	6.36	0.01	6.36										35	20.12	27.26	28.96	149	7

Table S2. Archaeological sample measurements and details. A/B for isotope measurements refers to individual replicates per sample. SD = standard deviation.

Site	Date	Sample	Position	Collagen Y (%C)	%N	CN_Ratio	Replicates	d13C_A	d13C_B	d13C_SD	d13C_mear	d15N_A	d15N_B	d15N_SD	d15N_mear	Replicates_%S	CN_Ratio	CS_Ratio	NS_Ratio	d34S_A	d34S_B	d34S_mear	d34S_SD	d34S_mear	Rank or Tyr	Height (mm)	Width (mm)	Length (mm)	Estimated FL (cm)		
Yenikapi, Is9-13th c.		MET12545	Inner Vertel	2.9	36	12.5	3.16	2	-15.17	-15.21	0.03	-15.19	7.58	7.54	0.03	7.56									8 to 18	41.06	48.94	37.64	213.1		
Yenikapi, Is9-13th c.		MET12545	Outer Vertel	5.2	30.4	11.4	3.14	2	-14.44	-14.45	0.01	-14.45	7.57	7.56	0.01	7.56									8 to 18	41.06	48.94	37.64	213.1		
Yenikapi, Is9-13th c.		MET14082	Inner Vertel	12.6	45	16.4	3.2	2	-15.01	-15.06	0.04	-15.03	6.89	6.86	0.02	6.88									13.1	8 to 18	30.8	36.54	36.82	165.7	
Yenikapi, Is9-13th c.		MET14082	Outer Vertel	14.4	41.2	14.8	3.25	2	-15.07	-15.09	0.02	-15.08	6.98	6.98	0	6.98	1	0.74	3.2	145	46	13.13			13.1	8 to 18	30.8	36.54	36.82	165.7	
Yenikapi, Is9-13th c.		MET14129	Inner Vertel	4.9	43.4	15.5	3.28	2	-14.99	-15.05	0.04	-15.02	6.34	6.32	0.01	6.33									24 to 31	33.9	42.15	31.6	168.8		
Yenikapi, Is9-13th c.		MET14129	Outer Vertel	8	43.1	15.7	3.21	2	-14.66	-14.68	0.01	-14.67	6.55	6.52	0.02	6.53									24 to 31	33.9	42.15	31.6	168.8		
Yenikapi, Is9-13th c.		MET16735	Inner Vertel	7.1	43.4	15.7	3.23	2	-15.26	-15.32	0.04	-15.29	6.24	6.18	0.04	6.21	1	0.71	3.1	156	50	11.35			11.35	24 to 31	47.53	59.4	46.53	229.9	
Yenikapi, Is9-13th c.		MET16735	Outer Vertel	8	40	14.7	3.16	2	-14.97	-15.06	0.07	-15.02	6.45	6.37	0.06	6.41	1	0.71	3.1	153	49	11.42			11.42	24 to 31	47.53	59.4	46.53	229.9	
Yenikapi, Is9-13th c.		MET1704	Inner Vertel	9.1	43.5	15.9	3.2	2	-13.68	-13.75	0.05	-13.71	9.04	8.92	0.08	8.98	1	0.71	3.1	155	50	12.59			12.59	30 to 32	34.13	44.86	41.47	168.4	
Yenikapi, Is9-13th c.		MET1704	Outer Vertel	5.8	41.5	14.9	3.25	2	-13.53	-13.59	0.04	-13.56	9.59	9.51	0.06	9.55	1	0.69	3.3	156	48	13.39			13.39	30 to 32	34.13	44.86	41.47	168.4	
Yenikapi, Is9-13th c.		MET17473	Inner Vertel	9.8	41.5	14.9	3.26	2	-14.87	-14.97	0.08	-14.92	7.12	6.94	0.13	7.03	1	0.62	3.2	176	55	13.85			13.85	30 to 32	48.24	55.22	51.37	198.4	
Yenikapi, Is9-13th c.		MET17473	Outer Vertel	7	39.3	14.2	3.23	2	-14.75	-14.75	0	-14.75	7.16	7.14	0.02	7.15	2	0.63	3.1	160	52	14.52	14.53	14.53	0.01	14.53	30 to 32	48.24	55.22	51.37	198.4
Yenikapi, Is9-13th c.		MET20124	Inner Vertel	9.1	44.4	15.9	3.25	2	-14.73	-14.81	0.06	-14.77	6.7	6.65	0.03	6.68	1	0.48	3.1	227	74	14.8			14.8	NA	NA	NA	NA	NA	
Yenikapi, Is9-13th c.		MET20124	Outer Vertel	10.1	34.1	12.6	3.15	2	-13.87	-13.88	0	-13.87	7.42	7.24	0.12	7.33	1	0.42	2.9	211	72	14.9			14.9	NA	NA	NA	NA	NA	
Yenikapi, Is9-13th c.		MET20737	Inner Vertel	7.3	42.5	14.9	3.29	2	-14.78	-14.81	0.02	-14.8	7.21	7.15	0.05	7.18	1	0.59	3.3	180	55	15.63			15.63	NA	NA	NA	NA	NA	
Yenikapi, Is9-13th c.		MET20737	Outer Vertel	7.6	36.3	13	3.24	2	-14.22	-14.23	0.01	-14.22	7.37	7.25	0.08	7.31	1	0.49	3.1	189	61	15.41			15.41	NA	NA	NA	NA	NA	
Yenikapi, Is9-13th c.		MET21093	Inner Vertel	3.1	43.8	15.6	3.21	2	-15.69	-15.96	0.04	-15.93	6.92	6.91	0.01	6.92	1	0.6	3.3	182	56	13.49			13.49	NA	NA	NA	NA	NA	
Yenikapi, Is9-13th c.		MET21093	Outer Vertel	3.4	32.2	11.5	3.22	2	-15.56	-15.61	0.03	-15.59	7.51	7.29	0.16	7.4	1	0.47	3.1	180	58	12.72			12.72	NA	NA	NA	NA	NA	
Yenikapi, Is9-13th c.		MET4187	Inner Vertel	13.4	43.8	15.9	3.21	2	-14.79	-14.8	0.01	-14.79	7.11	7.08	0.03	7.09	1	0.58	3.1	194	62	13.71			13.71	6	39.72	48.83	34.6	223.3	
Yenikapi, Is9-13th c.		MET4187	Outer Vertel	13.7	39.8	14.6	3.18	2	-14.22	-14.24	0.01	-14.23	7.17	7.11	0.04	7.14	2	0.47	3	213	70	14.31	14.33	14.32	0.01	14.32	6	39.72	48.83	34.6	223.3
Yenikapi, Is9-13th c.		METS7505	Outer Vertel	12	44	16.1	3.19	2	-15.31	-15.36	0.03	-15.34	6.75	6.73	0.01	6.74	1	0.55	3.2	205	65	15.5			15.5	8	39.11	46.1	31.94	204.7	
Yenikapi, Is9-13th c.		METS7505	Inner Vertel	11.6	43.2	15.3	3.19	2	-15.7	-15.7	0	-15.7	6.52	6.47	0.03	6.49	1	0.64	3.1	171	55	15.97			15.97	8	39.11	46.1	31.94	204.7	
Yenikapi, Is9-13th c.		MRY3265	Inner Vertel	11.2	43.9	15.2	3.27	2	-15.74	-15.74	0	-15.74	6.98	6.91	0.05	6.95									32	44.75	55.43	52.01	198.2		
Yenikapi, Is9-13th c.		MRY3265	Outer Vertel	10.7	33.5	12.1	3.24	2	-14.72	-14.74	0.01	-14.73	7.17	6.97	0.14	7.07									32	44.75	55.43	52.01	198.2		
Yenikapi, Is9-13th c.		MRY3964	Inner Vertel	12.6	42.4	15.5	3.18	2	-14.44	-14.52	0	-14.48	9.02	8.98	0.03	9	1	0.57	3.1	193	62	14.54			14.54	9	43.23	54.81	38.75	241.6	
Yenikapi, Is9-13th c.		MRY3964	Outer Vertel	12.5	32.2	11.9	3.16	2	-14.13	-14.14	0.01	-14.14	8.64	8.52	0.08	8.58	1	0.46	3	183	61	13.61			13.61	9	43.23	54.81	38.75	241.6	

## **Chapter 5**

Exploitation shifted trophic ecology and habitat preferences  
of Mediterranean and Black Sea bluefin tuna over centuries  
**(pages 140—187)**

1 Exploitation shifted trophic ecology and habitat preferences of Mediterranean and  
2 Black Sea bluefin tuna over centuries

3  
4 Adam J. Andrews<sup>\*1,2</sup>, Christophe Pampoulie<sup>3</sup>, Antonio Di Natale<sup>4</sup>, Piero Addis<sup>5</sup>, Darío Bernal-  
5 Casasola<sup>6</sup>, Veronica Aniceti<sup>7</sup>, Gabriele Carenti<sup>8</sup>, Verónica Gómez-Fernández<sup>9</sup>, Valerie  
6 Chosson<sup>3</sup>, Alice Ughi<sup>10</sup>, Matt Von Tersch<sup>10</sup>, Maria Fontanals-Coll<sup>10</sup>, Elisabetta Cilli<sup>2</sup>, Vedat  
7 Onar<sup>11</sup>, Fausto Tinti<sup>\*1</sup>, Michelle Alexander<sup>\*10</sup>

8  
9 1Department of Biological, Geological and Environmental Sciences, University of Bologna,  
10 Campus of Ravenna, Ravenna, Italy

11 2Department of Cultural Heritage, University of Bologna, Campus of Ravenna, Ravenna,  
12 Italy

13 3Marine and Freshwater Research Institute, Hafnarfjörður, Iceland

14 4Aquastudio Research Institute, Messina, Italy

15 5Department of Life and Environmental Sciences, University of Cagliari, Cagliari, Sardinia,  
16 Italy

17 6Department of History, Geography and Philosophy, Faculty of Philosophy and Letters,  
18 University of Cádiz, Cádiz, Spain

19 7Department of Natural History – University Museum, University of Bergen, Norway

20 8CEPAM, CNRS, Université Côte d'Azur, Nice, France

21 9Instituto Nacional de Investigaciones Científicas y Ecológicas, Salamanca, Spain

22 10BioArCh, Department of Archaeology, University of York, York, U.K.

23 11Osteoarchaeology Practice and Research Centre, Faculty of Veterinary Medicine, Istanbul  
24 University-Cerrahpaşa, Istanbul, Turkey

25  
26 \*Corresponding authors: [adam@palaeome.org](mailto:adam@palaeome.org), [fausto.tinti@unibo.it](mailto:fausto.tinti@unibo.it),  
27 [michelle.alexander@york.ac.uk](mailto:michelle.alexander@york.ac.uk)

28  
29 Keywords: *Thunnus thynnus*, historical baselines, anthropogenic impacts, trophic shifts,  
30 stable isotope analysis, Black Sea

31  
32 **Abstract**

33  
34 During recent decades, the health of ocean ecosystems and fish populations has been  
35 threatened by overexploitation, pollution, and anthropogenic-driven climate change. Due to a  
36 lack of long-term ecological data, we have a poor grasp of the true impact on the diet and  
37 habitat use of fishes. This information is vital if we are to recover depleted fish populations  
38 and predict their future dynamics. Here, we trace the long-term habitat use and diet of  
39 Atlantic bluefin tuna (*Thunnus thynnus*; BFT), a species that has had one of the longest and  
40 most intense exploitation histories, owing to its tremendous cultural and economic  
41 importance. Using carbon ( $\delta^{13}\text{C}$ ), nitrogen ( $\delta^{15}\text{N}$ ) and sulphur ( $\delta^{34}\text{S}$ ) stable isotope analyses  
42 of modern and ancient BFT including 98 archaeological and archival bones from 11  
43 Mediterranean locations ca. 1<sup>st</sup> century to 1941 CE, we reveal a hitherto unknown shift  
44 around the 16<sup>th</sup> century towards more pelagic BFT foraging. This likely reflects the early  
45 anthropogenic exploitation of inshore coastal ecosystems, as attested by historical literature  
46 sources. Further, we reveal that BFT which migrated to the Black Sea—and that disappeared  
47 during a period of intense exploitation and ecosystem changes in the 1980s—represented a  
48 unique component, isotopically distinct from BFT of NE Atlantic and Mediterranean locations.  
49 These data suggest that anthropogenic activities had the ability to alter the diet and habitat  
50 use of fishes in conditions prior to those of recent decades. Consequently, marine recovery

51 targets ought to be more ambitious and reflect the complexity of past ecosystems and  
52 populations, not their modern-day remnants.

53

## 54 1. INTRODUCTION

55

56 During the past century, a myriad of anthropogenic impacts such as fisheries exploitation,  
57 habitat modification, pollution, and climate change have had measurable and increasing  
58 consequences affecting habitat suitability, prey availability, individual life histories and in  
59 turn, the productivity, fitness and distribution of marine populations (Butchart et al., 2010;  
60 Casini et al., 2009; Howarth et al., 2014; Pauly et al., 1998; Planque et al., 2010). Due to a  
61 lack of long-term data, the onset of anthropogenic impacts remains unclear for many marine  
62 ecosystems and populations, as does their response (Jackson et al., 2001; Lotze et al.,  
63 2014; Schwerdtner Máñez et al., 2014). As such, historical baselines (e.g., population  
64 function and structure over centuries) would be useful to guide management targets on how  
65 complex populations were in the past, what more-natural distributions and behaviours looked  
66 like, and which anthropogenic impacts have driven change and should consequently be  
67 minimised to promote recovery (Caswell et al., 2020; Duarte et al., 2020; Engelhard et al.,  
68 2015).

69

70 As an exemplary case, the eastern Atlantic and Mediterranean population of bluefin tuna  
71 (*Thunnus thynnus*; BFT), is one of the longest and most heavily exploited pelagic predators  
72 (Porch et al., 2019). Consequently, BFT range contracted and its abundance was depleted  
73 by the 21<sup>st</sup> century, which included the loss of Black Sea habitats by the 1980s (MacKenzie  
74 et al., 2009; Worm & Tittensor, 2011). Since antiquity, the Black Sea has supported BFT  
75 fisheries from the Bosphorus to the Azov Sea, as attested by archaeological remains, the  
76 writings of classical authors, and the tuna-trap records over several centuries (Andrews, et  
77 al., 2022a; Cort & Abaunza, 2019; Di Natale, 2015; Karakulak & Oray, 2009; Karakulak &  
78 Yıldız, 2016). However, there is no information on the foraging ecology of Black Sea BFT,  
79 and little information on their distribution, or connectivity with Atlantic and Mediterranean  
80 BFT, which is vital to promote their return (Di Natale, 2015; Di Natale et al., 2019). Despite  
81 recoveries of BFT abundance during the last decade to 1970s levels (ICCAT, 2020), BFT is  
82 yet to recolonise habitats such as the Black Sea (Di Natale, 2019). Moreover, as for many  
83 consumers, questions exist around the broader impacts of ocean overexploitation over  
84 centuries. Such as, has the depletion of inshore species and forage fishes, especially in  
85 coastal areas, induced a shift in diets and distributions of BFT? (c.f. Hilborn et al., 2017;  
86 Jackson et al., 2001; Pauly et al., 1998) and, has the pollution of coastal areas shifted BFT  
87 migrations offshore (c.f. Addis et al., 2016)? Confidence in BFT sustainability is thus  
88 stymied, in part, by a limited understanding of its population structure and trophic niche(s)  
89 prior to the 1970s, which may improve recovery targets (ICCAT, 2020).

90

91 Nowadays, the eastern Atlantic and Mediterranean stock of BFT comprises individuals  $\leq 3.3$   
92 m in length and  $\leq 725$  kg in weight (Cort et al., 2013), and spawns predominantly in the  
93 Mediterranean from age 3-4 (Mather et al., 1995; Piccinetti et al., 2013). The majority of  
94 individuals undertake diverse feeding migrations to a range of habitats throughout the  
95 Atlantic (Druon et al., 2016; Mariani et al., 2016; Wilson & Block, 2009) from as early as age  
96 one (Dickhut et al., 2009), though tagging and fishery evidence suggests that a portion are  
97 resident in the Mediterranean all-year-round (Cermeño et al., 2015; De Metrio et al., 2004;  
98 Mather et al., 1995), and might be remnants of a population that migrated to the Black Sea

99 each spring and potentially spawned there (Di Natale, 2015; Karakulak & Oray, 2009). For  
100 this reason amongst others, it is hypothesised that BFT comprise more complexity than is  
101 currently reflected where BFT are managed as two stocks (Cort & Abaunza, 2019; Di Natale,  
102 2019; Fromentin, 2009). These are the eastern Atlantic and Mediterranean BFT and the  
103 genetically and isotopically distinct population of BFT spawning in the Gulf of Mexico and  
104 Slope Sea. Both stocks exhibit a high-degree of natal homing despite high-levels of  
105 population mixing (Brophy et al., 2020; Puncher et al., 2018; Richardson et al., 2016;  
106 Rodríguez-Ezpeleta et al., 2019; Rooker et al., 2008). Juvenile and adult BFT primarily  
107 inhabit the upper 200 m of neritic habitats (Druon et al., 2016; Walli et al., 2009; Wilson &  
108 Block, 2009), feeding on varied combinations of benthic-pelagic prey such as forage fishes,  
109 cephalopods and crustaceans (Karakulak et al., 2009; Logan et al., 2011), and occasionally  
110 diving offshore to feed at great depths (Battaglia et al., 2013; Olafsdottir et al., 2016; Rumolo  
111 et al., 2020; Sarà & Sarà, 2007; Wilson & Block, 2009). The greatest shift in BFT foraging  
112 strategy appears to be at age two, once the predation of zooplankton ends and the predation  
113 of fishes begins, after which, size-classes remain more isotopically similar (Rumolo et al.,  
114 2020; Sarà & Sarà, 2007).

115  
116 The study of stable isotopes using archaeological and archived bone, scales or otoliths to  
117 assess long-term population dynamics in fishes is well established (Barrett et al., 2011; Das  
118 et al., 2021; Hutchinson & Trueman, 2006; Newton & Bottrell, 2007). Recent studies have  
119 revealed the extinction of a resident trophic niche in Atlantic salmon (*Salmo salar*, Guiry et  
120 al. (2016), and indicated potential millennial-scale diet shifts in the highly exploited Atlantic  
121 cod (*Gadus morhua*, Ólafsdóttir et al. (2021)) and Atlantic populations of European hake  
122 (*Merluccius merluccius*, Llorente-Rodríguez et al. (2022)). Potential habitat productivity or  
123 usage shifts have also been suggested in Atlantic and Pacific fishes during the last 500  
124 years compared with the previous centuries (Misarti et al., 2009; Ólafsdóttir et al., 2021).

125  
126 A range of ecological and environmental variables will affect the  $\delta^{13}\text{C}$ ,  $\delta^{15}\text{N}$  and  $\delta^{34}\text{S}$  values  
127 of fish tissues.  $\delta^{15}\text{N}$  values increase with each trophic level and are thus used to estimate  
128 the trophic position of an organism in a food web (Sigman et al., 2009). In contrast,  $\delta^{13}\text{C}$  and  
129  $\delta^{34}\text{S}$  signatures pass between primary producers and consumers with low levels of  
130 fractionation. This lends them to being good indicators of provenance because distinct  $\delta^{13}\text{C}$   
131 and  $\delta^{34}\text{S}$  values are generally maintained across trophic levels (Guiry, 2019; Thode, 1991).  
132 Typically, habitats heavily influenced by low-salinity water (e.g., Black Sea) are lower in  $\delta^{15}\text{N}$   
133 and  $\delta^{13}\text{C}$  than saline habitats of the Mediterranean and especially NE Atlantic shelf seas due  
134 to increased terrestrially-derived or fixed (low- $\delta^{15}\text{N}$  and  $\delta^{13}\text{C}$ ) nitrogen and carbon and/or  
135 lower quantities of resuspended (remineralized, high- $\delta^{15}\text{N}$  and  $\delta^{13}\text{C}$ ) nitrogen and carbon  
136 from sediments or the deep-ocean (Barnes et al., 2009; Fulton et al., 2012; Magozzi et al.,  
137 2017; Rafter et al., 2019). For these reasons, pelagic habitats and consumers often contain  
138 lower  $\delta^{13}\text{C}$  than benthic and neritic ones (Amiriaux et al., 2023; DeNiro & Epstein, 1978) yet  
139 pelagic  $\delta^{15}\text{N}$  values are often higher due to high levels of fractionation and more complex  
140 food webs. It is important to note that many factors govern the complex variation in  $\delta^{15}\text{N}$  and  
141  $\delta^{13}\text{C}$  between consumers, including the environmental conditions, levels of benthic-pelagic  
142 coupling and the production in each habitat foraged (Barnes et al., 2009; Jennings et al.,  
143 2008; Sigman et al., 2009).  $\delta^{34}\text{S}$  is sometimes useful to disentangle these effects. For  
144 example, low  $\delta^{34}\text{S}$  values often reflect increased foraging on benthic or neritic prey while  
145 higher values indicate a greater degree of energy incorporated from pelagic production (Fry  
146 & Chumchal, 2011; Szpak & Buckley, 2020). Though, highly-stratified pelagic habitats such

147 as in the Black Sea can be expected to have relatively low  $\delta^{34}\text{S}$  values due to sulphate being  
148 partially derived from microbial sulphides in sub-oxic waters. Distance from shore also  
149 influences  $\delta^{34}\text{S}$  values, not because of freshwater input *per se*—even brackish water is  
150 dominated by marine high  $\delta^{34}\text{S}$  signatures (Cobain et al., 2022; Fry & Chumchal, 2011;  
151 Guiry et al., 2022)—but rather food webs associated with coastal habitats such as seagrass  
152 beds, salt marshes and mudflats where low  $\delta^{34}\text{S}$  is incorporated from anoxic marine  
153 sediments during production (Guiry et al., 2022; Szpak & Buckley, 2020; Thode, 1991).

154  
155 Since variables governing production change over time (e.g., changing environmental  
156 conditions and sources such as pollution), there is often intra- and inter-annual variation at  
157 the base of marine food-webs, which one needs to be aware of when drawing conclusions  
158 from temporal isotopic data—especially over the long-term (Jardine et al., 2014; Solomon et  
159 al., 2008). Some degree of temporal variation can be accounted for, like the long-term  
160 decrease in oceanic  $\delta^{13}\text{C}$  following industrialisation (Suess Effect: Gruber et al. (1999)),  
161 while tissue type can also improve temporal inferences. For instance, BFT vertebrae retain  
162 multiple years of isotopic foraging signatures across their growth axes (Andrews et al., 2023)  
163 and therefore bone isotope values dampen out intra- and inter-annual variation, providing an  
164 average across years of foraging prior to capture.

165  
166 In this study, we examine a long time series of isotopic data on Atlantic bluefin tuna,  
167 including 98 archaeological and archived bones from 11 eastern Atlantic, Mediterranean and  
168 Black Sea locations ca. 1<sup>st</sup> century to 1941 CE, and 20 modern samples. First, we analysed  
169 their  $\delta^{13}\text{C}$ ,  $\delta^{15}\text{N}$  and  $\delta^{34}\text{S}$  isotope composition to characterise the foraging ecology of Black  
170 Sea BFT, whose distribution and feeding habits remain unknown. Second, we investigated  
171 how Black Sea BFT functioned and was structured in relation to the eastern Atlantic and  
172 Mediterranean BFT, since the residency and role of BFT in the Black Sea region remains  
173 unknown (Di Natale, 2015; MacKenzie & Mariani, 2012). Finally, we investigated how BFT  
174 diet and/or migrations may have changed throughout the past two millennia in relation to  
175 commercial exploitation in light of evidence of offshore movement in the past few decades  
176 following noise pollution (Addis et al., 2016) and a shift in the size-structure of marine food  
177 webs (Baum & Worm, 2009; Pauly et al., 1998). It must be noted that temporal data  
178 produced using archaeological and historical samples can be complex to interpret since they  
179 are necessarily limited in number and might be influenced by changing fishing technologies  
180 and locations foraged available.

181

182

## 183 **2. METHODS**

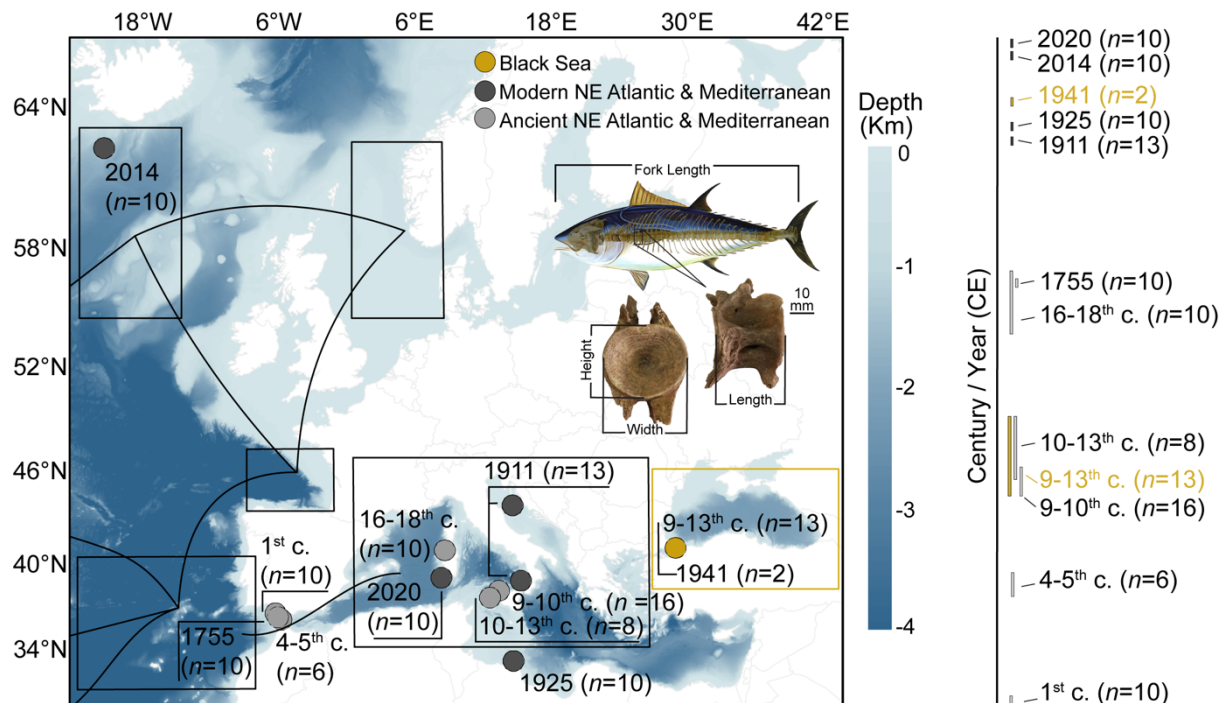
184

### 185 **2.1 Sampling and collagen extraction**

186

187 Ancient BFT bones (primarily vertebrae) were sampled from archaeological sites throughout  
188 the Mediterranean, each dated by context or  $^{14}\text{C}$  (Table S1, Figure S1), to between the 1<sup>st</sup>-  
189 18<sup>th</sup> century CE (Table 1, Figure 1: for details see Supplementary Materials). Care was taken  
190 to avoid sampling the same individual twice by selecting a range of specimens with different  
191 sizes or different stratigraphic units. Modern BFT bones comprise vertebrae pertaining to the  
192 20<sup>th</sup> c. Massimo Sella Archive, University of Bologna, Ravenna Campus (Italy) and those  
193 captured in the 21<sup>st</sup> century. Archival specimens were BFT captured in central  
194 Mediterranean tuna traps during the early-20<sup>th</sup> c. (Table 1, Figure 1), stored dry after the

195 removal of soft tissues by unknown means. BFT were sampled off southern Iceland in  
 196 September 2014 by long-line (fishing vessel: Jóhanna Gísladóttir, Vísir hf., Iceland) and Isola  
 197 Piana (Carloforte, Sardinia) in July 2020 by tuna trap (Carloforte Tonnare PIAM srl., Italy);  
 198 these were mechanically cleaned of soft-tissues, macerated in ambient-temperature water  
 199 for up to two months to remove remaining soft-tissues by microbial decomposition, then  
 200 dried.  
 201



202  
 203 **Figure 1. Locations and periods of capture of Atlantic bluefin tuna (*Thunnus thynnus*; BFT)**  
 204 **samples analysed herein** (coloured circles), illustrated in relation to ocean bathymetry, and major  
 205 BFT habitats (black, yellow rectangles) and migration strategies (black lines) in the eastern Atlantic  
 206 and Mediterranean, after (Mariani et al., 2016). Samples are coloured as follows: putative Black Sea,  
 207 yellow; modern NE Atlantic and Mediterranean, black; ancient (archaeological) NE Atlantic and  
 208 Mediterranean, grey. *n* = number successfully analysed. Map created using ESRI ArcMap (v.10.6,  
 209 <https://arcgis.com>). Illustration indicates fork length measurements used and provides an example of  
 210 a vertebra related to its vertebral position and measurements (Height, Width and Length) used to  
 211 reconstruct Fork Length of the modern and ancient samples.  
 212  
 213  
 214  
 215  
 216  
 217  
 218  
 219  
 220  
 221  
 222  
 223  
 224



Table 1. Summary details of modern and ancient Atlantic bluefin tuna ( <i>Thunnus thynnus</i> ) samples collected and analysed in the current study.									
Sample ID / Year CE	Location	Longitude (°E)	Latitude (°N)	n sampled	n analysed for $\delta^{13}\text{C}$ and $\delta^{15}\text{N}$	n analysed for $\delta^{34}\text{S}$	Fork Length min-max (mean) cm	Sample type	Skeletal elements
2020	Carloforte, Sardinia	8.31	39.18	10	10	10	111-196 (132)	Modern	Vertebrae
2014	Southwest Iceland	-21.42	62.42	10	10	9	198-238 (218)	Modern	Vertebrae
1941	Istanbul, Turkey	28.95	41.01	2	2	2	275 & 278	Archival	Vertebrae
1925	Zliten, Libya	14.66	33.25	10	10	10	158-204 (182)	Archival	Vertebrae
1911	Venice, Italy	14.59	43.93	7	6	5	88-152 (118)	Archival	Vertebrae
	Pizzo, Italy	15.34	38.97	7	7	6		Archival	Vertebrae
1755	Conil, Spain	-6.09	36.28	10	10	9	144-220 (176)	Archaeologica I	Vertebrae
16-18 <sup>th</sup> c.	Sassari, Sardinia	8.62	40.86	10	10	9	115-231 (178)	Archaeologica I	Vertebrae
10-13 <sup>th</sup> c.	Mazara del Vallo, Sicily	12.58	37.65	8	8	6	-	Archaeologica I	5 vertebrae, 3 cranial elements
9-10 <sup>th</sup> c.	Palermo, Sicily	13.37	38.11	18	16	12	101-185 (130)	Archaeologica I	15 vertebrae, 3 cranial elements
9-13 <sup>th</sup> c.	Istanbul, Turkey	28.95	41.01	14	13	12	165-241 (201)	Archaeologica I	Vertebrae
4-5 <sup>th</sup> c.	Baelo Claudia, Spain	-5.77	36.09	12	6	4	109-132 (124)	Archaeologica I	Vertebrae
1 <sup>st</sup> c.	Cadiz, Spain	-6.31	36.53	10	10	10	90-155 (130)	Archaeologica I	Vertebrae
<b>Total</b>				128	118	104			

N.B. 1911 sample groups were pooled for analyses. For further details of the archived and archaeological samples see Supplementary Materials. Samples from archaeological groups were not analysed if collagen yields <1%. Coordinates of 1911 and 1941 archival groups are approximations. n = the number of individual specimens included in analyses after quality-control.

225

226

227

228

To enable assessment of size effects on isotope values, we estimated the straight fork length (FL) of vertebrae specimens following (Andrews, et al., 2022b) using the online resource <https://tunaarchaeology.org/lengthestimations>. Briefly, vertebrae rank or type was

229 identified, vertebrae length/width/height was measured to the nearest mm, and the best-  
230 fitting power regression model was applied for each specimen (Table S2), which predicts FL  
231 to ca. 90% accuracy based on modern reference skeletons. It is assumed that relationships  
232 between vertebra size and FL were consistent between modern and historical specimens.  
233 FL was measured at sea for all modern Icelandic and three modern Sardinian samples  
234 (CF\_2020\_617, 667 and 673: Supplementary Materials), to the nearest cm.

235  
236 Isotope signatures from multiple years prior to catch are retained across the growth axes of  
237 BFT vertebrae (Andrews et al., 2023). Therefore, to obtain averages of foraging across  
238 seasons and avoid overrepresenting potential sporadic seasonal changes or foraging  
239 behaviours, we aimed to 1) sample the same element (vertebrae), whenever possible, and  
240 2) represent roughly equal portions of acellular (cortical) and cellular (spongy) bone across  
241 the growth-axis, between samples. Thus, we sampled bones using a diamond band saw to  
242 cut wedges across growth axes where the amount of inner material was lesser, but roughly  
243 proportional to the amount of outer material, between samples (Supplementary Materials,  
244 Figure S2). This resulted in a sample section which integrates collagen formed over the  
245 whole life of the fish. Cutting of vertebrae was prohibited for one sample group (9-13<sup>th</sup> c.  
246 Istanbul), thus we drilled into each vertebra at an inner and outer position, analysed the  
247 isotopic compositions separately, and averaged values for the final analyses (Table S2).

248  
249 Bone collagen was extracted following the modified Longin method (Brown et al., 1988).  
250 Briefly, cross-sections (ca. 250-1000 mg) of bone were mechanically cleaned to remove  
251 exogenous material. Modern and archaeological 1755 CE samples were defatted by  
252 sonication for 15 minutes in a 2:1 dichloromethane/methanol solution, repeated a minimum  
253 of three times until the solution remained clear. Residual solvents were then evaporated  
254 overnight before samples were rinsed three times with deionised water. Samples were  
255 demineralised at +4°C in 8 mL of 0.4 or 0.6 M HCl, depending upon if they were  
256 archaeological or modern samples, respectively. To remove non-collagenous proteins  
257 potentially retained in modern samples (Guiry & Szpak, 2020) we soaked demineralised  
258 modern samples in 0.25 M NaOH for 15 minutes. This was repeated until the solution  
259 remained clear, prior to refluxing back to 0.6 M HCl (Longin, 1971). Demineralised collagen  
260 was gelatinised at 80°C for 48 hours in 0.001 M HCl. Gelatinised collagen was filtered (60 to  
261 90 µm; Eze filters, Elkay, U.K.) and freeze-dried.

262

## 263 **2.2. Stable isotope analyses**

264

265 To determine carbon and nitrogen isotopic values, collagen (0.4 to 0.6 mg) was analysed in  
266 duplicate using a Sercon continuous flow 20-22 IRMS interfaced with a Universal Sercon  
267 gas solid liquid elemental analyser (Sercon, U.K.) at BioArCh, Department of Archaeology  
268 (York, U.K.). Sulphur isotope values were determined by analysing collagen (0.9 to 1.2 mg) in  
269 20% duplicate using a Delta V Advantage continuous-flow IRMS coupled via a ConFloIV to  
270 an IsoLink elemental analyser (Thermo Scientific, Germany) at SUERC (East Kilbride, U.K.)  
271 as described in Sayle et al. (2019). The obtained values were corrected from the isotopic  
272 ratio of the international standards, Vienna Pee Dee Belemnite (VPDB) for carbon, air (AIR)  
273 for nitrogen, and Vienna Cañon-Diablo Troilite (VCDT) for sulphur, using the  $\delta$  (‰) notation.

274

275 Uncertainties on the measurements were calculated by combining the standard deviation  
276 (SDs) of the sample replicates and those of International Atomic Energy Agency (IAEA)

277 reference material according to Kragten (1994) for carbon and nitrogen, and Sayle et al.  
278 (2019) for sulphur. The international standards used as reference material in analytical runs  
279 were; caffeine (IAEA-600), ammonium sulfate (IAEA-N-2), and cane sugar (IA-Cane) for  
280 carbon and nitrogen; and silver sulfide (IAEA-S-2 and IAEA-S-3) for sulphur. International  
281 standard average values and SD across the runs were as follows: IAEA-600 (n = 43),  $\delta^{13}\text{C}$   
282 raw =  $-27.71 \pm 0.09\text{‰}$  ( $\delta^{13}\text{C}$  true =  $-27.77 \pm 0.04\text{‰}$ ) and  $\delta^{15}\text{N}$  raw =  $+0.71 \pm 0.22\text{‰}$  ( $\delta^{15}\text{N}$   
283 true =  $1 \pm 0.2\text{‰}$ ); IAEA-N-2 (n = 43),  $\delta^{15}\text{N}$  raw =  $+20.38 \pm 0.38\text{‰}$  ( $\delta^{15}\text{N}$  true =  $20.3 \pm 0.2\text{‰}$ );  
284 and IA-CANE (n = 54),  $\delta^{13}\text{C}$  raw =  $-11.68 \pm 0.10\text{‰}$  ( $\delta^{13}\text{C}$  true =  $-11.64 \pm 0.03\text{‰}$ ); IAEA-S-  
285 2 (n=13),  $\delta^{34}\text{S}_{\text{VCTD}} = 22.62 \pm 0.08 \text{‰}$  and IAEA-S-3 (n=13)  $\delta^{34}\text{S}_{\text{VCTD}} = -32.49 \pm 0.08 \text{‰}$ . The  
286 maximum uncertainty across all samples (n = 118) was  $<0.20\text{‰}$  for  $\delta^{13}\text{C}$  and  $\delta^{15}\text{N}$ , and  
287 (n=104)  $0.36\text{‰}$  for  $\delta^{34}\text{S}$ .

288

289 Since BFT are highly migratory, it is challenging to predict the proportion of time foraging in  
290 each of their Atlantic and Mediterranean habitats. We therefore used a conservative  
291 approach to correct for the Suess Effect; the long-term decrease in oceanic  $\delta^{13}\text{C}$  due to the  
292 uptake of anthropogenic  $\text{CO}_2$  following industrialisation (Gruber et al., 1999). Our correction  
293 assumed that the majority of foraging was conducted in the NE Atlantic Ocean, which  
294 experienced the greatest degree of anthropogenic  $^{13}\text{C}$  change among BFT habitats (Eide et  
295 al., 2017). Therefore, applying corrections for this region would likely lead to an  
296 overcorrection but reduce the possibility of under-correction. Modern  $\delta^{13}\text{C}$  values were thus  
297 corrected for the influence of the Suess Effect, using Eq. 1 as per Hilton et al. (2006) and  
298 Ólafsdóttir et al. (2021):

299

$$300 \delta^{13}\text{C} \text{ Suess correction factor} = \alpha * \exp(\text{years from 1850} * b) \quad (1)$$

301

302 where  $\alpha$  = the annual rate of decrease for the study water body, approximated as  $-0.015\text{‰}$ ,  
303 based on previous estimates for the NE Atlantic Ocean (Quay et al., 2003), and  $b$  = the  
304 global decrease in oceanic  $\delta^{13}\text{C}$  established as 0.027 by Gruber et al. (1999). Thus, we  
305 added 0.08, 0.11, and 0.18 ‰ to 1911, 1925 and 1941  $\delta^{13}\text{C}$  values, and 1.26 ‰ and 1.48 ‰  
306 to 2014 and 2020  $\delta^{13}\text{C}$  values, respectively. An alternative approach assuming NE Atlantic  
307 residency (Clark et al., 2021) was not used but yielded similar estimates which did not alter  
308 the interpretation of our results.

309

310 Insufficient collagen (defined as  $<1\%$  total sample weight) resulted in 10 (13%)  
311 archaeological samples being excluded from analyses (six 4-5<sup>th</sup> c., one 9-13<sup>th</sup> C., two 9-10<sup>th</sup>  
312 c., one 1911, Table S2). The quality of  $\delta^{13}\text{C}$  and  $\delta^{15}\text{N}$  values for the remaining 118 samples  
313 was controlled by confirming atomic C:N ratios (3.0-3.4) fell within the accepted ranges for  
314 archaeological and modern samples (Guiry & Szpak, 2020, 2021). Since variation in lipid  
315 content between samples can potentially drive differences in  $\delta^{13}\text{C}$  values (Guiry & Szpak,  
316 2020), we studied the relationship between C:N Ratios and  $\delta^{13}\text{C}$  which revealed a non-  
317 significant correlation (Pearson's  $r = -0.12$ ,  $p = 0.23$ , Figure S3).

318

319 Quality control criteria for sulphur isotopes are relatively poorly defined for fishes. The quality  
320 of 104 samples analysed for  $\delta^{34}\text{S}$  (which passed the assessment above) was assessed by  
321 %S values. Following Nehlich & Richards (2009) we calculated the theoretical sulphur  
322 content of BFT collagen from its Type 1A and 2A collagen amino acid sequences (NCBI  
323 BioProject: PRJNA408269) following Nehlich & Richards (2009). We estimated the  
324 theoretical sulphur content of BFT collagen at 0.47% (Table S3), therefore two 9-13<sup>th</sup> c.

325 Istanbul samples (MRY3285 and MET12545, Table S2) were excluded from the dataset  
326 using the range (0.4-0.8%) suggested by Nehlich & Richards (2009). However, modern BFT  
327 fell outside of the C:S (125-225) and N:S (40-80) criteria for archaeological collagen  
328 suggested by (Nehlich & Richards, 2009), and consequently, this additional criteria was not  
329 applied. To confirm that our results were robust to variable C:S and N:S values (Table S2),  
330 we performed non-exact pairwise Wilcoxon tests in R (R Team, Core, 2013) which reported  
331 that BFT  $\delta^{34}\text{S}$  values do not significantly differ between samples falling inside or outside of  
332 the Nehlich & Richards (2009) C:S and N:S Ratio criteria (Wilcoxon,  $p > 0.05$ ). Finally, we  
333 returned to quality checks after final data analyses and found no significant differences were  
334 found in N:S or C:S between samples from the pre- vs. post 16<sup>th</sup> century (Wilcoxon,  $p$   
335  $> 0.05$ ).

336

### 337 **2.3 Statistical analyses**

338

339 We tested statistical pairwise differences in distribution between Black Sea, modern NE  
340 Atlantic and Mediterranean and ancient NE Atlantic and Mediterranean isotope values using  
341 non-exact pairwise Wilcoxon tests in R. To estimate the probability of a priori defined spatial  
342 groups being found within the same niche as each other we applied the overlap function  
343 using default settings and 10,000 iterations in the R package nicheROVER (Swanson et al.,  
344 2015). To avoid conflating temporal and spatial effects of Black Sea foraging, we used  
345 sample location to group all archaeological samples named 'Ancient NE Atlantic and  
346 Mediterranean', excluding 9-13<sup>th</sup> c. Istanbul samples, which formed their own group with  
347 1941 Istanbul samples, named 'Black Sea'. 21<sup>st</sup> c. samples were grouped with the remaining  
348 archival samples and named 'Modern NE Atlantic and Mediterranean'. We tested the  
349 relationship between Fork Length (FL) and each isotope value using the *lm* linear regression  
350 function in R, for each of the three sample groups. A base10 log-linear model was applied to  
351 FL values as per Nakazawa et al. (2010) and Jennings (2005). Black Sea regressions were  
352 calculated excluding the 1941 Istanbul individuals ( $n=2$ ) to avoid confounding spatial and  
353 temporal patterns. We tested the statistical differences between inner and outer vertebrae  
354 isotope values for the 9-13<sup>th</sup> c. Istanbul samples using exact pairwise Wilcoxon tests.

355

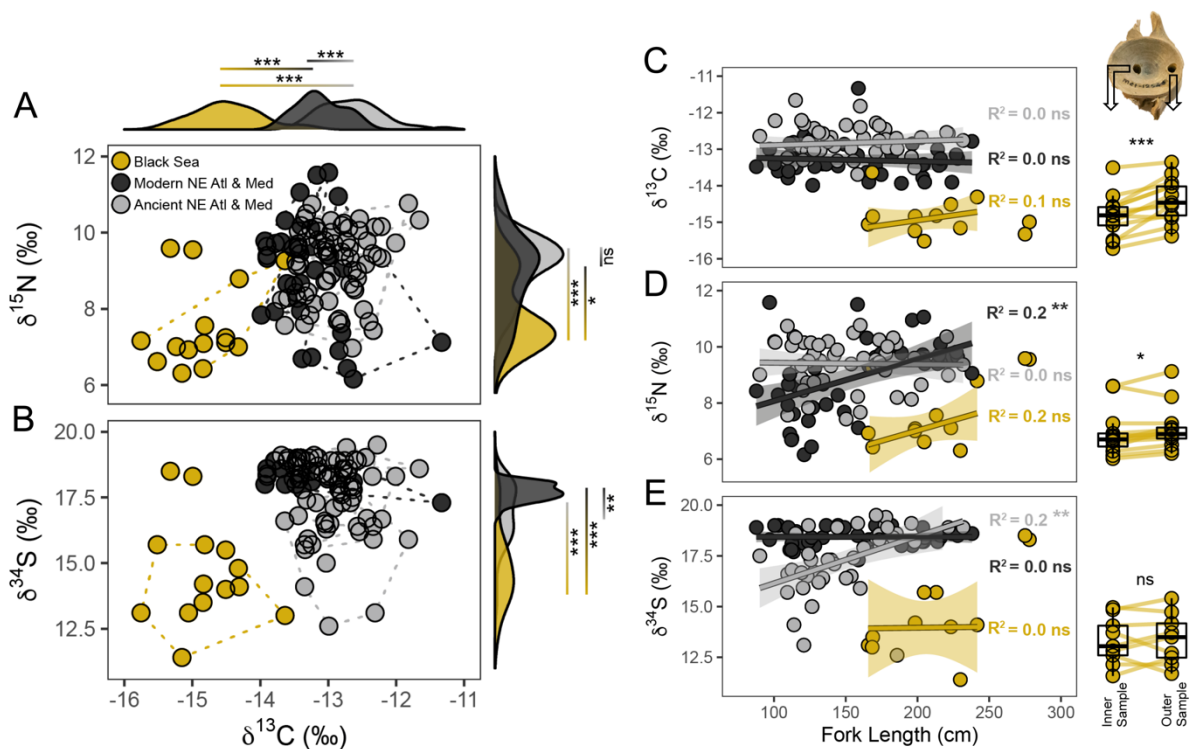
356 Generalised additive models (GAMs) were used to assess linear and non-linear relationships  
357 between time (Century / Year CE) and space (Longitude E), and  $\delta^{13}\text{C}$ ,  $\delta^{15}\text{N}$  and  $\delta^{34}\text{S}$  values.  
358 Following Zuur et al. (2009), we selected a model with the lowest Akaike information criterion  
359 (AIC) using a back-wards elimination of smoothed and unsmoothed factors (Table S4).  
360 Gaussian models with link functions were thus applied to a different suite of effects for each  
361 stable isotope as follows using the restricted maximum likelihood (REML) approach in the R  
362 package mgcv (Wood, 2012). The final models fitted for  $\delta^{13}\text{C}$  and  $\delta^{15}\text{N}$  was:  $\delta X \sim s(\text{longitude})$   
363  $+ \text{Year:group}$ , where group indicated a priori placement of samples into Black Sea or  
364 modern and ancient NE Atlantic and Mediterranean samples and only results for the latter  
365 were retained. This elimination of the Black Sea samples for temporal investigation reduced  
366 the possibility of spatial trends confounding temporal trends. The final model fitted for  $\delta^{34}\text{S}$   
367 was:  $\delta^{34}\text{S} \sim s(\text{longitude}, \text{by} = \text{group}) + s(\text{Year})$ , where the group indicated a placement of  
368 samples into pre-16<sup>th</sup> c. samples or post-16<sup>th</sup> c. samples, set based on visual observation of  
369 temporal changes in  $\delta^{34}\text{S}$  values to assess spatial variability for both periods. Plotting factor  
370 pairs confirmed that collinearity was absent. Residuals were observed to be randomly  
371 distributed, and observations were positively correlated with predicted values in each case.

372

373 **3. RESULTS**

374

375 Representing a temporal range of the last two millennia, we analysed a total of 118 BFT  
 376 bone samples for  $\delta^{13}\text{C}$  and  $\delta^{15}\text{N}$ , and 104 BFT bone samples for  $\delta^{34}\text{S}$ .  $\delta^{13}\text{C}$  values ranged  
 377 from -15.8 to -11.3‰,  $\delta^{15}\text{N}$  values ranged from 6.2 to 11.6‰, and  $\delta^{34}\text{S}$  values ranged from  
 378 11.4 to 19.5‰ (Figure 2A, 2B). We observed a distinct clustering of Black Sea samples  
 379 which were generally lower in  $\delta^{13}\text{C}$ ,  $\delta^{15}\text{N}$  and  $\delta^{34}\text{S}$ , than ancient or modern NE Atlantic and  
 380 Mediterranean samples. The Black Sea trophic niche was statistically significantly different  
 381 from Atlantic and Mediterranean sample niches across all three isotopes (Figure 2A, 2B,  $p$   
 382  $<0.05$  -  $<0.001$ ) and had low overlap probabilities with both ancient (0-3.5% CI) and modern  
 383 (0-12.0% CI) NE Atlantic and Mediterranean BFT niches (Figure S4).  
 384



385

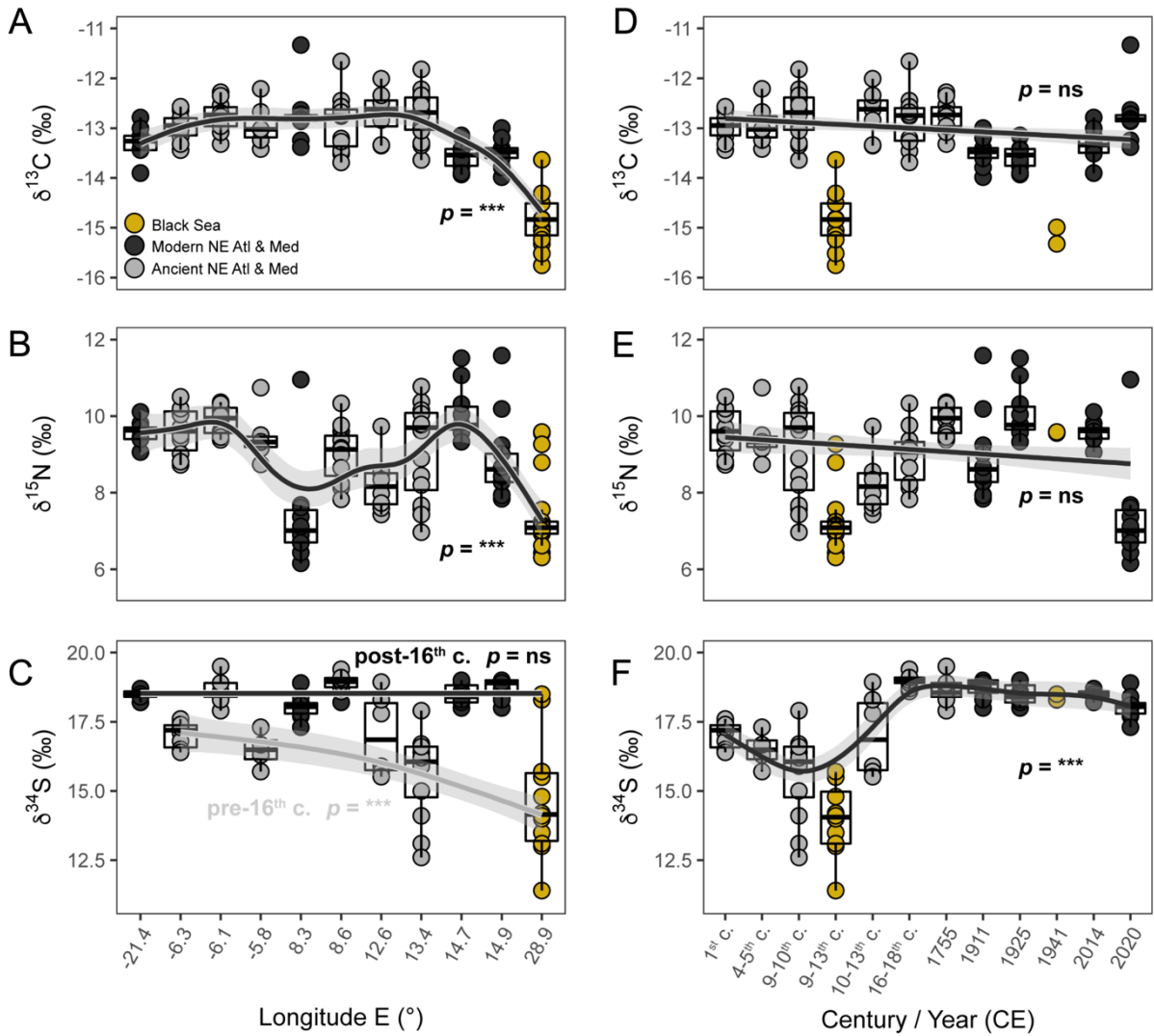
386 **Figure 2. Findings of an isotopically distinct Black Sea niche of Atlantic bluefin tuna (*Thunnus***  
 387 ***thynnus*; BFT) and the relationship between foraging behaviours and body size.**  $\delta^{13}\text{C}$  and  $\delta^{15}\text{N}$   
 388 scatterplots (A) and  $\delta^{13}\text{C}$  and  $\delta^{34}\text{S}$  scatterplots (B). Samples (symbols) are coloured according to their  
 389 provenance as putative Black Sea (yellow), modern (black), ancient (grey) NE Atlantic and  
 390 Mediterranean. Convex hull total areas (TA's) are shown for each sample group as dashed lines and  
 391 density distributions are shown for each isotope with significance between groups tested by non-rank  
 392 paired Wilcoxon tests. Relationships between Fork Length (FL) and isotope ratios (C,  $\delta^{13}\text{C}$ ; D,  $\delta^{15}\text{N}$   
 393 and E,  $\delta^{34}\text{S}$ ) are shown using scatterplots and a lm smooth estimated using ggplot geom\_smooth  
 394 where shading indicates 95% CI's. Relationships were tested using linear regressions after FL was  
 395 log10 transformed, where the regression coefficient ( $R^2$ ) and significance were calculated. Black Sea  
 396 regressions excluded the two 1941 Istanbul samples. Boxplots show differences in inner and outer  
 397 vertebrae sample values for ancient Black Sea samples and each isotope (C, D, E) with yellow lines  
 398 joining pairs of samples from the same specimen and significance between groups as tested by  
 399 ranked paired Wilcoxon tests. Boxplots show group means, 25<sup>th</sup> and 75<sup>th</sup> percentile as outer edges  
 400 and outliers illustrated outside of 95<sup>th</sup> percentiles (black whiskers). Significance is represented as 'ns'  
 401  $>0.05$ , '\*'  $<0.05$ , '\*\*'  $<0.01$  and '\*\*\*\*'  $<0.001$ .  
 402

402

403 Significant differences were also found between NE Atlantic and Mediterranean samples  
404 where modern samples were generally lower in  $\delta^{13}\text{C}$  ( $p < 0.001$ ) and higher in  $\delta^{34}\text{S}$  than  
405 ancient samples ( $p < 0.01$ , Figure 2C, 2E). Regressions revealed no significant relationships  
406 between  $\delta^{13}\text{C}$  and FL, though significant differences in  $\delta^{13}\text{C}$  and  $\delta^{15}\text{N}$  between inner and  
407 outer vertebrae pairs suggest the Black Sea niche is more different to NE Atlantic and  
408 Mediterranean niches at earlier than later life stages (Figure 2C, 2D). A significant positive  
409 relationship was found between  $\delta^{15}\text{N}$  and FL for modern NE Atlantic and Mediterranean  
410 samples ( $p < 0.01$ ) and between  $\delta^{34}\text{S}$  and FL for ancient NE Atlantic and Mediterranean ( $p <$   
411  $0.01$ ) and ancient Black Sea samples ( $p < 0.05$ ) whereas no significant relationship was  
412 found between  $\delta^{15}\text{N}$  and FL for ancient samples or between  $\delta^{34}\text{S}$  and FL for modern  
413 samples (Figure 2D, E).

414  
415 GAMS fitted spatial and temporal models across a wide range of sample locations. Ancient  
416 and modern sample distributions overlapped considerably, where ancient samples were  
417 mostly caught around the western and central Mediterranean (around the strait of Gibraltar  
418 and Sardinia) while modern samples the central Mediterranean (around Sicily and Sardinia  
419 but including the Adriatic Sea and off Libya) except for southwest Iceland. It is important to  
420 note that splitting data for pre- and post-16th c. inferences increased sample distribution  
421 overlap temporally. For spatial (longitude) models, distributions included Black Sea (Istanbul,  
422 Turkey) sample locations. GAMs indicated  $\delta^{13}\text{C}$  was significantly explained by longitude ( $p$   
423  $< 0.001$ , Table 2) whereby Atlantic locations and central Mediterranean and Black Sea  
424 locations had lower  $\delta^{13}\text{C}$  values than the western Mediterranean samples (Figure 3A). There  
425 was no significant relationship between  $\delta^{13}\text{C}$  or  $\delta^{15}\text{N}$  and time (year, Figure 3D, E).  $\delta^{15}\text{N}$  was  
426 significantly explained by latitude ( $p < 0.001$ ) whereby central Mediterranean locations and  
427 Black Sea locations had lower  $\delta^{15}\text{N}$  values (Figure 3B).  $\delta^{34}\text{S}$  was significantly explained by  
428 time ( $p < 0.001$ ) where post-16th c.  $\delta^{34}\text{S}$  values were greater (ca. 18-19%) than pre-16<sup>th</sup> c.  
429 values (ca. 12-18%, Figure 3F). Variation in pre-16<sup>th</sup> c.  $\delta^{34}\text{S}$  was significantly explained by  
430 longitude ( $p < 0.001$ ) where a gradient existed of decreasing  $\delta^{34}\text{S}$  with eastward  
431 Mediterranean locations (Figure 3C). However, it must be noted that  $\delta^{34}\text{S}$  and longitude  
432 trends follow those of FL and thus both factors contribute to  $\delta^{34}\text{S}$  variability in ancient  
433 samples. Predictions of GAM models (Figure S5) support that spatial and temporal factors  
434 did not co-vary and that across all temporal samples, there was no spatial relationship in  
435  $\delta^{34}\text{S}$ .

436



437  
 438  
 439  
 440  
 441  
 442  
 443  
 444  
 445  
 446  
 447  
 448  
 449  
 450  
 451  
 452  
 453  
 454  
 455  
 456

**Figure 3. Spatial and temporal relationships with isotope values explaining variation in Atlantic bluefin tuna (*Thunnus thynnus*) foraging ecology.** Relationships between isotope values and Longitude (A, B, C) or Century / Year CE (D, E, F) analysed using GAMs are illustrated as smoothed (non-linear) or non-smoothed (linear) lines of fit with 95% CI shading as calculated using the geom\_smooth function in ggplot2 with gam or lm specified, respectively. P-values are shown as estimated in GAM models where 'ns' > 0.05, '\*' < 0.05, '\*\*' < 0.01 and '\*\*\*' < 0.001. Black Sea samples were excluded from century/year lines of fit. Boxplots are shown for each BFT sample group with group means, 25<sup>th</sup> and 75<sup>th</sup> percentile as outer edges and outliers illustrated outside of 95<sup>th</sup> percentiles (black whiskers). Samples (circles) are coloured according to their provenance as putative Black Sea (yellow), modern (black) and ancient (grey) NE Atlantic and Mediterranean sample groups. Plots for each stable isotope are illustrated separately:  $\delta^{13}\text{C}$  (A, D),  $\delta^{15}\text{N}$  (B, E) and  $\delta^{34}\text{S}$  (C, F).

**Table 2.** GAM parameter estimates for BFT  $\delta^{13}\text{C}$ ,  $\delta^{15}\text{N}$  and  $\delta^{34}\text{S}$ , and variance structure of the data for the spatiotemporal models. Significant predictors are shown in boldface, judged at the 0.05 level. t/F indicates t or F statistic for each test. Results for Year are shown only for Mediterranean samples. Longitude pre/post-16<sup>th</sup> c. indicates samples pre and post 16<sup>th</sup> c. were pooled to assess the effect of latitude in both periods.

	$\delta^{13}\text{C}$			$\delta^{15}\text{N}$			$\delta^{34}\text{S}$		
Predictors	Estimate	t/F	p	Estimate	t/F	p	Estimate	t/F	p
Intercept	-13.01	-97.73	<0.001	8.44	28.45	<0.001	17.56	196.4	<0.001
Year: Mediterranean	-1.6e-4	-1.813	0.073	9.6e-5	0.482	0.63	3.99	46.81	<b>&lt;0.001</b>
Longitude	3.73	6.45	<b>&lt;0.001</b>	4.20	9.80	<b>&lt;0.001</b>			
Longitude:pre 16 <sup>th</sup> c.	-	-	-	-	-	-	1.00	46.26	<b>&lt;0.001</b>
Longitude:post 16 <sup>th</sup> c.	-	-	-	-	-	-	1.00	0.31	0.86
<b>Residual variance</b>	0.21			0.99			0.72		
<b>R<sup>2</sup></b>	0.66			0.36			0.78		
<b>Deviance explained</b>	68.0%			39.3%			78.9%		
<b>df</b>	8.11			8.52			8.39		

457

458

459

#### 4. DISCUSSION

460

461 Our results show, for the first time, that BFT increased in  $\delta^{34}\text{S}$  composition at around the 16<sup>th</sup>

462 century and that BFT which migrated to the Black Sea represented a unique component,

463 isotopically distinct from both modern and ancient BFT of the Mediterranean and NE Atlantic.

464 Low  $\delta^{13}\text{C}$ ,  $\delta^{15}\text{N}$  and  $\delta^{34}\text{S}$  values of BFT from Istanbul dating at 9-13th c. and 1941 are

465 indicative of sustained and consistent Marmara Sea and Black Sea foraging, due to the

466 hydrography of the region. One reasonably predicts that highly stratified, low surface salinity

467 waters, above an anoxic layer would result in low  $\delta^{15}\text{N}$  values due to primary nitrogen

468 fixation by phytoplankton (Fulton et al., 2012), low  $\delta^{13}\text{C}$  values due to low salinity (Magozzi

469 et al., 2017) and low  $\delta^{34}\text{S}$  where sulphate is derived from microbial sulphides in sub-oxic

470 waters (Neretin et al., 2003). These observations are unique throughout the BFT range and

471 indeed promote low  $\delta^{13}\text{C}$ ,  $\delta^{15}\text{N}$  and  $\delta^{34}\text{S}$  values at the ecosystem level in the Black Sea,

472 including in BFT prey (e.g., anchovy, *Engraulis encrasicolus*, ca. -20‰  $\delta^{13}\text{C}$ , 6‰  $\delta^{15}\text{N}$ )

473 (Bănaru et al., 2007; Çoban-Yıldız et al., 2006; Das et al., 2004; Lenin et al., 1997; Mutlu,

474 2021). Contextual  $\delta^{34}\text{S}$  isotope data from this region is limited though we theorise that



475 ancient BFT foraged on benthic-pelagic prey of Marmara, NW shelf ecosystems of the Black  
476 Sea and the Azov Sea, because BFT  $\delta^{34}\text{S}$  values were lower than the pelagic zones of  
477 these habitats (ca. 17‰, Lenin et al. (1997)). This may be explained by low  $\delta^{34}\text{S}$  being linked  
478 with neritic and benthic feeding in fishes (Cobain et al., 2022; Leakey et al., 2008; Szpak &  
479 Buckley, 2020), supporting archaeological bone finds and classical authors over millennia  
480 (Andrews, et al., 2022a; Karakulak & Oray, 2009).

481

#### 482 **4.1 BFT had an isotopically unique Black Sea niche**

483

484 Since BFT bone is likely to record multiple years of foraging behaviour (Andrews et al., in  
485 review), the observed significantly different Black Sea isotope values and low NE Atlantic  
486 and Mediterranean overlap proportions we found suggest that the majority of Black Sea BFT  
487 migrated consistently to—or were resident in—this region over multiple years for foraging while  
488 NE Atlantic and Mediterranean BFT seldomly used this region as a foraging habitat. Indeed,  
489 high-site fidelity has been reported in BFT (Block et al., 2005; Cermeño et al., 2015) but our  
490 findings would go further, supporting tagging data (De Metro et al., 2004) to suggest that  
491 current Atlantic foraging behaviours are probably not characteristic of all BFT, even at large  
492 body size (Rouyer et al., 2022).

493

494 From the 15<sup>th</sup> c., Bosphorus trap fisheries recorded BFT migrations into the Black Sea from  
495 April, with the majority believed to return to the Marmara Sea or Aegean Sea by September,  
496 due to poor winter conditions (Cort & Abaunza, 2019; Karakulak & Oray, 2009). We consider  
497 it likely that low  $\delta^{13}\text{C}$ ,  $\delta^{15}\text{N}$  and  $\delta^{34}\text{S}$  values in BFT from Istanbul were promoted by autumn  
498 or winter foraging in the Marmara or Black Sea, as predicted by early-20<sup>th</sup> c. scientists  
499 (Devedjian, 1926; Sara, 1964)—and supporting sparse catch data (Di Natale et al., 2019)—  
500 because the Aegean Sea and the Mediterranean proper are relatively high  $\delta^{13}\text{C}$   
501 environments (David Wells et al., 2021; Magozzi et al., 2017). Nonetheless, it remains  
502 challenging to assess proportions of time spent foraging in each habitat from isotope data  
503 alone. Since May-July is the spawning period for BFT in the Mediterranean, it therefore  
504 remains unknown if BFT individuals from the Black Sea skipped spawning or represented a  
505 separate spawning population (Di Natale, 2015; MacKenzie & Mariani, 2012).

506

507 Isotopic analysis of inner and outer Black Sea vertebrae samples suggests that earlier life  
508 stages (with lower  $\delta^{13}\text{C}$  and  $\delta^{15}\text{N}$ ), may have been more resident in the Black or Marmara  
509 Sea while later life stages (with higher  $\delta^{13}\text{C}$  and  $\delta^{15}\text{N}$ ) were more Mediterranean; which we  
510 theorise may indicative of increased spawning migrations to the Mediterranean with age.

511 Alternatively, our data may support spawning in the Black Sea where Mediterranean  
512 overwintering and/or foraging increased with age. There are uncertainties on reports of BFT  
513 eggs and larvae found in the Black Sea (Di Natale, 2015; Mather et al., 1995), although  
514 adaptation to spawn this low-salinity environment is possible for BFT (MacKenzie & Mariani,  
515 2012) and adults have been found in the Black Sea with ripe gonads (Di Natale, 2015).

516 Genomic analysis are required to exclude the possibility that Black Sea BFT represented a  
517 separate spawning population but since preliminary genetic results (Andrews et al., 2021)  
518 did not support this theory and juveniles have never been caught in this region (Di Natale,  
519 2015), we find it more likely that the Black Sea migration and the Marmara Sea residency  
520 was a prey-dependent, learned behaviour, as part of a collective memory, which takes time  
521 to rebuild (De Luca et al., 2014; Petitgas et al., 2010). Regardless, the return of Black Sea  
522 BFT will depend heavily on the recovery of ecosystems and trophic cascades in the  
523 Marmara Sea, Black Sea and Azov Sea, which remain poor after overexploitation (Demirel  
524 et al., 2020; Ulman et al., 2020). Climatic-cooling and the increase in alien species resulted

525 in heavy modification during the 20<sup>th</sup> c., and induced the collapse of multiple stocks  
526 (Karakulak & Oray, 2009; Oguz & Gilbert, 2007; Shiganova et al., 2001; Zaitsev, 1992).  
527 There is sparse evidence of Black Sea BFT returning (Di Natale et al., 2019), which may  
528 indicate that ecosystem recovery has begun.

529

#### 530 **4.2 Two millennia of stability in BFT trophic position**

531

532 Isotope values of BFT bone across centuries broadly reflected benthic-pelagic foraging, at  
533 moderate trophic levels ( $\delta^{15}\text{N}$ ) which increased significantly with size, supporting several  
534 studies (Estrada et al., 2005; Karakulak et al., 2009; Logan, 2009; Logan et al., 2011; Sarà &  
535 Sarà, 2007). Spatial relationships suggested that NE Atlantic and central-eastern  
536 Mediterranean fish foraged less in shelf waters, and more offshore (depleted  $^{13}\text{C}$ ); probably  
537 due to deep-diving opportunities in these locations (Battaglia et al., 2013; Olafsdottir et al.,  
538 2016; Wilson & Block, 2009), and/or their lower  $\delta^{13}\text{C}$  baselines as a result of less benthic-  
539 pelagic coupling (Magozzi et al., 2017; Pinzone et al., 2019). Spatial relationships in  $\delta^{15}\text{N}$   
540 values suggested that some Mediterranean catches, like the 2020 sample, may have  
541 resided mostly, or solely in this relatively low nitrogen environment (David Wells et al., 2021;  
542 Rafter et al., 2019). Relationships between size and  $\delta^{15}\text{N}$  in modern samples also support  
543 that smaller adults akin to 2020 catches (ca. 100-200 cm FL) may remain in the  
544 Mediterranean after spawning (Addis et al., 2016; Cermeño et al., 2015).

545

546 Lack of temporal  $\delta^{13}\text{C}$  and  $\delta^{15}\text{N}$  trends does not suggest that exploitation and climate have  
547 not shifted BFT diet and distribution over centuries—they surely have (Faillettaz et al., 2019;  
548 Fromentin et al., 2014). Perhaps more important, however, is that we found no isotopic  
549 evidence for a change in BFT trophic position across millennia despite recent ecosystem  
550 changes like exploitation restructuring fish populations to smaller individuals and  
551 predominantly depleting larger species (Baum & Worm, 2009; Pauly et al., 1998). This  
552 finding is especially striking considering that prey size has been shown to be an important  
553 driver of BFT condition (Golet et al., 2015), and that other tunas have shifted in isotope  
554 composition during the past two decades in the Atlantic (Lorrain et al., 2020). Since BFT  
555  $\delta^{15}\text{N}$  was relatively low (for predatory marine fish), we suggest that BFT is more generalist  
556 than previously thought. Highly generalist BFT foraging strategies have been hinted at  
557 recently with increasing evidence of the importance of gelatinous prey (Günther et al., 2021)  
558 which is likely to promote resilience to spatial changes in prey distribution or size, like in  
559 some marine cetaceans (Samarra et al., 2022). We acknowledge however that the presence  
560 of spatial and size relationships added noise to our dataset, which limits temporal  
561 observations. This issue may be overcome through the application of compound specific  
562 isotope analysis (CSIA) to disentangle source vs. trophic effects and confirm that despite  
563 regime shifts (Beaugrand et al., 2015; Conversi et al., 2010; Drinkwater, 2006; Siano et al.,  
564 2021; Tomasovych et al., 2020), BFT have been robust to ecosystem changes.

565

#### 566 **4.3 Early coastal degradation induced a pelagic shift in BFT**

567

568 Compared with carbon and nitrogen, sulphur offered greater sensitivity to detect temporal  
569 foraging shifts, probably due to its greater variation in benthic vs. pelagic prey (Fry et al.,  
570 1982). In BFT, we observed a novel post-16<sup>th</sup> c. shift in  $\delta^{34}\text{S}$ , to values indicative of  
571 predominantly pelagic energy sources (ca. 18-19‰, Thode (1991)) in the absence of  $\delta^{34}\text{S}$   
572 shifts at the base of marine food webs during the past two millennia (Newton & Bottrell,  
573 2007). Thus, we propose an increased preference for inshore and benthic opportunistic

574 foraging until the ~16<sup>th</sup> century, which may have reduced due to the early degradation of  
575 coastal ecosystems during this period (Hoffmann, 2005; Jackson et al., 2001). Within the  
576 Mediterranean and Black Sea, we found that  $\delta^{34}\text{S}$  declined with distance from the Atlantic.  
577 Yet, size-effects were also evident, perhaps reflecting that smaller individuals were  
578 residentary to a greater extent than larger individuals - and perhaps more so historically  
579 than today (Cermeño et al., 2015; Rouyer et al., 2022).  $\delta^{34}\text{S}$  values are relatively consistent  
580 among pelagic marine habitats worldwide (Thode, 1991), suggesting that our observation is  
581 benthic- rather than pelagic-related. Given that  $\delta^{34}\text{S}$  of benthic production (e.g., seagrass)  
582 varies spatially (Frederiksen et al., 2008), we cannot exclude that the observed  $\delta^{34}\text{S}$  shift  
583 may alternatively reflect reduced foraging locally in low  $\delta^{34}\text{S}$  Mediterranean habitats. GAM  
584 predictions nonetheless did not support this, showing a lack of a spatial relationship in  $\delta^{34}\text{S}$   
585 across all samples, while temporal patterns were indeed evident. Black Sea foraging of low  
586  $\delta^{34}\text{S}$  individuals is another unlikely explanation, given that  $\delta^{13}\text{C}$  values were consistent with  
587 higher  $\delta^{34}\text{S}$  Mediterranean individuals and unlike samples from Istanbul.

588

589 Whether BFT have shifted to forage on fewer inshore and/or benthic prey or in higher  $\delta^{34}\text{S}$   
590 habitats than previously, our observations are strongly supported by 16<sup>th</sup> c. transcripts  
591 documenting the overexploitation of BFT prey and disturbance of inshore habitats off  
592 Andalusia; specifically linking these with a lower productivity of Spanish tuna traps, which  
593 was not overcome until trap technology developed into more offshore operations (Andrews,  
594 et al., 2022a). We theorise that post-Middle Age exploitation induced an early tipping point in  
595 BFT foraging, while a second tipping point (perhaps more difficult to cross) in trophic position  
596 appears not to have been reached following more recent intensive exploitation of marine  
597 ecosystems. Today, BFT take varying degrees of benthic and sessile prey (Karakulak et al.,  
598 2009; Sarà & Sarà, 2007).

599

600 The recent dominance of invertebrates in anthropized marine ecosystems (Howarth et al.,  
601 2014) seems to contradict our novel  $\delta^{34}\text{S}$  conclusion. However, recent evidence suggests  
602 that BFT may be even more opportunistic than previously thought (Günther et al., 2021).  
603 Moreover, a similar shift in sulphur isotopes may explain differences between ancient and  
604 modern samples in the overexploited Atlantic cod (Nehlich et al., 2013), and therefore further  
605 research is required to better define the intensity of marine coastal exploitation during this  
606 period and provide baselines of modern habitat status. The  $\delta^{34}\text{S}$  shift appears to have  
607 occurred across BFT's range, as evident in the two archived specimens collected by M.  
608 Sella from Istanbul in 1941. This implies that a return of BFT to the Black Sea will not only be  
609 dependent on the re-establishment of inshore habitats.

610

#### 611 **4.4 Consequences for management and conservation**

612

613 While limited in sample size, the isotopic data presented here provide the first information on  
614 the foraging ecology of the extinct Black Sea niche of BFT, with which to guide their return.  
615 They suggest that limiting catches throughout the eastern Mediterranean may promote  
616 divergent migration strategies, even if these may have a behavioural rather than evolutionary  
617 basis. The potential need to manage Mediterranean BFT as more than one stock has been  
618 previously hinted at, in-part due to proposed Mediterranean residency of some individuals  
619 (Cermeño et al., 2015; Cort & Abaunza, 2019; De Metrio et al., 2004; Di Natale, 2019;  
620 Fromentin, 2009; Mather et al., 1995; Riccioni et al., 2010), and requires further genomic,  
621 CSIA and tagging studies. Our novel finding of a pre-industrial shift in BFT foraging

622 highlights the importance of recovering inshore habitats and benthic prey, which probably  
623 cannot be recovered to ancient levels (Atmore et al., 2021; Duarte et al., 2020), but are  
624 nonetheless likely to promote the recovery of BFT across its range. In addition, our results  
625 demonstrate the uniqueness of the isotopic niche of Black Sea BFT, which unfortunately  
626 disappeared due to exploitation, hence reducing the diversity of BFT life histories which  
627 potentially has consequences for the ability of BFT to adapt to dynamic environments. We  
628 conclude however that the inability to re-establish ancient inshore habitats should not hinder  
629 the return of BFT to the Black Sea. Instead, we find that effort should be made to recover the  
630 heavily overexploited and degraded shelf ecosystems of the Marmara Sea, Black Sea, and  
631 Azov Sea; which could promote occurrence of BFT in the region.

632

## 633 **ACKNOWLEDGEMENTS**

634

635 We thank Saadet Karakulak and Işık Oray for thoughtful discussions on Black Sea history.  
636 This work is a contribution to the <https://tunaarchaeology.org> project within the framework of  
637 the MSCA SeaChanges ITN, which was funded by EU Horizon 2020 (Grant Number:  
638 813383). Warm thanks to the two reviewers and editor whose comments improved the  
639 quality of this manuscript.

640

## 641 **AUTHOR CONTRIBUTIONS**

642

643 AJA, FT, and MA designed the study. AJA, PA, DBC, VA, VO, GC, VGF, VC and AS  
644 collected vertebrae samples for analysis. AJA, MVT, MFC, EC and AU conducted the  
645 laboratory work. AJA analysed the data. AJA, AD, FT, CP, and MA wrote the paper. All  
646 authors reviewed the paper.

647

## 648 **FUNDING INFORMATION**

649

650 This project was funded by the EU Horizon 2020 Grant Number 813383 as part of the MSCA  
651 ITN SeaChanges.

652

## 653 **CONFLICTS OF INTEREST**

654

655 No conflicts of interest exist.

656

## 657 **REFERENCES**

658

Addis, P., Secci, M., Biancacci, C., Loddo, D., Cuccu, D., Palmas, F., & Sabatini, A. (2016).

659

Reproductive status of Atlantic bluefin tuna, *Thunnus thynnus*, during migration off the coast of

660

Sardinia (western Mediterranean). *Fisheries Research*, 181, 137–147.

661

Amiriaux, R., Mundy, C. J., Pierrejean, M., Niemi, A., Hedges, K. J., Brown, T. A., Ehn, J. K., Elliott, K.

662

H., Ferguson, S. H., Fisk, A. T., Gilchrist, G., Harris, L. N., Iken, K., Jacobs, K. B., Johnson, K. F.,

663

Kuzyk, Z. A., Limoges, A., Loewen, T. N., Love, O. P., ... Yurkowski, D. J. (2023). Tracing carbon

664

flow and trophic structure of a coastal Arctic marine food web using highly branched isoprenoids

665

and carbon, nitrogen and sulfur stable isotopes. *Ecological Indicators*, 147, 109938.

666 Andrews, A.J., Orton, D., Onar, V., Addis, P., Tinti, F. and Alexander, M. (2023) Isotopic life-history  
667 signatures are retained in modern and ancient Atlantic bluefin tuna vertebrae. *Journal of Fish*  
668 *Biology. In Press. doi: 10.1111/jfb.15417.*

669 Andrews, A. J., Di Natale, A., Bernal-Casasola, D., Aniceti, V., Onar, V., Oueslati, T., Theodropoulou,  
670 T., Morales-Muñiz, A., Cilli, E., & Tinti, F. (2022a). Exploitation history of Atlantic bluefin tuna in  
671 the eastern Atlantic and Mediterranean—insights from ancient bones. *ICES Journal of Marine*  
672 *Science: Journal Du Conseil*, 79(2), 247–262.

673 Andrews, A. J., Mylona, D., Rivera-Charún, L., Winter, R., Onar, V., Siddiq, A. B., Tinti, F., & Morales-  
674 Muniz, A. (2022b). Length estimation of Atlantic bluefin tuna (*Thunnus thynnus*) using vertebrae.  
675 *International Journal of Osteoarchaeology*, 32(3), 645–653. <https://doi.org/10.1002/oa.3092>

676 Andrews, A. J., Puncher, G. N., Bernal-Casasola, D., Di Natale, A., Massari, F., Onar, V., Toker, N.  
677 Y., Hanke, A., Pavey, S. A., Savojardo, C., Martelli, P. L., Casadio, R., Cilli, E., Morales-Muñiz,  
678 A., Mantovani, B., Tinti, F., & Cariani, A. (2021). Ancient DNA SNP-panel data suggests stability  
679 in bluefin tuna genetic diversity despite centuries of fluctuating catches in the eastern Atlantic and  
680 Mediterranean. *Scientific Reports*, 11(1), 20744.

681 Atmore, L. M., Aiken, M., & Furni, F. (2021). Shifting Baselines to Thresholds: Reframing Exploitation  
682 in the Marine Environment. *Frontiers in Marine Science*, 8.  
683 <https://doi.org/10.3389/fmars.2021.742188>

684 Bănaru, D., Harmelin-Vivien, M., Gomoiu, M.-T., & Onciu, T.-M. (2007). Influence of the Danube River  
685 inputs on C and N stable isotope ratios of the Romanian coastal waters and sediment (Black  
686 Sea). *Marine Pollution Bulletin*, 54(9), 1385–1394.

687 Barnes, C., Jennings, Barry, J. T., & Simon. (2009). Environmental correlates of large-scale spatial  
688 variation in the  $\delta^{13}\text{C}$  of marine animals. *Estuarine, Coastal and Shelf Science*, 81(3), 368–374.

689 Barrett, J. H., Orton, D., Johnstone, C., Harland, J., Van Neer, W., Ervynck, A., Roberts, C., Locker,  
690 A., Amundsen, C., Enghoff, I. B., Hamilton-Dyer, S., Heinrich, D., Hufthammer, A. K., Jones, A. K.  
691 G., Jonsson, L., Makowiecki, D., Pope, P., O'Connell, T. C., de Roo, T., & Richards, M. (2011).  
692 Interpreting the expansion of sea fishing in medieval Europe using stable isotope analysis of  
693 archaeological cod bones. *Journal of Archaeological Science*, 38(7), 1516–1524.

694 Battaglia, P., Andaloro, F., Consoli, P., Esposito, V., Malara, D., Musolino, S., Pedà, C., & Romeo, T.  
695 (2013). Feeding habits of the Atlantic bluefin tuna, *Thunnus thynnus* (L. 1758), in the central  
696 Mediterranean Sea (Strait of Messina). *Helgoland Marine Research*, 67(1), 97–107.

697 Baum, J. K., & Worm, B. (2009). Cascading top-down effects of changing oceanic predator  
698 abundances. *The Journal of Animal Ecology*, 78(4), 699–714.

699 Beaugrand, G., Conversi, A., Chiba, S., Edwards, M., Fonda-Umani, S., Greene, C., Mantua, N., Otto,  
700 S. A., Reid, P. C., Stachura, M. M., Stemmann, L., & Sugisaki, H. (2015). Synchronous marine  
701 pelagic regime shifts in the Northern Hemisphere. *Philosophical Transactions of the Royal  
702 Society of London. Series B, Biological Sciences*, 370(1659), 20130272.

703 Block, B. A., Teo, S. L. H., Walli, A., Boustany, A., Stokesbury, M. J. W., Farwell, C. J., Weng, K. C.,  
704 Dewar, H., & Williams, T. D. (2005). Electronic tagging and population structure of Atlantic bluefin  
705 tuna. *Nature*, 434(7037), 1121–1127.

706 Brophy, D., Rodríguez-Ezpeleta, N., Fraile, I., & Arrizabalaga, H. (2020). Combining genetic markers  
707 with stable isotopes in otoliths reveals complexity in the stock structure of Atlantic bluefin tuna  
708 (*Thunnus thynnus*). *Scientific Reports*, 10(1), 14675.

709 Brown, T. A., Nelson, D. E., Vogel, J. S., & Southon, J. R. (1988). Improved Collagen Extraction by  
710 Modified Longin Method. *Radiocarbon*, 30(2), 171–177.

711 Butchart, S. H. M., Walpole, M., Collen, B., van Strien, A., Scharlemann, J. P. W., Almond, R. E. A.,  
712 Baillie, J. E. M., Bomhard, B., Brown, C., Bruno, J., Carpenter, K. E., Carr, G. M., Chanson, J.,  
713 Chenery, A. M., Csirke, J., Davidson, N. C., Dentener, F., Foster, M., Galli, A., ... Watson, R.  
714 (2010). Global biodiversity: indicators of recent declines. *Science*, 328(5982), 1164–1168.

715 Casini, M., Hjelm, J., Molinero, J.-C., Lövgren, J., Cardinale, M., Bartolino, V., Belgrano, A., &  
716 Kornilovs, G. (2009). Trophic cascades promote threshold-like shifts in pelagic marine  
717 ecosystems. *Proceedings of the National Academy of Sciences of the United States of America*,  
718 106(1), 197–202.

719 Caswell, B. A., Klein, E. S., Alleway, H. K., Ball, J. E., Botero, J., Cardinale, M., Eero, M., Engelhard,  
720 G. H., Fortibuoni, T., Giraldo, A.-J., Hentati-Sundberg, J., Jones, P., Kittinger, J. N., Krause, G.,  
721 Lajus, D. L., Lajus, J., Lau, S. C. Y., Lescrauwaet, A.-K., MacKenzie, B. R., ... Thurstan, R. H.  
722 (2020). Something old, something new: Historical perspectives provide lessons for blue growth  
723 agendas. *Fish and Fisheries*, 21(4), 774–796.

724 Cermeño, P., Quílez-Badia, G., Ospina-Alvarez, A., Sainz-Trápaga, S., Boustany, A. M., Seitz, A. C.,  
725 Tudela, S., & Block, B. A. (2015). Electronic tagging of Atlantic bluefin tuna (*Thunnus thynnus*, L.)  
726 reveals habitat use and behaviors in the Mediterranean Sea. *PLoS One*, 10(2), e0116638.

727 Clark, C. T., Cape, M. R., Shapley, M. D., Mueter, F. J., Finney, B. P., & Misarti, N. (2021). SuessR:  
728 Regional corrections for the effects of anthropogenic CO<sub>2</sub> on δ<sup>13</sup>C data from marine  
729 organisms. *Methods in Ecology and Evolution / British Ecological Society*, 12(8), 1508–1520.

730 Cobain, M. R. D., McGill, R. A. R., & Trueman, C. N. (2022). Stable isotopes demonstrate seasonally  
731 stable benthic-pelagic coupling as newly fixed nutrients are rapidly transferred through food  
732 chains in an estuarine fish community. *Journal of Fish Biology*. <https://doi.org/10.1111/jfb.15005>

733 Çoban-Yıldız, Y., Altabet, M. A., Yılmaz, A., & Tuğrul, S. (2006). Carbon and nitrogen isotopic ratios of  
734 suspended particulate organic matter (SPOM) in the Black Sea water column. *Deep-Sea*  
735 *Research. Part II, Topical Studies in Oceanography*, 53(17), 1875–1892.

736 Conversi, A., Fonda Umani, S., Peluso, T., Molinero, J. C., Santojanni, A., & Edwards, M. (2010). The  
737 Mediterranean Sea regime shift at the end of the 1980s, and intriguing parallelisms with other  
738 European basins. *PloS One*, 5(5), e10633.

739 Cort, J. L., & Abaunza, P. (2019). The Present State of Traps and Fisheries Research in the Strait of  
740 Gibraltar. In J. L. Cort & P. Abaunza (Eds.), *The Bluefin Tuna Fishery in the Bay of Biscay : Its*  
741 *Relationship with the Crisis of Catches of Large Specimens in the East Atlantic Fisheries from the*  
742 *1960s* (pp. 37–78). Springer International Publishing.

743 Cort, J. L., Deguara, S., Galaz, T., Mèlich, B., Artetxe, I., Arregi, I., Neilson, J., Andrushchenko, I.,  
744 Hanke, A., Neves dos Santos, M., Estruch, V., Lutcavage, M., Knapp, J., Compeán-Jiménez, G.,  
745 Solana-Sansores, R., Belmonte, A., Martínez, D., Piccinetti, C., Kimoto, A., ... Idrissi, M. (2013).  
746 Determination of L max for Atlantic Bluefin Tuna, *Thunnus thynnus* (L.), from Meta-Analysis of  
747 Published and Available Biometric Data. *Reviews in Fisheries Science*, 21(2), 181–212.

748 Das, K., Holsbeek, L., Browning, J., Siebert, U., Birkun, A., & Bouquegneau, J.-M. (2004). Trace metal  
749 and stable isotope measurements (δ<sup>13</sup>C and δ<sup>15</sup>N) in the harbour porpoise *Phocoena phocoena*  
750 *relicta* from the Black Sea. *Environmental Pollution*, 131(2), 197–204.

751 Das, S., Judd, E. J., Uveges, B. T., Ivany, L. C., & Junium, C. K. (2021). Variation in δ<sup>15</sup>N from shell-  
752 associated organic matter in bivalves: Implications for studies of modern and fossil ecosystems.  
753 *Palaeogeography, Palaeoclimatology, Palaeoecology*, 562, 110076.

754 David Wells, R. J., Rooker, J. R., Addis, P., Arrizabalaga, H., Baptista, M., Bearzi, G., Fraile, I.,  
755 Lacoue-Labarthe, T., Meese, E. N., Megalofonou, P., Rosa, R., Sobrino, I., Sykes, A. V., &  
756 Villanueva, R. (2021). Regional patterns of δ<sup>13</sup>C and δ<sup>15</sup>N for European common cuttlefish

757 (*Sepia officinalis*) throughout the Northeast Atlantic Ocean and Mediterranean Sea. *Royal Society*  
758 *Open Science*, 8(9), 210345.

759 De Luca, G., Mariani, P., MacKenzie, B. R., & Marsili, M. (2014). Fishing out collective memory of  
760 migratory schools. *Journal of the Royal Society, Interface / the Royal Society*, 11(95), 20140043.

761 De Metrio, G., Oray, I., Arnold, G. P., Lutcavage, M., Deflorio, M., Cort, J. L., Karakulak, S., Anbar, N.,  
762 & Ultanur, M. (2004). Joint Turkish-Italian research in the Eastern Mediterranean: bluefin tuna  
763 tagging with pop-up satellite tags. *Col. Vol. Sci. Pap. ICCAT*, 56(3), 1163–1167.

764 Demirel, N., Zengin, M., & Ulman, A. (2020). *First Large-Scale Eastern Mediterranean and Black Sea*  
765 *Stock Assessment Reveals a Dramatic Decline*. 7. <https://doi.org/10.3389/fmars.2020.00103>

766 DeNiro, M. J., & Epstein, S. (1978). Influence of diet on the distribution of carbon isotopes in animals.  
767 *Geochimica et Cosmochimica Acta*, 42(5), 495–506.

768 Devedjian, K. (1926). *Pêche et pêcheries en Turquie*. Imprimerie de l'Administration de la Dette  
769 Publique Ottomane.

770 Dickhut, R. M., Deshpande, A. D., Cincinelli, A., Cochran, M. A., Corsolini, S., Brill, R. W., Secor, D.  
771 H., & Graves, J. E. (2009). Atlantic bluefin tuna (*Thunnus thynnus*) population dynamics  
772 delineated by organochlorine tracers. *Environmental Science & Technology*, 43(22), 8522–8527.

773 Di Natale, A. (2015). Review of the historical and biological evidences about a population of bluefin  
774 tuna (*Thunnus thynnus* L.) in The Eastern Mediterranean and the black sea. *Col. Vol. Sci. Pap.*  
775 *ICCAT*, 71(3), 1098–1124.

776 Di Natale, A. (2019). Due to the new scientific knowledge, it it time to reconsider the stock  
777 composition of Atlantic bluefin tuna? *Col. Vol. Sci. Pap. ICCAT*, 75(6), 1282–1292.

778 Di Natale, A., Tensek, S., & García, A. P. (2019). Is the bluefin tuna slowly returning to the Black Sea?  
779 Recent evidences. *Col. Vol. Sci. Pap. ICCAT*, 75, 1261–1277.

780 Drinkwater, K. F. (2006). The regime shift of the 1920s and 1930s in the North Atlantic. *Progress in*  
781 *Oceanography*, 68(2), 134–151.

782 Druon, J.-N., Fromentin, J.-M., Hanke, A. R., Arrizabalaga, H., Damalas, D., Tičina, V., Quílez-Badía,  
783 G., Ramirez, K., Arregui, I., Tserpes, G., Reglero, P., Deflorio, M., Oray, I., Saadet Karakulak, F.,  
784 Megalofonou, P., Ceyhan, T., Grubišić, L., MacKenzie, B. R., Lamkin, J., ... Addis, P. (2016).  
785 Habitat suitability of the Atlantic bluefin tuna by size class: An ecological niche approach.  
786 *Progress in Oceanography*, 142, 30–46.



787 Duarte, C. M., Agusti, S., Barbier, E., Britten, G. L., Castilla, J. C., Gattuso, J.-P., Fulweiler, R. W.,  
788 Hughes, T. P., Knowlton, N., Lovelock, C. E., Lotze, H. K., Predragovic, M., Poloczanska, E.,  
789 Roberts, C., & Worm, B. (2020). Rebuilding marine life. *Nature*, 580(7801), 39–51.

790 Eide, M., Olsen, A., Ninnemann, U. S., & Eldevik, T. (2017). A global estimate of the full oceanic 13 C  
791 Suess effect since the preindustrial: Full Oceanic 13 C Suess Effect. *Global Biogeochemical*  
792 *Cycles*, 31(3), 492–514.

793 Engelhard, G. H., Thurstan, R. H., MacKenzie, B. R., Alleway, H. K., Bannister, R. C. A., Cardinale,  
794 M., Clarke, M. W., Currie, J. C., Fortibuoni, T., Holm, P., Holt, S. J., Mazzoldi, C., Pinnegar, J. K.,  
795 Raicevich, S., Volckaert, F. A. M., Klein, E. S., & Lescauwaet, A.-K. (2015). ICES meets marine  
796 historical ecology: placing the history of fish and fisheries in current policy context. *ICES Journal*  
797 *of Marine Science: Journal Du Conseil*, 73(5), 1386–1403.

798 Estrada, J. A., Lutcavage, M., & Thorrold, S. R. (2005). Diet and trophic position of Atlantic bluefin  
799 tuna (*Thunnus thynnus*) inferred from stable carbon and nitrogen isotope analysis. *Marine*  
800 *Biology*, 147(1), 37–45.

801 Faillettaz, R., Beaugrand, G., Goberville, E., & Kirby, R. R. (2019). Atlantic Multidecadal Oscillations  
802 drive the basin-scale distribution of Atlantic bluefin tuna. *Science Advances*, 5(1), eaar6993.

803 Frederiksen, M. S., Holmer, M., Pérez, M., Invers, O., Ruiz, J. M., & Knudsen, B. B. (2008). Effect of  
804 increased sediment sulfide concentrations on the composition of stable sulfur isotopes ( $\delta^{34}\text{S}$ )  
805 and sulfur accumulation in the seagrasses *Zostera marina* and *Posidonia oceanica*. *Journal of*  
806 *Experimental Marine Biology and Ecology*, 358(1), 98–109.

807 Fromentin, J.-M. (2009). Lessons from the past: investigating historical data from bluefin tuna  
808 fisheries. *Fish and Fisheries*, 10(2), 197–216.

809 Fromentin, J.-M., Reygondeau, G., Bonhommeau, S., & Beaugrand, G. (2014). Oceanographic  
810 changes and exploitation drive the spatio-temporal dynamics of Atlantic bluefin tuna (*Thunnus*  
811 *thynnus*). *Fisheries Oceanography*, 23(2), 147–156.

812 Fry, B., & Chumchal, M. M. (2011). Sulfur stable isotope indicators of residency in estuarine fish.  
813 *Limnology and Oceanography*, 56(5), 1563–1576.

814 Fry, B., Scalan, R. S., Winters, J. K., & Parker, P. L. (1982). Sulphur uptake by salt grasses,  
815 mangroves, and seagrasses in anaerobic sediments. *Geochimica et Cosmochimica Acta*, 46(6),  
816 1121–1124.

817 Fulton, J. M., Arthur, M. A., & Freeman, K. H. (2012). Black Sea nitrogen cycling and the preservation  
818 of phytoplankton  $\delta^{15}\text{N}$  signals during the Holocene. *Global Biogeochemical Cycles*, 26(2).  
819 <https://doi.org/10.1029/2011GB004196>

820 Golet, W. J., Record, N. R., Lehuta, S., Lutcavage, M., Galuardi, B., Cooper, A. B., & Pershing, A. J.  
821 (2015). The paradox of the pelagics: why bluefin tuna can go hungry in a sea of plenty. *Marine*  
822 *Ecology Progress Series*, 527, 181–192.

823 Gruber, N., Keeling, C. D., Bacastow, R. B., Guenther, P. R., Lueker, T. J., Wahlen, M., Meijer, H. A.  
824 J., Mook, W. G., & Stocker, T. F. (1999). Spatiotemporal patterns of carbon-13 in the global  
825 surface oceans and the oceanic suess effect. *Global Biogeochemical Cycles*, 13(2), 307–335.

826 Guiry, E.J. (2019). Complexities of Stable Carbon and Nitrogen Isotope Biogeochemistry in Ancient  
827 Freshwater Ecosystems: Implications for the Study of Past Subsistence and Environmental  
828 Change. *Frontiers in Ecology and Evolution*, 7, 313.

829 Guiry, E. J., Needs-Howarth, S., Friedland, K. D., Hawkins, A. L., Szpak, P., Macdonald, R.,  
830 Courtemanche, M., Holm, E., & Richards, M. P. (2016). Lake Ontario salmon (*Salmo salar*) were  
831 not migratory: A long-standing historical debate solved through stable isotope analysis. *Scientific*  
832 *Reports*, 6, 36249.

833 Guiry, E. J., Orchard, T. J., Needs-Howarth, S., & Szpak, P. (2022). Freshwater wetland–driven  
834 variation in sulfur isotope compositions: Implications for human paleodiet and ecological  
835 research. *Frontiers in Ecology and Evolution*, 10, 1207. <https://doi.org/10.3389/fevo.2022.953042>

836 Guiry, E. J., & Szpak, P. (2020). Quality control for modern bone collagen stable carbon and nitrogen  
837 isotope measurements. *Methods in Ecology and Evolution / British Ecological Society*, 11(9),  
838 1049–1060.

839 Guiry, E. J., & Szpak, P. (2021). Improved quality control criteria for stable carbon and nitrogen  
840 isotope measurements of ancient bone collagen. *Journal of Archaeological Science*, 132,  
841 105416.

842 Günther, B., Fromentin, J.-M., Metral, L., & Arnaud-Haond, S. (2021). Metabarcoding confirms the  
843 opportunistic foraging behaviour of Atlantic bluefin tuna and reveals the importance of gelatinous  
844 prey. *PeerJ*, 9, e11757.

845 Hilborn, R., Amoroso, R. O., Bogazzi, E., Jensen, O. P., Parma, A. M., Szuwalski, C., & Walters, C. J.  
846 (2017). When does fishing forage species affect their predators? *Fisheries Research*, 191, 211–

847 221.

848 Hilton, G. M., Thompson, D. R., Sagar, P. M., Cuthbert, R. J., Cherel, Y., & Bury, S. J. (2006). A  
849 stable isotopic investigation into the causes of decline in a sub-Antarctic predator, the rockhopper  
850 penguin *Eudyptes chrysocome*. *Global Change Biology*, 12(4), 611–625.

851 Hoffmann, R. C. (2005). A brief history of aquatic resource use in medieval Europe. *Helgoland Marine*  
852 *Research*, 59(1), 22–30.

853 Howarth, L. M., Roberts, C. M., Thurstan, R. H., & Stewart, B. D. (2014). The unintended  
854 consequences of simplifying the sea: making the case for complexity. *Fish and Fisheries*, 15(4),  
855 690–711.

856 Hutchinson, J. J., & Trueman, C. N. (2006). Stable isotope analyses of collagen in fish scales:  
857 limitations set by scale architecture. *Journal of Fish Biology*, 69(6), 1874–1880.

858 ICCAT. (2020). Report of the 2020 second ICCAT intersessional meeting of the bluefin tuna species  
859 group. Online, 20-28 July 2020. *Second BFT Intersessional Meeting - Online 2020*.  
860 [https://www.iccat.int/Documents/Meetings/Docs/2020/REPORTS/2020\\_2\\_BFT\\_ENG.pdf](https://www.iccat.int/Documents/Meetings/Docs/2020/REPORTS/2020_2_BFT_ENG.pdf)

861 Jackson, J. B., Kirby, M. X., Berger, W. H., Bjorndal, K. A., Botsford, L. W., Bourque, B. J., Bradbury,  
862 R. H., Cooke, R., Erlandson, J., Estes, J. A., Hughes, T. P., Kidwell, S., Lange, C. B., Lenihan, H.  
863 S., Pandolfi, J. M., Peterson, C. H., Steneck, R. S., Tegner, M. J., & Warner, R. R. (2001).  
864 Historical overfishing and the recent collapse of coastal ecosystems. *Science*, 293(5530), 629–  
865 637.

866 Jardine, T. D., Hadwen, W. L., Hamilton, S. K., Hladyz, S., Mitrovic, S. M., Kidd, K. A., Tsoi, W. Y.,  
867 Spears, M., Westhorpe, D. P., Fry, V. M., Sheldon, F., & Bunn, S. E. (2014). Understanding and  
868 overcoming baseline isotopic variability in running waters. *River Research and Applications*,  
869 30(2), 155–165.

870 Jennings, S. (2005). Size-based analyses of aquatic food webs. In *Aquatic Food Webs*, Belgrano, A.,  
871 Scharler, U.M., Dunne, J. and Ulanowicz, R.E. (Eds.), Oxford University Press. (pp. 86–97).  
872 <https://doi.org/10.1093/acprof:oso/9780198564836.003.0009>

873 Jennings, S., Barnes, C., & Sweeting, C. J. (2008). Application of nitrogen stable isotope analysis in  
874 size-based marine food web and macroecological research. *Rapid Communications in Mass*  
875 *Spectrometry*, 22(11), 1673–1680. <https://doi.org/10.1002/rcm.3497>

876 Karakulak, F. S., & Oray, I. K. (2009). Remarks on the fluctuations of bluefin tuna catches in Turkish

877 waters. *Col. Vol. Sci. Pap. ICCAT.*, 63, 153–160.

878 Karakulak, F. S., Salman, A., & Oray, I. K. (2009). Diet composition of bluefin tuna (*Thunnus thynnus*  
879 L. 1758) in the Eastern Mediterranean Sea, Turkey. *Journal of Applied Ichthyology*, 25(6), 757–  
880 761.

881 Karakulak, F. S., & yıldız, T. (2016). Bluefin Tuna Fishery In the Sea of Marmara. In *The Sea of*  
882 *Marmara Marine Biodiversity, Fisheries, Conservation and Governance*. Özsoy, E., Cagatay, M.,  
883 Balkis, N., Balkis, N., Öztürk, B. (Eds.), Publication no. 42, Turkish Marine Research Foundation  
884 (TÜDAV), Istanbul, Turkey.

885 Kragten, J. (1994). Tutorial review. Calculating standard deviations and confidence intervals with a  
886 universally applicable spreadsheet technique. *The Analyst*, 119(10), 2161–2165.

887 Leakey, C. D. B., Attrill, M. J., Jennings, S., & Fitzsimons, M. F. (2008). Stable isotopes in juvenile  
888 marine fishes and their invertebrate prey from the Thames Estuary, UK, and adjacent coastal  
889 regions. *Estuarine, Coastal and Shelf Science*, 77(3), 513–522.

890 Lenin, A. Y., Pimenov, N. V., Rysanov, I. I., Miller, Y. M., & Ivanov, M. V. (1997). Geochemical  
891 consequences of microbiological processes on the northwestern Black sea shelf. *Geokhimiya*,  
892 985–1004.

893 Llorente-Rodríguez, L., Craig, O. E., Colonese, A. C., Tersch, M., Roselló-Izquierdo, E., González  
894 Gómez de Agüero, E., Fernández-Rodríguez, C., Quirós-Castillo, J. A., López-Arias, B.,  
895 Marlasca-Martín, R., Nottingham, J., & Morales Muñiz, A. (2022). Elucidating historical fisheries'  
896 networks in the Iberian Peninsula using stable isotopes. *Fish and Fisheries*, 23(4), 862–873.  
897 <https://doi.org/10.1111/faf.12655>

898 Logan, J. M. (2009). *Tracking diet and movement of Atlantic bluefin tuna (Thunnus thynnus) using*  
899 *carbon and nitrogen stable isotopes. Doctoral Thesis*, University of New Hampshire, Durham,  
900 USA. <https://core.ac.uk/download/pdf/215517272.pdf>

901 Logan, J. M., Rodríguez-Marín, E., Goñi, N., Barreiro, S., Arrizabalaga, H., Golet, W., & Lutcavage, M.  
902 (2011). Diet of young Atlantic bluefin tuna (*Thunnus thynnus*) in eastern and western Atlantic  
903 foraging grounds. *Marine Biology*, 158(1), 73–85.

904 Longin, R. (1971). New method of collagen extraction for radiocarbon dating. *Nature*, 230(5291), 241–  
905 242.

906 Lorrain, A., Pethybridge, H., Cassar, N., Receveur, A., Allain, V., Bodin, N., Bopp, L., Choy, C. A.,

907 Duffy, L., Fry, B., Goñi, N., Graham, B. S., Hobday, A. J., Logan, J. M., Ménard, F., Menkes, C.  
908 E., Olson, R. J., Pagendam, D. E., Point, D., ... Young, J. W. (2020). Trends in tuna carbon  
909 isotopes suggest global changes in pelagic phytoplankton communities. *Global Change Biology*,  
910 26(2), 458–470.

911 Lotze, H. K., Hoffmann, R., & Erlandson, J. (2014). Lessons from historical ecology and management.  
912 In *The Sea, Volume 19: Ecosystem-Based Management*, Fogarty, M and McCarthy, J.J. (Eds.),  
913 Harvard University Press, USA.

914 MacKenzie, B. R., & Mariani, P. (2012). Spawning of bluefin tuna in the Black Sea: historical  
915 evidence, environmental constraints and population plasticity. *PLoS One*, 7(7), e39998.

916 MacKenzie, B. R., Mosegaard, H., & Rosenberg, A. A. (2009). Impending collapse of bluefin tuna in  
917 the northeast Atlantic and Mediterranean. *Conservation Letters*, 2(1), 26–35.

918 Magozzi, S., Yool, A., Vander Zanden, H. B., Wunder, M. B., & Trueman, C. N. (2017). Using ocean  
919 models to predict spatial and temporal variation in marine carbon isotopes. *Ecosphere*, 8(5),  
920 e01763.

921 Mariani, P., Křivan, V., MacKenzie, B. R., & Mullon, C. (2016). The migration game in habitat network:  
922 the case of tuna. *Theoretical Ecology*, 9(2), 219–232.

923 Mather, F. J., Mason, J. M., & Jones, A. C. (1995). *Historical document: life history and fisheries of*  
924 *Atlantic bluefin tuna*. NOAA Technical Memorandum NMFS-SEFSC-370. National Oceanic and  
925 Atmospheric Administration, USA (pp.165).  
926 [https://repository.library.noaa.gov/view/noaa/8461/noaa\\_8461\\_DS1.pdf](https://repository.library.noaa.gov/view/noaa/8461/noaa_8461_DS1.pdf)

927 Misarti, N., Finney, B., Maschner, H., & Wooller, M. J. (2009). Changes in northeast Pacific marine  
928 ecosystems over the last 4500 years: evidence from stable isotope analysis of bone collagen  
929 from archeological middens. *Holocene*, 19(8), 1139–1151.

930 Mutlu, T. (2021). Stable C and N Isotope Composition of European Anchovy, *Engraulis encrasicolus*,  
931 from the Marmara Sea and the Black Sea. *Turkish Journal of Agriculture - Food Science and*  
932 *Technology*, 9(6), 1087–1091.

933 Nakazawa, T., Sakai, Y., Hsieh, C.-H., Koitabashi, T., Tayasu, I., Yamamura, N., & Okuda, N. (2010).  
934 Is the relationship between body size and trophic niche position time-invariant in a predatory fish?  
935 First stable isotope evidence. *PLoS One*, 5(2), e9120.

936 Nehlich, O., Barrett, J. H., & Richards, M. P. (2013). Spatial variability in sulphur isotope values of

937 archaeological and modern cod (*Gadus morhua*). *Rapid Communications in Mass Spectrometry:*  
938 *RCM*, 27(20), 2255–2262.

939 Nehlich, O., & Richards, M. P. (2009). Establishing collagen quality criteria for sulphur isotope  
940 analysis of archaeological bone collagen. *Archaeological and Anthropological Sciences*, 1(1), 59–  
941 75.

942 Neretin, L. N., Böttcher, M. E., & Grinenko, V. A. (2003). Sulfur isotope geochemistry of the Black Sea  
943 water column. *Chemical Geology*, 200(1), 59–69.

944 Newton, R., & Bottrell, S. (2007). Stable isotopes of carbon and sulphur as indicators of environmental  
945 change: past and present. *Journal of the Geological Society*, 164(4), 691–708.

946 Oguz, T., & Gilbert, D. (2007). Abrupt transitions of the top-down controlled Black Sea pelagic  
947 ecosystem during 1960–2000: evidence for regime-shifts under strong fishery exploitation and  
948 nutrient enrichment modulated by climate-induced variations. *Deep Sea Research Part I:*  
949 *Oceanographic Research Papers*, 54(2), 220–242.

950 Olafsdottir, D., MacKenzie, B. R., Chosson-P, V., & Ingimundardottir, T. (2016). Dietary Evidence of  
951 Mesopelagic and Pelagic Foraging by Atlantic Bluefin Tuna (*Thunnus thynnus* L.) during Autumn  
952 Migrations to the Iceland Basin. *Frontiers in Marine Science*, 3.  
953 <https://doi.org/10.3389/fmars.2016.00108>

954 Ólafsdóttir, G. Á., Edvardsson, R., Timsic, S., Harrison, R., & Patterson, W. P. (2021). A millennium of  
955 trophic stability in Atlantic cod (*Gadus morhua*): transition to a lower and converging trophic niche  
956 in modern times. *Scientific Reports*, 11(1), 12681.

957 Pauly, D., Christensen, V., V., Dalsgaard, J., Froese, R., & Torres, F., Jr. (1998). Fishing down marine  
958 food webs. *Science*, 279(5352), 860–863.

959 Petitgas, P., Secor, D. H., McQuinn, I., Huse, G., & Lo, N. (2010). Stock collapses and their recovery:  
960 mechanisms that establish and maintain life-cycle closure in space and time. *ICES Journal of*  
961 *Marine Science: Journal Du Conseil*, 67(9), 1841–1848.

962 Piccinetti, C., Di Natale, A., & Arena, P. (2013). Eastern bluefin tuna (*Thunnus thynnus*, L.)  
963 reproduction and reproductive areas and season. *Col. Vol. Sci. Pap. ICCAT*, 69(2), 891–912.

964 Pinzone, M., Damseaux, F., Michel, L. N., & Das, K. (2019). Stable isotope ratios of carbon, nitrogen  
965 and sulphur and mercury concentrations as descriptors of trophic ecology and contamination  
966 sources of Mediterranean whales. *Chemosphere*, 237, 124448.

967 Planque, B., Fromentin, J.-M., Cury, P., Drinkwater, K. F., Jennings, S., Perry, R. I., & Kifani, S.  
968 (2010). How does fishing alter marine populations and ecosystems sensitivity to climate? *Journal*  
969 *of Marine Systems*, 79(3), 403–417.

970 Porch, C. E., Bonhommeau, S., Diaz, G. A., Haritz, A., & Melvin, G. (2019). The journey from  
971 overfishing to sustainability for Atlantic bluefin tuna, *Thunnus thynnus*. *The Future of Bluefin*  
972 *Tunas: Ecology, Fisheries Management, and Conservation*, 3–44.

973 Puncher, G. N., Cariani, A., Maes, G. E., Van Houdt, J., Herten, K., Cannas, R., Rodriguez-Ezpeleta,  
974 N., Albaina, A., Estonba, A., Lutcavage, M., Hanke, A., Rooker, J., Franks, J. S., Quattro, J. M.,  
975 Basilone, G., Fraile, I., Laconcha, U., Goñi, N., Kimoto, A., ... Tinti, F. (2018). Spatial dynamics  
976 and mixing of bluefin tuna in the Atlantic Ocean and Mediterranean Sea revealed using next-  
977 generation sequencing. *Molecular Ecology Resources*, 18(3), 620–638.

978 Quay, P., Sonnerup, R., Westby, T., Stutsman, J., & McNichol, A. (2003). Changes in the  $^{13}\text{C}/^{12}\text{C}$  of  
979 dissolved inorganic carbon in the ocean as a tracer of anthropogenic  $\text{CO}_2$  uptake. *Global*  
980 *Biogeochemical Cycles*, 17(1), 4–20.

981 Rafter, P. A., Bagnell, A., Marconi, D., & DeVries, T. (2019). Global trends in marine nitrate N isotopes  
982 from observations and a neural network-based climatology. *Biogeosciences*, 16(13), 2617–2633.

983 Riccioni, G., Landi, M., Ferrara, G., Milano, I., Cariani, A., Zane, L., Sella, M., Barbujani, G., & Tinti, F.  
984 (2010). Spatio-temporal population structuring and genetic diversity retention in depleted Atlantic  
985 Bluefin tuna of the Mediterranean Sea. *Proceedings of the National Academy of Sciences*,  
986 107(5), 2102–2107. <https://doi.org/10.1073/pnas.0908281107>

987 Richardson, D. E., Marancik, K. E., Guyon, J. R., Lutcavage, M. E., Galuardi, B., Lam, C. H., Walsh,  
988 H. J., Wildes, S., Yates, D. A., & Hare, J. A. (2016). Discovery of a spawning ground reveals  
989 diverse migration strategies in Atlantic bluefin tuna (*Thunnus thynnus*). *Proceedings of the*  
990 *National Academy of Sciences of the United States of America*, 113(12), 3299–3304.

991 Rodríguez-Ezpeleta, N., Díaz-Arce, N., Walter, J. F., III, Richardson, D. E., Rooker, J. R., Nøttestad,  
992 L., Hanke, A. R., Franks, J. S., Deguara, S., Laretta, M. V., Addis, P., Varela, J. L., Fraile, I.,  
993 Goñi, N., Abid, N., Alemany, F., Oray, I. K., Quattro, J. M., Sow, F. N., ... Arrizabalaga, H. (2019).  
994 Determining natal origin for improved management of Atlantic bluefin tuna. *Frontiers in Ecology*  
995 *and the Environment*, 17(8), 439–444.

996 Rooker, J. R., Secor, D. H., DeMetrio, G., Kaufman, A. J., Belmonte Ríos, A., & Ticina, V. (2008).

997 Evidence of trans-Atlantic movement and natal homing of bluefin tuna from stable isotopes in  
998 otoliths. *Marine Ecology Progress Series*, 368, 231–239.

999 Rouyer, T., Bernard, S., Kerzerho, V., Giordano, N., Giordano, F., Ellul, S., Ellul, G., Derridj, O.,  
1000 Canet, R., Deguara, S., Wendling, B., & Bonhommeau, S. (2022). Electronic tagging of Bluefin  
1001 Tunas from the Maltese spawning ground suggests size-dependent migration dynamics.  
1002 *Environmental Biology of Fishes*, 105(5), 635–644.

1003 R Team, Core. (2013). R development core team. *RA Lang Environ Stat Comput*, 55, 275–286.

1004 Rumolo, P., Bonanno, A., Genovese, S., Romeo, T., Mazzola, S., Basilone, G., Gherardi, S.,  
1005 Battaglia, P., Andaloro, F., & Barra, M. (2020). Growth-related trophic changes of *Thunnus*  
1006 *thynnus* as evidenced by stable nitrogen isotopic values in the first dorsal spine. *Scientific*  
1007 *Reports*, 10(1), 9899.

1008 Samarra, F. I. P., Borrell, A., Selbmann, A., Halldórson, S. D., Pampoulie, C., Chosson, V.,  
1009 Gunnlaugsson, T., Sigurðsson, G. M., Aguilar, A., & Víkingsson, G. A. (2022). Insights into the  
1010 trophic ecology of white-beaked dolphins *Lagenorhynchus albirostris* and harbour porpoises  
1011 *Phocoena phocoena* in Iceland. *Marine Ecology Progress Series*, 702, 139–152.

1012 Sarà, G., & Sarà, R. (2007). Feeding habits and trophic levels of bluefin tuna *Thunnus thynnus* of  
1013 different size classes in the Mediterranean Sea. *Journal of Applied Ichthyology*, 23(2), 122–127.

1014 Sara, R. (1964). Données, observations et commentaires sur la présence, le comportement, les  
1015 caractéristiques et les migrations des thons en Méditerranée. *Proc. Gen Fish. Coun. Medit. FAO*  
1016 *Débats et Documents*, 37(7), 371–388.

1017 Sayle, K. L., Brodie, C. R., Cook, G. T., & Hamilton, W. D. (2019). Sequential measurement of  $\delta^{15}\text{N}$ ,  
1018  $\delta^{13}\text{C}$  and  $\delta^{34}\text{S}$  values in archaeological bone collagen at the Scottish Universities  
1019 Environmental Research Centre (SUERC): A new analytical frontier. *Rapid Communications in*  
1020 *Mass Spectrometry: RCM*, 33(15), 1258–1266.

1021 Schwerdtner Máñez, K., Holm, P., Blight, L., Coll, M., MacDiarmid, A., Ojaveer, H., Poulsen, B., &  
1022 Tull, M. (2014). The future of the oceans past: towards a global marine historical research  
1023 initiative. *PloS One*, 9(7), e101466.

1024 Shiganova, T., Mirzoyan, Z., Studenikina, E., Volovik, S., Siokou-Frangou, I., Zervoudaki, S., Christou,  
1025 E., Skirta, A., & Dumont, H. (2001). Population development of the invader ctenophore  
1026 *Mnemiopsis leidyi*, in the Black Sea and in other seas of the Mediterranean basin. *Marine*



- 1027 *Biology*, 139(3), 431–445.
- 1028 Siano, R., Lassudrie, M., Cuzin, P., Briant, N., Loizeau, V., Schmidt, S., Ehrhold, A., Mertens, K. N.,  
1029 Lambert, C., Quintric, L., Noël, C., Latimier, M., Quéré, J., Durand, P., & Penaud, A. (2021).  
1030 Sediment archives reveal irreversible shifts in plankton communities after World War II and  
1031 agricultural pollution. *Current Biology*, 31(12), 2682–2689.e7.
- 1032 Sigman, D. M., Karsh, K. L., & Casciotti, K. L. (2009). Nitrogen Isotopes in the Ocean. *Encyclopedia*  
1033 *of Ocean Sciences*. 2009, pp. 40–54, <https://doi.org/10.1016/b978-012374473-9.00632-9>
- 1034 Solomon, C. T., Carpenter, S. R., Rusak, J. A., & Vander Zanden, M. J. (2008). Long-term variation in  
1035 isotopic baselines and implications for estimating consumer trophic niches. *Canadian Journal of*  
1036 *Fisheries and Aquatic Sciences*, 65(10), 2191–2200.
- 1037 Swanson, H. K., Lysy, M., Power, M., Stasko, A. D., Johnson, J. D., & Reist, J. D. (2015). A new  
1038 probabilistic method for quantifying n-dimensional ecological niches and niche overlap. *Ecology*,  
1039 96(2), 318–324.
- 1040 Szpak, P., & Buckley, M. (2020). Sulfur isotopes ( $\delta^{34}\text{S}$ ) in Arctic marine mammals: indicators of  
1041 benthic vs. pelagic foraging. *Marine Ecology Progress Series*, 653, 205–216.
- 1042 Thode, H. G. (1991). Sulphur isotopes in nature and the environment: An overview. In H. R. Krouse &  
1043 V. A. Grinenko (Eds.), *Stable Isotopes in the Assessment of Natural and Anthropogenic Sulphur*  
1044 *in the Environment*.
- 1045 Tomasovych, A., Albano, P., Fuksi, T., Gallmetzer, I., Haselmair, A., Kowalewski, M., Nawrot, R.,  
1046 Nerlovic, V., Scarponi, D., & Zuschin, M. (2020). *Data from: Ecological regime shift preserved in*  
1047 *the Anthropocene stratigraphic record Proceedings of the Royal Society B*, 287(1929),  
1048 p.20200695.
- 1049 Ulman, A., Zengin, M., Demirel, N., & Pauly, D. (2020). The Lost Fish of Turkey: A Recent History of  
1050 Disappeared Species and Commercial Fishery Extinctions for the Turkish Marmara and Black  
1051 Seas. *Frontiers in Marine Science*, 7. <https://doi.org/10.3389/fmars.2020.00650>
- 1052 Walli, A., Teo, S. L. H., Boustany, A., Farwell, C. J., Williams, T., Dewar, H., Prince, E., & Block, B. A.  
1053 (2009). Seasonal movements, aggregations and diving behavior of Atlantic bluefin tuna (*Thunnus*  
1054 *thynnus*) revealed with archival tags. *PloS One*, 4(7), e6151.
- 1055 Wilson, S. G., & Block, B. A. (2009). Habitat use in Atlantic bluefin tuna *Thunnus thynnus* inferred  
1056 from diving behavior. *Endangered Species Research*, 10, 355–367.

- 1057 Wood, S. (2012). *mgcv: Mixed GAM Computation Vehicle with GCV/AIC/REML smoothness*  
1058 *estimation*. [https://researchportal.bath.ac.uk/en/publications/mgcv-mixed-gam-computation-](https://researchportal.bath.ac.uk/en/publications/mgcv-mixed-gam-computation-vehicle-with-gcvaicreml-smoothness-est)  
1059 [vehicle-with-gcvaicreml-smoothness-est](https://researchportal.bath.ac.uk/en/publications/mgcv-mixed-gam-computation-vehicle-with-gcvaicreml-smoothness-est)
- 1060 Worm, B., & Tittensor, D. P. (2011). Range contraction in large pelagic predators. *Proceedings of the*  
1061 *National Academy of Sciences of the United States of America*, 108(29), 11942–11947.
- 1062 Zaitsev, Y. U. P. (1992). Recent changes in the trophic structure of the Black Sea. *Fisheries*  
1063 *Oceanography*, 1(2), 180–189.
- 1064 Zuur, A. F., Ieno, E. N., Walker, N., Saveliev, A. A., & Smith, G. M. (2009). *Mixed effects models and*  
1065 *extensions in ecology with R*. Springer, New York, USA.

# 1 **Supplementary Materials**

2

## 3 **Exploitation shifted trophic ecology and habitat preferences of Mediterranean** 4 **and Black Sea bluefin tuna over centuries**

5 Adam J. Andrews, Piero Addis, Darío Bernal-Casasola, Antonio Di Natale, Veronica Aniceti, Gabriele  
6 Carenti, Verónica Gómez-Fernández, Valerie Chosson, Christophe Pampoulie, Alice Ughi, Matt Von  
7 Tersch, Maria Fontanals-Coll, Elisabetta Cilli, Vedat Onar, Fausto Tinti, Michelle Alexander

8

9

10 *Archaeological and Archival sample details*

11

### 12 **1911-1941 CE Central Mediterranean Tonnare**

13 We analysed specimens collected from four locations in the early 20<sup>th</sup> century by the  
14 ecologist Massimo Sella (see Riccioni et al., 2010). All specimens consist of vertebrae that  
15 were air-dried by the collector after capture and processing at tuna traps (Tonnare). A total  
16 of seven samples were obtained from BFT vertebrae that were captured in the 1911 tonnara  
17 at Pizzo (Vibo Valentia, Italy), in the Tyrrhenian Sea. These samples were pooled for  
18 analysis with seven further BFT vertebrae samples that were caught in 1911 tuna traps in  
19 the Adriatic Sea off Istria / modern day Croatia, because initial analysis noted non-significant  
20 differences between the two sample sites. The pooled 1911 sample group is estimated to  
21 represent BFT between 88-152 cm FL, average 118 cm FL. A total of ten samples were  
22 obtained from BFT vertebrae captured in the tonnara at Zilten, Libya (Ionian Sea) in 1925,  
23 estimated to represent BFT between 158-204 cm FL, average 182 cm FL. Lastly, two large  
24 (275 and 278 cm FL, fork length) specimens were sampled that originated from tuna traps in  
25 the Bosphorus, Istanbul, Turkey in 1941. Aside from these two final specimens, fork length  
26 was calculated for the remaining individuals as detailed in the Materials and Methods.

27

28 **1755 CE La Chanca, Conil, Spain**

29 Ten vertebrae samples were obtained from the archaeological site of 'La Chanca' (Conil de  
30 la Frontera, Spain). La Chanca is a small salting factory belonging to the Duchy of Medina  
31 Sidonia that was built in the 16<sup>th</sup> century and was in operation until the 19<sup>th</sup> century. On  
32 November 1, 1755, an earthquake occurred with an epicentre in the Gulf of Cádiz, which  
33 generated a tsunami in the southeast of Andalusia (Huelva and Cádiz) and along the whole  
34 Iberian coast, leaving La Chanca completely destroyed, mid-operation. Excavations  
35 (Gutiérrez-Mas et al., 2016) confirmed the strata destroyed by the tsunami, where BFT  
36 vertebrae, scales and spines were recovered with an anatomical connection, although  
37 separated where presumably BFT were cut into spinal sections in preparation for the salting  
38 process. The dating of 1755 is corroborated by a letter from Miguel of Aragón and Serrano,  
39 who held the position of Corregidor of Conil in 1755 when he wrote to the Duke of Medina  
40 Sidonia detailing that BFT were in the salting piles at the time the catastrophe occurred, that  
41 the wave dragged them and that they remained buried under the ruins of the building, with  
42 no possibility of recovery (document 2326 of the General Archive of the Medina Sidonia  
43 Foundation). Fork lengths were estimated to range from 144-220 cm, average 176 cm.

44

45 **16-18<sup>th</sup> century CE Pedras de Fogu, Sardinia, Italy**

46 Ten vertebrae samples were obtained from the archaeological site of 'Pedras de Fogu'  
47 (Sassari, Sardinia, Italy). A tuna trap (tonnara) operated at this location from the 16<sup>th</sup> to the  
48 end of the 18<sup>th</sup> century where BFT vertebrae have been recovered in a midden at the back of  
49 the beach after they were revealed by coastal erosion (Delussu & Wilkens, 2001). These  
50 specimens were estimated to range from 115-231 FL, average 178 cm FL.

51

52 **10-13<sup>th</sup> century CE Mazara del Vallo, Sicily, Italy**

53 A total of nine samples (five vertebrae and four cranial elements) were obtained from the  
54 archaeological site of 'Mazara del Vallo' situated in the town (southwestern Sicily, Italy).  
55 Samples were recovered from urban 10-13<sup>th</sup> century layers, each dated by context as

56 detailed in Aniceti (2019), and identified as different individuals according to their range of  
57 sizes. FL estimates were not made for these individuals as the vertebrae selected were  
58 fragmented and could not be assigned to rank or accurately measured. Broadly, specimens  
59 represented small to large sized adult BFT.

60

### 61 **9-13<sup>th</sup> century CE Yenikapi, Istanbul, Turkey**

62 Fourteen vertebrae specimens were selected for analyses from a rescue excavation at a  
63 Byzantine site in the Yenikapi neighbourhood of Istanbul, Turkey. The Port of Theodosius  
64 operated at this site from 4-11<sup>th</sup> century CE before being filled in at the 15<sup>th</sup> century CE. Due  
65 to the specimens previously holding a conservative dated by stratigraphic unit between the  
66 4-15<sup>th</sup> century CE we opted to radiocarbon date a subset of the BFT vertebrae samples,  
67 archaeological context and according to the carbon dating of other specimens to obtain a  
68 more accurate date than from the context or associated fauna (Onar et al., 2008). It is  
69 unknown whether specimens were fished locally or transported to the city of Constantinople,  
70 which was a major trading hub throughout the Byzantine period. Specimens were estimated  
71 to range from 165-241 cm FL, average 201 cm FL.

72

73 Radiocarbon dating by AMS (Accelerator Mass Spectrometry) defined the <sup>14</sup>C age of the 9-  
74 13<sup>th</sup> century Istanbul samples from the Byzantine (4-15<sup>th</sup> century CE) archaeological site of  
75 Theodosius' Harbour (Yenikapi, Istanbul, Turkey). Briefly, 200 mg bone powder was  
76 obtained from each of the three BFT vertebrae specimens by drilling. Samples were then  
77 analysed using standard procedures and normalised against the IAEA Standard C<sup>6</sup> Sucrose  
78 (Quarta et al., 2021) at CEDAD (University of Salento, Salento, Italy).

79

80  $\delta^{13}\text{C}$  values were studied to take account of the marine reservoir effect (MRE). We applied  
81 the Mediterranean MRE correction of  $390 \pm 85$  y (Siani et al., 2000) to samples MRY 6374  
82 and MET18528 with low ( $\sim 12.5$  ‰)  $\delta^{13}\text{C}$  values (Table S1) indicative of Mediterranean  
83 residence and/or benthic feeding (i.e., causing a large overestimation of age due to the

84 incorporation of older carbon sources). We averaged the Mediterranean and Black Sea MRE  
85 of  $-180 \pm 40$  y (Siani et al., 2000) applied to sample MRY 3569 with a relatively high ( $\sim 17.0$   
86 ‰)  $\delta^{13}\text{C}$  value (Table S1), indicative of Black Sea residence and/or predominantly pelagic  
87 carbon sources (i.e. a small overestimation of age due to regenerated carbon sources). Note  
88 that BFT residents in the Black Sea necessarily migrated back to the Mediterranean during  
89 winter months due to the ecology of the Black Sea (Karakulak & Oray, 2009), therefore the  
90 full MRE correction for the Black Sea is not appropriate for BFT. Ages (Table S1) were  
91 corrected using OxCal v. 4.3 (Siani et al., 2000) with the marine20 curve (Heaton et al.,  
92 2020).

93

94 Mathematical corrections (Figure S2) indicate that this sample group dates towards the end  
95 of the site occupation from 9-13<sup>th</sup> century CE. This wide range was likely a consequence of  
96 the reservoir effect and error associated with MSE combined with measurement error.

97 Despite this, the context, size and condition of the BFT remains from this site implies a

98 single deposition event (Andrews et al., 2021; Onar et al., 2008), therefore the true date of

99 these specimens is likely to be where their dates overlap during the 10-12<sup>th</sup> century CE. To

100 be conservative, we recommend the use of 9-13<sup>th</sup> century CE.

101

102

103

104

105

106

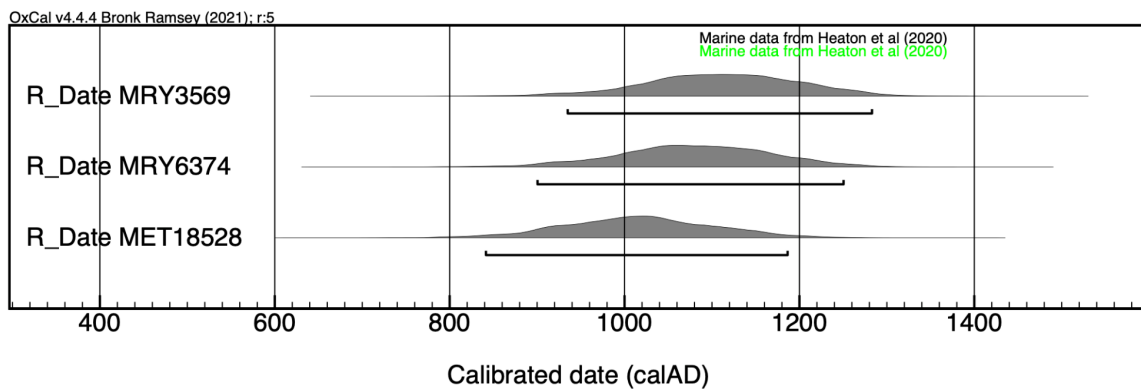
107

108

**Table S1.** Summary of raw and OxCal corrected  $^{14}\text{C}$  dates for three BFT samples from the archaeological site of Theodosius' Harbour (Yenikapi, Istanbul, Turkey, Onar et al. (2008)).

Sample	Raw Radiocarbon Age (years before 1950)	$\delta^{13}\text{C}$ (‰)	MRE correction ( $\delta\text{R}$ years)	CalAD years (95.4% probability)
MRY 3569	1667 $\pm$ 55	-17.1 $\pm$ 0.2	(-180 $\pm$ 40 + 390 $\pm$ 85 /2)	935-1283
MRY 6374	1880 $\pm$ 30	-12.7 $\pm$ 0.3	390 $\pm$ 85	900-1250
MET18528	1938 $\pm$ 45	-12.4 $\pm$ 0.3	390 $\pm$ 85	841-1186
<b>Total (95.4%) probable time span of cohort</b>				<b>841-1283</b>

109



110

**Figure S1.** Corrected  $^{14}\text{C}$  dates, produced using OxCal with the Marine20 curve for three Atlantic bluefin tuna (*Thunnus thynnus*) samples from the archaeological site of Theodosius' Harbour (Yenikapi, Istanbul, Turkey).

114

115 **9-10<sup>th</sup> century CE Palermo, Sicily, Italy**

116 A total of 18 samples (15 vertebrae and 3 cranial elements) were selected for analyses from  
117 urban 9-10<sup>th</sup> century layers in two different excavations in settlements in the city of Palermo,  
118 Sicily; Sant'Antonino and Corso dei Mille. The layers were dated by context as detailed in  
119 Bernal-Casasola et al. (2018). Samples were estimated to represent individuals ranging from  
120 101-185 cm FL, average 130 cm FL, believed to have been caught locally.

121

#### 122 **4-5<sup>th</sup> century CE Baelo Claudia, Andalusia, Spain**

123 A total of 12 vertebrae specimens were analysed from the Roman-era city of Baelo Claudia,  
124 Andalusia, Spain). Using the archaeological context of stratigraphic units, staples were dated  
125 to the late Roman era (4-5<sup>th</sup> century CE) from various stratigraphic units and contexts within  
126 the city, predominantly associated with the fish processing/salting facilities—called cetariae  
127 (Bernal-Casasola et al., 2018). Specimens analysed represented small-medium sized adult  
128 individuals (109-132 cm FL, average 124 cm FL). The Strait of Gibraltar supported large-  
129 scale fisheries for BFT from the Phoenician era (~8<sup>th</sup> century BCE) onwards, and thus these  
130 specimens are believed to have been caught locally.

131

#### 132 **1<sup>st</sup> century CE Olivillo, Cadiz, Spain**

133 Ten samples were selected for analysis from the archaeological site 'Olivillo', an Imperial  
134 Roman fish processing/salting facility within the city of Cádiz (Bernal-Casasola et al., 2020).  
135 Samples were selected from various stratigraphic units, dated by context to the 1<sup>st</sup> century  
136 CE. Specimens analysed represented individuals estimated to range from 90-155 cm FL, at  
137 an average of 130 cm FL, believed to have been caught locally.

138

139

140





141

142 **Figure S2.** A schematic showing how vertebrae (left) were sampled by cutting across the growth-axis  
143 to obtain cross-sections (right). Cross sections were occasionally sub-sampled by halving (dashed  
144 line) when the amount of material was excessive in the largest samples. Figure adapted from  
145 Calaprice (1986).

146

147

#### 148 **Sample details: length estimation and stable isotope measurements**

149

150 **Table S2** - external file.

151

152 *Theoretical sulphur content of Atlantic bluefin tuna (*Thunnus thynnus*) bone*

153

154 To confirm the quality of our samples we wanted to understand the quantity of sulphur that  
155 BFT bone should theoretically contain. First, we searched the Atlantic bluefin tuna (*Thunnus*  
156 *thynnus*) predicted proteome (NCBI BioProject: PRJNA408269) using blastn function with  
157 default settings, to retrieve the Collagen Type 1A and 1B (COL1A1, COL1A2) amino acid  
158 sequence of BFT, using six <https://www.ncbi.nlm.nih.gov/protein/> published records for  
159 fishes. Namely; *Cynoglossus semilaevis* (XP.008328838.1) *Lates calcarifer*  
160 (XP.018553992.1), *Oreochromis niloticus* (BAL40987.1) and *Thunnus orientalis*  
161 (BAN42671.1) for COL1A1; and *Cynoglossus semilaevis* (XP.008329548.1), *Lates calcarifer*  
162 (XP.018522130.1) and *Oreochromis niloticus* (BAL40988.1) for COL1A2. Retrieved amino  
163 acid sequences were then aligned and trimmed manually to confirm the same start and stop  
164 codon as the published records for the fishes *Cynoglossus semilaevis* (XP.008328838.1),  
165 *Dicentrarchus labrax* (CBN81647.1), *Haplochromis burtoni* (XP.005946024.1), *Larimichthys*

166 *crocea* (XP.010745684.1), *Lates calcarifer* (XP.018553992.1), *Maylandia zebra*  
167 (XP.004572575.1), *Neolamprologus brichardi* (XP.006808934.1), *Notothenia coriiceps*  
168 (XP.010767913.1), *Oreochromis niloticus* (BAL40987.1), *Paralichthys olivaceus*  
169 (BAD77968.1), *Pundamilia nyererei* (XP.005750908.1), *Stegastes partitus*  
170 (XP.008293593.1), *Takifugu rubripes* (XP.003964321.1) and *Thunnus orientalis*  
171 (BAN42671.1).

172

173 Amino acids were then counted from the resulting sequences (uploaded to NCBI: Accession  
174 ON142175 and ON142176) using <https://spin.niddk.nih.gov/clore/Software/A205.html> (Anthis  
175 & Clore, 2013). Theoretical mass of each amino acid and element was subsequently  
176 calculated using Table 8 and 9 of Nehlich & Richards (2009). This resulted in the following  
177 percentage calculations, including an estimated theoretical sulphur content of 0.47% for BFT  
178 bone (Table S2).

**Table S3.** Theoretical sulphur content of Atlantic bluefin tuna (*Thunnus thynnus*) bone calculated using COL1A1 and COL1A2 amino acid sequences, following Nehlich & Richards (2009).

Correlated chain			Chain $\alpha 1$		Chain $\alpha 2$							
AA	Mwt	In Protein (-H <sub>2</sub> O)	Number of residues	Molecular weight in protein (g mol <sup>-1</sup> )	Number of residues	Molecular weight in protein (g mol <sup>-1</sup> )	(2 × a1)+a2	C wt (g mol <sup>-1</sup> )	N wt (g mol <sup>-1</sup> )	O wt (g mol <sup>-1</sup> )	H wt (g mol <sup>-1</sup> )	S wt (g mol <sup>-1</sup> )
<b>OH-Pro</b>	131.13	122.12	0	0	0	0	0	0.00	0.00	0.00	0.00	0.00
<b>Asp</b>	131.09	122.08	28	3418.24	31	3784.48	10620.96	3897.89	1136.44	5183.03	403.60	0.00
<b>Thr</b>	119.12	110.11	33	3633.63	28	3083.08	10350.34	4171.19	1221.34	4171.19	786.63	0.00
<b>Ser</b>	105.09	96.09	37	3555.33	46	4420.14	11530.8	3955.06	1533.60	5269.58	772.56	0.00
<b>Glu</b>	147.13	138.12	55	7596.6	39	5386.68	20579.88	8396.59	1955.09	8952.25	1275.95	0.00
<b>Pro</b>	115.13	106.12	197	20905.64	189	20056.68	61867.96	32295.08	7547.89	17199.29	4887.57	0.00
<b>Gly</b>	75.07	66.06	353	23319.18	356	23517.36	70155.72	22449.83	13119.12	29886.34	4700.43	0.00
<b>Ala</b>	89.09	80.09	139	11132.51	120	9610.8	31875.82	12877.83	5004.50	11443.42	2518.19	0.00
<b>Cys</b>	121.16	112.15	0	0	0	0	0	0.00	0.00	0.00	0.00	0.00
<b>Val</b>	117.15	108.14	19	2054.66	23	2487.22	6596.54	3384.03	791.58	1800.86	626.67	0.00

<b>Met</b>	149.21	140.21	18	2523.78	13	1822.73	6870.29	2761.86	645.81	1470.24	508.40	1477.11
<b>Ile</b>	131.17	122.17	9	1099.53	12	1466.04	3665.1	2012.14	392.17	894.28	366.51	0.00
<b>Leu</b>	131.17	122.17	18	2199.06	28	3420.76	7818.88	4292.57	836.62	1907.81	781.89	0.00
<b>Tyr</b>	181.19	172.18	1	172.18	6	1033.08	1377.44	822.33	106.06	365.02	84.02	0.00
<b>Phe</b>	165.19	156.18	17	2655.06	10	1561.8	6871.92	4494.24	584.11	1333.15	460.42	0.00
<b>OH Lys</b>	162.19	153.18		0		0		0.00	0.00	0.00	0.00	0.00
<b>Lys</b>	146.19	137.18	37	5075.66	30	4115.4	14266.72	7033.49	2739.21	3124.41	1383.87	0.00
<b>His</b>	155.16	146.15	2	292.3	9	1315.35	1899.95	881.58	514.89	391.39	110.20	0.00
<b>Arg</b>	174.2	165.2	55	9086	58	9581.6	27753.6	11489.99	8936.66	5106.66	2248.04	0.00
<b>Asn</b>	132.12	123.11	12	1477.32	20	2462.2	5416.84	1971.73	1148.37	1966.31	330.43	0.00
<b>Gln</b>	146.15	137.14	25	3428.5	22	3017.08	9874.08	4058.25	1895.82	3238.70	681.31	0.00
<b>TRP</b>			0	0	0	0	3063.6	0.00	0.00	0.00	0.00	0.00
<b>Total</b>			<b>1055</b>	<b>103625.18</b>	<b>1040</b>	<b>102142.48</b>	<b>312456.44</b>	<b>131245.66</b>	<b>50109.29</b>	<b>103703.93</b>	<b>22926.69</b>	<b>1477.11</b>
<b>%</b>								<b>42.00</b>	<b>16.04</b>	<b>33.19</b>	<b>7.34</b>	<b>0.47</b>

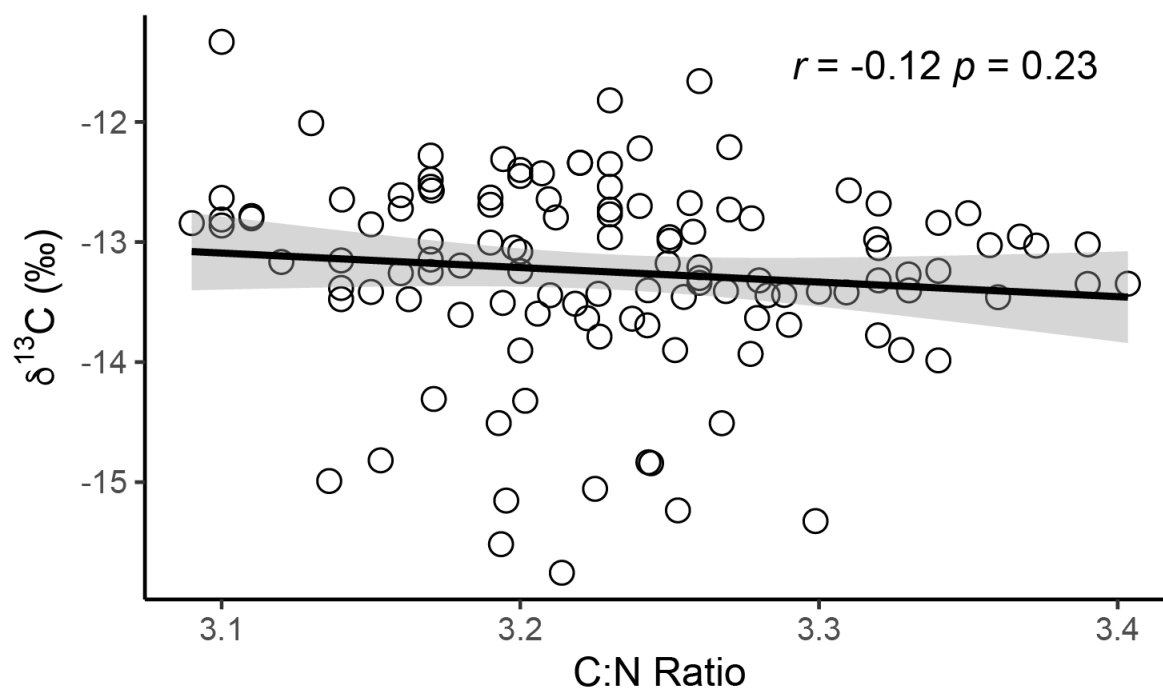


**Figure S3.** Scatterplot indicating a lack of correlation between C:N Ratio and  $\delta^{13}\text{C}$  across all samples (black circles), showing Pearson's  $r$  and statistical significance ( $p$ ) as tested in R.

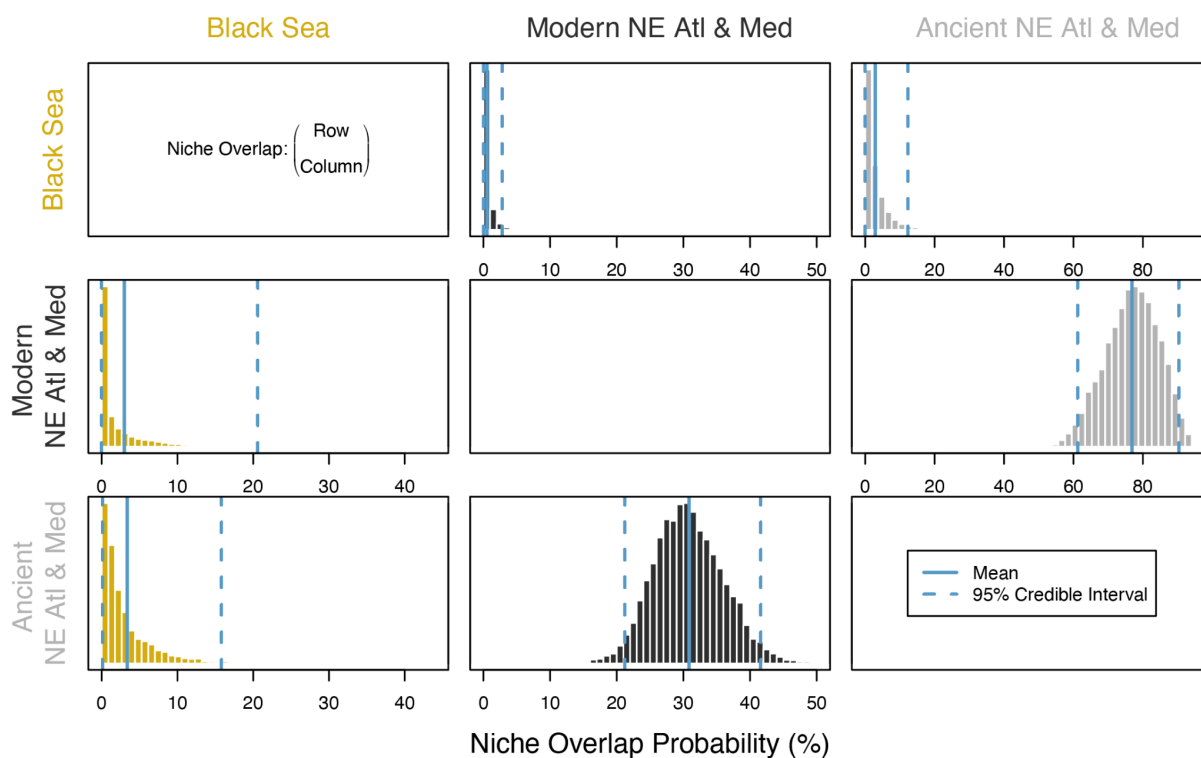


**Figure S4.** Overlap probabilities of each a priori defined spatial group, showing the mean and 95% CI for each group pairing as estimated using nicheROVER using 10,000 permutations.

**Table S4.** Generalised Additive Model AIC scoring, we used the model with the lowest AIC value, indicated in boldface. Year = Century/Year of sampling, group = spatial (Black Sea, NE Atlantic and Mediterranean) or temporal (pre-16<sup>th</sup> c., post 16<sup>th</sup> c., Black Sea) pools of sample groups.

<b>Stable isotope</b>	<b>Model</b>	<b>Degrees of freedom</b>	<b>AIC</b>
$\delta^{13}\text{C}$	<b><math>\delta^{13}\text{C} \sim \text{s(longitude)} + \text{year:group}</math></b>	<b>8.1</b>	<b>163.3</b>
	$\delta^{13}\text{C} \sim \text{longitude} + \text{year:group}$	5.0	187.9
	$\delta^{13}\text{C} \sim \text{longitude} + \text{s(year, by=group)}$	8.4	171.4
$\delta^{15}\text{N}$	<b><math>\delta^{15}\text{N} \sim \text{s(longitude)} + \text{year:group}</math></b>	<b>8.5</b>	<b>333.0</b>
	$\delta^{15}\text{N} \sim \text{longitude} + \text{year}$	4.0	369.9
	$\delta^{15}\text{N} \sim \text{s(longitude)} + \text{s(year, by=group)}$	11.9	342.8
$\delta^{34}\text{S}$	<b><math>\delta^{34}\text{S} \sim \text{s(longitude, by=group)} + \text{s(year)}</math></b>	<b>8.4</b>	<b>270.7</b>
	$\delta^{34}\text{S} \sim \text{longitude:group} + \text{s(year)}$	8.3	271.5
	$\delta^{34}\text{S} \sim \text{s(longitude, by=group)} + \text{year}$	8.7	271.5

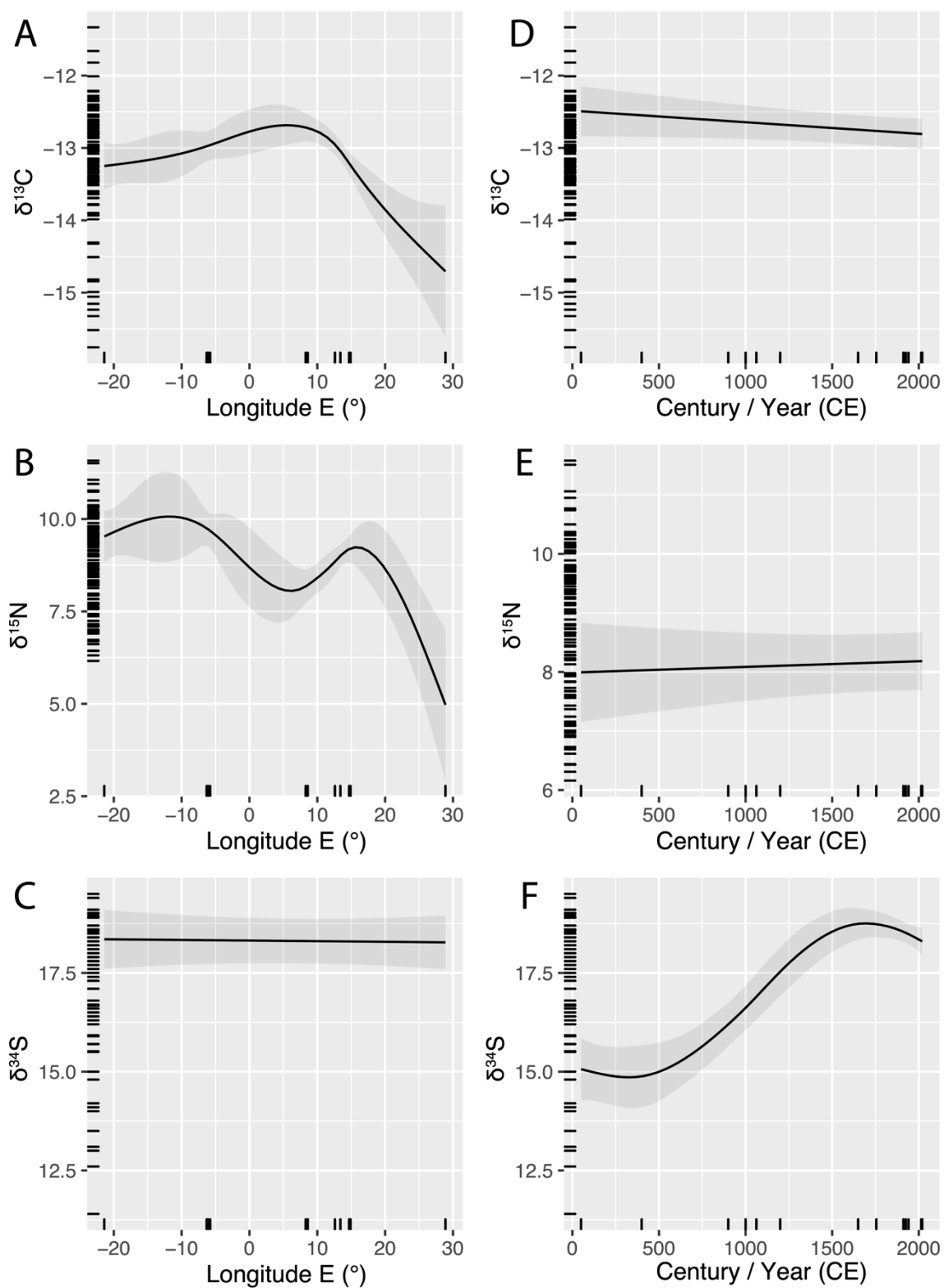


**Figure S5.** Predictions of GAM models for each stable isotope analysed and variable term (space and time) 95% CI (shaded band) as illustrated using the `plot_predictions` function in R. Plots for each stable isotope are illustrated separately:  $\delta^{13}\text{C}$  (A, D),  $\delta^{15}\text{N}$  (B, E) and  $\delta^{34}\text{S}$  (C, F).

## Supplementary References

- Andrews, A. J., Puncher, G. N., Bernal-Casasola, D., Di Natale, A., Massari, F., Onar, V., Toker, N. Y., Hanke, A., Pavey, S. A., Savojardo, C., Martelli, P. L., Casadio, R., Cilli, E., Morales-Muñiz, A., Mantovani, B., Tinti, F., & Cariani, A. (2021). Ancient DNA SNP-panel data suggests stability in bluefin tuna genetic diversity despite centuries of fluctuating catches in the eastern Atlantic and Mediterranean. *Scientific Reports*, *11*(1), 20744.
- Aniceti, V. (2019). *Animals and their roles in the medieval society of Sicily : from Byzantines to Arabs and from Arabs to Norman/Swabians* (U. Albarella (ed.)) [University of Sheffield].  
<https://ethos.bl.uk/OrderDetails.do?uin=uk.bl.ethos.805383>
- Anthis, N. J., & Clore, G. M. (2013). Sequence-specific determination of protein and peptide concentrations by absorbance at 205 nm. *Protein Science: A Publication of the Protein Society*, *22*(6), 851–858.
- Bernal-Casasola, D., Expósito, J. A., & Díaz, J. J. (2018). The Baelo Claudia paradigm: The exploitation of marine resources in Roman cetariae. *Journal of Maritime Archaeology*, *13*(3), 329–351.
- Bernal-Casasola, D., Vargas Girón, J. M., & Lara Medina, Y. (2020). Atunes en salazón y en conserva en las chancas gaditanas: perspectivas desde El Olivillo in 7 metros de la Historia de Cádiz. *Darío Bernal, José Manuel Vargas y Macarena Lara (eds.): 7 metros de la Historia de Cádiz... Arqueología en el Olivillo y en el Colegio Mayor Universitario. pp. 517 - 534., 726.*
- Calaprice, J. R. (1986). CV024000222 Calaprice1986.pdf. *Col.Vol.Sci.Pap. ICCAT*, *24*, 222–254.
- Delussu, F., & Wilkens, B. (2001). Analisi dei resti ossei della tonnara di Pedras de Fogu. *Archeologia Postmedievale*, *5*, 214.
- Gutiérrez-Mas, J. M., Gómez Fernández, V., García López, S., Morales González, J. A., Ibáñez Ageitos, J. M., & Others. (2016). Comparative analysis of the deposits left by the tsunami that followed to the Lisbon earthquake (1755 ad), on the Castilnovo beach and the old tuna factory of la Chança (Conil de la Frontera, SW Spain). *Revista de La Sociedad Geológica de España*, *29*(1), 21–33.
- Heaton, T. J., Köhler, P., Butzin, M., Bard, E., Reimer, R. W., Austin, W. E. N., Ramsey, C. B., Grootes, P. M., Hughen, K. A., Kromer, B., Reimer, P. J., Adkins, J., Burke, A., Cook, M. S., Olsen, J., & Skinner, L. C. (2020). Marine20—The Marine Radiocarbon Age Calibration Curve



(0–55,000 cal BP). *Radiocarbon*, 62(4), 779–820.

Karakulak, F. S., & Oray, I. K. (2009). Remarks on the fluctuations of bluefin tuna catches in Turkish waters. *Col. Vol. Sci. Pap. ICCAT*.

<http://citeseerx.ist.psu.edu/viewdoc/download?doi=10.1.1.519.468&rep=rep1&type=pdf>

Nehlich, O., & Richards, M. P. (2009). Establishing collagen quality criteria for sulphur isotope analysis of archaeological bone collagen. *Archaeological and Anthropological Sciences*, 1(1), 59–75.

Onar, V., Pazvant, G., & Armutak, A. (2008). Radiocarbon dating results of the animal remains uncovered at Yenikapı Excavations. *Istanbul Archaeological Museums, Proceedings of the 1st Symposium on Marmaray-Metro Salvage Excavations*, 249–256.

Quarta, G., Maruccio, L., D'Elia, M., & Calcagnile, L. (2021). Radiocarbon Dating of Marine Samples: Methodological Aspects, Applications and Case Studies. *WATER*, 13(7), 986.

Riccioni, G., Landi, M., Ferrara, G., Milano, I., Cariani, A., Zane, L., Sella, M., Barbujani, G., & Tinti, F. (2010). Spatio-temporal population structuring and genetic diversity retention in depleted Atlantic Bluefin tuna of the Mediterranean Sea. In *Proceedings of the National Academy of Sciences* (Vol. 107, Issue 5, pp. 2102–2107). <https://doi.org/10.1073/pnas.0908281107>

Siani, G., Paterne, M., Arnold, M., Bard, E., Métivier, B., Tisnerat, N., & Bassinot, F. (2000). Radiocarbon Reservoir Ages in the Mediterranean Sea and Black Sea. *Radiocarbon*, 42(2), 271–280.



Sample ID	Location	Period (year)	Inner/Outer	S:Collagen Y	C:N (ratio)	δ13C (‰)	δ15N (‰)	%S	CNMolar	CSMolar	NSMolar	δ34S (‰)	Comment
MET_12545	Yenikapi, ls 9-13th c.		Inner	2.9	3.2	-15.2	7.6						
MET_12545	Yenikapi, ls 9-13th c.		Outer	5.2	3.1	-14.4	7.6	0.47	3	178	60	15.7	
MET_14082	Yenikapi, ls 9-13th c.		Inner	12.6	3.2	-15.0	6.9	0.61	3.1	185	59	13.1	
MET_14082	Yenikapi, ls 9-13th c.		Outer	14.4	3.2	-15.1	7.0	0.74	3.2	145	46	13.1	
MET_14129	Yenikapi, ls 9-13th c.		Inner	4.9	3.3	-15.0	6.3						
MET_14129	Yenikapi, ls 9-13th c.		Outer	8	3.2	-14.7	6.5	0.65	3.1	165	53	13.5	
MET_15382	Yenikapi, ls 9-13th c.		Inner	<1. Not sufficient									Not included in final analyses
MET_15382	Yenikapi, ls 9-13th c.		Outer	<1. Not sufficient									Not included in final analyses
MET_16735	Yenikapi, ls 9-13th c.		Inner	7.1	3.2	-15.3	6.2	0.71	3.1	156	50	11.3	
MET_16735	Yenikapi, ls 9-13th c.		Outer	8	3.2	-15.0	6.4	0.71	3.1	153	49	11.4	
MET_1704	Yenikapi, ls 9-13th c.		Inner	9.1	3.2	-13.7	9.0	0.71	3.1	155	50	12.6	
MET_1704	Yenikapi, ls 9-13th c.		Outer	5.8	3.2	-13.6	9.6	0.69	3.3	156	48	13.4	
MET_17473	Yenikapi, ls 9-13th c.		Inner	9.8	3.3	-14.9	7.0	0.62	3.2	176	55	13.9	
MET_17473	Yenikapi, ls 9-13th c.		Outer	7	3.2	-14.7	7.1	0.63	3.1	160	52	14.5	
MET_20124	Yenikapi, ls 9-13th c.		Inner	9.1	3.2	-14.8	6.7	0.48	3.1	227	74	14.8	
MET_20124	Yenikapi, ls 9-13th c.		Outer	10.1	3.2	-13.9	7.3	0.42	2.9	211	72	14.9	
MET_20737	Yenikapi, ls 9-13th c.		Inner	7.3	3.3	-14.8	7.2	0.59	3.3	180	55	15.6	
MET_20737	Yenikapi, ls 9-13th c.		Outer	7.6	3.2	-14.2	7.3	0.49	3.1	189	61	15.4	
MET_21093	Yenikapi, ls 9-13th c.		Inner	3.1	3.2	-15.9	6.9	0.6	3.3	182	56	13.5	
MET_21093	Yenikapi, ls 9-13th c.		Outer	3.4	3.2	-15.6	7.4	0.47	3.1	180	58	12.7	
MET_4187	Yenikapi, ls 9-13th c.		Inner	13.4	3.2	-14.8	7.1	0.58	3.1	194	62	13.7	
MET_4187	Yenikapi, ls 9-13th c.		Outer	13.7	3.2	-14.2	7.1	0.47	3	213	70	14.3	
MET_57505	Yenikapi, ls 9-13th c.		Inner	12	3.2	-15.3	6.7	0.55	3.2	205	65	16	
MET_57505	Yenikapi, ls 9-13th c.		Outer	11.6	3.2	-15.7	6.5	0.64	3.1	171	55	15.5	
MRY_3285	Yenikapi, ls 9-13th c.		Inner	11.2	3.3	-15.7	6.9						
MRY_3285	Yenikapi, ls 9-13th c.		Outer	10.7	3.2	-14.7	7.1						
MRY_3964	Yenikapi, ls 9-13th c.		Inner	12.6	3.2	-14.5	9.0	0.57	3.1	193	62	14.5	
MRY_3964	Yenikapi, ls 9-13th c.		Outer	12.5	3.2	-14.1	8.6	0.46	3	183	61	13.6	

## **Chapter 6**

Ancient DNA SNP-panel data suggests stability in bluefin tuna genetic diversity despite centuries of fluctuating catches in the eastern Atlantic and Mediterranean  
**(pages 189—213)**



OPEN

# Ancient DNA SNP-panel data suggests stability in bluefin tuna genetic diversity despite centuries of fluctuating catches in the eastern Atlantic and Mediterranean

Adam J. Andrews<sup>1,2,11</sup>✉, Gregory N. Puncher<sup>1,3,11</sup>✉, Darío Bernal-Casasola<sup>4</sup>, Antonio Di Natale<sup>5</sup>, Francesco Massari<sup>1</sup>, Vedat Onar<sup>6</sup>, Nezir Yaşar Toker<sup>6</sup>, Alex Hanke<sup>7</sup>, Scott A. Pavey<sup>3</sup>, Castrense Savojardo<sup>8</sup>, Pier Luigi Martelli<sup>8</sup>, Rita Casadio<sup>8</sup>, Elisabetta Cilli<sup>2</sup>, Arturo Morales-Muñiz<sup>9</sup>, Barbara Mantovani<sup>10</sup>, Fausto Tinti<sup>1</sup> & Alessia Cariani<sup>1</sup>

Atlantic bluefin tuna (*Thunnus thynnus*; BFT) abundance was depleted in the late 20th and early 21st century due to overfishing. Historical catch records further indicate that the abundance of BFT in the Mediterranean has been fluctuating since at least the 16th century. Here we build upon previous work on ancient DNA of BFT in the Mediterranean by comparing contemporary (2009–2012) specimens with archival (1911–1926) and archaeological (2nd century BCE–15th century CE) specimens that represent population states prior to these two major periods of exploitation, respectively. We successfully genotyped and analysed 259 contemporary and 123 historical (91 archival and 32 archaeological) specimens at 92 SNP loci that were selected for their ability to differentiate contemporary populations or their association with core biological functions. We found no evidence of genetic bottlenecks, inbreeding or population restructuring between temporal sample groups that might explain what has driven catch fluctuations since the 16th century. We also detected a putative adaptive response, involving the cytoskeletal protein synemin which may be related to muscle stress. However, these results require further investigation with more extensive genome-wide data to rule out demographic changes due to overfishing, and other natural and anthropogenic factors, in addition to elucidating the adaptive drivers related to these.

Overfishing has reduced numerous fish populations to remnants of their historical levels<sup>1,2</sup>, yet we have a poor understanding of what impact this has had on their evolutionary potential and resilience<sup>3</sup>. This information is crucial to predict future demographic changes and thus promote sustainable fisheries management<sup>4,5</sup>. Studies of historical marine ecology offer an opportunity to learn and heed these past lessons<sup>5–7</sup>. In particular, genetic/genomic studies can infer past history from contemporary samples<sup>8</sup>, or directly test archaeological and archival samples<sup>9</sup> for losses in genetic diversity, population restructuring, or adaptive responses to natural factors e.g.,

<sup>1</sup>Department of Biological, Geological and Environmental Sciences, University of Bologna, Ravenna, Italy. <sup>2</sup>Department of Cultural Heritage, University of Bologna, Ravenna, Italy. <sup>3</sup>Department of Biological Sciences, Canadian Rivers Institute, University of New Brunswick, Saint John, NB, Canada. <sup>4</sup>Department of History, Geography and Philosophy, Faculty of Philosophy and Letters, University of Cádiz, Cádiz, Spain. <sup>5</sup>Aquastudio Research Institute, Messina, Italy. <sup>6</sup>Osteoarcheology Practice and Research Centre and Faculty of Veterinary Medicine, Istanbul University-Cerrahpaşa, Avcılar, Istanbul, Turkey. <sup>7</sup>St. Andrews Biological Station, Fisheries and Oceans Canada, St. Andrews, NB, Canada. <sup>8</sup>Biocomputing Group, University of Bologna, Bologna, Italy. <sup>9</sup>Department of Biology, Autonomous University of Madrid, Madrid, Spain. <sup>10</sup>Department of Biological, Geological and Environmental Sciences, University of Bologna, Bologna, Italy. <sup>11</sup>These authors contributed equally: Adam J. Andrews and Gregory N. Puncher. ✉email: adam@palaeome.org; gregpuncher@gmail.com

climate, or anthropogenic ones e.g., fisheries-induced evolution (FIE)<sup>10</sup>. A decade ago, Riccioni et al.<sup>11</sup> were the first to investigate temporal demographic changes in the key species Atlantic bluefin tuna (*Thunnus thynnus*, hereafter BFT) using archival early-20th century samples and microsatellite markers. Here, we build on this work by genotyping archival and archaeological samples to extend investigations into the pre-industrial era, when fishing may have also had the potential to impact BFT.

BFT is a highly migratory pelagic top predator, characterized by its large size (up to 3.3 m in length and 725 kg in weight), slow maturation (between 4 and 8 years)<sup>12,13</sup>, and inshore migration behaviour, that has made it vulnerable to overfishing. Recent genomic studies<sup>14,15</sup> support the delineation of two BFT populations. These are a western Atlantic component that spawns predominantly in the Gulf of Mexico<sup>16</sup>, and an eastern Atlantic and Mediterranean component that spawns predominantly in the Mediterranean Sea<sup>17</sup>. Individuals of both populations migrate into the Atlantic Ocean to feed, including as juveniles<sup>18</sup>, and exhibit high-levels of mixing<sup>14,15</sup>. The role of additional contemporary and historical spawning areas i.e. the Slope Sea (East of Cape Hatteras, USA)<sup>16</sup>, the Bay of Biscay<sup>19</sup>, and the Black Sea<sup>20,21</sup>, are yet to be clearly defined, especially regarding the Slope Sea where connectivity between populations was observed<sup>15</sup>.

During the last few years, the eastern Atlantic and Mediterranean population of BFT has recovered to 1970's levels following heavy overfishing that depleted spawning stock biomass, restructured the population toward younger individuals, and contracted the species range, in the late 20th and early 21st century<sup>22–25</sup>. However, reconstructions of 16th–20th century BFT trap catch records suggest abundance across the Mediterranean has been fluctuating for centuries<sup>23,26,27</sup>. Pelagic species are particularly susceptible to fluctuations in abundance since dynamic food and environmental conditions drive large variability in recruitment, but fishing magnifies poor recruitment and therefore population declines when large catches occur<sup>28</sup>. Multiple factors need to be taken into account to be able to interpret trap catch fluctuations as abundance<sup>29</sup>, though, it appears that catch numbers in the 16th and 18th century may be comparable to those during the industrial fishing of the last 50 years<sup>26,27</sup>. Hence, fishing appears to have been intense in this period.

The current study investigates genetic variability in eastern Atlantic and Mediterranean BFT prior to both their 21st century population collapse, and record trap catches in the 16th and 18th century, using archived early-20th century specimens, and archaeological remains, respectively. Despite overfished species having an overall lower genetic diversity when contemporary data are compared<sup>3</sup>, Riccioni et al.<sup>11</sup> were unable to detect losses in BFT genetic diversity when comparing contemporary and early-20th century samples. Likewise, no genetic erosion was observed following overfishing in the closely-related albacore (*Thunnus alalunga*)<sup>30</sup>, the Pacific herring (*Clupea pallasii*)<sup>31</sup>, or the European anchovy (*Engraulis encrasicolus*)<sup>32</sup>. Even marine species (e.g., sawfish, *Pristis* spp.) depleted to between 1 and 5% of their historical biomass appear to have retained genetic diversity<sup>33</sup>. However, several studies have noted genetic diversity declines or population losses following overfishing in Atlantic cod (*Gadus morhua*)<sup>34–36</sup>, Atlantic salmon (*Salmo salar*)<sup>37</sup>, and Chinook salmon (*Oncorhynchus tshawytscha*)<sup>38</sup>. In addition, adaptive responses to size- (in Walleye, *Sander vitreus*)<sup>39</sup>, and sex- (in Atlantic salmon)<sup>40</sup> selective harvesting, and environmental drivers (in Atlantic cod)<sup>41</sup> have also been reported in studies using archival or archaeological fish samples. It remains unclear to what extent the inability of some studies to detect these differences results from the selection of genetic markers with low resolution, or the resilience offered by complex life history traits during times of population decline. A recent whole genome sequencing (WGS) study<sup>42</sup>, that did not detect genetic erosion or adaptive responses in two Atlantic cod populations following 20th century overfishing, may indicate, however, that the latter is the case for some populations.

Here we test the hypotheses that the genetic diversity of BFT has declined and that their populations restructured following periods of intense fishing in the eastern Atlantic and Mediterranean. Further, we sought to identify adaptive responses that may be related to ecological or environmental conditions. To this end, our objectives were to genotype archaeological and archival specimens on a single nucleotide polymorphic (SNP) panel to (1) characterise their genetic diversity and population structure, (2) to compare those patterns to analogous ones from contemporary groups, and (3) to explore markers under putative selection and identify their associated function, if possible.

## Methods

**Samples.** We collected samples of contemporary, archival and archaeological BFT specimens for analysis as follows: Contemporary reference specimens (GOM: Gulf of Mexico, CMAS: Central Mediterranean Adriatic Sea, CMSI: Central Mediterranean Sicily, EABB: East Atlantic Bay of Biscay, EAGI: Eastern Atlantic Gibraltar, EMLS: Eastern Mediterranean Levantine Sea, WMBA: Western Mediterranean Balearic Islands, WTYY: Western Mediterranean Tyrrhenian Sea, n = 277, Table S1) at each life stage were collected across the species range between 2009 and 2012 (Fig. 1, Table S1) where tissue samples from each specimen were preserved in 96% ethanol or RNAlater (Thermo Fisher Scientific, USA) and stored at –20 °C until further processing. Archived vertebrae (HBOS: Historical Bosphorus, HADR: Historical Adriatic Sea, HION: Historical Ionian Sea, HTYR: Historical Tyrrhenian Sea: n = 147, Table S1) from the Massimo Sella Archive (see<sup>11</sup>) were collected between 1911 and 1941 (Fig. 1). Archaeological vertebrae (n = 136, Table S1) were retrieved from several excavations (Fig. 1) including 4th–15th century CE Yenikapi (HIST: Historical Istanbul, Turkey)<sup>43</sup>, 2nd century BCE–5th century CE Baelo Claudia (HBC: Historical Baelo Claudia, Spain)<sup>44</sup>, 2nd century BCE Tavira (HTAV: Historical Tavira, Portugal), and 4th–2nd century BCE Palacio de Justicia, (HPJ: Historical Palacio de Justicia, Spain)<sup>45</sup>. See Supplementary Materials 1 for more details on historical samples and their dating.

**Contemporary DNA extractions.** DNA was isolated from fin (adults) or muscle (juveniles, young-of-the-year) of contemporary samples (Table S1) as part of another study<sup>14</sup> using the Wizard<sup>SV96</sup> Genomic DNA Purification Kit (Promega, USA), following the manufacturer's instructions. Quantification was performed

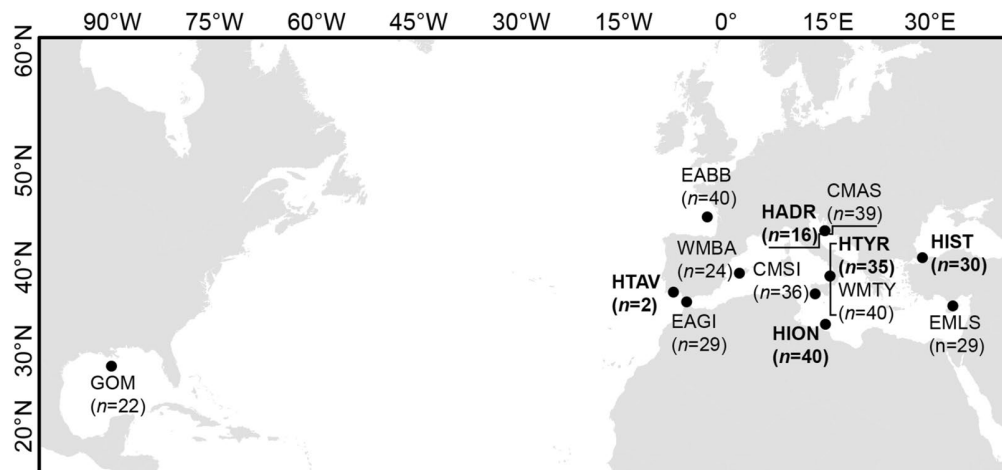


**Figure 1.** Map of the collection location for samples used in analyses. Historical (archival and archaeological) sample groups (in boldface, denoted with H) use approximate locations and the locations of archaeological sites where fish remains were recovered. Map created using ESRI ArcMap (v.10.6, <https://arcgis.com>). Only sample groups that were successfully genotyped and analysed are displayed. Numbers (*n*) represent those included in the final analysis for each sample group.

using a NanoDrop 2000 (Thermo Fisher Scientific, USA). Negative controls indicated that no cross-contamination took place between samples.

**Ancient DNA extractions.** Archival and archaeological samples underwent ancient DNA (aDNA) extraction in sterile, PCR-free conditions at the Ancient DNA Laboratory of the Department of Cultural Heritage (University of Bologna, Ravenna Campus, Italy), as part of another study which investigated their species identification via barcoding<sup>46</sup>. All bone specimens were sprayed with 1–2% sodium hypochlorite (bleach), left to soak for ten minutes, rinsed with distilled water and air-dried (as per<sup>47</sup>). Specimens were then mechanically cleaned using sandpaper, and the bleaching process was repeated. After, each specimen was exposed to UV light (254 nm) for 15 min before drilling to obtain ~200 mg bone powder. Bones that were too small for drilling were bisected, and their inner matrices were crushed.

Isolation of aDNA was performed using a modified version of Dabney et al.<sup>48,49</sup>. Briefly, ~200 mg of bone powder from each sample was divided in two and placed into separate tubes. After an overnight incubation in EDTA (0.5 M, pH 8.0) and proteinase K, lysates (1000 µl) of each sample were pooled and combined with 3000 µl binding buffer composed of guanidine thiocyanate (5 M), Tween 20 (0.05%), isopropyl alcohol (40% v/v), sodium acetate (90 mM, pH 5.2), and distilled water. This mixture was then centrifuged through a MinElute spin column (Qiagen, Germany), and washed twice with 720 µl PE buffer, before a final elution in 60 µl of distilled water.

The total DNA obtained from each extraction was quantified using a Qubit<sup>®</sup> dsDNA HS (High Sensitivity) Assay Kit (Thermo Fisher Scientific, USA). Negative controls employed for each batch of samples extracted indicated an undetectable level of contamination (< 500 pg/ml).

**DNA genotyping.** A total of 273 contemporary samples, and 280 historical (145 archival and 135 archaeological) samples contained sufficient quantities of DNA (100 ng total) for genotyping (Table S1). Samples were genotyped using a 96 SNP-panel we developed from SNP's identified by two studies<sup>14,30</sup> that were polymorphic between contemporary sample groups (see<sup>14</sup>) or matched with gene functions. To identify protein association we blasted the flanking regions of these loci against sequences for Atlantic cod<sup>50</sup>, sea bass (*Dicentrarchus labrax*)<sup>51</sup>, BFT<sup>52,53</sup> and an umbrella set of teleost sequences, on NCBI GenBank (<https://blast.ncbi.nlm.nih.gov/Blast.cgi>, Table S2) using the blastn option. Queries were considered matches if alignment coverage was > 80% and identity scores were > 80% (Table S2).

SNP genotyping was conducted first using Fluidigm 96.96 Dynamic Array<sup>™</sup> Integrated Fluidic Circuits (Probes: SNPtype-FAM:SNPtype-HEX, Passive reference: ROX) on the BioMarkHD034 platform (SGIKER, Spain). Historical samples were re-genotyped at a second facility using the Fluidigm EP1 platform (ABL, Bedford Institute of Oceanography, Canada) to assess genotype error rates. Genotyping employed two negative controls for each run, which confirmed no cross-contamination, and three positive controls (CMAS01, CMAS02, CMAS03), reporting identical genotypes. Similarly, 21 (7.5%) historical samples were extracted and genotyped twice and reported acceptable replicates at 97.8 ± 3.6% accuracy.

**Quality control filtering.** Prior to analyses, two loci (SNP85, SNP86, Table S2) with low call rates (98–100% missing data) were discarded. Individuals (148 out of 553, 26.7%) and two further loci (SNP45, SNP79) that contained > 10% missing data were then removed. Inconsistencies between the two facilities at the remain-

	Contemporary								Historical				
	GOM	CMAS	CMSI	EABB	EAGI	EMLS	WMBA	WMTY	HADR	HION	HTYR	HIST	HTAV
N	22	39	36	40	29	29	24	40	16	40	35	30	2
aR <sup>a</sup>	177	178	178	178	178	176	176	177	175	177	177	177	139
H <sub>e</sub> <sup>a</sup>	0.346	0.369	0.364	0.359	0.369	0.367	0.369	0.365	0.380	0.358	0.362	0.367	0.353
H <sub>o</sub> <sup>a</sup>	0.332	0.358	0.358	0.344	0.326	0.372	0.377	0.340	0.357	0.344	0.355	0.353	0.305
P <sub>HW</sub>	0.936	0.932	0.973	0.980	1.000	0.197	0.155	1.000	0.977	0.992	0.902	0.971	0.956
F <sub>IS</sub> <sup>a</sup>	0.032	0.024	0.033	0.034	0.137	-0.018	-0.022	0.066	0.052	0.041	0.023	0.038	-

**Table 1.** Genetic diversity, Hardy–Weinberg deviation, and F<sub>IS</sub> in contemporary and historical (archival and archaeological) sample groups. n, number of samples analysed, aR, allelic richness; H<sub>e</sub>, mean expected heterozygosity; H<sub>o</sub>, mean observed heterozygosity; P<sub>HW</sub>, P value of the Hardy–Weinberg equilibrium deviation test; F<sub>IS</sub>, inbreeding coefficient. <sup>a</sup>All unpaired t-test values between contemporary and historical samples (excluding GOM, HTAV) were non-significant.

	Contemporary								Historical			
	GOM	CMAS	CMSI	EABB	EAGI	EMLS	WMBA	WMTY	HADR	HION	HTYR	HIST
<b>Separate</b>												
n	14	32	27	30	-	14	16	36	-	24	24	18
N <sub>e</sub>	140	164	391	1454	-	2515	140	150	-	825	60	14
CI	56–∞	78–799	111–∞	158–∞	-	68–∞	46–∞	53–∞	-	118–∞	40–114	11–18
<b>Pooled</b>												
n	0	32	27	30	4	14	16	36	4	24	24	18
N <sub>e</sub>	939								298			
CI	497–5465								178–787			

**Table 2.** Effective population size (N<sub>e</sub>) and 95% confidence Intervals of contemporary and historical sample groups for samples (n) consistently scored across all 89 neutral loci analysed herein, under two approaches, where separate estimates were made for each sample group and for contemporary and historical pools.

ing 92 loci were then assessed. The remaining 146 historical individuals were subject to further filtering whereby they were removed if their genotypes were inconsistent between the two facilities at > 5% of loci. This removed a further 21 (14.4%) historical individuals achieved an overall genotyping success of 98.8% at 92 loci. Sample groups that contained a single individual as a result of filtering (HBOS, Table S1) were also removed. Historical duplicate samples resulting from the potential sampling of two or more bone specimens of the same individual were identified and removed by applying the function `clonecorrect` in the `Poppr` package<sup>54</sup> as implemented in R v.4.0.3<sup>55</sup>. A single clone was evident in the HIST archaeological sample group (Table 1).

**Loci evaluation.** Deviation from Hardy–Weinberg equilibrium (HWE) was assessed at each locus using the R package `Pegas`<sup>56</sup>. Linkage disequilibrium (LD) between loci was tested using the R package `Genepop`<sup>57</sup>. Outlier loci were identified using `Bayescan`<sup>58</sup> and `OutFLANK v0.2`<sup>59</sup> to obtain a neutral dataset and identify potential adaptive responses. Analysis was run excluding the western Atlantic sample group (GOM) between the following: all sample groups, pooled contemporary and historical sample groups, contemporary sample groups, and historical sample groups. Loci detected as outliers were removed from the dataset prior to demographic analyses and investigated as follows: gene association was inferred from the above `blastn` searches, and non-synonymous mutations were explored with the `Expassy Translation` tool as implemented online (<https://web.expassy.org/translate>). Default settings were used in the analyses. Significance was judged using the False Discovery Rate (FDR)<sup>60</sup> approach at the 5% level, as calculated using 999 permutations.

**Genetic diversity.** Allelic richness (aR), heterozygosity expected/observed (H<sub>e</sub>, H<sub>o</sub>), and the inbreeding coefficient F<sub>IS</sub>, were calculated for each sample group with the R package `Hierfstat`<sup>61</sup>. Significance of heterozygote excess was calculated with `Genepop` in R using the global excess method and default settings. Differences in aR, H<sub>e</sub>, H<sub>o</sub> and F<sub>IS</sub> between pooled contemporary and historical sample groups were assessed using unpaired t-tests in R. Significance was judged at the 5% level. Effective population size (N<sub>e</sub>) estimates were calculated only for samples consistently scored across all 89 neutral loci, as summarised in Table 2. Estimations were calculated using the linkage disequilibrium approach<sup>62</sup> as implemented in `NeEstimator v2.1`<sup>63</sup> and an allele frequency threshold of 0.01. A random down-sampling to generate and analyse equal-size groups is summarised in Table S3. Because N<sub>e</sub> estimates are often unreliable at low sample sizes<sup>64</sup>, we calculated per locus round-robin estimates of minor allele frequencies in R (as per<sup>65</sup>) and plotted trajectories between temporal sample groups. We performed a hierarchical analysis of molecular variance (AMOVA) in `Poppr`, with 10,000 permutations to assess



	$\Sigma$	% variance	<i>p</i> value
Within samples	31.203	96.010	<0.001
Between samples	1.203	3.703	0.001
Between sample groups	0.087	0.268	0.003
Between contemporary and historical groups	0.005	0.017	0.306

**Table 3.** Variance of the eastern Atlantic and Mediterranean BFT samples as computed by AMOVAs using a hierarchical approach as indicated by the four levels.

significance. AMOVAs were performed excluding the GOM sample group on the following levels: between periods; between sample groups; between samples (i.e., individuals); and within samples.

**Population structure.** A discriminant analysis of principal components (DAPC) was performed with the R package Adegenet<sup>66</sup> to explore how the historical groups relate to the contemporary reference groups. DAPC is a geometric clustering method free of HWE and LD assumptions, that attempts to maximise the inter-variation between clusters while minimising the intra-variation observed within clusters. DAPC clusters were set a priori to the number of sample groups. We retained 4 discriminant functions and the number of principal components (PC's) according to the function `optim.a.score`, based on an initial selection of all PC's before refinement. Population structuring was also evaluated using STRUCTURE v.2.3.4<sup>67</sup>, which implements a Bayesian clustering method to identify the most likely number of populations (K). We followed the Evano et al.<sup>68</sup> method, and thus, we carried out 10 runs per each value of K ranging from 1 to 10. Runs used the `locprior` and `admixture` models and assumed correlated allele frequencies. Each run used 500,000 burn-in and Markov Chain Monte Carlo replicates. We estimated the ad hoc statistic  $\Delta K$  in order to infer the most likely number of populations using STRUCTURE HARVESTER<sup>69</sup>. CLUMPAK<sup>70</sup> was used to merge the 10 runs from the most probable K, and reported similarity scores > 95. We used a hierarchical approach to improve resolution due to the identification of 5 outliers (EAGI 6 & 17, WMTY 52, 57 & 66) in two modern sample groups that constituted two distinct populations at K = 3 in the first run. Hence, these individuals were removed from the dataset and STRUCTURE was run a second time. Pairwise distances between sample groups were calculated with Nei's estimator of  $F_{ST}$ <sup>71</sup> in the `hierfstat` R package, using 999 permutations to calculate the respective p-values, which were judged for significance under the FDR approach at the 5% level.

## Results

**Loci evaluation.** Overall, 259 contemporary, and 123 historical (91 archival and 32 archaeological) samples were analysed at 92 loci (Table S1). No loci deviated from HWE or were in LD in more than a single population. BayeScan and OutFLANK both detected three loci (SNP41, SNP43 & SNP93, Table S1, Figure S1) as outliers. Loci SNP41 and SNP43 were outliers between contemporary sample groups and locus SNP93 was an outlier between historical sample groups. Locus SNP41 was identified as a putative adaptive response after being detected as an outlier between pooled contemporary and historical groups. Locus SNP41 was found to be in potential association with the gene *SYNM* that encodes Synemin, which is an intermediate filament protein. This putative adaptive locus was found to be under selection in all contemporary sample groups except CMSI, comprising a nucleotide mutation (T to A) that was non-synonymous, resulting in the production of glutamine instead of histidine. In contrast, SNP41 was not under selection in a single historical sample group.

**Genetic diversity.** We found no significant differences in gene diversity  $aR$  ( $p=0.181$ ,  $t(11)=1.426$ ),  $H_e$  ( $p=0.923$ ,  $t(11)=0.099$ ) and  $H_o$  ( $p=0.575$ ,  $t(11)=0.578$ ) between pooled contemporary and historical groups (Table 1). Heterozygote deficiency was not significant in any sample group (Table 1). Inbreeding ( $F_{IS}$ ) was rare within all sample groups (Table 1) and was not significantly different between pooled contemporary and historical samples ( $p=0.939$ ,  $t(9)=0.0791$ ). The dataset lacked power to define reliable estimates of  $N_e$  using both methods for each sample group i.e., our CIs contained infinity until they were pooled (Table 2). Randomly excluding samples to create equal size sample groups had minimal influence on estimations (Table S3).  $N_e$  estimates were higher for both contemporary sample groups, analysed separately, and the contemporary eastern Atlantic and Mediterranean when pooled (Table 2). Allele trajectories (Figure S1) showed stochastic fluctuations in minor allele frequencies between all sample groups, and no consistent drop-out or over-estimation in all contemporary or historical sample groups, respectively. Within the eastern Atlantic and Mediterranean samples, AMOVAs indicated significant differences in variance within and between samples, and between sample groups, but not between periods (Table 3, Figure S2).

**Population structure.** DAPC clustered eastern Atlantic and Mediterranean sample groups together while the western Atlantic (GOM) sample group was substantially separated (Fig. 2). Considerable overlap was observed between contemporary and historical clusters of the eastern Atlantic and Mediterranean.  $\Delta K$  suggested that the most likely number of populations identified with STRUCTURE was K = 3. All individuals shared mixed membership (q). Separate structuring of the GOM sample group was evident and the historical sample group HIST contained three individuals with this signature (Fig. 3). Overall, no evidence of population structure was evident between contemporary or historical sample groups of the eastern Atlantic and Mediterranean (Figs. 2,

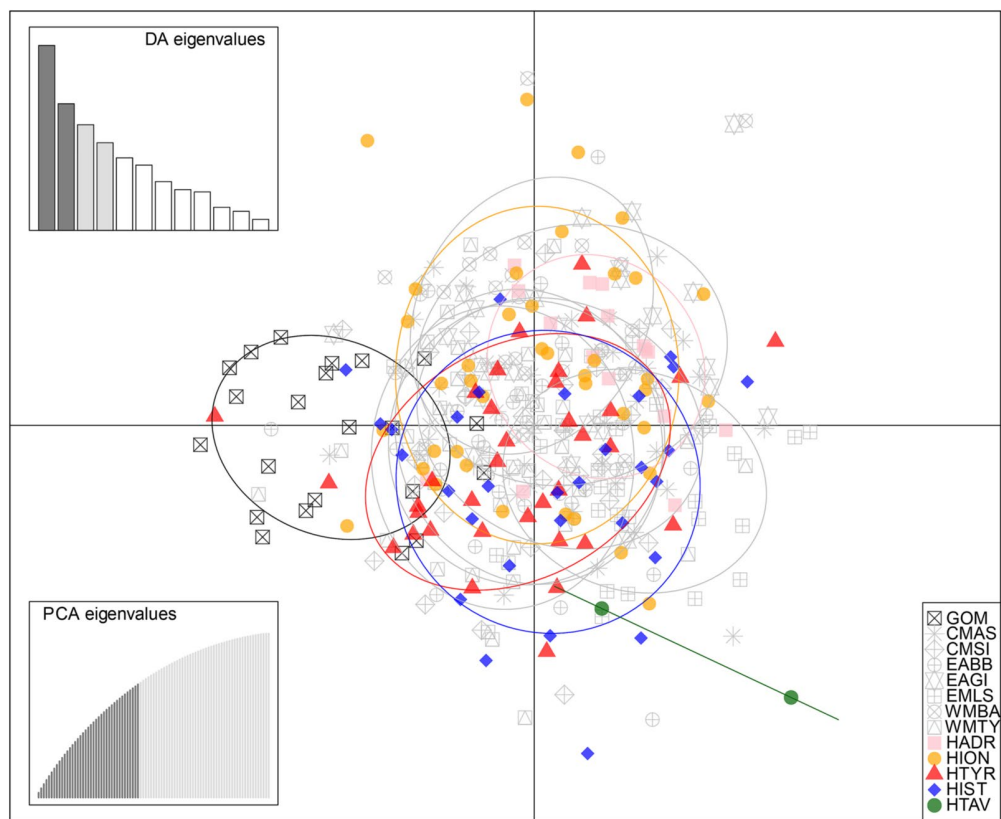


**Figure 2.** Discriminant analysis of principal components scatterplot showing how historical (archival and archaeological, denoted with H) sample groups relate to contemporary reference populations of the Gulf of Mexico (GOM) and the eastern Atlantic and Mediterranean. DAPC cluster ellipses were set to contain 95% of genotypes. Discriminant analysis (DA) eigenvalues and principal component analysis (PCA) eigenvalues were selected as displayed to avoid overfitting, utilising the *optim.a.score* approach within the R package *adegenet*.

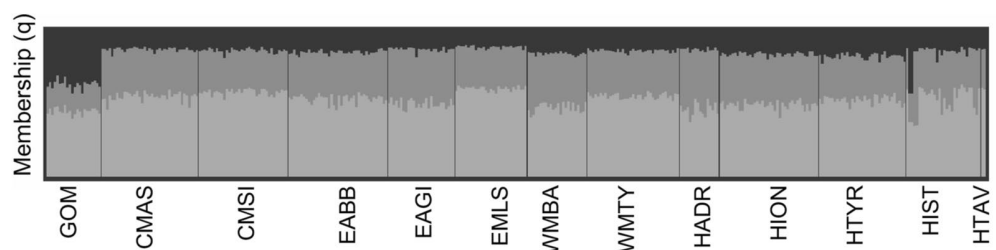


**Figure 3.** STRUCTURE barplot showing membership probabilities ( $q$ ) for each sample group analysed herein with  $K=3$  (each represented by a different shade).  $K=3$  was the most likely number of populations identified by the  $\Delta K$  method. Historical (archival and archaeological) sample groups are denoted with H).

3). Pairwise  $F_{ST}$  values were significant between the GOM sample group and all others (Table 4). In addition, the sample groups EMLS and WMBA, and EAGI and HIST were significantly different. No other significant differences were observed between contemporary and historical sample groups.

## Discussion

We found no evidence of genetic diversity loss or population restructuring in contemporary BFT sample groups of the eastern Atlantic and Mediterranean compared with those from the early 20th century CE prior to spawning biomass depletion and species range contraction<sup>22,25</sup>, and the 4th–15th century CE prior to a significant period of intense trap fishing marked by fluctuating catches<sup>26,27</sup>. If overfishing had resulted in a genetic bottleneck, we would expect to see significant decreases in minor allele frequencies, allelic richness, and observed heterozygosity<sup>72</sup> for contemporary samples compared with historical samples. Therefore, we would also expect to observe an increase in inbreeding and a decrease in effective population size<sup>8</sup>, which we did not. The impact

	Contemporary								Historical				
	GOM	CMAS	CMSI	EABB	EAGI	EMLS	WMBA	WMTY	HADR	HION	HTYR	HIST	HTAV
GOM		<b>0.001</b>	<b>0.001</b>	<b>0.001</b>	<b>0.001</b>	<b>0.001</b>	<b>0.001</b>	<b>0.001</b>	<b>0.001</b>	<b>0.001</b>	<b>0.001</b>	<b>0.001</b>	<b>0.001</b>
CMAS	0.0154		0.643	0.387	0.065	0.153	0.023	0.127	0.446	0.810	0.351	0.450	0.425
CMSI	0.0128	-0.0009		0.566	0.053	0.448	0.045	0.364	0.0295	0.602	0.029	0.538	0.221
EABB	0.0118	0.0006	-0.0004		0.108	0.111	0.174	0.416	0.749	0.635	0.593	0.625	0.702
EAGI	0.0240	0.0041	0.0046	0.0033		0.002	0.124	0.045	0.155	0.249	0.004	<b>0.001</b>	0.615
EMLS	0.0255	0.0027	0.0003	0.0034	0.0096		<b>0.001</b>	0.002	0.194	0.015	0.009	0.398	0.568
WMBA	0.0171	0.0064	0.0051	0.0029	0.0037	0.0109		0.116	0.689	0.273	0.007	0.085	0.103
WMTY	0.0167	0.0026	0.0007	0.0003	0.0047	0.0087	0.0035		0.099	0.022	0.197	0.597	0.413
HADR	0.0228	0.0004	0.0017	-0.0025	0.0040	0.0037	-0.0024	0.0048		0.853	0.248	0.876	0.211
HION	0.0129	-0.0018	-0.0006	-0.0008	0.0017	0.0059	0.0016	0.0049	-0.0040		0.217	0.562	0.238
HTYR	0.0117	0.0016	0.0053	-0.0004	0.0083	0.0070	0.0087	0.0019	0.0026	0.0017		0.155	0.351
HIST	0.0155	0.0003	-0.0003	-0.0007	0.0097	0.0008	0.0042	-0.0007	-0.0047	-0.0004	0.0027		0.594
HTAV	0.0350	0.0037	0.0183	-0.0127	-0.0079	-0.0046	0.0322	0.0035	0.0201	0.0168	0.0085	-0.0066	

**Table 4.** Pairwise  $F_{ST}$  (below the diagonal) and non-corrected P values (above the diagonal) between contemporary and historical sample groups.  $p$  values that were significant after FDR correction are presented in boldface.

of overfishing on genetic diversity and allele frequencies has been observed in a variety of studies that directly test archaeological and archival samples<sup>34–38</sup>. At its most extreme, overfishing has been observed to restructure marine fish populations<sup>36</sup>, yet we found no evidence of genetic restructuring in BFT. Likewise, a recent study found that Atlantic cod had not been impacted by 20th century overfishing at the genomic level<sup>42</sup>. Our findings are similar to those of Riccioni et al.<sup>11</sup> using microsatellite markers, though we did not observe significant sub-structuring within Mediterranean BFT as they did, and this is yet to be resolved to clarify alternative population structure hypotheses<sup>18,23,73</sup>. No recent genetic study, however, has detected population structure within the eastern Atlantic and Mediterranean BFT<sup>14,15,74</sup>. Perspectives from threatened populations of other taxa, inform us that a wide range of genomic responses are expected, along a continuous scale from resistance to collapse<sup>34,75–79</sup>, and recovery<sup>33,80–82</sup>. Despite differences between taxa, these data would suggest that there is likely no “one-size fits all” response to the depletion of marine fish populations, according to species life history traits and the extent and rate of overfishing.

The most common explanation for the maintenance of genetic diversity in threatened populations is that gene flow acts as a buffer<sup>72</sup>. This is plausible for BFT, though its western Atlantic population is smaller than the eastern Atlantic and Mediterranean population (ca. 1/10 the size) and was heavily fished itself since at least the early 19th century<sup>83,84</sup>. Connectivity with alternative spawning sites (e.g., the Slope Sea<sup>16</sup>, the Bay of Biscay<sup>19</sup>, Azores, Canary Islands, Ibero-Moroccan, Gulf of Guinea<sup>13,17</sup>) remains poorly understood, and the unresolved frequency and duration of spawning at these locations means we cannot assess its effect on gene flow. Likewise, introgression occurs at a low rate between *Thunnus* species<sup>85</sup> but could also act as a buffer. On the other hand, eastern BFT may be resilient towards genetic erosion due to their relatively large population size (enhanced by connectivity between spawning sites within the Mediterranean), and a long life cycle which promotes heavily overlapping generations<sup>13,17</sup>. In any case, our findings leave us with two possible explanations; either (1) overfishing was not severe enough to cause a genetic bottleneck in BFT, or (2) our observation of significant demographic changes was hindered by the methods we employed.

To address this first point, it is evident that BFT were overfished, at least in the 20th and early 21st century, if not as we suspect between the 16th–19th century. Studies by the management body ICCAT (the International Commission for the Conservation of Atlantic Tunas)<sup>25</sup>, and independent estimates e.g.,<sup>22</sup> suggested that BFT abundance and range declined by 70% and 46–53%, respectively, between 1960 and 2010. However, there is debate on the extent of the population decline, where on one hand, impending population collapse was predicted in 2009<sup>86</sup>, yet on the other, poorly understood population dynamics and incorrect assignments of catches has caused uncertainty in population estimates<sup>73,87</sup>. Hence, it is difficult to deduce whether we should expect to find evidence of a genetic bottleneck because the recent recovery of the population within just two generations from its lowest point in 2007<sup>88</sup> could suggest that either the population decline was not that severe, or that overfishing did trigger a severe population decline but BFT is remarkably resilient due to its complex life history traits.

Nonetheless, fishing effort is not the only factor that influences catches and abundance (as shown for the historical trap fishery data<sup>29</sup>), which one might expect to be reflected in genetic diversity and structure. Climate is likely the largest regulator of recruitment and thus fish abundance<sup>89,90</sup> and as a pelagic species, BFT are certainly no exception<sup>91,92</sup>. Therefore, one might expect to find evidence of fluctuating abundance—and potentially genetic diversity—that is merely exacerbated by fishing<sup>28</sup>. BFT’s Atlantic distribution varies with Atlantic multidecadal oscillation phases<sup>93</sup>, and thus gene flow and inbreeding is expected to vary accordingly because connectivity of populations is enhanced in warm years as ranges overlap, as attested by isotope data<sup>94</sup>. This is notwithstanding time-related effects driven by evolutionary processes i.e., mutation and genetic drift that we might expect to alter allele frequencies over time. Therefore, our observation of homogeneity between contemporary and historical BFT samples is somewhat striking. One might pose the question: at what rate should we expect to observe

demographic changes at the genomic level? We analysed moderate sample sizes from 1911 to 1926 (~20 generations ago) and the 4th–15th century (~100+ generations ago), yet we did not detect time-related effects. Thus, to address this, even at conservative mutation rates lower than those shown for marine fish<sup>95</sup>, we would expect to observe changes in allele frequencies as a result of genetic drift alone.

Alternatively, our observations may be explained by our methodological approach. By pre-selecting loci that were polymorphic in contemporary sample groups, our data are subject to an unknown degree of ascertainment bias. Theoretically, ascertainment bias could influence any analysis or inference based on SNP allele frequencies when SNPs are discovered in a limited sample but applied in another context (e.g., our historical sample groups)<sup>96</sup>. The expectation that this should inflate diversity in the ascertainment sample is a widely accepted hindrance of SNP-panel studies<sup>97–99</sup>. Studies usually correct for this by LD pruning<sup>100</sup> or modifying raw genotypes following maximum-likelihood simulations<sup>98</sup>, however this was not possible herein due to the few loci that were available. Indeed, the effect of ascertainment bias is likely to be exacerbated herein because we analysed few loci. This reduces the likelihood of detecting rare alleles and thereby erodes power<sup>97</sup> which is particularly crucial when differentiating marine samples due to high gene flow and low diversity in marine populations<sup>101</sup>. Theoretically, this might have inflated our estimates of genetic diversity among contemporary samples, and hence genetic diversity was comparatively low in historical samples. This theory is further supported by our AMOVA results and might explain why variance was lower than expected between temporal samples, and why structure was only observed between contemporary sample groups for which SNP discovery was made.

Moreover, our  $N_e$  estimate CIs often contained infinity, suggesting that we have little power to make any inferences on  $N_e$ . In many cases  $N_e$  was strikingly lower in (supposedly unimpacted) historical samples than the empirical rule-of-thumb threshold of  $N_e$  (500) proposed to maintain long-term genetic diversity in marine populations<sup>72</sup>. In any case,  $N_e$  is often unreliable when using sample sizes such as ours<sup>64</sup> and we caution the interpretation of our results for this reason. Additionally, our sampling strategy may have been limiting. For example, if genetic diversity had decreased following population declines (e.g., between 16th–18th century, and/or during the 20th and early 21st century) but was restored prior to our analogous archival samples of the early 20th century, or 2009–2012 contemporary samples, respectively. Species differ in their rates of genetic recovery according to their life history traits<sup>72</sup>, and as this rate is unknown in BFT, we cannot rule out this possibility.

Clearly aDNA approaches offer utility to fisheries management because long-term trends are understudied and we lack fisheries-independent indices<sup>7,90</sup>. However, genome-wide approaches are more likely to provide a better resolution to assess demographic impacts and adaptive responses. Assuming the availability of a reference genome, WGS approaches are increasingly cost-effective<sup>9</sup>, particularly for shallow sequencing<sup>102</sup>. This approach may also facilitate the recovery of data from arid Mediterranean specimens which were challenging to genotype herein due to their poor preservation<sup>46</sup>. Importantly, WGS would reduce ascertainment bias compared with SNP-genotyping. This is crucial where allele frequency distributions are used to infer demographic history, but also to scan for past targets of selection<sup>98</sup>. We were limited herein to detecting a single adaptive response in BFT: a potential change to the function of the protein synemin, which is a cytoskeletal protein that we speculate might be related to growth changes induced by size selective harvesting (FIE), although this remains to be tested. WGS studies able to detect additional loci under putative selection are ultimately required for the association of this response (and others) with natural or anthropogenic factors, in addition to discounting hitchhiking effects<sup>103</sup>.

## Conclusion

We identify that aDNA preserved within archival and archaeological fish remains has the potential to inform fisheries management by providing novel fisheries-independent baselines with which to observe unstudied long-term demographic and adaptive changes. We found no evidence that genetic diversity decreased or that populations restructured following several centuries of intense fishing, in line with a previous study<sup>11</sup>. This may hint at BFT's resilience which has been recently shown by rebounds in abundance<sup>25</sup> and a return to previous habitats<sup>88</sup>. However, we acknowledge limitations in our dataset i.e., few markers and the potential for ascertainment bias, and suggest that future studies might benefit from obtaining WGS data to observe rare alleles and reduce bias. Genome-wide data will be especially necessary to investigate adaptive responses, such as the putative selection on the cytoskeletal protein synemin found herein, and associate these with natural or anthropogenic factors to elucidate the drivers of change.

## Data availability

Flanking region sequences for each locus, and genotypes for all individuals, are attached as supplementary files.

Received: 7 May 2021; Accepted: 25 September 2021

Published online: 20 October 2021

## References

1. Pauly, D. *et al.* Towards sustainability in world fisheries. *Nature* **418**, 689–695 (2002).
2. Butchart, S. H. M. *et al.* Global biodiversity: Indicators of recent declines. *Science* **328**, 1164–1168 (2010).
3. Pinsky, M. L. & Palumbi, S. R. Meta-analysis reveals lower genetic diversity in overfished populations. *Mol. Ecol.* **23**, 29–39 (2014).
4. Neubauer, P., Jensen, O. P., Hutchings, J. A. & Baum, J. K. Resilience and recovery of overexploited marine populations. *Science* **340**, 347–349 (2013).
5. Lotze, H. K., Hoffmann, R. & Erlandson, J. Lessons from historical ecology and management. In *The Sea, Volume 19: Ecosystem-Based Management* (Harvard University Press, 2014).
6. Erlandson, J. M. & Rick, T. C. Archaeology meets marine ecology: The antiquity of maritime cultures and human impacts on marine fisheries and ecosystems. *Ann. Rev. Mar. Sci.* **2**, 231–251 (2010).

7. Schwerdtner Máñez, K. *et al.* The future of the oceans past: Towards a global marine historical research initiative. *PLoS ONE* **9**, e101466 (2014).
8. Palsbøll, P. J., Zachariah Peery, M., Olsen, M. T., Beissinger, S. R. & Bérubé, M. Inferring recent historic abundance from current genetic diversity. *Mol. Ecol.* **22**, 22–40 (2013).
9. Oosting, T. *et al.* Unlocking the potential of ancient fish DNA in the genomic era. *Evol. Appl.* **12**, 1513–1522 (2019).
10. Heino, M., Pauli, B. D. & Dieckmann, U. Fisheries-induced evolution. *Annu. Rev. Ecol. Evol. Syst.* **46**, 461–480 (2015).
11. Riccioni, G. *et al.* Spatio-temporal population structuring and genetic diversity retention in depleted Atlantic Bluefin tuna of the Mediterranean Sea. *Proc. Natl. Acad. Sci.* **107**, 2102–2107 (2010).
12. Cort, J. L. Age and growth of the bluefin tuna (*Thunnus thynnus*) of the Northeast Atlantic. In *Domestication of the bluefin tuna Thunnus thynnus thynnus. Cahiers Options Méditerranéennes (CIHEAM)* 45–49 (2003).
13. Mather, F. J., Mason, J. M. & Jones, A. C. *Historical document: life history and fisheries of Atlantic bluefin tuna.* (1995). NOAA Technical Memorandum NMFS-SEFSC – 370.
14. Puncher, G. N. *et al.* Spatial dynamics and mixing of bluefin tuna in the Atlantic Ocean and Mediterranean Sea revealed using next-generation sequencing. *Mol. Ecol. Resour.* **18**, 620–638 (2018).
15. Rodríguez-Ezpeleta, N. *et al.* Determining natal origin for improved management of Atlantic bluefin tuna. *Front. Ecol. Environ.* **17**, 439–444 (2019).
16. Richardson, D. E. *et al.* Discovery of a spawning ground reveals diverse migration strategies in Atlantic bluefin tuna (*Thunnus thynnus*). *Proc. Natl. Acad. Sci. USA* **113**, 3299–3304 (2016).
17. Piccinetti, C., Di Natale, A. & Arena, P. Eastern bluefin tuna (*Thunnus thynnus*, L.) reproduction and reproductive areas and season. *Collect. Vol. Sci. Pap. ICCAT/Recl. Doc. Sci. CICTA/Colecc. Doc. Cient. CICAA* **69**, 891–912 (2013).
18. Cort, J. L. & Abaunza, P. The present state of traps and fisheries research in the strait of Gibraltar. In *The Bluefin Tuna Fishery in the Bay of Biscay : Its Relationship with the Crisis of Catches of Large Specimens in the East Atlantic Fisheries from the 1960s* (eds. Cort, J. L. & Abaunza, P.) 37–78 (Springer International Publishing, 2019).
19. Alemany, F., Tensek, S. & Pagà García, A. ICCAT Atlantic-Wide Research programme for Bluefin Tuna (GBYP) activity report for the Phase 9 and the first part of Phase 10. *Collect. Vol. Sci. Pap. ICCAT/Recl. Doc. Sci. CICTA/Colecc. Doc. Cient. CICAA* **77**, 666–700 (2020).
20. MacKenzie, B. R. & Mariani, P. Spawning of bluefin tuna in the Black Sea: historical evidence, environmental constraints and population plasticity. *PLoS ONE* **7**, e39998 (2012).
21. Di Natale, A. The Eastern Atlantic bluefin tuna: Entangled in a big mess, possibly far from a conservation red alert. Some comments after the proposal to include bluefin tuna in CITES Appendix I. *Collect. Vol. Sci. Pap. ICCAT/Recl. Doc. Sci. CICTA/Colecc. Doc. Cient. CICAA* **65**(3), 1004–1043 (2010).
22. Worm, B. & Tittensor, D. P. Range contraction in large pelagic predators. *Proc. Natl. Acad. Sci. USA* **108**, 11942–11947 (2011).
23. Fromentin, J.-M. Lessons from the past: Investigating historical data from bluefin tuna fisheries. *Fish Fish.* **10**, 197–216 (2009).
24. Siskey, M. R., Wilberg, M. J., Allman, R. J., Barnett, B. K. & Secor, D. H. Forty years of fishing: Changes in age structure and stock mixing in northwestern Atlantic bluefin tuna (*Thunnus thynnus*) associated with size-selective and long-term exploitation. *ICES J. Mar. Sci.* **73**, 2518–2528 (2016).
25. ICCAT. Report of the 2020 second ICCAT intersessional meeting of the bluefin tuna species group. Online, 20–28 July 2020. *SECOND BFT INTERSESSIONAL MEETING – ONLINE 2020* (2020).
26. Ravier, C. & Fromentin, J.-M. Long-term fluctuations in the eastern Atlantic and Mediterranean bluefin tuna population. *ICES J. Mar. Sci.* **58**, 1299–1317 (2001).
27. Garcia, A. P. *et al.* Report on revised trap data recovered by ICCAT GBYP from Phase 1 to Phase 6. *Collect. Vol. Sci. Pap. ICCAT/Recl. Doc. Sci. CICTA/Colecc. Doc. Cient. CICAA* **73**, 2074–2098 (2017).
28. Anderson, C. N. K. *et al.* Why fishing magnifies fluctuations in fish abundance. *Nature* **452**, 835–839 (2008).
29. Di Natale, A. & Idrissi, M. Factors to be taken into account for a correct reading of tuna trap catch series. *Collect. Vol. Sci. Pap. ICCAT/Recl. Doc. Sci. CICTA/Colecc. Doc. Cient. CICAA* **67**, 242–261 (2012).
30. Laconcha, U. *et al.* New nuclear SNP markers unravel the genetic structure and effective population size of Albacore Tuna (*Thunnus alalunga*). *PLoS ONE* **10**, e0128247 (2015).
31. Speller, C. F. *et al.* High potential for using DNA from ancient herring bones to inform modern fisheries management and conservation. *PLoS ONE* **7**, e51122 (2012).
32. Montes, I. *et al.* No loss of genetic diversity in the exploited and recently collapsed population of Bay of Biscay anchovy (*Engraulis encrasicolus*, L.). *Mar. Biol.* **163**, 98 (2016).
33. Chapman, D. D. *et al.* Genetic diversity despite population collapse in a critically endangered marine fish: The smalltooth sawfish (*Pristis pectinata*). *J. Hered.* **102**, 643–652 (2011).
34. Hutchinson, W. F., van Oosterhout, C., Rogers, S. I. & Carvalho, G. R. Temporal analysis of archived samples indicates marked genetic changes in declining North Sea cod (*Gadus morhua*). *Proc. Biol. Sci.* **270**, 2125–2132 (2003).
35. Ólafsdóttir, G. Á., Westfall, K. M., Edvardsson, R. & Pálsson, S. Historical DNA reveals the demographic history of Atlantic cod (*Gadus morhua*) in medieval and early modern Iceland. *Proc. Biol. Sci.* **281**, 20132976 (2014).
36. Bonanomi, S. *et al.* Archived DNA reveals fisheries and climate induced collapse of a major fishery. *Sci. Rep.* **5**, 15395 (2015).
37. Nielsen, E. E., Hansen, M. M. & Loeschcke, V. Analysis of microsatellite DNA from old scale samples of Atlantic salmon *Salmo salar* : A comparison of genetic composition over 60 years. *Mol. Ecol.* **6**, 487–492 (1997).
38. Johnson, B. M., Kemp, B. M. & Thorgaard, G. H. Increased mitochondrial DNA diversity in ancient Columbia River basin Chinook salmon *Oncorhynchus tshawytscha*. *PLoS ONE* **13**, e0190059 (2018).
39. Bowles, E., Marin, K., Mogensen, S., MacLeod, P. & Fraser, D. J. Size reductions and genomic changes within two generations in wild walleye populations: associated with harvest?. *Evol. Appl.* **13**, 1128–1144 (2020).
40. Royle, T. C. A. *et al.* Investigating the sex-selectivity of a middle Ontario Iroquoian Atlantic salmon (*Salmo salar*) and lake trout (*Salvelinus namaycush*) fishery through ancient DNA analysis. *J. Archaeol. Sci. Rep.* **31**, 102301 (2020).
41. Therkildsen, N. O. *et al.* Microevolution in time and space: SNP analysis of historical DNA reveals dynamic signatures of selection in Atlantic cod. *Mol. Ecol.* **22**, 2424–2440 (2013).
42. Pinsky, M. L. *et al.* Genomic stability through time despite decades of exploitation in cod on both sides of the Atlantic. *Proc. Natl. Acad. Sci. USA* **118**, (2021).
43. Onar, V., Pazvant, G. & Armutak, A. Radiocarbon dating results of the animal remains uncovered at Yenikapi Excavations. In *Istanbul Archaeological Museums, Proceedings of the 1st Symposium on Marmaray-Metro Salvage Excavations* 249–256 (2008).
44. Bernal-Casasola, D., Expósito, J. A. & Díaz, J. J. The Baelo Claudia paradigm: The exploitation of marine resources in Roman ceterariae. *J. Marit. Archaeol.* **13**, 329–351 (2018).
45. Bernal, D. & Monclova, A. Pescar con Arte. Fenicios y romanos en el origen de los aparejos andaluces. *Monografías del Proyecto Sagena* **3**, (2011).
46. Puncher, G. N. *et al.* Comparison and optimization of genetic tools used for the identification of ancient fish remains recovered from archaeological excavations and museum collections in the Mediterranean region. *Int J Osteoarchaeol* **29**, 365–376 (2019).
47. Kemp, B. M. & Smith, D. G. Use of bleach to eliminate contaminating DNA from the surface of bones and teeth. *Forensic Sci. Int.* **154**, 53–61 (2005).

48. Dabney, J. *et al.* Complete mitochondrial genome sequence of a Middle Pleistocene cave bear reconstructed from ultrashort DNA fragments. *Proc. Natl. Acad. Sci. USA* **110**, 15758–15763 (2013).
49. Serventi, P. *et al.* Iron Age Italic population genetics: The Piceni from Novilara (8th–7th century BC). *Ann. Hum. Biol.* **45**, 34–43 (2018).
50. Star, B. *et al.* The genome sequence of Atlantic cod reveals a unique immune system. *Nature* **477**, 207–210 (2011).
51. Tine, M. *et al.* European sea bass genome and its variation provide insights into adaptation to euryhalinity and speciation. *Nat. Commun.* **5**, 5770 (2014).
52. Chini, V. *et al.* Genes expressed in bluefin tuna (*Thunnus thynnus*) liver and gonads. *Gene* **410**, 207–213 (2008).
53. Gardner, L. D., Jayasundara, N., Castilho, P. C. & Block, B. Microarray gene expression profiles from mature gonad tissues of Atlantic bluefin tuna, *Thunnus thynnus* in the Gulf of Mexico. *BMC Genomics* **13**, 530 (2012).
54. Kamvar, Z. N., Tabima, J. F. & Grünwald, N. J. Poppr: An R package for genetic analysis of populations with clonal, partially clonal, and/or sexual reproduction. *PeerJ* **2**, e281 (2014).
55. Team, R. C. R development core team. *RA Lang. Environ. Stat. Comput.* **55**, 275–286 (2013).
56. Paradis, E. pegas: An R package for population genetics with an integrated–modular approach. *Bioinformatics* **26**, 419–420 (2010).
57. Rousset, F. genepop'007: A complete re-implementation of the genepop software for Windows and Linux. *Mol. Ecol. Resour.* **8**, 103–106 (2008).
58. Foll, M. & Gaggiotti, O. A genome-scan method to identify selected loci appropriate for both dominant and codominant markers: A Bayesian perspective. *Genetics* **180**, 977–993 (2008).
59. Whitlock, M. C. & Lotterhos, K. E. Reliable detection of loci responsible for local adaptation: Inference of a null model through trimming the distribution of FST. *Am. Nat.* **186**, S24–S36 (2015).
60. Benjamini, Y. & Hochberg, Y. Controlling the false discovery rate: A practical and powerful approach to multiple testing. *J. R. Stat. Soc.* (1995).
61. Goudet, J. hierfstat, a package for r to compute and test hierarchical F-statistics. *Mol. Ecol. Notes* **5**, 184–186 (2005).
62. Waples, R. S. A bias correction for estimates of effective population size based on linkage disequilibrium at unlinked gene loci. *Conserv. Genet.* **7**, 167–184 (2006).
63. Do, C. *et al.* NeEstimator v2: Re-implementation of software for the estimation of contemporary effective population size (Ne) from genetic data. *Mol. Ecol. Resour.* **14**, 209–214 (2014).
64. Wang, J., Santiago, E. & Caballero, A. Prediction and estimation of effective population size. *Heredity* **117**, 193–206 (2016).
65. Jenkins, T. L., Ellis, C. D., Triantafyllidis, A. & Stevens, J. R. Single nucleotide polymorphisms reveal a genetic cline across the north-east Atlantic and enable powerful population assignment in the European lobster. *Evol. Appl.* **12**, 1881–1899 (2019).
66. Jombart, T. *et al.* Package 'adegenet'. *Bioinform. Appl. Note* **24**, 1403–1405 (2008).
67. Pritchard, J. K., Stephens, M. & Donnelly, P. Inference of population structure using multilocus genotype data. *Genetics* **155**, 945–959 (2000).
68. Evanno, G., Regnaut, S. & Goudet, J. Detecting the number of clusters of individuals using the software STRUCTURE: A simulation study. *Mol. Ecol.* **14**, 2611–2620 (2005).
69. Earl, D. A. & vonHoldt, B. M. STRUCTURE HARVESTER: A website and program for visualizing STRUCTURE output and implementing the Evanno method. *Conserv. Genet. Resour.* **4**, 359–361 (2012).
70. Kopelman, N. M., Mayzel, J., Jakobsson, M., Rosenberg, N. A. & Mayrose, I. Clumpak: A program for identifying clustering modes and packaging population structure inferences across K. *Mol. Ecol. Resour.* **15**, 1179–1191 (2015).
71. Nei, M. *Molecular Evolutionary Genetics*. (Columbia University Press, 1987). <https://doi.org/10.7312/nei-92038>.
72. Frankham, R., Scientist Emeritus Jonathan, Briscoe, D. A. & Ballou, J. D. *Introduction to Conservation Genetics*. (Cambridge University Press, 2002).
73. Di Natale, A. Due to the new scientific knowledge, is it time to reconsider the stock composition of the Atlantic bluefin tuna? *Collect. Vol. Sci. Pap. ICCAT/Recl. Doc. Sci. CICTA/Colecc. Doc. Cient. CICA* **75**, 1282–1292 (2019).
74. Di Natale, A., Tensek, S. & Pagá García, A. ICCAT Atlantic-wide research programme for bluefin tuna (GBYP) activity report for the last part of phase and the first part of phase (2016–2017). [https://www.iccat.int/Documents/CVSP/CV074\\_2017/n\\_6/CV074\\_063100.pdf](https://www.iccat.int/Documents/CVSP/CV074_2017/n_6/CV074_063100.pdf) (2017).
75. Leonard, J. A. Ancient DNA applications for wildlife conservation. *Mol. Ecol.* **17**, 4186–4196 (2008).
76. Alter, S. E., Newsome, S. D. & Palumbi, S. R. Pre-whaling genetic diversity and population ecology in eastern Pacific gray whales: Insights from ancient DNA and stable isotopes. *PLoS ONE* **7**, e35039 (2012).
77. Cole, T. L. *et al.* Ancient DNA of crested penguins: Testing for temporal genetic shifts in the world's most diverse penguin clade. *Mol. Phylogenet. Evol.* **131**, 72–79 (2019).
78. Dures, S. G. *et al.* A century of decline: Loss of genetic diversity in a southern African lion-conservation stronghold. *Divers. Distrib.* **25**, 870–879 (2019).
79. Thomas, J. E. *et al.* Demographic reconstruction from ancient DNA supports rapid extinction of the great auk. *Elife* **8**, (2019).
80. Colson, I. & Hughes, R. N. Rapid recovery of genetic diversity of dogwhelk (*Nucella lapillus* L.) populations after local extinction and recolonization contradicts predictions from life-history characteristics. *Mol. Ecol.* **13**, 2223–2233 (2004).
81. McEachern, M. B., Van Vuren, D. H., Floyd, C. H., May, B. & Eadie, J. M. Bottlenecks and rescue effects in a fluctuating population of golden-mantled ground squirrels (*Spermophilus lateralis*). *Conserv. Genet.* **12**, 285–296 (2011).
82. Jangjoo, M., Matter, S. F., Roland, J. & Keyghobadi, N. Connectivity rescues genetic diversity after a demographic bottleneck in a butterfly population network. *Proc. Natl. Acad. Sci. USA* **113**, 10914–10919 (2016).
83. Porch, C. E., Bonhommeau, S., Diaz, G. A., Haritz, A. & Melvin, G. The journey from overfishing to sustainability for Atlantic bluefin tuna, *Thunnus thynnus*. In *The Future of Bluefin Tunas: Ecology, Fisheries Management, and Conservation* 3–44 (2019).
84. Di Natale, A., Macias, D. & Cort, J. L. Atlantic bluefin tuna fisheries: temporal changes in the exploitation pattern, feasibility of sampling, factors that can influence our ability to understand spawning structure and dynamics. *Collect. Vol. Sci. Pap. ICCAT/Recl. Doc. Sci. CICTA/Colecc. Doc. Cient. CICA* **76**, 354–388 (2020).
85. Viñas, J. & Tudela, S. A validated methodology for genetic identification of tuna species (genus *Thunnus*). *PLoS ONE* **4**, e7606 (2009).
86. MacKenzie, B. R., Mosegaard, H. & Rosenberg, A. A. Impending collapse of bluefin tuna in the northeast Atlantic and Mediterranean. *Conserv. Lett.* **2**, 26–35 (2009).
87. Collette, B. B. Bluefin tuna science remains vague. *Science* **358**, 879–880 (2017).
88. Nøttestad, L., Bøge, E. & Ferter, K. The comeback of Atlantic bluefin tuna (*Thunnus thynnus*) to Norwegian waters. *Fish. Res.* **231**, 105689 (2020).
89. Lehodey, P. *et al.* Climate variability, fish, and fisheries. *J. Clim.* **19**, 5009–5030 (2006).
90. Kuwae, M. *et al.* Sedimentary DNA tracks decadal-centennial changes in fish abundance. *Commun Biol* **3**, 558 (2020).
91. Domingues, R. *et al.* Variability of preferred environmental conditions for Atlantic bluefin tuna (*Thunnus thynnus*) larvae in the Gulf of Mexico during 1993–2011. *Fish. Oceanogr.* **25**, 320–336 (2016).
92. Reglero, P. *et al.* Pelagic habitat and offspring survival in the eastern stock of Atlantic bluefin tuna. *ICES J. Mar. Sci.* **76**, 549–558 (2019).

93. Faillettaz, R., Beaugrand, G., Goberville, E. & Kirby, R. R. Atlantic Multidecadal Oscillations drive the basin-scale distribution of Atlantic bluefin tuna. *Sci. Adv.* **5**, eaar6993 (2019).
94. Hanke, A. *et al.* Stock mixing rates of bluefin tuna from Canadian landings: 1975–2015. *Collect. Vol. Sci. Pap. ICCAT/Recl. Doc. Sci. CICTA/Colecc. Doc. Cient. CICAA* **74**, 2622–2634 (2017).
95. Fraser, D. J. *et al.* Comparative estimation of effective population sizes and temporal gene flow in two contrasting population systems. *Mol. Ecol.* **16**, 3866–3889 (2007).
96. Albrechtsen, A., Nielsen, F. C. & Nielsen, R. Ascertainment biases in SNP chips affect measures of population divergence. *Mol. Biol. Evol.* **27**, 2534–2547 (2010).
97. Clark, A. G., Hubisz, M. J., Bustamante, C. D., Williamson, S. H. & Nielsen, R. Ascertainment bias in studies of human genome-wide polymorphism. *Genome Res.* **15**, 1496–1502 (2005).
98. Lachance, J. & Tishkoff, S. A. SNP ascertainment bias in population genetic analyses: Why it is important, and how to correct it. *BioEssays* **35**, 780–786 (2013).
99. Hofreiter, M. *et al.* The future of ancient DNA: Technical advances and conceptual shifts. *BioEssays* **37**, 284–293 (2015).
100. Malomane, D. K. *et al.* Efficiency of different strategies to mitigate ascertainment bias when using SNP panels in diversity studies. *BMC Genomics* **19**, 22 (2018).
101. Bradbury, I. R. *et al.* Evaluating SNP ascertainment bias and its impact on population assignment in Atlantic cod, *Gadus morhua*. *Mol. Ecol. Resour.* **11**, 218–225 (2011).
102. Lou, R. N., Jacobs, A., Wilder, A. & Therkildsen, N. O. A beginner's guide to low-coverage whole genome sequencing for population genomics. *Mol. Ecol.* <https://doi.org/10.1111/mec.16077> (2020).
103. Schlotterer, C. Hitchhiking mapping—functional genomics from the population genetics perspective. *Trends Genet.* **19**, 32–38 (2003).

## Acknowledgements

We thank two anonymous reviewers whose comments improved the quality of the manuscript. This work was carried out under the provision of the FARB Project (University of Bologna), the ICCAT Atlantic Wide Research Programme for Bluefin Tuna (GBYP) Data Recovery Plan, the International Governance Strategy of Fisheries and Oceans Canada (F5211-180183 and F5211-160166), and the MARES Joint Doctorate programme selected under Erasmus Mundus and coordinated by Ghent University (Grant Number: FPA 2011-0016). This work is also a contribution to the MSCA SeaChanges ITN and was part-funded by EU Horizon 2020 (Grant Number: 813383).

## Author contributions

A.C. & F.T. conceived the study. G.N.P., A.C., F.T., B.M., A.M.M., N.Y.T., V.O. and D.B.C. collected tissues for analysis. G.N.P., E.C., A.H., S.A.P. and F.M. conducted the lab work. A.D.N., C.S., P.L.M. and R.C. provided data. A.J.A. performed the statistical analysis. A.J.A., G.N.P., A.C. and F.T. wrote the manuscript. All authors reviewed the manuscript.

## Competing interests

The authors declare no competing interests.

## Additional information

**Supplementary Information** The online version contains supplementary material available at <https://doi.org/10.1038/s41598-021-99708-9>.

**Correspondence** and requests for materials should be addressed to A.J.A. or G.N.P.

**Reprints and permissions information** is available at [www.nature.com/reprints](http://www.nature.com/reprints).

**Publisher's note** Springer Nature remains neutral with regard to jurisdictional claims in published maps and institutional affiliations.



**Open Access** This article is licensed under a Creative Commons Attribution 4.0 International License, which permits use, sharing, adaptation, distribution and reproduction in any medium or format, as long as you give appropriate credit to the original author(s) and the source, provide a link to the Creative Commons licence, and indicate if changes were made. The images or other third party material in this article are included in the article's Creative Commons licence, unless indicated otherwise in a credit line to the material. If material is not included in the article's Creative Commons licence and your intended use is not permitted by statutory regulation or exceeds the permitted use, you will need to obtain permission directly from the copyright holder. To view a copy of this licence, visit <http://creativecommons.org/licenses/by/4.0/>.

© The Author(s) 2021

## SUPPLEMENTARY INFORMATION

### **Ancient DNA SNP-panel data suggests stability in bluefin tuna genetic diversity despite centuries of fluctuating catches in the eastern Atlantic and Mediterranean**

Adam J. Andrews, Greg N. Puncher, Darío Bernal-Casasola, Antonio Di Natale, Francesco Massari, Vedat Onar, Nezir Yaşar Toker, Alex Hanke, Scott A. Pavey, Castrense Savojardo, Pier Luigi Martelli, Rita Casadio, Elisabetta Cilli, Arturo Morales-Muñiz, Barbara Mantovani, Fausto Tinti, Alessia Cariani

#### Supplementary Materials 1: Details of historical specimens analysed

##### 1911-1941 CE Massimo Sella Archive

We analysed specimens collected from four separate locations in the early 20<sup>th</sup> century by the ecologist Massimo Sella<sup>11</sup>. All specimens consist of vertebrae that were air-dried by the collator after capture and processing at tuna traps (*Tonnare*). A total of 50 samples were obtained from BFT vertebrae that were captured in 1911 close to the shore at Messina, Pizzo, Italy. These samples were considered to represent the Tyrrhenian Sea as a whole (HTYR). A total of 46 samples were obtained from BFT vertebrae captured in Zilten, Libya in 1926, considered to represent the Ionian Sea as a whole and named HION. A total of 49 samples were obtained from BFT vertebrae captured in the north of the Adriatic Sea in 1927, off Istria / modern-day Croatia, and were named HADR. Lastly, two large (2.75 m FL, fork length) specimens were sampled that originated from tuna traps in the Bosphorus, Istanbul, Turkey in 1941, named HBOS. All specimens represented adult individuals, for an account of ages and sizes, see Riccioni et al.<sup>11</sup>.

##### 4<sup>th</sup>-15<sup>th</sup> century CE Yenikapi

67 vertebrae specimens were selected for analyses from a rescue excavation at a Byzantine site in the Yenikapi neighbourhood of Istanbul, Turkey. The Port of Theodosius operated at this site from 4-11<sup>th</sup> century CE before being filled in at the 16<sup>th</sup> century CE. The specimens used herein are conservatively dated by stratigraphic unit, archaeological context and according to the carbon dating of other specimens from the location<sup>43</sup>. The specimens consist of medium to large adult individuals (~2m FL), though thorough morphological analysis is yet to be conducted. It is unknown whether the vertebrae were transported to the site from other regions, or were caught locally in the Bosphorus, which supported a large Greek and Byzantine fishery. There is a potential for specimens to originate from different events by deposition in the harbour by way of the Lycus River from the city proper<sup>43</sup>. See Puncher et al.<sup>104</sup> for further details.

##### 2<sup>nd</sup> century BCE - 5<sup>th</sup> century CE Baelo Claudia

55 vertebrae specimens were analysed from the Roman-era city of Baelo Claudia, Andalusia, Spain). Using the archaeological context of stratigraphic units, a total of 10 specimens were dated to the Republican Rome era (2<sup>th</sup> century BCE - 1<sup>st</sup> century CE) and 45 samples were dated to the Imperial Rome era (1<sup>st</sup>-5<sup>th</sup> century CE) from various stratigraphic units and contexts within the city, predominantly associated with the fish processing facilities—called *cetariae*<sup>44</sup>. Specimens represented medium sized adult individuals (~1.5m FL). The Strait of Gibraltar supported large-scale fisheries for BFT from the Phoenician era (~8<sup>th</sup> century BCE) onwards, and thus specimens are believed to have been caught locally.



## 2<sup>nd</sup> century BCE Tavira

A total of 10 vertebrae representing medium sized adults (~1.5m FL) were analysed from excavations at a Republican Rome (2<sup>nd</sup> century BCE) site in Tavira, Algarve, Portugal. The archaeological context for this material is contained within an unpublished belonging to one of the co-authors, A. M-M. The vertebrae are dated according to stratigraphic units.

## 4<sup>th</sup>-2<sup>nd</sup> century BCE Palacio de Justicia

Four specimens were sampled from excavations at the Cadiz site 'Palacio de Justicia', which was a Punic and Roman era (4<sup>th</sup>-2<sup>nd</sup> century BCE) Palace, in Andalusia, Spain. Specimens represent medium sized adults believed to have been captured locally<sup>45</sup>.

## Supplementary Figures

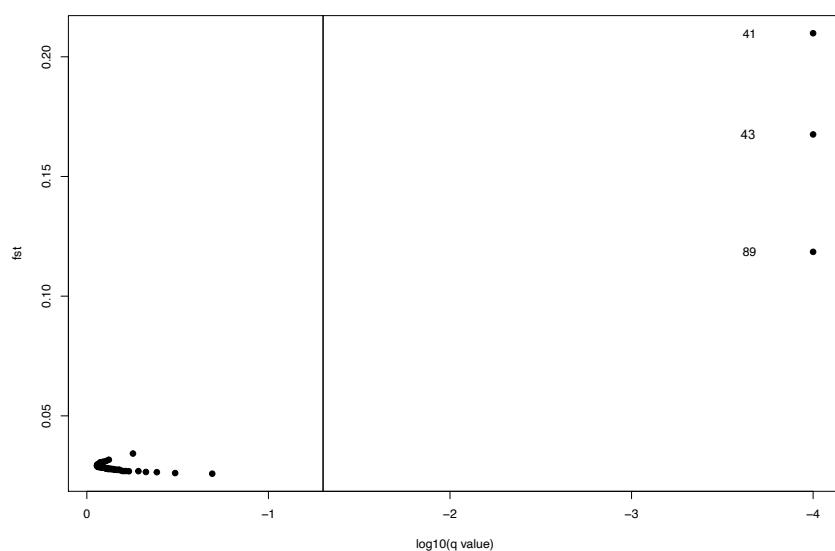


Figure S1. Scatterplot of the three outliers (black circles  $< -1.5 \log$ ) identified with BayeScan; SNP41, SNP43 and SNP89.

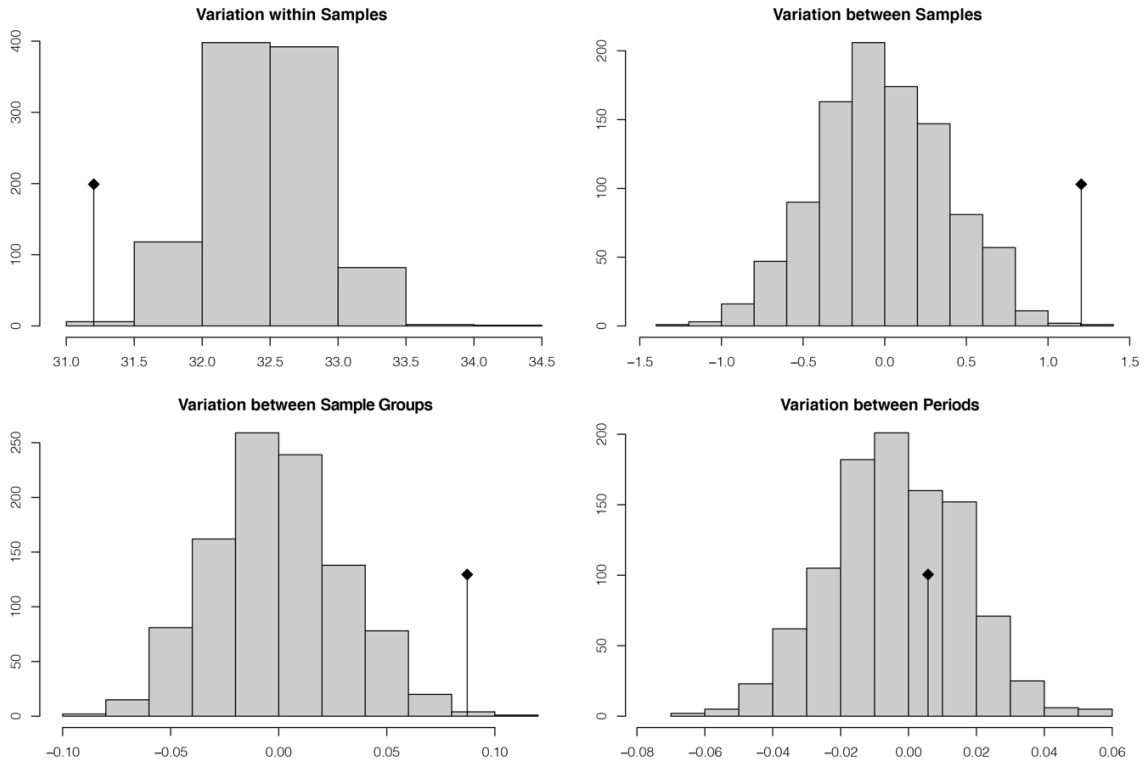


Figure S2. Barplots of variance estimated using AMOVAs using a hierarchical approach as indicated by the four levels; within samples, between samples, between sample groups and between periods (i.e. historical and contemporary). The black line indicates observed data in comparison with the expected variance from simulations (grey bars).

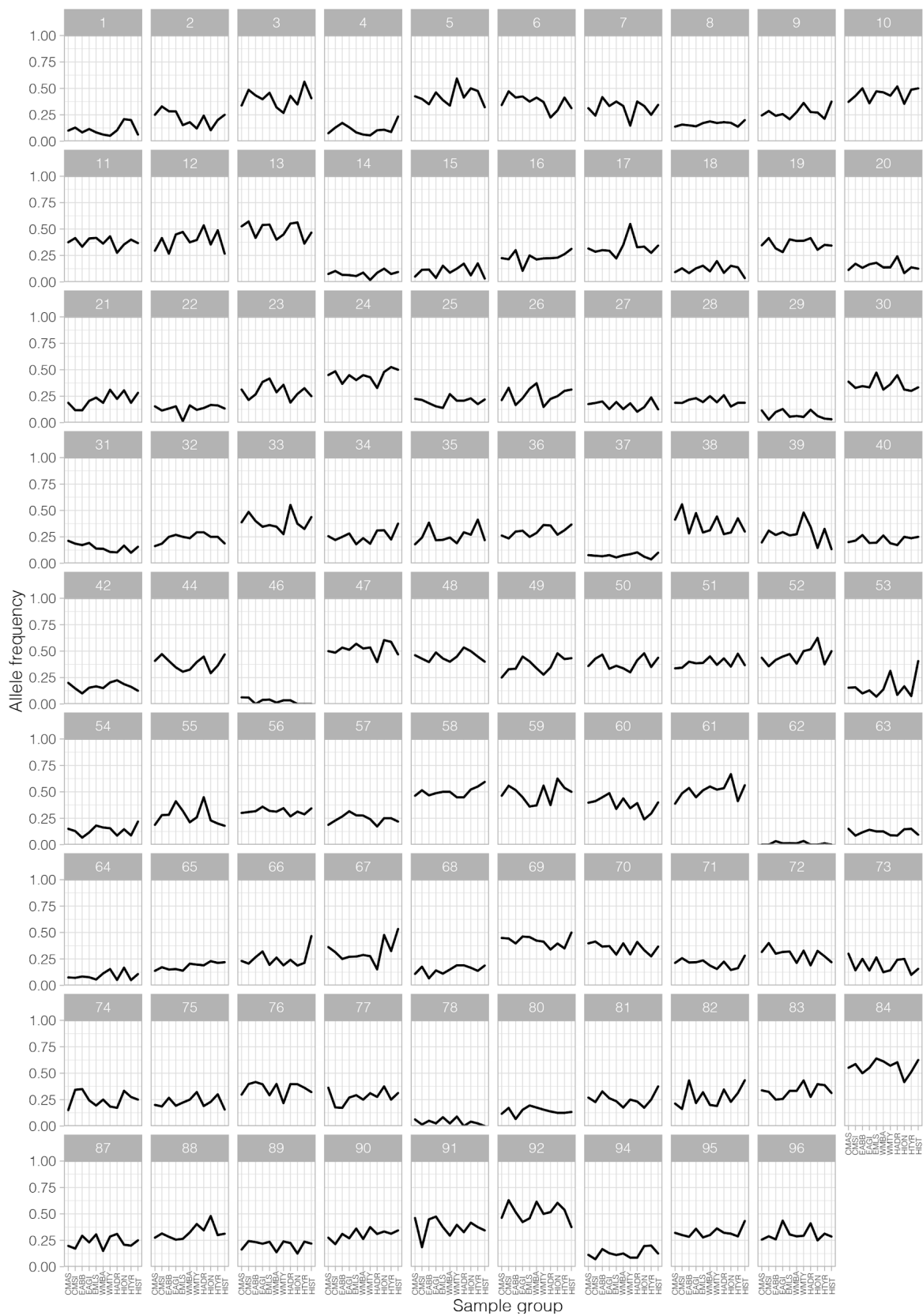


Figure S3. Line trajectory plot of minor allele frequencies per locus (excluding SNP41, SNP43 and SNP89 identified as outliers) as calculated with the round robin approach. Frequencies

course across each sample group from contemporary (left sided) progressing to the earliest sample group (right sided).

### Supplementary References

104. Puncher, G. N., Onar, V., Toker, N. Y. & Tinti, F. A multitude of byzantine era bluefin tuna and swordfish bones uncovered in Istanbul, Turkey. *Collect. Vol. Sci. Pap. ICCAT/Recl. Doc. Sci. CICTA/Colecc. Doc. Cient. CICA* **71**, 1626–1631 (2015).

### Supplementary Tables

Table S1. Details of contemporary, and historical (archived and archaeological) bluefin tuna (*Thunnus thynnus*) specimens collected, genotyped on the 96 loci panel, and included in the final dataset i.e. successfully genotyped. Genotype numbers of historical (archival and archaeological) samples represent those genotyped at two separate facilities to assess consistency.

Sampling Location	n sampled	n genotyped	n in final dataset	ID	Age class	Year	Type	Reference
Gulf of Mexico	24	24	24	GOM	YOY	2009	Contemporary	14
Central Mediterranean - Adriatic Sea	40	40	40	CMAS	Juvenile	2011	Contemporary	14
Central Mediterranean - Southern Sicily	38	38	38	CMSI	YOY	2012	Contemporary	14
Eastern Atlantic - Bay of Biscay	40	40	40	EABB	Juvenile	2011	Contemporary	14
Eastern Atlantic - Strait of Gibraltar	40	40	40	EAGI	Adult	2011	Contemporary	14
Eastern Mediterranean - Levantine Sea	29	29	29	EMLS	YOY	2011	Contemporary	14
Western Mediterranean - Balearic Islands	40	40	40	WMBA	YOY	2011	Contemporary	14
Western Mediterranean - Tyrrhenian Sea	40	40	40	WMTY	YOY	2012	Contemporary	14
Bosporus, Istanbul, Turkey	2	2	1	HBOS	Adult	1941	Massimo Sella Archive	11
Adriatic Sea, Istria, Croatia	49	49	21	HADR	Adult	1927	Massimo Sella Archive	11
Ionian Sea, Zliten, Libya	46	46	43	HION	Adult	1926	Massimo Sella Archive	11
Tyrrhenian Sea, Pizzo, Italy	50	48	39	HTYR	Adult	1911	Massimo Sella Archive	11
Yenikapi, Istanbul, Turkey	67	66	38	HIST	Adult	4 <sup>th</sup> -15 <sup>th</sup> CE	Archaeological	43

Baelo Claudia, Spain	4	4	0	HBC	Adult	5 <sup>th</sup> CE	Archaeological	44
Tavira, Portugal	10	10	2	HTAV	Adult	2 <sup>nd</sup> BCE	Archaeological	Roselló & Morales unpublished report
Baelo Claudia, Spain	45	45	0	HBC	Adult	2 <sup>nd</sup> BCE	Archaeological	44
Baelo Claudia, Spain	6	6	0	HBC	Adult	2 <sup>nd</sup> -1 <sup>st</sup> BCE	Archaeological	44
Palacio de Justicia, Cadiz, Spain	4	4	0	HPJ	Adult	4 <sup>th</sup> -2 <sup>nd</sup> BCE	Archaeological	45

n = number of individuals or archival/archaeological vertebrae

Reference indicates the primary reports detailing archival and archaeological specimens or where contemporary specimens were collected

YOY = Young-of-the-year

Table S2. The 96 loci genotyped and reasons behind their selection and association as inferred from NCBI Blastn analysis

SNP ID	Reason for selection	Associated Protein	Taxa alignment	% identity	% cover	E-value	NCBI Reference code
1	<i>Polymorphic between contemporary populations in Puncher et al.<sup>14</sup></i>						
2	<i>Gene association</i>	Phosphoglucomutase 1	<i>Dicentrarchus labrax teleosts</i>	95.92	80.99	6.00E-39	LG4:6467652-6467749
3	<i>Gene association</i>	Myoglobin	<i>Dicentrarchus labrax teleosts</i>	100	81.82	3.00E-11	E1CPX3_THUMA
4	<i>Gene association</i>						
5	<i>Gene association</i>	Vacuolar protein sorting-associated protein 28 homolog	<i>Dicentrarchus labrax teleosts</i>	91.74	100	1.00E-39	LG9:13694258-13694378
5	<i>Gene association</i>	Vacuolar protein sorting-associated protein 28 homolog	<i>teleosts</i>	94.29	86.78	3.00E-11	C1BLI6_OSMMO
6	<i>Gene association</i>	Betaine homocysteine methyltransferase isoform 3 OS	<i>teleosts</i>	97.14	86.78	3.00E-12	V9HXV7_SPAAU
7	<i>Gene association</i>	Amylo-6-4-alpha-glucanotransferase isoform 1	<i>Dicentrarchus labrax</i>	84.03	98.35	3.00E-16	LG10:1491505-1491623
8	<i>Polymorphic between contemporary populations in Puncher et al.<sup>14</sup></i>						
9	<i>Polymorphic between contemporary populations in Puncher et al.<sup>14</sup></i>						
10	<i>Polymorphic between contemporary populations in Puncher et al.<sup>14</sup></i>						
11	<i>Polymorphic between contemporary populations in Puncher et al.<sup>14</sup></i>						
12	<i>Polymorphic between contemporary populations in Puncher et al.<sup>14</sup></i>						
13	<i>Polymorphic between contemporary populations in Puncher et al.<sup>14</sup></i>						
14	<i>Gene association</i>	Phosphoglucomutase 1	<i>Dicentrarchus labrax</i>	90.6	96.69	1.00E-33	LG4:6464452-6464568
15	<i>Gene association</i>	RUVb-like 1-like	<i>Dicentrarchus labrax</i>	85.58	85.95	3.00E-16	LG1A:15592644-15592747

16	Gene association	Betaine-homocysteine S-methyltransferase 1-like	<i>Dicentrarchus labrax</i>	89.38	93.39	8.00E-32	LG20:4801689-4801801
16	Gene association	Betaine homocysteine methyltransferase isoform 4	teleosts	92.31	96.69	5.00E-16	V9HZ12_SPAAU
17	Gene association	T-complex protein 1 subunit epsilon	<i>Dicentrarchus labrax</i>	91.8	100	4.00E-37	LG18-21:6432507-6432628
18	Gene association	Trifunctional enzyme subunit mitochondrial	<i>Dicentrarchus labrax</i>	92.31	96.69	6.00E-39	LG17:12286073-12286189
18	Gene association	Hydroxyacyl-CoA dehydrogenase/3-ketoacyl-CoA thiolase/enoyl-CoA hydratase (trifunctional protein), beta subunit	<i>Gadus morhua</i>	95	99.17	2.00E-18	ENSGMOP000000019175
18	Gene association	Hydroxyacyl-Coenzyme A dehydrogenase	teleosts	97.5	99.17	2.00E-17	G1FKK0_EPIBR
19	Gene association	Calumenin isoform x2	<i>Dicentrarchus labrax</i>	85.09	94.21	2.00E-17	UN:33920969-33921082
20	Polymorphic between contemporary populations in Puncher et al. <sup>14</sup>						
21	Polymorphic between contemporary populations in Puncher et al. <sup>14</sup>						
22	Polymorphic between contemporary populations in Puncher et al. <sup>14</sup>						
23	Polymorphic between contemporary populations in Puncher et al. <sup>14</sup>						
24	Polymorphic between contemporary populations in Puncher et al. <sup>14</sup>						
25	Polymorphic between contemporary populations in Puncher et al. <sup>14</sup>						
26	Gene association	Xin actin-binding repeat-containing protein 2-like	<i>Dicentrarchus labrax</i>	88.03	96.69	2.00E-26	LG15:12489701-12489817

27	Gene association		M-protein, striated muscle	teleosts	82.05	96.69	2.00E-11	W5JUM88 ICTPU
28	Gene association		Reticulon-4-like isoform 1	<i>Dicentrarchus labrax</i>	94.12	98.35	6.00E-42	LG11:22112661-22112778
29	Gene association		SET and MYND domain containing protein 1a	teleosts	85	99.17	4.00E-15	W0M2F7_SINCH
30	Gene association		Myozenin 1	<i>Dicentrarchus labrax</i>	91.92	81.82	5.00E-30	LG1B:12030692-12030790
31	Gene association		COP9 constitutive photomorphogenic homolog subunit 5	<i>Gadus morhua</i>	100	84.3	2.00E-13	ENSGMOP00000018264
31	Gene association		COP9 signalosome complex subunit 5	teleosts	100	84.3	5.00E-12	C1BF76_ONCMY
32	Gene association	<i>Polymorphic between contemporary populations in Puncher et al.<sup>1,4</sup></i>						
33	Gene association	<i>Polymorphic between contemporary populations in Puncher et al.<sup>1,4</sup></i>						
34	Gene association	<i>Polymorphic between contemporary populations in Puncher et al.<sup>1,4</sup></i>						
35	Gene association	<i>Polymorphic between contemporary populations in Puncher et al.<sup>1,4</sup></i>						
36	Gene association	<i>Polymorphic between contemporary populations in Puncher et al.<sup>1,4</sup></i>						
37	Gene association	<i>Polymorphic between contemporary populations in Puncher et al.<sup>1,4</sup></i>						
38	Gene association		Eukaryotic translation initiation factor 3 subunit g	<i>Dicentrarchus labrax</i>	93.39	100	2.00E-44	LG8:11023666-11023786
39	Gene association		Proline-rich nuclear receptor coactivator 2	<i>Dicentrarchus labrax</i>	88.24	98.35	8.00E-26	LG16:4979463-4979579
40	Gene association		Thioredoxin interacting protein	Thunnus thynnus	100	100	3.00E-64	EC918814
40	Gene association		Thioredoxin-interacting protein	<i>Dicentrarchus labrax</i>	89.66	95.87	1.00E-30	LG9:3159022-3159137
40	Gene association		Thioredoxin-interacting protein	teleosts	97.5	99.17	5.00E-16	I7HH00_OPLFA
41	Gene association		Synemin isoform x1	<i>Dicentrarchus labrax</i>	85.95	100	1.00E-21	LG6:9865641-9865761
42	Gene association		Complement factor d-like	<i>Dicentrarchus labrax</i>	89.52	100	8.00E-32	LG12:21422927-21423050



42	Gene association		Complement factor D (adipsin)	<i>Gadus morhua</i>	82.5	96.69	3.00E-15	ENSGMOP000000005890
42	Gene association		Kallikrein like protein	<i>teleosts</i>	85	96.69	4.00E-15	Q2Z1R4_ORYLA
43	Gene association		Ryanodine receptor 3-like	<i>Dicentrarchus labrax</i>	86.73	93.39	2.00E-20	LG17:12874139-12874248
44	Polymorphic between contemporary populations in Puncher et al. <sup>14</sup>							
45	Polymorphic between contemporary populations in Puncher et al. <sup>14</sup>							
46	Polymorphic between contemporary populations in Puncher et al. <sup>14</sup>							
47	Polymorphic between contemporary populations in Puncher et al. <sup>14</sup>							
48	Polymorphic between contemporary populations in Puncher et al. <sup>14</sup>							
49	Gene association		Myosin heavy chain	<i>teleosts</i>	87.18	96.69	6.00E-13	Q98TQ4_9TELE
50	Gene association		Muscle-specific beta 1 integrin binding protein 2	<i>teleosts</i>	85.71	86.78	2.00E-11	B9V3X3_EPICO
51	Gene association		Platelet-derived growth factor receptor-like	<i>Thunnus thynnus</i>	93.97	94.21	1.00E-38	EH000371
52	Gene association		Heat shock protein 25 variant 1	<i>Dicentrarchus labrax</i>	90.74	89.26	1.00E-30	LG8:21804879-21804986
53	Gene association		Homeobox protein tgjf2	<i>Dicentrarchus labrax</i>	83.33	99.17	1.00E-12	LG1A:12106316-12106433
54	Gene association		High-mobility group box 1	<i>Thunnus thynnus</i>	100	93.39	2.00E-59	EC919262
54	Gene association		High mobility group-t	<i>Dicentrarchus labrax</i>	92.37	97.52	6.00E-39	LG14:17296613-17296730
55	Polymorphic between contemporary populations in Puncher et al. <sup>14</sup>							
56	Polymorphic between contemporary populations in Puncher et al. <sup>14</sup>							
57	Polymorphic between contemporary populations in Puncher et al. <sup>14</sup>							
58	Polymorphic between contemporary populations in Puncher et al. <sup>14</sup>							
59	Polymorphic between contemporary populations in Puncher et al. <sup>14</sup>							



77	Gene association		Eukaryotic translation elongation factor 2, like	teleosts	95	99.17	1.00E-15	Q7ZVM3_DANRE
78	Gene association		Elongation factor 1 alpha	Thunnus thynnus	95	99.17	6.00E-47	EL610929
78	Gene association		Elongation factor 1-alpha	<i>Dicentrarchus labrax</i>	97.5	99.17	2.00E-54	LG9:21157592-21157711
78	Gene association		Elongation factor 1-alpha	<i>Gadus morhua</i>	90	99.17	7.00E-16	ENSGMOP00000012846
78	Gene association		Elongation factor 1-alpha	teleosts	100	99.17	1.00E-16	A0A087XDA8_POEFO
79	<i>Polymorphic between contemporary populations in Puncher et al.<sup>14</sup></i>							
80	<i>Polymorphic between contemporary populations in Puncher et al.<sup>14</sup></i>							
81	<i>Polymorphic between contemporary populations in Puncher et al.<sup>14</sup></i>							
82	<i>Polymorphic between contemporary populations in Puncher et al.<sup>14</sup></i>							
83	<i>Polymorphic between contemporary populations in Puncher et al.<sup>14</sup></i>							
84	<i>Polymorphic between contemporary populations in Puncher et al.<sup>14</sup></i>							
85	Gene association		Phosphoglucomutase 1	<i>Dicentrarchus labrax</i>	86.09	94.21	4.00E-18	LG4:6461135-6461249
86	Gene association		Keratin 23 (histone deacetylase inducible)	<i>Gadus morhua</i>	94.59	91.74	1.00E-13	ENSGMOP00000015062
87	Gene association		Protein kinase c inhibitor aswz variant 5	<i>Dicentrarchus labrax</i>	88.46	85.95	5.00E-24	LG11:15886279-15886382
87	Gene association		Histidine triad nucleotide-binding protein	teleosts	82.86	86.78	2.00E-09	E3TGF9 ICTPU
87	Gene association		Protein FAM171b-like	<i>Dicentrarchus labrax</i>	90	100	1.00E-132	LG24:2370971-2371370
88	Gene association		Myozenin 1	<i>Dicentrarchus labrax</i>	96.69	100	1.00E-52	LG1B:12032167-12032287
88	Gene association		Myozenin-2	teleosts	82.5	99.17	5.00E-12	E3TCH3 ICTFU

89	Gene association		Calponin 1, basic, smooth muscle	<i>Gadus morhua</i>	91.67	89.26	3.00E-13	ENSGMOP000000016108
89	Gene association		Calponin	<i>teleosts</i>	88.89	89.26	4.00E-12	M4A2Z2_XIPMA
90	Gene association		Alpha cardiac-like isoform 1	<i>Dicentrarchus labrax</i>	93.44	100	2.00E-41	LG12:9448943-9449064
91	Polymorphic between contemporary populations in Pancher et al. <sup>14</sup>							
92	Polymorphic between contemporary populations in Pancher et al. <sup>14</sup>							
93	Polymorphic between contemporary populations in Pancher et al. <sup>14</sup>							
94	Polymorphic between contemporary populations in Pancher et al. <sup>14</sup>							
95	Polymorphic between contemporary populations in Pancher et al. <sup>14</sup>							
96	Polymorphic between contemporary populations in Pancher et al. <sup>14</sup>							

Table S3. Effective population size ( $N_e$ ) and 95% Confidence Intervals of contemporary and historical sample groups for samples (n) consistently scored across all 89 neutral loci analysed herein, under two approaches, where separate estimates were made for each sample group and for contemporary and historical pools. The number of samples analysed (n) per sample group were equalised by random down-sampling.

	Contemporary										Historical		
	GOM	CMAS	CMSI	EABB	EAGI	EMLS	WMBA	WMTY	HADR	HION	HTYR	HIST	
<b>Separate</b>													
<b>n</b>	14	14	14	14	-	14	14	14	-	14	14	14	
<b><math>N_e</math></b>	154	93	175	$\infty$	-	806	140	$\infty$	-	$\infty$	26	19	
<b>CI</b>	47 - $\infty$	38 - $\infty$	48 - $\infty$	76.7 - $\infty$	-	64 - $\infty$	46 - $\infty$	98 - $\infty$	-	244 - $\infty$	18 - 45	14 - 29	
<b>Pooled</b>													
<b>n</b>	0	14	15	17	0	2	7	15	4	24	24	18	
<b><math>N_e</math></b>					1049						285		
<b>CI</b>					321 - $\infty$						173 - 716		

## **Chapter 7**

Ancient DNA and genomics reveals exploitation induced pre-industrial biomass declines in Atlantic bluefin tuna but has not limited its adaptive potential  
**(pages 215—253)**

1 **Ancient DNA and genomics reveals exploitation induced pre-industrial biomass**  
2 **declines in Atlantic bluefin tuna but has not limited its adaptive potential**

3  
4 Adam J. Andrews<sup>\*1</sup>, Bastiaan Star<sup>\*2</sup>, Antonio Di Natale<sup>3</sup>, Estrella Malca<sup>4,5</sup>, Glenn Zapfe<sup>6</sup>,  
5 Vedat Onar<sup>7</sup>, Veronica Aniceti<sup>8</sup>, Gabriele Carenti<sup>9</sup>, Gäel Piques<sup>10</sup>, Federica Piattoni<sup>1</sup>, Sara  
6 De Fanti<sup>11</sup>, Francesco Fontani<sup>12</sup>, Emma Falkeid Eriksen<sup>2</sup>, Lane Atmore<sup>2</sup>, Oliver Kersten<sup>2</sup>,  
7 Fausto Tinti<sup>\*1</sup>, Elisabetta Cilli<sup>†12</sup>, Alessia Cariani<sup>†1</sup>

8  
9 1Department of Biological, Geological and Environmental Sciences, University of Bologna,  
10 Ravenna, Italy

11 2CEES - Centre for Ecology and Evolutionary Synthesis, University of Oslo, Oslo, Norway

12 3AquaStudio Research Institute, Messina, Italy

13 4Cooperative Institute for Marine and Atmospheric Studies, University of Miami, Miami,  
14 Florida, United States of America

15 5NOAA Fisheries, Populations and Ecosystems Monitoring Division, Miami, Florida, United  
16 States of America

17 6Southeast Fisheries Science Center, National Marine Fisheries Service, National Oceanic  
18 and Atmospheric Administration, Pascagoula, Mississippi, United States of America

19 7Osteoarchaeology Practice and Research Centre, Faculty of Veterinary Medicine, Istanbul  
20 University-Cerrahpaşa, Istanbul, Turkey

21 8Museum of Natural History, University of Bergen, Bergen, Norway

22 9CEPAM, CNRS, Université Côte d'Azur, Nice, France

23 10Archaeological-ichthyology Laboratory CEPAM, CNRS, Montpellier, France

24 11Department of Biological, Geological and Environmental Sciences, University of Bologna,  
25 Bologna, Italy,

26 12Department of Cultural Heritage, University of Bologna, Ravenna, Italy

27  
28 \*Corresponding authors: [adam@palaeome.org](mailto:adam@palaeome.org), [bastiaan.star@ibv.uio.no](mailto:bastiaan.star@ibv.uio.no),  
29 [fausto.tinti@unibo.it](mailto:fausto.tinti@unibo.it)

30 †EC and AC should be considered joint senior author

31  
32 Keywords: conservation genomics, ancient DNA, *Thunnus thynnus*, fisheries induced  
33 evolution, historical ecology, adaptation

34  
35 **Significance**

36 Although marine ecosystems have been exploited for millennia, for many species the history  
37 of exploitation and its intensity remains unknown leading to uncertainties in our understanding  
38 of the resilience of ecosystems today. Here, we evaluate human impacts on the iconic Atlantic  
39 bluefin tuna, which has a huge cultural and economic importance and has been intensely  
40 exploited for millenia. We observe genomic evidence for biomass declines between 1800-  
41 1950, predating current management recovery baselines; our observations therefore suggest  
42 that recovery targets should be more ambitious. Despite these declines in biomass, genetic  
43 variability has been retained; Finally, we find that several genomic regions show signals of  
44 recent adaptive responses, which we cannot rule out were caused by fisheries, and may  
45 represent positive selection to anthropized marine environments.

46  
47  
48

49 **Abstract**

50 Overexploitation has depleted numerous fish stocks during the past century, yet we have a  
51 poor understanding of when intensive exploitation began and what impact this has had. Such  
52 information is crucial to understand evolutionary factors limiting fish population recovery,  
53 maximise their productivity in-line with historical levels and predict future dynamics. Here, we  
54 evaluate human impacts on the iconic Atlantic bluefin tuna (*Thunnus thynnus*; BFT), one of  
55 the longest and most intensely exploited marine fishes, with a tremendous cultural and  
56 economic importance. Analysing whole genome data from ancient (n= 39) and modern (n=39)  
57 BFT, dating back ca. 1000 years, we uncover several findings with direct applicability to the  
58 management of BFT recovery. First, we resolve BFT population structure, identifying one  
59 western and one eastern population with extremely low levels of differentiation and near-  
60 identical demographic histories. These results imply that eastern recoveries may promote  
61 productivity in the smaller western stock. Second, models of effective population size across  
62 recent history suggest biomass declines by the 1800s, which is associated with a period of  
63 intensive exploitation. Therefore, BFT productivity should increase if low fishing mortality is  
64 maintained. Third, we find that the overexploitation of BFT has not resulted in genetic erosion,  
65 finding no evidence of strong genetic bottlenecks, inbreeding or population complexity loss.  
66 Finally, we observe putative selection signals between ancient and modern samples at 19  
67 locations across the genome, which might be associated with fisheries induced evolution.  
68 Further study is required to assess if adaptive responses are linked with changes in BFT  
69 juvenile growth, expected as a result of intensive fishing. In any case, adaptive responses can  
70 be considered as positive evidence that BFT is continuing to adapt to rapidly changing marine  
71 environments and has full capacity to do so.

72

73 **Main text**

74

75 As we restore our oceans, fundamental questions remain as to how productive fish  
76 populations were historically and whether recoveries will be hampered by genetic changes  
77 which have resulted from their overexploitation (1, 2). Between 1970-2007, the commercially  
78 important Atlantic bluefin tuna (*Thunnus thynnus*; BFT) was severely depleted, resulting in the  
79 loss of large size-classes and rarity across its range; where it even disappeared from habitats  
80 such as the North, Norwegian and Black Seas (3–8). Its abundance has recently recovered to  
81 1970s levels following several years of international management and favourable  
82 oceanographic conditions, while it has returned to most of its previous habitats in great  
83 numbers, except the Black Sea (9–13).

84

85 BFT recovery is duly considered a fisheries management success (3, 14); as a result, catch  
86 quotas have increased in recent years (13). However, BFT were commercially fished in the  
87 Mediterranean before ancient Greek times ca. 3000 YBP; and qualitative data from several  
88 sources would suggest that the intensification of their fisheries—and decline of their  
89 populations—had begun prior to the 1970s (15), as has been found in other marine populations  
90 and ecosystems (e.g., (16–19)). Nonetheless, little is known whether 1970 abundance  
91 baselines underestimate historical BFT productivity, and how centuries of exploitation have  
92 impacted its population structure, genetic diversity and evolution. This information is vital to  
93 maximise fisheries productivity, predict future dynamics and food security (20–23). With this  
94 work, we use ancient DNA and genomics to address these questions.

95



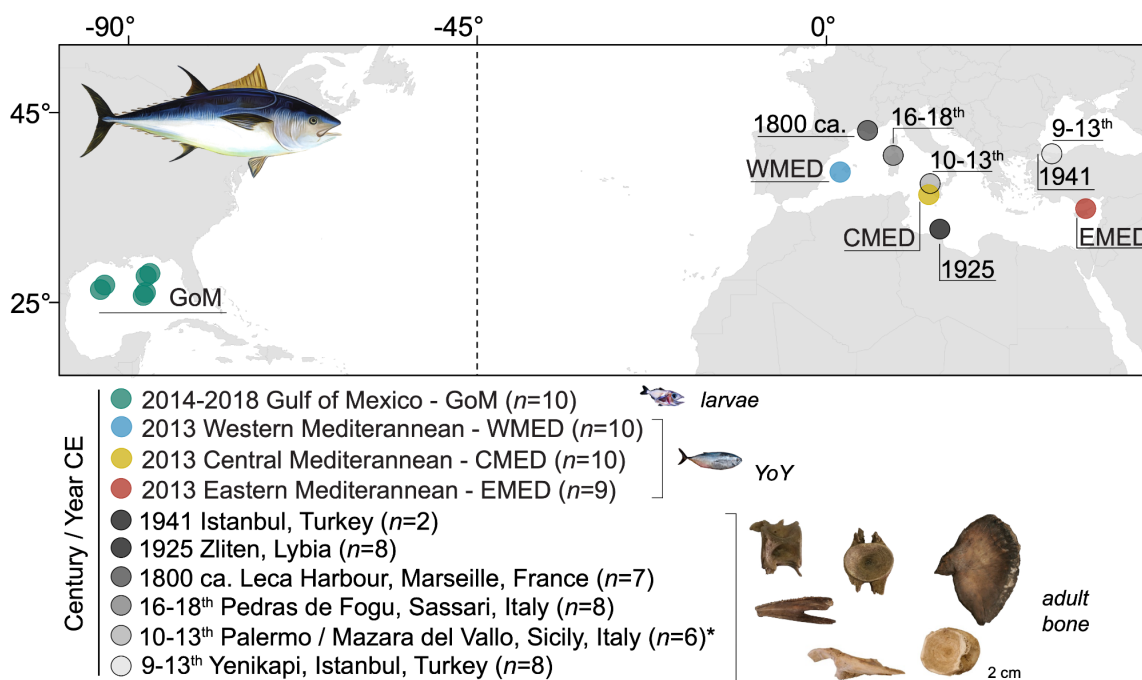
96 BFT is a pelagic predator characterised by its large size (up to 3.3 m in length and 725 kg in  
97 weight), far-reaching and inshore migration behaviour, and slow maturation (between 3-6  
98 years, [\(24, 25\)](#)). Recent genomic studies [\(26, 27\)](#) support the delineation of two BFT  
99 populations. These are a western Atlantic component that spawns predominantly in the Gulf  
100 of Mexico [\(28\)](#) and an eastern Atlantic and Mediterranean component that spawns  
101 predominantly in the Mediterranean Sea [\(25\)](#). Individuals of both populations migrate into the  
102 Atlantic Ocean to feed, including as juveniles [\(29, 30\)](#), and exhibit high-levels of mixing [\(26,](#)  
103 [27\)](#). The role of additional contemporary and historical spawning areas such as the Slope Sea  
104 (East of Cape Hatteras, USA, [\(28, 31\)](#)), the Bay of Biscay [\(32\)](#), and the Black Sea [\(33, 34\)](#) are  
105 yet to be clearly defined but BFT born in the Slope Sea appear to be a genetically mixed  
106 component of the two populations [\(27\)](#). Recent tagging data has fuelled a decades-old theory  
107 that a portion of Mediterranean BFT are resident all year round [\(6, 35, 36\)](#), potentially remnants  
108 of a spawning stock which migrated to the Black Sea [\(37, 38\)](#). Yet, the genetic origin of this  
109 stock is unknown.

110  
111 Since ancient Roman times, tuna traps lined eastern Atlantic and Mediterranean coasts and  
112 intercepted spawning migrations of highly-revered BFT between April-September [\(15, 29\)](#). By  
113 the 14th century, legislation controlling BFT catches existed, though to little effect since during  
114 the 18th century, when the Monk Martin Sarmiento proposed that they had been overfished in  
115 Spanish waters (see [\(15\)](#)). By the 1880s, trap records indicate that as many eastern BFT were  
116 landed as during the most intensive decades of BFT exploitation, which occurred between  
117 1980-2000 with huge advances in modern technology and effort [\(3, 39\)](#). By 1970, several case  
118 studies suggest that BFT productivity was not at maximum [\(6\)](#), though quantitative ecological  
119 and fisheries data has been lacking to evidence this.

120  
121 Genomic analyses of temporal samples before and after exploitation events provide key  
122 opportunities to test for the onset of intensive exploitation and its evolutionary impacts [\(22, 40,](#)  
123 [41\)](#). Indeed, recent demographic history has been modelled using contemporary samples to  
124 reveal pre-industrial exploitation impacts [\(16\)](#), but its combination with testing temporal  
125 samples [\(40\)](#) is imperative for revealing whether biomass declines result in genetic erosion–  
126 which might leave a population vulnerable to upcoming adaptive challenges [\(23, 41\)](#). Genetic  
127 erosion (increased homozygosity, inbreeding, mutational load) remains poorly studied in  
128 marine fishes, where temporal frame or the number/power of markers still hamper  
129 observations [\(42–45\)](#). The current study is the first to investigate temporal genomic changes  
130 in a fish population using whole genomes older than ~100 years. Consequently, detecting  
131 adaptive responses to natural factors (climate), or anthropogenic ones such as fisheries  
132 induced evolution (FIE; [\(46\)](#)) has been challenging, though some evidence exists from modern  
133 samples [\(47–49\)](#). Despite this, theory suggests that fishing drives phenotypic changes like  
134 earlier sexual maturation, increased reproductive investment, and slower adult growth, are  
135 underlied by evolution [\(1, 50\)](#). Laboratory experiments confirm this [\(51\)](#), detecting selective  
136 sweeps through dramatic shifts in allele frequencies, loss of genetic diversity, and increases  
137 in linkage disequilibrium at specific locations in the genome. Like other overfished species  
138 such as Atlantic cod (*Gadus morhua* [\(52\)](#)), 21st c. BFT are potentially reaching earlier  
139 maturation than their ancestors [\(53\)](#); though no study has before assessed genome-wide  
140 selection patterns in BFT.

141  
142 Here, we publish the first whole-genome data on Atlantic bluefin tuna including a long time  
143 series of genome-wide aDNA data, analysing 39 archaeological and archived bones from six

144 Mediterranean locations ca. 9<sup>th</sup> century to 1941 CE (Figure 1). Using modern whole-genome  
 145 resequencing data of a further 39 individuals of the Mediterranean and Gulf of Mexico, we  
 146 resolve population structure and model recent changes in effective population size—comparing  
 147 these with known historical fishing events to describe the onset of intensive exploitation and  
 148 population depletion. We directly test modern and ancient Mediterranean BFT for losses in  
 149 genetic diversity and population structure, including the genetic origin of individuals which had  
 150 an isotopically unique Black Sea niche (54) and potentially an extinct or heavily depleted  
 151 resident Mediterranean population. In addition, we use genome-wide scans to detect novel  
 152 selection signals and the potential for FIE during times of intense exploitation, in order to  
 153 assess what impact these events have had on the adaptive potential of the iconic and  
 154 overexploited BFT.  
 155



156  
 157 **Figure 1. Map of locations and periods of capture for Atlantic bluefin tuna (*Thunnus thynnus*; BFT) samples**  
 158 **resequenced.** Modern samples are coloured as follows: Gulf of Mexico (green, GoM); Western (blue, WMED),  
 159 Central (yellow, CMED) and Eastern (red, EMED) Mediterranean. Ancient samples are illustrated in greyscale  
 160 according to their period of capture. *n* = number successfully analysed. Stock management line at 45°W is  
 161 illustrated as a dashed black line. Insets illustrate sample types, cartoon fish not to scale. Map created using ESRI  
 162 ArcMap (v.10.6, <https://arcgis.com>). N.B. 1941 Istanbul sample location is approximately the same as 9-13th  
 163 Yenikapi, Istanbul samples. \*10-13<sup>th</sup> Sicilian samples pertain to three archaeological sites, for full details see  
 164 Supplementary.  
 165

166  
 167 **Results**

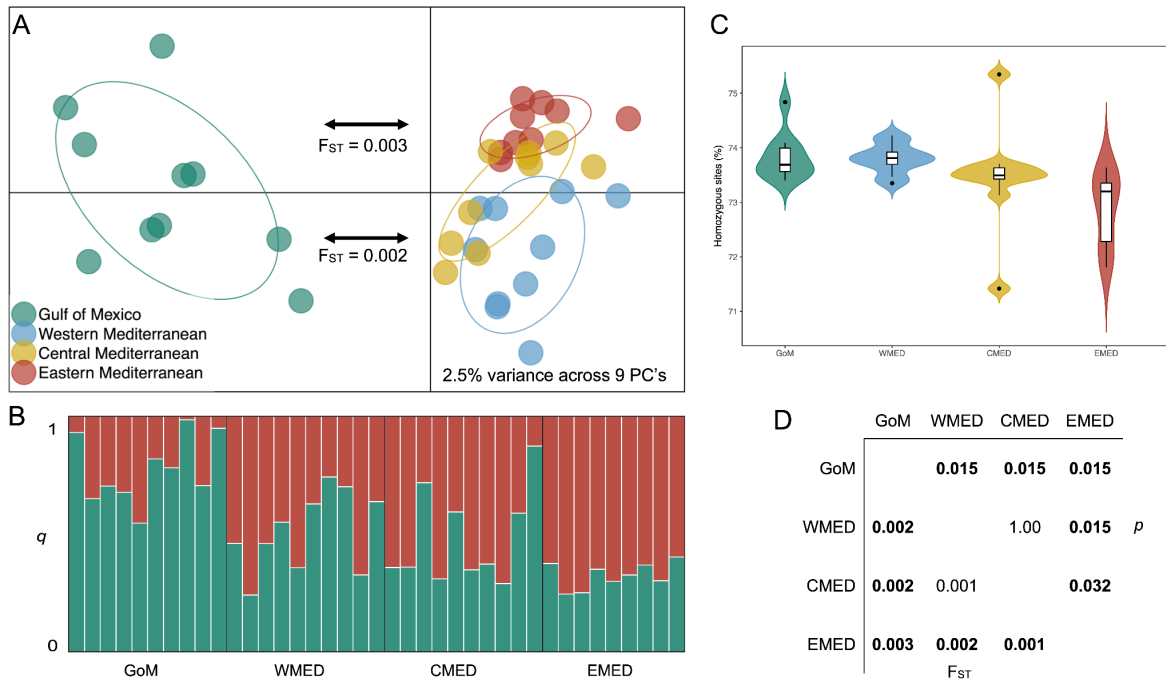
168  
 169 We analysed over 17.9 billion sequencing reads, obtaining an average of 9.7-fold nuclear  
 170 coverage for the ancient (*n* = 39; Table 1, S1) and 11.7-fold coverage for the modern samples  
 171 (*n* = 39; Table 1, S1). Ancient samples showed excellent potential for whole-genome  
 172 resequencing with high proportions of endogenous DNA (average 41%), and fragmentation  
 173 and sequence damage patterns (increases in C>T and G>A transitions) that are expected  
 174 from authentic, degraded DNA (Table 1, Fig. S1). We mapped all reads to a pseudo-

175 chromosome reference genome assembly produced from high-quality, short read data (NCBI  
176 BioProject: PRJNA408269) and—following an extensive set of quality-filtering steps (Materials  
177 and Methods)—we analysed single-nucleotide polymorphisms (SNPs) in 78 individuals using  
178 approaches based on hard called genotypes. Overall, these filters produced final datasets of  
179 39 modern individuals with 843,664 loci for demographic analysis and 1,064,265 for selection  
180 analysis, and combined ancient and modern datasets of 78 individuals with 106,210 loci for  
181 demographic analysis and 513,745 loci for selection analysis. This represented a ca. 60-fold  
182 increase in genomic representation compared to previous attempts investigating modern BFT  
183 population structure (27), a ca. 1000-fold increase on BFT aDNA resolution (43, 55) and the  
184 first genome-wide selection analyses on BFT.

185

### 186 **Modern population structure**

187 We resolved modern BFT population structure and found that the optimal number of BFT  
188 populations (K) described by DAPC and STRUCTURE was two, represented by one genomic  
189 cluster for the Gulf of Mexico and one for the Mediterranean (Fig. 2A, 2B). Membership  
190 probabilities suggest a large degree of overlap between the populations, yet, a genetic cline  
191 was observed between each of the spawning sites, where allele frequencies characteristic of  
192 the GoM decrease with geographical distance, eastwards into the Mediterranean (Fig. 2B).  
193 This pattern follows decreasing high levels (~75-71%) of homozygosity with distance from the  
194 GoM (Fig. 2C), where Eastern Mediterranean samples comprised significantly lower  
195 homozygosity overall, compared with the GoM and WMED (t-test's  $p < 0.05$ ). Pairwise  $F_{ST}$   
196 values (Fig. 2D) describe low but significant differentiation across the genetic cline where GoM  
197 and CMED/WMED samples differentiate by 0.002  $F_{ST}$  whereas GoM and EMED samples  
198 differentiate by 0.003  $F_{ST}$ . EMED Pairwise  $F_{ST}$  values were similarly significant within the  
199 Mediterranean, with WMED and CMED, respectively (0.002, 0.001  $F_{ST}$ , Fig. 2D). We note that  
200 the decreased homozygosity of EMED samples might simply reflect preferential mapping in  
201 complex regions (sequence bias) due to slight differences in read lengths between samples  
202 (Table 1).



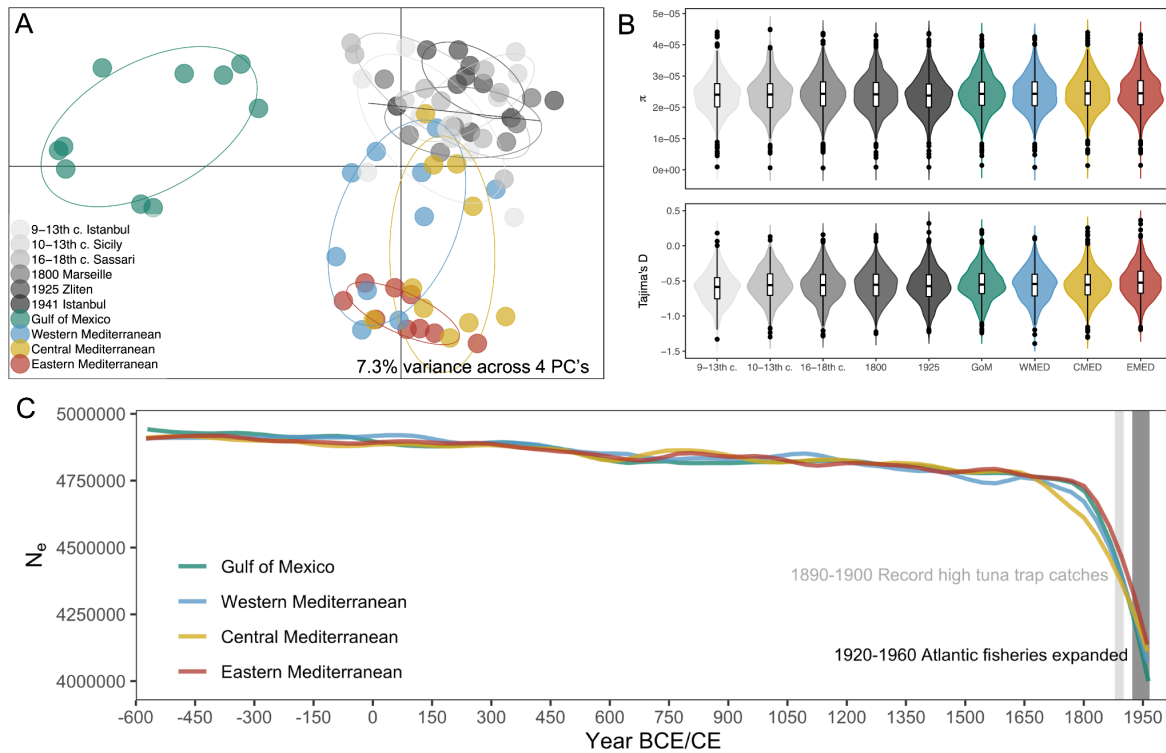
203  
204  
205  
206  
207  
208  
209  
210  
211  
212  
213  
214  
215

**Figure 2. Modern population genomic structure between Atlantic bluefin tuna (*Thunnus thynnus*) larvae/yoY sampled from spawning sites in the Gulf of Mexico (GoM, green), Western (WMED, blue), Central (CMED, yellow), and Eastern (EMED, red) Mediterranean. (A) DAPC scatterplots show how 39 modern samples (coloured circles) are clustered, using 9 PC's as indicated using the x.val function in adegenet, resulting in a total variance of 2.5% being retained where ellipses were set to contain 95% of genotypes. (B) STRUCTURE barplots show individual membership probabilities ( $q$ ) for the optimal  $K$  (2) tested using the Evanno Method. (C.) Violin boxplots show percentages of homozygous loci for each sample, with group means, 25<sup>th</sup> and 75<sup>th</sup> percentile as outer edges and outliers illustrated outside of 95<sup>th</sup> percentiles (black whiskers) as black circles. (D) Pairwise  $F_{ST}$ s (below the diagonal) show differentiation between samples and their statistical significance using FDR-corrected  $p$ -values (above the diagonal).**

### Temporal demographic analysis

216  
217 We found that all 39 ancient BFT samples, spanning over one millennia of commercial  
218 exploitation history, clustered with modern Mediterranean samples at 96,542 nuclear loci (Fig.  
219 3A); whether sites subject to potential post-mortem DNA damage were included, or not (Fig.  
220 S2). STRUCTURE analysis suggested the optimal  $K$  while ancient samples were present  
221 remained as two. Observations of membership probabilities at  $K = 3$  (Fig. S3) indicated that,  
222 regardless of time period, ancient BFT samples share similar allele frequencies, probably as  
223 a result of technical differences (degradation, read length) and thus represent origins of a  
224 single population. We found no significant differences in genetic diversity ( $\pi \sim 2.5e-5$ ) or  
225 Tajima's  $D$  ( $\sim -0.5$ ) between ancient and modern samples (Fig. 3B), which may have been  
226 indicative of a genetic bottleneck. Similarly, no significant differences in homozygosity were  
227 observed over one millennium (Fig. S4A), including when transition sites were removed (Fig  
228 S4A). Only EMED had significantly lower homozygosity than ancient samples (t-test  $p < 0.05$ );  
229 which was robust to differences in sequencing coverage (Fig. S5A,B). Despite temporal  
230 stability observed in summary statistics (Fig. 3B), historical  $N_e$  estimates reveal a significant  
231 decrease in effective population size in all samples between 1800-1950, whereas  $N_e$  remained  
232 stable during the two millennia prior to the 1800's (Fig. 3C). Demographic histories were nearly  
233 identical between modern populations over the 200 generation, 2.5 millennia period  
234 reconstructed (Fig. 3C).

235  
236



237  
238  
239  
240  
241  
242  
243  
244  
245  
246  
247  
248  
249  
250

**Figure 3. Genomic diversity retention despite declining effective population size between ancient and modern Atlantic bluefin tuna (*Thunnus thynnus*) larvae/yoY sampled from spawning sites in the Gulf of Mexico (GoM, green), Western (WMED, blue), Central (CMED, yellow), Eastern (EMED, red) Mediterranean, and ancient samples (greyscale) from 9-13th c. Istanbul, 10-13th c. Sicily, 16-18th c. Sassari, 1800 Marseille, 1925 Zliten and 1941 Istanbul.** (A) DAPC scatterplots show how ancient samples (greyscale circles) are clustered in relation to modern samples (coloured circles), using 4 PC's as indicated using the x.val function in adegenet, resulting in a total variance of 7.3% being retained where ellipses were set to contain 95% of genotypes. (B) Violin barplots show 100kb window estimates of  $\pi$  and Tajima's D for each sample with group means, 25<sup>th</sup> and 75<sup>th</sup> percentile as outer edges and outliers illustrated outside of 95<sup>th</sup> percentiles (black whiskers) as black circles. (C) GoNe estimates of historical effective population size ( $N_e$ ) for each modern sample, representing the previous 200 generations from 600 BCE to 1950, illustrated in relation to two potential causative exploitation events.

### 251 Spatio-temporal adaptations

252 Between ancient and modern Mediterranean samples, we detected 362 outlier loci in LD using  
253 both OutFlank and PCadapt (Fig. 4A,B; for a full summary see Table S2). Among them, 19  
254 genomic regions were considered under putative selection, where several loci appeared in  
255 each 1kb window. Major allele frequencies of one locus from each of the 19 genomic regions,  
256 representing 15 pseudo-chromosomes, show a lack or low frequency of minor alleles in  
257 ancient samples. Whereas, in 1941 or modern samples, the alternative allele was found in  
258 increased frequency, up to 50% among loci under putative selection, which were a  
259 combination of transitional and transversion mutations (Fig. 5C). The majority (12) of the 19  
260 sites were located in unannotated intergenic regions (Table S3) while seven sites were located  
261 within or 1kb away from genes, predominantly in introns or coding sequences (Table S3).  
262 Associated proteins of putative genic selection sites varied, including a tumour necrosis factor  
263 receptor, duodenase, Indoleamine dioxygenase, apoptosis-inducing factor, and three  
264 uncharacterised proteins (Table S3). Across the 19 sites under putative selection, the average

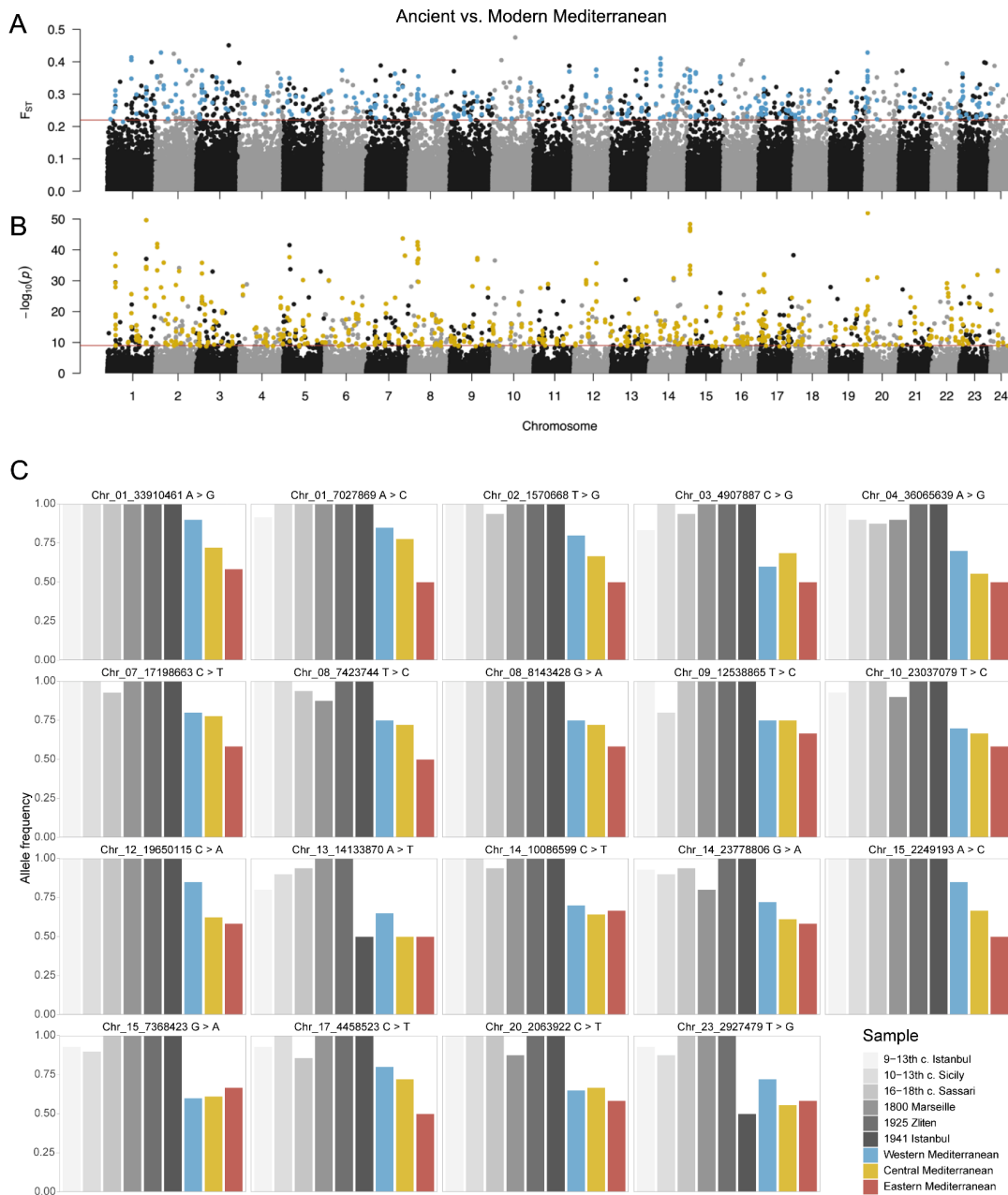
265 coverage of ancient and modern samples was 17.5 ( $\pm 2.3$ ) and 27.6 ( $\pm 5.3$ ) fold, respectively  
266 (Table S3).

267

268 Between modern GoM and Mediterranean samples, we found five loci under putative  
269 selection, which were in LD, and detected using both OutFlank and PCadapt (Supplementary,  
270 Fig. S8). Loci common to both methods did not display patterns of physical linkage with several  
271 outliers present within 1kb genomic windows (Table S4). In each case, GoM samples  
272 displayed increased frequency of the alternative allele (Fig. S8C). Two of the sites under  
273 putative selection were located within the coding sequence of genes, while two were in  
274 unannotated intergenic regions, and one was within 1kb of a gene. Associated proteins  
275 included a gamma-enolase isoform, and a mediator of RNA polymerase (Table S4). Outlier  
276 tests between Mediterranean samples resulted in no outlier loci common to both methods  
277 being detected (Table S4, Fig. S9).

278

279



280  
 281  
 282  
 283  
 284  
 285  
 286  
 287  
 288  
 289  
 290  
 291  
 292  
 293  
 294  
 295  
 296

**Figure 4. Putative loci under selection between ancient and modern Atlantic bluefin tuna (*Thunnus thynnus*) larvae/yoY sampled from spawning sites in the Gulf of Mexico (GoM, green), Western (WMED, blue), Central (CMED, yellow), Eastern (EMED, red) Mediterranean, and ancient samples (greyscale) from 9-13th c. Istanbul, 10-13th c. Sicily, 16-18th c. Sassari, 1800 Marseille, 1925 Zliten and 1941 Istanbul. (A) Genome-wide  $F_{ST}$ -based outliers detected using OutFlank where loci (circles) showing elevated ( $R^2 > 0.5$ ) linkage disequilibrium (LD) and statistically an outlier (above horizontal red line) were coloured in blue. (B) Genome-wide outliers detected using PCA-based PCAdapt where loci (circles) showing elevated ( $R^2 > 0.5$ ) linkage disequilibrium and statistically an outlier (above horizontal red line) were coloured in yellow. (C) Barplots of major allele frequencies per sample at 19 loci within genomic regions where multiple outliers were detected in 1kb windows which were both consistent between OutFlank and PCAdapt, and in LD. Annotations indicate the genomic location of outliers on pseudo-chromosomes (Chr) and the major allele nucleotide > alternative, novel mutated allele, in each region.**

## 297 Discussion

298

299 Here, we use unprecedented ancient and modern whole-genome data of Atlantic bluefin tuna  
300 (BFT), to resolve population structure, reveal that intensive exploitation had already  
301 contributed to population declines by the 1800s. Nonetheless, we do not find that  
302 overexploitation has resulted in genetic erosion and we provide evidence for recent, novel  
303 mutations across the genome, which may represent examples of fisheries-induced evolution.  
304 Here, we contextualise our results with ecological, evolutionary and historical perspectives to  
305 explain our findings in the broader narrative of marine population recovery.

306

307 Whole genomes settle a long-lasting debate that BFT constitutes more than two populations.  
308 Supporting recent research, the finding of a western (Gulf of Mexico) and eastern  
309 (Mediterranean) population suggests that spawning segregation cannot explain the resident  
310 behaviour of some Mediterranean individuals (6, 35, 36) or the disappearance of Black Sea  
311 BFT (33, 38, 56)—which we propose may recover if large size classes returned and if Black  
312 Sea habitats were improved. Despite this, we found very small but significant ( $F_{ST} < 0.003$ ,  $p =$   
313  $0.015$ ) differences between early-development stages collected from western and eastern  
314 spawning sites. Whole genome estimates were found to be similar to studies using large  
315 sample sizes and few markers under putative selection (26, 27). Since western BFT were  
316 likely not overexploited until the mid-20<sup>th</sup> century (3), near-identical GoNe demographic  
317 histories between stocks over the past two millennia suggest that BFT populations exhibit high  
318 levels of connectivity and gene flow, supporting recent work (26). This observation suggests  
319 that the recovery of either stock is partly dependent on the other due to genetic migrants,  
320 particularly so for the 10-fold smaller western stock, such that western productivity might be  
321 promoted by further recoveries of the eastern stock. The recent findings of a genetically mixed  
322 component of the two populations in the Slope Sea (27, 31), and increasing east to west  
323 migrants coinciding with eastern stock recovery (57) provides clear pathways for high-levels  
324 of connectivity reiterating that, in some aspects, BFT could be managed as a single stock (58).

325

326 Models of recent effective population size ( $N_e$ ) reveal that BFT started to noticeably decline in  
327 abundance during the 1800s and therefore that 1970s management baselines may  
328 underestimate historical productivity, as in Baltic herring (*Clupea harengus*, (16)). Given that  
329  $N_e$  was apparently stable across the two millennia prior to the 1800s, we suggest that the pre-  
330 industrial decline observed was caused by novel challenges like increased fishing effort,  
331 causing more dramatic fluctuations than is normally reflected by climate and other factors (6,  
332 59, 60). Increased fishing effort during this period is evident due to trap catches by the 1890s  
333 being at similar levels to those a century later which occurred after massive technological  
334 advances (39). Furthermore BFT fishing had expanded to year-round operations in the Atlantic  
335 by 1950, using highly effective long-lines, purse seines and gillnetting (3). Although a host of  
336 marine ecosystem changes likely occurred during this period including prey depletion (16) and  
337 habitat use changes (54) which may have contributed to biomass declines.

338

339 Reductions in  $N_e$  are indicative of losses in abundance, though the relationship between  $N_e$   
340 and  $N$  (census size) is complex for fish such as BFT with very large census sizes (61).  
341 Moreover,  $N_e$  estimates are influenced by many factors (62, 63), chiefly gene flow—which in  
342 the case of BFT is high. Due to the lack of pre-industrial western Atlantic overexploitation, we  
343 propose that gene flow from the western stock buffered the 20% drop in  $N_e$  we observed in  
344 BFT by 1950. Importantly,  $N_e$  estimates are robust to selection (64) and our findings suggest



345 sample size was not limiting. It should be noted that  $N_e$  is usually used as an estimate of  
346 population size, reflecting the potential for a population to lose genetic variation, not that  
347 genetic erosion has occurred (62).

348

349 Accordingly, we found that ancient and modern BFT do not differ significantly in genetic  
350 diversity, homozygosity or Tajima's D, indicating that there has been no genetic bottleneck  
351 and that the adaptive potential of BFT has been retained despite their overexploitation. These  
352 findings do not contradict the fact that BFT have been overexploited. Between 1960-2009,  
353 eastern BFT abundance and range declined by an estimated 70% and 46-53%, respectively  
354 (4, 5). Our demographic modelling suggests that this represents only the most recent impacts  
355 of intensive exploitation that began in the pre-industrial era. Nonetheless, our findings suggest  
356 that BFT has been genetically robust to overexploitation.

357

358 It is likely that a combination of BFT ecological features buffer against losses in genetic  
359 diversity such as high population connectivity, large population size and a long life cycle which  
360 promotes heavily overlapping generations (25, 65). Theoretically, each of these features limit  
361 the effect of genetic drift (61, 66), such that a larger number of generations would need to  
362 have elapsed in order to observe changes in heterozygosity (R. Waples, pers. comm.) as a  
363 result of biomass declines. The only other whole genome aDNA analysis on fishes showed  
364 genetic diversity retention in the overexploited Atlantic cod (42), though both genetic stability  
365 (43, 44, 55, 67-69) and loss (45, 70, 71) have been observed using fewer/weaker markers.  
366 The lack of exploitation impact on the BFT genome, should nonetheless be taken into account  
367 in fisheries management policies to provide confidence for recovery since it implies that BFT  
368 productivity can be maximised to historical levels.

369

370 Despite expectations that fisheries will induce the artificial selection of traits which favour  
371 smaller body sizes (1, 50), only two temporal investigations on genome-wide selection  
372 patterns exists for fishes; one which found a lack of adaptive responses (42), and the other,  
373 several adaptive responses coinciding with biomass and  $N_e$  declines in Atlantic salmon (*Salmo*  
374 *salar*, (72)). In the current study, we found 19 genomic regions under putative temporal  
375 selection. At each site, recent mutations promoted heterozygous genotypes which could not  
376 be explained by differences in sample depth. Due to varied gene function at these sites, it  
377 remains challenging to explain the driver of the increased frequency of alternative alleles and  
378 whether they indeed represent true selection signals which affect gene function.

379

380 While strong rises of novel alleles to high frequency and hard selective sweeps have been  
381 observed in laboratory experiments (51) and rare cases of rapid evolution in modern samples  
382 (47-49), we propose that our observations of novel alleles (or those previously at very low  
383 frequency) at moderate, rather than high frequency, are expected in wild fish populations. This  
384 is because novel, beneficial alleles are unlikely to rise to fixation unless hundreds of  
385 generations have elapsed under low levels of genetic drift (ca. two thousand years for BFT),  
386 or remain at moderate frequencies if representing polygenic or epistatic, global adaptation (66,  
387 73-76). Indeed, similar patterns have been observed in Atlantic salmon (72) and this  
388 reasoning may well explain difficulties in identifying adaptive responses, because lower  
389 frequency differences between temporal samples are more challenging to disentangle from  
390 sequence noise, and may not contribute to significant differences between temporal samples  
391 in Tajima's D across the genome (42).

392

393 We conclude that putative selection signals represent recent genomic changes, and that the  
394 most recent dramatic changes in marine environments which might induce evolution are  
395 anthropogenic ones; such as fisheries. To test whether our selection signals characterise  
396 fisheries induced evolution, and may explain recent changes in juvenile BFT growth and  
397 maturation (53), we would require larger sample sizes and an improved reference genome  
398 with complete annotation to 1) confirm that the current dataset is representative of both  
399 ancestral and modern populations, and 2) improve our understanding of function at these sites  
400 and whether mutations drive non-synonymous substitutions in amino acid sequences.

401

402 Our results provide further confidence for BFT stocks and clear relevance for management  
403 with findings that western and eastern stocks are not demographically independent; and that  
404 continued recovery of the eastern BFT stock is likely to promote western recoveries, which  
405 remains a smaller and less-well-recovered stock. Moreover, it is likely that BFT productivity  
406 was greater prior to 1970 and that therefore, sustained low fishing mortality will increase  
407 abundance and productivity from the current level. There is no genomic evidence to suggest  
408 that further recoveries will be hampered by a loss of genetic diversity, however it remains  
409 unclear what the cause or function of recent putative adaptive responses are across the BFT  
410 genome. In any case, adaptive responses can be considered as positive evidence that BFT is  
411 continuing to adapt to rapidly changing marine environments and could have full capacity to  
412 do so.

413

## 414 **Methods and Materials**

415

### 416 **Sample collection**

417 We collected samples of modern, archival and archaeological BFT specimens for analysis as  
418 follows: contemporary larvae or young-of-the-year specimens (GoM: Gulf of Mexico, WMED:  
419 Western Mediterranean Balearic Islands, CMED: Central Mediterranean Sicily, EMED:  
420 Eastern Mediterranean Levantine Sea, n = 40, Table 1) were collected from each of the major  
421 BFT spawning sites between 2013 and 2018 (Fig. 1, Table 1). Larvae and tissue samples from  
422 each specimen were preserved in 96% ethanol and stored at -20 °C until further processing.

423

424 Archived vertebrae (n = 12; Table 1) were retrieved from the Massimo Sella Archive (55) and  
425 pertained to two tuna-trap catches of the 20th c. (1925 Zliten, Libya; and 1941 Istanbul, Turkey:  
426 Table 1, Fig. 1). Archaeological vertebrae (n = 32, Table 1) retrieved from several  
427 Mediterranean excavations throughout the past two millennia (Fig. 1) including (~1800 Leca  
428 Harbour, Marseille, France; 16-18th c. Pedras de Fogu, Sassari, Italy; 10-13th c. Sicily, Italy;  
429 and 9-13th c. Yenikapi, Istanbul, Turkey). N.B. 10-13th c. Sicily samples are presented as a  
430 pooled group from several sites. See Supplementary Materials 1 for more details on historical  
431 samples and their dating.

432

433

434

435

436

437

438

439

440

441

**Table 1.** Summary details of ancient and modern Atlantic bluefin tuna samples resequenced herein. n = number. \*Gulf of Mexico samples pertain to several sites, for full details see Supplementary Fig. S1. Coordinates for all sites were rounded. YoY= Young-of-the-Year.

Sample ID / Year / Century CE	Location/archaeological site	Latitude	Longitude	Sample type	n sample	Sequence Length (mean bp)	Endogenous (mean%)	n in final analysis	Sequencing Coverage (mean X)
GoM 2014-2018	Gulf of Mexico	26.0*	-90.0*	Larvae	10	79±17	61±0	10	10.0±2.1
WMED 2013	Western Mediterranean	39.27	2.10	YoY	10	80±21	68±0	10	11.4±3.6
CMED 2013	Central Mediterranean	36.93	13.17	YoY	10	81±19	56±0	10	12.2±3.6
EMED 2013	Eastern Mediterranean	35.51	33.41	YoY	10	107±18	72±0	9	13.2±2.7
1941	Istanbul, Turkey	41.00	28.95	Archived adult bone	2	66±4	19±11	2	9.7±4.7
1925	Zliten, Lybia	41.00	14.65	Archived adult bone	8	70±10	41±5	8	10.3±4.0
~1800	Marseille, France	43.30	5.36	Archaeological adult bone	7	68±8	26±5	7	9.5±2.9
16-18 <sup>th</sup> c.	Sassari, Italy	40.86	8.62	Archaeological adult bone	9	72±7	50±7	8	8.3±0.9
10-13 <sup>th</sup> c.	Sicily, Italy	37.65, 38.10	12.58, 13.36	Archaeological adult bone	6	71±8	39±13	6	10.3±1.9
9-13 <sup>th</sup> c.	Istanbul, Turkey	41.00	28.95	Archaeological adult bone	10	74±6	54±5	8	9.1±5.2

443

444

#### Ancient DNA extraction

445

Archival and archaeological samples underwent ancient DNA (aDNA) extraction in dedicated, sterile, PCR-free conditions at the Ancient DNA Laboratory of the Department of Cultural Heritage (University of Bologna, Ravenna Campus, Italy), following strict criteria for aDNA analysis (77, 78). The outer surfaces of bones were cleaned with a ~20% sodium hypochlorite (bleach) solution and left to air-dry for 10 minutes. Specimens were then exposed to UV light

446

447

448

449

450 (254 nm) for 15 minutes on each side before drilling to remove an outer layer (~2 mm) of  
451 material. Between 100-350 mg bone powder was then collected by drilling at the same position  
452 where the outer layer had been removed. Care was taken to avoid overheating specimens by  
453 drilling at slow speeds with diamond-tipped drill-bits.

454

455 Isolation of aDNA was performed using a modified version of Dabney et al. (79, 80). Briefly,  
456 100-300 mg bone powder from each sample was pre-digested (81) for 20 minutes at 37°C in  
457 1-3 ml digestion buffer containing EDTA (0.45 M, pH 8.0) and proteinase K (0.25 mg/ml).  
458 Lysates were then discarded before samples were fully digested overnight in the same  
459 conditions. Once digested, lysates were combined with 10 ml of binding buffer (PB buffer,  
460 Qiagen, Germany) and bound to the High Pure Viral Nucleic Acid Large Volume silica spin  
461 columns (Roche, Basel, Switzerland) by centrifugation. Membrane-bound aDNA was then  
462 washed twice with 720 µl PE buffer (Qiagen), before elution in 30 µl of EB buffer (Qiagen).  
463 The total DNA obtained from each extraction was quantified using the Qubit® dsDNA HS (High  
464 Sensitivity) Assay Kit (Thermo Fisher Scientific, USA). Negative controls employed in each  
465 batch of samples extracted indicated an undetectable level of contamination (<500 pg/ml).  
466 Extractions were then stored at -20°C until library preparation.

467

#### 468 **Modern DNA extraction**

469 Modern specimens were extracted at the GenoDREAM laboratory of the Department of  
470 Biological, Geological and Environmental sciences (University of Bologna, Ravenna Campus,  
471 Italy), using a modified salt-based extraction protocol (82) using SSTNE extraction buffer (83),  
472 and treated with RNase (Qiagen) to remove residual RNA. After isolation, the total DNA  
473 obtained from each extraction was quantified using the Qubit® dsDNA BR Assay Kit (Thermo  
474 Fisher Scientific, USA). Negative controls employed for each batch of samples extracted  
475 indicated an undetectable level of contamination. Samples were diluted to 10 ng/ul. Prior to  
476 library preparation, 100 ul of DNA from each Modern extraction was sheared to maximum  
477 sizes of 500 bp using a Bioruptor® Pico sonicator (Diagenode) with the settings: Medium 30  
478 on/90 off for 10 minutes. Samples were precipitated using isopropanol, following a procedure  
479 from Qiagen (FAQ-ID-2953). Fragment lengths were confirmed by agarose gel  
480 electrophoresis and total DNA was re-quantified before precipitates were stored at -20°C until  
481 library preparation.

482

#### 483 **DNA library preparation and sequencing**

484 Single stranded libraries were built for both ancient and modern samples using the Santa Cruz  
485 Reaction (SCR) method (84) from 10-20 µl of DNA, up to a maximum input of 150 ng. Prior to  
486 indexing, aDNA libraries were prepared in sterile conditions at the Ancient DNA Laboratory of  
487 the Department of Cultural Heritage, separate to those used to prepare modern libraries.  
488 Library quality and the non-amplification of controls was confirmed using qPCR following the  
489 SCR method, which indicated the number of cycles required for indexing and inhibited  
490 samples to be discarded. Ligated DNA was double-indexed with sample-specific 6 bp indexes  
491 by amplification using 2X Amplitaq Gold 360 MM (Thermo Fisher Scientific, USA), and 25-50  
492 uM of each index for 10-14 cycles (2 min at 95°C, cycles of 30 s at 95°C, 30 s at 60°C, and  
493 70 s at 72°C with a final extension of 10 min at 72°C). Amplified products were cleaned by  
494 using AMPure XP beads (Agencourt) at a 1:1.2 ratio, eluted in 25 µl in EB buffer and quantified  
495 using a Bioanalyzer 2100 (Agilent Technologies). Libraries were screened to explore DNA  
496 preservation and library clonality by sequencing ~1 million reads per sample on the Illumina  
497 HiSeq X platform (100 bp paired-end), using a total of 4 lanes. Libraries were then re-

498 sequenced (150 bp paired-end) on the NovaSeq S4 Illumina platform, to the final sequencing  
499 depths reported, using a total of 7 lanes. Sequencing and demultiplexing (allowing zero  
500 mismatches in the index tags) was performed at the Norwegian Sequencing Center (Oslo,  
501 Norway) and Macrogen facilities (Seoul, South Korea/Amsterdam, Netherlands) with care  
502 taken to avoid batch effects by pooling varied combinations of samples (Table S1).

503

#### 504 **Reference assembly improvement**

505 The highly-scaffolded draft BFT genome assembly (NCBI BioProject: PRJNA408269), , was  
506 mapped against the fThuAlb1.1 chromosome-scale assembly of a sister-species, yellowfin  
507 tuna (*Thunnus albacares*, GCA\_914725855.1). Scaffolds were mapped using BMap (85)  
508 with the asm10 setting which successfully mapped 102,121 out of 103,645 (98.5%) scaffolds  
509 to yellowfin tuna chromosomes. Scaffolds were then binned into the 24 yellowfin tuna  
510 chromosomes by placing 200 N's between them, resulting in a 768 Mb pseudo-chromosome  
511 assembly. Non-mapped (unplaced) scaffolds were excluded from analyses.

512

#### 513 **Data processing and filtering**

514 Ancient and modern reads were processed by using PALEOMIX (86) which is a set of  
515 pipelines and tools designed to aid the rapid processing of high-throughput ancient  
516 sequencing data. Forward and reverse reads were collapsed with AdapterRemoval v1.5 (87)  
517 and aligned to our pseudo-chromosome BFT reference using BWA mem (85). Only reads that  
518 had a minimum length of 25 bp were aligned, and only with a minimum quality score (MapQ)  
519 of 30 i.e. a 0.1% chance each read was mis-aligned were used for subsequent analyses.  
520 Ancient DNA damage patterns were investigated by using mapDamage v.2.0.6 (88). Finally,  
521 we removed all clipped reads (or pairs of reads for which one read was clipped) and all  
522 duplicate reads (Picard Tools v. 1.96) and then realigned indels using GATK v. 3.7  
523 IndelRealigner (89). To reduce the influence of post-mortem taphonomic degradation on our  
524 downstream SNP analyses, we studied damage patterns (Supplementary Figure S1) and  
525 trimmed 3 bp from all ancient mapped reads using the TrimBam function of bamUtil v.1.0.6  
526 (90) and re-indexed using samtools v1.7 (91). This reduced the frequency of deamination to  
527 below 5% in all reads. Average read-depths were 9.7 and 11.7 fold coverage for ancient and  
528 modern samples, respectively.

529

530 We used GATK to jointly call SNPs (GATK HaplotypeCaller and GenotypeGVCFs) for ancient  
531 and modern samples using default settings, allowing a maximum of three alternative alleles.  
532 We were concerned with reference bias, as this is a common hindrance of genomic studies,  
533 especially those which map relatively short reads such as ours (42, 92, 93). Therefore, we  
534 filtered SNPs using conservative established approaches. First, SNPs were hard-filtered for  
535 strand bias (FS and SOR), mapping quality (MQ), quality by depth (QD), non-polymorphism  
536 (AC) using BCFTOOLS v. 1.6 with settings filter -i 'FS>60.0 || SOR>4 || MQ<30 || QD<2.0 ||  
537 AC==0 || AC==AN'. Then, we removed indels and retained only, bi-allelic SNPs using  
538 VCFtools v.0.1.16 (94) with settings --remove-indels --min-alleles 2 --max-alleles 2.

539

540 VCFtools was then used to filter for depth (minDP and max-meanDP) and minor allele  
541 frequency (MAF). MAF filters were used to remove singletons which may represent poor  
542 sequencing or DNA quality, and set depending on the number of samples present in multi-  
543 sample VCFs i.e --maf 0.05 or 0.02 if using modern (n=40) or modern and ancient (n=82)  
544 samples, respectively. Likewise, a --max-maf 0.95 or 0.98 filter was used to remove SNPs  
545 where the reference allele was not present at least twice, likely as a consequence of

546 insufficient reference quality in some regions. SNPs present in genomic regions where reads  
547 preferentially mapped more than twice the average (likely repetitive regions) were removed  
548 using a max-meanDP filter set to 30; double the coverage of our highest coverage samples.  
549 Unless otherwise mentioned, a minDP filter of 8 was used, to provide confidence that  
550 homozygous loci were not artefacts of insufficient coverage. A maximum of 5% missing data  
551 was tolerated for selection analyses (--missing-data 0.95) while no missing data was tolerated  
552 for demographic analyses (--missing-data 1) due to poor handling of missigness by programs  
553 which analyse differences in allele frequencies per sample group. Finally, to retain sufficient  
554 loci with this conservative approach, three ancient samples were dropped from analyses due  
555 to low coverage <6X (IST\_913C\_01, IST\_913C\_02 and PF\_1618C\_23, Table S1).

556  
557 For demographic analyses, we excluded loci that were out of hardy-weinberg equilibrium  
558 (HWE) due to the possibility that highly hetero- or homozygous loci represent non-biological  
559 sequencing artefacts or signatures of selection. We opted to remove loci if they yielded a p  
560 value <0.001 following a site-specific exact test across all samples as implemented in  
561 VCFtools, instead of removing loci which deviate from HWE per population; which is the  
562 recommended approach so as not to reduce population structure (95). Our justification for our  
563 approach was as follows: First, BFT is a highly-fecund, highly-mobile batch spawner which  
564 exhibits high-levels of population connectivity (26, 43), thus large (true biological) allele  
565 differences between populations which represent neutral demography were not expected.  
566 Second, analysing HWE per population with small-sample sizes would result in a large number  
567 of loci being falsely identified as out of HWE, which would have vastly reduced the number of  
568 informative loci for downstream analyses. Due to the potential that these sites may indeed  
569 represent biological selection signals, we employed a more relaxed HWE filter ( $p < 1e-6$ ) for  
570 selection analyses i.e. the threshold that is recommended for the detection of selection on  
571 quantitative traits (96).

572  
573 Due to the possibility that multiple ancient bones were sequenced from the same individual,  
574 or that modern tissues were sampled from closely-related individuals, we tested pairwise  
575 relatedness between samples in VCFtools using --relatedness2. This resulted in the removal  
576 of two ancient specimens from analyses (CDM\_10C\_07 and CDM\_10C\_11) due to their  
577 kinship coefficient >0.35 i.e. duplicate/twin with CDM\_10\_04. The modern sample CYPR-LS-  
578 331 was removed for the same reason due to its close-kinship >0.35 with CYPR-LS-330.

579  
580 Overall, these filters produced final datasets across the 768 Mb BFT pseudo-chromosome  
581 reference genome of 39 modern individuals with 843,664 loci for demographic analysis and  
582 1,064,265 for selection analysis, and combined ancient and modern datasets of 78 individuals  
583 with 106,210 loci for demographic analysis and 513,745 loci for selection analysis.

#### 584 585 **Population structure**

586 SNPs were pruned (--indep-pairwise 100 10 0.5) for linkage disequilibrium using PLINK  
587 v1.90b6.21 (97). Therefore, analyses were performed on two datasets; one modern dataset  
588 of 666,635 loci, and one modern and ancient dataset of 96,542 loci. A discriminant analysis of  
589 principal components (DAPC) was performed using the R package adegenet(98). DAPC is a  
590 geometric clustering method free of HWE assumptions that attempts to maximise variation  
591 between clusters, while minimising variation within clusters. DAPC was run by defining  
592 clusters a priori as sample groups. Cross-validation testing using the x.val function (n.rep =  
593 1000) indicated the number of principal components (PC's) to be retained was four for the

594 ancient and modern dataset, and nine for the modern dataset, while all discriminant functions  
595 were retained following (99). K-means clustering in adegenet was performed on the modern  
596 dataset using the function find.clusters, with default settings but specifying max.n.clust=4 i.e.  
597 the number of modern sample groups. We removed transition sites (C > T and G > A SNPs)  
598 which may be affected by post-mortem taphonomic degradation (Figure S1) and re-ran DAPC  
599 analyses on the remaining 27,915 loci to explore the potential impact of ancient DNA damage  
600 on our inference of population structure.

601

602 Population structure was also evaluated using STRUCTURE v.2.3.4 (100), which implements  
603 a Bayesian clustering method assuming HWE to identify the most likely number of populations  
604 (K). We followed the Evano *et al.* (101) method, and thus, we carried out 10 runs per each  
605 value of K ranging from 1 to 5. Runs used the locprior and admixture models and assumed  
606 correlated allele frequencies. Each run used 10,000 burn-in and 50,000 Markov Chain Monte  
607 Carlo replicates. We estimated the ad hoc statistic  $\Delta K$  in order to infer the most likely number  
608 of populations using STRUCTURE HARVESTER (102). CLUMPAK (103) was used to merge  
609 the 10 runs from the most probable K, which reported similarity scores >95%. Pairwise  
610 distances between localities and time periods were calculated with Nei's estimator of  $F_{ST}$   
611 (104) as implemented in the hierfstat R package, using 1000 permutations to calculate p-  
612 values, which were judged for significance under the FDR approach at the 5% level.

613

#### 614 **Genetic summary statistics**

615 Genetic summary statistics were calculated using the filtered, unpruned dataset.  
616 Heterozygosity was calculated for each individual using VCFtools --het. Nucleotide diversity  
617 ( $\pi$ ) and Tajima's D were then calculated per 100kb window for each sample group using  
618 VCFtools --windowpi and --TajimaD options, excluding the 1941 sample due to small sample  
619 size ( $n = 2$ ). T-tests were performed in R to judge the statistical significance of summary  
620 statistic differentiation between sample groups, at the 5% level. We removed transition sites  
621 (C > T and G > A SNPs) which may be affected by post-mortem taphonomic degradation and  
622 re-ran the analysis, details of which can be found in the Supplementary.

623

#### 624 **Effective population size**

625 We calculated historical effective population size ( $N_e$ ) using GoNe (63). GoNe assumes  
626 overlapping generations by applying the Jorde-Ryman modification to the temporal method to  
627 estimate  $N_e$  using linkage disequilibrium (LD) for the previous 200 generations. GoNe was run  
628 on the filtered dataset of modern samples comprising 843,664 loci, grouped by spawning-site  
629 ( $n = 9$  or  $10$ ). We converted GoNe outputs of  $N_e$  estimates per generation number to years  
630 (BCE/CE) using a generation length of 13 years, following (61) and <https://fishbase.se>. We  
631 discarded estimates of the previous 4 generations (~50 years) as these yielded extremely low  
632  $N_e$  estimates (~15-20k), likely as a function of methodological limitations (63). We tested for  
633 the effect of sample-size by pooling Mediterranean samples across sites ( $n = 29$ ) and all  
634 modern samples ( $n = 39$ ), which yielded near-identical  $N_e$  trajectories over time as when  
635 analysed separately (Fig. S5). We tested for the effect of sequencing depth on the stability of  
636 estimates, by increasing the --minDP 12 in VCFtools and re-running GoNe with 112,980 loci,  
637 which also yielded near-identical  $N_e$  trajectories.

638

639 As an alternative approach to infer relative changes in  $N_e$  using linkage patterns between  
640 ancient and modern samples, we estimated linkage ( $R^2$ ) across the genome in windows using  
641 PLINK ( --ld-window 10000 --ld-window-kb 500) for each ancient and modern sample group,

642 without setting an  $R^2$  threshold (--ld-window-r2 0). Results (Figure S6) suggested that linkage  
643 patterns were largely reflective of which individuals were present in a dataset and their kinship  
644 (105), such that combined cohorts in ancient samples had elevated LD patterns which are  
645 likely to downwardly bias  $N_e$  estimates (106) when census size is very large in comparison  
646 with  $N_e$ , as in the case of BFT. This precluded the opportunity to obtain meaningful single-  
647 sample  $N_e$  estimates for each temporal group using methods such as LDNe (107).

648

#### 649 **Tests for selection**

650 Selection presents itself in many forms in the genome including allele frequency changes and  
651 an increase in linkage disequilibrium (73, 108). We used the two SNP-based selection  
652 methods with the lowest false positive rates which detect outlier loci in allele frequency that  
653 may be under putative selection; OutFLANK (109) and pcadapt (110), and sought to identify  
654 which outlier loci show elevated levels of linkage to validate true positives. OutFLANK  
655 accounts for sampling error and nonindependence between sample groups provided a priori  
656 while inferring the  $F_{ST}$  distribution of loci and fitting a  $\chi^2$  model to the centre of the distribution.  
657 Loci under putative selection are those that deviate from this normal distribution. Pcadapt does  
658 not require sample groups to be defined, identifying outliers by ascertaining population  
659 structure via PCA and determining outlier loci as those excessively correlated with one or more  
660 ordination axes. OutFLANK was deemed to be the method most appropriate for the detection  
661 of large effect loci whereas pcadapt is likely to detect small effect loci in addition because  
662 these covary across multiple ordination axes which are taken into account with pcadapt.

663

664 First, SNPs were filtered using VCFtools (maf --0.1) to remove low heterozygous sites which  
665 have a high noise to signal ratio and are more likely to represent erroneous sites as a result  
666 of assembly artefacts (111). Therefore, we ran OutFLANK v.02 (109) and pcadapt (110) on a  
667 modern dataset of 1,064,265 loci including 1.2% missing data, and an ancient and modern  
668 dataset of 513,745 loci including 2.9% missing data. OutFLANK was run in R using suggested  
669 settings (LeftTrimFraction = 0.05, RightTrimFraction = 0.05) and a false discovery rate (FDR)  
670 of  $\leq 5\%$  (109). A 'qthreshold' of 0.05 was used for the modern dataset, while the 'qthreshold'  
671 was adjusted to 0.001 for the combined ancient and modern dataset to reflect relatively low  
672 levels of differentiation (109). pcadapt was run in R, we used population clustering results from  
673 DAPC and pcadapt to guide the choice of K latent factors, setting K=2 in the case of Ancient  
674 vs Contemporary Mediterranean, and Contemporary Gulf of Mexico vs. Contemporary  
675 Mediterranean, while K=3 was used within the Mediterranean, reflecting the three sample  
676 sites. QQ plots (data not shown) confirmed an expected distribution of the data which was  
677 skewed at the upper bounds indicating the presence of outliers. In all cases, we corrected  
678 significance ( $p < 0.001$ ) using the Bonferroni method, to conservatively limit the number of  
679 potential false positives identified by pcadapt (112).

680

681 Since loci under recent selection are likely to show elevated levels of linkage (113), we  
682 determined which outlier loci show elevated levels of linkage i.e.  $R^2$  values  $> 0.5$ , using PLINK  
683 (--indep-pairwise 100 10 0.5). To explore the spatial and temporal rise to fixation of alleles at  
684 selected putative loci under selection we calculated allele frequencies for loci in LD and  
685 common between the methods in R using an uncorrected approach (as per (114)) and plotted  
686 MAFs for each sample group. For the combined ancient and modern dataset we plotted the  
687 best candidates only i.e. genomic regions where  $> 3$  outlier loci were present in a 1kb window.  
688 To identify the function of genomic regions under putative selection we first isolated loci with  
689 150bp upstream and downstream flanking regions and converted coordinates to the original



690 scaffold assembly gene annotations using the blastn –query function (settings: -evalue 0.001  
691 -outfmt 6 -ungapped), selecting only matches where the entire fragment length was retrieved.  
692 Second, we searched annotated predicted proteins within 2kb of loci using the blastp –query  
693 function (default settings) against the NCBI Protein Database (ncbi.nlm.nih.gov/protein),  
694 reporting the top hit in each instance.  
695

#### 696 **Author Contributions**

697 AJA, FT, EC and AC designed the study. AJA, FT, EM, GZ, VO, AS, VA, GC, and GP collected  
698 samples for analysis. AJA, FP, SDF, FF and EC conducted the laboratory work. AJA, BS,  
699 EFE, LA, OK and AC analysed the data. AJA, BS, ADT, EFE, FT, EC and AC wrote the paper.  
700 All authors reviewed the paper.  
701

#### 702 **Acknowledgements**

703 The authors would like to thank the NOAA Restore Project which aided the collection of  
704 western Atlantic samples. This work is a contribution to the <https://tunaarchaeology.org> project  
705 within the framework of the MSCA SeaChanges ITN, which was funded by EU Horizon 2020  
706 (Grant Number: 813383).  
707

#### 708 **Funding Information**

709 This project was funded by the EU Horizon 2020 Grant Number 813383 as part of the MSCA  
710 ITN SeaChanges.  
711

#### 712 **Conflict of Interest**

713  
714 No conflicts of interest exist.  
715

#### 716 **References**

- 717 1. A. Kuparinen, J. A. Hutchings, Consequences of fisheries-induced evolution for  
718 population productivity and recovery potential. *Proc. Biol. Sci.* **279**, 2571–2579 (2012).
- 719 2. C. M. Duarte, *et al.*, Rebuilding marine life. *Nature* **580**, 39–51 (2020).
- 720 3. C. E. Porch, S. Bonhommeau, G. A. Diaz, A. Haritz, G. Melvin, The journey from  
721 overfishing to sustainability for Atlantic bluefin tuna, *Thunnus thynnus*. *The future of*  
722 *bluefin tunas: Ecology, fisheries management, and conservation*, 3–44 (2019).
- 723 4. B. R. MacKenzie, H. Mosegaard, A. A. Rosenberg, Impending collapse of bluefin tuna  
724 in the northeast Atlantic and Mediterranean. *Conserv. Lett.* **2**, 26–35 (2009).
- 725 5. ICCAT, Report of the 2006 Atlantic bluefin tuna stock assessment session. *Collect.*  
726 *Vol. Sci. Pap. ICCAT* **60**, 652–880 (2007).
- 727 6. J.-M. Fromentin, Lessons from the past: investigating historical data from bluefin tuna  
728 fisheries. *Fish Fish* **10**, 197–216 (2009).
- 729 7. M. R. Siskey, M. J. Wilberg, R. J. Allman, B. K. Barnett, D. H. Secor, Forty years of  
730 fishing: changes in age structure and stock mixing in northwestern Atlantic bluefin tuna  
731 (*Thunnus thynnus*) associated with size-selective and long-term exploitation. *ICES J.*  
732 *Mar. Sci.* **73**, 2518–2528 (2016).
- 733 8. B. Worm, D. P. Tittensor, Range contraction in large pelagic predators. *Proc. Natl.*  
734 *Acad. Sci. U. S. A.* **108**, 11942–11947 (2011).

- 735 9. L. Nøttestad, E. Boge, K. Ferter, The comeback of Atlantic bluefin tuna (*Thunnus*  
736 *thynnus*) to Norwegian waters. *Fish. Res.* **231**, 105689 (2020).
- 737 10. T. W. Horton, *et al.*, Evidence of increased occurrence of Atlantic bluefin tuna  
738 in territorial waters of the United Kingdom and Ireland. *ICES J. Mar. Sci.* (2021)  
739 <https://doi.org/10.1093/icesjms/fsab039> (April 21, 2021).
- 740 11. A. Di Natale, S. Tensek, A. P. García, Is the bluefin tuna slowly returning to the  
741 Black Sea? Recent evidences. *Collect. Vol. Sci. Pap. ICCAT* **75**, 1261–1277 (2019).
- 742 12. C. Carrano, *et al.*, 2022 asap stock assessment of The Eastern Atlantic and  
743 Mediterranean bluefin tuna. *Collect. Vol. Sci. Pap. ICCAT*, 79(3): 551-586 (2022)
- 744 13. ICCAT, Report of the 2020 second ICCAT intersessional meeting of the bluefin  
745 tuna species group. Online, 20-28 July 2020. *Collect. Vol. Sci. Pap. ICCAT*, 77(2): 441-  
746 567(2020).
- 747 14. M. J. Juan-Jordá, *et al.*, Seventy years of tunas, billfishes, and sharks as  
748 sentinels of global ocean health. *Science* **378**, eabj0211 (2022).
- 749 15. A. J. Andrews, *et al.*, Exploitation history of Atlantic bluefin tuna in the eastern  
750 Atlantic and Mediterranean—insights from ancient bones. *ICES J. Mar. Sci.* **79**, 247–262  
751 (2022).
- 752 16. L. M. Atmore, *et al.*, Population dynamics of Baltic herring since the Viking Age  
753 revealed by ancient DNA and genomics. *Proc. Natl. Acad. Sci. U. S. A.* **119**, e2208703119  
754 (2022).
- 755 17. J. B. Jackson, *et al.*, Historical overfishing and the recent collapse of coastal  
756 ecosystems. *Science* **293**, 629–637 (2001).
- 757 18. H. K. Lotze, R. Hoffmann, J. Erlandson, “Lessons from historical ecology and  
758 management” in *The Sea, Volume 19: Ecosystem-Based Management*, (Harvard  
759 University Press, 2014) (October 20, 2020).
- 760 19. E. J. Guiry, *et al.*, Early evidence for historical overfishing in the Gulf of Mexico.  
761 *Sci Adv* **7** (2021).
- 762 20. K. Schwerdtner Máñez, *et al.*, The future of the oceans past: towards a global  
763 marine historical research initiative. *PLoS One* **9**, e101466 (2014).
- 764 21. G. L. Britten, M. Dowd, B. Worm, Changing recruitment capacity in global fish  
765 stocks. *Proc. Natl. Acad. Sci. U. S. A.* **113**, 134–139 (2016).
- 766 22. E. L. Jensen, *et al.*, Ancient and historical DNA in conservation policy. *Trends*  
767 *Ecol. Evol.* **37**, 420–429 (2022).
- 768 23. M. Kardos, *et al.*, The crucial role of genome-wide genetic variation in  
769 conservation. *Proc. Natl. Acad. Sci. U. S. A.* **118** (2021).
- 770 24. G. Heinisch, H. Rosenfeld, J. M. Knapp, H. Gordin, M. E. Lutcavage, Sexual  
771 maturity in western Atlantic bluefin tuna. *Sci. Rep.* **4**, 7205 (2014).
- 772 25. C. Piccinetti, A. Di Natale, P. Arena, Eastern bluefin tuna (*Thunnus thynnus*,  
773 L.) reproduction and reproductive areas and season. *Collect. Vol. Sci. Pap. ICCAT* **69**,  
774 891–912 (2013).

- 775 26. G. N. Puncher, *et al.*, Spatial dynamics and mixing of bluefin tuna in the Atlantic  
776 Ocean and Mediterranean Sea revealed using next-generation sequencing. *Mol. Ecol.*  
777 *Resour.* **18**, 620–638 (2018).
- 778 27. N. Rodríguez-Ezpeleta, *et al.*, Determining natal origin for improved  
779 management of Atlantic bluefin tuna. *Front. Ecol. Environ.* **17**, 439–444 (2019).
- 780 28. D. E. Richardson, *et al.*, Discovery of a spawning ground reveals diverse  
781 migration strategies in Atlantic bluefin tuna (*Thunnus thynnus*). *Proc. Natl. Acad. Sci. U.*  
782 *S. A.* **113**, 3299–3304 (2016).
- 783 29. J. L. Cort, P. Abaunza, “The Present State of Traps and Fisheries Research in  
784 the Strait of Gibraltar” in *The Bluefin Tuna Fishery in the Bay of Biscay : Its Relationship*  
785 *with the Crisis of Catches of Large Specimens in the East Atlantic Fisheries from the*  
786 *1960s*, J. L. Cort, P. Abaunza, Eds. (Springer International Publishing, 2019), pp. 37–78.
- 787 30. R. M. Dickhut, *et al.*, Atlantic bluefin tuna (*Thunnus thynnus*) population  
788 dynamics delineated by organochlorine tracers. *Environ. Sci. Technol.* **43**, 8522–8527  
789 (2009).
- 790 31. C. M. Hernández, *et al.*, Support for the Slope Sea as a major spawning ground  
791 for Atlantic bluefin tuna: evidence from larval abundance, growth rates, and particle-  
792 tracking simulations. *Can. J. Fish. Aquat. Sci.* **79**, 814–824 (2022).
- 793 32. J. M. Rodriguez, C. Johnstone, D. Lozano-Peral, Evidence of Atlantic bluefin  
794 tuna spawning in the Bay of Biscay, north-eastern Atlantic. *J. Fish Biol.* **99**, 964–969  
795 (2021).
- 796 33. B. R. MacKenzie, P. Mariani, Spawning of bluefin tuna in the Black Sea:  
797 historical evidence, environmental constraints and population plasticity. *PLoS One* **7**,  
798 e39998 (2012).
- 799 34. A. Di Natale, The Eastern Atlantic bluefin tuna: Entangled in a big mess,  
800 possibly far from a conservation red alert. Some comments after the proposal to include  
801 bluefin tuna in CITES appendix I. *Collect. Vol. Sci. Pap. ICCAT*, **65** (3): 1004–1043.  
802 (2010).
- 803 35. P. Cermeño, *et al.*, Electronic tagging of Atlantic bluefin tuna (*Thunnus thynnus*,  
804 L.) reveals habitat use and behaviors in the Mediterranean Sea. *PLoS One* **10**, e0116638  
805 (2015).
- 806 36. G. De Metrio, *et al.*, Joint Turkish-Italian research in the Eastern Mediterranean:  
807 bluefin tuna tagging with pop-up satellite tags. *Collect. Vol. Sci. Pap. ICCAT* **56**, 1163–  
808 1167 (2004).
- 809 37. A. Di Natale, Review of the historical and biological evidences about a  
810 population of bluefin tuna (*Thunnus thynnus* L.) in The Eastern Mediterranean and the  
811 black sea. *Collect. Vol. Sci. Pap.* **71**, 1098–1124 (2015).
- 812 38. F. S. Karakulak, I. K. Oray, Remarks on the fluctuations of bluefin tuna catches  
813 in Turkish waters. *Collect. Vol. Sci. Pap. ICCAT* (2009).
- 814 39. A. Pagá Garcia, *et al.*, Report on revised trap data recovered by ICCAT GBYP  
815 from Phase 1 to Phase 6. *Collect. Vol. Sci. Pap. ICCAT* **73**, 2074–2098 (2017).
- 816 40. T. Oosting, *et al.*, Unlocking the potential of ancient fish DNA in the genomic

- 817 era. *Evol. Appl.* **12**, 1513–1522 (2019).
- 818 41. D. Díez-Del-Molino, F. Sánchez-Barreiro, I. Barnes, M. T. P. Gilbert, L. Dalén,  
819 Quantifying Temporal Genomic Erosion in Endangered Species. *Trends Ecol. Evol.* **33**,  
820 176–185 (2018).
- 821 42. M. L. Pinsky, *et al.*, Genomic stability through time despite decades of  
822 exploitation in cod on both sides of the Atlantic. *Proc. Natl. Acad. Sci. U. S. A.* **118** (2021).
- 823 43. A. J. Andrews, *et al.*, Ancient DNA SNP-panel data suggests stability in bluefin  
824 tuna genetic diversity despite centuries of fluctuating catches in the eastern Atlantic and  
825 Mediterranean. *Sci. Rep.* **11**, 20744 (2021).
- 826 44. L. Hauser, G. J. Adcock, P. J. Smith, J. H. B. Ramírez, G. R. Carvalho, Loss of  
827 microsatellite diversity and low effective population size in an overexploited population of  
828 New Zealand snapper (*Pagrus auratus*). *Proc. Natl. Acad. Sci. U. S. A.* **99**, 11742–11747  
829 (2002).
- 830 45. W. F. Hutchinson, C. van Oosterhout, S. I. Rogers, G. R. Carvalho, Temporal  
831 analysis of archived samples indicates marked genetic changes in declining North Sea  
832 cod (*Gadus morhua*). *Proc. Biol. Sci.* **270**, 2125–2132 (2003).
- 833 46. M. Heino, B. D. Pauli, U. Dieckmann, Fisheries-Induced Evolution. *Annual*  
834 *Review of Ecology, Evolution, and Systematics* **46**, 461–480 (2015).
- 835 47. N. O. Therkildsen, *et al.*, Microevolution in time and space: SNP analysis of  
836 historical DNA reveals dynamic signatures of selection in Atlantic cod. *Mol. Ecol.* **22**,  
837 2424–2440 (2013).
- 838 48. E. Bowles, K. Marin, S. Mogensen, P. MacLeod, D. J. Fraser, Size reductions  
839 and genomic changes within two generations in wild walleye populations: associated with  
840 harvest? *Evolutionary Applications* **13**, 1128–1144 (2020).
- 841 49. Y. Czorlich, T. Aykanat, J. Erkinaro, P. Orell, C. R. Primmer, Rapid evolution in  
842 salmon life history induced by direct and indirect effects of fishing. *Science* **376**, 420–423  
843 (2022).
- 844 50. J. A. Hutchings, A. Kuparinen, Throwing down a genomic gauntlet on fisheries-  
845 induced evolution. *Proc. Natl. Acad. Sci. U. S. A.* **118** (2021).
- 846 51. N. O. Therkildsen, *et al.*, Contrasting genomic shifts underlie parallel  
847 phenotypic evolution in response to fishing. *Science* **365**, 487–490 (2019).
- 848 52. E. M. Olsen, *et al.*, Maturation trends indicative of rapid evolution preceded the  
849 collapse of northern cod. *Nature* **428**, 932–935 (2004).
- 850 53. A. J. Andrews, Vertebrae reveal industrial-era increases in Atlantic bluefin tuna  
851 catch-at-size and juvenile growth. *ICES J. Mar. Sci.*
- 852 54. A. J. Andrews, Exploitation shifts trophic ecology and habitat preferences of  
853 Mediterranean and Black Sea bluefin tuna over centuries. Under review.
- 854 55. G. Riccioni, *et al.*, Spatio-temporal population structuring and genetic diversity  
855 retention in depleted Atlantic Bluefin tuna of the Mediterranean Sea. *Proceedings of the*  
856 *National Academy of Sciences* **107**, 2102–2107 (2010).
- 857 56. A. Di Natale, Review of the historical and biological evidences about a

- 858 population of bluefin tuna (*Thunnus thynnus* L.) in the eastern Mediterranean and the  
859 Black Sea. *Col Vol. Sci. Pap. ICCAT* **71**, 1098–1124 (2015).
- 860 57. G. N. Puncher, *et al.*, Individual assignment of Atlantic bluefin tuna in the  
861 northwestern Atlantic Ocean using single nucleotide polymorphisms reveals an  
862 increasing proportion of migrants from the eastern Atlantic Ocean. *Can. J. Fish. Aquat.*  
863 *Sci.* **79**, 111–123 (2022).
- 864 58. A. Di Natale, Due to the new scientific knowledge, is it time to reconsider the  
865 stock composition of Atlantic bluefin tuna? *Collect. Vol. Sci. Pap. ICCAT* **75**, 1282–1292  
866 (2019).
- 867 59. A. Di Natale, M. Idrissi, Factors to be taken into account for a correct reading  
868 of tuna trap catch series. *Collect. Vol. Sci. Pap. ICCAT* **67**, 242–261 (2012).
- 869 60. C. Ravier, J.-M. Fromentin, Long-term fluctuations in the eastern Atlantic and  
870 Mediterranean bluefin tuna population. *ICES J. Mar. Sci.* **58**, 1299–1317 (2001).
- 871 61. R. S. Waples, P. M. Grewe, M. W. Bravington, R. Hillary, P. Feutry, Robust  
872 estimates of a high Ne/N ratio in a top marine predator, southern bluefin tuna. *Sci Adv* **4**,  
873 eaar7759 (2018).
- 874 62. R. S. Waples, What is Ne, anyway? *J. Hered.* (2022)  
875 <https://doi.org/10.1093/jhered/esac023> (May 19, 2022).
- 876 63. J. A. Coombs, B. H. Letcher, K. H. Nislow, GONe: software for estimating  
877 effective population size in species with generational overlap. *Mol. Ecol. Resour.* **12**, 160–  
878 163 (2012).
- 879 64. I. Novo, E. Santiago, A. Caballero, The estimates of effective population size  
880 based on linkage disequilibrium are virtually unaffected by natural selection. *PLoS Genet.*  
881 **18**, e1009764 (2022).
- 882 65. F. J. Mather, J. M. Mason, A. C. Jones, Historical document: life history and  
883 fisheries of Atlantic bluefin tuna (1995).
- 884 66. R. Frankham, Genetics and extinction. *Biol. Conserv.* **126**, 131–140 (2005).
- 885 67. T. Oosting, *et al.*, Mitochondrial genomes reveal mid-Pleistocene population  
886 divergence, and post-glacial expansion, in Australasian snapper (*Chrysophrys auratus*).  
887 *Heredity* (2022) <https://doi.org/10.1038/s41437-022-00579-1>.
- 888 68. L. Martínez-García, *et al.*, Historical Demographic Processes Dominate  
889 Genetic Variation in Ancient Atlantic Cod Mitogenomes. *Frontiers in Ecology and*  
890 *Evolution* **9**, 342 (2021).
- 891 69. C. F. Speller, *et al.*, High potential for using DNA from ancient herring bones to  
892 inform modern fisheries management and conservation. *PLoS One* **7**, e51122 (2012).
- 893 70. S. Bonanomi, *et al.*, Archived DNA reveals fisheries and climate induced  
894 collapse of a major fishery. *Sci. Rep.* **5**, 15395 (2015).
- 895 71. E. E. Nielsen, M. M. Hansen, V. Loeschcke, Analysis of microsatellite DNA from  
896 old scale samples of Atlantic salmon *Salmo salar* : a comparison of genetic composition  
897 over 60 years. *Mol. Ecol.* **6**, 487–492 (1997).
- 898 72. S. J. Lehnert, *et al.*, Genomic signatures and correlates of widespread

- 899 population declines in salmon. *Nat. Commun.* **10**, 2996 (2019).
- 900 73. N. Barghi, J. Hermisson, C. Schlötterer, Polygenic adaptation: a unifying  
901 framework to understand positive selection. *Nat. Rev. Genet.* **21**, 769–781 (2020).
- 902 74. M. Dehasque, *et al.*, Inference of natural selection from ancient DNA. *Evol Lett*  
903 **4**, 94–108 (2020).
- 904 75. M. Kimura, Attainment of Quasi Linkage Equilibrium When Gene Frequencies  
905 Are Changing by Natural Selection. *Genetics* **52**, 875–890 (1965).
- 906 76. S. Yeaman, Evolution of polygenic traits under global vs local adaptation.  
907 *Genetics* **220** (2022).
- 908 77. B. Llamas, *et al.*, From the field to the laboratory: Controlling DNA  
909 contamination in human ancient DNA research in the high-throughput sequencing era.  
910 *STAR: Science & Technology of Archaeological Research* **3**, 1–14 (2017).
- 911 78. E. Cilli, *Archaeogenetics* (2023).
- 912 79. J. Dabney, *et al.*, Complete mitochondrial genome sequence of a Middle  
913 Pleistocene cave bear reconstructed from ultrashort DNA fragments. *Proc. Natl. Acad.*  
914 *Sci. U. S. A.* **110**, 15758–15763 (2013).
- 915 80. P. Serventi, *et al.*, Iron Age Italic population genetics: the Piceni from Novilara  
916 (8th-7th century BC). *Ann. Hum. Biol.* **45**, 34–43 (2018).
- 917 81. P. B. Damgaard, *et al.*, Improving access to endogenous DNA in ancient bones  
918 and teeth. *Sci. Rep.* **5**, 11184 (2015).
- 919 82. V. P. Cruz, *et al.*, Identification and validation of single nucleotide  
920 polymorphisms as tools to detect hybridization and population structure in freshwater  
921 stingrays. *Mol. Ecol. Resour.* **17**, 550–556 (2017).
- 922 83. A. Blanquer, Phylogéographie intraspécifique d'un poisson marin, le flet  
923 *Platichthys flesus* L. (Heterosomata): Polymorphisme des marqueurs nucléaires et  
924 mitochondriaux. *PhD Thesis, Montpellier, France* (1990)  
925 <https://doi.org/http://www.theses.fr>. <http://www.theses.fr/1990MON20015>.
- 926 84. J. D. Kapp, R. E. Green, B. Shapiro, A Fast and Efficient Single-stranded  
927 Genomic Library Preparation Method Optimized for Ancient DNA. *J. Hered.* **112**, 241–  
928 249 (2021).
- 929 85. B. Bushnell, “BBMap: A fast, accurate, splice-aware aligner” (Lawrence  
930 Berkeley National Lab. (LBNL), Berkeley, CA (United States), 2014) (October 5, 2022).
- 931 86. M. Schubert, *et al.*, Characterization of ancient and modern genomes by SNP  
932 detection and phylogenomic and metagenomic analysis using PALEOMIX. *Nat. Protoc.*  
933 **9**, 1056–1082 (2014).
- 934 87. M. Schubert, S. Lindgreen, L. Orlando, AdapterRemoval v2: rapid adapter  
935 trimming, identification, and read merging. *BMC Res. Notes* **9**, 88 (2016).
- 936 88. H. Jónsson, A. Ginolhac, M. Schubert, P. L. F. Johnson, L. Orlando,  
937 mapDamage2.0: fast approximate Bayesian estimates of ancient DNA damage  
938 parameters. *Bioinformatics* **29**, 1682–1684 (2013).

- 939 89. A. McKenna, *et al.*, The Genome Analysis Toolkit: a MapReduce framework for  
940 analyzing next-generation DNA sequencing data. *Genome Res.* **20**, 1297–1303 (2010).
- 941 90. G. Jun, M. K. Wing, G. R. Abecasis, H. M. Kang, An efficient and scalable  
942 analysis framework for variant extraction and refinement from population-scale DNA  
943 sequence data. *Genome Res.* **25**, 918–925 (2015).
- 944 91. H. Li, *et al.*, The Sequence Alignment/Map format and SAMtools.  
945 *Bioinformatics* **25**, 2078–2079 (2009).
- 946 92. L. Orlando, *et al.*, Recalibrating Equus evolution using the genome sequence  
947 of an early Middle Pleistocene horse. *Nature* **499**, 74–78 (2013).
- 948 93. S. Gopalakrishnan, *et al.*, The wolf reference genome sequence (*Canis lupus*  
949 *lupus*) and its implications for *Canis* spp. population genomics. *BMC Genomics* **18**, 495  
950 (2017).
- 951 94. P. Danecek, *et al.*, The variant call format and VCFtools. *Bioinformatics* **27**,  
952 2156–2158 (2011).
- 953 95. W. S. Pearman, L. Urban, A. Alexander, Commonly used Hardy-Weinberg  
954 equilibrium filtering schemes impact population structure inferences using RADseq data.  
955 *Mol. Ecol. Resour.* **22**, 2599–2613 (2022).
- 956 96. A. T. Marees, *et al.*, A tutorial on conducting genome-wide association studies:  
957 Quality control and statistical analysis. *Int. J. Methods Psychiatr. Res.* **27**, e1608 (2018).
- 958 97. S. Purcell, *et al.*, PLINK: a tool set for whole-genome association and  
959 population-based linkage analyses. *Am. J. Hum. Genet.* **81**, 559–575 (2007).
- 960 98. T. Jombart, S. Devillard, F. Balloux, Discriminant analysis of principal  
961 components: a new method for the analysis of genetically structured populations. *BMC*  
962 *Genet.* **11**, 94 (2010).
- 963 99. T. Jombart, adegenet: a R package for the multivariate analysis of genetic  
964 markers. *Bioinformatics* **24**, 1403–1405 (2008).
- 965 100. J. K. Pritchard, M. Stephens, P. Donnelly, Inference of population structure  
966 using multilocus genotype data. *Genetics* **155**, 945–959 (2000).
- 967 101. G. Evanno, S. Regnaut, J. Goudet, Detecting the number of clusters of  
968 individuals using the software STRUCTURE: a simulation study. *Mol. Ecol.* **14**, 2611–  
969 2620 (2005).
- 970 102. D. A. Earl, B. M. vonHoldt, STRUCTURE HARVESTER: a website and program  
971 for visualizing STRUCTURE output and implementing the Evanno method. *Conservation*  
972 *Genetics Resources* **4**, 359–361 (2012).
- 973 103. N. M. Kopelman, J. Mayzel, M. Jakobsson, N. A. Rosenberg, I. Mayrose,  
974 Clumpak: a program for identifying clustering modes and packaging population structure  
975 inferences across K. *Mol. Ecol. Resour.* **15**, 1179–1191 (2015).
- 976 104. M. Nei, Molecular Evolutionary Genetics (1987) [https://doi.org/10.7312/nei-](https://doi.org/10.7312/nei-92038)  
977 92038.
- 978 105. F. Marandel, *et al.*, Estimating effective population size of large marine  
979 populations, is it feasible? *Fish Fish* **20**, 189–198 (2019).

- 980 106. R. S. Waples, T. Antao, G. Luikart, Effects of overlapping generations on  
981 linkage disequilibrium estimates of effective population size. *Genetics* **197**, 769–780  
982 (2014).
- 983 107. R. S. Waples, C. Do, Idne: a program for estimating effective population size  
984 from data on linkage disequilibrium. *Mol. Ecol. Resour.* **8**, 753–756 (2008).
- 985 108. V. Buffalo, G. Coop, The Linked Selection Signature of Rapid Adaptation in  
986 Temporal Genomic Data. *Genetics* **213**, 1007–1045 (2019).
- 987 109. M. C. Whitlock, K. E. Lotterhos, Reliable Detection of Loci Responsible for  
988 Local Adaptation: Inference of a Null Model through Trimming the Distribution of FST.  
989 *Am. Nat.* **186**, S24–S36 (2015).
- 990 110. K. Luu, E. Bazin, M. G. B. Blum, pcadapt: an R package to perform genome  
991 scans for selection based on principal component analysis. *Mol. Ecol. Resour.* **17**, 67–77  
992 (2017).
- 993 111. E. Linck, C. J. Battey, Minor allele frequency thresholds strongly affect  
994 population structure inference with genomic data sets. *Mol. Ecol. Resour.* **19**, 639–647  
995 (2019).
- 996 112. X. Qin, C. W. K. Chiang, O. E. Gaggiotti, Deciphering signatures of natural  
997 selection via deep learning. *Brief. Bioinform.* **23** (2022).
- 998 113. M. Slatkin, Linkage disequilibrium—understanding the evolutionary past and  
999 mapping the medical future. *Nat. Rev. Genet.* **9**, 477–485 (2008).
- 1000 114. T. L. Jenkins, C. D. Ellis, A. Triantafyllidis, J. R. Stevens, Single nucleotide  
1001 polymorphisms reveal a genetic cline across the north-east Atlantic and enable powerful  
1002 population assignment in the European lobster. *Evol. Appl.* **12**, 1881–1899 (2019).
- 1003 115. G. Piquès, “Étude de l’ichtyofaune : déchets de préparation de thons et autres  
1004 restes de poissonS” in *Provence-Alpes-Côte d’Azur, Bouches-Du-Rhône, Marseille, 22*  
1005 *Rue Jean-François Leca, Le Castel, Avant Le Port de La Joliette*, A. Richier, Ed. (INRAP  
1006 Rapport final d’opération, 2020), p. 448.
- 1007 116. F. Delussu, B. Wilkens, Analisi dei resti ossei della tonnara di Pedras de Fogu.  
1008 *Archeologia Postmedievale* **5**, 214 (2001).
- 1009 117. V. Aniceti, “Animals and their roles in the medieval society of Sicily : from  
1010 Byzantines to Arabs and from Arabs to Norman/Swabians,” University of Sheffield. (2019)  
1011 (March 25, 2022).
- 1012 118. V. Onar, G. Pazvant, A. Armutak, Radiocarbon dating results of the animal  
1013 remains uncovered at Yenikapı Excavations in *Istanbul Archaeological Museums,*  
1014 *Proceedings of the 1st Symposium on Marmaray-Metro Salvage Excavations*, (2008), pp.  
1015 249–256.



## Supplementary Materials

### Ancient DNA and genomics reveals exploitation induced pre-industrial biomass declines in Atlantic bluefin tuna but has not limited its adaptive potential

Adam J. Andrews<sup>\*1</sup>, Bastiaan Star<sup>\*2</sup>, Antonio Di Natale<sup>3</sup>, Estrella Malca<sup>4,5</sup>, Glenn Zapfe<sup>6</sup>, Vedat Onar<sup>7</sup>, Veronica Aniceti<sup>8</sup>, Gabriele Carenti<sup>9</sup>, Gäel Piques<sup>10</sup>, Federica Piattoni<sup>1</sup>, Sara De Fanti<sup>11</sup>, Francesco Fontani<sup>12</sup>, Emma Falkeid Eriksen<sup>2</sup>, Lane Atmore<sup>2</sup>, Oliver Kersten<sup>2</sup>, Fausto Tinti<sup>\*1</sup>, Elisabetta Cilli<sup>\*12</sup>, Alessia Cariani<sup>\*1</sup>

#### Sample Details

**Table 1** - external file Supplementary Table S1

#### *Gulf of Mexico samples*

Gulf of Mexico larval samples were collected as part of the NOAA Restore project (<https://restoreactscienceprogram.noaa.gov/projects/bluefin-tuna-larvae>). Larvae were randomly selected for resequencing from three sampling surveys conducted in 2014, 2017 and 2018 from the north and western shelf of the Gulf of Mexico. Multiple years and locations were sampled to obtain maximum genomic variability among few final samples analysed (n=10). Full details of sampling are found in Table S1.

**Table S1.** Sampling details of the Gulf of Mexico (GoM) 2014-2018 samples resequenced herein, collected across multiple years and locations.

ID	Station	Ship	Gear	Sample_No	SL_m m etoh	developmental stage	depth collected , m	Longitude	Latitude	Date
N1704 0108	4	NOAA SHIP NANCY FOSTER	90 cm quadrangular bongo, 505 mesh	D0376 0	7.19	postflexion	0-25	- 87.77 73	26.1 198	10- May -17
N1704 0501	21	NOAA SHIP NANCY FOSTER	90 cm quadrangular bongo, 505 mesh	D0379 1	5.5	flexion	0-25	- 88.13 28	25.8 438	12- May -17
N1802 1808	91	NOAA SHIP NANCY FOSTER	90 cm quadrangular bongo, 505 mesh	D0466 4	not meas ured	larvae	0-25	- 87.24 97	28.3 327	15- May -18
N1802 1809	91	NOAA SHIP NANCY FOSTER	90 cm quadrangular bongo, 505 mesh	D0466 4	not meas ured	larvae	0-25	- 87.24 97	28.3 327	15- May -18
N1802 1810	91	NOAA SHIP NANCY FOSTER	90 cm quadrangular bongo, 505 mesh	D0466 4	not meas ured	larvae	0-25	- 87.24 97	28.3 327	15- May -18
W1405 0007	23	F.G. Walton Smith (UNOLS Ship)	1x2m rectangular net, 505 mesh	47654	4.28	larvae	0-10	- 93.58 2	26.5 346	7- May -14
W1405 0014	23	F.G. Walton Smith (UNOLS Ship)	1x2m rectangular net, 505 mesh	47654	4.32	larvae	0-10	- 93.58 2	26.5 346	7- May -14

W1405 0029	27	F.G. Walton Smith (UNOLS Ship)	1x2m rectangular net, 505 mesh	47659	5.05	larvae	0-10	- 93.00 33	27.0 388	8- May -14
W1405 0096	69	F.G. Walton Smith (UNOLS Ship)	1x2m rectangular net, 505 mesh	47701	6.68	larvae	0-10	- 87.76 1	27.9 963	20- May -14
W1405 0097	69	F.G. Walton Smith (UNOLS Ship)	1x2m rectangular net, 505 mesh	47701	5.94	larvae	0-10	- 87.76 1	27.9 963	20- May -14

### *Ancient samples*

Archival and archaeological sample details are listed below along with body size estimates calculated using the online tool <https://tunaarchaeology.org/lengthestimations/> in the publication (53).

#### *1911-1941 CE Archival samples*

We analysed specimens collected from two locations in the early 20<sup>th</sup> century by the ecologist Massimo Sella (55). All specimens consist of vertebrae that were air-dried by the collector after capture and processing at tuna traps (Tonnare). A total of 8 vertebrae specimens were obtained from BFT captured in the tonnara at Zilten, Libya (Ionian Sea) in 1925, estimated to represent BFT between 158-204 cm FL, average 182 cm FL. Two large (275 and 278 cm FL, fork length) specimens were also sampled from tuna traps in the Bosphorus, Istanbul, Turkey in 1941.

#### *1800 CE Leca Harbour, Marseille, France*

A total of seven BFT bones (6 opercula and 1 vertebra) were obtained from the archaeological site of Leca Harbour, Marseille, France which was dated to between the late 18<sup>th</sup> and early 19<sup>th</sup> century (115). An approximate date of 1800 CE is shown for these sample groups in analyses. FL estimates were not made for these individuals as the vertebra selected was fragmented and could not be assigned to rank or accurately measured. Broadly, specimens represented large ~2 m sized adult BFT.

#### *16-18<sup>th</sup> century CE Pedras de Fogu, Sassari, Italy*

Ten vertebrae samples were obtained from the archaeological site of 'Pedras de Fogu' (Sassari, Sardinia, Italy). A tuna trap (tonnara) operated at this location from the 16<sup>th</sup> to the end of the 18<sup>th</sup> century where BFT vertebrae have been recovered in a midden at the back of the beach after they were revealed by coastal erosion (116). These specimens were estimated to range from 115-231 FL, average 178 cm FL.

#### *10-13<sup>th</sup> century CE Sicily, Italy*

A total of 3 specimens (2 vertebrae and 1 cranial element) were obtained from the archaeological site of 'Mazara del Vallo' situated in the town (southwestern Sicily, Italy). Samples were recovered from urban 10-13<sup>th</sup> century layers, each dated by context as detailed in (117), and identified as different individuals according to their range of sizes. FL estimates were not made for these individuals as the vertebrae selected were fragmented and could not be assigned to rank or accurately measured. Broadly, specimens represented small-large

sized adult BFT. A total of 3 samples (2 vertebrae and 1 cranial element) were selected for analyses from urban 9-10<sup>th</sup> century layers in two different excavations in settlements in the city of Palermo, Sicily; Sant'Antonino and Corso dei Mille. The layers were dated by context as detailed in [\(117\)](#). Samples were estimated to represent individuals ranging from 101-185 cm FL, average 130 cm FL, believed to have been caught locally.

*9-13<sup>th</sup> century CE Yenikapi, Istanbul, Turkey*

Ten vertebrae specimens were selected for analyses from a rescue excavation at a Byzantine era site in the Yenikapi neighbourhood of Istanbul, Turkey. The Port of Theodosius operated at this site from 4-11<sup>th</sup> century CE before being filled in at the 15<sup>th</sup> century CE [\(118\)](#). The 9-13<sup>th</sup> c. origin of the samples is proposed from carbon dating achieved in a separate study [\(54\)](#). It is unknown whether specimens were fished locally or transported to the city of Constantinople, which was a major trading hub throughout the Byzantine period.

## Supplementary Analysis Figures and Tables

### Mapping and sample quality

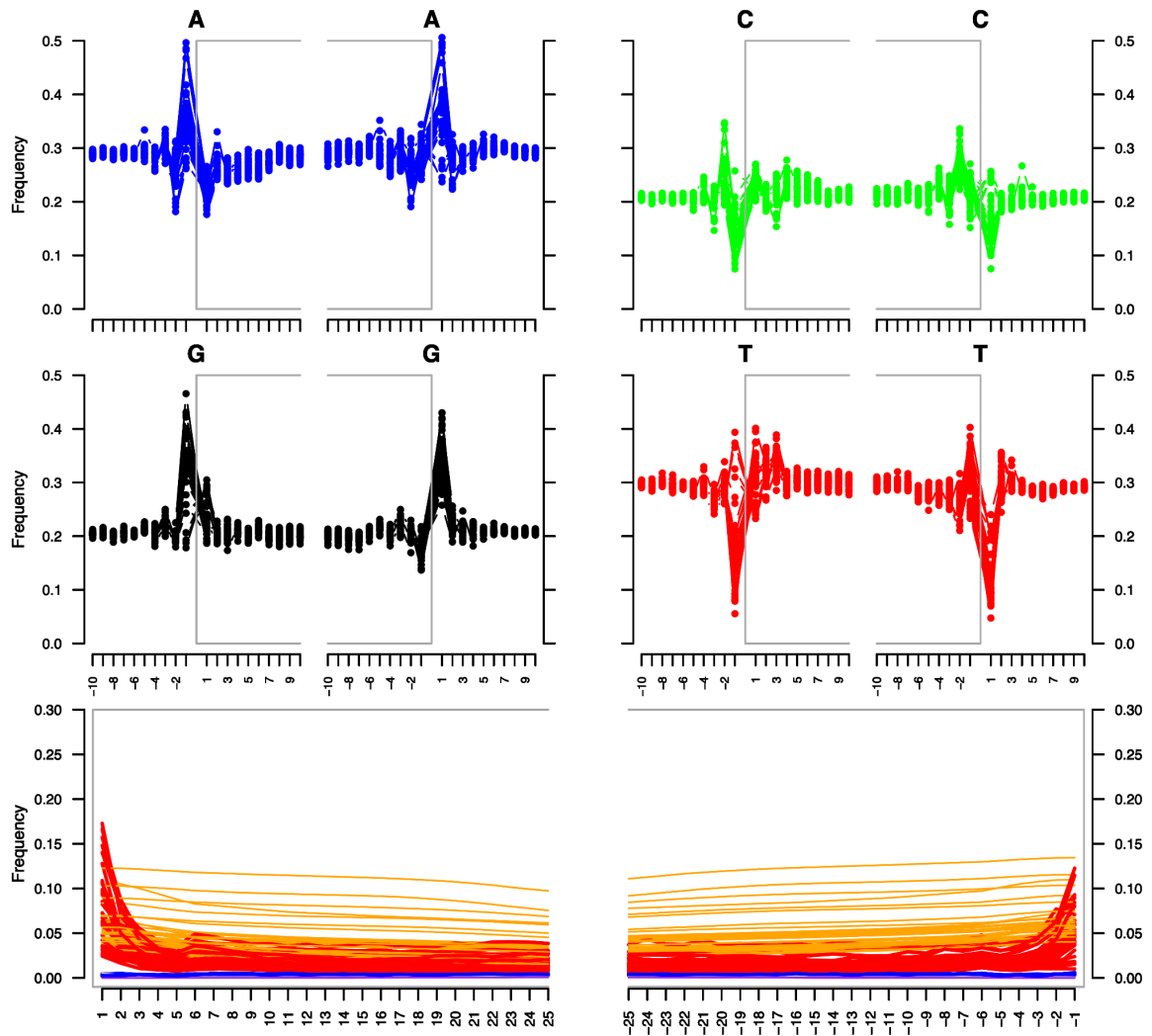


**Figure S1.** MapDamage fragment length plots for all ancient Atlantic bluefin tuna (*Thunnus thynnus*) samples analysed (n=39). X-axes represent base pair number from terminal ends of sequence reads to the BFT pseudo-chromosome assembly.

## Demographic analyses

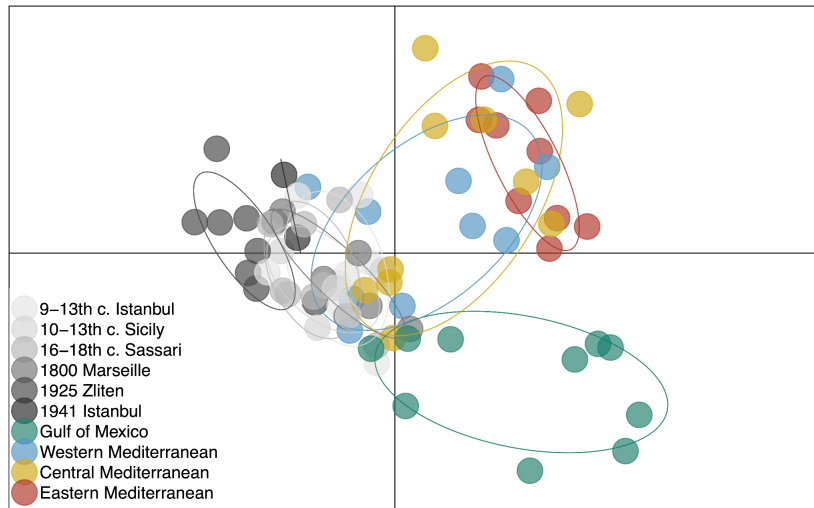


**Figure S2.** Impact of removing transition sites potential subject to post-mortem DNA damage on the population genomic structure of ancient and modern Atlantic bluefin tuna (*Thunnus thynnus*) larvae/yoys sampled from spawning sites in the Gulf of Mexico (GoM, green), Western (WMED, blue), Central (CMED, yellow), Eastern (EMED, red) Mediterranean, and ancient samples (greyscale) from 9-13th c. Istanbul, 10-13th c. Sicily, 16-18th c. Sassari, 1800 Marseille, 1925 Zliten and 1941 Istanbul. (A) DAPC scatterplots show how ancient samples (greyscale circles) are clustered in relation to modern samples (coloured circles), using 4 PC's as indicated using the `x.val` function in `ade4`, where ellipses were set to contain 95% of genotypes.

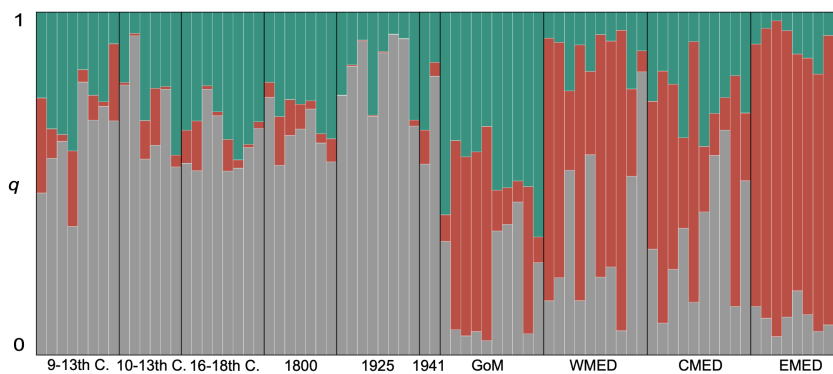


**Figure S3.** STRUCTURE barplot of individual membership probabilities ( $q$ ) for  $K=3$  using the ancient and modern dataset of Atlantic bluefin tuna (*Thunnus thynnus*) larvae/yoys sampled from spawning sites in the Gulf of Mexico (GoM), Western (WMED), Central (CMED), Eastern (EMED) Mediterranean, and ancient samples (greyscale) from 9-13th c. Istanbul, 10-13th c. Sicily, 16-18th c. Sassari, 1800 Marseille, 1925 Zliten and 1941 Istanbul.

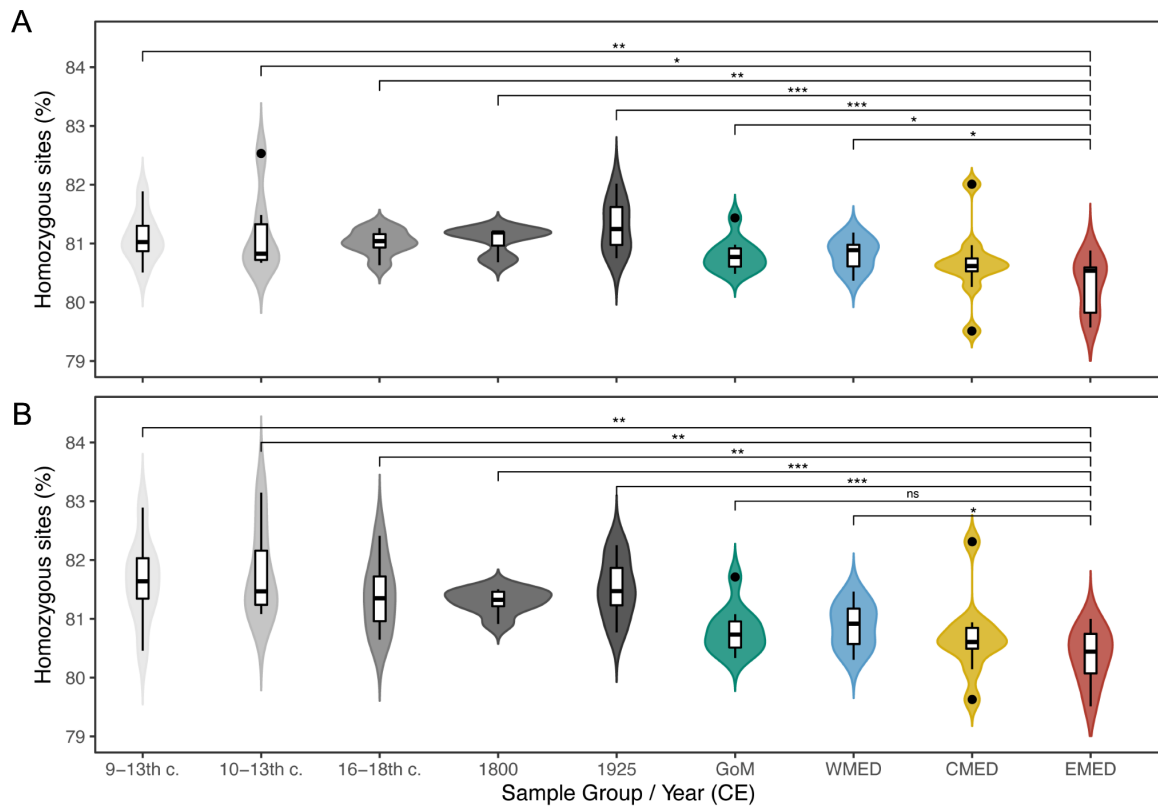


**Figure S4.** Violin boxplots show percentages of homozygous loci for each ancient and modern sample with group means, 25<sup>th</sup> and 75<sup>th</sup> percentile as outer edges and outliers illustrated outside of 95<sup>th</sup> percentiles (black whiskers) as black circles. (A) Homozygosity using the full dataset and (B) where transition sites were removed to explore the influence of loci potentially subject to post-mortem DNA damage. Significance is represented as 'ns' >0.05, '\*' < 0.05, '\*\*' < 0.01 and '\*\*\*' < 0.001 as tested between sample groups using t-tests in R. Only significant pairs were shown.

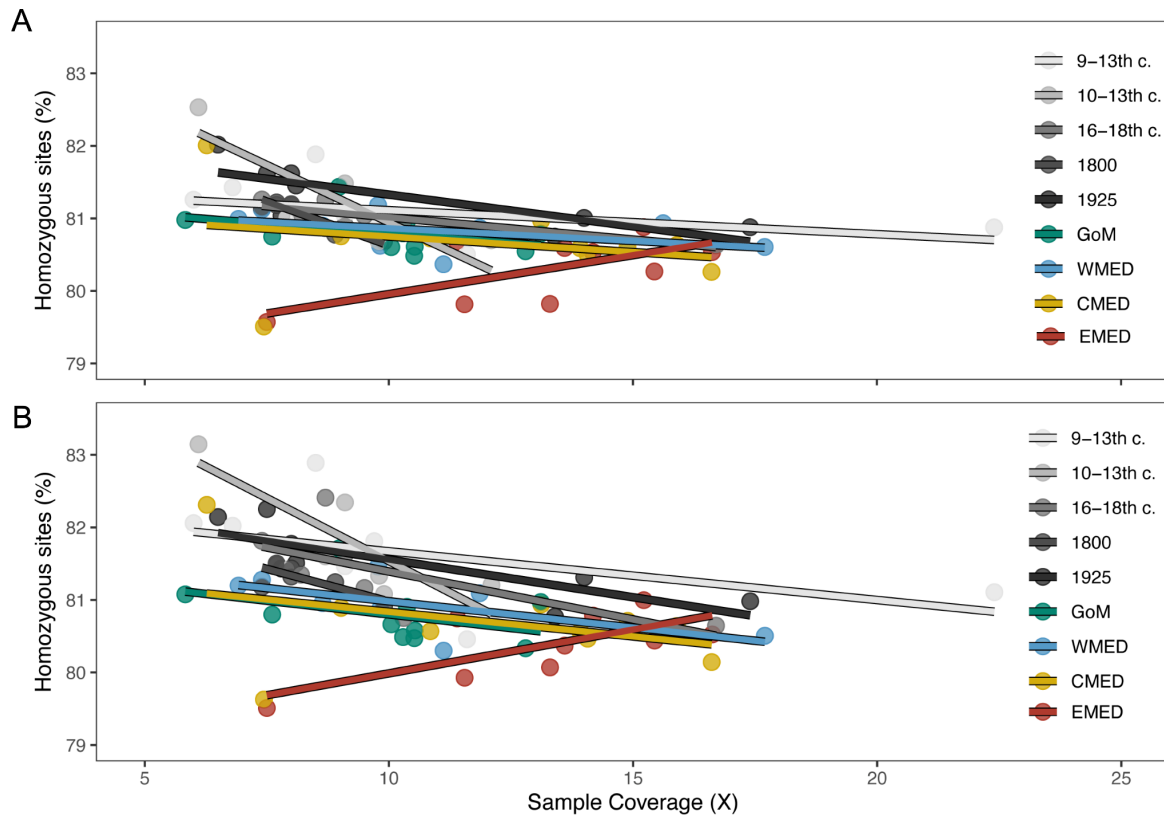


**Figure S5.** Scatterplots show relationship between homozygosity (% sites) and sample coverage (fold) per for each ancient and modern sample. (A) Homozygosity vs. sample coverage using the full dataset and (B) homozygosity vs. sample coverage where transition sites were removed to explore the influence of loci potentially subject to post-mortem DNA damage.

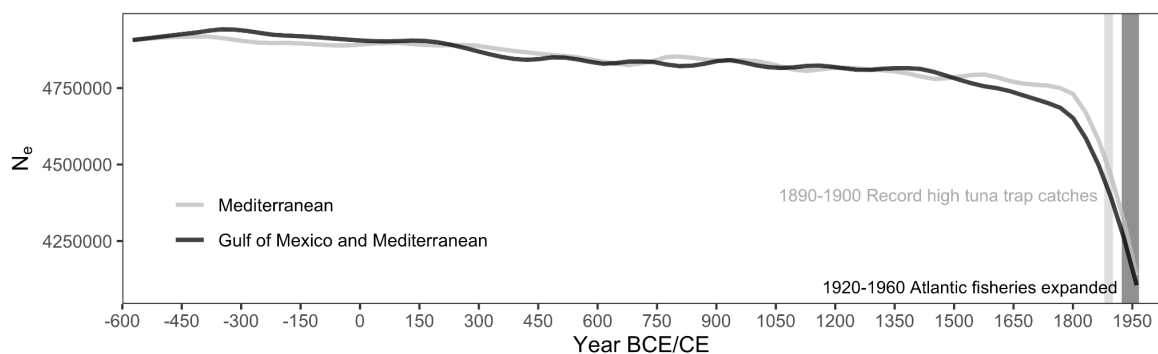


**Figure S6.** GoNe estimates of historical effective population size ( $N_e$ ) for pooled modern samples to confirm lack of sample size influence on estimates, produced using Mediterranean spawning sites (grey) and Gulf of Mexico and Mediterranean spawning sites combined (black), representing the previous 200 generations from 600 BCE to 1950, illustrated in relation to two potential causative exploitation events.

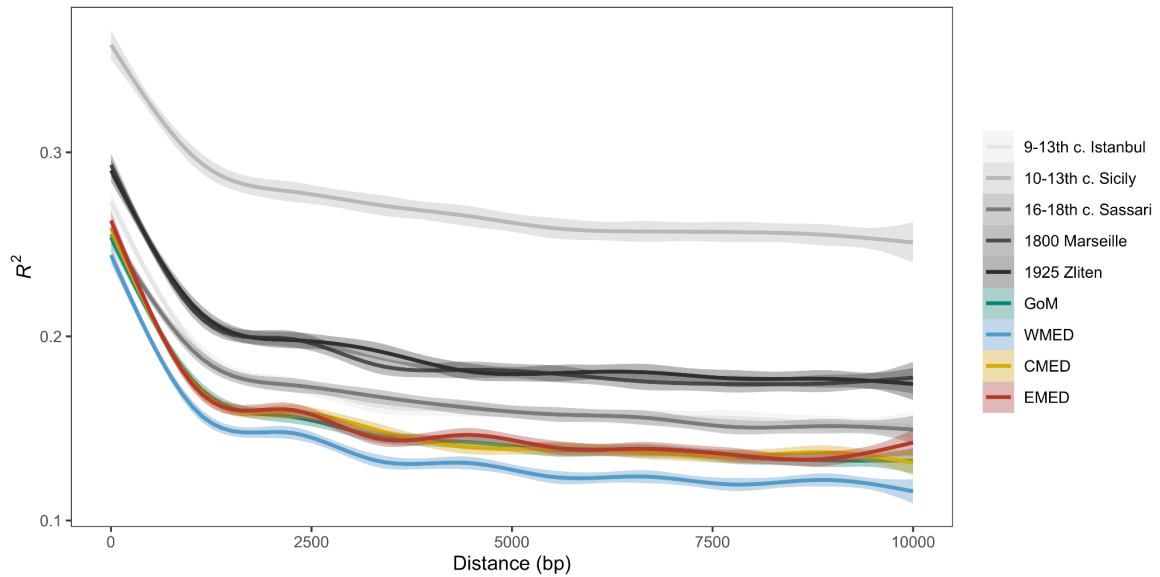


**Figure S7.** Linkage ( $R^2$ ) decay per sample calculated using PLINK in 0.5kb sliding windows to 10kb distances, revealing that relatedness impacts LD but not decay, due to combined cohorts in ancient samples representing multiple generations.

### Selection analyses

**Table S2.** Summary of loci detected as outliers and considered to be under putative selection for each dataset analysed between the methods of OutFlank and PCadapt.

Dataset	Outlier detection method	Number of loci detected	Number of loci detected in LD	Number of common outliers in LD	Regions were >3 loci in 1kb window
Ancient and Modern	OutFlank	1019	423	362	19
Ancient and Modern	PCadapt	1259	703		
Modern	OutFlank	213	80	5	-
Modern	PCadapt	254	137		
Modern Mediterranean	OutFlank	0	-	-	-
Modern Mediterranean	PCadapt	166	85	0	-



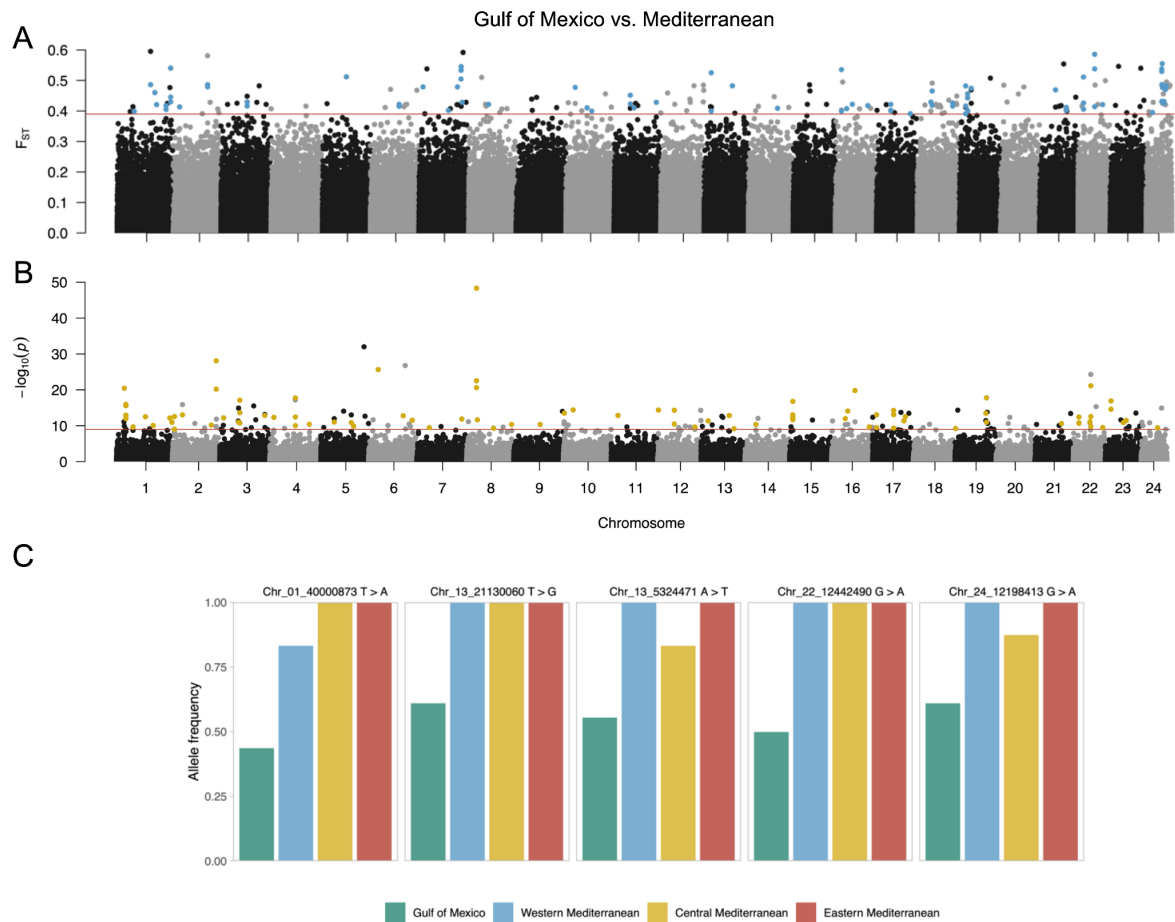


**Figure S8.** Putative loci under selection between modern Atlantic bluefin tuna (*Thunnus thynnus*) larvae/yoys sampled from spawning sites in the Gulf of Mexico (GoM, green), Western (WMED, blue), Central (CMED, yellow), Eastern (EMED, red) Mediterranean. (A) Genome-wide  $F_{ST}$ -based outliers detected using OutFlank where loci (circles) showing elevated ( $R^2 > 0.5$ ) linkage disequilibrium (LD) and statistically an outlier (above horizontal red line) were coloured in blue. (B) Genome-wide outliers detected using PCA-based PCAdapt where loci (circles) showing elevated ( $R^2 > 0.5$ ) linkage disequilibrium and statistically an outlier (above horizontal red line) were coloured in yellow. (C) Barplots of major allele frequencies per sample at 5 loci which were both consistent between OutFlank and PCAdapt, and in LD. Annotations indicate the genomic location of outliers on pseudo-chromosomes (Chr) and the minor allele nucleotide > major, predominantly Mediterranean derived allele, in each region.

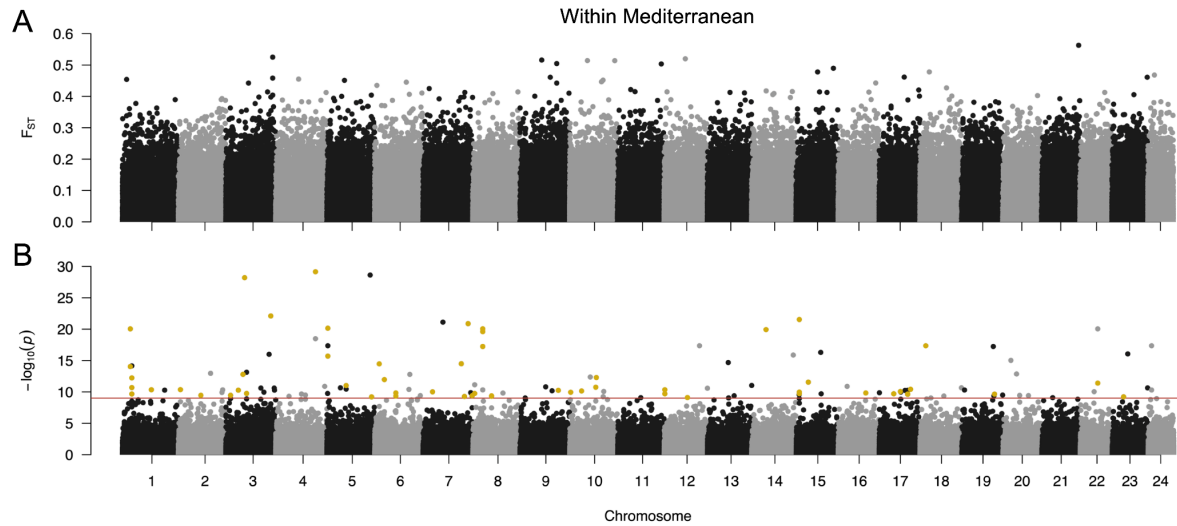


**Figure S9.** Putative loci under selection between modern Atlantic bluefin tuna (*Thunnus thynnus*) larvae/yoY sampled from spawning sites in Western (WMED, blue), Central (CMED, yellow), Eastern (EMED, red) Mediterranean. (A) Genome-wide  $F_{ST}$ -based outliers detected using OutFlank where loci (circles) showing elevated ( $R^2 > 0.5$ ) linkage disequilibrium (LD) and statistically an outlier (above horizontal red line) were coloured in blue. (B) Genome-wide outliers detected using PCA-based PCAdapt where loci (circles) showing elevated ( $R^2 > 0.5$ ) linkage disequilibrium and statistically an outlier (above horizontal red line) were coloured in yellow.

**Table S3.** Gene ontology blastn and blastp results for each locus under putative selection between ancient and modern Mediterranean samples. Original assembly and predicted proteome can be found in NCBI BioProject: PRJNA408269.

Locus	Original position in scaffold assembly	Blast e-value score	Genic location	Gene ID	Blast hit similarity and record	Putative function	Annotated in species	Ancient sequence coverage (mean, SD)	Modern sequence coverage (mean, SD)
Chr_01_7027869	scaffold 434_134-434	9e-162	Intergenic					15.9±2.5	20±3.3
Chr_01_33910461	scaffold 19186_3583-3883	9e-162	Intergenic					19.7±2.5	33.6±5.7
Chr_02_1570668	scaffold 20_215461-215761	9e-162	Intergenic					16.2±2.3	25.7±4.7
Chr_03_4907887	scaffold 446_505	9e-162	Intergenic					16.4±1.4	34.4±3.8

	92-50892								
Chr_04_36065639	scaffold66856_373-673	9e-162	Intergenic					16.1±2.5	18.2±3.1
Chr_07_17198663	scaffold2468_12080-12380	9e-162	Intergenic					14.4±3.6	20.2±6.0
Chr_08_7423744	scaffold627_49698-49998	9e-162	Intron	g5323	100% XP_044040228.1	Uncharacterized protein	<i>Siniperca chuatsi</i>	17.9±1.8	27.6±2.9
Chr_08_8143428	scaffold731_74142-74442	9e-162	Intergenic ~1kb downstream of	g5909	100% XP_044213927.1	tumor necrosis factor receptor superfamily member 11B-like	<i>Thunnus albacares</i>	15.9±1.5	31.9±4.9
Chr_09_12538865	scaffold1378_44638-44938	9e-162	Between CDS and start codon	g9077	93.6% XP_042272948.1	duodena se-1-like	<i>Thunnus maccoyii</i>	15.9±2.2	27.6±3.1
Chr_10_23037079	scaffold7521_14157-14457	9e-162	Intergenic					15.9±2.6	31.9±5.4
Chr_12_19650115	scaffold7533_375-675	9e-162	Exon	g22732	85% XP_044223499.1	uncharacterized protein LOC122993417 isoform X1	<i>Thunnus albacares</i>	20.4±3.2	31.1±5.5
Chr_13_14133870	scaffold8521_3891-4192	9e-162	Intergenic					16.8±2.4	25.3±1.4
Chr_14_10086599	scaffold1026_103093-103393	2e-159	Intergenic ~1kb downstream of	g7506	100% XP_042289735.1	indoleamine 2,3-dioxygenase 2-like	<i>Thunnus maccoyii</i>	16.4±2.0	17.6±4.3
Chr_14_23778806	scaffold8818_8418-8718	9e-162	Intron	g24316	100% XP_042290005.1	apoptosis-inducing factor 2	<i>Thunnus maccoyii</i>	20.8±2.6	31.5±9.4
Chr_15_2249193	scaffold150_217907-218207	9e-162	Intergenic					16.2±3.4	26.7±4.8

Chr_17_4458523	scaffold 428_49191-49491	9e-162	Intron	g4119	No record			18.4±3.2	29.6±6.2
Chr_20_2063922	scaffold 226_173166-173466	9e-162	Intergenic					23.5±10.6	29.8±7.4
Chr_23_2927479	scaffold 456_85372-85672	9e-162	Intergenic					14.2±1.9	29.8±7.1

**Table S4.** Gene ontology blastn and blastp results for each locus under putative selection between modern Gulf of Mexico and Mediterranean samples. Original assembly and predicted proteome can be found in NCBI BioProject: PRJNA408269.

Locus	Original position in scaffold assembly	Blast e-value score	Genic location	Gene ID	Blastp hit similarity and record	Putative function	Annotated in species
Chr_01_4000873	Scaffold73 600_523-823	2e-163	Intergenic				
Chr_13_5324471	scaffold207_115070-115370	2e-163	CDS	g2463	86% KAG72244 71.1	hypothetical protein	<i>Caranx melampygus</i>
Chr_13_21130060	scaffold448 9_21846-22147	4e-157	CDS	g17877	91% XP_04229 2575.1	gamma-enolase isoform X1	<i>Thunnus maccoyii</i>
Chr_22_12442490	scaffold645 9_2274-2574	2e-163	Intergenic ~1kb downstream of	g46416	100% XP_04226 2015.1	mediator of RNA polymerase II transcription subunit 20 isoform X1	<i>Thunnus maccoyii</i>
Chr_24_12198413	scaffold11740_8491-8791	2e-163	Intergenic				

**Table S1. Sampling and sequencing details of genomic samples resequenced for WG analyses**

Sample ID	Species	Sample Group	Sample typ	Location	Longitude	Latitude	Life stage	Year	Reads Obtain	Endogenous	Read Length	Nuclear Coverage (fold)
IST_415C_16	Thunnus thynnus	9-13th c.	Archaeolog	Yenikapi	28.95227	41.00601	Adult	9-13th c.	129536799	50.0	73	6.8
IST_415C_23	Thunnus thynnus	9-13th c.	Archaeolog	Yenikapi	28.95227	41.00601	Adult	9-13th c.	231830205	46.9	66	9.7
IST_415C_13	Thunnus thynnus	9-13th c.	Archaeolog	Yenikapi	28.95227	41.00601	Adult	9-13th c.	259277713	61.0	73	6.0
IST_415C_12	Thunnus thynnus	9-13th c.	Archaeolog	Yenikapi	28.95227	41.00601	Adult	9-13th c.	386660574	53.0	78	22.4
IST_415C_10	Thunnus thynnus	9-13th c.	Archaeolog	Yenikapi	28.95227	41.00601	Adult	9-13th c.	160138093	59.0	68	9.1
IST_415C_05	Thunnus thynnus	9-13th c.	Archaeolog	Yenikapi	28.95227	41.00601	Adult	9-13th c.	141218038	57.0	72	7.9
IST_415C_04	Thunnus thynnus	9-13th c.	Archaeolog	Yenikapi	28.95227	41.00601	Adult	9-13th c.	237180201	45.0	85	11.6
IST_415C_02	Thunnus thynnus	9-13th c.	Archaeolog	Yenikapi	28.95227	41.00601	Adult	9-13th c.	85247221	Not included in final ana	3.6	
IST_415C_01	Thunnus thynnus	9-13th c.	Archaeolog	Yenikapi	28.95227	41.00601	Adult	9-13th c.	109403461	Not included in final ana	5.5	
IST_415C_24	Thunnus thynnus	9-13th c.	Archaeolog	Yenikapi	28.95227	41.00601	Adult	9-13th c.	132066947	54.7	84	8.5
SAN_10C_10	Thunnus thynnus	10-13th c.	Archaeolog	Sant'Antonio	13.36481	38.10961	Adult	10th c.	163296705	59	66	9.9
CDM_10C_07	Thunnus thynnus	10-13th c.	Archaeolog	Corso dei Mille	13.36998	38.10933	Adult	10th c.	437023789	17.0	75	6.9
CDM_10C_06	Thunnus thynnus	10-13th c.	Archaeolog	Corso dei Mille	13.36998	38.10933	Adult	10th c.	404338085	19.0	60	6.1
CDM_10C_04	Thunnus thynnus	10-13th c.	Archaeolog	Corso dei Mille	13.36998	38.10933	Adult	10th c.	524748537	17.0	72	8.7
CDM_10C_11	Thunnus thynnus	10-13th c.	Archaeolog	Corso dei Mille	13.36998	38.10933	Adult	10th c.	333454528	20.7	80	7.5
MZ_13C_12	Thunnus thynnus	10-13th c.	Archaeolog	Mazara del Vallo	12.589	37.653	Adult	10-13th c.	162081768	52.4	79	9.8
MZ_13C_13	Thunnus thynnus	10-13th c.	Archaeolog	Mazara del Vallo	12.589	37.653	Adult	10-13th c.	346826115	21.6	86	9.1
MZ_13C_15	Thunnus thynnus	10-13th c.	Archaeolog	Mazara del Vallo	12.589	37.653	Adult	10-13th c.	224210622	58.5	67	12.1
PF_1618_02	Thunnus thynnus	16-18th c.	Archaeolog	Pedras de Fogu	8.624177	40.8631	Adult	16-18th c.	275133758	57.3	71	16.7
PF_1618_05	Thunnus thynnus	16-18th c.	Archaeolog	Pedras de Fogu	8.624177	40.8631	Adult	16-18th c.	203126677	39.4	77	9.1
PF_1618_23	Thunnus thynnus	16-18th c.	Archaeolog	Pedras de Fogu	8.624177	40.8631	Adult	16-18th c.	84770223	Not included in final ana	4.6	
PF_1618_21	Thunnus thynnus	16-18th c.	Archaeolog	Pedras de Fogu	8.624177	40.8631	Adult	16-18th c.	180357636	56.7	73	10.3
PF_1618_19	Thunnus thynnus	16-18th c.	Archaeolog	Pedras de Fogu	8.624177	40.8631	Adult	16-18th c.	234745788	49.2	73	11.4
PF_1618_18	Thunnus thynnus	16-18th c.	Archaeolog	Pedras de Fogu	8.624177	40.8631	Adult	16-18th c.	170354508	57.9	85	9.5
PF_1618_24	Thunnus thynnus	16-18th c.	Archaeolog	Pedras de Fogu	8.624177	40.8631	Adult	16-18th c.	189521908	35.6	81	7.4
PF_1618_07	Thunnus thynnus	16-18th c.	Archaeolog	Pedras de Fogu	8.624177	40.8631	Adult	16-18th c.	208238351	39.9	76	8.7
PF_1618_10	Thunnus thynnus	16-18th c.	Archaeolog	Pedras de Fogu	8.624177	40.8631	Adult	16-18th c.	204549484	39.4	74	8.2
ML_18C_02B	Thunnus thynnus	1800	Archaeolog	Marseille Leca	5.366698	43.30201	Adult	1800	185930362	35.2	80	7.4
ML_18C_04B	Thunnus thynnus	1800	Archaeolog	Marseille Leca	5.366698	43.30201	Adult	1800	328889414	21.7	78	7.7
ML_18C_09	Thunnus thynnus	1800	Archaeolog	Marseille Leca	5.366698	43.30201	Adult	1800	441434027	25.0	66	8.9
ML_18C_07B	Thunnus thynnus	1800	Archaeolog	Marseille Leca	5.366698	43.30201	Adult	1800	356909645	27.5	66	8.6
ML_18C_01	Thunnus thynnus	1800	Archaeolog	Marseille Leca	5.366698	43.30201	Adult	1800	278236664	34.0	62	8.0
ML_18C_10B	Thunnus thynnus	1800	Archaeolog	Marseille Leca	5.366698	43.30201	Adult	1800	374549711	17.9	71	9.9
ML_18C_05B	Thunnus thynnus	1800	Archaeolog	Marseille Leca	5.366698	43.30201	Adult	1800	346448656	23.7	67	7.7
ION_1925_40	Thunnus thynnus	1925	Archival	Ziiten	14.65777	33.25315	Adult	1925	157680443	49.0	69	7.8
ION_1925_27	Thunnus thynnus	1925	Archival	Ziiten	14.65777	33.25315	Adult	1925	197619377	45.0	57	7.5
ION_1925_22	Thunnus thynnus	1925	Archival	Ziiten	14.65777	33.25315	Adult	1925	217493567	37.0	58	6.5
ION_1925_11	Thunnus thynnus	1925	Archival	Ziiten	14.65777	33.25315	Adult	1925	397637695	46.0	59	14.0
ION_1925_09	Thunnus thynnus	1925	Archival	Ziiten	14.65777	33.25315	Adult	1925	370419792	40.0	72	13.4
ION_1925_08	Thunnus thynnus	1925	Archival	Ziiten	14.65777	33.25315	Adult	1925	302195775	33.0	56	8.0
ION_1925_04	Thunnus thynnus	1925	Archival	Ziiten	14.65777	33.25315	Adult	1925	264014574	36.0	62	8.1
ION_1925_01	Thunnus thynnus	1925	Archival	Ziiten	14.65777	33.25315	Adult	1925	579104421	38.0	58	17.4
IST_1941_02	Thunnus thynnus	1941	Archival	Istanbul	28.95	41	Adult	1941	277052784	27.0	63	6.3
IST_1941_01	Thunnus thynnus	1941	Archival	Istanbul	28.95	41	Adult	1941	1321362576	11.0	69	13.0
N18021808	Thunnus thynnus	GoM	Modern	Gulf of Mexico	-87.2497	28.3327	Larvae	15-May-18	139541381	51.4	88	10.52
N18021809	Thunnus thynnus	GoM	Modern	Gulf of Mexico	-87.2497	28.3327	Larvae	15-May-18	172754062	58.4	87	12.8
N18021810	Thunnus thynnus	GoM	Modern	Gulf of Mexico	-87.2497	28.3327	Larvae	15-May-18	116693740	58.1	115	10.29
N17040501	Thunnus thynnus	GoM	Modern	Gulf of Mexico	-88.1328	25.8438	Larvae	12-May-17	187146187	42.5	82	10.53
N17040108	Thunnus thynnus	GoM	Modern	Gulf of Mexico	-87.7773	26.1198	Larvae	10-May-17	188911025	69.6	63	10.37
W14050096	Thunnus thynnus	GoM	Modern	Gulf of Mexico	-87.761	27.9963	Larvae	20-May-14	152783501	62.0	62	13.11
W14050097	Thunnus thynnus	GoM	Modern	Gulf of Mexico	-87.761	27.9963	Larvae	20-May-14	105816601	63.5	90	8.98
W14050029	Thunnus thynnus	GoM	Modern	Gulf of Mexico	-93.0033	27.0388	Larvae	8-May-14	175222894	68.4	60	5.83
W14050007	Thunnus thynnus	GoM	Modern	Gulf of Mexico	-93.582	26.5346	Larvae	7-May-14	108745683	70.8	73	7.4
W14050014	Thunnus thynnus	GoM	Modern	Gulf of Mexico	-93.582	26.5346	Larvae	7-May-14	182858567	72.0	70	10.05
CYPR-LS-315	Thunnus thynnus	EMED	Modern	Eastern Mediterranean	33.41961	35.51136	YoY	2013	97896709	75.2	105	17.49
CYPR-LS-330	Thunnus thynnus	EMED	Modern	Eastern Mediterranean	33.41961	35.51136	YoY	2013	107324817	73.3	119	20.44
IEO-BA-104	Thunnus thynnus	WMED	Modern	Western Mediterranean	2.068465	39.27089	YoY	2013	143129257	72.7	76	11.12
IEO-BA-107	Thunnus thynnus	WMED	Modern	Western Mediterranean	2.068465	39.27089	YoY	2013	144642227	73.5	106	15.62
IEO-BA-109	Thunnus thynnus	WMED	Modern	Western Mediterranean	2.068465	39.27089	YoY	2013	96241790	65.1	91	8.64
IEO-BA-110	Thunnus thynnus	WMED	Modern	Western Mediterranean	2.068465	39.27089	YoY	2013	97782879	73.4	76	7.4
IEO-BA-113	Thunnus thynnus	WMED	Modern	Western Mediterranean	2.068465	39.27089	YoY	2013	155133760	70.1	114	17.7
IEO-BA-121	Thunnus thynnus	WMED	Modern	Western Mediterranean	2.068465	39.27089	YoY	2013	160129608	68.8	68	9.82
IEO-BA-63	Thunnus thynnus	WMED	Modern	Western Mediterranean	2.068465	39.27089	YoY	2012	207719516	63.2	57	9.78
IEO-BA-67	Thunnus thynnus	WMED	Modern	Western Mediterranean	2.068465	39.27089	YoY	2012	166718453	61.8	54	6.92
IEO-BA-68	Thunnus thynnus	WMED	Modern	Western Mediterranean	2.068465	39.27089	YoY	2012	171334592	71.4	87	14.9
IEO-BA-77	Thunnus thynnus	WMED	Modern	Western Mediterranean	2.068465	39.27089	YoY	2012	217771014	69.6	62	11.86
UNIB-SI-65	Thunnus thynnus	CMED	Modern	Central Mediterranean	13.17898	36.93424	YoY	2013	224072082	36.9	91	15.9
UNIB-SI-67	Thunnus thynnus	CMED	Modern	Central Mediterranean	13.17898	36.93424	YoY	2013	187286567	39.8	90	13.12
UNIB-SI-70	Thunnus thynnus	CMED	Modern	Central Mediterranean	13.17898	36.93424	YoY	2013	173517705	67.0	59	9.02
UNIB-SI-74	Thunnus thynnus	CMED	Modern	Central Mediterranean	13.17898	36.93424	YoY	2013	195783542	46.5	100	14.07
UNIB-SI-77	Thunnus thynnus	CMED	Modern	Central Mediterranean	13.17898	36.93424	YoY	2013	135696808	65.5	61	7.44
UNIB-SI-79	Thunnus thynnus	CMED	Modern	Central Mediterranean	13.17898	36.93424	YoY	2013	145693992	75.3	100	14.89
UNIB-SI-81	Thunnus thynnus	CMED	Modern	Central Mediterranean	13.17898	36.93424	YoY	2013	179052561	59.8	87	13.92
UNIB-SI-84	Thunnus thynnus	CMED	Modern	Central Mediterranean	13.17898	36.93424	YoY	2013	191490646	45.2	101	16.61
UNIB-SI-89	Thunnus thynnus	CMED	Modern	Central Mediterranean	13.17898	36.93424	YoY	2013	194564289	63.5	66	10.85
UNIB-SI-92	Thunnus thynnus	CMED	Modern	Central Mediterranean	13.17898	36.93424	YoY	2013	156174048	62.0	51	6.27
CYPR-LS-331	Thunnus thynnus	EMED	Modern	Eastern Mediterranean	33.41961	35.51136	YoY	2013	104811752	Not included in final ana	18.96	
CYPR-LS-343	Thunnus thynnus	EMED	Modern	Eastern Mediterranean	33.41961	35.51136	YoY	2013	103487327	60.7	102	20.34
CYPR-LS-347	Thunnus thynnus	EMED	Modern	Eastern Mediterranean	33.41961	35.51136	YoY	2013	173458587	55.2	95	14.18
CYPR-LS-352	Thunnus thynnus	EMED	Modern	Eastern Mediterranean	33.41961	35.51136	YoY	2013	149595935	75.9	97	15.22
CYPR-LS-41	Thunnus thynnus	EMED	Modern	Eastern Mediterranean	33.41961	35.51136	YoY	2012	147452659	75.6	97	15.44
CYPR-LS-45	Thunnus thynnus	EMED	Modern	Eastern Mediterranean	33.41961	35.51136	YoY	2012	115427698	73.6	97	1



## Discussion

This thesis documents a long-term eco-evolutionary investigation into one of the most ecologically, culturally, and economically important marine fishes. My aim was to promote a better understanding of BFT exploitation and recovery. I created empirical datasets that rival temporal investigations on better studied fishes, such as Atlantic cod. Through the establishment of an online domain for the open access of data and information sharing (<https://tunaarchaeology.org>), I provided a pathway for further research. To facilitate this, I delivered the first detailed account of the number and whereabouts of BFT remains, and how to identify BFT vertebrae to skeletal position and estimate body size in past environments. I performed the first ecological studies on long-term BFT size and growth, diet and habitat use, and demography and adaptation, and in doing so, produced the first genome-wide data on this species. Moreover, my thesis is the first to investigate temporal genomic changes in any fish population using whole genomes older than ~100 years.

BFT remains have been excavated from a total of 114 archaeological settlements across northern Europe and the Mediterranean. Here, BFT remains were studied from a total of 14 archaeological settlements and 10 modern sites, dating back over two millennia, to the 3<sup>rd</sup> century BCE. I analysed a total of 286 samples using length estimations, 133 using annuli (growth marks), 118 using stable isotopes, 382 using SNP-genotyping and 78 samples using whole genome sequencing. The multidisciplinary and interdisciplinary approach I took was challenging in that it required careful spatio-temporal experimental design including planning to limit the destruction of specimens and prioritise the maximum morphological and biomolecular information harvested. While difficult, this approach provided novel value and could only be implemented by growing and merging scientific and technical knowledge, skills and competences in archaeology, history, biology, molecular and chemical biology, fish ecology and biology, and fishery science. I consider my experimental design unique, seldom seen in fishes, or marine fauna for that matter. It allowed me to deliver previously undocumented insights into the long-term population dynamics of BFT and the eco-evolutionary consequences of their exploitation and anthropogenic impacts on marine environments, more broadly. With the proceeding section I seek to find common threads between insights from the different multidisciplinary approaches I took in each of my papers.

### Eco-evolutionary consequences of exploitation

Historical ecological data is often complex to interpret since it is subject to limited sources (in our case, bones), spread unevenly across time and space, which are each influenced by multiple variables. To provide robust conclusions, it is therefore useful if multiple lines of evidence corroborate. I found that multiple indicators, namely literature, size, growth, isotopes and DNA point towards eco-evolutionary consequences of exploitation on BFT populations, beginning prior to recent decades, which were previously undocumented. Therefore, my findings have important implications for the management of BFT due to novel perceptions provided of the onset and impact of exploitation, and recovery from it. My findings also implicate the recovery of fishes more broadly, since they are likely to be transferable to species

with similar ecologies and life histories. Furthermore, BFT exploitation has likely operated in concert with a variety of anthropogenic impacts and natural climatic changes that marine ecosystems of the Atlantic, Mediterranean and Black Sea have experienced throughout the past two millennia. Therefore, my results also represent, in part, the health of marine ecosystems and allow for a novel perspective on the onset of their modification and its extent today.

Regarding the onset of intensive exploitation and biomass decline, the literature review (**Chapter 1**) suggested that there was some concern or awareness of the potential to overfish BFT by the 14<sup>th</sup> c., when legislation controlling BFT catches existed. It also highlighted that the Monk Martin Sarmiento proposed that BFT had been overfished and their habitats had been degraded, in Spanish waters during the 16<sup>th</sup> c., following declines in Spanish trap catches. By the 1880s, tuna trap records indicated that as many eastern BFT were landed as during the most intensive decades of BFT exploitation, which occurred between 1980-2000 with huge advances in modern technology and effort. By 1970, several 20<sup>th</sup> c. case studies i.e. fewer catches off Brazil, Norway, Bay of Biscay, Black Sea, declining trap catches across the Mediterranean, suggested that BFT productivity was not at maximum.

The genomic reconstructions of effective population size I performed (**Chapter 7**) provide robust evidence that BFT biomass began to decline in the eastern Atlantic and Mediterranean—and potentially across its entire range—during the 19<sup>th</sup> century. While it cannot be concluded that a biomass decline did not begin earlier, I suggest that if it did, it was not severe enough to impact the BFT genome. Increases in juvenile BFT growth by the 20<sup>th</sup> c., but not the 16-18<sup>th</sup> century corroborates this finding, since juvenile growth is likely to increase under lower population biomass (**Chapter 3**). Indeed, I find that an alternative hypothesis of diet shifts inducing early maturation/increased juvenile growth are not supported by isotopic data which show BFT have been trophically stable across two millennia (**Chapter 5**). In addition, historical estimates of catch-at-size indicated that prior to ~18<sup>th</sup> century, smaller BFT were being caught, and since size has often been used as a proxy for fishing effort (**Chapter 3**), it can be deduced that it was indeed around the 19<sup>th</sup> century when exploitation began to deplete the biomass of BFT. Stable isotopic data (**Chapter 5**) provided an explanation for why then, tuna-trap catches may have fluctuated prior to the 19<sup>th</sup> century, why early legislation on BFT exploitation was necessary, and why BFT were perceived to have been overexploited by the 16<sup>th</sup> century. A shift in sulphur isotopes revealed that BFT began to feed further offshore on more pelagic prey from around the 16<sup>th</sup> century, potentially due to the degradation of coastal marine habitats and prey. Therefore, my results point to wider marine exploitation impacts during the pre-industrial era which had consequences for BFT behaviour, and their coastal trap fisheries.

My results revealed that exploitation has not only induced biomass declines in BFT, occurring earlier than previously realised, but it has also altered their foraging behaviour. Further evidence of this is that of BFT which previously migrated to the Black Sea up until the 1980s. Indeed, the genetic (**Chapter 6**) and genomic (**Chapter 7**) data indicated Black Sea BFT do not represent a separate spawning population. Instead, stable isotope data show (**Chapters 4, 5**) that Black Sea BFT were trophically distinct from eastern Atlantic and Mediterranean BFT, and probably engaged in residentiary behaviours which, since the 1980s have been very rare.



By investigating both phenotypic and genotypic temporal responses in BFT (**Chapters 3, 7**), I find that exploitation impacts may have extended further still, to inducing novel selection pressures on the BFT genome. While further investigations are required, the finding of increased juvenile growth (**Chapter 3**) may be explained by an earlier maturation, which fisheries induced evolution theory suggests may be underlied by evolutionary responses to size-selective exploitation. Indeed, I found putative evidence for adaptive responses across the BFT genome between ~1800 and the mid-20<sup>th</sup> or the early 21<sup>st</sup> century. Certainly, the timing of these responses coincides with catch-at-size and genomic evidence of intensified, size-selective exploitation, but further study is required to confirm that phenotypic and genotypic responses are linked.

Somewhat strikingly, I found no evidence for a genetic bottleneck (**Chapters 6, 7**) nor a significant recent shift in trophic position (**Chapter 5**) following the intense exploitation of BFT, and their prey, during the past half century. In overexploited terrestrial taxa, genetic variability is readily lost when biomass declines (Khan *et al.*, 2021; Femerling *et al.*, 2022; Robin *et al.*, 2022). Despite the depletion of BFT throughout the past half-century, and as I show a long exploitation history with genomic impacts evident by the 1800s, BFT has retained its genetic variability. I acknowledge that the loss of genetic variation in the marine environment may not be equivocal to that in terrestrial ecosystems, such that Atlantic cod appear to be genomically stable across one century (Pinsky *et al.*, 2021), and not even the vaquita (*Phocoena sinus*) has developed inbreeding depression after being depleted to handfuls of individuals (Robinson *et al.*, 2022). Despite evidence of exploitation restructuring fish populations to smaller individuals and predominantly depleting larger species (Pauly *et al.*, 1998), which is thought to have an impact on BFT specifically (Golet *et al.*, 2015), my results show BFT trophic position has probably not significantly changed recently to reflect this. Perhaps more surprising is that throughout several regime shifts that have occurred (Drinkwater, 2006; Conversi *et al.*, 2010; Beaugrand *et al.*, 2015; Siano *et al.*, 2021; Vollset *et al.*, 2022), and particularly since other tunas have shifted in isotope composition during the past two decades in the Atlantic (Lorrain *et al.*, 2020), BFT trophic position has not changed over millennia. While further investigations are required, these results, when considered in concert, speak of the robustness of BFT, able to flex around changes in its environment.

## Revising Atlantic bluefin tuna ecology with history

We may amend the opening section 'Study system: the eastern Atlantic and Mediterranean bluefin tuna' with several novel insights following my research effort. First, I find that the intensification of BFT exploitation probably occurred sometime during the 1800s, consistent with increases in catch-at-size, growth, and genomic footprints. This implies that although eastern Atlantic and Mediterranean BFT have recovered in recent years, their historical productivity is underestimated, and recovery is overestimated. It is therefore likely that perceptions of BFT abundance fluctuation prior to this date (Ravier and Fromentin, 2001; Fromentin, 2009) are more affected by behavioural responses to ecosystem exploitation than previously thought, where BFT moved offshore and temporarily decreased tuna trap efficiency. I find that BFT are robust to high levels of exploitation, where even a long exploitation history, intensifying in the 1800s and driving BFT close to collapse by the early 2000s (MacKenzie, Mosegaard and Rosenberg, 2009) was not sufficient to limit their adaptive potential. I found

that BFT had the potential to take increased proportions of benthic and inshore prey, than is currently recognised. This is important, as it reflects Pauly's (Pauly, 1995) 'shifting baseline theory', in that, not only is historical BFT productivity underestimated, but also perceptions of in which habitats we should expect to find BFT.

Genomic data support that BFT are composed of two populations as previously shown, and reveal for the first time that theories of a Black Sea spawning population (MacKenzie and Mariani, 2012; Di Natale, 2015) are ungrounded. Genomic data address previous debate of a portion of Mediterranean BFT being residentary (De Metrio *et al.*, 2004; Fromentin, 2009; Cermeño *et al.*, 2015; Medina *et al.*, 2022), likely being driven by behavioural variation in life histories, rather than spawning divergence. As isotope data show, residentary life-history behaviours extend further still, where BFT inhabited more distant habitats such as the Black Sea, for considerable parts of the year, doing this consistently between years, and probably did not migrate into the Atlantic. I find it likely that Black Sea residency will increase, only that it takes time to rebuild collective memory of migration routes (Petitgas *et al.*, 2010; De Luca *et al.*, 2014), particularly if density remains below historical thresholds because migration behaviours are then less heritable (Crespel *et al.*, 2021) and individuals are less averse to risk (investigating new habitats, Sbragaglia *et al.*, 2021). Certainly, BFT have rebounded in a variety of habitats historically used by a greater majority of the population (Porch *et al.*, 2019; Nøttestad, Bøge and Ferter, 2020; Horton *et al.*, 2021).

My findings suggest that BFT uses a (tremendously) high degree of variation in life histories to limit dependence on few habitats and prey. This probably reflects highly dynamic pelagic environments that it inhabits (DeFilippo and Ohlberger, 2021), evident for example from larval predation patterns under good recruitment years which compound recruitment success and provide striking advantages when conditions are favourable (Ottmann *et al.*, 2022). Considerable variation in BFT life histories has long been known but is perhaps more evident here than previously shown c.f. (Mather, Mason and Jones, 1995; Bolnick *et al.*, 2007). As observed herein, BFT appears more generalist, feeding on a wide degree of prey, than has previously been appreciated. We find relatively low  $\delta^{15}\text{N}$  isotope values that support BFT being large, but not an apex predator, as (Logan, Golet and Lutcavage, 2015). Recent works support this, such as a greater proportion of gelatinous prey being ingested (Günther *et al.*, 2021). The results I obtained add that it is likely that these traits have stabilised BFT trophic position across millennia and made BFT robust to the recent depletion of prey, prey size, and entire ecosystems within the Atlantic, Mediterranean and Black Sea.

I confirm that genomic differentiation between stocks is extremely low, where Gulf of Mexico and Mediterranean spawning sites share near-identical demographic histories despite different exploitation histories (**Chapter 1**). This suggests that from a management point of view, BFT could be managed as a single unit in some respects, where further recoveries in the eastern Atlantic and Mediterranean may promote greater abundance in the western Atlantic - which is less well recovered (ICCAT, 2020). Again, this feature is one that reiterates BFT robustness, promoting genomic diversity retention by spawning in a wide range of locations and time periods (Piccinetti, Di Natale and Arena, 2013) where individuals from both populations (and a range of age classes) occasionally mix. During BFT recoveries of recent years, increased numbers of migrants from the Mediterranean to the western Atlantic evidence this (Puncher *et al.*, 2022) and suggest that gene flow between spawning sites is variable in time, being greater when biomass is high. Low genomic population differentiation observed

also suggests that differences in maturation between stocks are likely to be plastic and related to environmental conditions. Few outlier loci were found across the genome, between stocks, which not only suggests a lack of evolutionary basis for differences in maturation schedules, but also a lack of differential responses to size-selective exploitation between stocks which might be expected if stocks were more ecologically distinct due to differences in age, growth and life histories undertaken (Ahti *et al.*, 2021; Sbragaglia *et al.*, 2021).

Finally, I find that BFT juvenile growth varies temporally (**Chapter 3**) and has increased in recent centuries. Growth may increase if driven by climate warming but may decrease if it reflects more competition for resources and recent declines in biomass. Alternatively, increased juvenile growth may represent earlier maturation driven by fisheries induced evolution (FIE) and require careful consideration in management plans (Kuparinen and Merilä, 2007).

### Digging deeper

It would be remiss of us to neglect a discussion on how to further our important works and their applicability in the real world. I identified that major questions remain as to whether past properties of fish populations can be restored. It is expected that since a lack of evolutionary changes have occurred to BFT (excluding the potential for FIE), that past states such as increased biomass, slower juvenile growth/late maturation, larger size classes, residentiary Mediterranean and Black Sea behaviours, and inshore feeding; should in theory be possible to return. As Duarte *et al.* (2020) state, we can only recover ecosystems and populations to recent decades but this clearly depends on which (natural and anthropogenic) processes have occurred, and which of them are irreversible (Pinnegar and Engelhard, 2008). Therefore, further works are required to assess whether all, or any of the exploitation impacts we discover on BFT can be rectified. Nonetheless, my results point to wide-ranging and far-reaching but reversible exploitation impacts in the marine realm, such as predominantly (or entirely) plastic responses which puts fish populations at a greater conservation standing compared to highly vulnerable terrestrial taxa (Cowie, Bouchet and Fontaine, 2022).

There are specific ways in which each of the eco-evolutionary indicators studied in this thesis might be further explored to increase resolution - here I identified what I see as the most fruitful opportunities. First, temporal growth patterns could benefit from fine-scale biochronological analyses using otoliths, such as archival specimens from Schloesser *et al.* (2009). This may address the onset of growth changes throughout the last century and disentangle the influence of temperature and biomass on BFT growth, since we have temperature and biomass data for this period and may elucidate if evolutionary forces are potential drivers. Second, diet and habitat use should be studied using additional stable isotopes such as mercury and lithium which may be more variable spatially (Tseng *et al.*, 2021; Thibon *et al.*, 2022) and allow for disentangling spatial vs. temporal factors - though this may require otolith mineral rather than bone collagen. Further, compound specific stable isotope analysis (CSIA) of individual amino acids has been recently shown as a way to disentangle trophic vs. source effects on the  $\delta^{15}\text{N}$  variability of bulk isotope values in contemporary fish studies (Bradley *et al.*, 2015; Le-Alvarado *et al.*, 2021). Therefore, CSIA could eliminate the possibility of baseline shifts clouding observations of diet and habitat shifts in BFT. In theory, CSIA can be applied to

archaeological and archival samples, providing that preservation is sufficient (for many of our samples, it was).

Finally, focus should be placed on improving genomic investigations, across several fronts. First, attempts should be made to reconstruct recent estimates of effective population size ( $N_e$ ) such as those since 1960 that I could not produce. This is especially important because it remains difficult (but not impossible (MacKenzie *et al.* 2022)) to assess population size from fishery catches, let alone for the historical period (Pauly, Hilborn and Branch, 2013). This would provide quantitative data on the demographic decline of BFT during the most intense decades of exploitation and complement studies from recent years using catch-mark-recapture techniques e.g., McDowell *et al.* (2022). One potential solution is to use single sample methods (estimating  $N_e$  for one year and comparing with others) following Waples and Do (2008) and Waples *et al.* (2018), with the consideration that these require large sample sizes and archived samples from a single cohort (Marandel *et al.*, 2019). Indeed, archived samples from the western Atlantic should be interrogated in addition to the eastern Atlantic and Mediterranean to support that BFT stocks are not demographically independent. In addition, long-term  $N_e$  methods should be employed to estimate the source population of modern BFT and when the two stocks diverged e.g., Shchur *et al.* (2022). Further, ancient DNA approaches should be extended to track mutational load, which can also be a consequence of population depletion e.g., Femerling *et al.* (2022), and may explain differences in allele frequency between ancient and modern samples.

## Conclusion

The highly multidisciplinary approach undertaken in this thesis to investigate eco-evolutionary consequences of exploitation in BFT was challenging, but certainly fruitful. Through investigating temporal changes in size and growth, diet and habitat use, and demography and adaptation, I provide novel insights which revise our perspectives of BFT ecology, and the onset of impactful marine exploitation. The findings of my thesis point toward exploitation impacting BFT foraging behaviour by the ~16<sup>th</sup> century when coastal ecosystem degradation induced a pelagic shift in diet and habitat use. Empirical data show that BFT biomass began to decline much earlier than hitherto documented, by the 1800s, consistent with intensive tuna trap catches during this period and catch-at-size increasing. Further, the results I obtained show that BFT juvenile growth had increased by the early 1900s (and more dramatically by the 2000s) which may reflect fisheries induced evolution to size selective harvest, temperature, or density effects during this early industrial period. I observed that BFT foraging behaviours have been modified following overexploitation during the 20<sup>th</sup> century, which previously included an isotopically distinct, Black Sea niche which could not be explained by spawning divergence. Finally, I provide evidence for BFT being robust to exploitation in that genomic diversity has been retained, which provides confidence for their continued recovery. Indeed, my research indicates that BFT productivity was historically greater than it is today suggesting that management plans can be ambitious with their recovery targets. I sincerely hope that my findings contribute to the cultural transition towards sustainable oceans and the recognition for historical perspectives to guide this process, which reflect the wisdom of people using and enjoying ocean life over millennia.

## References

- Aarestrup, K. *et al.* (2022) 'First tagging data on large Atlantic bluefin tuna returning to Nordic waters suggest repeated behaviour and skipped spawning', *Scientific reports*, 12(1), p. 11772.
- Addis, P. *et al.* (2016) 'Reproductive status of Atlantic bluefin tuna, *Thunnus thynnus*, during migration off the coast of Sardinia (western Mediterranean)', *Fisheries research*, 181, pp. 137–147.
- Ahti, P.A. *et al.* (2021) 'Age is not just a number-Mathematical model suggests senescence affects how fish populations respond to different fishing regimes', *Ecology and evolution*, 11(19), pp. 13363–13378.
- Atmore, L.M. *et al.* (2022) 'Population dynamics of Baltic herring since the Viking Age revealed by ancient DNA and genomics', *Proceedings of the National Academy of Sciences of the United States of America*, 119(45), p. e2208703119.
- Atwood, T.B. and Hammill, E. (2018) 'The Importance of Marine Predators in the Provisioning of Ecosystem Services by Coastal Plant Communities', *Frontiers in plant science*, 9, p. 1289.
- Barrett, J.H. *et al.* (2011) 'Interpreting the expansion of sea fishing in medieval Europe using stable isotope analysis of archaeological cod bones', *Journal of archaeological science*, 38(7), pp. 1516–1524.
- Barrett, J.H. (2019) 'An environmental (pre)history of European fishing: past and future archaeological contributions to sustainable fisheries', *Journal of fish biology*, 94(6), pp. 1033–1044.
- Barrett, J.H., Locker, A.M. and Roberts, C.M. (2004) 'The origins of intensive marine fishing in medieval Europe: the English evidence', *Proceedings. Biological sciences / The Royal Society*, 271(1556), pp. 2417–2421.
- Battaglia, P. *et al.* (2013) 'Feeding habits of the Atlantic bluefin tuna, *Thunnus thynnus* (L. 1758), in the central Mediterranean Sea (Strait of Messina)', *Helgoland marine research*, 67(1), pp. 97–107.
- Baum, J.K. and Worm, B. (2009) 'Cascading top-down effects of changing oceanic predator abundances', *The Journal of animal ecology*, 78(4), pp. 699–714.
- Beaugrand, G. *et al.* (2015) 'Synchronous marine pelagic regime shifts in the Northern Hemisphere', *Philosophical transactions of the Royal Society of London. Series B, Biological sciences*, 370(1659), p. 20130272.
- Bennema, F.P. (2018) 'Long-term occurrence of Atlantic bluefin tuna *Thunnus thynnus* in the North Sea: contributions of non-fishery data to population studies', *Fisheries research*, 199, pp. 177–185.
- Bianchi, D. *et al.* (2021) 'Estimating global biomass and biogeochemical cycling of marine fish with and without fishing', *Science advances*, 7(41), p. eabd7554.
- Blankholm, H.P. *et al.* (2020) 'Dangerous food. Climate change induced elevated heavy metal levels in Younger Stone Age seafood in northern Norway', *Quaternary international: the journal of the International Union for Quaternary Research*. Available at:

<https://doi.org/10.1016/j.quaint.2020.01.019>.

Bolle, L.J. *et al.* (2004) 'Growth changes in plaice, cod, haddock and saithe in the North Sea: a comparison of (post-)medieval and present-day growth rates based on otolith measurements', *Journal of sea research*, 51(3), pp. 313–328.

Bolnick, D.I. *et al.* (2007) 'Comparative support for the niche variation hypothesis that more generalized populations also are more heterogeneous', *Proceedings of the National Academy of Sciences of the United States of America*, 104(24), pp. 10075–10079.

Bonanomi, S. *et al.* (2015) 'Archived DNA reveals fisheries and climate induced collapse of a major fishery', *Scientific reports*, 5, p. 15395.

Bradley, C.J. *et al.* (2015) 'Trophic position estimates of marine teleosts using amino acid compound specific isotopic analysis', *Limnology and oceanography, methods / ASLO*, 13(9), pp. 476–493.

Britten, G.L., Dowd, M. and Worm, B. (2016) 'Changing recruitment capacity in global fish stocks', *Proceedings of the National Academy of Sciences of the United States of America*, 113(1), pp. 134–139.

Brophy, D. *et al.* (2020) 'Combining genetic markers with stable isotopes in otoliths reveals complexity in the stock structure of Atlantic bluefin tuna (*Thunnus thynnus*)', *Scientific reports*, 10(1), p. 14675.

Butchart, S.H.M. *et al.* (2010) 'Global biodiversity: indicators of recent declines', *Science*, 328(5982), pp. 1164–1168.

Casini, M. *et al.* (2009) 'Trophic cascades promote threshold-like shifts in pelagic marine ecosystems', *Proceedings of the National Academy of Sciences of the United States of America*, 106(1), pp. 197–202.

Caswell, B.A. *et al.* (2020) 'Something old, something new: Historical perspectives provide lessons for blue growth agendas', *Fish and fisheries*, 21(4), pp. 774–796.

Cermeño, P. *et al.* (2015) 'Electronic tagging of Atlantic bluefin tuna (*Thunnus thynnus*, L.) reveals habitat use and behaviors in the Mediterranean Sea', *PloS one*, 10(2), p. e0116638.

Conversi, A. *et al.* (2010) 'The Mediterranean Sea regime shift at the end of the 1980s, and intriguing parallelisms with other European basins', *PloS one*, 5(5), p. e10633.

Cort, J.L. and Abaunza, P. (2019) 'The Present State of Traps and Fisheries Research in the Strait of Gibraltar', in J.L. Cort and P. Abaunza (eds) *The Bluefin Tuna Fishery in the Bay of Biscay : Its Relationship with the Crisis of Catches of Large Specimens in the East Atlantic Fisheries from the 1960s*. Cham: Springer International Publishing, pp. 37–78.

Cowie, R.H., Bouchet, P. and Fontaine, B. (2022) 'The Sixth Mass Extinction: fact, fiction or speculation?', *Biological reviews of the Cambridge Philosophical Society*, 97(2), pp. 640–663.

Crespel, A. *et al.* (2021) 'Density influences the heritability and genetic correlations of fish behaviour under trawling-associated selection', *Evolutionary applications*, 14(10), pp. 2527–2540.

- Crozier, L.G. and Hutchings, J.A. (2014) 'Plastic and evolutionary responses to climate change in fish', *Evolutionary applications*, 7(1), pp. 68–87.
- DeFilippo, L.B. and Ohlberger, J. (2021) 'Stochastic recruitment alters the frequencies of alternative life histories in age-structured populations', *Fish and fisheries*, 22(6), pp. 1307–1320.
- De Luca, G. *et al.* (2014) 'Fishing out collective memory of migratory schools', *Journal of the Royal Society, Interface / the Royal Society*, 11(95), p. 20140043.
- De Metrio, G. *et al.* (2004) 'Joint Turkish-Italian research in the Eastern Mediterranean: bluefin tuna tagging with pop-up satellite tags', *Col. Vol. Sci. Pap. ICCAT*, 56(3), pp. 1163–1167.
- Denechaud, C. *et al.* (2020) 'A century of fish growth in relation to climate change, population dynamics and exploitation', *Global change biology*, 26(10), pp. 5661–5678.
- Dickhut, R.M. *et al.* (2009) 'Atlantic bluefin tuna (*Thunnus thynnus*) population dynamics delineated by organochlorine tracers', *Environmental science & technology*, 43(22), pp. 8522–8527.
- Di Natale, A. (2010) 'The Eastern Atlantic bluefin tuna: Entangled in a big mess, possibly far from a conservation red alert. Some comments after the proposal to include bluefin tuna in cites appendix I', *Col. Vol. Sci. Pap. ICCAT*, 65(3), pp. 1004–1043.
- Di Natale, A. (2012) 'The iconography of tuna traps: Essential information for the understanding of the technological evolution of this ancient fishery', *Col. Vol. Sci. Pap. ICCAT*, 67(1), pp. 33–74.
- Di Natale, A. (2014) 'The ancient distribution of bluefin tuna fishery: how coins can improve our knowledge', *Col. Vol. Sci. Pap. ICCAT*, 70, pp. 2828–2844.
- Di Natale, A. (2015) 'Review of the historical and biological evidences about a population of bluefin tuna (*Thunnus thynnus* L.) in the eastern Mediterranean and the Black Sea', *Col Vol. Sci. Pap. ICCAT*, 71(3), pp. 1098–1124.
- Drinkwater, K.F. (2006) 'The regime shift of the 1920s and 1930s in the North Atlantic', *Progress in oceanography*, 68(2), pp. 134–151.
- Druon, J.-N. *et al.* (2016) 'Habitat suitability of the Atlantic bluefin tuna by size class: An ecological niche approach', *Progress in oceanography*, 142, pp. 30–46.
- Duarte, C.M. *et al.* (2020) 'Rebuilding marine life', *Nature*, 580(7801), pp. 39–51.
- Engelhard, G.H. *et al.* (2015) 'ICES meets marine historical ecology: placing the history of fish and fisheries in current policy context', *ICES journal of marine science: journal du conseil*, 73(5), pp. 1386–1403.
- Erlandson, J.M. and Rick, T.C. (2010) 'Archaeology meets marine ecology: the antiquity of maritime cultures and human impacts on marine fisheries and ecosystems', *Annual review of marine science*, 2, pp. 231–251.
- Faillottaz, R. *et al.* (2019) 'Atlantic Multidecadal Oscillations drive the basin-scale distribution of Atlantic bluefin tuna', *Science advances*, 5(1), p. eaar6993.

- Femerling, G. *et al.* (2022) 'Genetic load and adaptive potential of a recovered avian species that narrowly avoided extinction', *bioRxiv*. Available at: <https://doi.org/10.1101/2022.12.20.521169>.
- Ferrari, G. *et al.* (2021) 'The preservation of ancient DNA in archaeological fish bone', *Journal of Archaeological Science*, 126, p. 105317.
- Fiksen, Ø. and Reglero, P. (2022) 'Atlantic bluefin tuna spawn early to avoid metabolic meltdown in larvae', *Ecology*, 103(1), p. e03568.
- Finney, B.P. *et al.* (2002) 'Fisheries productivity in the northeastern Pacific Ocean over the past 2,200 years', *Nature*, 416(6882), pp. 729–733.
- Finney, B.P. *et al.* (2010) 'Paleoecological studies on variability in marine fish populations: A long-term perspective on the impacts of climatic change on marine ecosystems', *Journal of Marine Systems*, 79(3), pp. 316–326.
- France, R.L. (2021) 'Historical anecdotes of fishing pressure: Misconstrued “sea serpent” sightings provide evidence for antecedent entanglement of marine biota in the British Isles', *Fish and fisheries*, 22(1), pp. 54–71.
- Fromentin, J.-M. (2009) 'Lessons from the past: investigating historical data from bluefin tuna fisheries', *Fish and fisheries*, 10(2), pp. 197–216.
- Fromentin, J.-M. and Powers, J.E. (2005) 'Atlantic bluefin tuna: population dynamics, ecology, fisheries and management', *Fish and Fisheries*, pp. 281–306. Available at: <https://doi.org/10.1111/j.1467-2979.2005.00197.x>.
- Galland, G., Rogers, A. and Nickson, A. (2016) 'Netting billions: a global valuation of tuna', *The Pew Charitable Trusts*, pp. 1–22.
- Golet, W.J. *et al.* (2015) 'The paradox of the pelagics: why bluefin tuna can go hungry in a sea of plenty', *Marine ecology progress series*, 527, pp. 181–192.
- Guiry, E.J. *et al.* (2021) 'Early evidence for historical overfishing in the Gulf of Mexico', *Science advances*, 7(32). Available at: <https://doi.org/10.1126/sciadv.abh2525>.
- Guiry, E.J. and Hunt, B.P.V. (2020) 'Integrating fish scale and bone isotopic compositions for “deep time” retrospective studies', *Marine environmental research*, 160, p. 104982.
- Günther, B. *et al.* (2021) 'Metabarcoding confirms the opportunistic foraging behaviour of Atlantic bluefin tuna and reveals the importance of gelatinous prey', *PeerJ*, 9, p. e11757.
- Hazen, E.L. *et al.* (2019) 'Marine top predators as climate and ecosystem sentinels', *Frontiers in ecology and the environment*, 17(10), pp. 565–574.
- Heinisch, G. *et al.* (2014) 'Sexual maturity in western Atlantic bluefin tuna', *Scientific reports*, 4, p. 7205.
- Heino, M., Pauli, B.D. and Dieckmann, U. (2015) 'Fisheries-Induced Evolution', *Annual Review of Ecology, Evolution, and Systematics*, pp. 461–480.
- Heithaus, M.R. *et al.* (2008) 'Predicting ecological consequences of marine top predator



declines', *Trends in ecology & evolution*, 23(4), pp. 202–210.

Hernández, C.M. *et al.* (2022) 'Support for the Slope Sea as a major spawning ground for Atlantic bluefin tuna: evidence from larval abundance, growth rates, and particle-tracking simulations', *Canadian journal of fisheries and aquatic sciences. Journal canadien des sciences halieutiques et aquatiques*, 79(5), pp. 814–824.

Hilborn, R. *et al.* (2003) 'Biocomplexity and fisheries sustainability', *Proceedings of the National Academy of Sciences of the United States of America*, 100(11), pp. 6564–6568.

Hilborn, R. *et al.* (2020) 'Effective fisheries management instrumental in improving fish stock status', *Proceedings of the National Academy of Sciences of the United States of America*, 117(4), pp. 2218–2224.

Horton, T.W. *et al.* (2021) 'Evidence of increased occurrence of Atlantic bluefin tuna in territorial waters of the United Kingdom and Ireland', *ICES journal of marine science: journal du conseil*. Available at: <https://doi.org/10.1093/icesjms/fsab039>.

Howarth, L.M. *et al.* (2014) 'The unintended consequences of simplifying the sea: making the case for complexity', *Fish and fisheries*, 15(4), pp. 690–711.

ICCAT (2007) 'Report of the 2006 Atlantic bluefin tuna stock assessment session', *Col. Vol. Sci. Pap. ICCAT*, 60(3), pp. 652–880.

ICCAT (2020) 'Report of the 2020 second ICCAT intersessional meeting of the bluefin tuna species group. Online, 20-28 July 2020', *Second BFT Intersessional Meeting - Online 2020* Available at: [https://www.iccat.int/Documents/Meetings/Docs/2020/REPORTS/2020\\_2\\_BFT\\_ENG.pdf](https://www.iccat.int/Documents/Meetings/Docs/2020/REPORTS/2020_2_BFT_ENG.pdf).

Jackson, J.B. *et al.* (2001) 'Historical overfishing and the recent collapse of coastal ecosystems', *Science*, 293(5530), pp. 629–637.

Jennings, S., Reynolds, J.D. and Mills, S.C. (1998) 'Life history correlates of responses to fisheries exploitation', *Proceedings. Biological sciences / The Royal Society*, 265(1393), pp. 333–339.

Jørgensen, C. *et al.* (2007) 'Ecology: managing evolving fish stocks', *Science*, 318(5854), pp. 1247–1248.

Juan-Jordá, M.J. *et al.* (2022) 'Seventy years of tunas, billfishes, and sharks as sentinels of global ocean health', *Science*, 378(6620), p. eabj0211.

Karakulak, F.S., Salman, A. and Oray, I.K. (2009) 'Diet composition of bluefin tuna (*Thunnus thynnus* L. 1758) in the Eastern Mediterranean Sea, Turkey', *Zeitschrift fur angewandte Ichthyologie = Journal of applied ichthyology*, 25(6), pp. 757–761.

Kardos, M. *et al.* (2021) 'The crucial role of genome-wide genetic variation in conservation', *Proceedings of the National Academy of Sciences of the United States of America*, 118(48). Available at: <https://doi.org/10.1073/pnas.2104642118>.

Khan, A. *et al.* (2021) 'Genomic evidence for inbreeding depression and purging of deleterious genetic variation in Indian tigers', *Proceedings of the National Academy of Sciences of the United States of America*, 118(49). Available at: <https://doi.org/10.1073/pnas.2023018118>.

- Kuparinen, A. and Hutchings, J.A. (2012) 'Consequences of fisheries-induced evolution for population productivity and recovery potential', *Proceedings. Biological sciences / The Royal Society*, 279(1738), pp. 2571–2579.
- Kuparinen, A. and Merilä, J. (2007) 'Detecting and managing fisheries-induced evolution', *Trends in ecology & evolution*, 22(12), pp. 652–659.
- Le-Alvarado, M. *et al.* (2021) 'Yellowfin tuna (*Thunnus albacares*) foraging habitat and trophic position in the Gulf of Mexico based on intrinsic isotope tracers', *PloS one*, 16(2), p. e0246082.
- Llorente-Rodríguez, L. *et al.* (2022) 'Elucidating historical fisheries' networks in the Iberian Peninsula using stable isotopes', *Fish and fisheries* [Preprint]. Available at: <https://doi.org/10.1111/faf.12655>.
- Logan, J.M. *et al.* (2011) 'Diet of young Atlantic bluefin tuna (*Thunnus thynnus*) in eastern and western Atlantic foraging grounds', *Marine biology*, 158(1), pp. 73–85.
- Logan, J.M., Golet, W.J. and Lutcavage, M.E. (2015) 'Diet and condition of Atlantic bluefin tuna (*Thunnus thynnus*) in the Gulf of Maine, 2004–2008', *Environmental biology of fishes*, 98(5), pp. 1411–1430.
- Longo, S.B. and Clark, B. (2012) 'The commodification of bluefin tuna: The historical transformation of the Mediterranean fishery', *Journal of agrarian change*, 12(2-3), pp. 204–226.
- Lorrain, A. *et al.* (2020) 'Trends in tuna carbon isotopes suggest global changes in pelagic phytoplankton communities', *Global change biology*, 26(2), pp. 458–470.
- Lotze, H.K., Hoffmann, R. and Erlandson, J. (2014) 'Lessons from historical ecology and management', in *The Sea, Volume 19: Ecosystem-Based Management*. Harvard University Press.
- Lotze, H.K. and Worm, B. (2009) 'Historical baselines for large marine animals', *Trends in ecology & evolution*, 24(5), pp. 254–262.
- MacKenzie, B.R. *et al.* (2022) 'Neglected fishery data sources as indicators of pre-industrial ecological properties of Mediterranean swordfish (*Xiphias gladius*, Xiphiidae)', *Fish and Fisheries*, 23(4), pp.829-846.
- MacKenzie, B.R. and Mariani, P. (2012) 'Spawning of bluefin tuna in the Black Sea: historical evidence, environmental constraints and population plasticity', *PloS one*, 7(7), p. e39998.
- MacKenzie, B.R., Mosegaard, H. and Rosenberg, A.A. (2009) 'Impending collapse of bluefin tuna in the northeast Atlantic and Mediterranean', *Conservation letters*, 2(1), pp. 26–35.
- MacKenzie, B.R. and Myers, R.A. (2007) 'The development of the northern European fishery for north Atlantic bluefin tuna *Thunnus thynnus* during 1900–1950', *Fisheries research*, 87(2), pp. 229–239.
- Marandel, F. *et al.* (2019) 'Estimating effective population size of large marine populations, is it feasible?', *Fish and fisheries*, 20(1), pp. 189–198.
- Mariani, P. *et al.* (2016) 'The migration game in habitat network: the case of tuna', *Theoretical*

*Ecology*, 9(2), pp. 219–232.

Mather, F.J., Mason, J.M. and Jones, A.C. (1995) 'Historical document: life history and fisheries of Atlantic bluefin tuna'. Available at: [https://repository.library.noaa.gov/view/noaa/8461/noaa\\_8461\\_DS1.pdf](https://repository.library.noaa.gov/view/noaa/8461/noaa_8461_DS1.pdf).

McClanahan, T., Allison, E.H. and Cinner, J.E. (2015) 'Managing fisheries for human and food security', *Fish and fisheries*, 16(1), pp. 78–103.

McClatchie, S. *et al.* (2017) 'Collapse and recovery of forage fish populations prior to commercial exploitation', *Geophysical research letters*, 44(4), pp. 1877–1885.

McDowell, J.R. *et al.* (2022) 'Low levels of sibship encourage use of larvae in western Atlantic bluefin tuna abundance estimation by close-kin mark-recapture', *Scientific reports*, 12(1), p. 18606.

Medina, A. *et al.* (2022) 'Monitoring the reproductive status of resident and migrant Atlantic bluefin tuna in the Strait of Gibraltar', *Marine ecology progress series* [Preprint]. Available at: <https://doi.org/10.3354/meps14129>.

Morales-Muñiz, A. *et al.* (2018) 'Hindcasting to forecast. An archaeobiological approach to the European hake (*Merluccius merluccius*, Linnaeus 1758) fishery: Iberia and beyond', *Regional Studies in Marine Science*, 21, pp. 21–29.

Myers, R.A. and Worm, B. (2003) 'Rapid worldwide depletion of predatory fish communities', *Nature*, 423(6937), pp. 280–283.

Mylona, D. (2021) 'Catching tuna in the Aegean: biological background of tuna fisheries and the archaeological implications', *Anthropozoologica*, 56(2). Available at: <https://doi.org/10.5252/anthropozoologica2021v56a2>.

Neubauer, P. *et al.* (2013) 'Resilience and recovery of overexploited marine populations', *Science*, 340(6130), pp. 347–349.

Nøttestad, L., Bøge, E. and Ferter, K. (2020) 'The comeback of Atlantic bluefin tuna (*Thunnus thynnus*) to Norwegian waters', *Fisheries research*, 231, p. 105689.

Ólafsdóttir, D. *et al.* (2016) 'Dietary Evidence of Mesopelagic and Pelagic Foraging by Atlantic Bluefin Tuna (*Thunnus thynnus* L.) during Autumn Migrations to the Iceland Basin', *Frontiers in Marine Science*, 3. Available at: <https://doi.org/10.3389/fmars.2016.00108>.

Ólafsdóttir, G.Á. *et al.* (2014) 'Historical DNA reveals the demographic history of Atlantic cod (*Gadus morhua*) in medieval and early modern Iceland', *Proceedings. Biological sciences / The Royal Society*, 281(1777), p. 20132976.

Ólafsdóttir, G.Á. *et al.* (2017) 'A millennium of north-east Atlantic cod juvenile growth trajectories inferred from archaeological otoliths', *PLoS one*, 12(10), p. e0187134.

Ólafsdóttir, G.Á. *et al.* (2021) 'A millennium of trophic stability in Atlantic cod (*Gadus morhua*): transition to a lower and converging trophic niche in modern times', *Scientific reports*, 11(1), p. 12681.

Oosting, T. *et al.* (2019) 'Unlocking the potential of ancient fish DNA in the genomic era',

*Evolutionary applications*, 12(8), pp. 1513–1522.

Örenc, A.F. *et al.* (2014) 'Tentative GBYP bluefin tuna data recovery from the Ottoman Archives, the Maritime Museum Archives and the Archives of the Istanbul Municipality', *Col. Vol. Sci. Pap. ICCAT*, 70(2), pp. 447–458.

Orton, D.C. *et al.* (2011) 'Stable Isotope Evidence for Late Medieval (14th–15th C) Origins of the Eastern Baltic Cod (*Gadus morhua*) Fishery', *PLoS one*, 6(11), p. e27568.

Orton, D.C. (2016) 'Archaeology as a Tool for Understanding Past Marine Resource Use and Its Impact', in K. Schwerdtner Máñez and B. Poulsen (eds) *Perspectives on Oceans Past*. Dordrecht: Springer Netherlands, pp. 47–69.

Ottmann, D. *et al.* (2022) 'Small fish eat smaller fish: A model of interaction strength in early life stages of two tuna species', *Limnology and oceanography letters*, 7(3), pp. 227–234.

Pauly, D. (1995) 'Anecdotes and the shifting baseline syndrome of fisheries', *Trends in ecology & evolution*, 10(10), p. 430.

Pauly, D. *et al.* (1998) 'Fishing down marine food webs', *Science*, 279(5352), pp. 860–863.

Pauly, D. *et al.* (2002) 'Towards sustainability in world fisheries', *Nature*, 418(6898), pp. 689–695.

Pauly, D., Hilborn, R. and Branch, T.A. (2013) 'Fisheries: Does catch reflect abundance?', *Nature*, 494(7437), pp. 303–306.

Pauly, D., Watson, R. and Alder, J. (2005) 'Global trends in world fisheries: impacts on marine ecosystems and food security', *Philosophical transactions of the Royal Society of London. Series B, Biological sciences*, 360(1453), pp. 5–12.

Pedersen, T., Amundsen, C. and Wickler, S. (2022) 'Characteristics of early Atlantic cod (*Gadus morhua* L.) catches based on otoliths recovered from archaeological excavations at medieval to early modern sites in northern Norway', *ICES journal of marine science: journal du conseil*, 79(10), pp. 2667–2681.

Petitgas, P. *et al.* (2010) 'Stock collapses and their recovery: mechanisms that establish and maintain life-cycle closure in space and time', *ICES journal of marine science: journal du conseil*, 67(9), pp. 1841–1848.

Piccinetti, C., Di Natale, A. and Arena, P. (2013) 'Eastern bluefin tuna (*Thunnus thynnus*, L.) reproduction and reproductive areas and season', *Col. Vol. Sci. Pap. ICCAT*, 69(2), pp. 891–912.

Pinnegar, J.K. and Engelhard, G.H. (2008) 'The "shifting baseline" phenomenon: a global perspective', *Reviews in fish biology and fisheries*, 18(1), pp. 1–16.

Pinsky, M.L. *et al.* (2021) 'Genomic stability through time despite decades of exploitation in cod on both sides of the Atlantic', *Proceedings of the National Academy of Sciences of the United States of America*, 118(15). Available at: <https://doi.org/10.1073/pnas.2025453118>.

Planque, B. *et al.* (2010) 'How does fishing alter marine populations and ecosystems sensitivity to climate?', *Journal of Marine Systems*, 79(3), pp. 403–417.

- Porch, C.E. *et al.* (2019) 'The journey from overfishing to sustainability for Atlantic bluefin tuna, *Thunnus thynnus*', *The future of bluefin tunas: Ecology, fisheries management, and conservation*, pp. 3–44.
- Puncher, G.N. *et al.* (2015) 'A multitude of Byzantine era bluefin tuna and swordfish bones uncovered in Istanbul, Turkey', *Col. Vol. Sci. Pap. ICCAT*, 71(4), pp. 1626–1631.
- Puncher, G.N. *et al.* (2016) 'Unlocking the evolutionary history of the mighty bluefin tuna using novel paleogenetic techniques and ancient tuna remains', *Col. Vol. Sci. Pap. ICCAT*, 72(6), pp. 1429–1439.
- Puncher, G.N. *et al.* (2018) 'Spatial dynamics and mixing of bluefin tuna in the Atlantic Ocean and Mediterranean Sea revealed using next-generation sequencing', *Molecular ecology resources*, 18(3), pp. 620–638.
- Puncher, G.N. *et al.* (2019) 'Comparison and optimization of genetic tools used for the identification of ancient fish remains recovered from archaeological excavations and museum collections in the Mediterranean region', *International Journal of Osteoarchaeology*, 29(3), pp. 365–376.
- Puncher, G.N. *et al.* (2022) 'Individual assignment of Atlantic bluefin tuna in the northwestern Atlantic Ocean using single nucleotide polymorphisms reveals an increasing proportion of migrants from the eastern Atlantic Ocean', *Canadian journal of fisheries and aquatic sciences. Journal canadien des sciences halieutiques et aquatiques*, 79(1), pp. 111–123.
- Ravier, C. and Fromentin, J.-M. (2001) 'Long-term fluctuations in the eastern Atlantic and Mediterranean bluefin tuna population', *ICES journal of marine science: journal du conseil*, 58(6), pp. 1299–1317.
- Riccioni, G. *et al.* (2010) 'Spatio-temporal population structuring and genetic diversity retention in depleted Atlantic Bluefin tuna of the Mediterranean Sea', *Proceedings of the National Academy of Sciences*, pp. 2102–2107. Available at: <https://doi.org/10.1073/pnas.0908281107>.
- Richardson, D.E. *et al.* (2016) 'Discovery of a spawning ground reveals diverse migration strategies in Atlantic bluefin tuna (*Thunnus thynnus*)', *Proceedings of the National Academy of Sciences of the United States of America*, 113(12), pp. 3299–3304.
- Richter, K.K. *et al.* (2011) 'Fish 'n chips: ZooMS peptide mass fingerprinting in a 96 well plate format to identify fish bone fragments', *Journal of Archaeological Science*, 38(7), pp. 1502–1510.
- Robin, M. *et al.* (2022) 'Ancient mitochondrial and modern whole genomes unravel massive genetic diversity loss during near extinction of Alpine ibex', *Molecular ecology*, 31(13), pp. 3548–3565.
- Robinson, J.A. *et al.* (2022) 'The critically endangered vaquita is not doomed to extinction by inbreeding depression', *Science*, 376(6593), pp. 635–639.
- Rochet, M.-J. (1998) 'Short-term effects of fishing on life history traits of fishes', *ICES journal of marine science: journal du conseil*, 55, pp. 371–391.
- Rodríguez-Ezpeleta, N. *et al.* (2019) 'Determining natal origin for improved management of

- Atlantic bluefin tuna', *Frontiers in ecology and the environment*, 17(8), pp. 439–444.
- Rodriguez, J.M., Johnstone, C. and Lozano-Peral, D. (2021) 'Evidence of Atlantic bluefin tuna spawning in the Bay of Biscay, north-eastern Atlantic', *Journal of fish biology*, 99(3), pp. 964–969.
- Rooker, J.R. *et al.* (2008) 'Evidence of trans-Atlantic movement and natal homing of bluefin tuna from stable isotopes in otoliths', *Marine ecology progress series*, 368, pp. 231–239.
- Sbragaglia, V. *et al.* (2021) 'Fisheries-induced changes of shoaling behaviour: mechanisms and potential consequences', *Trends in ecology & evolution*, 36(10), pp. 885–888.
- Schijns, R. *et al.* (2021) 'Five centuries of cod catches in Eastern Canada', *ICES journal of marine science: journal du conseil*, 78(8), pp. 2675–2683.
- Schloesser, R.W. *et al.* (2009) 'Interdecadal variation in seawater d13C and d18O recorded in fish otoliths', *Limnology and oceanography*, 54(5), pp. 1665–1668.
- Schwerdtner Máñez, K. *et al.* (2014) 'The future of the oceans past: towards a global marine historical research initiative', *PloS one*, 9(7), p. E101466.
- Sella, M. (1929) 'Migrazioni e habitat del tonno (*Thunnus thynnus*, L.) studiati col metodo degli ami, con osservazioni su l'accrescimento, sul regime delle tonnare', *Memoria, R. Comitato Talassografico Italiano*, 156, pp. 511–542.
- Shchur, V. *et al.* (2022) 'Estimating population split times and migration rates from historical effective population sizes', *bioRxiv*. Available at: <https://doi.org/10.1101/2022.06.17.496540>.
- Siano, R. *et al.* (2021) 'Sediment archives reveal irreversible shifts in plankton communities after World War II and agricultural pollution', *Current biology: CB*, 31(12), pp. 2682–2689.e7.
- Siskey, M.R. *et al.* (2016) 'Forty years of fishing: changes in age structure and stock mixing in northwestern Atlantic bluefin tuna (*Thunnus thynnus*) associated with size-selective and long-term exploitation', *ICES journal of marine science: journal du conseil*, 73(10), pp. 2518–2528.
- Smoliński, S. *et al.* (2020) 'Century-long cod otolith biochronology reveals individual growth plasticity in response to temperature', *Scientific reports*, 10(1), p. 16708.
- Sodeland, M. *et al.* (2022) 'Stabilizing selection on Atlantic cod supergenes through a millennium of extensive exploitation', *Proceedings of the National Academy of Sciences of the United States of America*, 119(8). Available at: <https://doi.org/10.1073/pnas.2114904119>.
- Spiers, E.K.A. *et al.* (2016) 'Potential role of predators on carbon dynamics of marine ecosystems as assessed by a Bayesian belief network', *Ecological informatics*, 36, pp. 77–83.
- Steneck, R.S. (2012) 'Apex predators and trophic cascades in large marine ecosystems: learning from serendipity', *Proceedings of the National Academy of Sciences of the United States of America*, pp. 7953–7954.
- Thibon, F. *et al.* (2022) 'The ecology of modern and fossil vertebrates revisited by lithium isotopes', *Earth and planetary science letters*, 599, p. 117840.

- Thurstan, R.H., Hawkins, J.P. and Roberts, C.M. (2014) 'Origins of the bottom trawling controversy in the British Isles: 19th century witness testimonies reveal evidence of early fishery declines', *Fish and fisheries*, 15(3), pp. 506–522.
- Tseng, C.-M. *et al.* (2021) 'Bluefin tuna reveal global patterns of mercury pollution and bioavailability in the world's oceans', *Proceedings of the National Academy of Sciences of the United States of America*, 118(38). Available at: <https://doi.org/10.1073/pnas.2111205118>.
- Tzadik, O.E. *et al.* (2017) 'Chemical archives in fishes beyond otoliths: A review on the use of other body parts as chronological recorders of microchemical constituents for expanding interpretations of environmental, ecological, and life-history changes', *Limnology and oceanography, methods / ASLO*, 15(3), pp. 238–263.
- Van Neer, W. *et al.* (2002) 'Fish Otoliths and their Relevance to Archaeology: An Analysis of Medieval, Post-Medieval, and Recent Material of Plaice, Cod and Haddock from the North Sea', *Environmental Archaeology*, 7(1), pp. 61–76.
- Van Neer, W. *et al.* (2004) 'Fish remains from archaeological sites as indicators of former trade connections in the Eastern Mediterranean', *Paléorient*, 30(1), pp. 101–147.
- Vollset, K.W. *et al.* (2022) 'Ecological regime shift in the Northeast Atlantic Ocean revealed from the unprecedented reduction in marine growth of Atlantic salmon', *Science advances*, 8(9), p. eabk2542.
- Walli, A. *et al.* (2009) 'Seasonal movements, aggregations and diving behavior of Atlantic bluefin tuna (*Thunnus thynnus*) revealed with archival tags', *PloS one*, 4(7), p. e6151.
- Waples, R.S. *et al.* (2018) 'Robust estimates of a high Ne/N ratio in a top marine predator, southern bluefin tuna', *Science advances*, 4(7), p. eaar7759.
- Waples, R.S. and Do, C. (2008) 'Idne: a program for estimating effective population size from data on linkage disequilibrium', *Molecular ecology resources*, 8(4), pp. 753–756.
- Williams, N. (2007) 'Tuna crisis looms', *Current biology: CB*, 17(4), pp. R108–R109.
- Wilson, S.G. and Block, B.A. (2009) 'Habitat use in Atlantic bluefin tuna *Thunnus thynnus* inferred from diving behavior', *Endangered species research*, 10, pp. 355–367.
- Worm, B. *et al.* (2009) 'Rebuilding global fisheries', *Science*, 325(5940), pp. 578–585.
- Worm, B. and Tittensor, D.P. (2011) 'Range contraction in large pelagic predators', *Proceedings of the National Academy of Sciences of the United States of America*, 108(29), pp. 11942–11947.
- WWF (2006) *The plunder of bluefin tuna in the Mediterranean and East Atlantic in 2004 and 2005 - Uncovering the real story*. WWF. Available at: [https://wwfeu.awsassets.panda.org/downloads/wwfbftreportfinalaeditionreducido\\_final.pdf](https://wwfeu.awsassets.panda.org/downloads/wwfbftreportfinalaeditionreducido_final.pdf).
- Zeller, D., Froese, R. and Pauly, D. (2005) 'On losing and recovering fisheries and marine science data', *Marine Policy*, 29(1), pp. 69–73.

**Adam J. Andrews**

## **Unlocking ecological history using fish remains**

### **Eco-evolutionary consequences of exploitation in the Atlantic bluefin tuna**

During recent decades, the health of ocean ecosystems and fish populations has been threatened by overexploitation, pollution, and anthropogenic-driven climate change. Due to a lack of long-term data, we have a poor understanding of when intensive exploitation began and what impact anthropogenic activities have had on the ecology and evolution of fishes. Such information is crucial to recover degraded and depleted marine ecosystems and fish populations, maximise their productivity in-line with historical levels, and predict their future dynamics. In this thesis, I evaluate anthropogenic impacts on the iconic Atlantic bluefin tuna (*Thunnus thynnus*; BFT), one of the longest and recently most intensely exploited marine fishes, with a tremendous cultural and economic importance. Using a long-time series of archaeological and archived faunal remains (bones) dating back to approximately two millennia ago, I apply morphological, isotopic, and genomic techniques to perform the first studies on long-term BFT size and growth, diet and habitat use, and demography and adaptation, and produce the first genome-wide data on this species. My findings suggest that exploitation had impacted BFT foraging behaviour by the ~16<sup>th</sup> century when coastal ecosystem degradation induced a pelagic shift in diet and habitat use. I reveal that BFT biomass began to decline much earlier than hitherto documented, by the 19<sup>th</sup> century, consistent with intensive tuna trap catches during this period and catch-at-size increasing. I find that BFT juvenile growth had increased by the early 1900s (and more dramatically by the 21<sup>st</sup> century) which may reflect an evolutionary response to size selective harvest—which I find putative genomic signatures of. Further, I observed that BFT foraging behaviours have been modified following overexploitation during the 20<sup>th</sup> century, which previously included an isotopically distinct, Black Sea niche. Finally, I show that despite biomass declining from centuries ago, BFT has retained genomic diversity. This provides confidence for its long-term recovery, suggesting that management plans can be ambitious with their recovery targets. However, the loss of a Black Sea trophic niche, and potential for fisheries-induced evolution is concerning and requires further investigation. Unfortunately, all in all my findings show that modern marine ecosystems may be more heavily modified than previously thought, therefore further multidisciplinary long-term investigations are warranted to study the wide-ranging and far-reaching effects of marine exploitation.

**Dissertation for the degree of PhD 2023**

PhD Programme in Cultural and Environmental Heritage

Alma Mater Studiorum – University of Bologna